9/8-94 9 8 (2)

ANL/RERTR/TM-13
CONF-8809221--

ANL/RERTR/TM-13
CONF-8809221--

Proceedings of the 1988 International Meeting on REDUCED ENRICHMENT FOR RESEARCH AND TEST REACTORS

San Diego, California

September 19–22, 1988

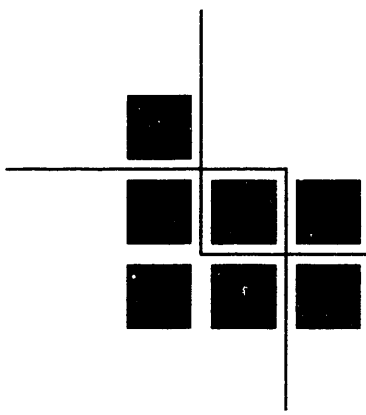

Reduced Enrichment
Research and Test Reactor
Program

ARGONNE NATIONAL LABORATORY, ARGONNE, ILL.
Operated by THE UNIVERSITY OF CHICAGO

Prepared for the U. S. DEPARTMENT OF ENERGY

Office of Intelligence and National Security,
Office of Arms Control and Nonproliferation
under Contract W-31-109-Eng-38

DISTRIBUTION OF THIS DOCUMENT IS UNLIMITED

Argonne National Laboratory, with facilities in the states of Illinois and Idaho, is owned by the United States government, and operated by The University of Chicago under the provisions of a contract with the Department of Energy.

DISCLAIMER

This report was prepared as an account of work sponsored by an agency of the United States Government. Neither the United States Government nor any agency thereof, nor any of their employees, makes any warranty, express or implied, or assumes any legal liability or responsibility for the accuracy, completeness, or usefulness of any information, apparatus, product, or process disclosed, or represents that its use would not infringe privately owned rights. Reference herein to any specific commercial product, process, or service by trade name, trademark, manufacturer, or otherwise, does not necessarily constitute or imply its endorsement, recommendation, or favoring by the United States Government or any agency thereof. The views and opinions of authors expressed herein do not necessarily state or reflect those of the United States Government or any agency thereof.

Reproduced from the best available copy.

Available to DOE and DOE contractors from the
Office of Scientific and Technical Information
P.O. Box 62
Oak Ridge, TN 37831
Prices available from (615) 576-8401

Available to the public from the
National Technical Information Service
U.S. Department of Commerce
5285 Port Royal Road
Springfield, VA 22161

Distribution Category
Nuclear Energy (UC-940)

ANL/RERTR/TM-13
CONF-8809221

ARGONNE NATIONAL LABORATORY
9700 South Cass Avenue
Argonne, Illinois 60439

Proceedings of the 1988 International Meeting on

REDUCED ENRICHMENT FOR RESEARCH AND TEST REACTORS

San Diego, California
September 19-22, 1988

Armando Travelli
Program Chairman

Administrative Arrangements

Carole Simpson
Eileen Johnson

July 1993

MASTER

DISTRIBUTION OF THIS DOCUMENT IS UNLIMITED

The previous Reduced Enrichment for Research and Test Reactor meetings were held at:

Argonne National Laboratory - November 1978

Saclay, France - December 1979

Argonne National Laboratory - November 1980

Juelich, FRG - September 1981

Argonne National Laboratory - November 1982

Tokai, Japan - October 1983

Argonne National Laboratory - October 1984

Petten, The Netherlands - October 1985

Gatlinburg, Tennessee - November 1986

Buenos Aires, Argentina - September 1987

San Diego, California - September 1988

Berlin, Germany - September 1989

Newport, Rhode Island - September 1990

Jakarta, Indonesia - November, 1991

Roskilde, Denmark - September, 1992

PREFACE

The international effort to develop and implement new research reactor fuels utilizing low-enriched uranium, instead of highly-enriched uranium, continues to make solid progress. This effort is the cornerstone of a widely shared policy aimed at reducing, and possibly eliminating, international traffic in highly-enriched uranium and the nuclear weapon proliferation concerns associated with this traffic.

The effort involves scientists, reactor operators, commercial fuel suppliers, research centers, and government organizations from at least 35 different countries, each sharing our common goal and each unique in its contributions.

To foster direct communication and exchange of ideas among the specialists in this area, the Reduced Enrichment Research and Test Reactor (RERTR) Program, at Argonne National Laboratory, sponsored this meeting as the eleventh of a series which began in 1978. All previous meetings of this series are listed on the facing page.

The focus of this meeting was the General Atomics Company, which championed utilization of LEU fuels in its greatly successful TRIGA reactors, and whose new high-density LEU fuels were licensed by the NRC in 1987. On behalf of all attendees, I would like to thank the General Atomics Company for many years of successful and continuing cooperation, and for the interesting tour of their facilities which they provided on this occasion.

It was with much sadness that we learned, on the second day of the meeting, of the untimely death of Dr. Richard A. Lewis in an airplane crash. Dick pioneered the concept of the RERTR program and for many years supported our efforts with his advice and indomitable energy. With a great feeling of loss, I dedicate these proceedings to his memory.

Armando Travelli
Program Manager

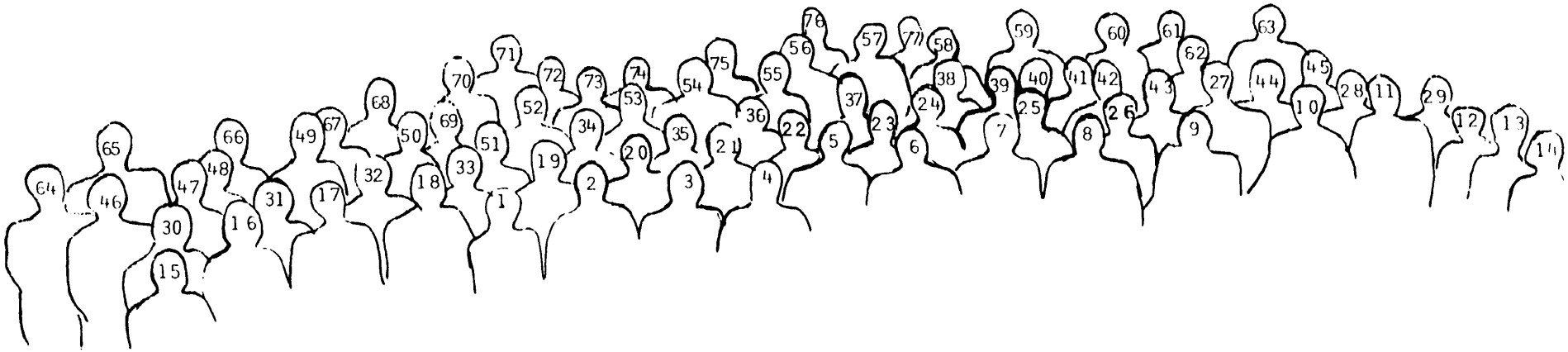

1. J. Kwok, ANL, U.S.
2. J. Colton, ACDA, U.S.
3. K. Kanda, KURRI, Japan
4. J. Rest, ANL, U.S.
5. G. Thamm, KFA-Jülich, FRG
6. A. Travelli, ANL, U.S.
7. S. Ceja, DOE, U.S.
8. J. Jaspert, Euratom, Belgium
9. F. DiMeglio, RINSC, U.S.
10. S. Mo, ANL, U.S.
11. M. Madariaga, INVAP S.E., Argentina
12. I. Concha, IAN, Colombia
13. C. Simpson, ANL, U.S.
14. E. Johnson, ANL, U.S.
15. H-t. Kung, INER, Taiwan
16. D. Thom, UKAEA-Dounreay, Scotland
17. A. Tissier, CERCA, France
18. P. Porte, CERCA, France
19. D. Giorsetti, CNEA, Argentina
20. J-C. Marguin, CERCA, France
21. H. Hassel, CERCA/NUKEM, FRG
22. M. Cundy, JRC-Petten, The Netherlands
23. B. Horn, NRC, U.S.
24. K. Saltvedt, Studsvik Nuc., Sweden
25. K. Haack, Risø Natl. Lab., Denmark
26. R. Domagala, ANL, U.S.
27. J. Matos, ANL, U.S.
28. J. Deen, ANL, U.S.
29. M. Bretscher, ANL, U.S.
30. I. Bornstein, ANL, U.S.
31. P. Blum, Transnucleaire, France
32. J. Schreader, AECL, CRNL, Canada
33. A. Wares, UKAEA-Dounreay, Scotland
34. J. DeVries, IRI, The Netherlands
35. A. Strömich, Interatom GmbH, FRG
36. J. Ahlf, JRC-Petten, The Netherlands
37. W. Krull, GKSS, FRG
38. J. Snelgrove, ANL, U.S.
39. Y. Fanjas, CERCA, France
40. J-F. Poupard, CERCA, France
41. O. Gallar, Purdue University, U.S.
42. E. Bauer, Inst. Laue-Langevin, France
43. G. Gruber, NUKEM GmbH, FRG
44. R. Muranaka, IAEA, Austria
45. G. West, GA, U.S.
46. F. Merchie, CEA-Grenoble, France
47. Y. Futamura, JAERI, Japan
48. W. Krug, KFA-Jülich, FRG
49. I. Kennedy, AECL, CRNL, Canada
50. P. Ernst, McMaster Univ., Canada
51. W. Ruzicka, Cintichem, U.S.
52. W. Byszewski, IAEA, Austria
53. R. Rydin, Univ. of Virginia, U.S.
54. H. Fuchs, CERCA/NUKEM, FRG
55. G. Hofman, ANL, U.S.
56. G. Vandegrift, ANL, U.S.
57. A. Sameh, KFK-Karlsruhe, FRG
58. W. Woodruff, ANL, U.S.
59. R. DeLaBarre, DOS, U.S.
60. E. Adolph, Risø Nat. Lab., Denmark
61. A. Beeckmans, CEN/SCK, Belgium
62. G. Copeland, ORNL, U.S.
63. J. Borring, Risø, Denmark
64. F. Sakurai, JAERI, Japan
65. H. Tschiesche, Nuc.Cargo & Serv., FRG
66. J-H. Guiheux, COGEMA, France
67. K. Parker, UKAEA-Risley, U.K.
68. A. Röhrmoser, Tech. Univ. Munich, FRG
69. T. Wiencek, ANL, U.S.
70. B. Horn, NRC, U.S.
71. H. Preble, B&W, U.S.
72. K. Brown, DOE, U.S.
73. J. DeFelice, Precision Componts., U.S.
74. R. Knight, ORNL, U.S.
75. S. Fukushima, Nissho Iwai Corp., Japan
76. J. Marks, B&W, U.S.
77. A. Ballagny, CEA-CEN-Saclay, France

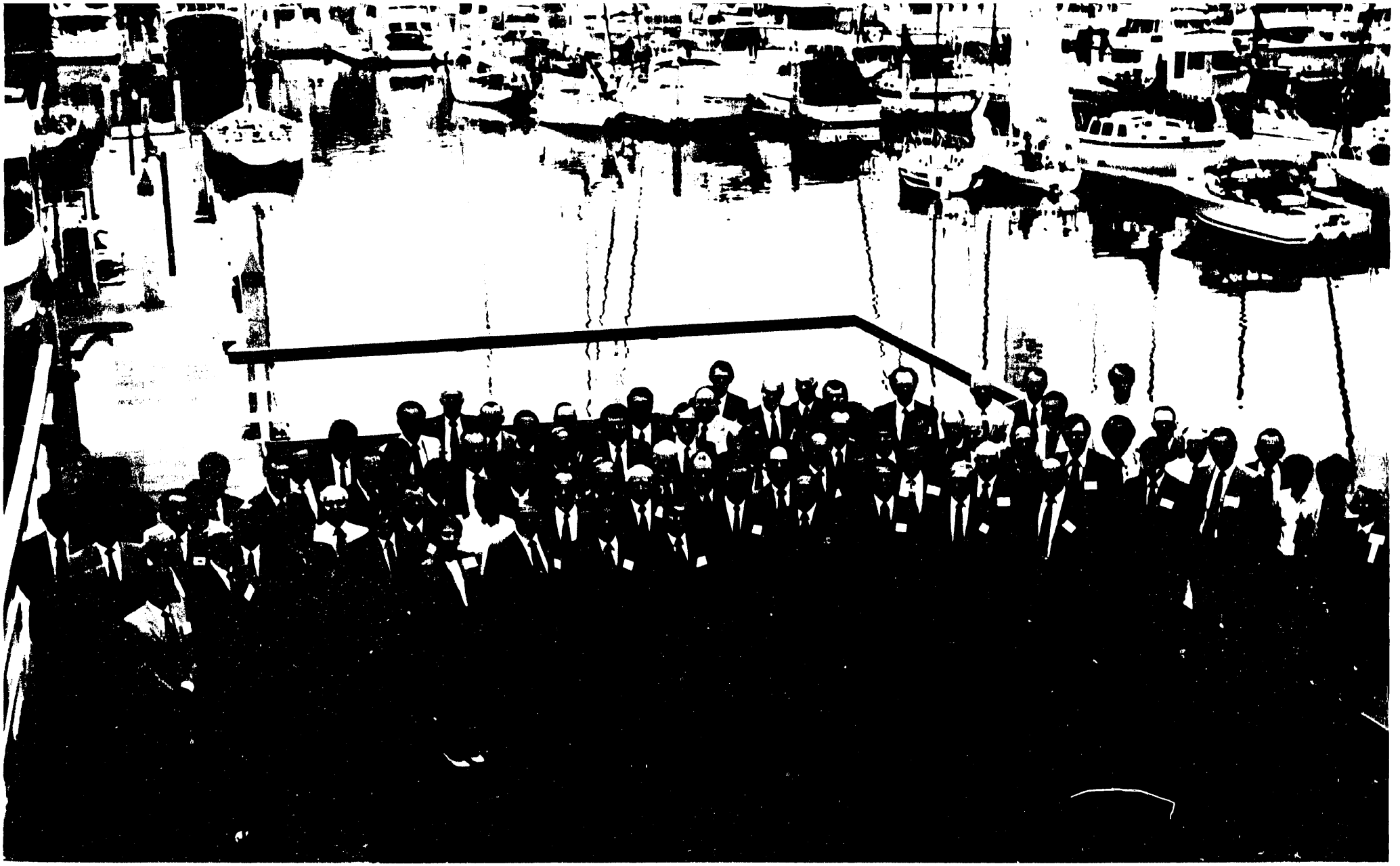

1988 INTERNATIONAL MEETING ON REDUCED ENRICHMENT FOR RESEARCH AND TEST REACTORS SEPT. 19-22, 1988
KONA KAI BEACH AND TENNIS RESORT, SAN DIEGO, CALIFORNIA USA

Table of Contents

SESSION I

September 19, 1988

NATIONAL PROGRAMS
Chairman: A. Travelli (ANL, USA)

Page

STATUS OF THE RERTR PROGRAM
A. Travelli, ANL 3

THE STATUS OF THE GERMAN AF PROGRAM, PROSPECTS WITH RESPECT TO PROGRAM TERMINATION, FURTHER INTERNATIONAL RERTR COOPERATION, AND -HEU -LEU RESEARCH REACTOR CONVERSIONS
G. Thamm, KFA-Jülich 14

PRESENT STATUS AND OBJECTIVES OF THE REDUCED ENRICHMENT PROGRAM FOR RESEARCH REACTORS IN FRANCE
F. Merchie, CEA-CEN-Grenoble 24

STATUS OF REDUCED ENRICHMENT PROGRAM FOR RESEARCH REACTORS IN JAPAN
K. Kanda* and H. Nishihara, KURRI
Y. Futamura, H. Sakurai, and Y. Iso, JAERI 31

NATIONAL PROGRAMS (Continued)
Chairman: K.Haack, (Risø National Laboratory, Denmark)

STATUS OF CANADIAN LOW-ENRICHED URANIUM CONVERSION PROGRAM
J.W. Schreader*, I.C. Kennedy, and D.F. Sears, AECL . . . 39

IAEA ACTIVITIES IN RESEARCH REACTOR SAFETY
W. Byszewski, IAEA 48

SESSION II

September 19, 1988

CHANGES IN THE FUEL FABRICATION INDUSTRY
Chairman: G. Thamm (KFA-Jülich, FRG)

WHY NUKEM STEPS OUT OF THE MTR-FUEL ELEMENT MARKET AND HOW TO SOLVE THE PROBLEMS RESULTING FROM THAT
H. Hassel, CERCA/NUKEM, FRG 69

RECENT EVOLUTION IN THE MTR FUEL INDUSTRY
Y. Fanjas* and J.C. Marguin, CERCA 73

---

*Denotes speaker

SESSION III

September 19, 1988

FUEL DEVELOPMENT
Chairman: G. Thamm (KFA-Jülich, FRG)

FABRICATION OF HIGH-DENSITY FUEL PLATES BY HOT ISOSTATIC PRESSING
T.C. Wiencek*, R.F. Domagala, and H. R. Thresh, ANL . . . 85

SOME RECENT OBSERVATIONS ON THE RADIATION BEHAVIOR OF URANIUM SILICIDE DISPERSION FUEL
G. L. Hofman, ANL 92

FUEL DEVELOPMENT (Continued)
Chairman: K. Saltvedt (Energiteknik AB, Sweden)

THE EFFECT OF CRYSTAL STRUCTURE STABILITY ON SWELLING IN INTERMETALLIC URANIUM COMPOUNDS
J. Rest., G.L. Hofman, and R.C. Birtcher, ANL 111

FINAL RESULTS OF TEST-IRRADIATIONS WITH LEU-PLATES AT KFA JüLICH
W. Krug*, E. Groos, J. Seferiadis, and G. Thamm, KFA-Jülich 155

IRRADIATION BEHAVIOR OF THE CNEA'S EXPERIMENTAL URANIUM SILICIDE DISPERSION FUEL PLATES
G. L. Hofman*, ANL
A. Marajofsky and C. Kohut, CNEA 182

SESSION IV

September 20, 1988

FUEL FABRICATION
Chairman: W. Krull (GKSS, FRG)

ADAPTION OF INSPECTION METHODS TO LEU FUEL
J. F. Poupard, CERCA 209

MANUFACTURE OF RESEARCH REACTOR FUELS
R. W. Knight, ORNL 225

LEU FUEL ELEMENT PRODUCTION PLANT AT RISφ NATIONAL LABORATORY
E. Adolph*, P. Toft, and J. Borring, Risø 228

PREPARATION OF REDUCED ENRICHMENT FUELS FOR KOREA MULTIPURPOSE RESEARCH REACTOR AND THE EFFORTS TO REDUCE THE DIFFICULTIES IN COMMINUTION OF U_3SI-AL DISPERSED FUEL
I. H. Kuk, C.K. Kim, and J. T. Lee, KAERI 239

SESSION V

September 20, 1988

CONVERSION EXPERIENCES
Chairman: F. Merchie (CEA-CEN-Grenoble, France)

FUEL ELEMENT POWERS, ^{235}U MASSES, AND BURNUPS FROM GAMMA-SCANNING DATA (PRELIMINARY ANALYSIS OF IRRADIATED ORR LEU FUEL ELEMENTS)
M. M. Bretscher* and J. L. Snelgrove, ANL
R. W. Hobbs, ORNL 257

ENRICHMENT REDUCTION ACTIVITIES FOR THE FRG-1 AND FRG-2 RESEARCH REACTORS
W. Krull, GKSS 273

LICENSE APPROVAL ON THE CONVERSION OF DR-3 TO LEU
K. Haack, Risø 282

SESSION VI

September 20, 1988

CONVERSION PLANS AND STUDIES
Chairman: K. Kanda (KURRI, Japan)

FULL CORE MEU FUEL DEMONSTRATION IN THE JRR-2
Y. Futamura*, J. Tsunoda, and T. Koganezawa, JAERI 293

REDUCED ENRICHMENT FUEL CONVERSION EFFORTS AT THE SWEDISH R2 RESEARCH AND TEST REACTOR
E. Kaffehr and K. Saltvedt, Studsvik AB 304

LEU FUEL CYCLE ANALYSES FOR THE BELGIAN BR2 RESEARCH REACTOR
J. R. Deen* and J. L. Snelgrove, ANL 313

CONVERSION AIMS ON THEIR WAY FROM PHYSICS TO ECONOMY
A. Strömich and H-J. Rögler, Interatom GmbH 324

CONVERSION PLANS AND STUDIES (Continued)
Chairman: F. DiMeglio (RINSC, USA)

ANALYTICAL, ENGINEERING AND LICENSING ASPECTS OF THE OSURR LEU CONVERSION/UPGRADE
J. Talnagi*, T. Aldemir, and D. W. Miller,
Ohio State University 335

STATUS OF THE UNIVERSITY OF VIRGINIA REACTOR CONVERSION TO LEU FUEL
R. A. Rydin*, S. Wasserman, M. Fehr, D. Freeman,
and B. Hosticka, University of Virginia 346

NEUTRONIC CALCULATIONS FOR THE IAN-R1 RESEARCH REACTOR CORE CONVERSION
I. A. Concha, IAN 358

SESSION VII

September 21, 1988

CONVERSION PLANS AND STUDIES (Continued)
Chairman: A. Beeckmans (CEN-SCK, Belgium)

PRELIMINARY SAFETY ANALYSIS FOR JMTR CORE CONVERSION TO LEU FUEL
F. Sakurai*, E. Ishituka, H. Ando, M. Saito, and R. Oyamada, JAERI 375

PHYSICS OF THE MUNICH COMPACT CORE DESIGN
A. Röhrmoser, K. Böning, and W. Gläser, TUM 393

SOME OBSERVATIONS REGARDING RESEARCH REACTOR COMPARISONS TO THE SPERT TRANSIENT EXPERIMENTS
W. L. Woodruff, ANL 404

SESSION VIII

September 21, 1988

TARGETS
Chairman: J. E. Matos (ANL, USA)

PRODUCTION CYCLE OF FISSION MOLYBDENUM-99
A. A. Sameh* and H. J. Ache, KFK 417

PROCESSING OF LOW-BURNUP LEU SILICIDE TARGETS
J. Kwok*, G. F. Vandegrift, and J. E. Matos, ANL 434

CONTINUING INVESTIGATIONS ON ELECTROCHEMICAL PREPARATION OF LEU TARGETS FOR ^{99}MO PRODUCTION
S. L. Marshall, L. Redey, D. R. Vissers*, G. F. Vandegrift, and J. E. Matos, ANL 443

TRANSNUCLÉAIRE INTRODUCTION TO THE TRANSPORTATION PANEL 459

FINAL LIST OF ATTENDEES 461

SESSION I

September 19, 1988

NATIONAL PROGRAMS

Chairmen:

A. Travelli
(ANL, USA)

K. Haack
(RISØ, Denmark)

STATUS OF THE RERTR PROGRAM

A. Travelli
Argonne National Laboratory
Argonne, Illinois 60439 U.S.A.

ABSTRACT

The progress of the Reduced Enrichment Research and Test Reactor (RERTR) Program is described. After a brief summary of the results which the RERTR Program, in collaboration with its many international partners, had achieved by the end of 1987, the major events, findings, and activities of 1988 are reviewed.

The U.S. Nuclear Regulatory Commission issued a formal and generic approval of the use of U_3Si_2-Al dispersion fuel in research and test reactors, with densities up to 4.8 g U/cm^3.

New significant findings from postirradiation examinations, from ion-beam irradiations, and from analytical modeling, have raised serious doubts about the potential of LEU U_3Si-Al dispersion fuel for applications requiring very high uranium densities and high burnups (>6 g U/cm^3, >50% burnup).

As a result of these findings, the fuel development efforts have been redirected towards three new initiatives: 1) a systematic application of ion-beam irradiations to screen new materials; 2) application of Hot Isostatic Pressing (HIP) procedures to produce U_3Si_2-Al plates with high uranium densities and thin uniform cladding; and 3) application of HIP procedures to produce plates with U_3Si wires imbedded in an aluminum matrix, achieving stability, high uranium density, and thin uniform cladding. The new fuel concepts hold the promise of extraordinary performance potential and require approximately five years to develop. The first results are encouraging but not conclusive. More concrete results are needed before a decision can be reached about the desirability of bringing these efforts to conclusion.

As the RERTR Program embarks in a period of renewed fuel development, with exciting new tools, techniques, and concepts, the importance of international cooperation continues to be essential.

INTRODUCTION

The Reduced Enrichment Research and Test Reactor (RERTR) Program was established in 1978 by the Department of Energy (DOE). It was managed and funded by DOE through 1986. Beginning in 1987, funding responsibility for the program was assumed by the Arms Control and Disarmament Agency (ACDA) with management responsibility shared between ACDA and DOE. The primary objective of the program is to develop the technology needed to use Low-Enrichment Uranium (LEU) instead of High-Enrichment Uranium in research and test reactors, and to do so without significant penalties in experiment performance, economics, or safety aspects.

Excellent progress has been made toward the achievement of this objective through the close cooperation which has existed since the beginning between the program and the many organizations represented at this meeting. In particular, cooperation with General Atomics has been active since 1978. As part of this cooperation, rods of several advanced LEU TRIGA fuel types were developed and fabricated by General Atomics and demonstrated by the RERTR Program through an extensive series of irradiations in the Oak Ridge Research Reactor (ORR). It is a pleasure to report here, in close proximity to General Atomics and to their Mark-F reactor which will be refueled next month with one of the new LEU fuels, on the status of the RERTR Program, on last year's progress, and on our plans.

OVERVIEW OF THE SEPTEMBER 1987 PROGRAM STATUS

By September 1987, when the last International RERTR Meeting was held,[1] the main results achieved in the fuel development area were:

(a) The qualified uranium densities of the three main fuels which were in operation with HEU in research reactors when the program began (UAl_x-Al with up to 1.7 g U/cm^3; U_3O_8-Al with up to 1.3 g U/cm^3; and $UZrH_x$ with 0.5 g U/cm^3) had been significantly increased. The new uranium densities extended up to 2.3 g U/cm^3 for UAl_x-Al, 3.2 g U/cm^3 for U_3O_8-Al, and 3.7 g U/cm^3 for $UZrH_x$. Each fuel had been tested extensively for up to these densities and, in some cases, beyond them. All the data needed to qualify these fuel types with LEU and with the higher uranium densities had been collected.

(b) For U_3Si_2-Al, all the data needed to qualify this fuel type with LEU and with densities up to 4.8 g U/cm^3 had been collected and submitted to the U.S. Nuclear Regulatory Commission (NRC) for review. In addition, a whole-core demonstration using this fuel had been successfully completed in the ORR using a mixed-core approach.

(c) For U_3Si-Al, miniplates with up to 6.1 g U/cm^3 had been fabricated by ANL and the CNEA, and irradiated to 84-96% in the ORR. PIE of these miniplates had given good results, but had shown that some burnup limits might need to be imposed for the higher densities.

A large number of miniplates (54) had been irradiated in the ORR as part of the second miniplate series. These miniplates had densities up to 7.2 g U/cm^3, enrichments up to 93%, greater than stochiometric Si contents, and other variations. Only partial postirradiation examinations had been completed, with inconclusive results.

Four full-size plates, fabricated by CERCA with up to 6.0 g U/cm^3 had been successfully irradiated to 53-54% burnup in SILOE.

Irradiation testing of a full-size U_3Si-Al (6.0 g U/cm^3) element, fabricated by CERCA, had been successfully completed in SILOE with 55% burnup.

In other important program areas, reprocessing studies at the Savannah River Laboratory had concluded that the RERTR fuels could be successfully reprocessed at the Savannah River Plant and DOE had defined the terms and conditions under which these fuels will be accepted for reprocessing.

Extensive studies had been conducted, with favorable results, on the performance, safety, and economic characteristics of LEU conversions. These studies included many joint study programs, which were in progress for 28 reactors from 17 different countries.

A new analytical/experimental program had begun to determine the feasibility of using LEU, instead of HEU, in fission targets dedicated to the production of ^{99}Mo for medical applications.

Coordination of the safety calculations and evaluations had begun for the U.S. university reactors planning to convert to LEU as required by the recent NRC rule. Calculations for seven reactors were in progress.

PROGRESS OF THE RERTR PROGRAM IN 1988

1. Fuel Development

The past year was marked by several significant events, findings and initiatives in the fuel development area. These factors have strongly affected the entire program's activities, objectives, schedule, and plans for the future.

1) In July 1988 the U. S. Nuclear Regulatory Commission issued a formal and generic approval[2] of the use of U_3Si_2-Al fuel in research and test reactors, with uranium densities up to 4.8 g/cm^3.

This approval is the coronation of many years of work on U_3Si_2-Al fuel by the entire RERTR effort, both in the United States and abroad. It paves the way for several research reactor core conversions that are already in progress in the U.S. It also provides foreign licensors with convincing evidence that the methods, procedures, and results used to qualify this fuel are valid, because they have passed with flying colors one of the most demanding reviews to which they could be subjected.

With the addition of U_3Si_2-Al fuel to the list of the LEU fuels which were successfully qualified since the RERTR Program began, it can be safely concluded that at least 90% of the research reactors which were using HEU fuel in 1978 can now use LEU fuels without significant penalties. Most of the program's efforts are now to be devoted to the higher uranium densities needed to convert the remaining reactors, which use approximately 30% of the HEU dedicated to research reactor fuels. It is in this area that three important findings were made at the beginning of 1988.

2) As the postirradiation examinations of the second miniplate series progressed[3] (including U_3Si, $U_3Si_{1.5}$, U_3SiCu, and other plates containing U_3Si as their primary component), the results failed to indicate that the tendency of U_3Si to swell under irradiation could be suppressed by any of the modifications which had been tried.

3) A technique based on ion bombardment and in-situ transmission electron microscopy (TEM) of U_3Si samples[4], revealed that this material undergoes a crystalline-to-amorphous transformation when irradiated under conditions very similar to those encountered by fuel operating in a research reactor. After the transformation, U_3Si loses nearly all of its structural stability and flows plastically as observed in the past in several miniplates subjected to high burnups during in-pile irradiations.

4) An analytical model was developed[5] to predict the behavior of amorphous U_3Si under irradiation. The model predicts correctly the swelling and bubble distribution of U_3Si under in-pile irradiation, and the very different behavior observed for U_3Si_2.

These findings forced a thorough reevaluation of the potential of U_3Si fuel, as developed so far, for achieving the long-term goals of the program. It was concluded that the evidence available to date indicates that U_3Si can be used safely with densities of up to 6 g U/cm^3 and intermediate burnups ($\leq$50%), as indicated by miniplate results and by full-size element irradiations in SILOE. However, there are strong indications that the material as currently developed cannot be used safely outside these limits. Furthermore, the problems associated with U_3Si-Al appear to stem from a fundamental property of the material (its amorphous structure, after the irradiation-induced transformation) which does not appear to be sensitive to the type of adjustments considered so far.

As a result, many of the program's activities, which up to that time had been directed at the demonstration of U_3Si fuels in the high-burnup, high-uranium-density range, had to be redirected. Since the traditional processes had already been extensively pursued and applied to the very limits of fabricability, new and fresh approaches were required to achieve the higher uranium loadings which are the goal of the program. The experiences and ideas of many years were brought to bear on this exercise, and the result was a new set of initiatives and activities which have now been in progress for almost six months.

5) Continue ion-beam irradiations of U_3Si specimens and of other specimens, to observe the behavior of their crystalline structure and physical properties under irradiation.

A general objective of this task is to gain a fundamental understanding of how, when, and why the crystalline-to-amorphous transformation occurs in U_3Si. A specific objective is to identify treatments or alloying additions which might prevent the transformation from occurring. It has already been noticed during ion-beam irradiations that the onset of the transformation is strongly dependent on temperature and prior irradiations. It may be possible to identify procedures or additions which prevent the transformation, or new promising fuel materials. The potential usefulness of this tool for the evaluation of nuclear fuels is enormous and largely untapped. The results are obtained nearly one hundred times faster, and nearly one hundred times less expensively, than those obtained through in-pile testing. Of course, in-pile testing will still be required to confirm the good behavior of promising candidate fuels.

6) Pursue development of a U_3Si_2-Al fuel with greater fuel volume fraction than achieved in the past, and a greatly improved fuel homogeneity, allowing use of thinner nominal cladding.

The goal of this activity is to develop plates with a uranium density of up to 6.8 g/cm^3 in the fuel meat, and with a uniform clad thickness of 0.25 mm.

7) Pursue development of a rodded-plate U_3Si fuel concept compatible with the amorphous structure of this material.

In this concept, the U_3Si is shaped into wires imbedded in the aluminum matrix. The structural strength of the matrix prevents the swelling of the wires, as evidenced by the AECL experience with U_3Si-Al rods[6] and by the small forces observed at work on the amorphous material. The goal of this activity is to develop plates with a uranium density of up to 8.6 g/cm^3 in the fuel meat, and with a uniform clad thickness of 0.25 mm.

A key element of the last two activities is the replacement of plate rolling with Hot Isostatic Pressing (HIP), in which the entire plate is subjected simultaneously to very high, uniform, and controlled temperatures and pressures. HIPping promises to make it possible to achieve reliably the very thin uniform cladding thicknesses which are pursued in both activities. Thin cladding, combined with high uranium density in the fuel meat, holds the promise for research reactor fuels of extraordinary performance. For instance, a typical MTR plate with 0.38 mm clad and 0.51 mm meat would require 10.2 g U/cm^3 and 12.9 g U/cm^3, respectively, to achieve the same uranium loading as the fuels which are the goal of the activities described in items 6 and 7 for a plate of the same thickness.

It is too soon to predict with confidence the outcome of these efforts, but the preliminary results are encouraging[7].

2. Fuel Demonstration

Detailed analyses of the experiments which were performed during the whole-core demonstration of U_3Si_2-Al fuel in the Oak Ridge Research Reactor (ORR) have made good progress.

The importance of these experiments transcends the particular fuel which was used in the demonstration. The ORR demonstration was accomplished on purpose through the mixed-core approach which is likely to be followed by the majority of research reactors undergoing conversion to reduced enrichment fuels. This process is more cost-effective and less disruptive of reactor operations than a simultaneous enrichment change of the whole core, but is also more difficult to calculate. The results of the ORR demonstration analyses[8] provide convincing evidence that the physics and analytical tools needed to predict accurately the behavior of a research reactor undergoing a mixed-core conversion are well at hand.

Postirradiation examinations of representative elements used in the ORR demonstration have been initiated, and are planned for conclusion in 1989. The channel gap measurements are consistent with the excellent behavior observed in past U_3Si_2-Al miniplate and full-size element postirradiation examinations.

Demonstration activities for fuels with densities in excess of 4.8 g U/cm^3 have been postponed to match the pace of the new activities of the fuel development area. Demonstration activities of U_3Si_2-Al fuel with intermediate enrichments have been deferred because of a determination by the Executive Branch that such enrichments would not meet current nuclear non-proliferation goals.

3. Generic Analysis and Specific Support

Analyses of the feasibility to convert the many foreign reactors with which the RERTR Program has joint study agreements have continued. As in previous years, some of these studies concern high-power, high-performance reactors like the HFR-Petten (The Netherlands), the BR-2 (Belgium), and the RHF (France), which require special considerations and methods. The results obtained to date are generally positive, and prototype elements with reduced enrichment will soon begin to be tested in at least one of these reactors.

A significant fraction of the analytical effort was dedicated to the coordination of the safety calculations and evaluations for U.S. university reactors planning to convert to LEU as required by the NRC. Of these reactors, one (the Rensselaer Polytechnic Institute Reactor Critical Facility, RPI-RCF) has already been successfully converted to LEU SPERT fuel.* The safety analyses for four other reactors (at Worcester Polytechnic Institute, Ohio State University, Manhattan College, and University of Missouri at Rolla) have been completed. Conversion of the first two of these reactors is expected to occur before the end of the year. Calculations for five more reactors (at Iowa State University, University of Virginia, Rhode Island Nuclear Science Center, University of Lowell, and University of Florida) are in progress.

*The RERTR Program support for the RPI-CRF conversion was limited to the qualification of its fuel.

4. LEU Targets

Experimental studies related to the separation of ^{99}Mo from irradiated LEU targets with very low burnup have been performed[9]. The targets contained uranium in both silicide and metal form, and the results were favorable.

Application of electrolytic deposition of uranium metal on a stainless steel base, for the production of targets with enhanced uranium content, has made good progress[10]. However, several problems remain to be solved before this method can be applied to an industrial process. During the forthcoming year, we plan to pursue the same goal by applying Hot Isostatic Pressing procedures to the bonding of LEU metal foils to a Zircaloy base.

PLANNED ACTIVITIES

The new developments which have occurred in the fuel area have had a strong impact on our plans for future program activities. The intense, short-duration activities which were planned last year to demonstrate and qualify an already developed fuel (U_3Si-Al) have been replaced by less intense, long-duration efforts aiming at the development of the new fuel concepts.

The U.S. Government agencies responsible for managing the RERTR Program have approved and support the current fuel development activities of the program. The major activities which are already in progress, and which are planned for continuation in the near term are:

1. Complete postirradiation examinations of the ORR demonstration elements.

2. Continue ion bombardment and TEM examinations to identify possible treatments or modifications of U3Si-Al fuel that would prevent it from losing its crystalline structure under irradiation.

3. Use HIP procedures to prepare U_3Si_2-Al miniplates with high fuel volume fractions in the fuel meat and thin uniform cladding.

4. Use HIP procedures to prepare miniplates with wires of U_3Si (or similar materials) imbedded in the fuel meat and thin uniform cladding.

5. Make preparations for subsequent in-pile irradiations of the miniplates.

6. In parallel with these activities, complete documentation of the fuels which have already been qualified, and support their implementation.

7. Perform calculations and evaluations for reactors preparing to undergo conversion, to assist in improving performance and in resolving safety issues.

8. Develop a viable process, based on LEU, for the production of fission ^{99}Mo in research reactors.

It is estimated that qualification of the new fuels will require approximately five years. More concrete results from the ongoing fuel development activities must be obtained before a long-term fuel development plan can be finalized and approved.

Figure 1 illustrates a conceptual unapproved schedule for the long-term activities that would be required to bring to fruition the ongoing fuel development efforts.

SUMMARY AND CONCLUSION

1988 has been an intense and stimulating year for the RERTR Program. New findings, difficult decisions, and bold new initiatives have altered much of the program's activities and plans, and may revolutionize future fuel fabrication processes for research reactors.

A very important event occurred when the NRC issued a formal generic approval of the LEU U_3Si_2-Al dispersion fuel with meat densities up to 4.8 g U/cm^3, for use in research and test reactors. The NRC approval was the coronation of many years of effort, and paves the way for the extensive application of this new fuel in research reactors worldwide.

Three significant findings raised serious doubts about the potential of LEU U_3Si-Al dispersion fuel for application in reactors requiring more than 4.8 g U/cm^3 to convert. Postirradiation examinations of the second miniplate series continued to show excessive swelling at high burnups for all the U_3Si-Al variants which had been tried; a technique based on ion bombardment disclosed that the swelling is due to a fundamental property of U_3Si, namely, the disintegration of its crystalline structure under irradiation; and, finally, an analytical model confirmed that the assumption of an irradiation-induced disintegration of the crystalline structure is consistent with the observed morphology of irradiated U_3Si-Al miniplates. It was concluded that U_3Si-Al dispersion fuel appears to be usable with densities no greater than 6 g U/cm^3 and burnups no greater than 50%, but that different fuels are needed for reactors with requirements beyond this range.

A meaningful effort was initiated to develop viable LEU research reactor fuels that could operate in the very-high-uranium-density, very-high-burnup range. The ideas and experiences of many years were brought to bear on this exercise, and the result was a diversified approach based on several new techniques and concepts, each with different strengths and weaknesses, and each holding extraordinary performance potential. The main techniques and concepts of this approach are:

1) A systematic application of ion-beam irradiations and in-situ TEM observations to gain fundamental understanding of the amorphization process, to learn how to control it, and to screen new fuel materials. The potential usefulness of this tool for testing and screening new reactor fuels is enormous because of its simplicity, speed, and low cost.

2) Application of Hot Isostatic Pressing (HIP) procedures to U_3Si_2-Al dispersion fuel. This concept holds the promise of overcoming the loading limitations of U_3Si_2-Al due to the rolling process, while retaining the advantage of its excellent irradiation behavior. Fuel meat densities up to 6.8 g U/cm^3 appear feasible, with uniform cladding thickness of 0.25 mm. This combination could be used to achieve fuel plate loadings in excess of those required for the conversion of any HEU research reactor currently in operation.

3) Application of Hot Isostatic Pressing procedures to a fuel plate containing U_3Si wires imbedded in an aluminum matrix. Fuel meat densities up to 8.6 g U/cm^3 appear feasible, with uniform cladding thickness of 0.25 mm. The fuel plate loadings which can be achieved with this combination are even higher than those achievable with the U_3Si_2-Al HIP concept.

The first results obtained in each of these activities are encouraging, but not conclusive A set of miniplates, reflecting the best that can be achieved in each concept, will be assembled during the next year and preparations for their irradiation will be made. At that time, it will be possible to define the desirability, requirements, and schedule for a long-term fuel development activity which would bring these concepts to fruition. A conceptual schedule indicates that five years would be required to achieve this goal.

The other major program activities have made solid progress during the past year, without startling developments comparable to those which have marked the fuel area. Analyses of the ORR demonstration have shown that the neutronics properties of mixed-core conversions can be predicted with the required reliability and precision. Several safety analyses for U.S. university research reactors planning to convert to LEU have been completed. One of these reactors has already converted, and two more are planning to convert within the next three months. Finally, in the LEU target area, tests on irradiated, low-burnup samples have been successfully conducted and application of HIPping procedures to the fabrication of targets with very high uranium content is planned.

Active cooperation among international fuel developers, commercial vendors, and reactor operators has been instrumental to the success which the overall RERTR effort has already achieved. As we embark in a period of renewed fuel development, with exciting new tools, techniques, and concepts, the importance of continued international cooperation continues to be essential.

REFERENCES

1. A. Travelli,"The RERTR Program: Progress and Plans", Proc. X Int'l Mtg. on RERTR, Buenos Aires, Argentina, Sep. 28-Oct. 1, 1987 (to be published).

2. U.S. Nuclear Regulatory Commission, "Safety Evaluation Report Related to the Evaluation of Low-Enriched Uranium Silicide-Aluminum Dispersion Fuel for Use in Non-Power Reactors", NUREG-1313, July 1988.

3. G. L. Hofman, "Some Recent Observations on the Irradiation Behavior of Uranium Silicide Dispersion Fuel", These Proceesings.

4. R. C. Birtcher, C. W. Allen, L. E. Rehn, and G. L. Hofman, "Simulation of the Swelling of Intermetallic Reactor Fuels", J. Nucl. Mat. 152, 1988.

5. J. Rest, G. L. Hofman and R. C. Birtcher, "The Effect of Crystal Structure Stability on the Mobility of Gas Bubbles in Intermetallic Uranium Compounds", Proc. Symp. on Effects of Radiation on Materials, June 27-29, 1988, Andover, MA.

6 D. F. Sears, "Fabrication and Irradiation Testing of LEU at CNRL - Status as of September 1987", Proc. X Int'l Mtg. on RERTR, Buenos Aires, Argentina, Sep.28-Oct.1, 1987 (to be published).

7. T. C. Wiencek, R. C. Domagala, and H. R. Thresh, "High Density Fuel Plates by Hot Isostatic Pressing", These Proceedings.

8. M. M. Bretscher, "Fuel Element Powers, ^{235}U Masses, and Burnups from Gamma-Scanning Data Preliminary Analysis of Irradiated ORR LEU Fuel Elements", These Proceedings.

9. J. Kwok and G. F. Vandegrift, "Processing of Low-Burnup LEU Silicide Targets", These Proceedings.

10. S. Marshall, L. Redey, D. Vissers, G. Vandegrift, and J. Matos, "Electrochemical Formation of LEU Targets for the Production of ^{99}Mo", These Proceedings.

Fig. 1. Conceptual Fuel Development Schedule

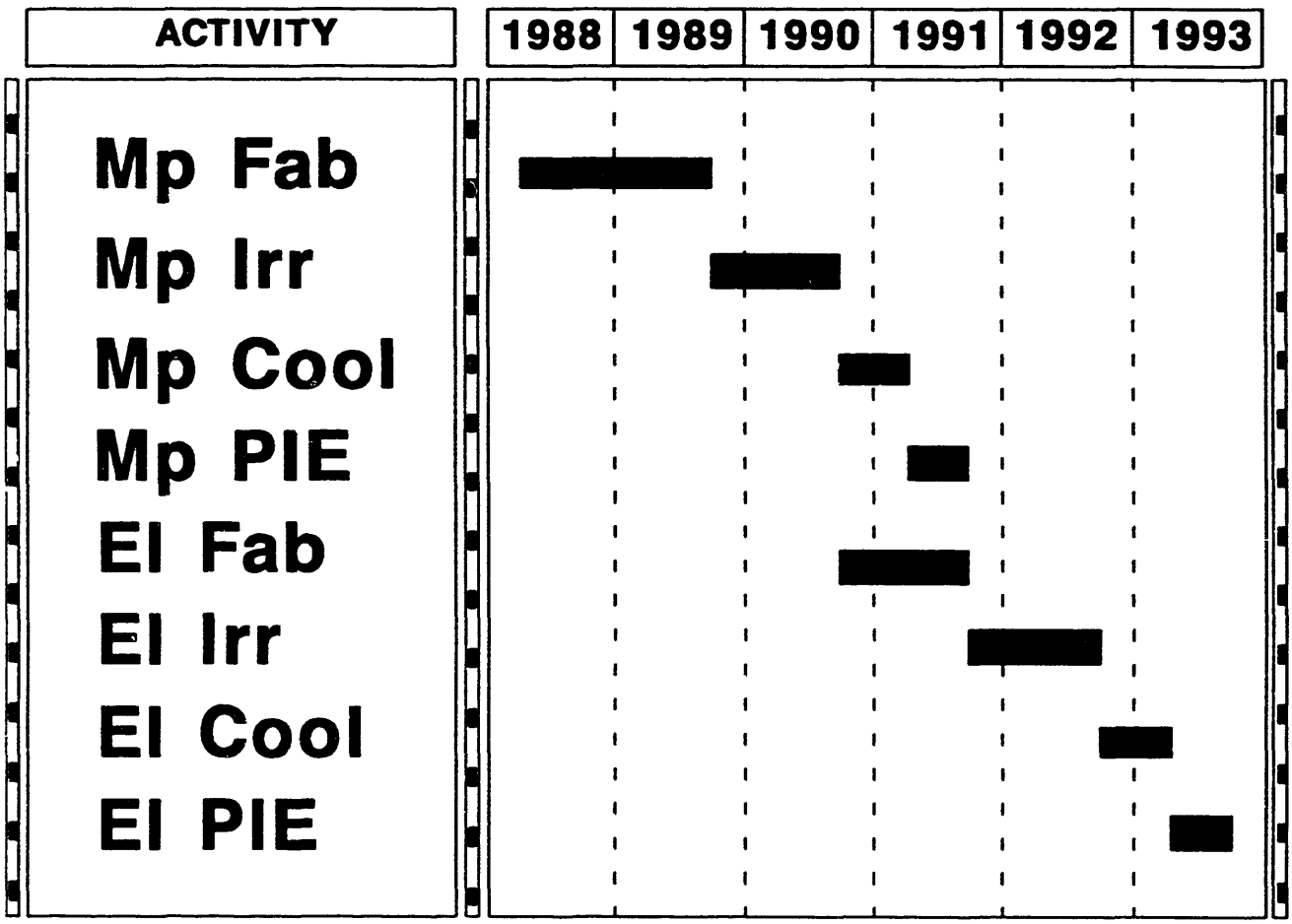

The Status of the German AF Program

Prospects with Respect to
– Program Termination
– Further Int. RERTR Cooperation and
– HEU–LEU Research Reactor Conversions

G. Thamm
Kernforschungsanlage Jülich GmbH,
Federal Republic of Germany

Abstract

In the past year work on the topics of **LEU fuel and fuel element fabrication technology as well as LEU fuel and fuel element qualification** within the German AF Program has been concluded so that the corresponding individual projects can be formally terminated at the end of 1988. The difficulties experienced at Nukem finally leading to the decision to discontinue fuel element fabrication for research reactors consequently means that the essential goal of the AF Program, namely of constructing an LEU fabrication line operating under industrial/commercial conditions, cannot be realized in Germany. However, the know–how for the required methods and procedures, and also for the equipment, has been developed and in part the preparation of this equipment has reached such an advanced stage that it would be possible to realize the LEU fabrication line at a different fuel element manufacturer. The **studies on the HEU–LEU conversion concepts** have largely been completed for the German research reactors.

1. Introduction

In spite of considerable difficulties with the program partner Nukem, mainly caused by the suspension for almost three months of the operating license for fuel element fabrication, it was largely possible to conclude work within the AF program according to plan and on schedule. As already reported last year /1/, it will therefore be possible to formally terminate the program at the end of 1989.

In the following sections, a report will be given on the status of work and then the outlook with respect to completion of the program, possible further international RERTR cooperation after terminating the program, and the possibilities emerging for the short– and medium–term HEU–LEU conversion of research reactors.

2. Status

One year ago, work was still continuing on 7 major tasks within the AF program (see /1/). This was distributed between the existing main fields of activity as follows:

- **3 LEU fuel and fuel element technology**
- **3 LEU fuel and fuel element qualification**
- **1 HEU–LEU conversion studies.**

One of these projects was already completed at the end of 1987. Five further projects will be terminated in 1988 so that only one single project remains for 1989. The following sub–sections present information on the status of work for the three different fields.

2.1 LEU fuel development and fuel element fabrication

As is well known, work in this field is concentrated on discovering technically optimized, low–cost solutions for the 6 essential process steps in the manufacture of LEU–MTR fuel elements using uranium silicide fuel, and after completing this work on installing an LEU fuel element fabrication line operating under commercial/industrial conditions (see /2/ and /3/).

The work has been successfully completed for **fuel conversion**. The procedures or

technical devices have been developed and constructed to reduce dust release with an increased throughput of uranium material in the LEU case to such an extent that increased radiation exposure for the personnel can be avoided during later operation. On the basis of previous good operating experience with the prototype devices, the corresponding systems have already been ordered for later incorporation into the LEU fabrication line. The associated major task was completed by Nukem at the end of 1987.

In a further individual task, Nukem was able to employ the procedures and technical systems developed for the overall process of LEU fuel element fabrication by the **series production of 78 LEU fuel elements** for the HEU–LEU conversion of the Geesthacht research reactors. The technical know–how and also to a very great extent the technical devices are therefore already available for incorporation into the LEU fuel element fabrication line to be installed. The goal of this major task – to be concluded at the end of 1988 – has thus been achieved. It was not possible to continue any further work within the framework of the third Nukem major task in 1988 – namely **the final assembly of the LEU fuel element fabrication line**. This project will have to be prematurely terminated in 1988. The results gathered so far will be presented in a final report.

2.2 LEU fuel qualification

LEU fuel plates and elements have been tested in Germany within the framework of the AF program, primarily in Geesthacht and Jülich.

After concluding the irradiation of 25 plates of reduced size in previous years, the post–examinations were completed this year both at Geesthacht and also Jülich. The results will be presented at this RERTR Meeting (see /4/ and /5/). Only a few brief details will therefore be presented in the following.

At Geesthacht, 5 U_3Si_2 plates with increased (approx. 40 %) and normal (< 25 %) fine grain fraction (40 μm) were irradiated up to a burn–up of about 1.5×10^{21} f/cm^3. The post–examinations revealed excellent irradiation behavior. Due to the greater initial porosity, the swelling behavior of the plates with an increased fine grain fraction is lower than for the reference plates. Furthermore, the low swelling rates determined are in good agreement with the data obtained in corresponding studies in America (see /6/ and /7/). According to the results of these studies, it therefore seems admissible to permit a higher (than 25 %) fine grain fraction in the LEU fuel element fabrication specifications.

As is well known, plates of reduced size were irradiated in the FRJ–2 (DIDO) at Jülich in two irradiation campaigns of 10 plates each. The post–examinations of the plates had already progressed well last year (examinations were actually completed for the first campaign) so that it was possible to communicate the essential results in Buenos Aires (see /8/). After finishing the post–irradiation examinations, the complete results are now available. It became apparent that the plates from the second campaign (5 x $U_3Si_{1.5}$ with 6 gU/cm³, and 5 with $U_3Si_{1.3}$ with 6.5 gU/cm³) already display microstructure behavior characterized by the irradiation behavior of the U_3Si fraction even with moderate burn–ups (approx. 1.2 x 10^{21} f/cm³). The interlinkage of fission gas bubbles typical of U_3Si occurred – naturally only weakly characterized in accordance with the burn–up rate. The B_4C poisoning present in some plates did not exert any perceptible influence. One plate became leaky due to mechanical defects (around the groove designed to accommodate a thermocouple with a very great reduction in cladding thickness) and as is known led to the premature termination of irradiation due to increased releases of fission products into the coolant water of the irradiation device. Reactions between the water, or the decomposition products of the water, with the fuel only took place in the immediate area around the leak and led to considerable pillowing of the fuel plate there. Even in the immediate vicinity of this area, the microstructure of the fuel still displayed completely normal behavior. Studies on the release of fission products were carried out on selected plates from both irradiation campaigns by cutting open the plates. The measured relative release rates for Kr 85 were about 1 x 10^{-4} for the plates with U_3Si_2 or $U_3Si_{1.3}$ and $U_3Si_{1.5}$ fuel. In the case of U_3Si plates with incipient breakaway swelling and strong interlinkage of fission gas bubbles in the fuel meat, on the other hand, release rates higher by about three orders of magnitude were determined. The releases of solid fission products (Cs–137 and Ce–144) were significantly lower and only amounted to a few 10^{-7}. Release behavior very similar to the UAl_x fuel thus results for U_3Si_2 fuel.

2.3 HEU–LEU conversions, studies and preparatory work

In the meantime **basic studies**, by means of which all data essential for the HEU–LEU conversion were to be determined, have also been completed for the BER–II (see also /9/). Calculations were undertaken for two fuel elements with different loads (323 g of U–235; 3.7 gU/cm³ and 402 g of U–235; 4.6 gU/cm³). The higher fuel element load would have been expected to lead to a significant increase in the mean burn–up, but on the other hand would have reduced the thermal neutron flux in the reflector or irradiation positions by up to 20 %. The operator has meanwhile decided in favor of the

323 g element. This element requires an HEU–LEU transition phase of approx. 250 full–power days, in which case temporary power reductions will be required with the first "mixed cores" in the transitional phase due to very high power density form factors. It will not be possible to begin conversion of the reactor before 1992.

The GKSS obtained the license for the HEU–LEU conversion of their reactors FRG–1 and FRG–2 in May 1988. Conversion will only be able to take place in early 1989 since a cold neutron source still has to be installed (see also /4/).

The **operating– and licensing–specific studies** have been started for the FRJ–2 in Jülich, primarily providing the data required for the licensing procedure. It will not be possible to effect conversion before 1992 since due to the withdrawal of Nukem a different fuel element manufacturer will have to be qualified by corresponding test irradiations with fuel elements in HEU and LEU of the design type required for later LEU operation.

The FRM in Garching is currently being mainly operated with an MEU element. Final LEU conversion is only envisaged here if the project of a new modern beam tube reactor with a compact cylindrical core cannot be realized – the plant design and safety analysis report are being drawn up for this project at present (see /10/).

3. Prospects

In the following sections a survey will be given of the termination of the AF program, discussing in detail the **achievable goals** after the Nukem decision to discontinue production of fuel elements for research reactors. The possible form of **further international RERTR cooperation** after the formal completion of the AF program will be outlined and also the **possibilities at present (or in the medium term) of the HEU–LEU conversion of research reactors.**

3.1 Termination of the AF program

It was reported at the international RERTR meeting at Buenos Aires, Argentina /1/, last year that the German AF program will be terminated according to plan at the end of 1989. The major reasons for this decision were also presented. This is naturally still the case today and has been reinforced by work in the past year.

A year ago, 7 of the total of 15 individual projects within the AF program were still under way (3 fuel and fuel element technology, 3 fuel and fuel element qualification, and

1 HEU–LEU conversion studies). Even if from a formal point of view 6 projects are still operative, nevertheless only one project will remain at the end of 1988. This involves work with Interatom on the HEU–LEU conversion studies. As already mentioned in 2.3, this work will be **completed according to plan and on schedule** next year.

The remaining 5 major tasks will be completed at the end of 1988. The 3 tasks on LEU fuel and fuel element qualification by irradiations and post–examinations will be completed **according to plan and on schedule** since, as reported in 2.2, the post–irradiation examinations of all plates of reduced size have been completed in Geesthacht and Jülich, and also the irradiation tests with LEU fuel elements (mainly at Geesthacht). All further irradiations with LEU fuel elements, primarily in Jülich and later also in Berlin, will be carried out with LEU fuel elements of a prototype character for the respective reactor so that their application is only of signficance for the subsequent HEU–LEU conversion and no longer "formally" serves for fuel or fuel element qualification as defined in the AF program.

The 2 individual tasks still existing on LEU fuel and fuel element technology were affected to varying extents by the situation at Nukem in Hanau (see /7/). As is well known, at the height of a campaign in the German media culminating in the accusation based on rumor that Nukem had infringed the non–proliferation treaty by supplying weapons grade uranium material to Libya and Pakistan, the competent atomic regulatory commission suspended Nukem's license for the processing of nuclear fuel in mid–January 1988 on the grounds of alleged violations in handling radioactive waste. In spite of subsequent intensive efforts by Nukem, which also very rapidly revealed that the accusations of passing on "bomb material" proved to be without foundation, it was nevertheless not possible to recover the operating license in such good time that all deadlines for existing fuel element supply contracts could be fulfilled. Nukem therefore announced on March 10, 1988 after time–consuming internal discussions, their decision to discontinue altogether the fabrication of fuel elements for research reactors. Even though the German research reactor operators and the AF program greatly regretted this decision due to the resulting consequences nevertheless they appreciated the reasons for it. After all, Nukem would also have to reckon in future with similar interventions in the operation of their facilities, which would no longer permit contractual obligations to be fulfilled on time. In the final analysis, this would also have led to the loss of international competitiveness. Only after this decision in early April 1988 was the license restored to Nukem with the proviso that radioactive material should be removed from

the facility by the end of 1988. In spite of the major obstacles and restrictions thus caused, Nukem was still able to successfully complete one of its two individual tasks, namely "testing the fabrication technology for LEU–MTR fuel elements by producing a fairly large series of fuel elements". As reported in 2.1, 78 LEU fuel elements have already been fabricated and delivered for the HEU–LEU conversion of the GKSS research reactors. The task will therefore be completed **according to plan and on schedule** at the end of 1988.

In contrast, it was not possible to work on the final Nukem task – "Installation of an LEU fuel element fabrication line on the basis of uranium silicide fuel" – in the current year. Although a great deal of essential knowledge on fabricating elements for the GKSS has been obtained for the installation of a final LEU fuel element fabrication line, nevertheless the corresponding work on the actual hardware construction of this line could understandably no longer be carried out. In principle, the know–how for the method to be used and in part also for the technical devices to be incorporated into the fabrication process has been acquired. The results will of course be compiled in a final report after the premature termination of the project. A total of only about 30 % of the funds of almost DM 10 million envisaged for this uncompleted task have been spent. The overall cost of the AF program will thus be reduced to a little over DM 50 million in comparison to the figure represented at the last RERTR meeting in Buenos Aires (see /1/). The precise figures will only be available in early 1989.

3.2 Further international RERTR cooperation

On the assumption that all national programs currently under way would be formally terminated at the latest at the end of 1990, the RERTR activities which would be necessary after this period and possible measures for their implementation were discussed at the final round–table discussion at the last international RERTR meeting in Buenos Aires. Three major fields were determined for these activities:

1. The continuation of an exchange of information by further RERTR meetings from 1991 onwards.

2. Assistance in HEU–LEU conversions for those countries unable to convert their reactors by the early nineties and not having at their disposal the necessary technical or scientific capacities.

3. The qualification of LEU fuels by irradiation and post–irradiation examinations by manufacturers in countries only now or in future building up their LEU fabrication lines.

Representatives from America, France, Japan and Germany (with two further observers from Belgium and Indonesia) met at the IAEA in Vienna at the end of May 1988 in order, as agreed, to compile proposals for further action to be submitted at this meeting. It became apparent at Vienna that primarily for budgetary reasons America would most probably continue the RERTR program beyond the end of 1990 for a further two to three years. During this phase, work should be intensified on the development and qualification of uranium fuels with particularly high densities (above 7 gU/cm^3) to be undertaken on the basis of current design or by modifying the construction of MTR fuel plates using U_3Si. Test plates are to be subsequently manufactured and tested under irradiation. Germany will not be participating in such work, not least due to the decision by Nukem described in 3.1. Test irradiations will also not be possible in Germany due to the termination of these projects (irradiation facilities are no longer available for these tests at Geesthacht and Jülich). However, these tests are to be carried out in high–performance reactors anyway, as for example the HFIR at Oak Ridge.

It is assumed in Germany that if the US RERTR program should continue in existence then the "leading role" in further international cooperation will be taken over by the Americans. Even if a number of staff from the German AF program have already undertaken or will in the foreseeable future take over other tasks, at least representatives of the German research reactors will continue to participate in the international RERTR meetings and report on preparations for implementing or the implementation itself and the operating experience subsequently obtained in HEU–LEU conversions. This is possible in any case even without the formal existence of the German AF program. However, the extent to which, if at all, RERTR work can be undertaken by the German partners in accordance with international coordination will be extremely limited.

3.3 HEU–LEU conversion of research reactors

At the beginning of the AF program 7 research reactors with a total power of 63 MW and annual requirements of 50 to 60 kg of HEU were in operation in Germany. Of these, the FRJ–1 in Jülich (10 MW) has in the meantime been shut down and the long–term further operation of the FRG–2 (15 MW) in Geesthacht is uncertain at present. All German reactors – including the two mentioned above – could be converted to

operation with LEU by using U_3Si_2–Al dispersion fuel. The license has already been granted for the reactors at Geesthacht. The conversion at Geesthacht will probably only take place in early 1989 primarily due to the installation of a cold neutron source in the FRG–1 which still has to be undertaken (see also /4/). The respective conversion concept has already been decided for the reactors in Berlin (BER–II, 10 MW) and in Jülich (FRJ–2, 23 MW) and preparations are already under way so that it will be possible to convert the reactors in the early nineties. The Munich reactor (FRM, 4 MW) can also be converted to LEU in its present form. It is currently being operated with MEU. A complete conversion to LEU will probably only be undertaken if the concept of a modern beam tube reactor (see also /10/) with a cylindrical compact core (20 MW), presently being studied, cannot be implemented. The reactor in Braunschweig (FMRB, 1 MW) is similarly convertible but due to its low fuel consumption will probably continue to be operated with HEU until its final shutdown at the end of the nineties. Due to the work of the AF program, fuel requirements in Germany will thus be completely covered by LEU material from about the mid–nineties[1]. Only if the Munich plans are realized will annual requirements of approx. 15 kg of HEU be maintained for the Federal Republic of Germany.

About 450 kg of HEU are required outside the USA at present for use in research reactors (see /11/). Of this, a quantity of between 300 and 350 kg can be replaced by LEU material. This means a reduction in the total HEU material requirements to about 30 %. This quantity is distributed between a few facilities (in Europe for example between the HFR, Grenoble, the ORPHEE, Saclay, and the BR–II in Mol) and should thus represent a low proliferation risk on the basis of specific monitoring for a few facilities. The HEU material for the operation of these facilities should therefore be guaranteed in any case until the new development work starting in America for particularly high uranium densities has been concluded. Such a guarantee is therefore considered appropriate since in America a number of high–performance research reactors (including HFIR, HFBR, ATR...) with a total power of more than 400 MW and annual requirements of more than 300 kg of HEU are not going to be converted to operation with LEU either. After all, this is about three times the HEU material requirements compared with that outside the USA.

[1] The shutdown of research reactors previously operated with HEU is naturally also to be regarded as a constructive contribution towards reducing the proliferation risk.

References

/1/ G. Thamm, "The Status of the German AF Program and Thoughts Toward a Nationally and Internationally Coordinated Termination of the Programs", Int. RERTR Meeting, Buenos Aires, Argentina, Sept. 28 – Oct. 01, 1987

/2/ H.W. Hassel, E. Wehner, "Series Production in a Standardized Fabrication Line for Silicide Fuels and Commercial Aspects", Int. RERTR Meeting, Buenos Aires, Argentina, Sept. 28 – Oct. 01, 1987

/3/ H.W. Hassel, "Why Nukem Steps out of the HTR–Fuel–Element Market and how to Solve Problems Resulting from that", this Conference

/4/ W. Krull, "Enrichment Reduction Activities for the FRG–1 and FRG–2 Research Reactors – Status and Future Plans", this Conference

/5/ W. Krug, E. Groos, J. Seferiadis, G. Thamm, "Final Results of the Test Irradiations with LEU Plates at KFA Jülich", this Conference

/6/ J.L. Snelgrove, "Qualification Status of LEU Fuels", Int. RERTR Meeting, Buenos Aires, Argentina, Sept. 28 – Oct. 01, 1987

/7/ G.L. Hofmann, L.A. Neimark, "Prospects for Stable High–Density Dispersion Fuels", Int. RERTR Meeting, Buenos Aires, Argentina, Sept. 28 – Oct 01, 1987

/8/ E. Groos, W. Krug, G. Thamm, "LEU Fuel Testing at KFA Jülich under the German AF Program, Plate Irradiation and PIE". Int. RERTR Meeting, Buenos Aires, Argentina, Sept. 28 – Oct. 01, 1987

/9/ A. Strömich, H.J. Roegler, "Conversions on their Way from Physics to Economy", this Conference

/10/ K. Böning, W. Gläser, A. Röhrmoser, "Neutron Physics of the New Munich Compact Core Design", this Conference

/11/ Nuclear Fuel – June 27, 1988 – 11

PRESENT STATUS AND OBJECTIVES OF THE REDUCED ENRICHMENT PROGRAM FOR RESEARCH REACTORS IN FRANCE

F. MERCHIE
CEA, France

ABSTRACT

After a brief presentation of the policy followed by the CEA in the field of its multipurpose research reactors, the paper describes the present status of the RERTR program in France and the results of the LEU conversion studies performed for OSIRIS and SILOE.

1. GENERAL

Before describing the present state of progress of the CEA's program for reduction of enrichment, it is no doubt valuable to briefly recall the major principles of the policy adopted over the past few years by the CEA on the subject of research reactors.

The desire to have a range of research reactors at its disposal which comply with the most recent and the most stringent safety criteria, and which are perfectly adapted in both number and quality to the current and future requirements of the different research programs indeed emerges very clearly from the latest decisions and directions set by the CEA, namely:

- modification of the pool lining and of the internal structures of SILOE in order to withstand the BORAX accident
- standardization of the fuel elements for SILOE and OSIRIS with the adoption of a 20 % enriched U_3Si_2 fuel, while ORPHEE for its part has to retain its 93 % enriched compact core in order to continue to provide the highest possible thermal fluxes required by the fundamental physics experiments set up on its beams.
- definitive shut down of MELUSINE on June 30th, 1988 after 30 years of operation, with extremely satisfactory results in all respects, in particular in the experimental field.

The CEA thus currently has at its disposal a coherent set of 3 modern and complementary high performance reactors :

- OSIRIS (70 MW) for testing materials and production of radio-isotopes
- SILOE (35 MW) for testing materials, production of radio-isotopes and fundamental research, as a new tangential beam tube in addition to the two existing radial tubes has been installed to compensate for the shut down of MELUSINE
- ORPHEE (14 MW) designed and built to be totally devoted to fundamental research on beams tubes and equipped with very high performance experimental facilities (cold sources, hot source, neutron guides etc.).

A system of pluriannual management of the irradiation programs enables coordination of the experimental loading schedules and the annual operating programs of the three reactors. In collaboration with the MOL Centre (Belgium), harmonization of the operating programs has since 1988 been extended to the BR2 reactor, so as to guarantee good consistency of Mo-99 production in Europe.

2. THE CEA CONTRIBUTION TO THE RERTR PROGRAM

From the very beginning, the CEA has participated in the RERTR international program, signing collaboration agreements with the DOE/ANL and the CERCA. These agreements have given rise to numerous qualification tests for high density LEU fuel elements, carried out principally in SILOE.

It was in fact in about 1975 that the CEA launched a study program on the reduction of the enrichment of its research reactor fuel elements, based on the utilization of a 7 % enriched UO_2 fuel in the form of very thin rectangular pellets called CARAMEL. This resulted in the conversion in 1979 of the OSIRIS reactor (70 MW) located at Saclay, which since then uses the CARAMEL fuel exclusively. Ten years later, OSIRIS still remains the most powerful research reactor in the world to have carried out the HEU to LEU conversion.

Table 1 hereafter summarizes the principal qualification tests carried out in SILOE and OSIRIS on silicon-based fuel elements, the first tests in the program having been carried out on UAlx und U_3O_8 fuels, then subsequently abandoned in view of the highly promising prospects offered by silicides. It should be noted that immersed metrology benches were developed on this occasion to measure under water the variations in plate thickness and width of the cooling channels, so as to guarantee close monitoring of any possible swelling under irradiation. These dimensional readings, together with flux measurements, cladding failure detection and burn-up measurements by gamma scanning also carried out between cycles, enable relatively detailed monitoring to be obtained virtually on line for the different qualification tests.

The prospects opened up by silicides fairly rapidly gave rise to preliminary neutron studies to evaluate the consequences for each reactor of a possible change in fuel.

Once the qualification of the U_3Si_2 fuel element at 4.8 g/cm^3 was considered to be established in 1987, detailed technical and economic studies were undertaken for the introduction of this new fuel in SILOE and OSIRIS. In view of the results, the conversion of SILOE and OSIRIS has been decided, and all the appropriate measures have been taken to prepare supplies of the fuel materials and the first fuel element fabrications.

While the conversion of OSIRIS and SILOE appears globally to be acceptable both technically and economically, as will be shown hereafter, the special situation of ORPHEE does not allow the same conclusions to be drawn.

Indeed, in order to satisfy the requirements of fundamental research to which it is entirely devoted, the ORPHEE reactor is designed to produce the highest possible fluxes in the heavy water reflector where all the beam tubes are set up. Consequently, the configuration of the core is extremely compact and includes only 8 elements loaded with a UAlx fuel enriched to 93 % with a density of 1.2 g/cm^3, that is to say identical to that of the RHF, which is hardly surprising given that the two reactors were designed with the same objectives. The invariable geometry of the core of ORPHEE is fixed by the reduced dimensions (25 x 25 cm) of the zincalloy caisson separating the core from the heavy water vessel. Hence, any modification of the core which may be made necessary by the adoption of the U_3Si_2 fuel at 4.8 g/cm^3 would inevitably impose a change in the principal internal structures of the reactor (caisson,

heavy water vessel, set-up of the beam tubes and various cold and hot sources etc..), all of which represent large-scale, difficult and highly costly alterations. This choice of course cannot be convincing, knowing that the only benefit of such an operation will be a strong decrease in all the reactor's current performances, with its consequences for the research programs.

Even with a fuel with a density greater than 4.8 g/cm^3, such as a U_3Si_2 with a density equal to 6.1 g/cm^3 for example, the deterioration of fluxes would still be significant, while the reduction in the efficiency of the control rods would diminish the reactivity shutdown margin to an unacceptable degree at the beginning of the core life-time.

In comparison with SILOE and OSIRIS, whose situations are less restrictive in this respect, the HEU remains an essential condition for ORPHEE to reach the objective for which it was designed and built.

3. LEU CONVERSION STUDIES APPLIED TO OSIRIS AND SILOE

3.1 Technical aspects

Given that detailed neutron studies of new cores are always very long and thus extremely costly, the first objective set was to obtain with a maximum degree of confidence all the results needed to establish reliable technical and economic comparisons between reference cores made of CARAMEL and U_3Si_2 for OSIRIS, UAl at 93 % and U_3Si_2 for SILOE.

Preliminary calculations carried out with U_3Si_2 at different densities up to 5.3 g/cm^3 have confirmed that a density of 4.8 g/cm^3 may be definitively accepted both for OSIRIS and for SILOE. This offers the advantage of having the same basic fuel for both reactors and being able to use the results of the majority of the qualification tests performed to date on U_3Si_2 in support of the safety documents to be submitted to the safety authorities before any change.

With this same concern for standardization, identical thicknesses of meat, cladding and plate were chosen on the two reactors. At one point, an increase from 23 to 25 had been considered in the number of plates of the standard elements of SILOE. Finally for both technical, economic and safety reasons, the present geometry of the plates and the elements has been maintained. On OSIRIS, the situation is different in that the CARAMEL plates are thicker (e = 2.25 mm). Thermohydraulic optimization leads to the acceptance of 22 plates for the standard U_3Si_2 elements as against 17 for the CARAMEL elements. It should also be remembered that the pitch of the OSIRIS lattice is square, the cross-section of the elements being 82 x 82 mm, whereas the section of the standard MTR lattice elements is 76 x 80 mm. The height determined for the U_3Si_2 core of OSIRIS is also slightly different : 630 mm as against 600 mm for SILOE.

Although SILOE uses UAl elements containing boron and OSIRIS also used boron before its conversion to CARAMEL, all the reference calculations are made without burnable poison, for reasons of simplification of implementation and interpretation. The codes used are those developed by the CEA and known by the name of APOLLO and ICARE.

Table 2 summarizes the principal characteristics of the U_3Si_2 cores and elements of SILOE and OSIRIS.

In comparison with the performances of the UAl and CARAMEL reference cores of SILOE and OSIRIS, the conversion to U_3Si_2 fuel elements will have the following consequences :

- for SILOE, the thermal fluxes available in the reflector will be on average 5 % less, while the fast fluxes in the special irradiation sites of the core will be preserved, with however a harder neutron spectrum in particular in the core (the ratio ϕ_{epi} / ϕ_{th} will increase by 35 %).

- for OSIRIS the thermal fluxes in the reflector will be about 8 % greater on average, while the fast fluxes in the core sites will be about 12 % less, with gamma heating in the core which is about 50 % greater, which is not without causing problems for certain experiments.

The detailed studies are continuing so as to determine the optimal concentrations of burnable poison to be introduced in the elements and to fix the final configurations.

As far as the strategy for building the LEU cores is concerned: progressive transfer by regular introduction of new U_3Si_2 elements in the present HEU core of SILOE and CARAMEL core of OSIRIS, or direct passage from the present configurations to the new LEU configurations, a preference is beginning to emerge in favour of a direct passage, so as to perturb the experiments and irradiation programs in progress for the shortest possible period.

3.2 Safety Aspects

As far as safety is concerned, the authorities in question wished to obtain an "industrial" confirmation of the qualification of U_3Si_2, by requesting the fabrication and the irradiation of a few first series elements, produced with technical specifications and procedures which are absolutely identical to those to be applied for series commercial manufacturing.

In addition, the authorities verified that the consequences of a BORAX type reactivity accident on a U_3Si_2 core would remain within the limits of those arising on a UAl core, and that the dimensionning of the reactor main structures was therefore not brought into question. (The explosive BORAX type accident is taken as the design basis accident in research reactors in France).

Lastly, the consequences of a classic cladding failure or of a localised fuel melting (burn out or flow blockage) must be subjected to a comparative evaluation with UAl (release of fission products, contamination of pools and circuits).

3.3 Economic Aspects

From the economic point of view, the neutron studies have provided all the data necessary for setting up comparative calculations for the cost of HEU and LEU cycles at the equilibrium (spent fuel burn-up, annual consumption etc...).

Taking the enrichment and reprocessing prices currently applied by the DOE, i.e.

Enrichment :	UTS < 10 %, 157 Dollars
	UTS > 10 %, 492 Dollars
Reprocessing :	UAl at 93 %, 1000 Dollars/kg
	U_3Si_2 at 20 %, 835 Dollars/kg

as well as the COGEMA's ruling prices for its different services (transport and conversion of UF_6 to U metal, recovery and processing of production waste, dispatch and transport of irradiated fuel elements etc...), and the prices published by CERCA for the industrial manufacture of U_3Si_2 elements (that is 1.3

times the price of UAl elements), the following conclusions may be reached, taking into account valorization of the uranium credit after reprocessing : the cost of the 20 % enriched U_3Si_2 cycle, at OSIRIS and at SILOE, is identical to that of the 93 % enriched UAl cycle, to within less than 4 % on the basis of an annual operation of about 200 days.

The recent increase of the price of UTS > 10 % from 492 to 922 dollars which will be enforced by the DOE as from 1.1.1989, leads to an increase in the cost of cycles of 3.5 % for UAl 93 % and 1 % for U_3Si_2 20 %.

4. CONCLUSIONS

After evaluation of the technical and economic consequences of the use of a 20 % enriched U_3Si_2 fuel with 4.8 g/cm^3, in OSIRIS and SILOE, the CEA has decided not to place any new order of 93 % enriched UAl fuel elements for SILOE and of CARAMEL fuel elements for OSIRIS.

Once the supplies and production under way have been consumed, the two reactors will then use the same 20 % enriched U_3Si_2 fuel. The safety documents are in preparation with a view to approval within 18 months. In parallel, the operations of an industrial nature associated with the supply of material and series production have been defined and are progressively being established.

A few important points however remain to be elucidated. The first question concerns the conditions for the reprocessing after 1988 of the 93 % enriched irradiated fuel elements from ORPHEE and SILOE until its conversion to U_3Si_2. Before defining a final position on what is to become of these irradiated elements, we are waiting for the announcement of the new DOE provisions to be made for the 10 years to come on the one hand, and on the other hand to know under what conditions the HEU credits thus generated could be valorized and utilized.

The next question concerns the SRP reprocessing conditions for irradiated U_3Si_2 fuel elements dispatched after 1992, at which date the conditions currently applied by the DOE expire.

Independently of the considerable economic aspects associated with these questions, our safety authorities are indeed concerned about what becomes of the irradiated LEU elements, and their final agreement remains in any case subject to the establishment of a satisfactory solution for the end of the cycle.

TABLE 1. U_3Si and U_3Si_2 FUEL TESTINGS IN SILOE AND OSIRIS

REACTOR	FUEL	DENSITY g/cm³	AVERAGE BURN-UP %	MAX. SWELLING mm	MAX. FISSIONS 10^{21}/cm³
SILOE	U_3Si 4 plates	5.5	46	0.05	2.21
		5.5	53	0.06	2.07
		6.0	54	0.105	2.19
		6.0	43	0.095	2.19
SILOE	U_3Si_2 4 plates	2.0	78	0.035	0.88
		3.7	76	0.045	1.54
		5.2	75	0.045	2.15
		5.4	75	0.055	2.27
SILOE	U_3Si 1 elt with 2 removable plates	6.0	52	0.070	1.76
			59	0.095	2.06
SILOE	U_3Si_2 1 elt with 2 removable plates	5.2	54	0.015	1.4
			54	0.025	1.4
OSIRIS	U_3Si_x 1 elt	4.66	83		2.25

TABLE 2 - SILOE AND OSIRIS LEU CORES

	SILOE (35 MW)	OSIRIS (70 MW)
FUEL	U_3Si_2	U_3Si_2
ENRICHMENT, %	20	20
DENSITY, g/cm^3	4.8	4.8
THICKNESS, mm		
MEAT	0.5	0.5
CLADDING	0.38	0.38
PLATE	1.27	1.27
PLATE SIZES, mm	600 x 65.5	630 x 68.4
WATER CHANNEL,mm	2.10	2.48
NUMBER OF PLATES	23	22
U_5 per STD. ELT., g	416	458
U_T per STD. ELT., g	2106	2320
CORE configuration	32 (28S + 4 C)	44 (38S + 6 C)
U_5 IN THE CORE, g		
BOL	9.300	12.500
EOL	8.200	10.800
CYCLE DURATION, d	2 x 14	21

STATUS OF REDUCED ENRICHMENT PROGRAM FOR RESEARCH REACTORS IN JAPAN

Keiji Kanda, Hideaki Nishihara

Research Reactor Institute, Kyoto University
Kumatori-cho, Sennan-gun, Osaka 590-04, Japan

and

Yoshiaki Futamura, Hiroshi Sakurai and Yasuhiko Iso

Japan Atomic Energy Research Institute
Uchisaiwai-cho, Chiyoda-ku, Tokyo 100, Japan

ABSTRACT

The reduced enrichment programs for the JRR-2, JRR-3, JRR-4 and JMTR of Japan Atomic Energy Research Institute (JAERI), and the KUR and KUHFR of Kyoto University Research Reactor Institute (KURRI) are in progress under the Joint Study Programs with Argonne National Laboratory (ANL).

The post irradiation examination on the MEU/LEU aluminide full-size fuel elements has been completed or is in progress in JAERI. The full core demonstration using MEU aluminide fuel was achieved in the JRR-2 in November 1987. The feasibility studies for use of LEU silicide fuel in the JMTR and KUR are in progress.

INTRODUCTION

Among eighteen research reactors and critical assemblies in Japan (Tables 1 and 2), those which are relevant to the RERTR program are the JRR-2, JRR-3, JRR-4 and JMTR of JAERI and the KUR and KUHFR of KURRI (Table 3). The RERTR program in Japan has been pursued extensively under the direction of the Five Agency Committee on Highly Enriched Uranium, which consists of the Science and Technology Agency, the Ministry of Education, Science and Culture, the Ministry of Foreign Affairs, JAERI and KURRI. It has played a remarkable role in deciding policies related to the program and in close cooperation with ANL

through Joint Studies.

The program in JAERI for the first step, in which the JRR-2 and JMTR are being converted to the use of 45% enriched uranium aluminide fuels and the [illegible] and JFT-[illegible] to the use of 20% enriched uranium aluminide fuels, has been completed or in progress. Further core conversion of the JMTR for use of 20% enriched uranium silicide fuel with burnable poison has been studied since [illegible] in accordance with the Joint Study with ANL. Along with this direction, silicide miniplates were irradiated in the JMTR. Hydraulic tests using dummy fuel elements and release/born measurements of fission products on silicide fuel are under way in cooperation with KURRI.

On the other hand, in KURRI the same efforts as in JAERI to reduce enrichment of the KUR fuel are in progress. In order that the safety review application for full core fuel demonstration is accepted, the present data on LEU silicide fuel are regarded to be insufficient. Therefore, JAERI is planning to perform a thermal-hydraulic experiment of miniplates in cooperation with KURRI, and KURRI also planning to demonstrate to use two full size LEU silicide fuel elements among the current HEU elements, prior to the safety review application for full core conversion with LEU silicide fuel.

JAERI

JRR-2

According to the RERTR program, the core conversion from HEU(93%) fuel to MEU (45%) fuel was carried out in the JRR-2. The safety review for the conversion was over in December 1986. The following items were required to be installed additionally considering the latest LWR-based safety criteria.

1. An additional emergency heavy water supply equipment.
2. Safety circuits of high flux at low power mode and fuel failure.

Operation of the JRR-2 had been carried out with HEU fuel until April 24, 1987. The installation works were performed from May to October 1987. The first criticality with MEU fuel was achieved on November 25, 1987. After the critical examination, several kinds of experiments concerning with reactor characteristics were performed.

Now the JRR-2, converted to use MEU fuel, has been smoothly operated with the rated power (10 MW) under the annual schedule from February 8, 1988. Detailed descriptions of the test results are presented at this meeting.

JRR-3

The applications of the upgraded JRR-3 for design and construction permit were completed and the construction works have been started in May 1987. The

installation works for the reactor components are in progress and will be finished in 1990. The design of the upgraded JRR-3 fuel (LEU, 2.2 gU/cc) was completed, and the fuel fabrication will be started in 1988. The first criticality of the upgraded JRR-3 will be scheduled in 1990.

JRR-4

The post irradiation experiments of the full-sized UAl_x-Al fuel element loaded with 20% enriched uranium (2.2 gU/cc) irradiated in the JRR-2 have been completed with good results. The results of scanning electron microscopy (SEM) and X-ray micronalysis (XMA) of the fuel plates are being compiled. Another LEU full-sized UAl_x-Al fuel element in the JRR-4 has been irradiated with a good in-core behavior and will be finished at the end of November 1988.

The core conversion from HEU fuel to LEU fuel is under consideration including the upgrade of utilization capability.

JMTR

The full core demonstration with MEU fuel (UAl_x-Al, 1.6 gU/cc) elements in the JMTR was successfully carried out August 1986. The JMTR has been in steady operation with MEU fuel. The application of safety review for further core conversion from MEU fuel to LEU fuel is in preparation.

1. The miniplate irradiation tests (U_3Si_2, 5.0 and 5.3 gU/cc) were completed in 1986 with satisfactory results.

2. The safety analysis of LEU core is in progress, and the results so far are presented in this meeting.

3. The hydraulic tests for confirming mechanical integrity will be carried out in 1988 using two dummy fuel elements.

4. The measurements of temperature-dependent LEU silicide fuel properties will be carried out in Fiscal 1988.

5. The irradiation of LEU silicide fuel specimens measuring release/born (R/B) of fission products at high temperature will be started in November 1988. Experiments for fuel behavior in a reactor accident condition and basic studies on compatibility of U_xSi_y particle and aluminum matrix, fission product release mechanism, etc. are scheduled.

KURRI

KURRI has had the Joint Study Program with ANL since May 1977. The KUR has been successful in operation with HEU (93%) alloy fuel since 1964, and

will be converted to use LEU silicide fuel. Neutronics calculations and thermal hydraulic analysis for use of LEU fuel in the KUR have been almost completed, and it has been confirmed that the KUR core can be converted to use LEU silicide fuel without major design change. Before the full core conversion with LEU silicide fuel, two elements will be irradiated and tested in the current HEU core in Fiscal 1990, for which safety analysis is in preparation. The full core conversion will be anticipated in 1993. As to the KUHFR, no significant progress has been made in the past year.

REFERENCES

1. K. Kanda, "Reducing Enrichment Program for Research Reactors in Japan", in Proceedings of the International Meeting of Research and Test Reactor Core Conversion from HEU to LEU Fuels, Argonne, USA, November 8-10, ANL/RERTR/TM-4 CONF-821155, pp.24-32 (September 1983).

2. K. Sato, "Opening Statement to the Internation Meeting on Reduced Enrichment for Research and Test Reactors", in Proceedings of the Internation Meeting on Reduced Enrichment for Research and Test Reactors, Tokai, Japan, October 24-27, 1983, JAERI-M 84-073, pp.8-10 (May 1984).

3. K. Kanda, T. Shibata, I. Miyanaga, H. Sakurai and M. Kanbara, "Status of Reduced Enrichment Program for Research Reactor Fuels in Japan", in Proceedings of International Meeting on Reduced Enrichment of Research Reactor and Test Reactors, Argonne, USA, October 15-18, 1984, ANL/RERTR/TM-6 CONF-8410173, pp.11-20 (July 1985).

4. I. Miyanaga, K. Kamei, K. Kanda and T. Shibata, "Present Status of Reduced Enrichment Program for Research and Test Reactor Fuels in Japan", in Reduced Enrichment for Research and Test Reactors, Proceedings of an International Meeting, Petten, The Netherlands, October 14-16, 1985, D. Reidel Publishing Company, Dordrecht/Boston/Lancaster/Tokyo, pp.21-32, (March, 1986).

5. K. Kanda, T. Shibata, Y. Iso, H. Sakurai and Y. Okamoto, "Status of Reduced Enrichment Program for Research and Test Reactor Fuels in Japan", in Proceedings of the 1986 International Meeting on Reduced Enrichment for Research and Test Reactors, Gatlinburg, USA, November 3-6, 1986, ANL/RERTR/TM-9 CONF-861185, pp.14-22.

6. Y. Futamura, H. Sakurai, Y. Iso, K. Kanda and I. Kimura, "Status of Reduced Enrichment Program for Research and Test Reactor Fuels in Japan", in Proceedings of the 10th RERTR Meeting, Buenos Aires, Argentina, September 28 - October 1, 1987, in press.

Table 1. Japanese Research Reactors in Operation

Name	Owner	Site	Type and enrichment			Max. power	Start-up data
JRR-2	JAERI	Tokai	D_2O (CP-5)	U-Al	93 %	10 MW	1960.11
				UAl_x	45 %	10 MW	1987.11
UTR-KINKI	Kinki Univ.	Higashiosaka	H_2O (UTR)	U-Al	90%	1 W	1961.11
TRIGA-II	Rikkyo Univ.	Yokosuka	H_2O (TRIGA)	U-ZrH	20%	100 kW	1961.12
TTR	Toshiba	Yokosuka	H_2O (pool)	U-Al	20%	100 kW	1962.3
JRR-3	JAERI	Tokai	D_2O (tank)	NU		10 MW	1962.9
				UO_2	1.5%		
			H_2O (pool)	UAl_x-Al	20%	20 MW	1990
TRIGA-II MUSASHI	Musashi Inst. Tech.	Kawasaki	H_2O (TRIGA)	U-ZrH	20%	100 kW	1963.3
KUR	KURRI	Kumatori	H_2O (tank)	U-Al	93%	5 MW	1964.6
JRR-4	JAERI	Tokai	H_2O (pool)	U-Al	93%	3.5 MW	1965.1
JMTR	JAERI	Oarai	H_2O (MTR)	U-Al	93%	50 MW	1968.3
				UAl_x	45%	50 MW	1986.8
YAYOI	Univ. of Tokyo	Tokai	fast (horizontally movable)	U	93%	2 kW	1971.4
NSRR	JAERI	Tokai	H_2O (TRIGA)	U-ZrH	20%	300 kW	1975.6

Table 2. Japanese Critical Assemblies in Operation

Name	Owner	Site	Type and enrichment	Max. power	Start-up date
VHTRC	JAERI	Tokai	Graphite U 20% horizontally split	10 W	1961.1
TCA	JAERI	Tokai	H_2O(tank) UO_2 2.6% UO_2-PuO_2 2.6%	200 W	1962.8
NCA	NAIG	Kawasaki	H_2O(tank) UO_2 1-4.9%	200 W	1963.12
JMTRC	JAERI	Oarai	H_2O(pool) U-Al 93% UAl_x 45%	100 W	1965.10 1983. 8
FCA	JAERI	Tokai	fast U 93% U 20% Pu horizontally split	2 kW	1967.4
DCA	PNC	Oarai	D_2O(tank) UO_2 0.22% UO_2-PuO_2 1.5%	1 kW	1969.12
KUCA	KURRI	Kumatori	various U-Al 93% multi-core UAl_x 45%	100 W 1 kW (short time)	1974.8 1981.5

Table 3. Research Reactors Relevant to RERTR in Japan

Name	Power (MW)	First Critical	Fuel Enrichment	Conversion
KUR (KURRI)	5	1964	HEU → LEU	1993
KUHFR (KURRI)	30	?	HEU → MEU	?
JRR-2 (JAERI)	10	1960	HEU → MEU	1987
JRR-3 (JAERI)	20	1962	LEU → LEU	1990
JRR-4 (JAERI)	3.5	1965	HEU → LEU	?
JMTR (JAERI)	50	1968	MEU → LEU	1993
Related Critical Assemblies				
KUCA (KURRI)	0.0001	1974	HEU → MEU	1981
JMTRC (JAERI)	0.0001	1965	HEU → MEU	1983

Table 4. History of Reduced Enrichment Program for Research and Test Reactors in Japan

1977. 11.	Japanese Committee on INFCE WG-8 was started.
1977. 11.	Joint Study Program was proposed at the time of the application of export license of HEU for the KUHFR.
1978. 5.	ANL-KURRI Joint Study Phase A was started.
1978. 6.	Five Agency Committee on Highly Enriched Uranium was organized.
1978. 10.	Five Agency Committee tentatively agreed to reduce the KUHFR fuel enrichment from 93% to 45% as recommended by INFCE WG-8 in Japan.
1979. 2.	ANL-KURRI Joint Study Phase A was completed.
1979. 5.	Project team for RERTR was formed in JAERI.
1979. 7.	ANL-KURRI Joint Study Phase B was started.
1980. 1.	ANL-JAERI Joint Study Phase A was started.
1980. 8.	ANL-JAERI Phase A was completed.
1980. 9.	ANL-JAERI Phase B was started.
1981. 5.	MEU UAl_x-Al full core experiment was started in the KUCA.
1983. 3.	ANL-KURRI Phase B was completed.
1983. 8.	MEU UAl_x-Al full core experiment in the JMTRC was started.
1983. 11.	ANL-KURRI Phase C was started.
1984. 3.	ANL-JAERI Phase B was completed.
1984. 4.	ANL-JAERI Phase C was started.
1984. 4.	MEU-HEU mixed core experiment in the KUCA was started.
1984. 9.	Irradiation of 2 MEU and 1 LEU UAl_x-Al full size elements in the JRR-2 was started.
1984. 10.	Irradiation of LEU UAl_x-Al full size element in the JRR-4 was started.
1984. 11.	Thermal-hydraulic calculations for the KUR core conversion from HEU to LEU was performed.
1985. 1.	Irradiation of MEU UAlx-Al full size elements in the JMTR was started.
1985. 3.	Irradiation of MEU UAl_x-Al full size elements in the JMTR was completed.
	Irradiation of LEU U_xSi_y-Al miniplates in the JMTR was started.
1985. 6.	Irradiation of LEU U_xSi_y-Al miniplates in the JMTR was completed.
1985. 10.	Neutronics calculations for the KUR core conversion from HEU to LEU was performed.
1986. 1.	Irradiation of MEU UAl_x-Al full size elements in the JRR-2 was completed.
1986. 5.	Irradiation of MEU UAl_x-Al full size elements in the JRR-2 was completed.
1986. 8.	The JMTR was fully converted from HEU to MEU fuels.
1987. 11.	MEU UAl_x-Al full core in the JRR-2 was started.
1988. 7.	PIE of MEU, LEU UAl_x-Al full size element in the JRR-2 was completed.

STATUS OF CANADIAN LOW-ENRICHED URANIUM CONVERSION PROGRAM

J.W. Schreader, I.C. Kennedy, and D.F. Sears
Atomic Energy of Canada Limited
Chalk River Nuclear Laboratories
Chalk River, Ontario, Canada
K0J 1J0

Presented at

The International Meeting on
Reduced Enrichment for
Research and Test Reactors (RERTR)
September 19-22, 1988
San Diego, California, USA

ABSTRACT

Despite a dramatic increase in the cost of our new LEU fuel fabrication shop and setbacks in its construction schedule, AECL's program to convert the NRU Reactor to LEU fuel has moved ahead significantly. Thirty-one prototype LEU fuel rods are nearly ready for installation in the reactor, and construction work on the new fuel shop has begun. According to the current schedule, full-scale production of LEU fuel for NRU will begin during 1990. In our continuing fuel development program, a mini-element test irradiation is in progress to assess the behaviour of U_3Si_2 fuel with various particle size distributions, as an alternative to the U_3Si dispersion fuel already developed for the NRU and MAPLE-X10 reactors.

INTRODUCTION

This status report is an update on the program to convert Atomic Energy of Canada Limited's NRU reactor, situated at Chalk River Nuclear Laboratories (CRNL), from a highly-enriched uranium (93.15 wt% U-235, HEU) fueled reactor to a low-enriched uranium (19.75 wt% U-235, LEU) fueled reactor. NRU is a powerful and versatile heavy-water moderated and cooled reactor used for research and radioisotope production. It features on-power refueling, and typically contains about 95 fuel rods (assemblies) each having an initial fuel content of 0.5 kg U-235. The reactor operates on the average 80% of the time at approximately 130 MW (Th).

We regret to inform this meeting that delays in the construction of our new LEU fuel fabrication building and a re-evaluation of the time needed for equipment installation and commissioning have caused a slippage of approximately eight months in our conversion program. However, we are now installing the foundations for the building, and full-scale fuel fabrication is expected to begin in 1990.

FABRICATION OF U_3Si FUEL

Prototype Fuel Rods

Using industrial-scale manufacturing equipment housed in several CRNL buildings, we have completed the extrusion of uranium silicide cores for 31 additional NRU prototype rods. Cladding of the aluminum sheaths onto the extruded cores has been completed, most of the end plugs have been welded, and 25 of 31 complete fuel bundle assemblies have been produced. In addition, extruded cores for four prototype fuel bundles have been produced for our new MAPLE-X10 reactor, construction of which begins in 1989.

LEU Fuel Fabrication Facility

At the same time, work has proceeded toward the construction of a new building dedicated to the production of LEU fuel.

Increased demands by the regulatory agencies on criticality and safety, and a need for additional in-process storage capacity, required a re-design of certain areas of the original building plan. Also, equipment used in the temporary facilities for the production of the 31 prototype LEU fuel rods had to be optimized for larger-scale production. The latter forced re-design and, in some cases, procurement of additional equipment. All of this increased the estimated cost of the building and equipment from $3.8M (CDN) to $6.5M (CDN). Management, of course, then requested a complete review of all estimates and further presentations to our Board of Directors

who just recently approved our proceeding, even at the increased costs. All of this has taken valuable time.

The estimate of the time required for the moving and installation of equipment and commissioning of the new fabrication processes has been increased to approximately seven months. The LEU process, particularly the "front end" (from casting to extrusion) involves many more operations than the HEU process (see Figure 1). Our experience thus far has been working in a "batch" production mode with the various operations located in several buildings and, as noted earlier, using methods and equipment that must be changed somewhat for full-scale production. Our experience makes us optimistic about our final success but we need the additional time to ensure that our staff is fully familiar and competent with the new equipment and processes.

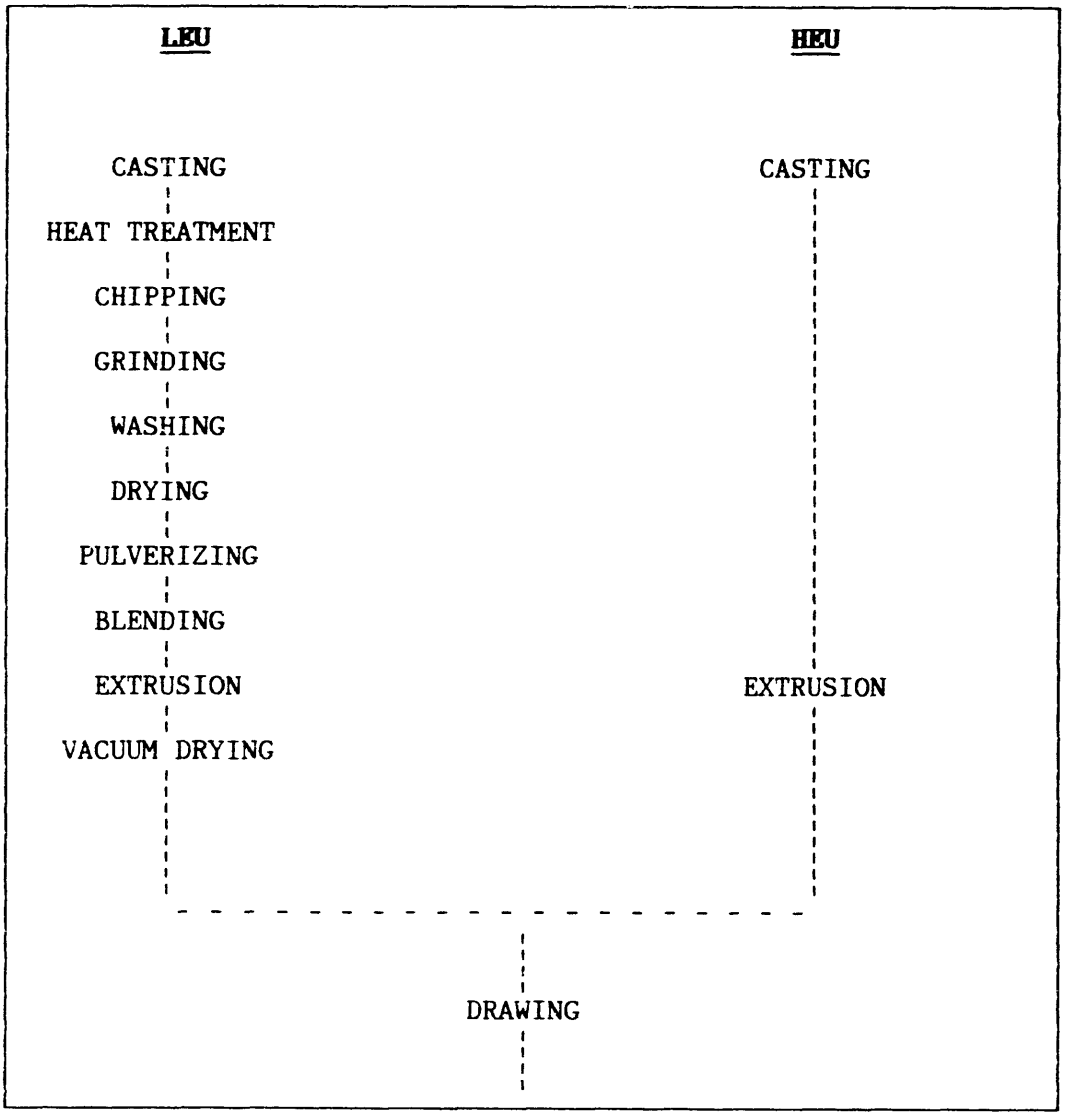

Fig. 1. Major Steps in Fuel Fabrication Processes.

We are pleased to report that the final pour of concrete for the foundation of the new fabrication building is being readied as we meet here today and the first of the prototype LEU rods is ready for insertion in NRU this week. Programming for the computerized nuclear materials accounting and control system for the new LEU facility has also been completed. This will provide real-time data for the various accounting zones in the LEU fabrication process and building storage areas. Our Nuclear Materials Control Branch, responsible for all nuclear material accounting on site, will also have a computer terminal giving direct access to inventory/accounting within the new building, the first CRNL facility with that capability.

PLANS FOR NRU REACTOR CONVERSION TO LEU FUEL

Philosophy of Conversion

Early in the LEU conversion program, it was decided that an essential intermediate step would be the on-site manufacture of a large-enough number of fuel assemblies (about 30) to give us confidence that our fuel production rate could exceed our fuel usage rate. When all of the 31 assemblies which were subsequently fabricated are installed in NRU, this "partial core" of LEU fuel rods will allow us to evaluate effects on the D_2O and its helium cover gas. Heavy water is the coolant as well as the moderator of NRU, and a purification system continuously cleans the D_2O as it picks up corrosion products from aluminum and steel reactor components.

The 31 prototype LEU fuel rods will be inserted at the usual fueling rate of about two per week beginning in 1988 September, until by 1989 January we will have approximately one-third of the reactor fueled with LEU. Normal fuel management practice will be followed, whereby the fuel is initially installed in a relatively low-flux location and subsequently moved several times to other higher-flux locations until it reaches full burnup after about a year.

In deciding on the fuel rod movements needed to satisfy the various experimental and isotope production rods in NRU, the reactor physicists will treat the HEU and LEU fuel rods as completely interchangeable. Based on our good experience with the first seven prototype LEU rods irradiated in 1984 to 1986, we expect to see no differences in individual fuel rod behavior or handling, but we will be looking for any magnified effect on bulk parameters such as coolant/moderator chemistry or overall reactivity. Barring the occurrence of any adverse bulk effects, we will proceed toward converting the whole NRU core as LEU fuel rods become available.

Revised Schedule for Converting NRU to LEU Fuel

After construction and commissioning of the new fuel fabrication facility, we expect to manufacture NRU LEU rods in 1990 and to begin the full core conversion when a stable production rate is achieved by 1990 September.

The current schedule is:

- Begin construction of LEU Fuel Fabrication building - 1988 Summer
- Install first of 31 LEU prototype rods in reactor - 1988 September
- Complete LEU Fuel Fabrication building - 1989 June
- Commence equipment installation and commissioning - 1989 July
- Commence production of NRU LEU fuel - 1990 February
- Introduce first LEU production fuel rods into NRU - 1990 September

Fuel Supply

By 1988 October, CRNL will issue requests for quotations for the supply of the approximately 400 kg LEU required for the first NRU LEU core. Recognizing the slippage of approximately eight months in the conversion program, we are monitoring our HEU supply very closely and will be considering various contingencies to ensure the continued operation of NRU Reactor through the conversion process.

TEST IRRADIATION PROGRAM

General

As reported at the previous RERTR conference[1], we have successfully completed the test irradiation program to qualify U_3Si dispersion fuel for use in the NRU Reactor. In the extruded rod form, U_3Si performs well in-reactor up to very high burnup (6-8 vol% swelling at 93 atomic % burnup). It appears that U_3Si dispersions are mainly being considered elsewhere for similar, large, high-power research reactors; by contrast, most low- to medium-power reactors are being converted to a U_3Si_2 dispersion instead, because the plate-type fuel design provides insufficient restraint to maintain acceptable swelling with U_3Si dispersions. Considering the number of smaller reactors scheduled for conversion to U_3Si_2, the potential database which could be generated on U_3Si_2 fuel performance as a result, the generic approval for use of this fuel in USNRC licenced research reactors, and the implications of safety and licencing precedents based on U_3Si_2 , CRNL has decided to evaluate U_3Si_2 as a backup dispersion fuel. Also, since U_3Si_2 is friable and more easily reduced into powders than U_3Si , it is economically attractive from a fuel manufacturing viewpoint and could serve as a good candidate fuel for smaller Canadian reactors.

During the last year the U_3Si_2 fuel fabrication effort has been concentrated on developing gentle powder manufacturing methods to minimize the amount of fines produced, and on optimizing the core fabrication process for the higher loading of U_3Si_2 required. The challenge is to extrude cores with the higher volume fraction of dispersant required, while maintaining the U-235 homogeneity and uniformity, and minimizing the porosity and segregation in the long NRU fuel elements.

Experiment Exp-FZZ-921

In order to evaluate the behavior of the U_3Si_2 dispersion fuel and qualify it for use in Canadian reactors, a new test irradiation, experiment Exp-FZZ-921, was initiated. As reported previously[1], the test vehicle for irradiating LEU silicide dispersion fuels in NRU has been the mini-element (except for the full-scale demonstration irradiation of seven prototype 12-element NRU rods, Exp-FZZ-913). The mini-element fuel core diameter (5.5 mm) and clad wall thickness (0.76 mm) are the same as full-size NRU elements. The mini-elements are, however, only 184 mm long compared with 2.9 m for NRU elements. The mini-elements also resemble NRU elements in that they have six cooling fins at 60° intervals around the cladding.

Twelve mini-elements containing approximately 64 wt% U_3Si_2 dispersed in Al (3.15 gU/cm^3, the loading required for NRU) were fabricated for the test irradiation in NRU. The U_3Si_2 was cast using a high-frequency vacuum induction furnace. Since we know from previous test irradiations that the particle size is an important variable which can affect dispersion fuel swelling, we were also interested in determining its effect on U_3Si_2 fuel performance. For example, a previous experiment Exp-FZZ-918 confirmed that swelling was proportional to the percentage of fine (< 44 μm) particles contained (see Figure 2).

The mini-elements for Exp-FZZ-921 were divided into 3 groups of 4 elements, each containing a range of particle size distributions. Group 1 contained the size distribution which resulted from U_3Si_2 pulverization trials with a laboratory-scale hammer mill. The U_3Si_2 is brittle and easily reduced into powders, but hammer-milled powders contain a high percentage of fines as can be seen in Figure 3. Normally the amount of fines in a dispersion fuel would be kept to a minimum, to minimize the damage to the matrix material from fission product recoil, and to reduce the fuel surface area and thus the amount of solid-state reaction with the matrix material. However, it was reported that tests at the Oak Ridge Reactor show as much as 50% fines could be accommodated in U_3Si_2 fuel elements with no detrimental effects[2], so the hammer-milled powders were included. If this were found to be suitable, then little further development would be required to manufacture CRNL's annual powder requirements.

Group 3 contained a size distribution close to that currently used with U_3Si. It is felt that with the development of gentler size-reduction methods such as jaw- or roll-crushing, the percentage of fines could be reduced to the Group 3 fraction.

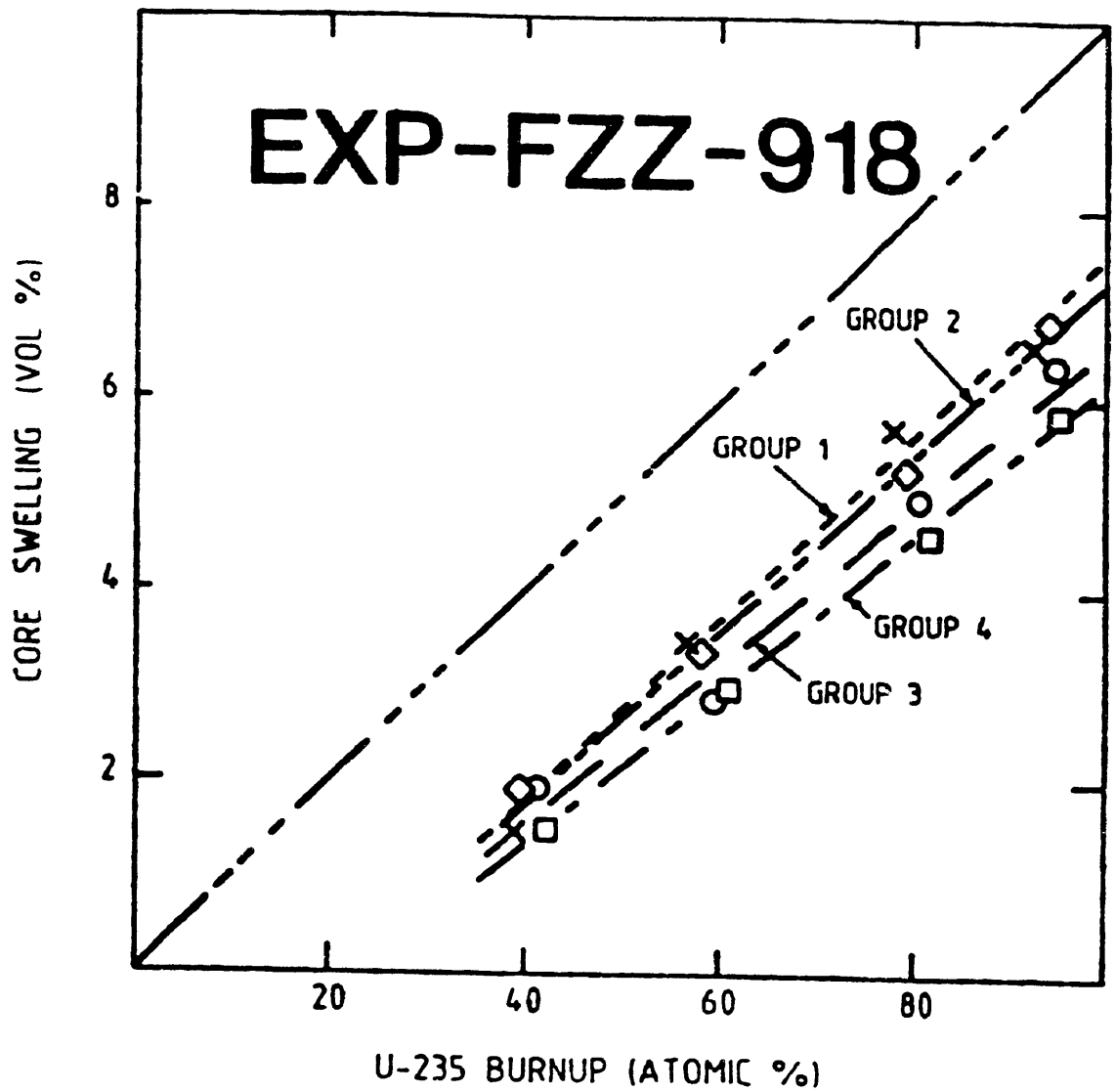

Fig. 2. Swelling dependence on particle size distribution and burnup for mini-elements containing Al-61.4 wt% uranium silicide (EXP-FZZ-918). Group 1 contained the highest fraction of fines, Groups 2 and 3 had progressively lower fractions and Group 4 contained the fraction used at CRNL.

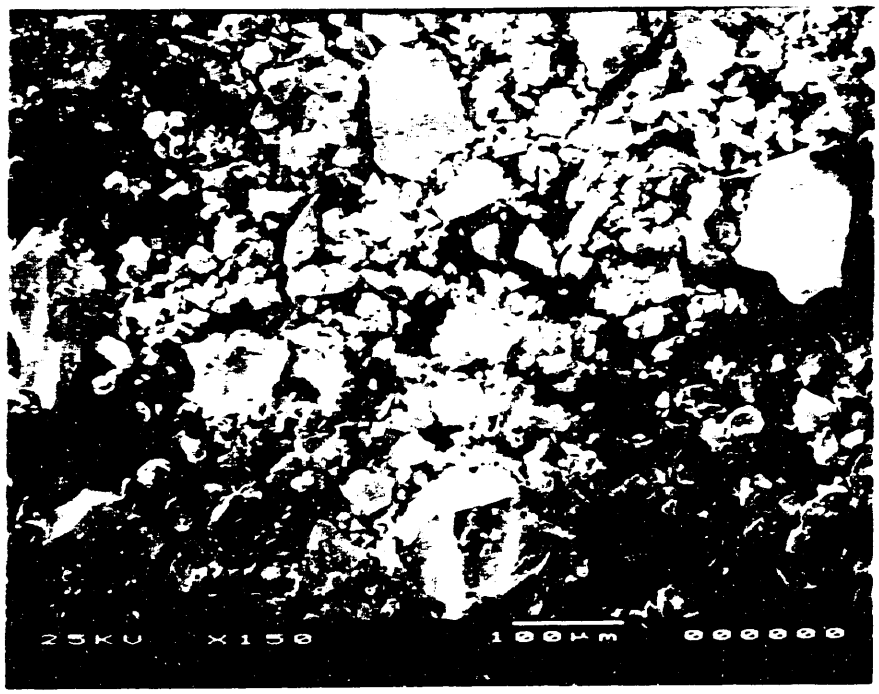

Fig. 3. SEM micrograph of typical powders produced by the hammer-mill.

The mini-elements in Group 2 contained an intermediate size distribution between Group 1 and Group 3.

The mini-elements were installed in NRU in 1988 June, and were irradiated under typical NRU driver fuel operating conditions at linear power ratings between 86-92 kW/m. The assembly was removed after reaching approximately 60% burnup of the original U-235. After cooling, three of the mini-elements, one from each group, will be removed from the assembly for post-irradiation examinations in the reactor bays and the hot-cells. The remaining elements will be returned to the reactor for further irradiation, and will be removed for interim and final examinations after 80 and 93% burnup respectively.

CONCLUSIONS

1) Despite the slippage in the overall conversion program we are confident that most major hurdles have been overcome. We have committed ourselves to dealing with any others that come along, with the ultimate goal still being the conversion of NRU to LEU fuel.

2) Barring any unforeseen complications, the complete conversion of the NRU Reactor to LEU fuel should be achieved by 1991.

3) In our continuing fuel development program, twelve Al-64 wt% U_3Si_2 mini-elements containing a variety of particle size distributions were irradiated up to 60 at% burnup in NRU, without incident. Three of the elements will be removed for PIE and the remaining elements will be irradiated up to 80 and 93 at% burnup, after which they will be examined similarly.

REFERENCES

1. D.F. Sears, L.C. Berthiaume, L.N. Herbert, "Fabrication and Irradiation Testing of LEU Fuels at CRNL - Status as of 1987 September", Proceedings of the International RERTR Meeting, Buenos Aires, Argentina, September 28 - October 2, 1987 (to be published).

2. G.L. Copeland, et al., "Performance of LEU U_3Si_2-Al Dispersion Fuel Elements in the Oak Ridge Research Reactor", ANL/RERTR/TM-10, October 1987.

IAEA ACTIVITIES IN RESEARCH REACTOR SAFETY

W. Byszewski
International Atomic Energy Agency
Vienna, Austria

ABSTRACT

The paper presents activities of the IAEA in two areas of research reactor safety; safety inspections to research reactors and development of safety standards.

Safety inspections are preformed mainly to countries under Agency sponsored projects, but also on request to other Member States.

The paper first presents the scope and objectives of the inspection.

Secondly, the Agency programme of Safety Standards development is described.

1. INTRODUCTION

There are presently about 326 research reactors operating in 55 countries (see Table 1). The total number of research reactor years of operating experience is 9474, 6555 of these with units still operating.

The range of the research reactors is large, varying from very small ones including those used for teaching, to development or prototype plant of many hundreds of megawatts capacity.

Four more research reactors were shut down in 1987, making a total of 204 shut down. These reactors offer the potential for experience to be gained on decommissioning.

In 1987 seventeen were under construction and 18 were planned.

Developing countries are operating 76 research reactors, constructing 12 and planning 16. More than 63% of the operating research reactors have an operating history of over 20 years. It means that a large number of the research reactors were constructed 20-25 years ago and many of them are nearing or have reached the end of their useful life. The age distribution of current reactors is shown in Fig.1.

The Agency has given an appropriate consideration to nuclear safety of research reactors.

In 1972 the Agency started safety advisory missions to research reactors which are under the Agency sponsored projects (see Table 2), whereby the Agency is entitled to examine the operational and radiological safety aspects of Agency assisted projects.

The IAEA's statute authorizes it to establish and adopt safety standards and the Agency countinues to play an important role in this area. However, for research reactors many safety standards are still lacking.

The main document, Code of Practice "Safe operation of Research Reactors and Critical Assemblies", Safety Series No 35 has been revised and published in 1984 as a new edition. A few other documents have been initiated recently.

This paper sets out some of the activities at the Agency in the field of Research Reactor Safety.

2. SAFETY INSPECTIONS TO RESEARCH REACTORS

Operational safety advisory programme was created to provide useful assistance and advice from an international perspective to research reactor operators and regulators on how to enhance operational safety and radiation protection on their reactors.

In the most comprehensive form of safety mission, a team of experts assesses all areas affecting the ultimate safety of a particular research reactor. These missions are conducted regularly, about once each four years. Each mission comprises IAEA staff and if necessary external consultants.

Safety missions cover not only the operational safety of reactors themselves, but also the safety of associated experimental loops, isotope laboratories and other experimental facilities.

Safety missions are also performed on request in other Member States which are interested in receiving impartial advice and assistance in order to enhance the safety of research reactors.

2.1. Objectives of the Mission

The objectives of a safety mission are to conduct a comprehensive integrated safety assessment of the research reactor facility and to compare the safety of the reactor with the Agency's safety standards.

The evaluation is also aimed at facilitating an exchange of knowledge and experience between the experts and reactor personnel.

Safety missions are intended not to be a regulatory-type inspection that checks compliance with national requirements, but to achieve enhanced operational safety through application of effective practices used at other facilities around the world.

2.2. Areas of the Inspection

2.2.1 General

The mission checks whether the safety at the reactor is subject to review by a regulatory organisation independent of the operating organisation and noting the frequency of regular inspections and any non-compliance observed by the inspectors. Does a reactor safety committee, or equivalent advisory group exist to review safety problems arising in reactor operations and in planning of experiments.

The mission also checks whether the Safety Analysis Report (SAR) is up to date including accident analysis and whether the SAR addresses current deterministic and probabilistic methodologies for safety assessment.

2.2.2. Nuclear Safety

The nuclear safety review is mainly based on the requirements of the "Safe operation Research Reactor and Critical Assemblies" as it appears in the Agency's Safety Series No.35, 1984 edition.

The review examines the following areas:

2.2.2.1. Safety Specifications --The mission checks whether there are approved safety specifications, including limits and conditions for the conduct of operations and experiments, and corrective actions in case of violation of the safety limits.

2.2.2.2. Periodic Testing and Inspection --The mission checks the surveillance test intervals established for the different reactor systems, the availability of written procedures for testing and inspection and the compliance of test results with safety specifications.

2.2.2.3. Management --The mission verifies the organisational structure of the Research Centre and Reactor Department for clearly defined duties and responsibilities in implementing and controlling facility activities. Particular attention is paid to training and retraining programmes, staff size, qualification and licencing of the operators, programmes for reactor utilization, quality assurance for operation, physical security and housekeeping.

2.2.2.4. Operating instructions --During the inspection the mission checks whether all normal and emergency operating procedures required for guiding the operating personnel are in place, that the personnel are trained and retrained in these procedures, and a system has been astablished for regular review of all procedures and for the communication of any revisions to the operating personnel and other holders of the document.

2.2.2.5. Records and Reports --The mission checks whether all essential records on design and operation related to safety are being maintained.

2.2.2.6. Maintenance --The mission checks primarily the preventive maintenance programme for the reactor, the organisation of maintenance, the equipment available, and the procedures and documentation for maintenance. It also checks whether a system of work permits and approval after the maintenance is completed exists.

2.2.2.7. Experiments and modification --The mission checks the assurance of safety in routine experiments and irradiations and the safety review process for new experiments or modifications in the reactor systems.

2.2.2.8. Physical security --The mission checks whether a physical security plan exists for the facility and whether it has been approved by the regulatory body.

2.2.2.9. Quality Assurance Programme for Operation --The mission checks whether the operating organisation has a quality assurance programme duly reviewed and approved by the regulatory body that will govern the quality at all safety related items during the operations. Does the quality assurance programme cover periodic testing and inspection of components and equipment at a determined frequency.

2.2.2.10. Conduct of Operations --The mission conducts a walk-through of the facility and asks questions of reactor personnel on matters relating to the reactor systems and the safety of reactor operation.

The mission checks :

a) Housekeeping in the facility
b) Operational status of components and equipment important to safety
c) Leak tightness of containment/confinement
d) Proper demarcation of high radiation areas, e.g. experimental facilities, spent fuel storage, etc.
e) Following up the approved procedures by the operators and accomplishment of the required checklists and forms.
f) Function and calibration of instruments and systems.
g) Knowledge of operating limits of the reactor and, of its operational characteristics by the operators
h) Reactor incidents and abnormal occurences with safety significances which may have occurred.
i) Number of unplanned scrams per year (for the last three years)
j) Future plans for the reactor facility (conversion, increase in power level)

2.2.3.Radiation Protection

The mission examines the following areas :

2.2.3.1. Roles and responsibilities of management, the line organisation and the authority of the radiation protection staff with regard to the operating personnel.

2.2.3.2. Staff selection, training and qualification.

2.2.3.3. Occupational radiation control including equipment, facilities and procedures for external and internal dose control, and surveillance activities including dosimetry and monitoring activities.

2.2.3.4. Public radiation control including equipment, facilities and procedures for control and monitoring of liquid gaseous and solid waste discharged into environment and environmental monitoring.

2.2.3.5. Emergency planning and preparedness at on-site and off-site organizations responsible for responding to nuclear accidents and radiological emergencies.

2.3. Performance of the Mission

The members of a mission study information provided in advance by the research reactor organisation to familiarize themselves with the reactor, its main design features, operating characteristics, and the organisation of the reactor operation. This information is contained in a questionnaire which is filled out by the reactor operator.

At the reactor site members of the mission :

- examine the safety documentation of the facility,
- review the oprational status of the reactor,and observe, if possible, a reactor start-up and shutdown,
- discuss technical details with the responsible personnel.

At the conclusion the mission's principal findings and recommendations are discussed with the senior management of the operating organisation and representatives of the regulatory authority.

2.4. Reporting Policy

After examining in depth the operational safety and the radiation protection aspects of the reactor operation the mission orally convey their findings and recommendations to the relevant authorities (operating organisation and regulatory body) during the final meeting. Shortly afterwards, a final mission report with conclusions is submitted through official channels to the Member State concerned. Further distribution of the report is at the discretion of the requesting Member State.

2.5. Some Conclusions from Inspections

The results of the inspections have shown that in some countries there are problems with radiation protection practices and nuclear safety.

Very often the Safety Analysis Report is not updated, regulatory supervision needs clarification and improvement, maintenance procedures should be more formalised and records and reports are not maintained properly. In many cases population density around the facility has increased affecting the validity of the original safety analysis.

3. SAFETY STANDARDS AND REGULATIONS

Until now little safety guidance was available to facilitate national efforts to update safety at reserach reactor facilities. To meet that need the IAEA has initiated a safety standards programme for reseach reactors. For the past 4 years the IAEA has collected information and experience on this subject.

3.1. Published Documents

The first document, the Safety Guide on "Safety in Decommissioning of Research Reactors", Safety Series No 74 has been published in 1986. With the increasing age of many research reactors much more attention has been given to decommissioning. This Safety Guide was issued in response to this need as part of the Agency's programme for establishing Codes of Practice and Safety Guides for research reactors. It supplements the existing Code of Practice on the Safe Operation of Research Reactors and Critical Assemblies, Safety Series No 35 (1984 Edition).

Additionally some TECDOS's have been published in the areas where the needs were recognized (see Table 3).

3.2. New Documents

According to the Research Reactor Safety Publications programme the Agency had started to develop such Safety Guides as :

- Research Reactor Safety Criteria
- Research Reactor Safety Assessment
- Safety Aspects of Research Reactor Modification,

and the following documents are planned for the future:

- Siting of Research Reactors (revision of TECDOC-403)
- Regulatory Aspects of Research Reactors

An Advisory Group Meeting on Research Reactor Publications (AGM) was held in Vienna in June 1988 to review the Agency's proposed Research Reactor Safety Publications programme and the existing documents for Research Reactor Safety.

The AGM has categorized all documents according to the new proposed structure for safety-related publications at the Agency. A number of technical areas are identified to group together those documents which are mainly devoted to one topic, e.g. to waste management, radiation protection or research reactor safety. Within each of these groups, called an Application Area, a hierarchical structure of the following four levels is established :

- Safety Fundamentals
- Safety Standards
- Safety Guides
- Safety Practices

Publications which are not part of the Safety Series as they address subjects additional to those of safety are:
- Technical Reports
- TECDOC's

According to the proposed structure the AGM has developed a list of Safety Standards, Safety Guides and Safety Practices giving for each the objectives, topics to be covered, priority, related documentation and status/follow-up/recommendations where appropriate.

A general survey of all the above documents is shown in Table 4. Some changes and additions, taking into account the new approved structure for safety-related documents have been introduced in the programme. For example, the Safety Guide on Research Reactor Safety Principles and Criteria has been split into two guides - design and operation. Commissioning, Emergency Planning and Utilization are now new guides. The old guide on Modification has been "downgraded" to a safety practice under the safety guide on Operation.

The remaining Safety Practices are new documents. However, the majority of them will be based on existing documents (TECDOCs and contributions by experts participating in activities of the previous progrmme).

In Table 5 is shown a schedule of the steps to produce the mentioned documents and the recommendations on how to proceed for their development.

The mentioned recommendations take into account the fact that almost all the proposed documents can be prepared from existing documents. For this reason, small working groups of experts at only one meeting will be able to prepare drafts to be presented directly to Technical Committee Meeting. The AGM also recommended that the Chairman of the Working Group also chair the corresponding Technical Committee for consistency. This would streamline the process by eliminating one or two Advisory Group Meetings which otherwise would be required to prepare the first draft.

A particular recommendation was that a specific Quality Assurance Guide for Research Reactors not be produced. The adopted approach has been to incorporate QA requirements into each specific safety standard, guide or practice. The NUSS QA documents could be utilized for Research Reactors up to a certain extent.

After finalizing all safety guides the Advisory Group Meeting on Research Reactor Publications should be reconvened to initiate the overall safety standard for research reactor (old Safety Series No 35).

The entire process is expected to take about 3 years with current Agency resources. In some cases it may be necessary to send the working group drafts to specific advisory groups for review.

Table 1. Research Reactors in Operation (22 April 1988)

	Number		Number
Argentina	5	Libyan Arab Jamahiriya	1
Australia	2	Malaysia	1
Austria	3	Mexico	3
Belgium	6	Netherlands	2
Brazil	3	Norway	2
Bangladesh	1	Pakistan	1
Bulgaria	1	Peru	1
Canada	14	Philippines	1
Chile	1	Poland	3
China	9	Portugal	1
Colombia	1	Romania	2[a]
Czechoslovakia	3	South Africa	1
Dem. People's Rep. of Korea	1[a]	Spain	1
Denmark	2	Sweden	2
Egypt	1	Switzerland	4
Finland	1	Taiwan, China	5
France	21	Thailand	1
German Democratic Republic	5	Turkey	2
Germany, Federal Republic of	21	United Kingdom	15
Greece	2	USA	99
Hungary	3	USSR	24[a]
India	5	Venezuela	1
Indonesia	3	Viet Nam	1
Iran, Islamic Republic of	1	Yugoslavia	3
Iraq	2	Zaire	1
Israel	2[a]		
Italy	7[b]		
Jamaica	1		
Japan	18		
Korea, Republic of	3	TOTAL	326

a Information incomplete.
b Includes a CEC reactor.
Source: IAEA Research Reactor Database.

Table 2. RECORDS OF IAEA RESEARCH REACTOR SAFETY MISSIONS

COUNTRY	FACILITY DESCRIPTION	FACILITY LOCATION	DATES OF SAFETY MISSION VISIT															
			72	73	74	75	76	77	78	79	80	81	82	83	84	85	86	87
Argentina	5MW RAEP reactor	Ezeiza Atomic Centre Buenos Aires		x					x									
	Siemens SUR-100 Zero power reactor	Univ. of Rosario		x					x									
Brazil	10MW pool type reactor	Instituto de Energia Atomica Sao Paolo		x				x										
Chile	5MW Herald type reactor	La Reina Nuclear Centre Santiago		x				x									x	
Columbia	20KW pool type reactor	Instituto de Asuntos Nucl. Bogota						x						x				x
Egypt	2 MW WWR-C	INSHAS														x	x	
Finland	100KW TRIGA	Finland Inst. of Technology Otaniemi					x					x						x
Greece	5 MW GRR-1	Democritos Nuclear Res. Centre Athens	x				x						x				x	
Indonesia	1 MW TRIGA MK II	Bandung Res. Centre	x		x				x	x			x				x	
	250 KW TRIGA MK II	Yogyakarta Res. Centre								x			x				x	
Iran	5MW Pool type reactor	Teheran Nucl. Centre, Univ. of Teheran	x				x											
Jamaica	20 KW Slowpoke res. reactor	University of West Indies, Kingston															x	

N.A. : Not Applicable, x - has taken place,

RECORDS OF IAEA RESEARCH REACTOR SAFETY MISSIONS

COUNTRY	FACILITY DESCRIPTION	FACILITY LOCATION	DATES OF SAFETY MISSION VISIT																
			72	73	74	75	76	77	78	79	80	81	82	83	84	85	86	87	88
Japan	10MW JRR-3	JAERI Tokai - Mura						x											
Korea, Rep of	100KW TRIGA MK II 2MW TRIGA MK III	Korea Atomic Energy Res. Inst. Seoul						x						x x					
Malaysia	1 MW TRIGA MK II	Tun Ismail Atomic Res. Centre							x					x			x		
Maroco	TRIGA MK I	Rabat																	
Mexico	1MW TRIGA MK III,MX-A SUR -100, MX-B	Mexican Natio. Nucl.Ener.Com. Natio. Autonomous, U.of Mexico	x	x				x x				x x					x x		
	Nucl.Chicago SCA,MX-C	Natio. Polytechnic Inst.		x				x				x					x		
	Nucl.Chicago SCA,MX-C	School of Eng. Zacatecas		x				x				x					x		
Norway	20 MW, NORA Reactor HBWR	Institute of Atomic Energy, Kjeller																x	x
Pakistan	5MW Pooltype reactor	PINSTECH Rawal Phindi					x									x			
Peru	Zero power Res. reactor	Nuclear Res. Centre, Lima							x			x						x	

COUNTRY	FACILITY DESCRIPTION	FACILITY LOCATION	DATES OF SAFETY MISSION VISIT																
			72	73	74	75	76	77	78	79	80	81	82	83	84	85	86	87	88
Philippines	1MW Pool type	Phil. Atomic Energy Comm. Quezon City	x		x			x					x						
Romania	14 MW Dual Core TRIGA	Romanian Inst. for Nucl. Technology, Pitesti											x						
Spain	Zero energy fast reactor CORAL-I	Spanish Nuclear Energy Comm. Madrid											x				x		
Thailand	2MW TRIGA MK III	Off. of Atomic Energy for Peace, Bangkok			x				x				x					x	
Turkey	2MW Pool type reactor	Cekmece Nuclear Res. & Training Centre, Istanbul					x									x			
Uruguay	100KW RV-1 res. reactor	Nuclear Research Centre, Montevideo			x			x	x					x			Decommissioning		
Vietnam	0,5 MW res. reactor	Nucl. Research Inst., Da Lat														x			
Venezuela	3 MW RV-1 res. reactor	Venezuelan Scientific Res. Institute			x				x					x					x
Yugoslavia	100 KW TRIGA MK II	Nucl. Inst. Josef Stefan Ljubljana					x									x			
	10 MW, HWR	Boris Kidric Vinca, Belgrade														x			
Zaire	1 MW TRIGA MK I	Lovanium Univ. of Kinshasa Leopoldville								x					x				

Table 3. IAEA TECDOCS on Research Reactor Safety

1. IAEA TECDOC-348

   Earthquake resistant design of nuclear facilities with limited radioactive inventory (1985 Edition)

2. IAEA TECDOC-400

   Probabilistic safety assessment for research reactors (1987 Edition)

3. IAEA TECDOC-403

   Siting of research reactors (1987 Edition)

4. IAEA TECDOC-233

   Research reactor core conversion from the use of highly enriched uranium to the use of low enriched uranium fuels Guidebook (1980 Edition)

5. IAEA TECDOC-448

   Analysis and upgrade of instrumentation and control systems for the modernization of research reactors (1988 Edition)

Table 4 Research Reactor Safety Documents - Survey Sheet

SAFETY STANDARD	SAFETY GUIDES	SAFETY PRACTICES
	SG 1 Regulatory Aspects	
	SG 2 Safety Analysis Report	SP 2.1 Methods and Tools for Nuclear and Thermal Safety Analysis
		SP 2.2 Source Term Derivation and Radiological Consequence Analysis
		SP 2.3 Accident Analysis
	SG 3 Emergency Planning	
	SG 4 Siting	
	SG 5 Design for Safety	SP 5.1 Earthquake Resistant Design
		SP 5.2 Design Information
		SP 5.3 Instrumentation and Control Systems
	SG 6 Commissioning	
	SG 7 Safe Operation	SP 7.1 Personnel Qualifications and Training
		SP 7.2 Operational Safety Documentation
		SP 7.3 Safety Aspects of Modifications
	SG 8 Safety Aspects of Utilization	
	SG 9 Decommissioning	

Table 5 Recommended Schedule for Research Reactor Publications

1988

AG on Publications No. 1/June 1988/1 week
TC on Design (Safety Guide)/October 1988/1 week
CS on Design (Safety Guide and Practices)/December 1988/1 week

1989

AG on Safety Analysis Report (Safety Guide)/February 1989/2 weeks
AG on Operational Safety (Safety Guide and Practices)/April 1989/ 2 weeks
AG on Publications No. 2/September 1989/1 week
TC on Safety Analysis Report (Safety Guide)/December 1989/1 week

1990

AG on Safe Utilization (Safety Guide and Practices)/Spring 1990/2 weeks
AG on Commissioning, Decommissioning and Emergency Planning (Safety Guides)Summer 1990/2 weeks
AG on Regulatory Aspects and Siting (Safety Guides)/Fall 1990/2 weeks
TC on Operational Safety (Safety Guide)/Winter 1990/1 week

1991

AG on Publications No. 3/early 1991/2 weeks
TC on Safe Utilization (Safety Guide)/Spring 1991/1 week
Mail review of the Safety Guides on Commissioning, Decommissioning, Emergency Planning, Siting and Regulatory Aspects/Spring 1991
TC on the Safety Standard/Summer 1991/1 week

Fig. 1 The Age Distribution of Research Reactors (Source: IAEA RRDB, May 1988)

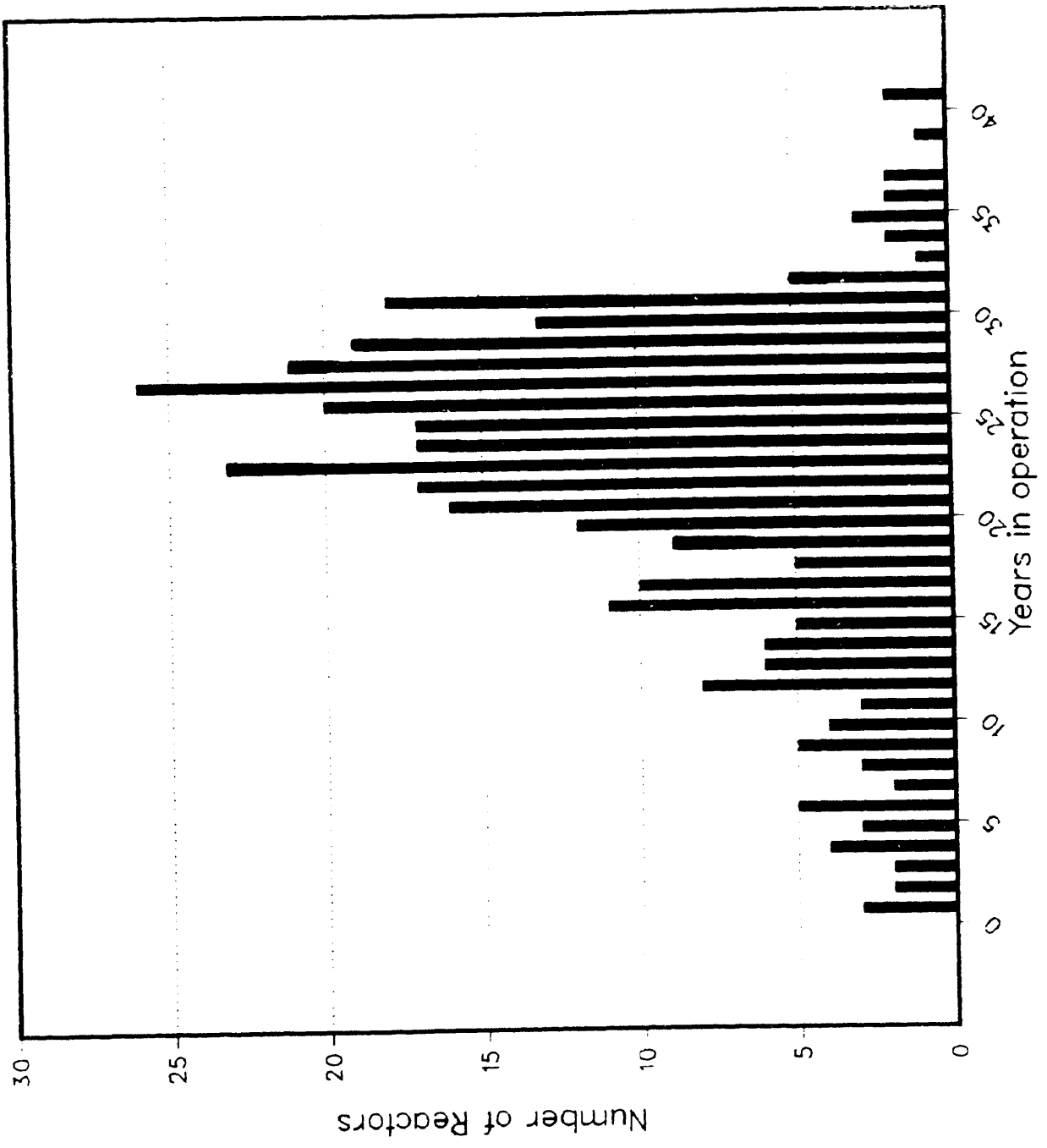

SESSION II

September 19, 1988

CHANGES IN THE FUEL FABRICATION INDUSTRY

Chairman:

G. Thamm
(KFA, Federal Republic of Germany)

WHY NUKEM STEPS OUT OF THE MTR-FUEL ELEMENT MARKET AND HOW TO SOLVE THE PROBLEMS RESULTING FROM THAT

Horst W. Hassel
NUKEM GmbH
and
C.E.C.C.N.
D-6450 Hanau/Main, Hessen, Federal Republic of Germany

ABSTRACT

Since NUKEM has been forced by political circumstances to stop any kind of handling and converting radioactive materials, mainly enriched and depleted uranium, the most important question arising from that decision, had to be answered: How to avoid major difficulties which NUKEM's customers within this field of business may run into by such an unexpected event? There was just one reasonable answer: A quick and smooth transfer of current contracts, know-how, materials, tools, equipments and documents to a close-by European company, experienced enough to step into NUKEM's MTR- and depleted uranium business.

After many years of strong and permanent attacks, the West German anti-nuclear movement has won an important battle: NUKEM's operation licence for fabricating nuclear fuel was withdrawn by the German authorities on January 15, 1989. After Tshernobyl and the Hanau bribery scandal it was just a question of time to feed the pro and contra discussion with more and more hysteric argumentation and extremely unfair rumors against that company which almost everybody saw as the center of the nuclear fuel cycle in Germany.

End of February, after a permanent discussion with the authorities, it was for sure not to reobtain the operation licence within a period which could have allowed to continue all work contracted. Also the risk of further production stops due to unpredictable actions of various authorities under the permanent pressure of the media forming the so called public opinion could no longer be accepted, neither by NUKEM nor by its customers!

Therefore it was decided not to continue in the long run but only to fight for a limited operation licence which allows at least two important steps:

1) To finish the most important fabrication under current contracts in Hanau, and in parallel to that,

2) To transfer the business to CERCA by the help of CECCN and to train CERCA personnel at NUKEM's Hanau facilities (fabrication + QA) up to the end of 1988 using the restricted operation licence.

1) For finalizing the most important fabrication under current contracts NUKEM was allowed by the restricted licence, obtained in April, only to perform the work for which the uranium was available already at Hanau at least in the form of purified metal. All scraps had to be collected, identified and packed for the transfer to a European facility for chemical recovery. For several reasons NUKEM chose COGEMA in France.

2) The work for which there was no purified uranium metal available at Hanau at the time of obtaining the restricted licence had to be transferred to CERCA after entering into a corresponding agreement between the two companies.

Why did NUKEM choose CERCA?

- CERCA is a very well experienced company in this field, which has fabricated around 250000 fuel plates within the past 30 years, always being up to date concerning the needs and requirements of the market, and already having performed all necessary r + d for LEU/silicide fuel.

- CERCA can make available the necessary capacity without major problems (see the presentation of M. Yves Fanjas/CERCA).

- It is a company within the EC and close-by.

- Both companies already have cooperated in the field of supplying advanced fuel to European High Flux Research Reactors such as for the research centers in Ispra, Grenoble, Petten and Studsvik.

All this has given the best guarantee for an immediate and effective transfer of current contracts, i.e. avoiding major delays in the supply of fuel elements. Any delay until now only was caused by the very restricted way of granting export- and transport-licences by various German authorities which felt very much irritated by the rumors and accusations coming from the anti-nuclear movement and the major part of the West German press and mass media.

Anyway, export licences were necessary not only for uranium but also for aluminum materials, tools, equipments, know-how, drawings and specs. Aluminum, for example, had become some kind of strategic material for which an export licence was not easy to get.

In order to handle all these transfer questions in front of the customers, CERCA and NUKEM have founded a common marketing company called CECCN (Compagnie Européenne de Combustibles CERCA NUKEM) for a limited period of time. All in all the transfer period has been calculated with approx. two and a half years, starting mid of 1988, ending around December 1990.

More details will be given by the Appendix and within the CERCA-presentation.

The "surviving" parts of NUKEM, which already have had 75 % of the total turn over within the past 3 years, are divisions such as process engineering electronic non-destructive testing equipments, nuclear fuel service,

alternative energy products, environmental protection systems, other equipments and toolings.

For the High Temperature fuel element fabrication NUKEM is still trying hard to find a solution together with other companies interested in this field in order to form a new HTR-fuel company which then allows NUKEM to continue without having the need of any licence for the handling of radioactive material.

Appendix

Article 9 of the CERCA-NUKEM Agreement: Marketing Company

9.1 The Parties agree to establish a Marketing Company to be called Compagnie Européene de Combustible CERCA NUKEM (CECCN), SARL (hereinafter referred to as "the Company").

This Company shall be organized under the laws of France and the form of such Company shall be a Société à responsabilité limitée (SARL). The by-laws of this Company are attached as Appendix F.

Sixty percent (60 %) of the shares of the Company shall be held by CERCA and forty percent (40 %) of the shares by NUKEM. The total share capital of the Company shall be 50.000 FF. The Company shall have its registered place of business in Creteil, France, and the representatives of the Company shall have the use of office space at Hanau made available by NUKEM.

9.2 The business purpose of the Company is restricted to the rights and obligations stipulated under the exclusive Sales Representative Contract to be signed with CERCA, the translation thereof is attached hereto as Appendix G. As provided in the Sales Representative Contract the Company shall have the responsibility for the commercialization of CERCA's activities in the areas of fuel production for MTR and the manufacturing of depleted uranium. In consequence CERCA shall not address and contact any customers without the involvement of the Company except in cases where CERCA can demonstrate that the customer wishes expressively to deal directly with CERCA. The Sales Representative Contract covers all countries except France, provided, however that Institut Max von Laue - Paul-Langevin -, Grenoble, shall be covered by the Contract.

9.3 CERCA and NUKEM shall put at the disposal of the Company the necessary staff to ensure smooth operations according to the needs of the market; in the beginning two professionals and one secretary from NUKEM and one professional plus secretary from CERCA shall be put at the disposal of the Company for full time services. The personnel will remain employees of NUKEM and CERCA respectively.

The Managing Director shall be Mr. Paul Quinton of CERCA, whose services for the Company shall without any charges to the Company.

Mr. Hassel shall be the representative of the office of the Company at Hanau and at the same time the deputy of Mr. Quinton.

RECENT EVOLUTION IN THE MTR FUEL INDUSTRY

Y.FANJAS
C.E.R.C.A.
ROMANS - FRANCE

J.C.MARGUIN
C.E.C.C.N.
CRETEIL - FRANCE

ABSTRACT

The take over of NUKEM MTR fuel activities by CERCA requires the adaptation of the commercial organization and the industrial equipment to the new situation. The creation of a marketing company and the evolution of CERCA MTR workshop are reported.

The paper also gives the latest results of CERCA silicide irradiation program.

INTRODUCTION

The recent events in Germany have significantly modified the landscape of the MTR fuel industry. NUKEM's withdrawal from this field has left several customers with a problem of short term supply.

In order to minimize the inconvenience of such a situation for the customers, we had to manage a quick and efficient transfer of NUKEM's activities. "A quick and efficient transfer" : this was meaning two things :

- To help the customers in making a smooth transition from one supplier to the other.

- To adapt our workshop to take over NUKEM's fabrications within a short period of time.

In view of meeting the above two goals, CERCA and NUKEM have set up an agreement by which :

- A new marketing company was created to help meeting the first goal.

- Complementary equipments, toolings, materials and documents would be transfered from NUKEM to CERCA to help meeting the second goal.

The main purpose of this paper is to keep everybody informed of the agreement signed between the two companies and to explain how CERCA is adapting its production capacity to the new situation.

The second purpose is to give the latest results about the CERCA silicide irradiation program.

After a few words about the agreement itself, we will present :

- The new marketing company,

- The evolution of CERCA MTR workshop.

Finally, we will say a few words about the irradiation of a mixed U3Si/U3Si2 prototype fuel element in the OSIRIS reactor core.

THE CERCA-NUKEM AGREEMENT

Following NUKEM's decision to step out of the MTR fuel business, the two companies NUKEM and CERCA started negotiations which were concluded by the signature of an agreement on the 27th of April.

By this agreement, CERCA takes over NUKEM's basis of business in the fields of MTR fuels and depleted uranium products. As a result, NUKEM will move some equipments and toolings to CERCA. It will also transfer the contracts entered into with customers, provided customers agree with such a transfer. In such cases, uranium, materials, structural parts and documents (specifications,drawings, procedures...) will be delivered to CERCA. This applies to any contract NUKEM cannot achieve within the restricted time available for NUKEM to perform the remaining work under the restricted governmental operating license.

Such a transmission of contracts and the negotiation of future contracts will be greatly facilitated by the creation of the marketing company CECCN which employs the salesmen from NUKEM and CERCA.

NEW MARKETING COMPANY (Slide 1)

NUKEM and CERCA agreed to establish a marketing company to be called COMPAGNIE EUROPEENNE DE COMBUSTIBLES CERCA-NUKEM, in short CECCN. Sixty percent of the shares of the company are held by CERCA and forty percent by NUKEM. The company has its registered place of business in Créteil, France and another place of business in Hanau, Germany. The managing director is Mr QUINTON, president of CERCA.

The company is set up for a period of time of two and a half years, until December 1990.

Scope of activity of the Company

CERCA appoints CECCN as a world wide representative for the MTR fuel elements and civil applications of depleted uranium.

Obligations of the Company

The Company has the responsibility for commercial relations with customers. All inquiries should be addressed to this company which has to prepare and submit the offers. After the negotiations with the customer, the order has to be submitted or sent to CECCN but will be confirmed and signed by CERCA which has to perform the contracted work and to give the necessary garanties.

ADAPTATION OF CERCA MTR WORKSHOP

The quantity of fuel plates to be produced in 1989 corresponds to twice the quantity produced in 1988. The doubling of the production output is not worrying in itself. On the one hand, the CERCA workshop has a large extra capacity and we have already fabricated in the past more than twice the present annual quantity. On the other hand, the flexibility of our people and our equipments is so that the management of great variations in production level can be well kept under control.

However, the simultaneous arrival of many new orders coming from new customers requires to improve further the flexibility. The difficulty arises from the great variety of products resulting from the various enrichments (HEU, MEU, LEU), various compounds (uranium aluminium alloy, aluminide, silicide), various compositions and various plate and components dimensions of products, to be manufactured simultaneously.

We are overcoming such a difficulty by improving the flexibility of our production facility in three fields : the workshop building, the personnel and the equipments.

The MTR workshop building

We are now finishing the modifications of the workshop which are resulting in a 25 % increase in ground area (slide 2).

The extra space is mainly used for increasing our semi-finished and finished products storage capacity and setting up new equipments. The workshop extension work will be completed in October of this year.

Increase in personnel

The doubling of the production output involves a significant increase in personnel, both in offices and on the production line. Such an increase is greatly facilitated by the presence of the FBFC company (PWR fuel manufacturer) on the same site. This related company employs in Romans five time as many people as CERCA. It is thus possible to obtain its help by transfer of qualified personnel accustomed to work in the nuclear fuel industry.

We have already moved most of the necessary additional people from FBFC to CERCA in order to give them the necessary specific training. Several new workers are already operational.

Work in two shifts is already in practice for some operations. It is going to be generalized.

In parallel, we have reinforced our development team by a new R&D engineer.

Equipments

In order to fulfill our task, we need two kinds of additional fabrication and inspection equipments :

- Machines which will increase the flexibility of our workshop by allowing simultaneous production or inspection of different products and avoiding long interruptions due to equipment cleaning or adjusting.

- Machines, and mainly toolings, which are specific to a given type of fuel element or to a given customer.

NUKEM equipments : Most of above two kinds of equipments are existing in NUKEM. The list of those which will be transfered to CERCA is given in Slide 3. The transfer will take place as soon as the necessary permits are obtained from the German authorities.

CERCA equipments : Other equipments which are CERCA designed have already been or will soon be installed in our facility. Among them, we particularly mention two new powder lines : one so-called mini-line and one full size line. The mini-line is already operational. The full size line was designed two years ago by CERCA. The corresponding glove boxes and machines have been ordered. Taking into account the time necessary for delivery, the new line will be fully operational at the beginning of next year. Thus, we will have four powder production units able to produce simultaneously HEU, MEU and LEU aluminides and LEU silicides.

STATUS OF CERCA SILICIDE IRRADIATION PROGRAM (Slide 4)

Since the last RERTR meeting, the main evolution in our silicide program has been the irradiation of mixtures of U3Si2 and U3Si :

- In the OSIRIS reactor one test element loaded to 4.8 g U/cm^3 has been successfully burned to an average 83 % burn-up. The proportion of U3Si in the fuel powder was 30 w.%.
  This result clearly shows that the presence of U3Si even in large amounts is not detrimental to the fuel behaviour even at a very high burn-up level.

- In the HFR reactor another fuel element loaded to 5.5 g U/cm^3 will start irradiation in October of this year. In this element the proportion of U3Si phase is even higher than in the OSIRIS element since it reaches 47 w.% (calculated value).

CONCLUSION

The new situation in the MTR fuel industry was requiring a very quick reaction in order to minimize the consequences for the customer. The actions we have undertaken both from the marketing and from the production points of view show that CERCA is ready to assume its new obligations.

As always in the past, our main concern is to fully satisfy our customers'needs. This new challenge will give CERCA the opportunity to prove its reliability once more.

The recent reinforcement of our research and development team also demonstrates our firm intention to improve further our products and to always be in a position to propose the best adapted fuel to our customers.

CERCA

SLIDE 1

CECCN
A NEW MARKETING COMPANY

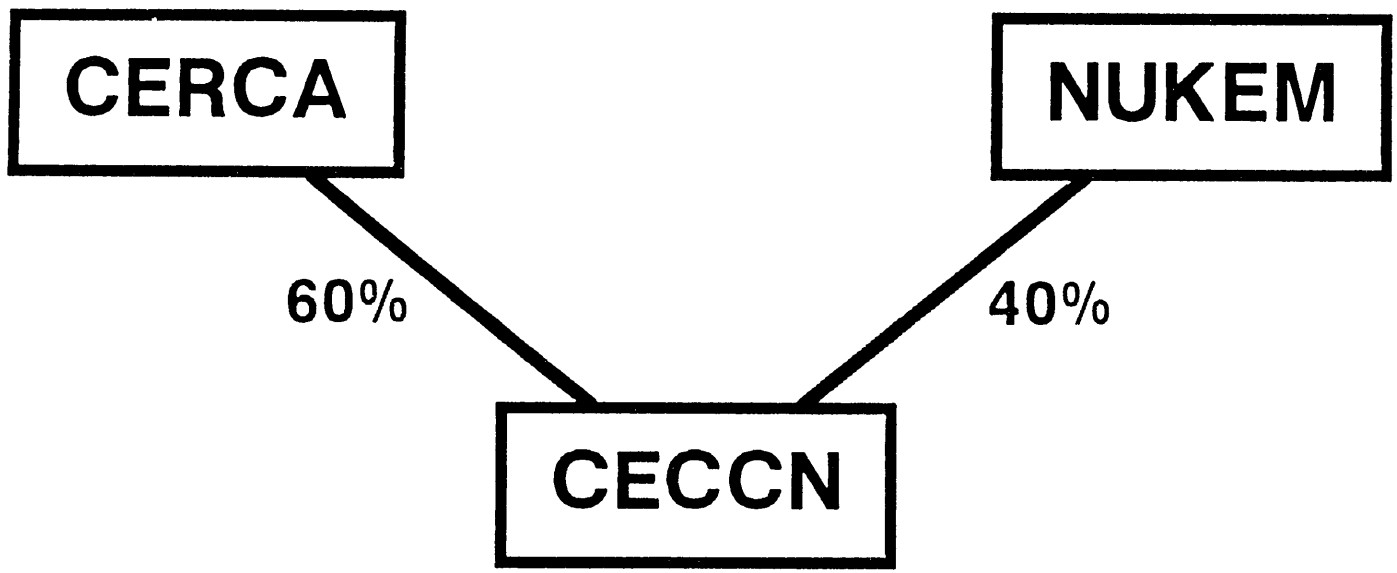

COMPAGNIE EUROPEENNE DE COMBUSTIBLES CERCA-NUKEM

Head-Office : CRETEIL, FRANCE
German-Office : HANAU, GERMANY

CERCA
SLIDE 2

MTR WORKSHOP BUILDING

A 25% INCREASE IN GROUND SPACE

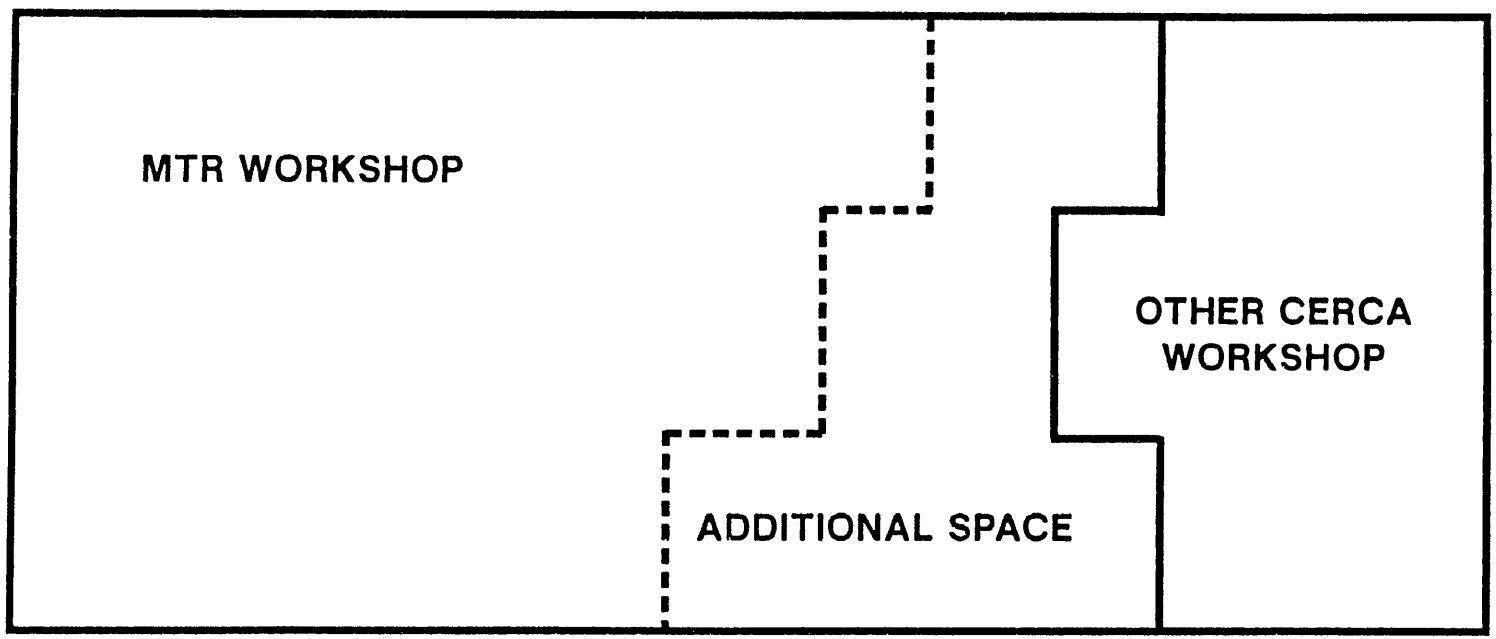

CERCA

SLIDE 3

MAIN EQUIPMENTS TO BE TRANSFERED FROM NUKEM TO CERCA

MACHINES :

MELTING FURNACE
FUEL CORES PRESSING MACHINE
ROLLING MILL
ELECTRON BEAM WELDING MACHINES

GAMMA COUNTING MACHINE
ULTRASONIC TESTING MACHINE
X-RAY HOMOGENEITY SCANNING MACHINE
WATER CHANNELS INSPECTION MACHINE
SEMI AUTOMATIC CLADDING MEASURING DEVICE

TOOLINGS :

TOOLINGS ADAPTED TO TRANSFERED EQUIPMENTS
TOOLINGS SPECIFIC TO PARTICULAR FUEL ELEMENTS

CERCA
SLIDE 4

CERCA U_3Si_2 and U_3Si IRRADIATION PROGRAM STATUS - ENRICHMENT 20%

SEPT. 88

FUEL	REACTOR	URANIUM DENSITY (g/cm^3)	NUMBER OF Elt	IRRADIATION		AVERAGE BURN-UP (%)
				START	END	
U_3Si_2	ORR	4.8	1 Element 1 Element	Apr. 83 Apr. 83	Oct. 83 Aug. 84	56 (54)* 82
	SILOE	2.0 3.7 5.2 5.4	1 Plate 1 Plate 1 Plate 1 Plate	Jul. 84	Jan. 86	78 76 75 75
	SILOE	5.2	1 Element	Feb. 86		54
	R2	4.8	1 Element	Nov. 86		28
	ORR	4.8	20 Elements	Jan. 86	Mar. 87	Up to 52
	HFR Petten	4.8	1 Element	Oct. 88		
U_3Six	OSIRIS	4.7	1 Element	Nov. 86	Jun. 88	83
	HFR Petten	5.5	1 Element	Oct. 88		
U_3Si	SILOE	5.5 6.0	2 Plates 2 Plates	Jun. 82 Jun. 82	Nov. 83 Nov. 83	56 (53)* 58 (54)*
	SILOE	6.0	1 Element	Sept. 84	Oct. 85	55

* NUMBER BETWEEN ( ) : MEASURED VALUE

SESSION III

September 19, 1988

FUEL DEVELOPMENT

Chairmen:

G. Thamm
(KFA, Federal Republic of Germany)

K. Saltvedt
(Studsvik Nuclear, Sweden)

FABRICATION OF HIGH-DENSITY FUEL PLATES BY HOT ISOSTATIC PRESSING

T. C. Wiencek, R. F. Domagala and H. R. Thresh
Fabrication Technology Section
Materials and Components Technology Division
Argonne National Laboratory
Argonne, Illinois U.S.A.

ABSTRACT

The loading limits of U_3Si AND U_3Si_2 dispersion fuel plates fabricated by conventional techniques have been reached. Fuel densities of up to 7.0 gU/cm^3 have been successfully produced. These loadings are sufficient for the needs of most research reactors, but a few reactors require higher fuel densities. Two concepts are presented which may lead to loadings beyond 7.0 gU/cm^3: a wire concept in which 0.030 in. (0.76 mm) uranium silicide wire is bonded within an aluminum plate and a dispersion concept in which a highly loaded (>50 volume percent fuel), uniformly clad fuel plate is produced. In both concepts hot isostatic pressing is a key processing technique.

INTRODUCTION

The loading limits of conventional fabrication techniques have been reached for U_3Si and U_3Si_2 powder metallurgy fuel plates. On a laboratory scale, fuel densities of up to 7.0 gU/cm^3 have been successfully produced. However, a few reactors require higher fuel densities. As a point of reference, for reactors loaded with HEU (93% enriched) UAl_x with a fuel density of 1.7 gU/cm^3 and a fuel zone thickness of 0.020 in. (0.51 mm), the equivalent loading for LEU (20% enriched) fuel would be as follows:

Ratio of Enrichment x Original Loading x Reactivity Factor

$$(93/20) \times 1.7 \times 1.15 = 9.1\ gU/cm^3$$

In terms of quality and fabricability, this is well beyond the loading range possible for conventionally produced powder metallurgy core fuel plates, irrespective of the fuel alloy chosen.

Other innovative techniques were examined to meet the low-enrichment needs of these high-performance reactors. Two concepts have been proposed to address this issue. The first effort involves the generation of wires of U_3Si and/or $U_{75}Ga_{10}Si_{15}$. These wires would be used as filaments bonded into Al in such a geometry as to generate plates with loadings approaching 9.0 gU/cm^3 in the fuel zone. The second effort involves a dispersion concept in which a highly loaded (>50 volume percent U_3Si_2), uniformly clad fuel plate is produced with areal loadings equivalent to 9.0 gU/cm^3.

The most common problem with highly loaded fuel plates is the limited ability of the material system to respond uniformly to the rolling process. The major cause of this is the difference in the hardness of the fuel and the matrix. The fuel particles are very hard and resist deformation; the matrix is soft and flows very easily. When the volume fraction of the harder fuel phase reaches about 40-50%, the classic "dog-bone" effect is seen. This is a thickening of the ends of the fuel zone such that when viewed in longitudinal cross section, the fuel zone resembles a dog-bone. The ends of the fuel zone are where the greatest discontinuities occur. In these regions the aluminum clad is forced over the fuel zone without reducing the fuel zone thickness. In the center of the fuel zone during the rolling process, the constraint, and therefore the deformation, is uniform. Dog-boning is minimal in shaped (tapered) compacts containing up to about 55 volume percent fuel. At higher fuel percentages, the differences in hardness between fuel zone and cladding are so great that the fuel appears as a series of dog-bones, with alternating thick and thin areas throughout the whole zone. Because of minimum clad thickness requirements and limits on the uniformity of uranium loading, plates with a fuel zone of this shape are not acceptable.

The root of this problem is the rolling process, which is a line contact deformation system. Dog-boning occurs because the fuel zone is constrained from lateral motion but can move in the rolling direction, which is the least restrained direction. This flow is probably greatest during the early rolling passes when the fuel zone is the least constrained by the thickness and geometry. At later passes there is more resistance and probably less dog-boning. If a uniform pressure could be applied to the fuel plate to deform it, this problem would be minimized and perhaps eliminated.

PROCESS

The process we chose to apply to this problem is hot isostatic pressing (HIPping). Over the last fifteen years, this process equipment has become more readily available and HIPping has gone from being a specialized laboratory technique to a commercially used process. In this fabrication method, the workpiece is hermetically sealed in a deformation container, placed in a high-pressure environment [approximately 30 ksi (207 MPa)] and heated to an appropriate temperature in the range of 200-1500°C. The combination of heat and pressure densifies, sinters and bonds the workpiece. A schematic representation of a HIP unit is shown in Figure 1.

All of the HIP experiments to date have been conducted on a Conaway unit manufactured in ~1980. The HIP chamber is approximately 4.5 in. (11.4 cm) in diameter and 6 in. (15.2 cm) high. A molybdenum heater permits heating to as high as 1500°C. Since all our work has been and will be with Al and Al alloy clad, we plan never to exceed ~500°C.

The potential advantages of a HIPped fuel plate are uniform clad and fuel zone thickness as well as control of the fabrication atmosphere, temperature and pressure. With the appropriate HIP, plates can be batch processed. However, a complete installation capable of batch processing full-size plates could easily cost over a half million dollars (U.S.A.).

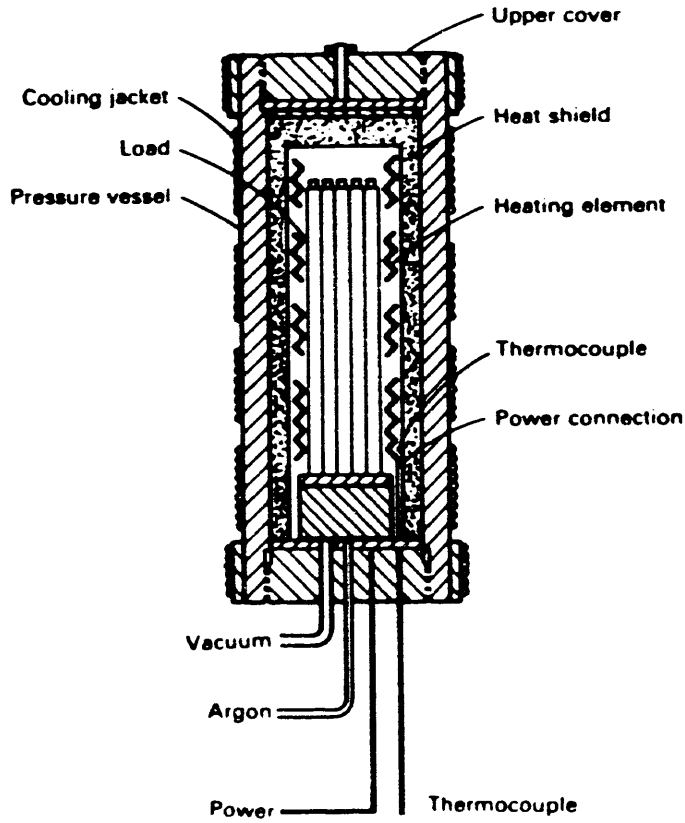

Fig. 1. Schematic Representation of HIP Unit.

CONCEPTS

Wire Concept

Figure 2 shows a schematic cross section of a "wire-concept" fuel plate. This design can be fabricated with a solid cover plate and a base plate in which cavities are machined to accept the fuel wires. Alternatively, top and bottom cover plates can be machined with grooves to accept one-half the wire diameter and the cover plates placed together to totally surround the wire. If such a configuration with U_3Si or $U_{75}Ga_{10}Si_{15}$ wires of 0.030 in. (0.76 mm) diameter, can be successfully bonded, the uranium density in the fuel zone will be 8.6 g/cm^3.

The wire concept provides a system (plate) with the following advantages:

- The mechanical constraint on the fuel will be much greater than in a conventional dispersed-phase plate configuration.

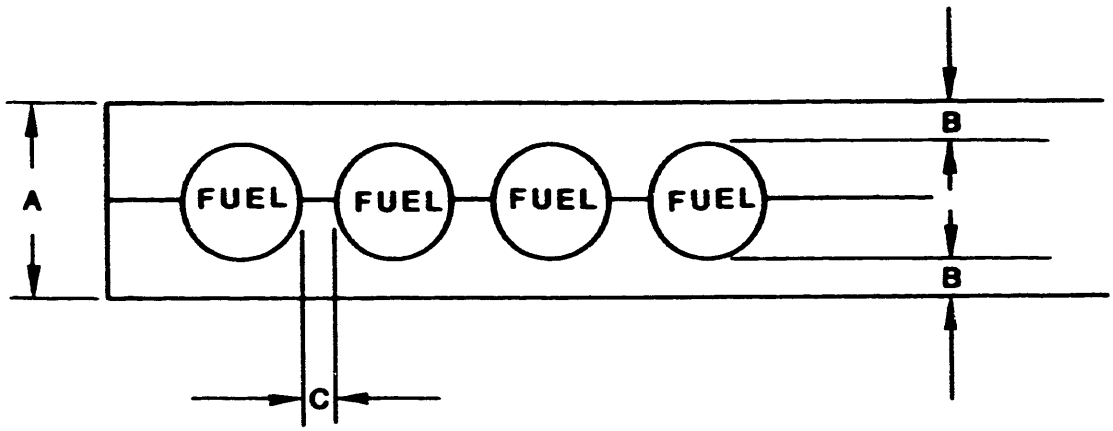

Fuel: U_3Si or $U_{75}Ga_{10}Si_{15}$; 0.030 in. (0.76 mm) Diameter
U Loading: 8.6 g/cm^3
A:0.050 in. (1.27 mm) B:0.010 in.(0.25 mm) C:0.010 in. (0.25 mm)

Fig. 2. Cross Section of "Wire Concept" Fuel Plate

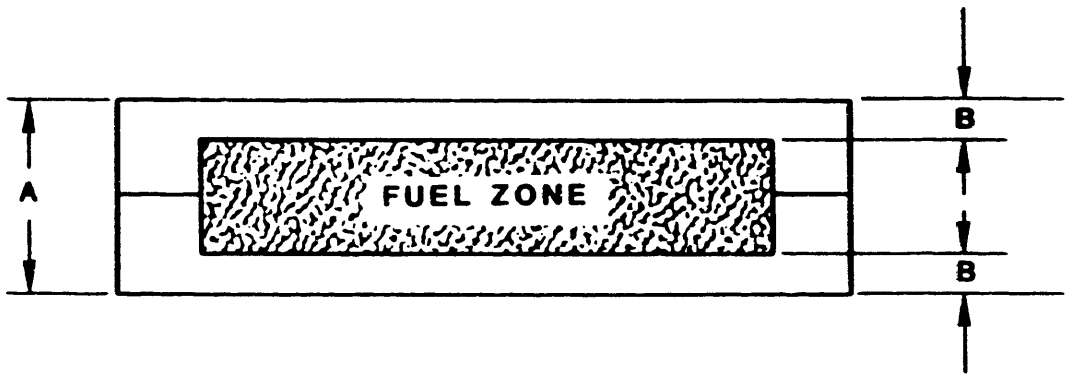

Fuel: U_3Si_2, 55 vol.%, <1% Porosity
U Loading: 6.2 g/cm^3
A:0.050 in. (1.27 mm) B:0.010 in. (0 25 mm)

Fig. 3. Cross Section of "Dispersion Concept" Fuel Plate

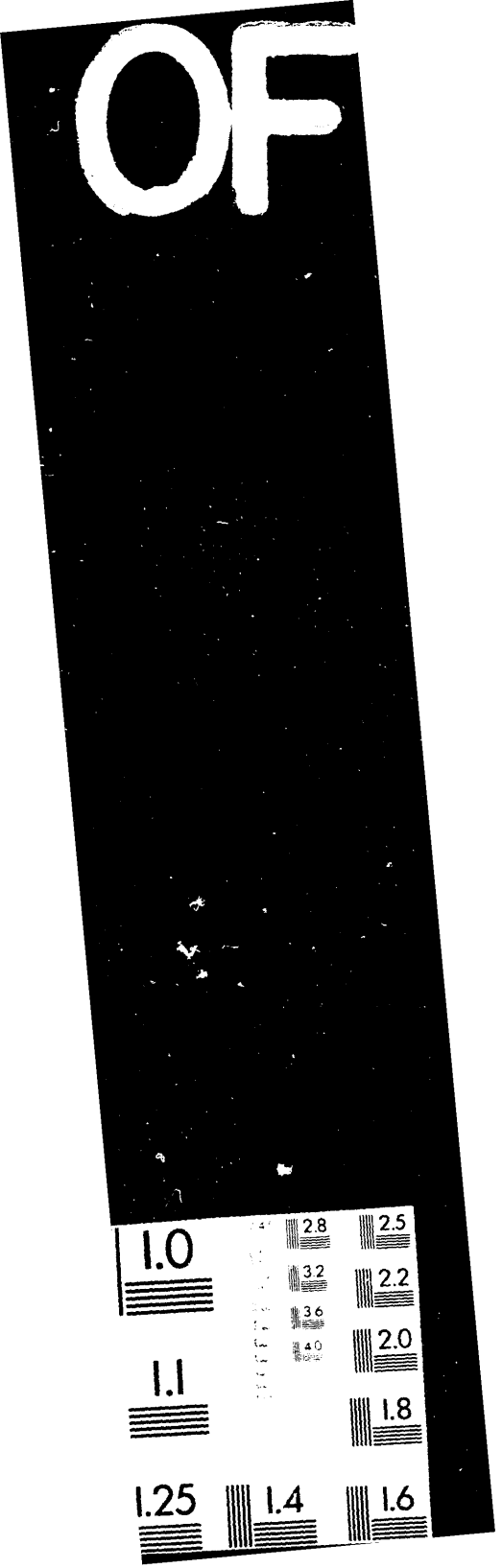
OF
1.0
1.1
1.25
1.4
1.6
1.8
2.0
2.2
2.5
2.8
3.2
3.6
4.0

- The fuel phase has relatively little surface area, compared with a dispersed phase, to react with the Al matrix.
- Precise positioning of fuel is possible.
- Shaped fuel distributions may be achieved.

The two major challenges in producing such fuel plates are to produce U_3Si and $U_{75}Ga_{10}Si_{15}$ wires of the indicated diameter and to HIP-bond them to a suitable aluminum alloy such as 6061. (HIP bonding of aluminum alloys is not a trivial task.)

The fuels chosen for experimental work were U_3Si with a density of 15.2 g/cm^3 and a composition of 96 wt.% U and $U_{75}Ga_{10}Si_{15}$ with a density of 15.6 g/cm^3 and a composition of 94.1 wt.% U. U_3Si has been chosen as one candidate for the wire concept because so much is known about its irradiation behavior as well as the chemical, physical, and mechanical properties of this phase. U_3Si in an Al matrix is known to be relatively stable under irradiation up to at least 50% burnup. No irradiation data for $U_{75}Ga_{10}Si_{15}$ are available; it was chosen because it represents a simple modification of U_3Si and, most important, can be cold rolled at least 40% at room temperature. With successive rolling and 800°C annealing steps, it is presumed that wire of the required dimensions can be fabricated. Both compositions require a prolonged heat treatment (72 h, 800°C) to form the intermetallic compounds by a peritectoid reaction.

Dispersion Concept

A cross section of the HIPped "dispersion-concept" fuel plate is shown schematically in Figure 3. For this concept, the fuel of choice is U_3Si_2. The strategy underlying the dispersion concept is simply to increase the thickness of the fuel zone to 0.030 in. (0.76 mm); with 55 vol.% U_3Si_2, this thickness would provide an equivalent areal loading of 9.3 gU/cm^3. Since the total plate thickness cannot exceed 0.050 in. (1.27 mm), a clad thickness of 0.010 ± 0.002 in. (0.25 ± 0.051 mm) will be required. By its nature, the HIP process may be expected to produce a plate with final dimensions that are very nearly those of the assembled components before HIPping, so a uniform clad thickness can reasonably be expected. In contrast, such a uniformity is never guaranteed in a rolled plate. The two major challenges in the dispersion concept are, then, to produce thin powder metallurgy compacts of U_3Si_2 + Al with uniform thickness and acceptable homogeneity and to HIP bond them within a suitable Al alloy clad.

RESULTS AND DISCUSSION

Work on the concepts described above is in its early stages. Trial runs were made with an argon atmosphere and pieces of solid 6061 Al alloy to demonstrate that the newly installed HIP unit was functioning properly. After this, several archive Argonne miniplates and compatibility study plates, originally fabricated by standard rolling procedures, were HIPped. The object was to determine whether the porosity in the fuel zone could be reduced by the process. Several plates were treated and porosity values of

much less than 2% were calculated from immersion density measurements.

Several attempts to HIP-bond 6061 to itself were only moderately successful; bonding was inadequate. However, instead of devoting time and effort to developing the proper surface preparation parameters and operating temperatures and pressures, we chose at this time to use 1100 Al (99.00 min. Al) for further HIP experiments. Pieces of 1.5 in. (38.1 mm) diameter 1100 Al rod were HIPped end-to-end and tensile bars were machined from the product. Three such bars were produced, machined, and tested to failure. Values for ultimate tensile strength and percent elongation measured for the HIP-bonded specimens were within the normal scatter band for solid wrought pieces of 1100 Al in the 0-temper (soft) condition. Metallographic examinations of the zone of the original interface showed some recrystallization across the interface and what appeared to be a sound metallurgical bond.

Wire Concept

Generating 0.030 in. (0.76 mm) wire of the aforementioned U-base alloys for the wire-concept plates is currently being addressed. "Bare" $U_{75}Ga_{10}Si_{15}$ round/oval rods ~0.4 in. (~10 mm) in diameter have been rolled at several temperatures. As stated earlier, we have already demonstrated that stock of this alloy can be reduced in thickness by up to ~40% by flat rolling at room temperature. With intermediate anneals of 1 h at 800°C, we have successfully produced sheet of this alloy as thin as 0.016 in. (0.4 mm). This thickness is obviously less than the 0.76-mm target diameter. Flat rolling produces sheet from which wires with a square cross section can, of course, be cut. However, wire with a circular cross-section would presumably be better constrained from swelling during irradiation because of the hoop stresses in the surrounding clad. Square cross section wire could be reshaped into a round with appropriate additional processing steps.

To obviate the necessity for intermediate anneals, hot-rolling experiments at 400° and 800°C were conducted with the U-Ga-Si alloy. For the 400°C experiments, an oil bath served to both heat the alloy and partially protect the surface from contact with air (oxygen). However, the amount of reduction in thickness before cracking occurred was the same as for rolling at room temperature. Therefore, use of an oil bath appears to provide no advantage.

For rolling at 800°C, a salt bath was used. The salt, a mixture of 65 wt.% KCO_3, 10 wt.% $NaCO_3$ and 25 wt.% $LiCO_3$, is used commercially for hot rolling of U metal. No improvement in the rolling characteristics was observed and severe corrosive attack of the alloy by the carbonate salt occurred. It has been concluded that cold rolling at room temperature with intermediate anneals is the most expeditious procedure for fabricating $U_{75}Ga_{10}Si_{15}$ wire; no further hot rolling experiments with this alloy are contemplated.

The currently planned procedure is rod rolling followed by swaging to convert the round/oval ingot bars into wire of the desired diameter. All operations will be conducted at room temperature, with intermediate 800°C anneals at approximately every 30 to 35% reduction in cross-sectional area.

Efforts to produce U_3Si wire have just been initiated. Our previous experience has shown that it is not possible to accommodate more than one or two percent reduction of U_3Si at room temperature, so all working processes are planned for temperatures above room temperature. No increase in workability of U_3Si has been observed up to ~600°C. At 600°C and above, where the carbonate salt bath was used, severe corrosive attack of U_3Si by the salt outweighed any improvement in ductility.

The plan for further deformation experiments with U_3Si involves "canning" cast and heat-treated rods in an appropriate material (304 stainless steel, for example); working the canned assembly at, say, 800°C, and then stripping away the protective layer.

Dispersion Concept

The dispersion concept requires a thin compact. To test the feasibility of this approach, a compact of 55 vol.% W and balance Al and void was inserted into a cavity machined into a piece of 0.080 in. (2.03 mm) thick 1100 Al plate. A flat 1100 Al plate of the same dimensions was used as a cover and the assembly was TIG-welded peripherally; Cu chills and clamps were used to minimize heating of the internal mating surfaces of the compact and clad. The 1100 Al pieces were chemically cleaned in an Oakite-160 solution, following practices identical to those employed for cleaning Al hardware for conventional rolling of fuel plates. This assembly was HIP-bonded at 500°C and ~11,000 psi (~76 MPa) for two hours. The chamber was not pressurized until the internal thermocouple indicated 500°C. The product appeared to be well bonded. Immersion density measurements were conducted, and calculations based on the data indicated 7.6% voids in the fuel zone. A full transverse section of this plate was cut and the sample mounted and polished for metallographic study. The clad thicknesses on either side of the fuel zone were remarkably uniform. The bond at the 1100 Al interface appeared to be sound.

Additional experiments with W+Al compacts HIP bonded into Al alloy frame and cover assemblies are planned. When procedural parameters are established, depleted-uranium U_3Si_2 + Al powder compacts will be prepared and HIPped.

SUMMARY AND CONCLUSIONS

New concepts and fabrication procedures are being addressed for fabricating plate-type fuel elements with U densities approaching 9.0 g/cm^3, or increasing the fuel zone thickness of a 0.050 in. (1.27 mm) thick plate to a point where the equivalent loading can be achieved. Hot isostatic pressing is the procedure of choice at present. Concepts involving the utilization of U_3Si or $U_{75}Ga_{10}Si_{15}$ wire and the direct HIPping of high-U-density compacts in a near-net-shape geometry are being investigated.

Some Recent Observations on the Radiation Behavior of Uranium Silicide Dispersion Fuel

by
Gerard L. Hofman

Abstract

Addition of B_4C burnable poison results in higher plate swelling in both U_3Si_2 and U_3Si-Al dispersion fuel plates and also decreases the blister threshold temperature of these plates. Prolonged annealing of U_3Si_2-Al fuel plates produced no blister after 696 hours at 400°C. Blister formation started between 257 hours and 327 hours at 425°C and between 115 hours and 210 hours at 450°C.

Operation with breached cladding resulted in pillowing of an U_3Si-Al fuel plate due to reaction of the fuel core with coolant water.

I. Introduction

The miniplate irradiation program carried out in the Oak Ridge Research Reactor (ORR) has come to an end. Postirradiation analysis of the last batch of miniplates, as well as re-evaluation of previously reported results is in progress and will be reported in the next RERTR meeting.

This paper deals with some selected recent observations, the timely reporting of which may be important to the RERTR community. Specifically, we will discuss the effect of burnable poison (B_4C) on the irradiation behavior of silicide dispersion fuel, the nature of blister formation during extended postirradiation annealing, and the behavior of a U_3Si fuel plate that operated with breached cladding.

II. Effect of B_4C

Some reactor core designs require the addition of burnable poison in their fuel elements. The most convenient way of incorporating a burnable poison such as ^{10}B is by mixing an appropriate amount of powdered B_4C with the fuel powder. In order to assess the possible effects of such a mixture on the irradiation behavior of silicide dispersion fuel, several U_3Si_2 and U_3Si miniplates containing typical amount of B_4C were fabricated. After irradiation in the ORR to approximately 80% ^{235}U burnup, postirradiation analysis was performed. The results were compared to postirradition data from previously irradiated sibling miniplates that contained no B_4C.

The difference in irradiation behavior between fuel plates with and without B_4C is appreciable. As shown in Table I, the B_4C-containing plates had an average thickness increase of 0.15 mm vs. 0.05 mm for plates without B_4C at approximately the same ^{235}U burnup. Likewise the average meat swelling was 8.6 vs. 2.4%. Metallographic examination reveals the reason for the larger swelling of the B_4C-containing plates. Comparison of polished cross section, (Figs. 1 and 2) clearly show a much larger fraction of retained as-fabricated porosity in the B_4C-containing plates, as well as many clusters of large pores in the fuel particles. The retained as-fabricated porosity was measured with an image analyzer and found to have decreased during irradiation from 10% to 4.5% for the B_4C-containing plates and from 10% to less than 1% for the sibling plates without B_4C (see Table I). Calculating the amount of fuel particle swelling ΔV^F, with the following formula:

$$\Delta V^F = \frac{\Delta V^m + (V_o^P - V^P)}{V_o^F}$$

one obtains, respectively, 31% and 25%. The difference in fuel swelling is presumably due to the presence of pore clusters in the fuel particles of B_4C-containing plates.

In order to further investigate this apparent effect of B_4C on swelling, selected samples were examined with a scanning electron microscope (SEM) including energy dispersive x-ray analysis, and with a scanning Auger electron microprobe (SAM).

Figure 3 shows the distribution of B_4C particles (dark angular features) in an unirradiated fuel plate. The B_4C particles are clearly identified by the boron Auger-electron dot-map shown in Fig. 3.

The meat microstructure after irradiation is also shown in Fig. 3. Again clearly identified by SAM are the B_4C particles, which now appear less angular in shape presumably as a result of irradiation damage. Bigger B_4C particles are found at residual as-fabricated porosity suggesting that the presence of B_4C prevents closure of the pores. Detailed SAM analysis did not detect boron, carbon, or the reaction product lithium in the residual pores. The only other element involved is helium produced through α generation by the reaction:

$$^{10}B\ (n, \alpha)^{7}Li$$

The amount of helium generated in a particle of the size shown in Fig. 3 at complete burnup of the ^{10}B isotope is approximately 7×10^{-10} moles. If all this helium is released into the pore shown in Fig. 1, a pressure of approximately 800 psi could be generated at 100°C. Such a high pressure would certainly prevent closure of the pore, but a lower pressure due to only fractional helium release from the B_4C particle might well be sufficient to prevent pore closure. Without further analyses it seems nevertheless plausible at this point to conclude that helium release is responsible for the observed retention of as-fabricated porosity.

Next we examined the clusters of large pores in the fuel particles that account for the larger fuel particle swelling in the B_4C-containing plates. Optical metallography of etched meat microstructure and a SAM micrograph shown in Fig. 4 reveal a different fuel microstructure around the clusters. The appearance of this etched fuel microstructure is similar to that of fuel that has reacted with aluminum; however, SEM analysis found no difference in composition between the

phase around the pores and the bulk of the fuel. SAM analysis again showed no evidence of boron or carbon but a faint indication of lithium was detected.

High magnification SEM examination of the fuel, also shown in Fig. 4 shows the typical small,-regular-spaced fission gas bubbles in the bulk U_3Si_2, but absence of these small bubbles in the different structure around the large pore clusters. Apparently fission gas diffusivity in the cluster area was much higher leading to the growth of large bubbles. We can only speculate that a small amount of lithium and possibly also helium diffused from B_4C particles into adjacent fuel causing a increase to fission gas diffusivity. We believe that there is enough circumstantial evidence to state that activation products from the B_4C particles are the root-cause of the higher swelling of B_4C-containing fuel plates. The effect of B_4C on U_3Si plates was similar to that in U_3Si_2 plates.

III. Blister Formation During Postirradiation Annealing

Blister annealing tests are routinely performed on experimental fuel plates as part of the postirradiation analysis. These tests consist of 1/2 hour annealing steps of 50°C starting at 350°C until blisters are observed. The temperature at which blisters are first formed is called the blister threshold temperature and is a figure of merit to assess the high temperature stability of fuel plates.

To better characterize blister formation long time anneals are performed to study the time-temperature relation of blister formation as well as the behavior of blisters after continued annealing.

The test results are shown in Table II for LEU U_3Si_2 plates with high loading (5.2-5.6 g cm^{-3}) after approximately 85% ^{235}U burnup. The normal blister threshold temperature for this type of plate is 525°C for the standard 1/2 hour anneal. The data in Table II shows that the plates are very stable at 400°C, for no blisters formed after a total time of 696 hours at temperature. The time to form blisters decreases to 327 hours at 425°C and 210 hours at 450°C. No measurable change in plate thickness occurred prior to blister formation at any temperature.

An example of blister formation is shown in Fig. 5. Blisters form typically first at the edges of the fuel core an then at locations throughout the fuel plate. These locations coincide with oxide inclusions at the fuel core-cladding interface (see Fig. 6). Inclusions are usually larger and more numerous at the core edges, hence, the predominant formation of blisters in these areas. During continued annealing blisters, particularly those at the ends of the fuel core grow in size and evenually rupture, as shown in metallographic cross-section in Fig. 7. Fig. 7 also shows the correlation of a large amount of oxide inclusions and large blister formation. Apparently for a blister to continue to grow and rupture, a large amount of oxide needs to be present. This oxide evidently reacts with aluminum and fuel. Fission gas released as a result of this reaction pressurized the blister, eventually rupturing the cladding.

Plates containing B_4C (see previous section) were also subjected to the blister test and were found to have a 100°C lower threshold than plates without B_4C. The blisters in these plates were also more numerous after prolonged annealing (see Fig. 8). A cross-section though some blisters, also shown in Fig. 8, reveals that the blisters form at the fuel core-cladding interface. Oxide inclusions are the most likely initiation sites; however, it seems plausible that helium originating from the n-α reaction in the B_4C particles diffused to these sites and pressurized the blisters, thereby promoting their growth.

IV. Operation with Breached Cladding

Coolant channel width between miniplates is routinely measured during scheduled shutdowns in the ORR irradiation program. During one of these measurements a significant decrease in channel width was observed in two adjacent channels in irradiation module 34. The change was not large enough to require removal of the module and the irradiation was continued. After an additional reactor run, the same channels were found to have changed drastically and the module was removed for examination. Photography of the module using backlighting through the coolant channels showed one severely pillowed plate, see Fig. 9. The plate in question was an LEU U_3Si plate with a loading of 6.1 g cm^{-3} that had accummulated a ^{235}U burnup of 55%. Visual examination of this plate after removal

from the module revealed a transverse crack at one end of the pillow near the end of the fuel core. Also, the channel width probe had gouged the cladding on the pillow, as shown in Fig. 9.

A metallographic section was taken at the end of the pillow transecting the crack as shown in Fig. 10. The crack is located at the "dog bone" end of the fuel core where the cladding is rather thin. There is a large amount of two phase reaction product in the area and this reaction product contains large fission gas bubbles. The cladding breached probably early on during the irradiation in a very thin spot over the dog bone end. Ingress of water during continued irradiation resulted in the reaction (most likely oxidation) of the silicide - Al dispersion. Fission gas bubbles evidently grow easily in the reaction product, although hydrogen originating from the decomposition of H_2O may also have contributed to bubble growth. The reaction product, including its gas bubbles, appears similar to the fuel core phases found in high burnup - highly loaded U_3O_8-Al fuel plates where the U_3O_8 has completely reacted with the aluminum matrix.[1] It is of interest to note that predefected fuel plates when soaked in hot water for prolonged periods [2] do not show the formation of interaction product and do not swell; evidenty radiation is necessary for the reaction to occur. No unusual fission gas activity was detected during the irradation and release of fission gas through the crack, which must have occurred to some extent, was evidently of such a low rate that the ORR instrumentation could not measure it.

German investigators have reported on operation with a failed U_3Si_2 miniplate [3]. The cladding of this plate had cracked at a thermocouple attachment point and also had also developed a pillow at the crack site.

It is interesting to note that experimental UAl_x-Al dispersion miniplates irradiated in the Advanced Fast Reactor, ATR, with cladding corrosion defects also developed pillows [4].

References

1. G. L. Hofman et al., Nucl. Technol. Vol. 72, Mar. 1986, pp. 330-344.
2. R. F. Domagala, Argonne National Laboratory, Private Communication.
3. C. Thamm, KFA, Jülich personal communication, and W. Krug etc., this meeting.
4. J. M. Beeston et al., Idaho National Engineering Laboratory, EGG-SE-6696, Oct. 1984.

TABLE I. Comparison of LEU, U_3Si_2 Miniplates With and Without B_4C

	With B_4C	Without B_4C
^{235}U Loading, g cm^{-3}	5.1	5.1
Δt, in. (mm)	0.005 (0.15)	0.0021 (0.05)
ΔV^m, %	8.6	2.4
ΔV^F, %	31	25
V_o^F, %	46	46
V_o^P, %	10	10
V^P, %	4.5	1.0
FD^m, 10^{21}	1.9	2.2
Bu, %	79	84
Blister Temp, °C	425	525

---

where:

Δt is plate thickness increase, including oxide layer.

ΔV^m is meat volume change $\frac{V^m - V_o^m}{V_o^m}$

ΔV^F is fuel particle volume change.

V_o^F is the original fuel volume fraction in meat.

V_o^P is the original as-fabricated porosity in meat.

V^P is the fraction of as-fabricated porosity remaining after irradiation.

FD is the accumulated fission density.

TABLE II. Postirradition Annealing Data of U_3Si_2 Miniplates

Plate A-99, 5.2 g cm^{-3}, 79% Bu, 400°C

time, hours	Thickness, mils Grid Point* 5	6	7	Comments
0	62.0	61.5	61.4	
6	62.0	61.5	61.4	
47	62.0	61.3	61.3	
117	62.0	61.3	61.3	
313	62.5	61.3	61.3	
531	61.8	61.3	61.3	
696	--	61.2	61.4	No Blisters

Plate A-91, 5.6 g cm^{-3}, 84% Bu, 425°C

0				
257	50.0	50.3	50.2	
327	50.6	50.2	50.0	One Blister
423	50.0	61.0	50.2	3 Blisters Warping
517	58.0	61.0	50.2	7 Blisters Warping

Plate A-85, 5.0 g cm^{-3}, 84% Bu, 450°C

0	51.0	51.0	51.4	
20	51.0	51.0	51.4	
115	51.8	51.2	51.5	
210	53.0	53.1	53.0	Blister in Center
278	54.1	55.0	54.8	U + Warping
490	73.0	68.0	60.7	Many Small Blisters and Warping

*These points are spaced on the longitudinal center line of the plates.

Fig. 1. Microstructure of Plate A-199P, U_3Si_2 & B_4C, Showing Retained As-Fabricated Porosity and Bubble Clusters in Fuel After Irradiation

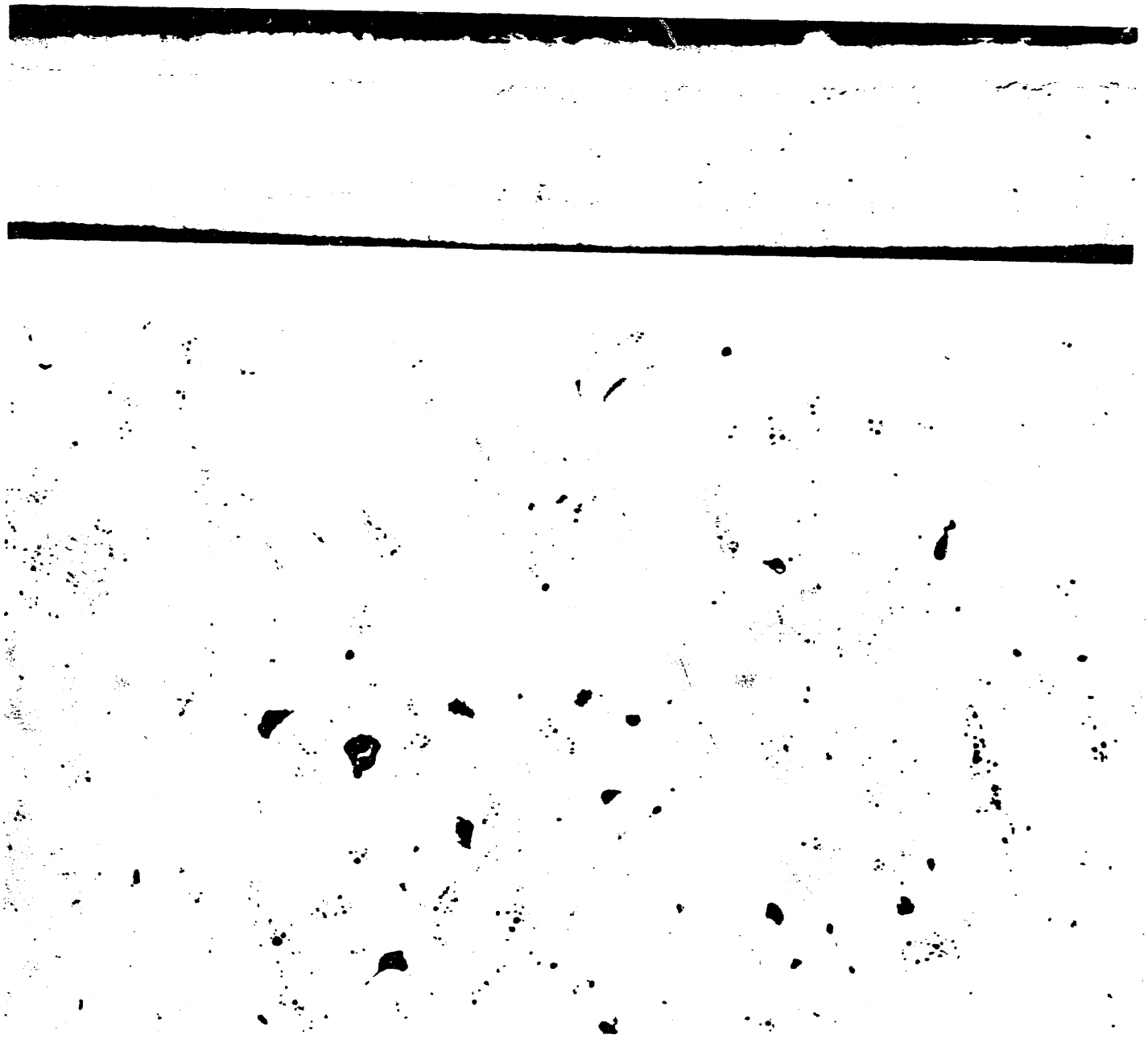

Fig. 2. Microstructure of Plate A, U_3Si_2 Without B_4C, Showing Nearly Complete Closure of As-Fabricated Porosity and Absence of Bubble Clusters

(210716) SAM, Specimen Current

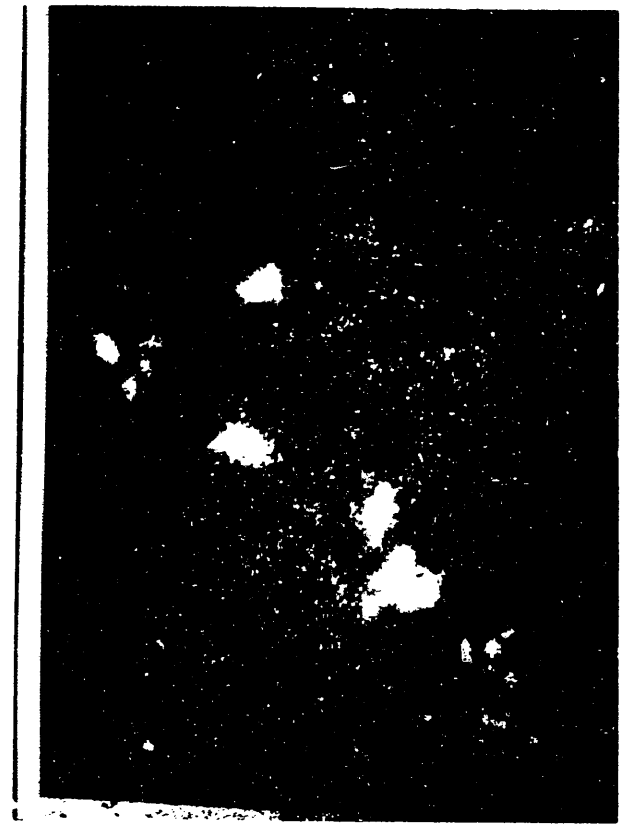

(210717) SAM, Boron

SEM

(210739) SAM, Boron, Detail

Fig. 3. Fuel Core Microstructure Showing B_4C Particles,

Upper: Unirradiated; Lower: Irradiated

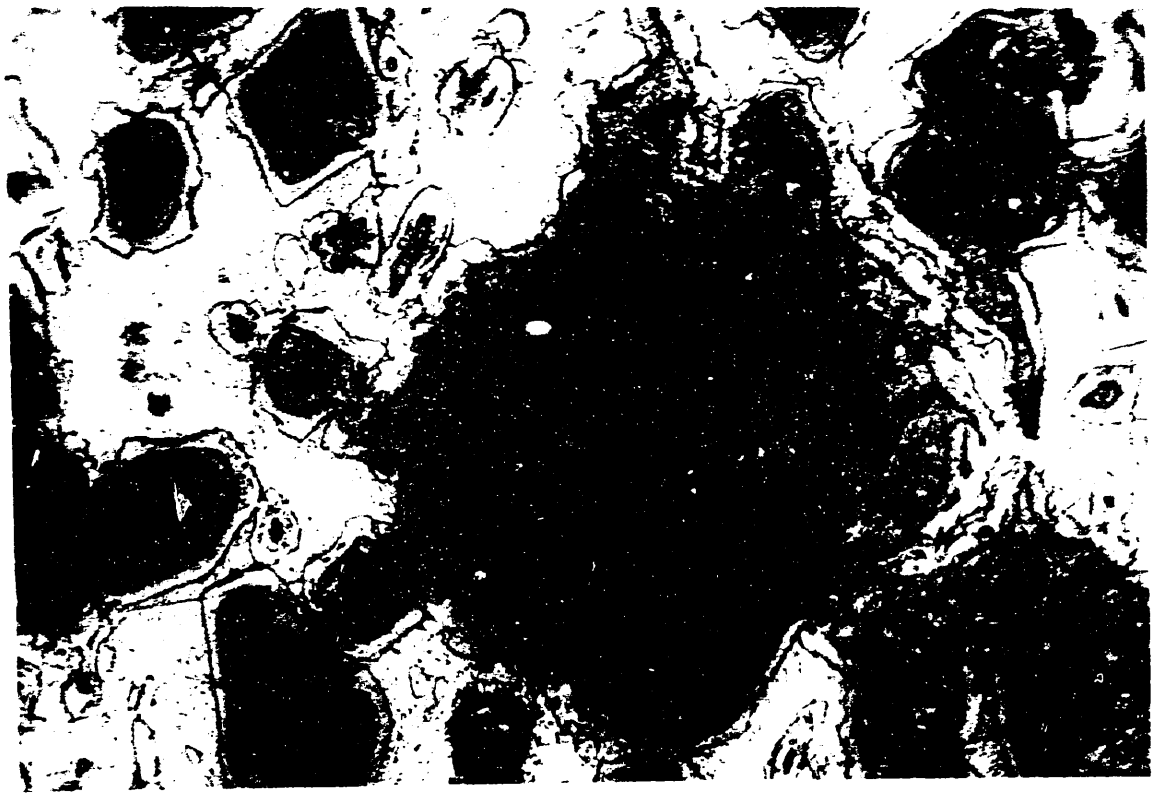

Optical Etched

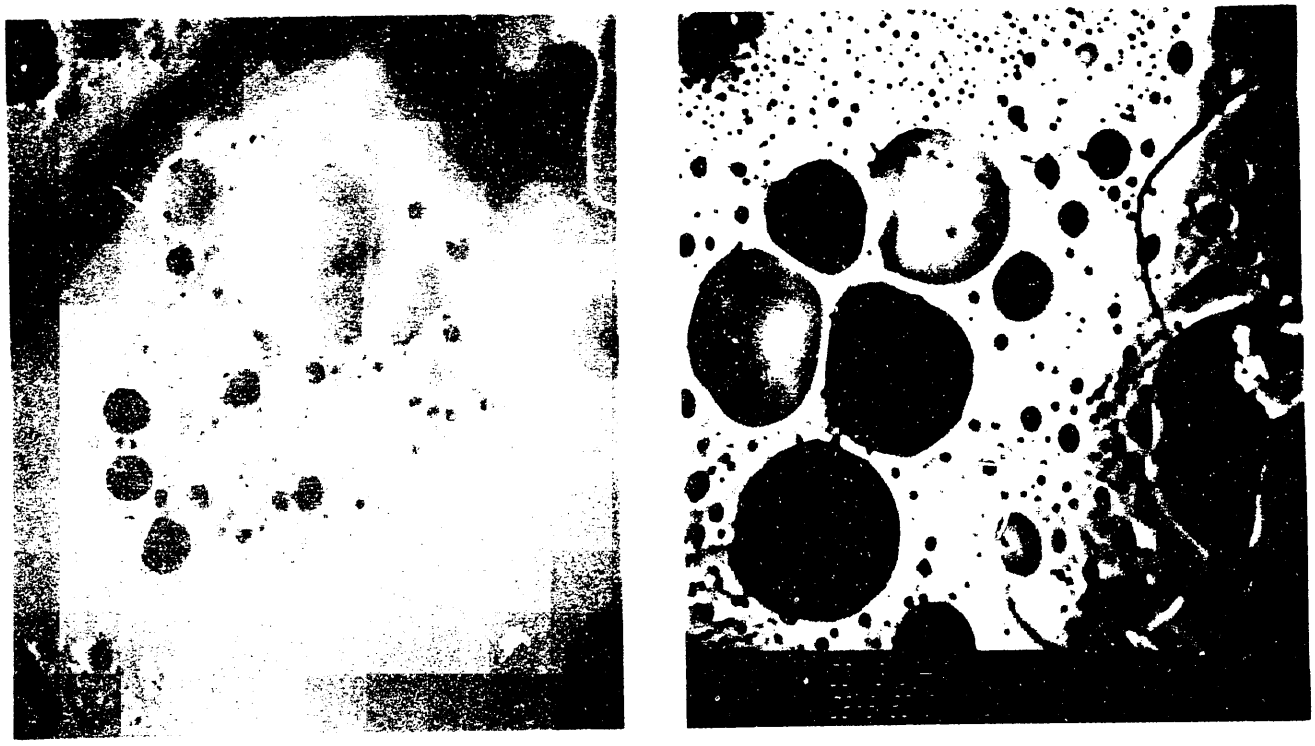

SAM

SEM

Fig. 4. Fuel Microstructure Showing Structural Difference Around Bubble Clusters in Fuel Particles

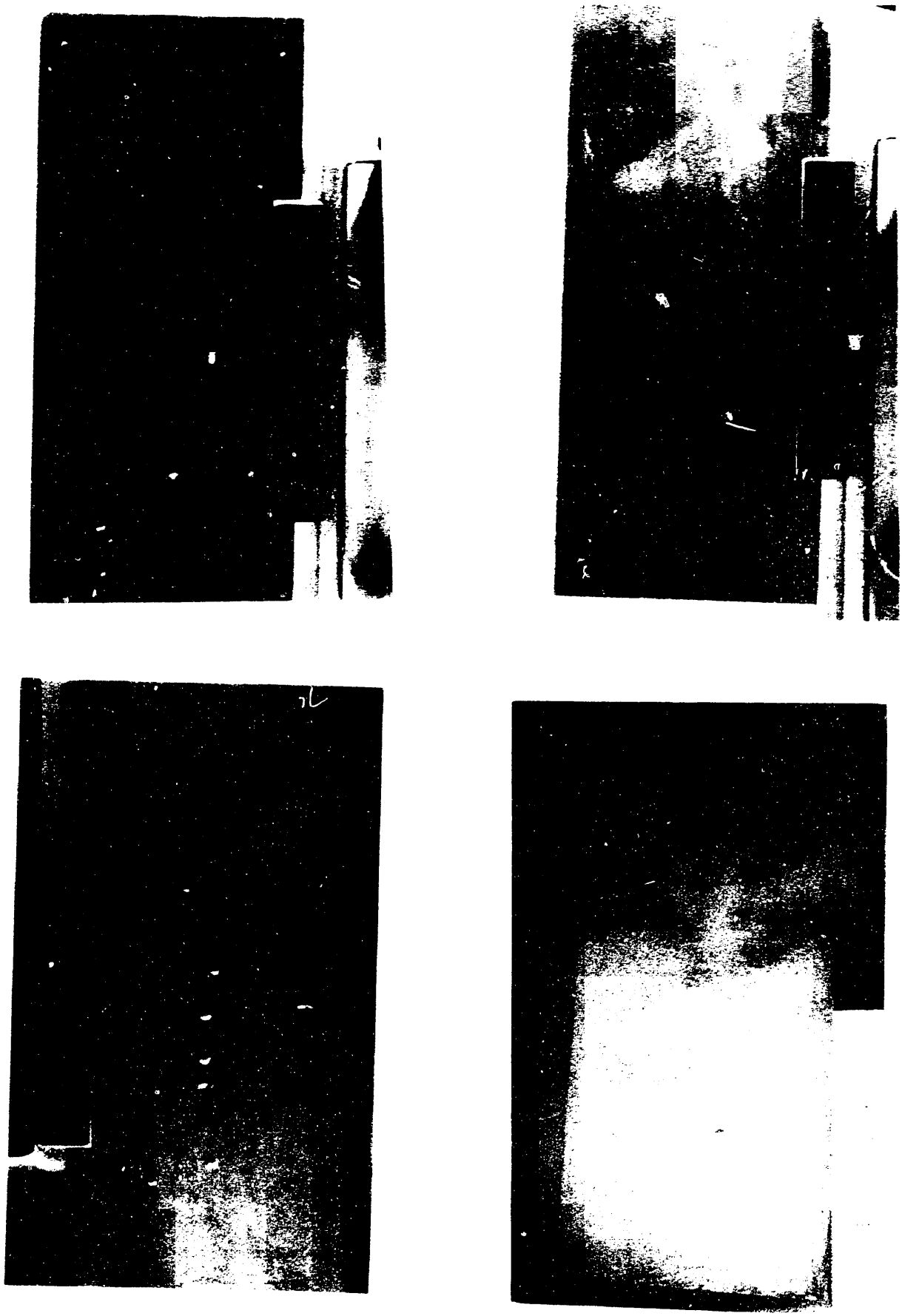

Fig. 5. Location of Blisters in Irradiated U_3Si_2 Plates After 1/2 Hour at 525°C

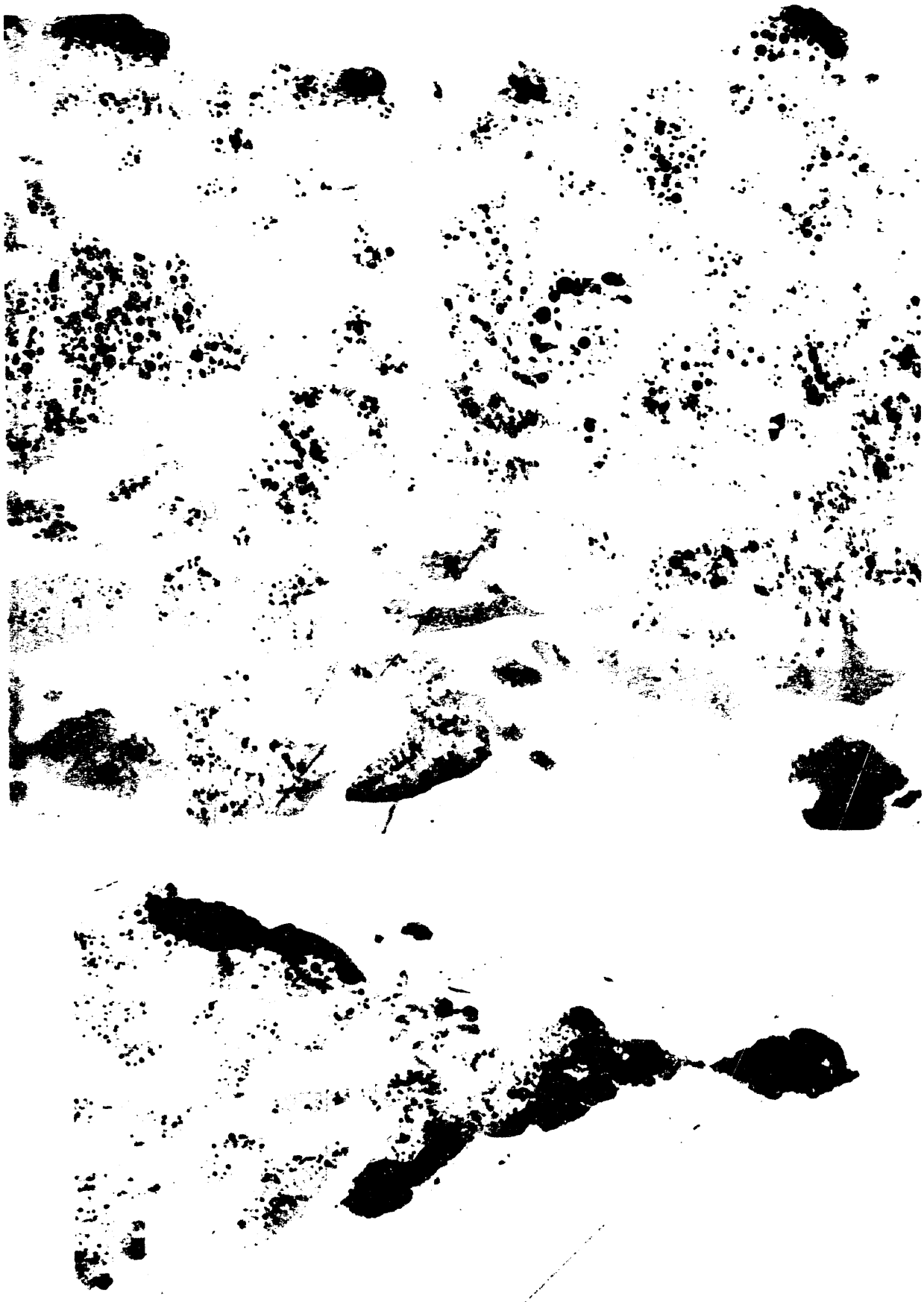

Fig. 6. Fuel Core Microstructure of Irradiated U_3Si Plate Showing Location of Oxide Particles at Core Edge and Dog Bone End

Fig. 7. Crossection of Ruptured Blister at Dog Bone End of Irradiated U_3Si_2 Plate After Prolonged Annealing at 450°C

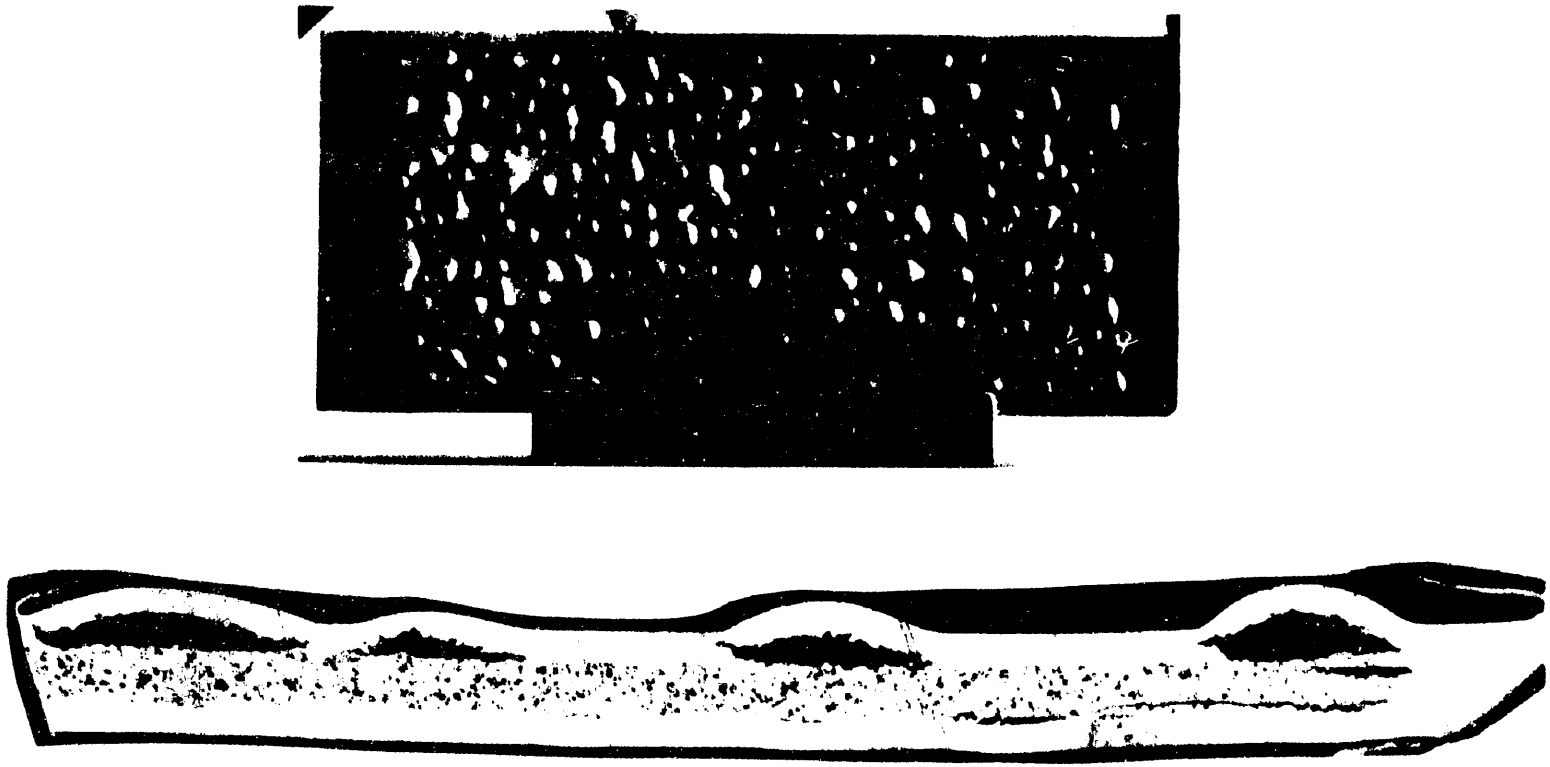

Fig. 8. Blisters and Crossection Through Blisters of B_4C Containing U_3Si_2 Plate after Prolonged Annealing at 450°C

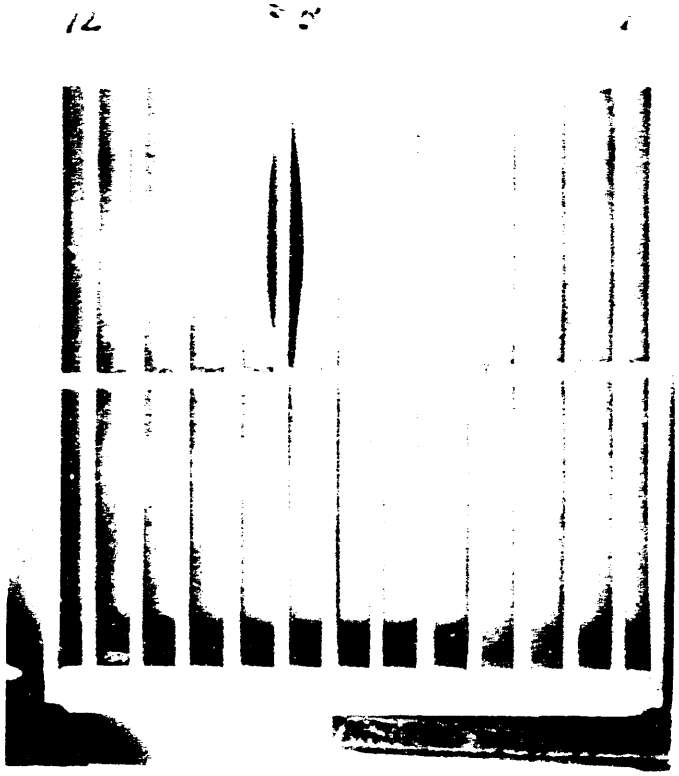

Back lightening through module

Edge on view of pillowed plate

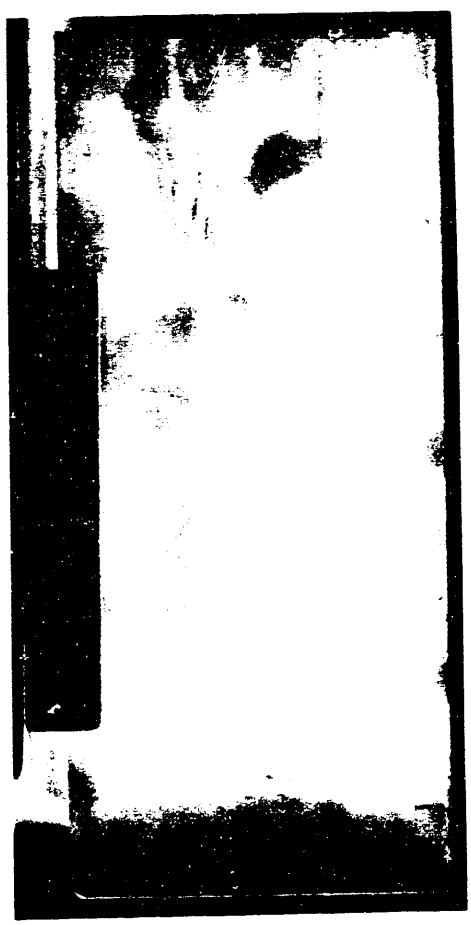

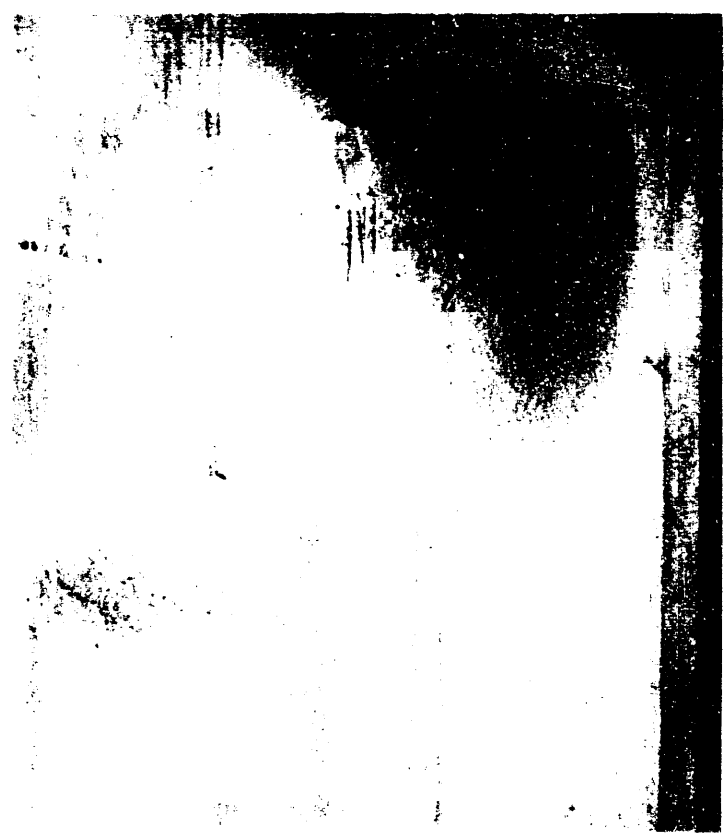

Fig. 9. Views of Pillowed U_3Si Plate A211, Showing Crack of Edge of Pillow

Detail

Fig. 10. Crossection of Pillowed Region of Plate 211, Including Crack Showing Remnants Reaction Product

THE EFFECT OF CRYSTAL STRUCTURE STABILITY ON SWELLING IN INTERMETALLIC URANIUM COMPUNDS

by

J. Rest, G. L. Hofman, and R. C. Birtcher

ABSTRACT

Irradiation experiments with certain low-enrichment, high-density, uranium-base intermetallic alloys that are candidate reactor fuel materials, such as U_3Si and U_6Fe, have revealed extraordinarily large voids at low and medium fuel burnup. This phenomenon of breakaway swelling does not occur in other fuel types, such as U_3Si_2 and UAl_3, where a distribution of relatively small and stable fission gas bubbles forms. In situ transmission electron microscope observations of ion radiation-induced rapid swelling of intermetallic materials are consistent with growth by plastic flow. Large radiation enhancement of plastic flow in amorphous materials has been observed in several independent experiments and is thought to be a general materials phenomenon.

The basis for a microscopic theory of fission gas bubble behavior in irradiated amorphous compounds has been formulated. The assumption underlying the overall theory is that the evolution of the porosity from that observed in the crystalline material to that observed in irradiated amorphous U_3Si as a function of fluence is due to a softening of the irradiated amorhpus material. Bubble growth in the low-viscosity material has been approximated by an effective enhanced diffusivity. Mechanisms are included for the radiation-induced softening of the amorphous material, and for a relation between gas atom mobilities and radiation-induced (defect-generated) changes in the material. Results of the analysis indicate that the observed rapid swelling in U_3Si arises directly from enhanced

bubble migration and coalescence due to plastic flow.

I. Introduction

Fission gas bubbles have recently been shown to exhibit extremely high growth rates at relatively low temperatures in certain uranium compounds [1]. It was proposed that this accelerated swelling phenomenon occurs only in compounds that undergo a crystalline-to-amorphous transformation, and that it is a manifestation of radiation enhancement of diffusion and plastic flow in amorphous solids.

The classical model of radiation-enhanced diffusion and creep in crystals, based on the generation of vacancies in excess of their thermal equilibrium concentration, does not apply in a noncrystalline solid where, strictly speaking, the vacant lattice site or vacancy does not exist. In amorphous solids, a model of a radiation-enhanced free volume can be used to interpret the very large flow rates observed. We will draw together here the results of several seemingly unrelated experimental studies in an attempt to generalize this large radiation effect in amorphous solids, and explore a model that describes the effect in particular as it relates to nuclear fuel.

Mineralogists have long recognized the presence of radiation-induced crystalline-to-amorphous transformations in natural radioacative compounds. The extent of this so-called metamict condition is used to determine the age of minerals and was first described by Pellas [2], who showed that partially covalent crystals can undergo this transformation. This bond-type criterion for amorphization has more recently been confirmed in an extensive ion bombardment study of compounds by Naguib and Kelly [3], who fouond that amorphization is quite common and should occur whenever the ionicity is <0.47.

In an attempt to extend the range of compounds in which the metamict condition can be used to determine the age of minerals, Cartz and co-workers [4,5] carried out an ion bombardment and transmission electron microscopy (TEM) study of a number of silicides and nitrides and made some remarkable observations. They found that $ZrSiO_4$ particles irradiated with 1-3.5 MeV Kr ions became amorphous at a dose of 2×10^{19} ions m^{-2}, and that further irradiation caused the non-crystalline particles to bloat into extended disc shapes, quadrupling in diameter at irradiation doses of between 6 and 60×10^{19} ions m^{-2}. A similar large glassy flow occurred in α-quartz after amorphization, whereas Si_3N_4 particles, which remained crystalline after exposure to the same irradiation, retained their original shape and size.

During approximately the same time period, Porter et al. [6] and Fowler et al. [7] studied radiation damage in glass ceramics for fusion reactor applications. They independently observed rapid void or bubble growth in the amorphous phases of these materials under electron bombardment. An example of Porter's observation in the form of time-lapse TEM images, illustrating the rapidity of the growth, is shown in Fig. 1. Void diameter changes estimatged from both Refs. 6 and 7 are similar in magnitude and increase linearly with electron dose. Inferences were also drawn as to the effectiveness of ionization damage, versus the largely displacement damage imposed during previous neutron exposures, in producing bubble growth in ionic crystals. Note that DeNatale and Horwitt [8] have recently observed the same type of radiation-damage phenomenon in previously unirradiated nuclear waste glasses.

The ion bombardment work of Klaumünzer and co-workers is of particular interest because it extends the observation of extraordinarily high radiation-induced growth to

metallic glasses. From a series of papers published from 1982 [9-11], it appears likely that all amorphous alloys (metallic glasses) are susceptible to large plastic flow under heavy ion bombardment. Recently, Klaumünzer et al. performed an ion bombardment experiment with borosilicate glass [12] and again found a very large plastic flow, comparable to that seen in the metallic glasses.

In reactor irradiation experiments with intermetallic uranium compounds, Hofman [1] showed that an enormous increase in gas bubble growth occurs when a compound becomes amorphous during irradiation. An example of this rapid bubble growth in U_3Si is illustrated in Fig. 2. Evidence of very large plastic flow in neutron-irradiated materials has also been reported in U_6Fe by Bloch [13], in PU_6 Fe by Coffinberry and Waldron [14] and in BeO by Yeniscavich and Bleiberg [15]. In every one of these experiments, the material exhibiting excessive flow was found to be amorphous after irradiation.

Finally, the ion bombardment and in situ TEM experiments of Birtcher et al. on U_3Si [16] underscore the general nature of the effect. During irradiation of the amorphous phase, the initial specimen perforation increased rapidly in size. This did not occur in the crystalline phase. Figure 3 shows the behavior of a strip of material between two holes in amorphous U_3Si during 1-MeV Kr irradiation. This material is under tension during the irradiation and undergoes plastic flow. Small holes within the strip grow and coalesce. This growth stops when the irradiation is interrupted. The overall behavior is identical to that displayed by reactor-irradiated U_3Si (Fig. 2). These observations suggest that plastic flow induced by a large radiation dose is not restricted to partially covalent materials but can occur in any amorphous solid.

The deformation measurements obtained in the ion bombardment experiments of Cartz, Klaumünzer, and Birtcher are combined in the plot shown in Fig. 4. The close grouping of the data should be considered coincidental and not indicative of a functional relationship, since no corrections for experimental differences have been made. However, Fig. 4 does illustrate the magnitude of observed deformations as well as the apparent linear relationship between deformation and irradiation dose. This linear dose dependence, which was also found during the electron irradiations of Porter and Fowler, indicates that atomic displacements control the deformation rate.

This summary of results of widely different experiments strongly suggests a unique radiation effect in glassy materials. The very large plastic flows suggest low viscosities characteristic of glass near its softening point. However, all experiments were performed below 0.3 T_m, temperatures where the materials in question are hard and have high viscosities. Indeed, after irradiation these amorphous materials are found to be hard and brittle. For example, the microhardness of U_3Si (measured after irradiation), increased slightly after prolonged neutron irradition, during which the compound became amorphous and experienced excessive swelling. The drastic difference between elastic properties during and after irradiation is graphically shown in Fig. 5, which is a scanning electron microscope (SEM) image of the surface of a large fission gas bubble in U_3Si. The smooth flow patterns on the bubble surface indicate viscous behavior, whereas the fractured "ligaments" which had connected two sides of the bubble, and which were broken during SEM sample preparation after irradiation, indicate brittle behavior. It may be concluded that viscous flow occurs under ion, electron, and neutron irradiation and fissioning in the glassy (amorphous) state only, whether this state is pre-existing or is formed during the irradiation.

As suggested in the proceding discussions, the underlying mechanisms affecting swelling behavior in intermetallic compounds involve mechanical instability under irradiation. As we shall show, radiation-enhanced diffusion and plastic flow are key determinants of swelling behavior. Figure 6 is a plot of the fuel swelling, obtained from immersion density measurements, for U_6Fe, U_3Si, U_3Si_2, and UAl_3 dispersion fuels. The UAl_3 and U_3Si_2 show little swelling after very high U burnup, but the higher density U_6Fe and U_3Si experience rapid swelling at medium and low burnup.

The differences in fission gas bubble behavior are illustrated in Fig. 7 for the four fuels shown in Fig. 6. Typically, UAl_3 does not develop resolvable fission gas bubbles, but U_3Si_2 contains bubbles which have an extremely narrow size distribution and uniform spacing, and which appears to be arranged in rows. The U_3Si develops large bubbles which interconnect and result in rapid swelling. At low burnup, U_6Fe likewise develops large irregular bubbles which interconnect, causing a sharp increase in the swelling curve. As will be shown in Section II, the swelling behavior of the stable compounds UAl_3, U_3Si_2, and USi can be explained with current models of fission gas behavior in nuclear fuels, models that include such effects as radiation-enhanced diffusion and nucleation and growth of fission gas bubbles on grain boundaries, subgrain boundaries and dislocations in a crystalline solid.

In Section III, it will be shown that the gas bubble growth observed in U_6Fe, U_3Si, and U_6Mn at low temperature can be explained by assuming that under irradiation, properties of the fuel approach those of the liquid state. Results will be presented which suggest that extraordinarily low viscosity occurs in amorphous solids under irradiation. An

analytical model will be presented which relates the migration energy for diffusion within a defect cascade to the level of damage sustained in the material. Measurements by Okamota et al. [17] of the change in sound velocity in irradiated intermetallic compounds have shown that substantial elastic softening of the intermetallic compounds occurs in the crystalline state and is associated with the progressive destruction of the chemical long-range order which precedes the onset of amorphization in these materials. The shear constant decreases linearly by as much as 50% with increasing volume dilation, and extrapolates to zero at a volume dilatation of about 4.7%.

II. Fission Gas Bubble Behavior in Crystalline Intermetallic Compounds

A. Models

Estimates of the quantity of gas that can be accounted for in the observed U_3Si_2 bubble population (Fig. 7) fall far short of the total amount generated. As the limit of resolution in the SEM is about 50 nm, it is likely that a high density of small bubbles and/or a high concentration of gas in solution is present within the U_3Si_2 matrix. A mechanistic fission gas release and swelling mode, GRASS-SST [18,19], has been utilized to interpret the observations.

For the purpose of calculation (i.e., reasonable code running times), the bubbles are represented by a set of size classes defined in terms of the number of gas atoms per bubble. This method of grouping significantly reduces the number of equations needed to describe the bubble size distributions. The bubble classes are ordered so that the first class refers to bubbles that contain only one gas atom. If S_i denotes the average number of atoms per bubble for bubbles in the ith class (henceforth, called i bubbles), then the bubble

size classes are defined by

$$S_i = mS_{i-1} \tag{1}$$

where $m \geq 1.6$, $i \geq 2$, and $S_1 = 1$. The S_1 class is assumed to consist of a single gas atom associated with one or more vacancies or vacancy clusters. P_{ij} is the probability of an i bubble coalescing with a j bubble when the bubbles move by random motion, and is given by

$$P_{ij} = 4\pi(r_i + r_j)(D_i + D_j) \tag{2}$$

where r_i is the average i-bubble radius and D_i is the average i-bubble diffusion coefficient in the lattice.

The rate of coalescence, C_{ij}, of bubbles with j bubbles is given by

$$C_{ij} = P_{ij}F_iF_j \tag{3}$$

where F_i is the number of i bubbles per unit volume. Details of the bubble growth calculation are given in the Appendix.

Dislocations can act as trapping sites for fission gas and bubbles. The fission gas atoms diffuse by random motion to dislocations at a rate

$$R^d = \frac{2\pi D_1 \rho c}{ln(r_c/r_i)} \tag{4}$$

where ρ is the dislocation density, c is the concentration of fission gas in the lattice, r_1 is the radius of a single gas atom, and r_c is the radius of the cylindrical capture volume around the dislocation, i.e.,

$$(\pi r_c^2)\rho = 1. \tag{5}$$

Once the fission gas is pinned to dislocations, the gas can coalesce with both lattice and dislocation bubbles (re-solution causes gas atoms to be knocked back into the lattice). Coalescence probabilities for bubbles on dislocations can be derived from a solution of the one-dimensional, time-dependent diffusion equation, and are given by

$$P_{ij} = (D_i^d + D_j^d)/\sqrt{\rho}, \tag{6}$$

where D_i^d is the average i-bubble diffusion coefficient on dislocations.

Bubble growth in crystalline U_3Si_2 during low-temperature (<200°C) irradiation occurs primarily by the diffusion of gas atoms to existing bubbles, i.e., the bubbles are basically immobile. Gas atom diffusion in U_3Si_2 at 100°C is primarily athermal, i.e., irradiation enhanced. The gas atom diffusivities used in GRASS-SST are taken from those reported by Höh and Matzke [20], and are given by

$$D_a = 3.5 \bullet 10^{-40} m^5 \bullet f \tag{7}$$

where f is the fission rate.

Bubble growth is limited not only by the gas atom and gas bubble densities and diffusivities, but by radiation-induced gas atom re-solution, i.e., the rate, b, at which gas atoms are ejected from a bubble owing either to direct or to indirect collisions by fission fragments.

The re-solution rate is calculated with the assumption that gas atom re-solution from a spherical bubble is isotropic and proceeds by the knocking out of single gas atoms. Thus, from geometrical considerations

$$b_i = \frac{2b_0 f}{r_i^3} \int_{r_i - \lambda}^{r_i} \left(\frac{1 + \cos\theta_i}{2}\right) R^2 \, dR \tag{8}$$

where $\cos\theta = (r_i^2 - \lambda^2 - R^2)/2R\lambda$, λ is the distance an average ejected atom travels, and b_o is an experimentally determined constant [19].

For bubbles on dislocations, equilibrium is reached when the diffusion flux of gas atoms from the local concentration gradients is balanced by the flux owing to re-solution. If instantaneously there are N_i bubbles per unit length of dislocation, the re-solution flux is $N_i b/2$. If the gas atom concentration is zero at the dislocation and C^λ a distance λ from it, the diffusion flux is approximately given by $D\, C^\lambda/\lambda$ from Fick's law. Thus, at equilibrium, when the two fluxes are equal.

$$(1 - C^\lambda/C^\circ) = 1 - \sum_i N_i b_i \lambda/2DC^\circ \qquad (9)$$

where C° is the gas atom concentration far from the dislocation.

Within the rate theory approach used in GRASS-SST, the rate of gas atom re-solution from dislocation bubbles, $bN_i/2$, is multiplied by the factor $C_o^\lambda = C^\lambda/C^\circ$ to obtain the backward flux of gas atoms. Good agreement between theory and experiment is obtained only for small values of C_o^λ ($C_o^\lambda << 1$). Physically, these results are interpreted as due to a small value of the penetration depth, λ. The value of λ used in GRASS-SST (λ = 5 nm) and by Dowling et al. [21] is consistent with this conclusion and is on the order of a defect cascade size.

A system of coupled equations for the evolution of the size distribution of fission gas bubbles in the lattice and on dislocations can be derived [19] on the basis of the models discussed above. The equations have the form

$$F_i^\alpha = - A_i^\alpha F_i^\alpha F_i^\alpha - B_i^\alpha F_i^\alpha + C_i^\alpha (i = 1, ..., N; \alpha = 1,2) \qquad (10a)$$

where F_i^{α} is the number of α-type bubbles in the ith size class per unit volume; α = 1,2 represents the lattice and dislocation distributions, respectively; and the coefficients B_i^{α} and C_i^{α} obey functional relationships of the form

$$C_i^{\alpha} = C_i^{\alpha}(F_i^{\beta}, ..., F_{i-1}^{\beta}, F_i^{\alpha}, F_{i+1}^{\beta} ..., F_N^{\beta}) \qquad (10b)$$

$$B_i^{\alpha} = B_i^{\alpha}(F_1^{\beta}, ..., F_{i+1}^{\beta}, F_i^{\alpha}, F_{i+1}^{\beta} ..., F_N^{\beta})$$

where $\alpha = 1; \beta = 1,2; \alpha = 2$

$\alpha = 2; \beta = 1,2; \alpha = 1.$

In Eq. 10, A_i^{α} represents the rate at which α-type bubbles grow out of the ith size class due to coalescence with other bubbles in the ith class; B_i^{α} represents the rate at which α-type bubbles are lost from the ith size class owing to coalescence with bubbles in other size classes, change in bubble type owing to bubble migration processes, and re-solution; and C_i^{α} represents the rate at which bubbles are being added to the ith size class owing to fission gas absorption, bubble nucleation, bubble growth resulting from bubble coalescence, and bubble shrinkage from the i+1 class due to gas atom re-solution.

Figure 8 is a GRASS-SST flow chart. Given the operating conditions, such as the time step, temperature, stress, grain size and dislocation densities, GRASS-SST calculates the equilibrium bubble radii for the size classes of bubbles under consideration (the initial number of size classes is an input) by using a modified hard-sphere equation of state for xenon as well as the generalized capillary relation

$$P_i(T) = \frac{2\gamma}{r_i} + \sigma_H \qquad (11)$$

where $P_i(T)$ is the gas pressure in a bubble with radius r_i, γ is the surface energy, and σ_H is the local hydrostatic stress.

After the bubble radii have been determined, the bubble diffusivities and coalescence probabilities are calculated. The code then solves for the bubble size distributions (Eqs. 10) incrementally by using a modified midpoint rule to generate a sequence of approximations; every sequence is interpolated by rational functions to obtain a "trial" solution until specified convergence criteria are satisfied. (If required, the code will increment the number of size classes involved in the calculation.) Finally, the fission gas released and the swelling due to retained gas are calculated. The intragranular swelling due to retained fission gas is calculated from the bubble size distributions, F_i^{α}, using

$$\Delta V = \frac{4\pi}{3} \sum_{i,d} r_i^3 \, F_i^{\alpha} \tag{12}$$

B. Results of GRASS-SST Calculations

The observed bubble distribution in crystalline U_3Si_2 contains bubbles having a relativey uniform separation, with many of the bubbles lying along straight lines (Fig. 7). Electron microscope observations of intragranular bubble distributions in uranium dioxide irradiated at temperatures in excess of about 700°C have also shown bubbles lying in straight lines [22]. Calculations of homogeneous bubble nucleation suggest that heterogeneous nucleation is most likely to occur when nuclei are present with a spacing of less than a micron [23]. This led Speight [24] to the supposition that dislocations or, more likely, dislocation networks that form low-angle subgrain boundaries act as favorable nuclei for bubble growth under these conditions, since they are present on this scale and their effective binding energy with fission gas atoms is large. Studies of helium precipitation in

metals have shown directly that He precipitates at dislocations [25]. In fissile materials, it would appear that as the bubbles nucleate and grow, their associated dislocations will climb by adsorption of excess interstitials remaining after vacancies are absorbed by bubbles and other sinks (equal numbers of vacancies and interstitials are produced). The climb is such that a bubble transfers from the tensile to the compressive side of the dislocation and away from the region of high gas density. The only locations that remain as good nucleation and growth centers throughout the irradiation are the dislocation nodes, and it is to be expected that the largest bubbles will be located at these sites, with small ones on or near dislocation lines.

Figure 9 shows the GRASS-SST-calculated bubble size distribution in U_3Si_2 at 16 U at.% burnup. Also shown is the average observed bubble diameter. The calculation shown in Fig. 9 was made with the assumption that gas atom re-solution from bubbles on dislocations is a factor of 10 smaller than re-solution of bubbles in the lattice. This difference is due to a larger knock-out distance required to separate a gas atom from a bubble located on a dislocation. For gas-atom knock-out distances, λ, less than the gas-capture radius for a dislocation, r_c, the gas associated with bubbles on dislocations is effectively trapped. Thus bubbles on dislocations grow at a faster rate. As can be seen from Fig. 9, the GRASS-SST-calculated distribution of bubbles on dislocations is in good alignment with the average bubble diameter. The majority of the generated fission gas is predicted to be in very small bubbles not on dislocations (radii less than about 5 nm). However, the small bubbles are responsible for only 50% of the total swelling.

Figure 10 compares the measured and GRASS-SST-calculated gas bubble swelling as a function of fluence for U_3Si_2. The calculation closely matches the linear dependence of the observed swelling on fluence. The constant difference between the

straight-line approximation to the data and the GRASS-SST-calculated values can be associated with solid fission products (i.e., fission products other than the noble gases) not included in the GRASS-SST calculations. Sensitivity studies performed with GRASS-SST indicate that the calculated results shown in Fig. 9 are relatively insensitive to the value of the athermal diffusivity, D_a, and the assumed value for the dislocation density, ρ. However, the size distribution of bubbles on dislocations is very sensitive to the assumed value for the dislocation gas atom re-solution rate, i.e., b_o in Eq. 8. The reason for the relative insensitivity to D_a of the calculated distribution of bubbles on dislocations and in the lattice is related to the dominance of re-solution of gas atoms originally contained within highly concentrated bubbles in the lattice. The motion of gas in the lattice is dominated by a high number of trapping (by bubbles) and detrapping (via re-solution) events. Increasing D_a increases the gas atom mobility while at the same time increasing the trapping rate at small bubbles in the lattice. These two interrelated and competitive processes result in a relatively weak D_a dependence of the gas atom flux to dislocations.

On the other hand, the gas atom re-solution rate from dislocation bubbles directly affects the growth rate of the bubbles on dislocations. A decreased value for the dislocation gas atom re-solution rate allows the dislocation bubbles to effectively retain their gas. Reasonable agreement is obtained for re-solution from dislocation bubbles at a rate that is a factor 10 lower than that used for bulk gas atom re-solution. This observation is consistent with the gas atom capture properties of dislocations.

III. FISSION GAS BUBBLE BEHAVIOR IN IRRADIATED AMORPHOUS INTER-METALLIC COMPOUNDS

As discussed in Section I, observations of certain low-enrichment, high-density, uranium-base intermetallic alloys, such as U_3Si and U_6Fe, have revealed extraordinarily large voids at low and medium fuel burnup. This phenomenon of breakaway swelling does not occur in other fuel types, such as U_3Si_2 and UAl_3, where instead a distribution of relatively small, stable fission gas bubbles forms. The in situ observations of ion-radiation-induced rapid swelling of intermetallic materials (see Fig. 3) are consistent with growth by plastic flow.

A microscopic theory of fission gas bubble behavior in irradiated amorphous compounds is proposed in this section. The assumption underlying the overall theory is that the difference in evolution of the porosity between crystalline and amorphous U_3Si is due to a softening of the irradiated amorphous material with a concurrent orders-of-magnitude increase in the effective gas bubble diffusivity due to plastic flow. The coupling of changes in shear modulus with radiation-induced softening of amorphous material and gas atom mobility within defect cascades is discussed.

A. Model for Irradiation-induced Softening of Amorphous Materials

The major differences between the crystalline and amorphous phases are due to changes in the elastic properties. In a number of recent studies discussed in Section I, elastic softening of irradiated glasses was reported. P. R. Okamoto et al. [26] show that substantial elastic softening of intermetallic compounds occurs in the crystalline phase and is associated with the progressive destruction of the chemical long-range order. Brillouin scattering experiments and transmission electron diffraction studies [27] have shown that

single-crystal silicon and polycrystalline intermemtallic compounds undergo dramatic elastic softening after irradiation with charged-particle beams. Measurements of the change in sound velocity show that the average shear constant decreases by as much as 30% in silicon and by as much as 50% in intermetallics. These results point to a strong coupling between strain and order parameter as a possible origin of the elastic softening and to strain accumulation as an important prerequisite for the amorphization of these intermetallics.

The degree of long-range atomic order, S, has an exponential dependence on the total dose ϕt,

$$S/S_o = \exp(-K\phi t). \tag{12}$$

Measurements by Okamoto et al. [17] of the Zr_3Al lattice dilation, $\Delta a/a$, determined from the change in spacings of the (400) fundamental reflection, showed that $\Delta a/a$ increases with increasing dose, reaches a maximum value of about 0.8% at the dose where amorphization starts, then drops abruptly to ~0.7% (S~0) and thereafter remains approximately constant. For doses up to 0.2 dpa, the percentage lattice dilatation is a quadratic function of S:

$$\Delta a/a = (\Delta a/a)_m [1 - (S/S_o)^2] \tag{13}$$

where $S/S_o = \exp[-11.6\ \phi t]$ is the observed dose dependence of S and $(\Delta a/a)_m = 0.775\%$ is the maximum lattice dilatation due to disordering. The results of Brillouin scattering measurements (post-irradiation) on the same material showed that a large (~50%) decrease in the shear constant occurs after chemical disordering. The decrease occurs prior to the onset of amorphization, and hence the elastic softening is a precursor effect rather than a consequence of amorphization. This result is significant since it strongly suggests that an elastic instability triggers the onset of amorphization. For doses up to 0.15 dpa, the shear

constant is a quadratic function of S:

$$C/C_0 = 0.5\,[1 + (S/S_o)^2]. \qquad (14)$$

The S^2 dependence of both the elastic softening and lattice dilatation can be understood-qualitatively in terms of phenomenological theories of order-disorder based on central pair-wise interactions, as described in Refs. 12 and 13 of the paper by Okamato et al. [26].

The S^2 dependence described by Eqs. 13 and 14 implies that the shear constant is a linear function of volume dilation, $3\Delta a/a$. Eliminating $(S/S_o)^2$ in Eqs. 13 and 14 yields

$$C/C_o = [1 - (3\Delta a/a)/4.65]. \qquad (15)$$

As described by Eq. 15, the shear constant decreases linearly with volume dilatation and extrapolates through the glass gap (i.e., the change in the density between the partially disordered crystalline phase and the amorphous phase is ~2.5% to zero at $3\Delta a/a$ (~4.7%), which is very close the value of $4 \pm 1\%$ measured by Schulson for total volume expansion of amorphous Zr_3Al [28]. The loss of resistance to shearing at a dilatation of 4.7% indicates that the partially disordered material ($S \sim 0.2$) is mechanically unstable with respect to density fluctuations comparable in magnitude to the glass expansion gap. Since density fluctuations of comparable magnitude may occur in the cores of energetic cascades, the irradiation itself can provide the additional density fluctuation required to trigger an elastic instability in the partially disordered material. An estimate of these density fluctuations in U_3Si is presented inSection IIIC.

Okamoto et al. [26] emphasize that the elastic instability which occurs during irradiation is not one in which the entire crystal transforms catastrophically to an amor-

phous phase at some critical disorder. The glass expansion gap represents a nucleation barrier against glass formation in the highly-strained, metastable, disordered crystalline material. Although the dilatational strain will have a well-defined average value, local dilatation fluctuations result in regions of mechanical instability, i.e., amorphization, and not everywhere simultaneously. In the context of the theory being developed in this paper, the important point is that disorder results in a volume-dependent shear coefficient during irradiation similar to that associated with the heating and melting of metals.

B. Calculation of Gas-Atom Diffusivities Within Defect Cascades

Measurements of ion beam mixing of tracer impurities in metallic glasses and in the pure crystalline elements comprising the glasses performed by Hahn et al. [29] at 80 K demonstrated that the ion mixing efficiency of the tracer impurities was greater in the metallic glasses than in either of the constituent elements for the NiZr and CuEr systems. The athermal diffusivities of the tracer impurities in the metallic glasses was within a factor of 10 of those measured in the crystalline materials. Although in the right direction, a factor of 10 increase in the gas-atom diffusivities is not sufficient to explain the breakaway swelling observed in the irradiated U_3Si material (Fig. 2). However, the Hahn et al. results are consistent with the picture of cascade dynamics provided by recent molecular dynamics computer simulations [30]. The simulations show that the cascade region has a "liquid-like" structure during the thermal spike phase of the cascade evolution.

C. P. Flynn [31] has developed a simple picture for the relationship between the migration energy for diffusion and the elastic constants of the material. A diffusion jump introduces a lattice strain. One may expect the strain caused by the jump to be mainly a shear. An estimate of the energy in this shear strain can be obtained by treating

the material as a Hookeian solid. For Hookeian shear, the work done per unit volume of strain energy in the body is given by

$$W = \frac{1}{2}\,\varepsilon^2 C' \tag{16}$$

where C' is the shear modulus and ε is the strain caused by the jump. The energy in the shear strain is obtained by multiplying W by the strained volume. Choosing a volume given by $\frac{4}{3}\,\pi a^3$, where a is the atomic spacing, results in

$$E_m = \frac{4}{3}\,\pi a^3 C' \varepsilon^2 \tag{17}$$

In Flynn's more rigorous elastic theory, large atomic displacements causing diffusion jumps in monatomic crystals are treated as a summation of phonon amplitudes. Using the harmonic approximation, Flynn derived an expression for a Gibbs function for the migration energy given by

$$E_m = C\,\Omega\,\delta^2 \tag{18}$$

where C is an average elastic constant for migration, Ω is the atomic volume, $\delta^2 = q^2/s^2$, where q measures the energy fluctuation needed for a jump to continue to completion and s is a measure of the jump path. Equations 17 and 18 have the same functional dependence on the shear modulus. A decrease in the shear modulus will result in a proportional decrease in the migration energy for diffusion.

The thermally activated gas atom diffusivities in the amorphous phase can be described by an exponential dependence on tempreature, i.e.,

$$D_a = D_o \exp(-E_m/RT). \tag{19}$$

Gas atom mobility in irradiated crystalline material at relatively low temperatures is dominated by athermal diffusion. However, a decrease in E_m may result in thermal activation dominating the diffusion process. From Eqs. 18 and 15, the migration energy in the damaged material is reduced to

$$E_d = E_m [1 - (3\Delta a/a)/4.65] \tag{20}$$

where E_m is on the order of the migration energy in the undamaged material. The diffusivity in the damaged material is thus increased to

$$D_d = D_a \exp [(E_m/RT) \bullet (3\Delta a/a)/4.65]. \tag{21}$$

For a 3% dilatation, the diffusivity at 150°C would be enhanced by about ten orders of magnitude over thermal diffusion.

It is important to note that the gas atom diffusivity as given by Eq. 21 is appropriate only for local regions of the amorphous (or crystalline) material which are sustaining damage. The dilatation, $\Delta a/a$ in Eq. 21, applies to this damaged region (e.g., the volume of the damage cascade), and is estimated to have a lifetime on the order of the defect cascade, 10^{-10} s. From the analysis presented in section III A on the irradiation-induced softening of amorphous materials, it follows that Eq. 21 applies as well to damaged regions in partially disordered crystalline materials. The key difference in bubble behavior between irradiated crystalline and amorphous materials suggested by the experimental results presented in section I is that the amorphous materials can undergo substantial plastic flow. In irradiated amorphous materials containing fission gas (e.g., U_3Si), overpressurized bubbles can provide the driving force for flow. In addition, density fluctuations produced by the damage cascade can provide a driving force for microscopic deformation. Plastic flow, in turn, results in enhanced bubble coalescence and bubble sweeping of gas

atoms out of solution.

The calculation of bubble growth in irradiated amorphous materials is complicated by the interplay between bubble growth (driven by plastic flow) and plastic flow (e.g., driven by bubble overpressure). In order to provide for a computationally tractable description of this phenomenon, the assumption is made that bubble motion in a material undergoes plastic flow can be described by an effective bubble diffusivity on the basis of random motion in a liquid where the bubbles move by volume diffusion. The diffusivity of a bubble of radius r_i migrating by volume diffusion is given by

$$D_i = \frac{3\Omega}{4\pi r_i^3} D_u \qquad (22)$$

where Ω is a molecular volume and D_u is the diffusivity of the diffusing atoms. This diffusion is qualitatively described by the Stokes-Einstein equation:

$$D_u = kT/(6\pi r_u \eta) \qquad (23)$$

where r_u is the radius of the diffusing species and η is the viscosity. A softening of the material produces a decrease in η and a corresponding increase in D_u. The assumption is made here that in irradiated amorphous materials, the effect of plastic flow can be described by using an effective atomic diffusivity D_u equal to D_d (Eq. 21).

C. Results of GRASS-SST Calculation

The reader should keep in mind that several key physical processes are occurring simultaneously as damage is sustained in the material. The first process is radiation-induced crystalline to amorphous transitions, which occur in certain materials when long-range order in the crystal is destroyed. The loss of long-range order, directly

observed by Okamoto et al. [26], has been qualitatively correlated with compound stability, as expressed by the free energy of formation [1]. The amorphization process occurs on a microscopic scale when the local dilatation due to a damage cascade exceeds the glass expansion gap. Subsequently, the number density of these microscopic amorphous regions increases with time until they begin to overlap. The dose dependence of the amorphous volume fraction can be estimated by using a statistical overlap model [32] which assumes that each fission event produces many cascades that are amorphous.

The second process is the softening of the amorphous regions. This irradiation-induced softening process was noted by Klaumunzer [9-11] and others [4,5], and can be understood in terms of local density fluctuations which increase the free volume. Bethune [33] has observed an anomalous volume increase of 2.4% in U_3Si irradiated at temperatures below 100°C. Although he has interpreted his observations in terms of small vacancy clusters of diameter < 2 nm, they could be interpreted as an overall increase in free volume.

The third process is the increase in the motion of gas bubbles in material undergoing plastic flow. This motion has been qualitatively described by the use of effective atomic mobilities in the irradiated amorphous regions as described by Eq. 22. (Note that these atomic mobilities are directly applicable to the damage cascade region.) The increased atomic mobilities result in an enhanced growth rate of small gas bubbles and a reduction in the effectiveness of gas atom re-solution. The resultant overpressurized bubbles provide a driving force for plastic flow. Subsequently, the growing bubbles interconnect and the result is substantial porosity and deformation.

Approximately 5 MeV of damage energy is liberated by each fission event, and each event consists of about 200 cascades having individual energies of 5 to 30 keV. The increase of the amorphous volume fraction, V_A, is given by

$$\frac{dV_A}{dn} = V_c\,[1-V_A] \tag{24}$$

where V_c is the average cascade volume and n is the number of cascades produced. Integrating Eq. 24 yield

$$V_A = 1 - \exp[-V_c n] \tag{25}$$

For a fission rate of 1×10^{21} $m^{-3}s^{-1}$ and cascades with diameters of 10 nm, the material will be 99 percent amorphous after a dose of 4.4×10^{22} fissions$\cdot m^{-3}$ or a time of 45 sec. Within a relatively short time the crystalline U_3Si is rendered amorphous. Subsequently, the fission gas atoms and bubbles undergo motion in the flowing material. This motion has been qualitatively characterized by enhanced diffusivities given by Eqs. 21 and 22, respectively. If we assume an average dilatation, $3\Delta a/a$, of 3%, Eq. 21 predicts a diffusivity of about 6×10^{-14} m^2s^{-1}. This value for the gas atom diffusivity is equivalent to a viscosity of about 350 poises. The reader should note that the effective diffusivities (Eq. 21 and 22) used to characterize bubble motion in plastically flowing material are not related to the viscosity through the Stokes-Einstein equation (eq. 23). Although these diffusivities are characteristic of those within the "liquid-like" damage cascade regions, as discussed in Ref. 29, they are not observed in the bulk irradiated amorphous material. This apparent anomaly has been addressed by van den Beuhel [34], where violations of the Stokes-Einstein relation (from linear to parabolic behavior) has been measured. The violation of the Stones-Einstein relation is attributed to high concentrations of flow defects in irradiated amorphous materi-

als in response to applied stress.

Following the above discussion, GRASS-SST has been used to simulate fission gas behavior in U_3Si. The amorphous U_3Si was treated as if it were a low-melting-point (150°C) material. A gas atom diffusivity of 6×10^{-14} m^2s^{-1} was used, and bubbles were assumed to move by volume diffusion as given by Eq. 22. Figure 11 shows the GRASS-SST-calculated evolution of the gas-bubble size distribuiton in amorphous U_3Si. The calculations show that the bubble size distribution evolves to larger sizes as the irradiation proceeds. This results in an unrestrained fractional volume swelling of about 135% at 6×10^{27} fissions$\cdot m^{-3}$.

Although the bubble sizes calculated for amorphous U_3Si are substantially larger than those calculated for crystalline U_3Si_2, the model does not describe the extreme porosity and frothing observed in Fig. 2. This discrepancy is due to the absence of a realistic model to describe swelling in a material that exhibits plastic flow characteristic of a low viscosity. Small bubbles, formed from the precipitation of gas atoms, act as sinks for the continusously generated fission gas. The persistent radiation damage provides a sustained softening of the amorphous material. Upon bubble coalescence, the number of gas atoms and the bubble volume are conserved. Thus, these newly formed bubbles are in an over-pressurized state. Subsequently, the bubbles grow toward their equilibrium configuration by deforming the relatively soft surrounding material. Upon reaching equilibrium, the total surface area of the bubbles is conserved and a significant volume increase results.

IV. CONCLUSIONS

We have reviewed the irradiation behavior of intermetallic uranium alloys and have found similarities with the irradiation behavior of other intermetallics. Several of these systems undergo a crystalline-to-amorphous transformation during irradiation at low temperatures. The amorphous phases soften and are mechanically unstable during irradiation, even though they are brittle after irradiation. The mechanical instability arises from an elastic softening which increases the ductility by many orders of magnitude. In reactor fuels, this mechanical instability results in the rapid nucleation and growth of fission gas bubbles. Because of the decreased viscosity of the amorphous material under irradiation, fission-gas bubbles coalesce to form extremely large cavities, and the material swells at an uncontrollable rate (frothing). This swelling can be as much as three orders of magnitude greater than that observed in crystalline material.

Insight into the mechanisms involved has been gained through computer modeling with the GRASS-SST computer code. The kinetics of swelling in crystalline U_3Si_2 have been studied. The majority of fission gas is found to be in small bubbles (diameters <5 nm) which are dispersed throughout the crystal lattice. However, the swelling arises equally from the high density of small bubbles and a low density of large bubbles which are pinned to dislocations. Calculations show that the growth of the bubbles on dislocations is very sensitive to irradiation-induced re-solution of gas atoms from the bubble back into the crystal lattice. Re-solution from bubbles on dislocations is predicted to occur at a rate that is ten times lower than that from bubbles dispersed in the crystal lattice. This difference is due to a larger knock-out distance required to separate a gas atom from a bubble located on a dislocation. For gas atom knock-out distances less than the gas-capture radius for a dislocation, the gas associated with bubbles on dislocations is effectively trapped. Thus,

bubbles on dislocations are more effective at retaining their gas and grow at a higher rate than bubbles dispersed in the crystal lattice. The peaks in the bubble distribution at small and large sizes (Fig. 11) result from a balance between bubble nucleation, growth driven by diffusion, and shrinkage driven by re-solution (the latter two are linearly dependent on fission rate). Thus, the bubble size distribution is independent of fission gas generation rate but dependent on the total number of fission events or on the amount of gas generated. Changes in dislocation density or fuel chemistry during irradiation will strongly affect the distribution of large bubbles.

Analysis of fission gas behavior in irradiated amorphous U_3Si suggests that irraditaion softening combined with bubble overpressurization results in very large plastic flow. The effect of plastic flow has been modeled by an effective diffusivity. Enhanced diffusion leads to very rapid nucleation of gas bubbles, a rapid coarsening of the bubble-size distribution, and an enhanced fuel swelling rate. This model does not fully describe the observed extent of bubble growth and frothing, which arise from very rapid bubble migration and coalescence due to plastic flow.

APPENDIX

Coalescence between bubbles causes bubbles to change from one size class to another. The probability that a coalescence between an i bubble and a j bubble will result in a k bubble is given by the array T_{ijk}. Assume that $i \geq j$ in all cases. The number of gas atoms involved in one such coalescence is $S_i + S_j$. The array T_{ijk} is defined by the following three conditions:

1. The total probability of producing a bubble is unity; i.e., $\sum_k T_{ijk} = 1$.

2. The number of gas atoms, on the average, is conserved; i.e. $\sum_k T_{ijk} S_k = S_i + S_j$.

3. For a given pair, i and j, only two of the T_{ijk} array elements (corresponding to k and k + 1, where $S_k \leq S_i + S_j \leq S_{k+1}$; i.e, $m \geq 1.6$) can be nonzero.

From these three conditions, it follows that k = i, and

$$T_{ijk} S_k + (1 - T_{ijk}) S_{k+1} = S_i + S_j . \qquad \text{(A1)}$$

Thus, the probability that a coalescence between an i bubble and a j bubble results in a k bubble is given by

$$T_{ijk} = \frac{S_{k+1} - S_i - S_j}{S_{k+1} - S_k} = 1 - \frac{S_j}{S_{k+1} - S_k} . \qquad \text{(A2)}$$

The array T_{ijk} may be considered as the probability that an i bubble becomes a k bubble as a result of its coalescence with a j bubble. The rate N_{ik} at which i bubles become k bubbles is given by

$$N_{ik} = \sum_{j \le i} C_{ij} T_{ijk} . \qquad \text{(A3)}$$

The j bubble is assumed to disappear; gas atoms are absorbed into the i bubble. The rate x_x of disappearance is given by

$$x_j = \sum_{i \ge j} C_{ij} , \qquad \text{(A4)}$$

The rate N_{ik} at which i bubbles become k bubbles, with k = i+1, is reduced by re-solution of gas atoms. Re-solution is the rsult of a direct (or possibly indirect) collision between a fission fragment and a gas bubble. From Eqs. A2 and A3

$$N_{ik} = \sum_{j \le i} C_{ij} T_{ijk}$$

$$= \sum_{j \le i} P_{ij} F_i \frac{S_j}{S_k - S_i} \qquad \text{(A5)}$$

$$= \frac{F_i}{S_k - S_i} \sum_{j \le i} P_{ij} F_j S_j ,$$

The expression

$$\sum_{j \le i} P_{ij} F_j S_j ,$$

gives the rate at which gas atoms are added to an i bubble. Re-solution causes an i bubble to lose gas atoms at a rate given by $b_i S_i$, where b_i is the probability that a gas atom in an i bubble is redisolved. The reduced N_{ij} becomes

$$N_{ik} = \frac{F_i}{S_k - S_i} \left[\sum_{j \leq i} (P_{ij} F_j S_j) - b_i S_i . \right]. \qquad \text{(A6)}$$

If the expression within parentheses is negative, then N_{ik} is zero, and $N_{ik'}$, the rate at which i bubbles become i - 1 bubbles, with $k' = i - 1$, is

$$N_{ik'} = \frac{F_i}{S_i - S_{k'}} (b_i S_i - \sum_{j \leq i} P_{ij} F_j S_j). \qquad \text{(A7)}$$

Equations A6 and A7 are proportional to the probabilities that any particular i bubble becomes an i + 1 or an i - 1 bubble, respectively; the ratio of the probabilities is equal to the ratio of the rates. Clearly, the above definitions of N_{ik} converve the total number of gas atoms.

REFERENCES

1. Hofman, G. L., *Journal of Nuclear Materials*, Vol. 140, 1986, pp. 256-263.
2. Pellas, P., *Comptes Rendus Hebdomadaires des Seances de l'Academie des Sciences*, Vol. 233, 1969, pp. 1369-1371.
3. Niguib, H. M. and Kelly, R., *Radiation Effects*, Vol. 25, 1975, pp. 1-12.
4. Cartz, L. and Fournelle, R., *Radiation Effects*, Vol. 41, 1979, pp. 211-217.
5. Cartz, L., Karkoris, F. C., and Fournelle, R. A., *Radiation Effects*, Vol. 54, 1981, pp. 57-64.
6. Porter, D. L., Pascussi, M. R., and Olbert, B. H., *Journal of Nuclear Materials*, Vol. 103-104, 1981, pp. 767-772.
7. Fowler, J. D., Jr., Hurley, C. F., Kennedy, J. C., and Clinard F. W., Jr., *Journal of Nuclear Materials*, Vol. 103-104, 1981, pp. 755-760.
8. DeNatale, J. F. and Howitt, D. G., *American Ceramic Society, Bulletin*, Vol. 66, No. 9, 1987, pp. 1393-1396.
9. Klaümunzer, S., Schumacher, C., Rentzsch, S., and Vogel, G., *Acta Metallurgica*, Vol. 30, 1982, pp. 1493-1502.
10. Klaümunzer, S., and Schumacher, C., *Physical Review Letters*, Vol. 51, No. 21, 1983, pp. 1987-1990.
11. Klaümunzer, S., Schumacher, C., Hou, Ming-dong, and Vogel, C., *Rapidly Quenched Metals*, Vol. 1, S. Steeb and H. Warlimont, Eds., North Holland, New York, 1985.
12. Klaümunzer, S., Liu, Li Chang, and Schmacher, C., *Applied Physics Letters* (in press).
13. Bloch, J., *Journal of Nuclear Materials*, Vol. 6, 1962, pp. 203-212.

14. Coffinberry, A. S. and Waldron, M. B., *Progress in Nuclear Energy*, Vol. 1, 1956, p. 399.

15. Yeniscavich W. and Bleiberg, M. L., WAPD-BT-20.

16. Birtcher, R. C., Allen, C. W., Rehn, L. E., and Hofman, G. L., *Journal of Nuclear Materials*, Vol. 152, 1988, pp. 73-76.

17. Okomoto, P. R., Rehn, L.E., Pearson, J., Bhadra, R., and Grimsditch, M., In *Proc. Int. Symposium on Solid-State Amorphizing Transformations*, Los Alamos National Laboratory, August 1987, (in press).

18. Rest, J., *GRASS-SST: A Comprehensive, Mechanistic Model for the Prediction of Fission-Gas Behavior in UO_2-Base Fuels during Steady-State and Transient Conditi ons*, NUREG/CR-0202, ANL-78-53, Argonne National Laboratory, 1978.

19. Rest, J. and Cronenberg, A.W., *Journal of Nuclear Materials*, Vol. 150, 1987, pp. 203-225.

20. Hoh, A. and Matzke, Mj., *Journal of Nuclear Materials*, Vol. 48, 1973, pp. 157-164.

21. Dowling, D. M., White, R. J., and Tucker, M. O., *Journal of Nuclear Materials*, Vol. 110, No. 1, 1982, pp. 37-47.

22. Turnbull, J. A., *Journal of Nuclear Materials*, Vol. 38, 1971, pp. 203-212.

23. Greenwood, C. W., Foreman, A. J. E., and Rimmer, D. E., *Journal of Nuclear Materials*, Vol. 4, 1959, pp. 305-324.

24. Speight, M. V. and Greenwood, C. W., *Journal of Nuclear Materials*, Vol. 16, 1965, pp. 327-332.

25. Krishan, K., *Radiation Effects*, Vol. 66, 1987, pp. 122-155.

26. Okamoto, P. R., Rehn, L. E., Pearson, J., Bhadra, R., and Grimsditch, M., *Procedures of Materials Research Society Meeting*, Boston, Mass., Nov. 1987, (in press).

27. Grimsditch, M., Coray, K. E., Bhadra, R., Kampwirth, R. T., and Rehn, L. E., *Physical Review*, Vol. B35, 1987, p. 883.

28. Schulson, E. M., *Journal of Nuclear Materials*, Vol. 83, 1979, pp. 239-264.

29. Hahn, H., Averback, R. S., and Rothman, S. J., Physical Review Letters, Vol. 59, 1982, pp. 1930-1933.

30. Diaz de la Ruban, T., Averback, R. S., Benedek, R., and Kins, W.E., Physical Reveiw Letters, Vol. 59, 1987, pp. 1930-1933.

31. Flynn, C. P., *Physical Review*, Vol. 171, No. 3, 1960, pp. 682-698.

32. Brimhall, J. L., Kissinger, H. E., and Pelton, A. R., *Radiation Effects*, Vol. 90, 1985, pp. 241-258.

33. Bethune, B., *Journal of Nuclear Materials*, Vol. 40, 1971, pp. 205-212.

34. Van den Beuhel, A., *Scripta Metallurgica*, Vol. 22, 1988, pp. 877-880.

LIST OF FIGURES

1. Void and Bubble Growth in Preirradiated Borosilicate Glass During Electron Irradiation.
2. Formation of Large Gas Bubbles in Irradiated U_3Si Dispersed in Aluminum.
3. Deformation of U_3Si (Black) as a Function of Kr Dose.
4. Deformation in Several Amorphous Materials After Ion Bombardment.
5. Scanning Microscope Image of the Surface of a Large Bubble Shown in Fig. 2.
6. Swelling of Various Intermetallic Low-Enriched Uranium Compounds Verses Fission Density in the Compound.
7. Characteristic Fission Gas Bubble Morphology in Various Intermetallic Uranium Compounds after Reaching the Indicated Fission Density (FD).
8. GRASS-SST Flow Chart.
9. Bubble Size Distribution in Crystalline U_3Si_2 at 16 at.% Burnup.
10. Comparison of Measured (Symbols) and Calculated Swelling in Crystalline U_3Si_2.
11. Calculated Bubble Size Distribution in Amorphous U_3Si as a Function of Fission Density.

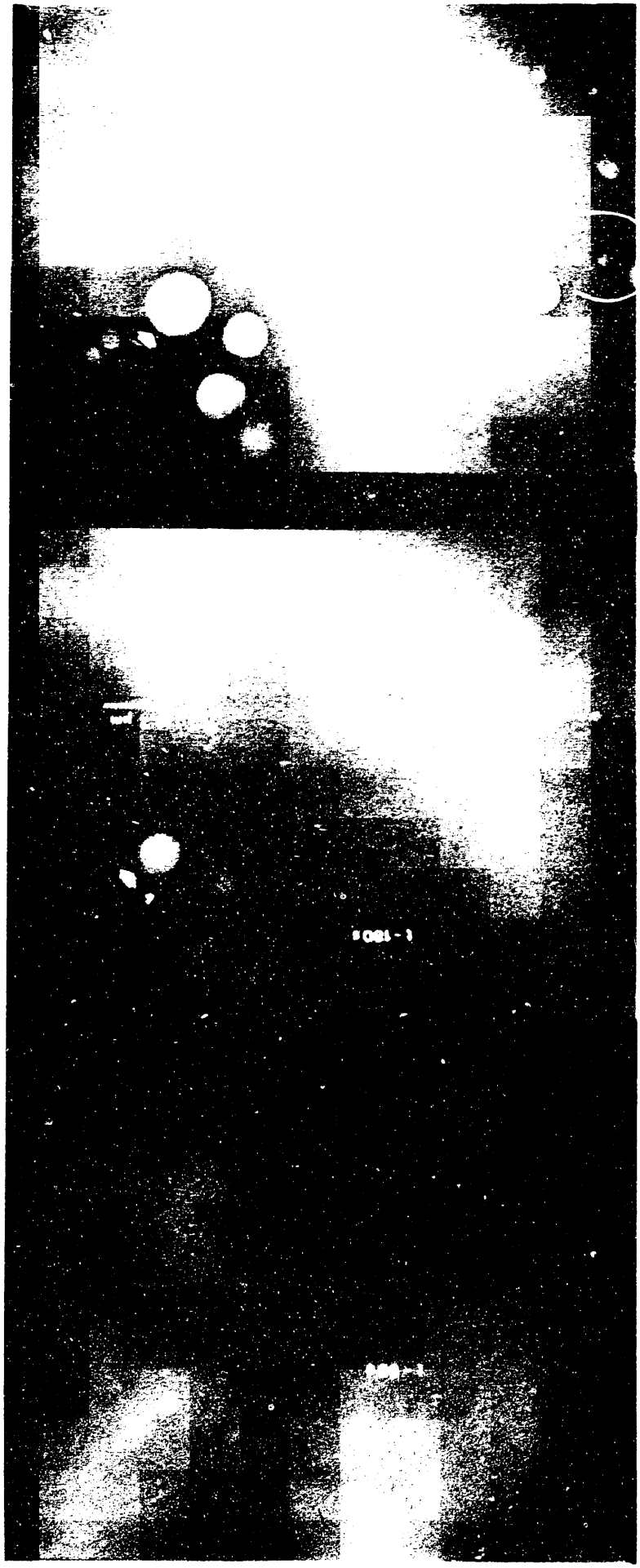

Fig. 1

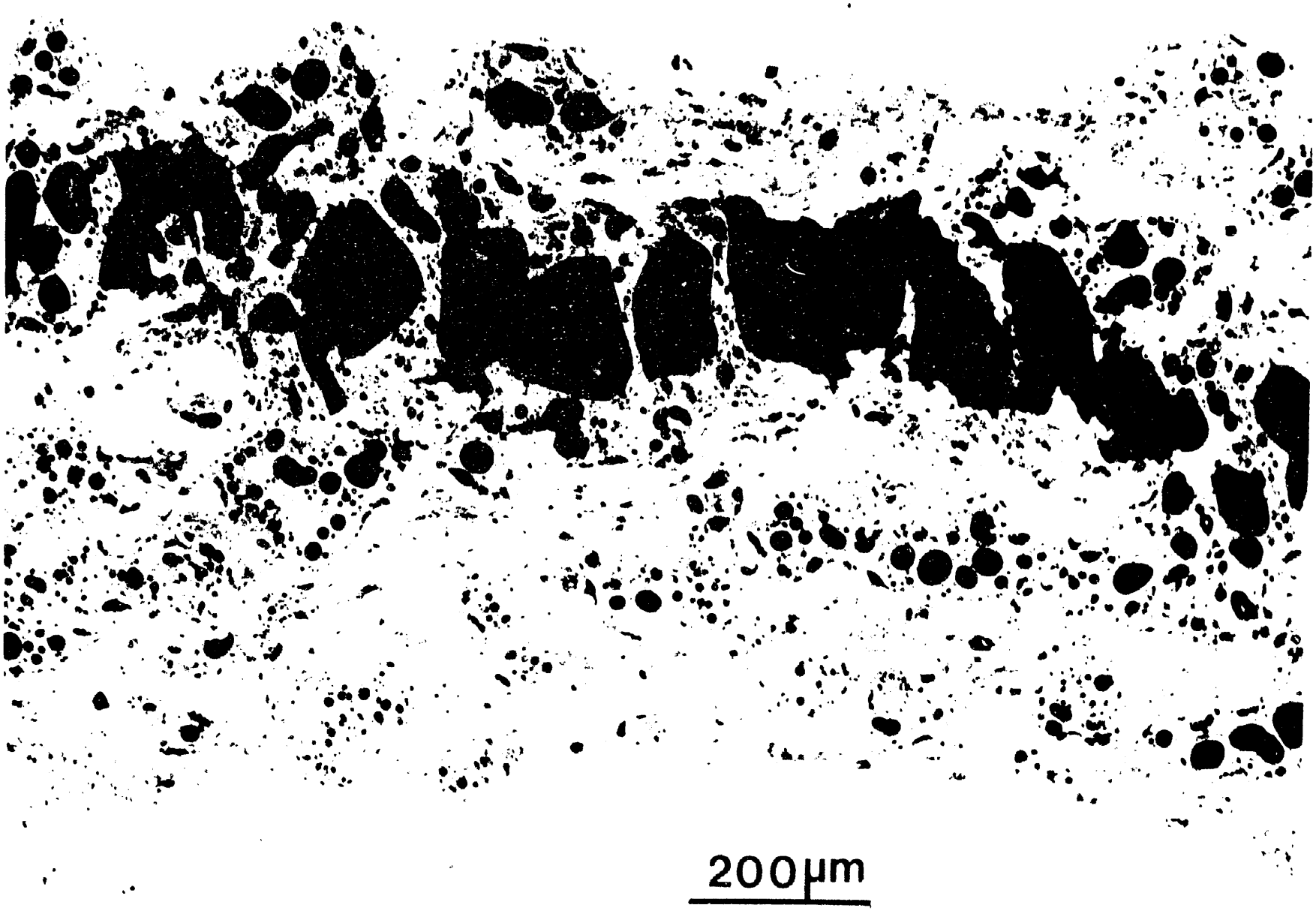

Fig. 2

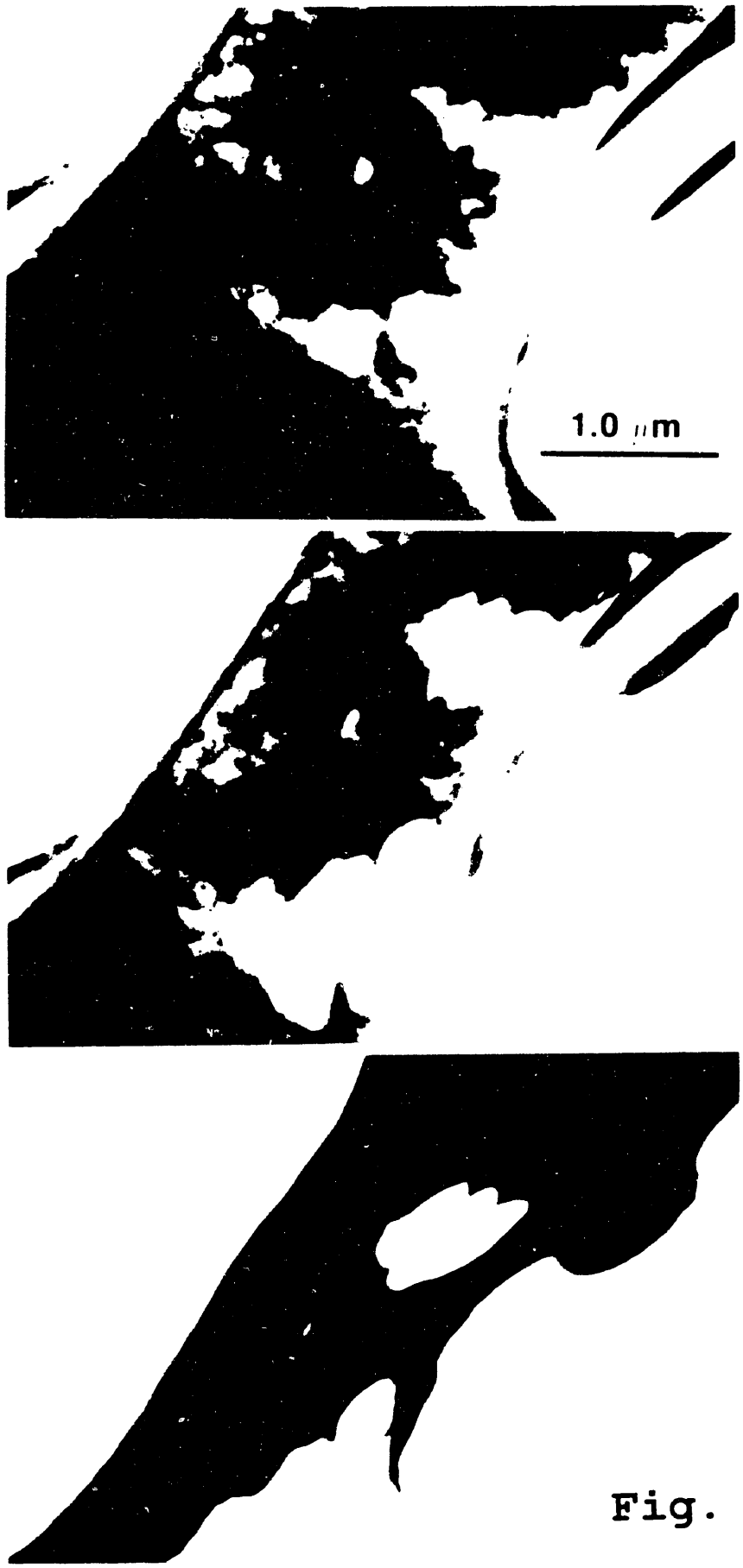

Fig. 3

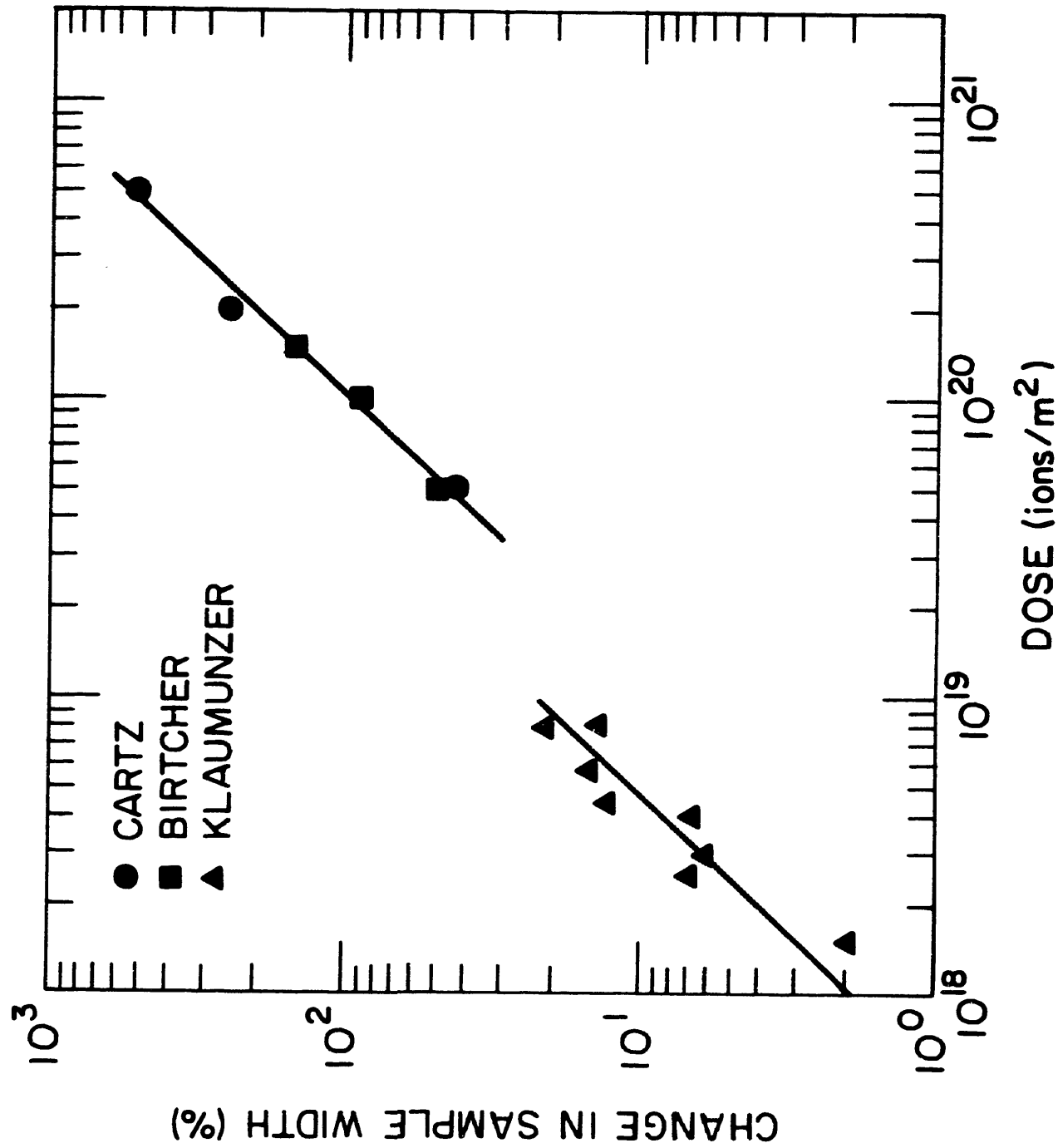
CHANGE IN SAMPLE WIDTH (%)
10^3
10^2
10^1
10^0
10^{18}
10^{19}
10^{20}
10^{21}
DOSE (ions/m^2)
CARTZ
BIRTCHER
KLAUMUNZER

Fig. 4

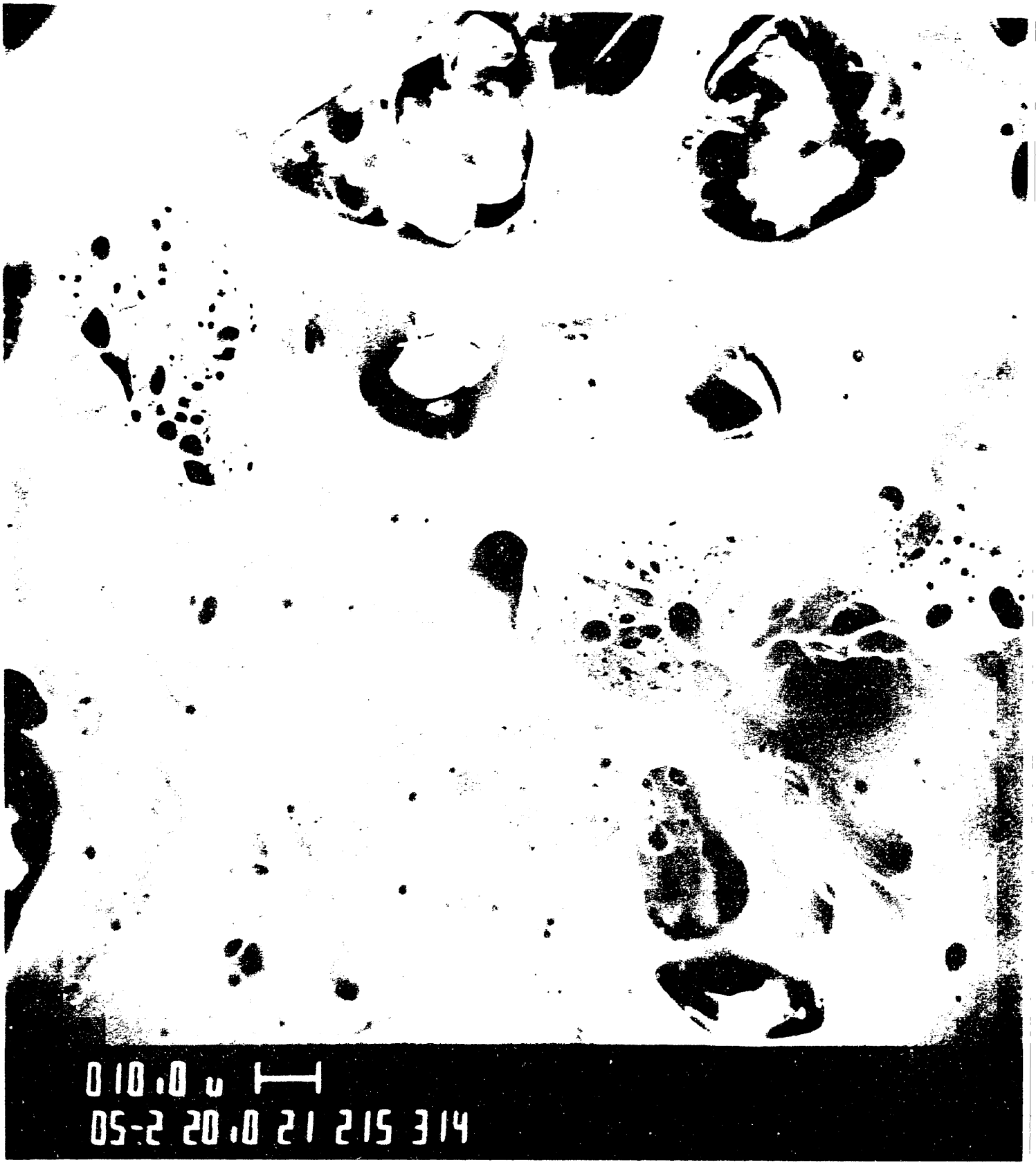

Fig. 5

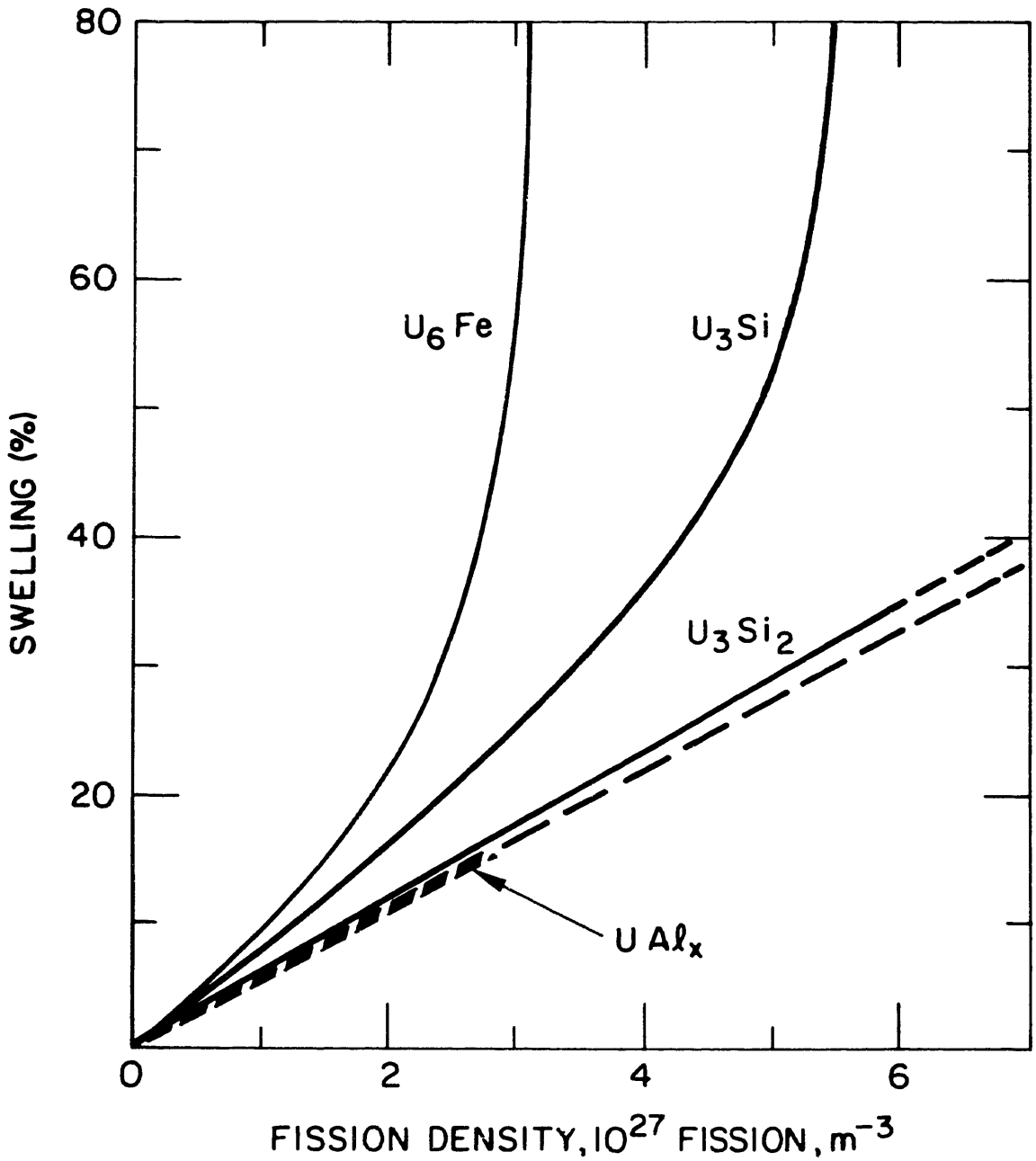
80
60
40
20
0
2
4
6
SWELLING (%)
U_6Fe
U_3Si
U_3Si_2
UAl_x
FISSION DENSITY, 10^{27} FISSION, m^{-3}

Fig. 6

UAl_x, FD = $6 \cdot 10^{27}$ m^{-3}

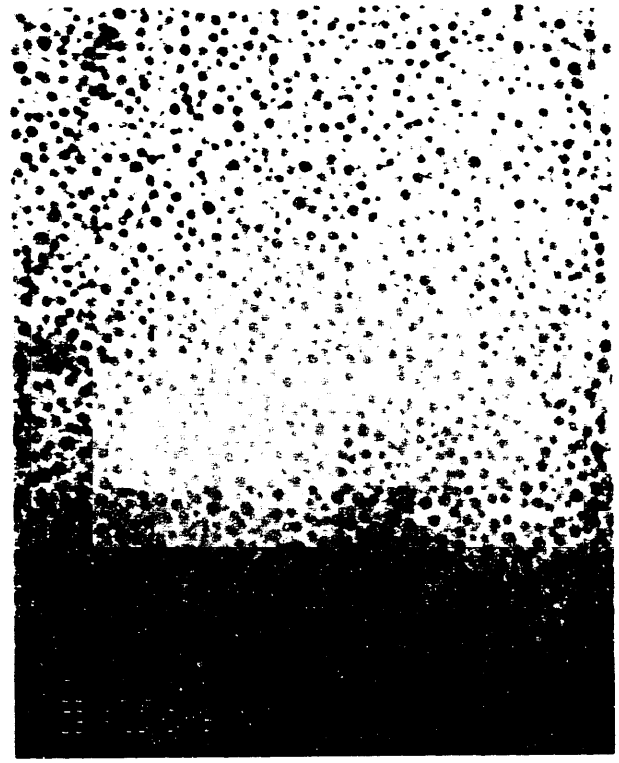

U_3Si_2, FD = $15 \cdot 10^{27}$ m^{-3}

U_3Si, FD = $5 \cdot 10^{27}$ m^{-3}

U_6Fe, FD = $2 \cdot 10^{27}$ m^{-3}

Fig. 7

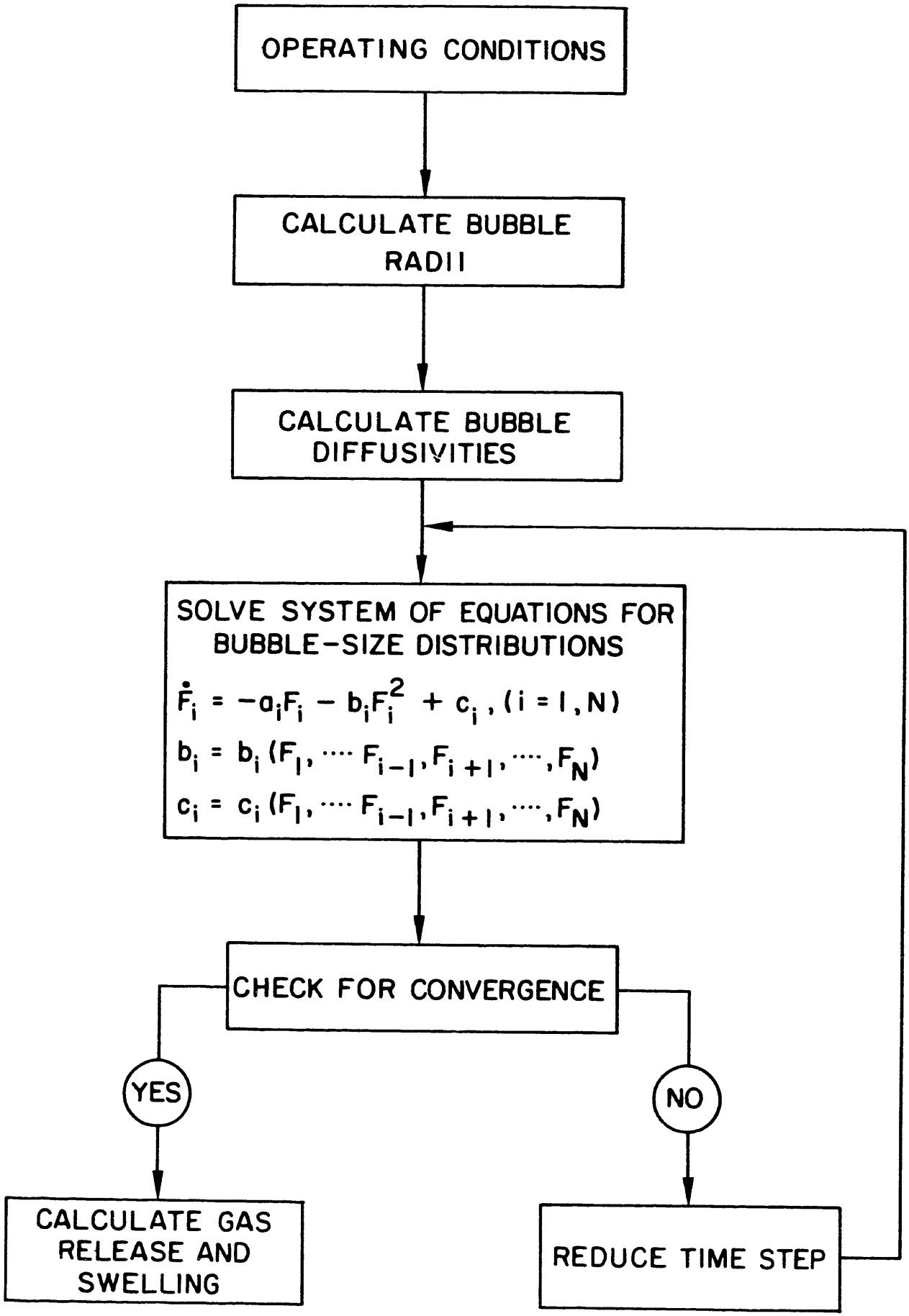
OPERATING CONDITIONS
CALCULATE BUBBLE RADII
CALCULATE BUBBLE DIFFUSIVITIES
SOLVE SYSTEM OF EQUATIONS FOR BUBBLE-SIZE DISTRIBUTIONS
$\dot{F}_i = -a_i F_i - b_i F_i^2 + c_i$, (i = 1, N)
$b_i = b_i(F_1, \cdots F_{i-1}, F_{i+1}, \cdots, F_N)$
$c_i = c_i(F_1, \cdots F_{i-1}, F_{i+1}, \cdots, F_N)$
CHECK FOR CONVERGENCE
YES
NO
CALCULATE GAS RELEASE AND SWELLING
REDUCE TIME STEP

Fig. 8

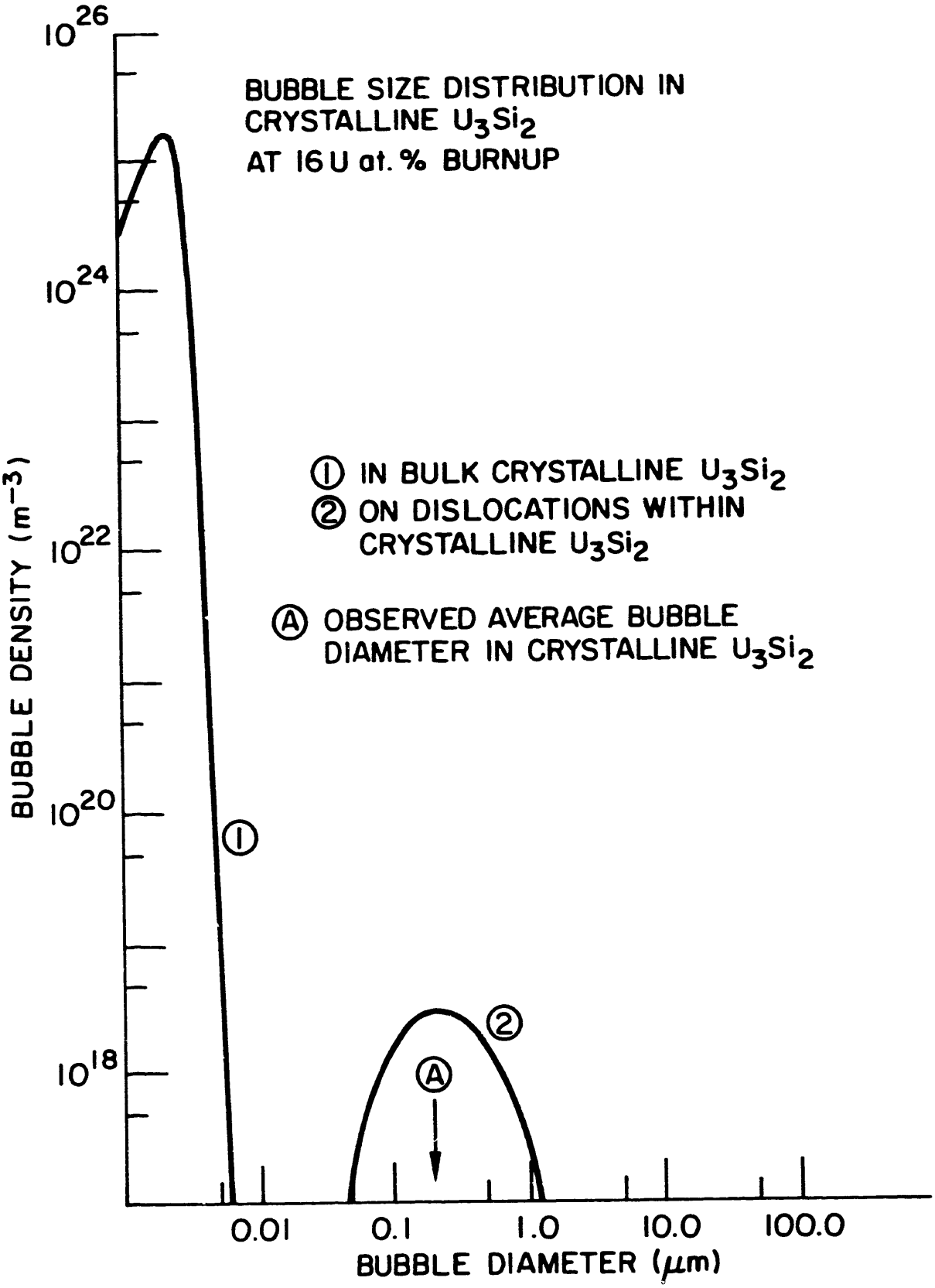
BUBBLE SIZE DISTRIBUTION IN
CRYSTALLINE U_3Si_2
AT 16 U at. % BURNUP
① IN BULK CRYSTALLINE U_3Si_2
② ON DISLOCATIONS WITHIN
CRYSTALLINE U_3Si_2
Ⓐ OBSERVED AVERAGE BUBBLE
DIAMETER IN CRYSTALLINE U_3Si_2
BUBBLE DENSITY (m^{-3})
10^{26}
10^{24}
10^{22}
10^{20}
10^{18}
0.01
0.1
1.0
10.0
100.0
BUBBLE DIAMETER (μm)

Fig. 9

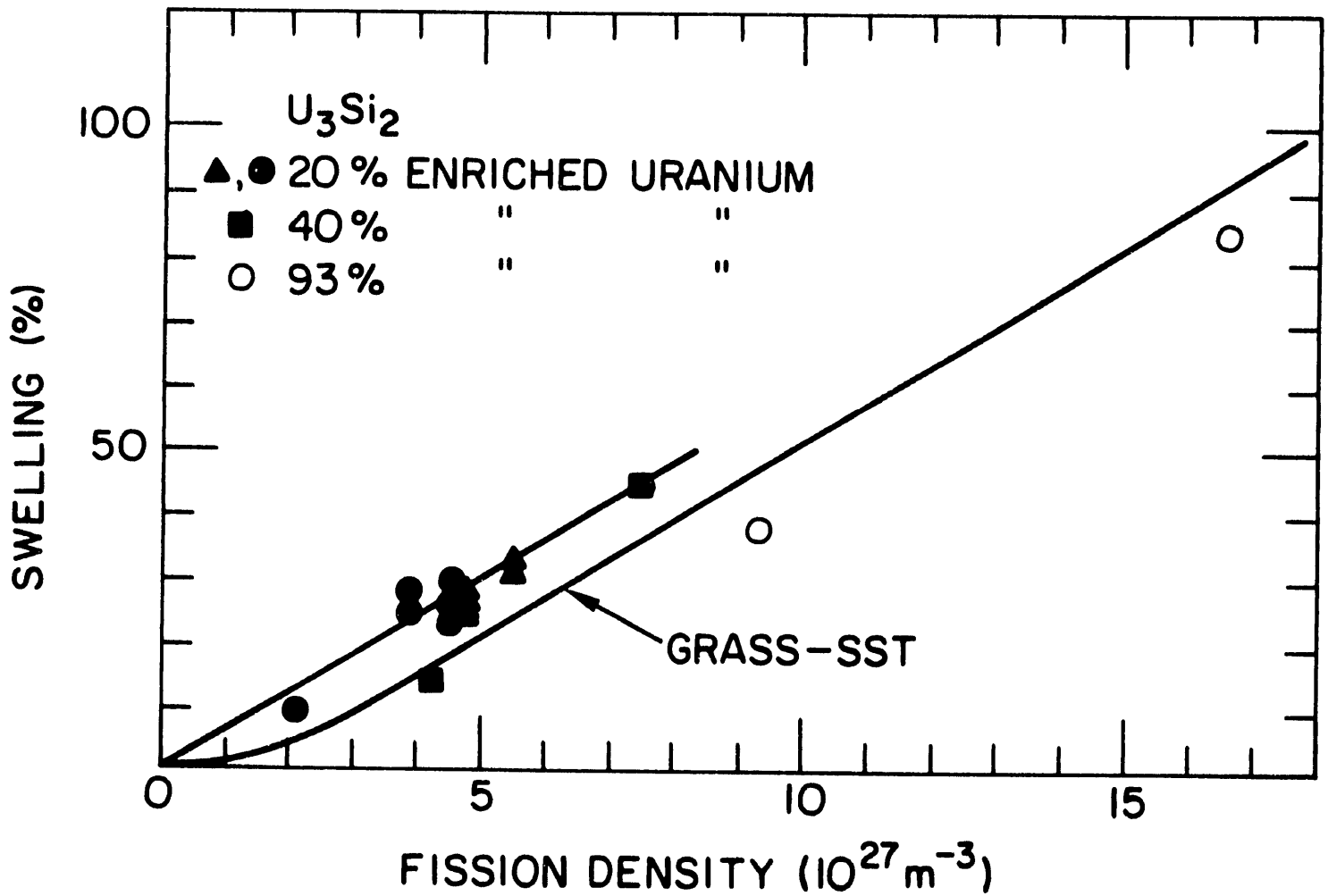
U_3Si_2
▲,● 20 % ENRICHED URANIUM
■ 40 % " "
○ 93 % " "
GRASS-SST
SWELLING (%)
100
50
0
5
10
15
FISSION DENSITY (10^{27} m^{-3})

Fig. 10

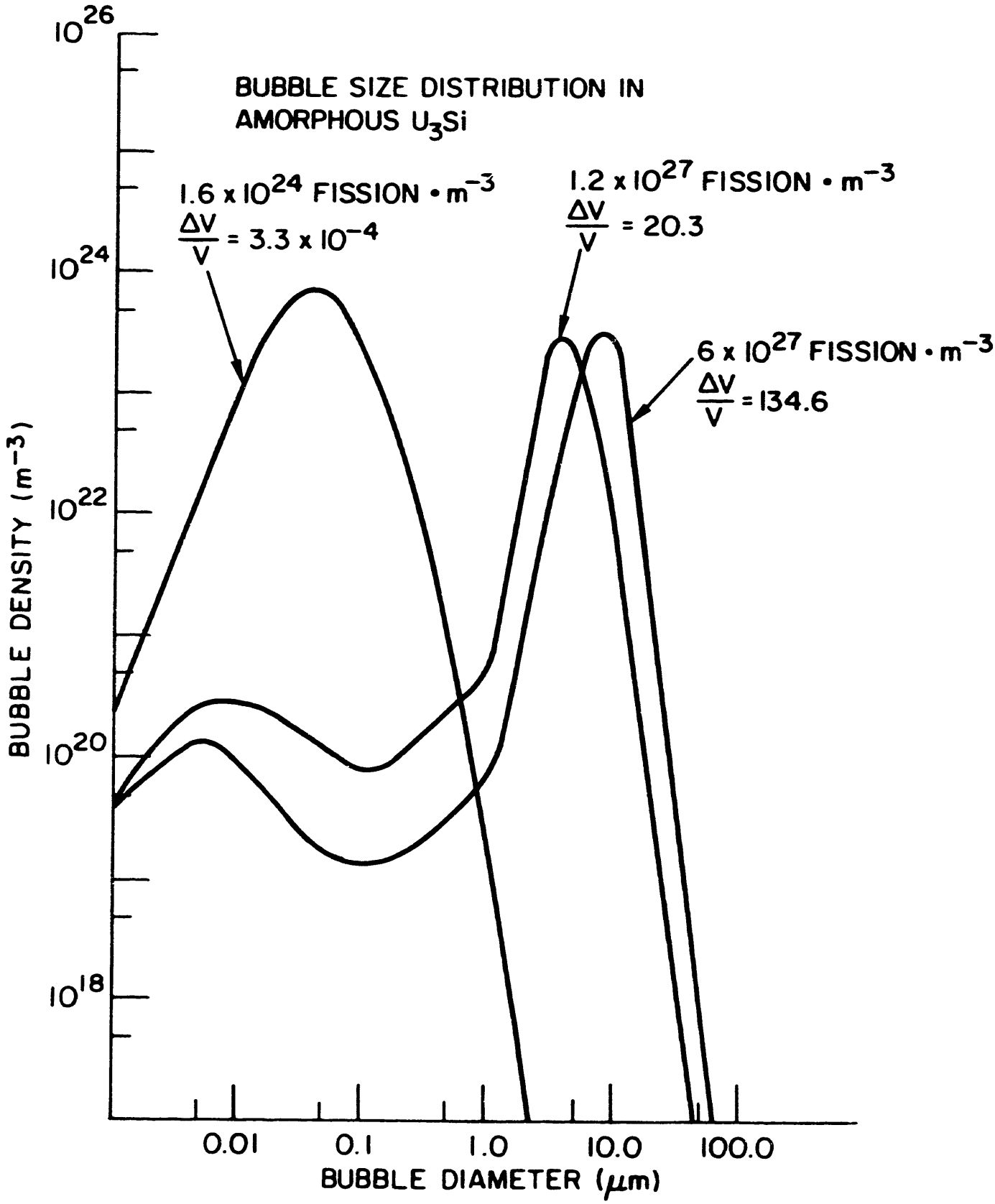
BUBBLE SIZE DISTRIBUTION IN
AMORPHOUS U_3Si
1.6×10^{24} FISSION • m^{-3}
$\frac{\Delta V}{V} = 3.3 \times 10^{-4}$
1.2×10^{27} FISSION • m^{-3}
$\frac{\Delta V}{V} = 20.3$
6×10^{27} FISSION • m^{-3}
$\frac{\Delta V}{V} = 134.6$
BUBBLE DENSITY (m^{-3})
10^{26}
10^{24}
10^{22}
10^{20}
10^{18}
0.01
0.1
1.0
10.0
100.0
BUBBLE DIAMETER (μm)

Fig. 11

Final Results of Test-Irradiations with LEU-Plates at KFA Jülich

W. Krug, E. Groos, J. Seferiadis, and G. Thamm
Kernforschungsanlage Jülich
Federal Republic of Germany

1. Introduction

The irradiation program of the German AF-Program has been terminated recently.

Two irradiation campaigns have been accomplished at the DIDO-reactor at KFA-Jülich.

In total 20 test plates have been irradiated and investigated in the hot cells at KFA-Jülich. Some results have been reported in earlier meetings.

The final results and a summary of all results will be presented.

2. Irradiations

The irradiations have been performed with the so called AF-Loop-Jülich.
Ten test-plates can be inserted in each inpile-section. They are arranged in two groups of five plates each, one above the other with coolant flow upwards.

The first irradiation experiment AF1 was in operation from July 1983 to October 1984.
After 321 full power days (fpd) an average burn-up (U-235 consumption) of more than 80 % had been achieved.

The second irradiation experiment AF2 has been operated from march 1986 to January 1987. It had to be stopped unscheduled after 130 full power days because of a plate failure, which caused a significant increase of the cooling water activity by fission products. An average burn-up (U-235 consumption) of 42 % has been reached. Test-plate and irradiation data are summarized in fig. 1 and fig. 2.

3. Post Irradiation Examinations (PIE)

The post irradiation examinations have been performed in the hot cells of KFA-Jülich corresponding to the PIE-program shown in fig. 3. The numbers behind the titles of the different chapters indicate the number of investigated plates, representing AF1, AF2.

3.1 Visual Inspections

AF1:

All plates were covered with a brittle reddish layer of 1 tenth of a mm ore more, which partly started to peel off. Along the border of the meat small blisters could be seen, also at the thermocouple attachments. Analysis showed, that this layer consisted of Al_2O_3 coloured by 1 % iron. At the start-up of this experiment the cooling water quality came out of control for about 24 hours. Because of a wrong filling of the deionisation filter, a pH-value of 9,1 was reached, which caused the formation of this Al_2O_3-layer.

At the end of the meat zone of one U_3O_8-plate a swelling of about 25 mm in diameter with about the double of the normal plate thickness could be identified. Other deformations could not be seen.

AF2:

All plates were monotonous grey coloured with a thin oxide layer as it is normal for Aluminium-surfaces after irradiation.
At one $U_3Si_{1,3}$-plate a small crack was found at a thermocouple attachment combined with local bulging of lenticular size on both sides of the plate. This crack was identified, also lateron by micrographs as the source of the fission product release.

3.2 Analysis of the plate layer (AF1)

The reddish brown layer of the AF1-plates has been analyzed by three different methods:

- Gamma spectroscopy:

  The main components were Zn65 ($3,6 \cdot 10^6$ Bq/g) and Co6 ($2,0 \cdot 10^6$ Bq/g. Minor components were Mn54, Sc46, Fe59 Sb124 and Cr51. These are all activated products, no fission products were found.

- Quantitative optic-emission spectroscopic analysis:

  Aluminium was found as the main component (32 %), Nickel and Iron as minor components.

- Micro-probe-scanning:

  The same results than before, but in addition oxygen was found.

The layer was identified as consisting of Al_2O_3, coloured by about 1 % of Fe.

3.3 Gamma Scanning

The distribution of the fission products along the area of all test plates of AF1 were measured by gamma-scanning. Based on these results the gamma-scanning for AF2 could be abandoned.
Camma scans have been performed along the length and transvers for the total Gamma-emission (130 to 1470 keV) and for the Nuclides Nb95, Rh106, Cs134, Cs137, Ce144. The plots are showing the relative activity distribution at the date of measurement.

The course of curves of the total Gamma-emission as well of the single Nuklids are equal in the tendency of the respective test plate. This is valid for the highly mobile isotopes (Cs134 and 137) as well as for the isotopes of low mobility (Nb95, Rh106, Ce144), and it means, that local differences of activity are caused by inhomogeneities from the fabrication. There are for instance higher activities at one or both ends of the plates (dog boning), rather clear at the U_3Si-plates, with differences up to 25 % (fig. 4).
The transvers scans for the same plates are showing more or less a clear depression of activity via the middle of the plate (fig. 5).

3.4 Dimensional Measurements

Dimensional measurements have been performed by

- mechanical measurements of plate thicknes (AF1),
- optical measurements of plate thickness (micrographs, AF1),
- volume change determination (AF1, AF2).

The mechanical measurements of the plate thicknes has been performed by two movable feelers. The distance between them (plate thickness) has been recorded via an inductive displacement pick-up. The accuracy of these measurements was ± 0,001 mm.
The measurements for each plate have been made along three lines, on which also the five measuring points of the pre-irradiation measurements were lying.
The five U_3Si_2-plates alltogether showed a reduction of thickness, caused by a chemical attack of the cooling water at the start of the irradiation. The average value is -(4,3±1,7)%. Also the two U_3O_8-plates still showed a small decrease of thickness, except the distinct local swelling at one plate with 53 % in maximum.

The average value was -(1,15±2,87)%. Against them all U_3Si-plates showed a significant swelling with an average value of +(7,9±10,0)%. The large scattering is regarded by the great standard deviation.

The optical measurements of plate thickness have been performed at micrographs by an ocularmicrometer. In addition to the measurements of the total plate thickness also the thickness of the meat could be measured. The results of the mechanical and optical measurements are in a good agreement.
The optical measurements indicate, that for the U_3Si_2-plate there is a small but significant swelling of the meat of about 6 % concealed by the decrease of the total thickness of this plate.
The swelling of the meat of the U_3Si-plate was much more stronger, in minimum 13 %, in maximum 110%.

Regarding these values for the particular pure fuel the following values of relative swelling are determined:

U_3Si_2 (45 Vol.%)	:	14 %,
U_3Si (42 Vol.%)	:	31 % min,
		260 % max.

The swelling of the fuel zone has been also determined by the volume change of the plates during irradiation. The volume of the plates as well as their weight have been determined before and after irradiation. The volume change provides a mean value for the whole plate which can be corrected by the cladding loss out of the weight difference. Oxide layer removal (Aloca Bright Dip) and volume change determination (immersion) were performed according to procedures used for PIE of LEU plates at ANL.

The following results were found:

AF1:

Weight and volume of all plates had decreased. The weight losses are refered to the loss of cladding by corrosion.

The average weight decrease of (5,4 $\pm$ 0,8)% corresponds to a reduction of cladding betweeen 0,04 to 0,05 mm on each side. This is in good agreement with the optical measurements (0,045 mm). The average weight decrease for the U_3Si_2- and U_3O_8-plates was (5,1 $\pm$0,8)%, for the U_3Si-plates only 1,4 %.

As a result of the swelling of the fuel zone the netto volume increase of the test plates was for U_3O_8- and U_3Si_2-plates (1,9$\pm$0,8)% and for U_3Si-plates 7,0 %.

AF2:

As expected the volume and weight changes are remarkably lower than for AF1. The volume decrease was measured between 1,7 and 3,2 %, which was correlated with a weight decrease between 1,3 and 2,3 %. Particularly low are the values for the swelling of the fuel zone, which are between -0,2 and +0,3 %.

In fig. 6 the main results of the dimensional measurements are listed up.

The volume increase of the different fuel-types are shown in fig. 7 as a function of the fuel fission density. The solid lines represent the results of the US-RERTR-program. The consistency of the results of both programs looks very good.

U_3Si_2 and $U_3Si_{1,3}$, $U_3Si_{1,5}$ are lying in the range of linear swelling, where a good irradiation behavior can be expected. The U_3Si-plates are highly in the range of break away swelling, so that a bad irradiation behavior must be expected.

3.5 Metallographic Examinations

Four plates of AF1 and AF2 respectively have been used for metallographic examinations. The microstructures of the fuel were investigated by optical microscopy up to magnifications of 500x.

A transvers section through the swelled area of the defect plate (AF2) showed, that a crack has developed in the edge of the thermocouple groove. The rest of the cladding was to thin to withstand all stresses during irradiation. About 15 mm around the leak the

microstructure of the meat is totally destroyed. The lenticular swelling to both sides of the plate seems to be caused by steam generated from penetrating water. Beyond this reaction zone the fuel remained completely uninfluenced. This makes clear that the defect has a mechanical reason caused by the cutting of the croove.

Typical pictures of transvers sections of all four types of fuel (AF1) are shown in fig. 8, 9, 10 and 11 (magnification 50 and 500). The U_3Si_2-plates (4,75 resp. 5,04 gU/cm³) behaved very well (fig. 8, 9). Only small fission gas bubbles have been formed, which are uniformly distributed within the fuel particles. The bonding between fuel particles and the metallic phase (Al) or the cladding is completely intact.

U_3Si (6,05 gU/cm³, fig. 10), however, is in the range of break away swelling. Fuel particles have linked up to a high extent loosing their identity. Large gas bubbles (up to 0,5 mm) have accumulated, opening extended cavities in the central region of the fuel meat. The occurance of pillowing without further irradiation due the thermal cycling effects only seems highly probable. Also these results are in an excellent agreement with the ANL-PIE results.

The U_3O_8 plate (fig. 11) which pillowed during irradiation shows large gas bubble formation only in the region of the pillowed blister and here only betweeen meat and cladding, not in the centre region. At one side cladding and meat are separated by a large gap. The remaining parts of the meat (non-pillowed) show a quite normal microstructure similar to that of U_3Si_2 resp. unirradiated U_3O_8.

The micrographs of the $U_3Si_{1,3/1,5}$-plates with and without B_4C show a rather undisturbed microstructure of the meat, which indicates a low burn-up (40 % U235). Only a low amount of small gas bubbles can be recognized, which don't influence the microstructure anyway.

Remarkable however ist the presence of singular larger gas bubbles, which cannot be accumulated by diffusion due to the achieved burn-up. This must explained by the influence of the contained U_3Si. An influence on the integrity of the meat with this burn-up can be neglected. But these bubbles can be the origin of damages at higher burn-ups.

An influence of the B_4C has not been found.

3.6 Blister Tests

One plate of each fuel type has been selected for the blister test, i.e. four plates of AF1 and AF2 respectively. Four plates have been heated up together in each case in air to the desired temperature, starting with 350°C, increasing in 50° and above 500° in 25° steps, and held there for 30 minutes. After cooling down to room temperature, the plates were inspected visually. Plates with blisters were removed and testing was continued.

The results are listed up in fig. 12. The order of the listing indicates the behaviour of the plates starting with the worst plate and ending with the best.

Beside the dimensional measurements also the blister tests indicate clearly, that U_3Si_2 as fuel is superior to the other alternatives, particularly if it is considered, that the $U_3Si_{1,3}$-, $U_3Si_{1,5}$-plates had only achieved half the burn-up.

3.7 Fission Product Release Tests

The aim of these tests was to investigate the release of gaseous (Kr85) and solid (Cs137) fission products from defect plates during transport or storage. Therefore 4 plates have been cut through (simulation of a mechanical damage) and the halfs were heated up to 300°C in steps of 100°C. The pieces were standing in a small oven with the cutting areas two cm deep in a loose charcoal bed for removing solid fission products.
The results of Kr85 release are shown in fig. 13, those of Cs137 and Ce144 in fig. 14.

In general the results for the U_3Si_2-plates show a lower release as well for Kr85 ($1 \cdot 10^{-4}$ of the inventory) as for Cs137 and Ce144 (1 to $2 \cdot 10^{-7}$ of the inventory). It is of importance, that the very low release of the solid fission products for both isotopes has nearly the same fraction. This means, that there is no temperature dependant diffusion. Both fission products probably came into the charcoal by mechanical abrasion of fuel from the cut areas. In principle it is a dust contamination.

The U_3Si-plate released nearly the same Kr85-activity as the U_3Si_2-plates, although a higher release could be expected caused by the changed micro structure.

The reason is, that Kr has diffused into the large and combined gas bubbles even during irradiation. When the plate has been cut through, this gas released immediately. It has been registrated in the vent system of the hot cells. A recalculation resulted in a Kr85-release of about 10 % at that time, which is about a factor of 1000 more than during the annealing test.
The results of these annealing tests can be summarized as follows:

- Fission gases: At normal temperature (< 30 °C), no release can be measured, at higher temperatures (up to 300 °C) for an undisturbed microstructure the available reservoir is quickly discharged so that the release is reduced to zero soon. J131 could not be measured. With the presence of water it is expected that it will behave like fission gases.

- Solid fission products: At temperatures up to 300 °C no release by diffusion must be expected, even for the high mobile Cs. But at all temperatures a dust contamination by abrasion must be taken in account.

4. Conclusion

This irradiation program was mainly concentrated on the investigation of uranium silicides. 4 uranium silicides (U_3Si, $U_3Si_{1,3}$, $U_3Si_{1,5}$, U_3Si) an U_3O_8 (as a reference fuel) have been irradiated and examined in hot cells at KFA-Jülich.
Significantly different irradiation behavior have been found between U_3Si_2 and U_3Si.
All results of the German AF-program are in a good agreement with the respective results of the ANL-PIE results (G.L. Hofman, L.A. Neimark).

U_3Si_2 showed

- lower swelling (well below 10 %), far away from break away swelling,
- moderate microstructure changes,
- higher blister thresholds (> 500 °C),
- lower release rates of fission products for defect fuel elements.

Based on these results, no burn-up limits have to be considered, as also stated by J.L. Snelgrove.

Also $U_3Si_{1,3/1,5}$ has shown a good irradiation behavior, but only the half of burn-up has been reached. Nevertheless the microstructure contains agglomerations of fission gas bubbles, which are typical for U_3Si. Therefore it must be expected, that the further irradiation behavior will be dominated by the U_3Si component. That means, that also for this fuel the same limits of burn-up will be valid ($1{,}8 \cdot 10^{21}$ cm^{-3}), as stated by J.L. Snelgrove for U_3Si.

As the essential result of this irradiation program U_3Si_2 has been proven as a pontential fuel for the conversion to low enriched fuel elements for test reactors. Therefore no further activities to investigate alternative fuels are necessary for us and therefor the irradiation programs have been terminated.

5. References

/1/ E. Groos, H.J. Bücker, H. Derz, R. Schröder
Nachbestrahlungsuntersuchungen an Testplatten für niedrig angereicherte Brennelemente für Forschungsreaktoren
KFA-HZ, Mai 1988

/2/ G. Thamm
The Status of the German AF-Program
This Conference

/3/ G. Thamm
The Status of the German AF-Program and Thoughts Toward a Nationally and Internationally Coordinated Termination of the Programs
Int. RERTR-Meeting, Buenos Aires, Argentina, Sept. 28 - Oct. 01, 1987

/4/ J.L. Snelgrove
Qualification Status of LEU Fuels
Int. RERTR-Meeting, Buenos Aires, Argentina, Sept. 28 - Oct. 01, 1987

/5/ G.L. Hofmann, L.A. Neimark
Prospects for Stable High-Density Dispersion Fuels
Int. RERTR-Meeting, Buenos Aires, Argentina, Sept. 28 - Oct. 01, 1987

/6/ E. Groos, W. Krug, G. Thamm
LEU Fuel Testing at KFA-Jülich under the German AF-Program, Plate Irradiation and PIE
Int. RERTR-Meeting, Buenos Aires, Argentina, Sept. 28 - Oct. 01, 1987

Final Results of Test-Irradiations with LEU-Plates at KFA Jülich

Fig. 1

Test-Plate Data

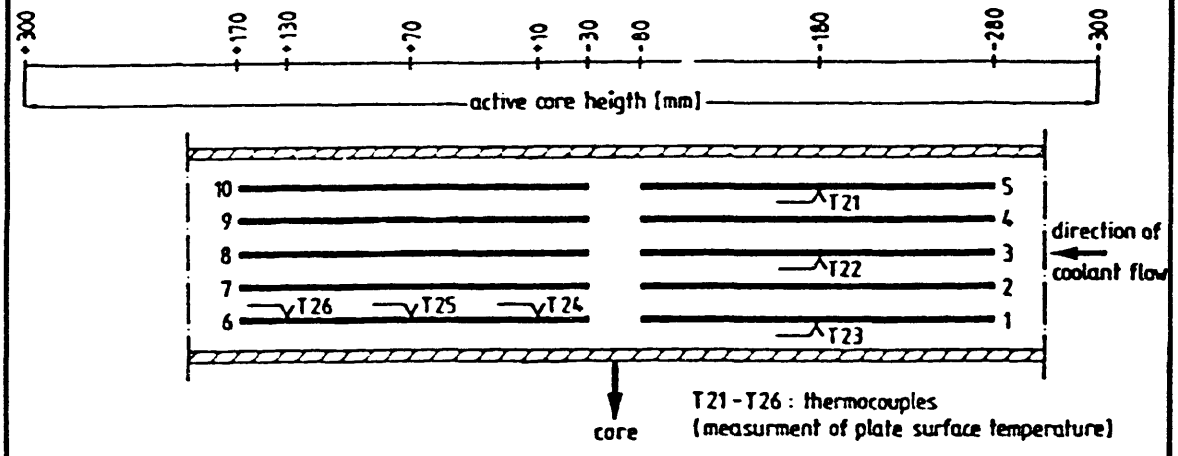

Test Plates: 200 × 60 × 1,27 mm
Meat: 190 × 50 mm
Cladding: AlMg2

U-235 – Content:
- **AF1:** 4,38 g/plate
- **AF2:** 6,00 g/plate

Final Results of Test-Irradiations with LEU-Plates at KFA Jülich	Fig. 2

Test-Plate and Irradiation Data

Fuel	Nr.	Meat thickness mm	U-Density g/cm³	U-235 Enrichm. %	Burn-up fiss./cm³	Exp.
U_3Si_2	3	0,51	4,75	19,75	1.9×10^{21}	AF1
U_3Si_2	2	0,48	5,04	19,75	$2,0 \times 10^{21}$	
U_3Si	3	0,40	6,05	19,75	$2,4 \times 10^{21}$	
U_3O_8	2	0,51	2,34	40,00	$1,9 \times 10^{21}$	
$U_3Si_{1,5}$*	4	0,56	6,0	19,70	$1,1 \times 10^{21}$	AF2
$U_3Si_{1,3}$*	6	0,52	6,5	19,78	$1,2 \times 10^{21}$	

* 2 resp. 3 plates with B_4C

AF1: July 1983 to Oct. 1984, 321 fpd

AF2: March 1986 to Jan. 1987, 130 fpd

Final Results of Test-Irradiations with LEU-Plates at KFA Jülich	Fig. 3

PIE - Program

- Visual inspections (10, 10),
- analysis of the plate layer (AF1),
- gamma scanning (10,0),
- dimensional measurements (10,4),
- metallographic examinations (4,4),
- blister tests (4,4),
- fission product annealing tests (3,1).

Final Results of Test-Irradiations with LEU-Plates at KFA Jülich	Fig. 4

Gamma Scans U_3Si-plate (along the length)

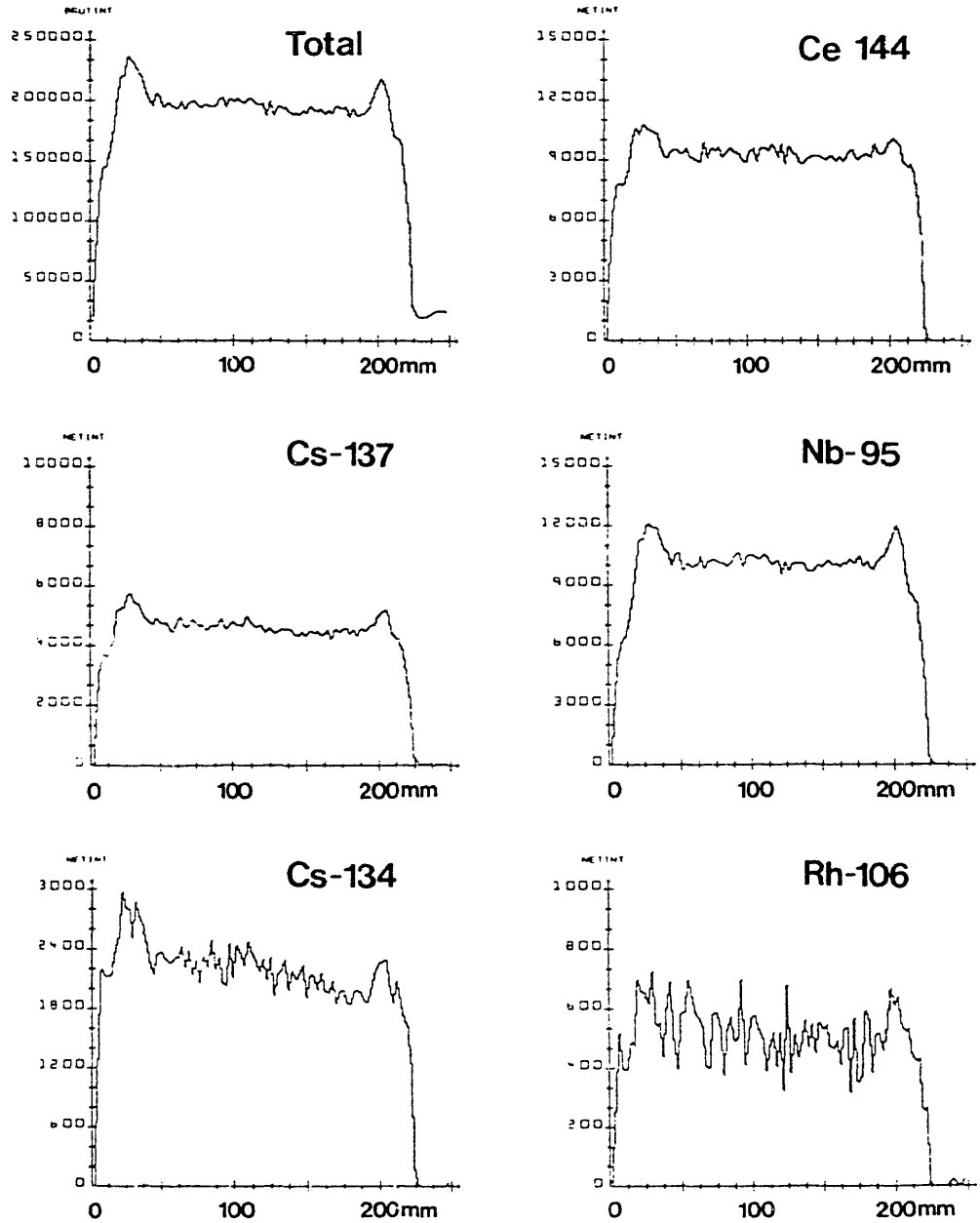

Final Results of Test-Irradiations with LEU-Plates at KFA Jülich	Fig. 5

Gamma Scans U_3Si-plate (transvers)

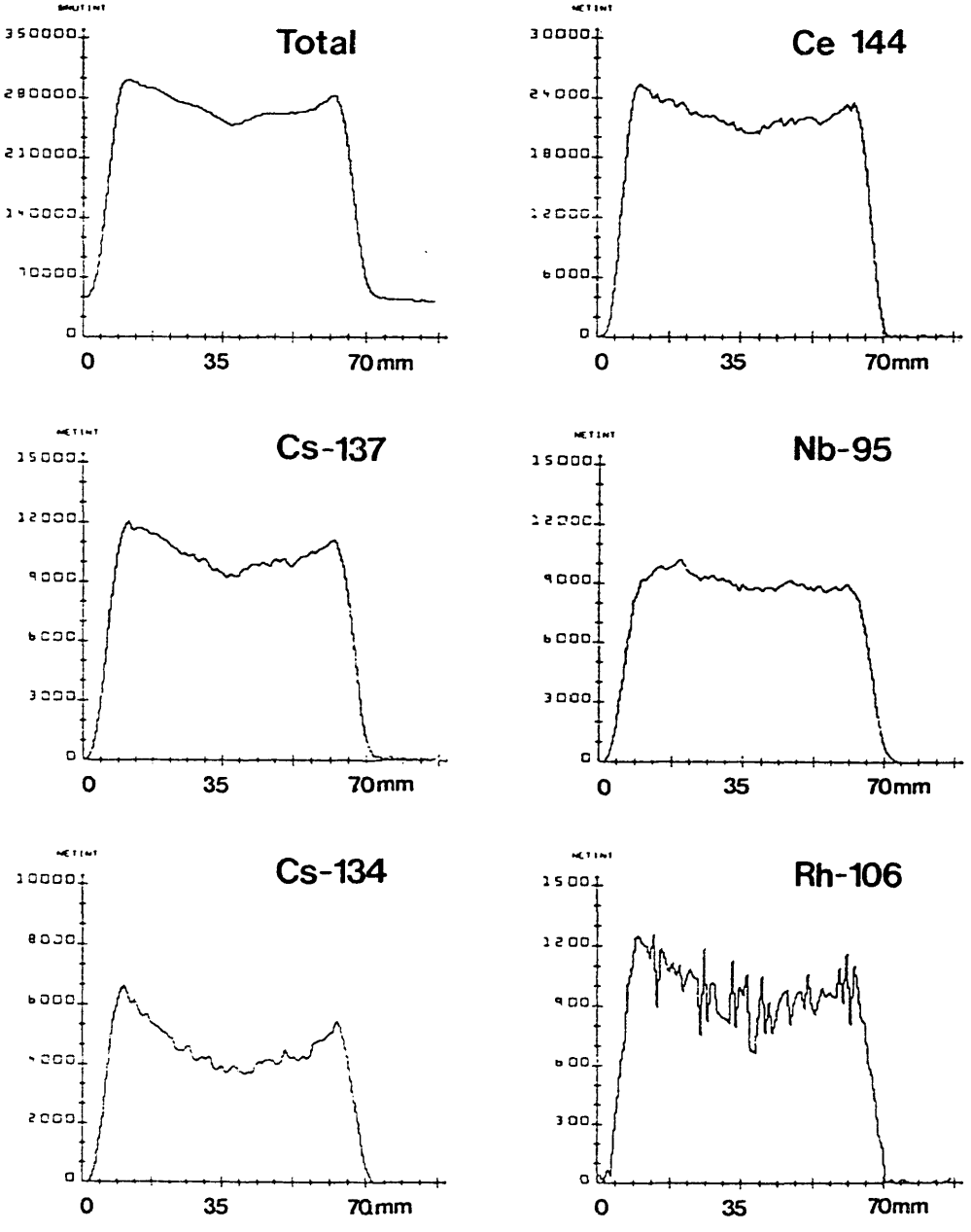

Final Results of Test-Irradiations with LEU-Plates at KFA Jülich	Fig. 6

Results of Dimensional Measurements

Exp.	Fuel (U-density)	Cladding reduction (one side) mm	Rel. swelling of fuel zone %	Rel. swelling of fuel %
AF1	U_3Si_2 (4.75)	0.04	7.3	29.6
	U_3Si_2 (5.04)	0.04	4.3	28.0
	U_3Si (6.05)	0.05	32.4	85.5
	U_3O_8 (2.34)	0.05	5.7 (13.1)	26.9 (49.0)
AF2	$U_3Si_{1.3}$ (6.5)	0.02	1.45	16.2
	$U_3Si_{1.5}$ (6.0)	0.01	0.55	13.2

Final Results of Test-Irradiations with LEU-Plates at KFA Jülich	Fig. 7

Volume Change of Fuel as Function of Fuel Fission Density

(Curves according to G.L. Hofman and L.A. Neimark, ANL)

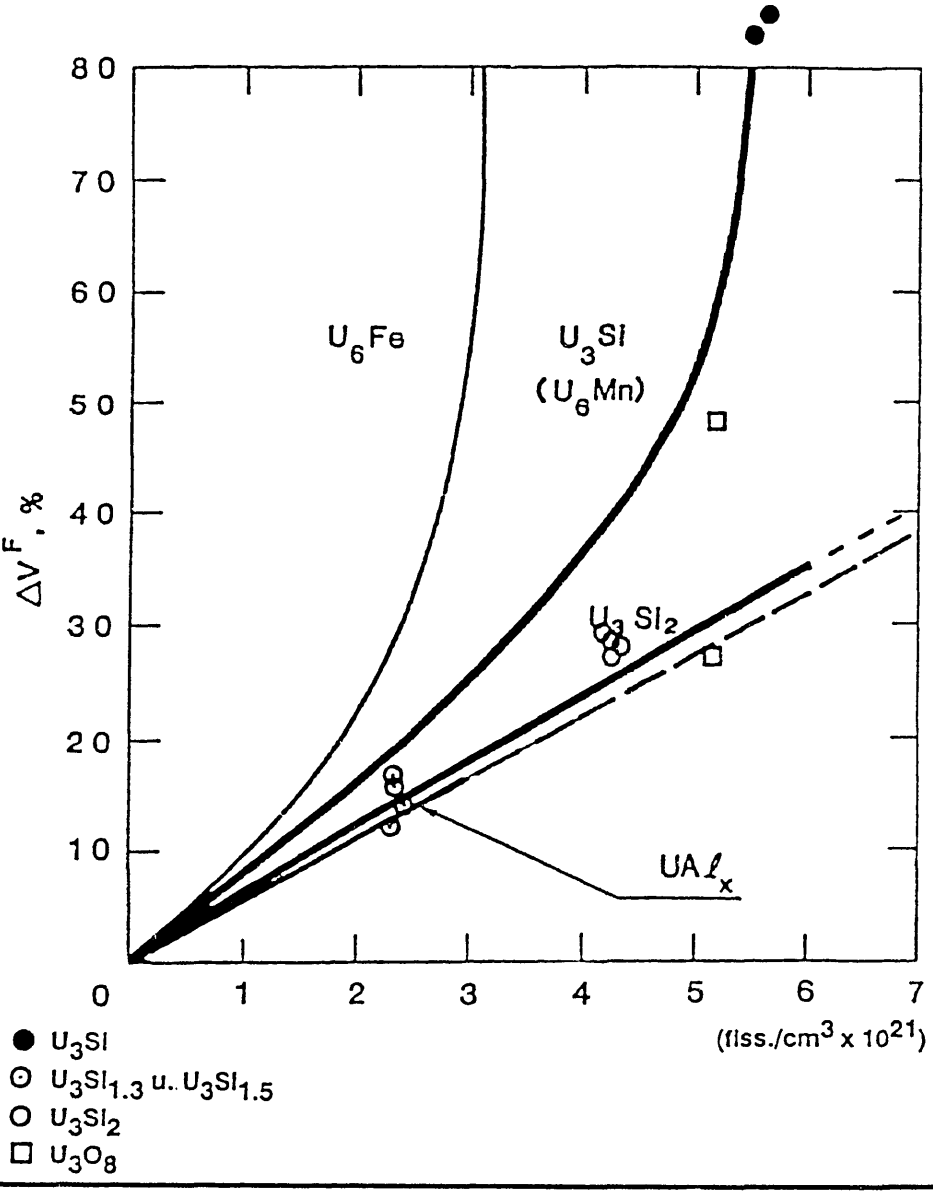

Final Results of Test-Irradiations with LEU-Plates at KFA Jülich

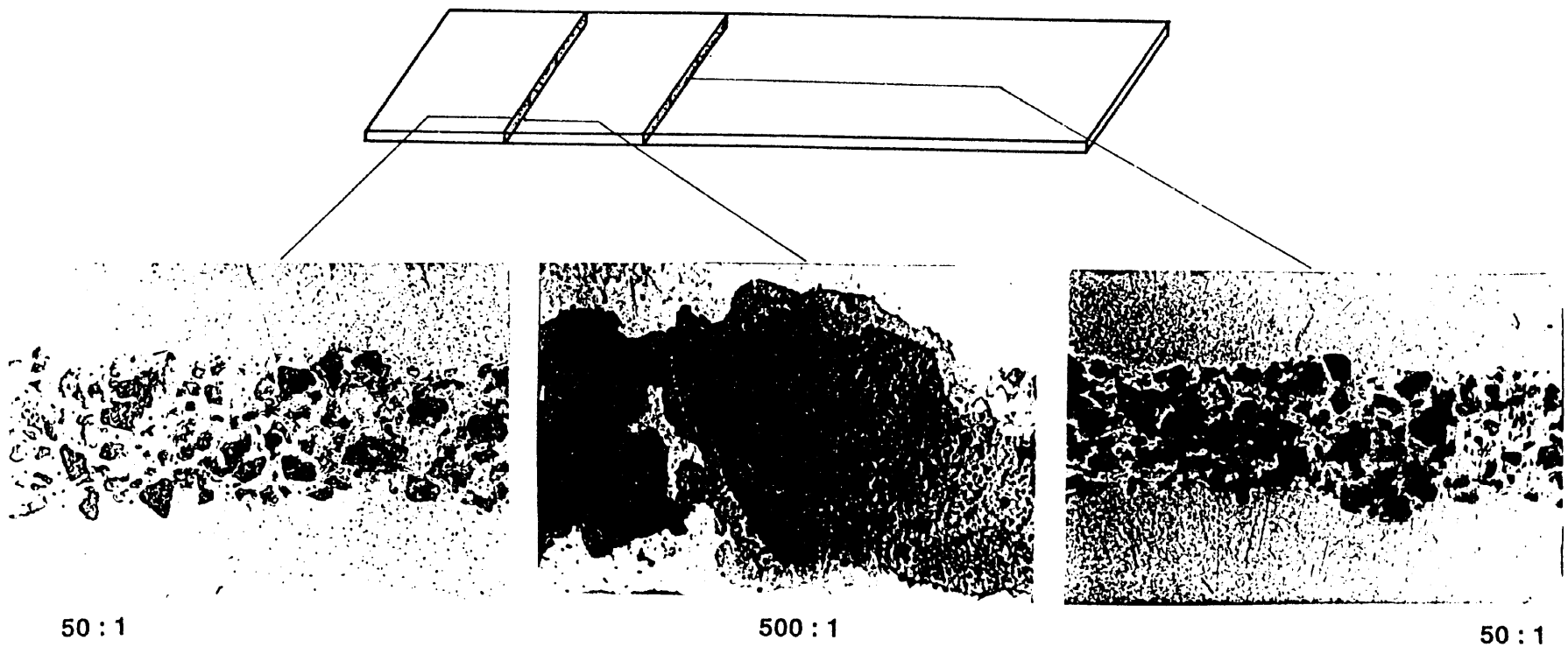

Fig. 8 Microstructure of a U_3Si_2 fuel plate (No. 10) with fission densities of 1.9×10^{21} f/cm^3 (4.75 gU/cm^3, U-35: 19,75 %)

Final Results of Test-Irradiations with LEU-Plates at KFA Jülich

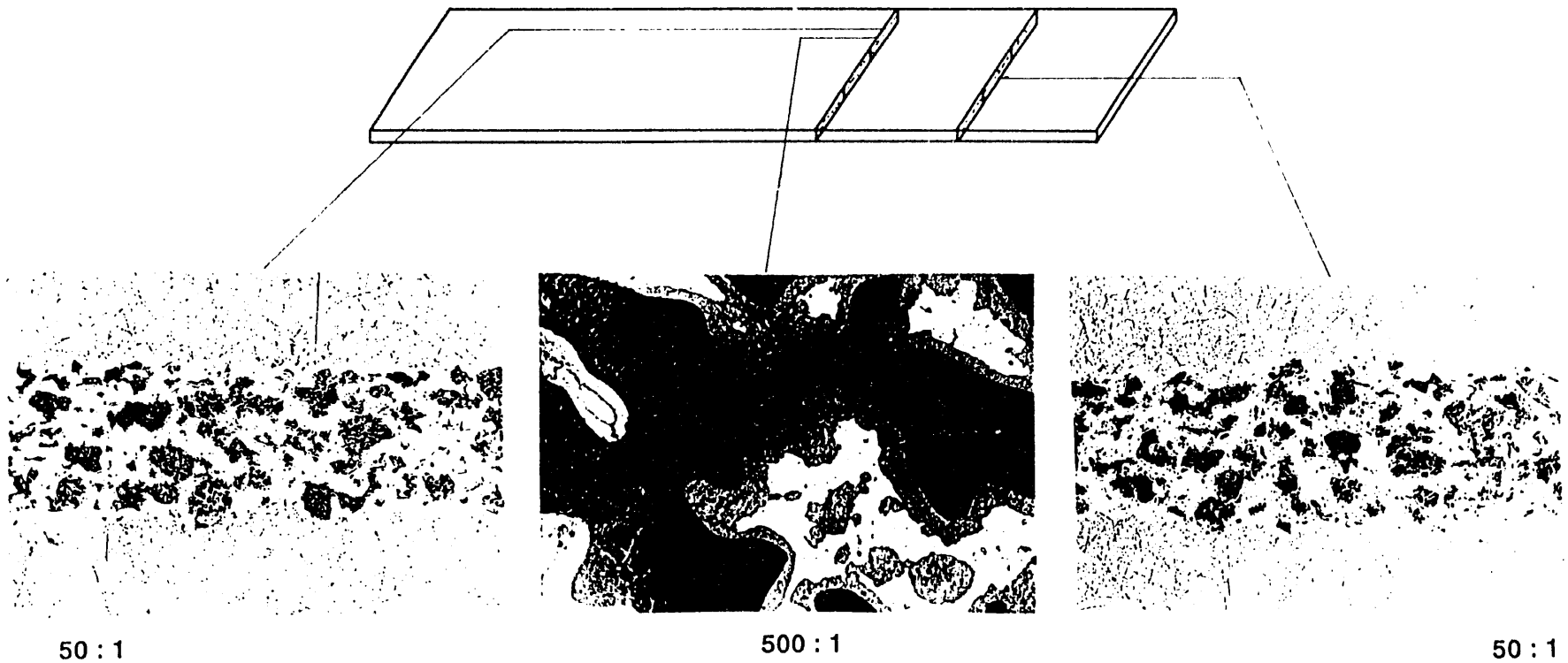

Fig. 9 Microstructure of a U_3Si_2 fuel plate (No. 3) with fission densities of 2.0×10^{21} f/cm^3 (5.04 gU/cm^3, U-35: 19,75 %)

Final Results of Test-Irradiations with LEU-Plates at KFA Jülich

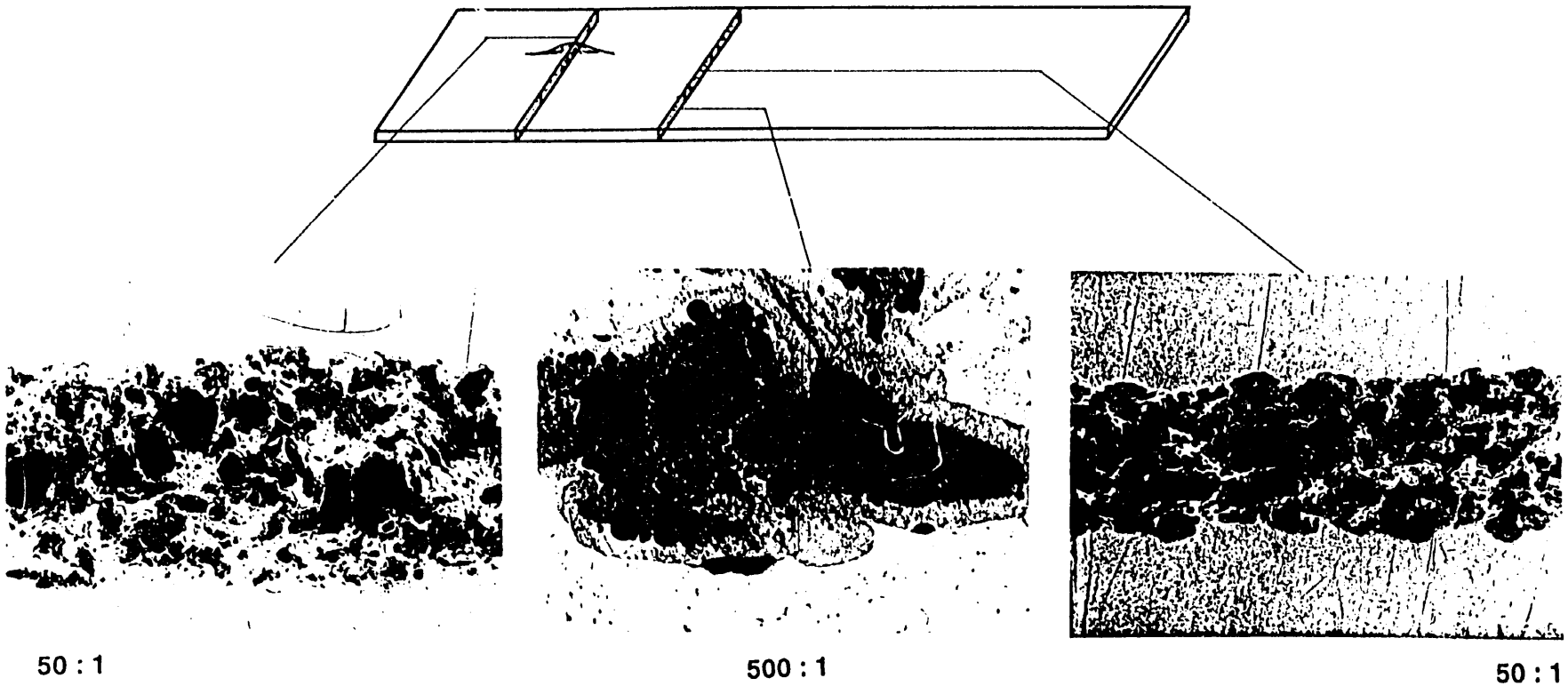

Fig. 10 Microstructure of a U_3Si fuel plate (No. 4) with fission densities of 2.4×10^{21} f/cm^3 (6.05 gU/cm^3, U-35: 19,75 %)

Final Results of Test-Irradiations with LEU-Plates at KFA Jülich

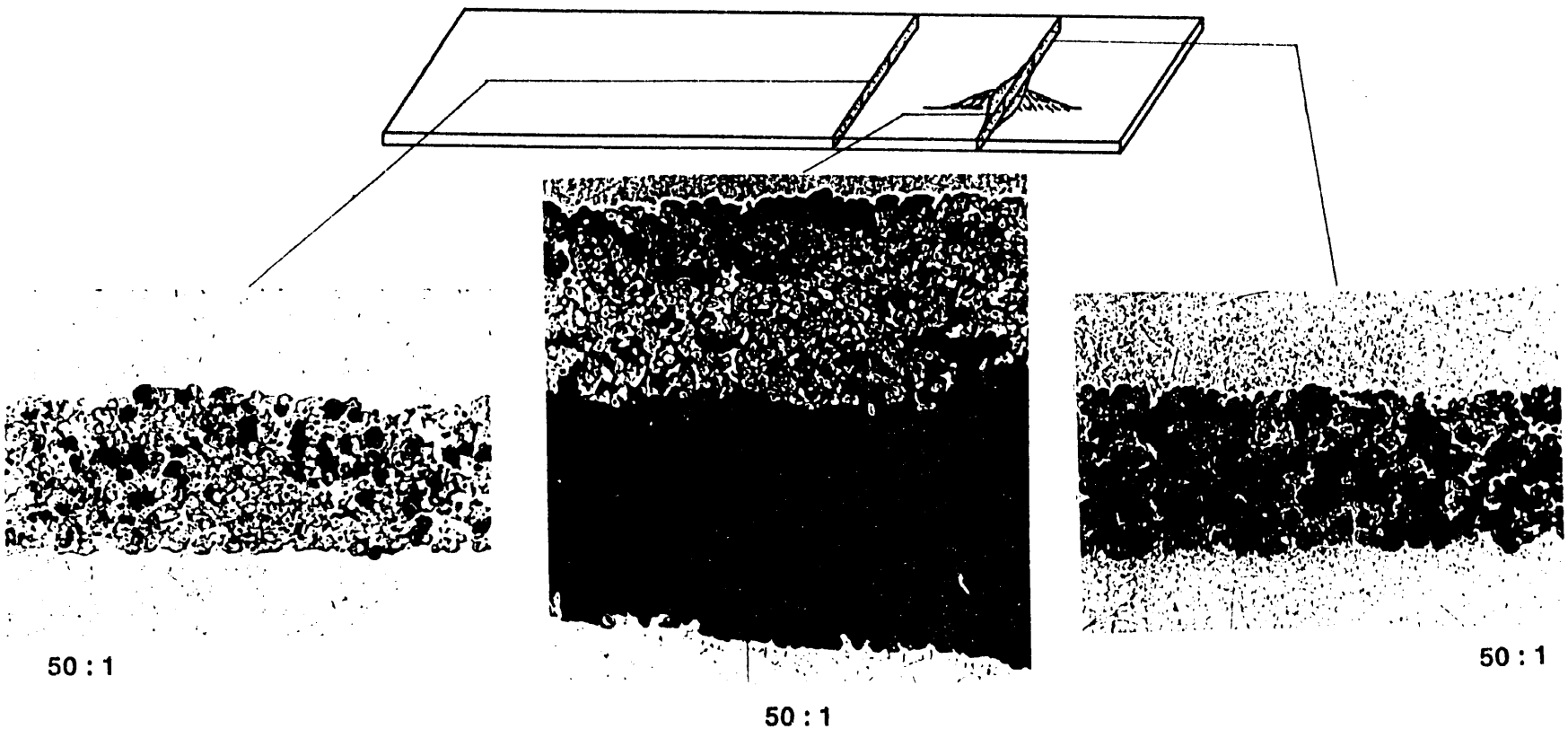

Fig. 11 Microstructure of a U_3O_8 fuel plate (No. 1) with fission densities of 1.9×10^{21} f/cm^3 (2.30 gU/cm^3, U-35: 40.00 %)

Final Results of Test-Irradiations with LEU-Plates at KFA Jülich	Fig. 12

Results of Blister Tests

Temp. °C	Fuel type	Fuel density g/cm³	Results
400	U_3O_8	2.34	Irradiation blister enlarged (leak)
500	$U_3Si_{1.5}$	6.0	Plate strongly bended,large blister with two holes
	U_3Si	6.05	Very large blister covering half of plate. Plate bended like a S.
	$U_3Si_{1.3}$ (B_4C)	6.5	(At 400° C start of bending, strong bending at 450° C). Strongly bended, large blister.
	$U_3Si_{1.3}$	6.5	(Bending like before). Strongly bended.
525	U_3Si_2	5.04	Many small blisters mainly along the meat border and a small hole. Slightly bended.
	$U_3Si_{1.5}$ (B_4C)	6.0	1 large blister, strongly bended like a S.
	U_3Si_2	4.75	Many small blisters mainly along the meat border, slightly bended.

Final Results of Test-Irradiations with LEU-Plates at KFA Jülich	Fig. 13

Kr-85-Release from Defect Plates

Fuel (density)	Temp. °C	Duration heating h	Duration release h	Act. peak Amplit. Bq x 10^4	Act. peak Area Bq x 10^4	total release Bq x 10^5	Kr-85 inventory Bq x 10^{10}	Relat. release 10^{-4}
U_3Si_2 (4.75)	200	2.5	0.5	0.4	0.4			
	300	2.0	2.0	5.9	39.0	39	3.8	1.0
U_3Si_2 (5.04)	208	4.0	1.0	7.3	7.0			
	257	19.0	1.7	13.6	25.0			
	307	5.0	0.8	3.4	3.1	35	3.7	0.95
U_3Si (6.05)	200	4.5	1.5	0.4	3.2			
	300	4.5	4.5	4.6	43.0	46	3.8	1.2 (1200)
$U_3Si_{1.3}$ (6.5)	200	22.0	4.7	20	104			
	300	4.0	1.1	16	27	121	2.9	4.2

Final Results of Test-Irradiations with LEU-Plates at KFA Jülich	Fig. 14

Cs-137- and Ce-144-Release from Defect Plates

Fuel (density)	Temp. °C	Release (10^4 Bq)		Inventory (10^{12} Bq)		Relat. Release (10^{-7})	
		Cs-137	Ce-144	Cs-137	Ce-144	Cs-137	Ce-144
U_3Si_2 (4.75)	200	4.1	11.5	0.40	0.60	1.0	1.9
	300	3.7	13.7			0.9	2.3
U_3Si_2 (5.04)	200						
	250						
	300	3.3	2.6	0.40	0.40	0.8	0.6
U_3Si (6.05)	200	11.6	12.9	0.40	0.60	2.9	7.2
	300	51.8	146			13.1	24.4
$U_3Si_{1.3}$ (6.50)	200						
	300	5.2	13.7	0.26	2.3	2.0	0.6

Irradiation Behavior of the CNEA's Experimental Uranium Silicide Dispersion Fuel Plates

by
Adolfo Marajofsky, Carlos Kohut (CNEA)
and Gerard L. Hofman (ANL)

1. INTRODUCTION

Since 1978 the CNEA ECBE project has been involved in the development of dispersion fuel plates with four types of fuel materials-UAl_x, U_3O_8, U_3Si, and U_3Si_2-to be used in low enriched (LEU < 20% ^{235}U) fuel elements for research reactors. Miniplates with these fuel materials were manufactured at CNEA and were irradiated in the ORR in three series of irradiations as part of the RERTR miniplate irradiation program. The first irradiation contained U_3O_8 and UAl_x fuel, the second U_3O_8, UAl_x and U_3Si, while the third irradiation test consisted of six U_3Si_2 miniplates and one U_3Si miniplate. This third test is the subject of this paper. The present results compare favorably with other irradiations performed in the RERTR program[1,2] showing in particular the excellent behavior of the U_3Si_2. The overall data accumulated support the qualification of the CNEA fabrication techniques.

2. EXPERIMENTAL

The ORR irradiation module No. 30 contained seven CNEA miniplates-six with U_3Si_2 and one with U_3Si, as well as three ANL miniplates. The standard dimensions of these miniplates are 4.5 in. (114 mm) long, 2.0 in. (51 mm) wide and either 0.06 (1.52 mm) or 0.05 in. (1.27 mm) thick. More detailed characteristics are given in Table 1.

Module 30 was irradiated in the ORR between November 27, 1985 and November 8, 1986, for a total irradiation time of 272.32 full-power days. The peak plate burnup achieved was 81% of the original ^{235}U.

The fuel alloys consisted of metallic U enriched to 45%, purchased from the USDOE and alloyed with natural U metal to achieve an enrichment of 19.70 wt.% ^{235}U, and pure Si. The fuel ingots were produced by induction melting in alumina (A1203) crucibles under inert gas atmos-

phere (Ar or He) at low pressure (530 mba) followed by casting in graphite molds. The fuel alloy ingots were annealed for 72 h at 800°C in fused-quartz tubes, prior to comminution to fuel alloy powder. The fuel powder particle size ranged from 44 to 90 μm, plus 25 w/o fines (particle size <44 μm). The Al powder used was a commercially available atomized powder (Arquimex). The average particle size was 8 μm, with 100% less than 45 μm and 99.5% less than 38 μm. The minimum Al content was 99.5% wt.%. The cladding and frame material was 6061 Al alloy, produced by KICSA Co. Arg. conforming to ASTM B209-67 (aluminum alloy sheet).

The fuel plate specifications conformed to the fuel plate specification for RERTR irradiation tests in the ORR Reactor and were in accordance with the inspection and QA documentation stated by the ORR Engineering Technology Division,[3].

The fabrication sequence of the miniplates was as follows:

(1) Weighing and blending fuel and aluminum powder for each compact.
(2) Cold pressing at 450 MPa for all the blends. The surface of the die was lubricated with stearic acid.
(3) Cleaning the frames and cover plates by caustic etching followed by neutralizing with nitric acid.
(4) Placing the compacts in the frames and welding the cover plates (TIG welding) to the frames.
(5) Hot roll bonding after preheating for one hour in air at 490°C or 510°C. Intermediate heating between successive passes was 15-30 minutes.
(6) Annealing the plates for one hour at 490°C or 510°C at the conclusion of hot rolling to soften the plates and test for blister formation (unbonded areas).
(7) Cold rolling to final dimensions (85% total reduction in hot plus cold rolling).
(8) Finishing operations - radiographing for core locations, shearing to size, cleaning, and inspecting for dimensional requirements.

A description of the postirradiation examination methods employed can be found in [5] and the purpose of each one of the steps in [2]. Briefly, the examination included:

- Visual examination and photography of the as-received module.
- Visual examination and photography of individual plates after dismantling of the module.

- Longitudinal and transverse γ-scanning.
- Plate thickness measurements.
- Plate immersion volume measurement after oxide scale removed.
- Blister annealing of selected plate.
- Sectioning of selected plates for optical metallography, scanning electron microscopy and burnup analysis.

3.0 DISCUSSION OF RESULTS

Visual inspection of the irradiation module in the as-received condition using backlighting through the coolant channels revealed no unusual features. No bowing, warping or pillowing or the plates and no coolant channel obstructions were observed.

As is usually the case for high burnup modules, the plates could not be removed from the intact module and required cutting off of one of the side plates of the module. Visual examination showed each plate to be in excellent condition.

The longitudinal and transverse γ scans of each plate yielded very regular γ intensity traces indicating uniform fuel distribution and absence of dog boning. Representative longitudinal gross γ scan traces are shown in Fig. 1.

Plate thickness measurements were made with a micrometer having a 1/4 inch anvil. Nine measurements were taken on each plate spaced on a square grid on the plate. The maximum, minimum, and average values measured on each plate are given in Table 2. The thickness increase of the U_3Si_2 plates was very uniform ranging from 3 to 4 mils (0.08 to 0.10 μm). The sole U_3Si plate also had a uniform thickness increase of 4 to 5 mils (0.10 to 0.13 mm). These data indicate that the fuel swelling is very uniform along the plates.

Prior to measuring the plate volume increase, ΔV_p, by the Archemedian method, a layer of oxidation product that has a much lower density than aluminum must be removed. This layer consists primarily of Beomite and can be removed with a hot acid treatment, called bright dipping. With the assumption that no significant swelling of the aluminum has occurred, the volume increase of the core or meat, ΔV_m, may be calculated using the as-built core volume fraction of the plate. If it is further assumed that the as-built core porosity has been consumed by the swollen fuel, an assumption that must be confirmed by metallography, the actual fuel swell-

OF
1.0
2.8
2.5
3.2
2.2
3.6
1.1
4.0
2.0
1.8
1.4
1.6

ing, ΔV_f, may be computed as follows:

$$\Delta V_f = \frac{(\Delta V_m + \Delta V_p^o)}{V_f^o}$$

where: ΔV_p^o is the as-built porosity fraction in the core and ΔV_f^o the as-built fuel volume fraction in the core. The swelling data, together with average ^{235}U burnup and accumulated fission density, for each plate are given in Table 4. The swelling behavior of the CNEA fuel can be accessed by comparison to swelling data of previously irradiated miniplates of similar fissile loading. This is done graphically for U_3Si_2 in Fig. 2 and for U_3Si in Fig. 3. It may be concluded that the CNEA-produced fuel compares very favorably in this respect.

Metallographic examination was performed on two U_3Si_2 plates, one 0.05 in. (1.27 mm) and 0.06 in. (1.52-mm)-thick plate, and on the sole U_3Si plate. Figure 4 shows a transverse section taken from the midpoint of the plate. The fuel core is very uniform in thickness, and the as-built porosity has, except for some very small remnant, been consumed by fuel swelling. Oxidized fuel particles are present at the core-cladding interface toward the fuel edge (see details in Fig. 4), and to a minor degree throughout the fuel core (see Fig. 5). Oxide particles like these are introduced during plate fabrication and occur to various degrees in silicide fuel made by all manufacturers. They do not appear to affect the irradiation behavior of the fuel but are the nucleation sites for blisters that occur during high temperature blister testing. Figure 6 shows a longitudinal section starting at the center of the trailing end (with respect to the rolling direction) of the plate. Again the fuel core is very uniform without significant dog boning, which is consistent with the γ-scanning results. A relatively large amount of oxidized fuel is present (see detail), which is not uncommon at the end of fuel cores. This oxidization as mentioned before, has never been found to affect the irradiation behavior of the fuel plate. The majority of the fuel microstructure is represented by the sections shown in Figs. 7, 8, and 9 taken from a 1.52-mm-thick (7,8) and 1.27-mm-thick (9) plate, respectively. The fuel contains a few oxide particles and a very small fraction of retained as-fabricated porosity. The vast majority of the fuel particles exhibited typical U_3Si_2 behavior, i.e., they contain a dense population of very small fission gas bubbles and patches of larger bubbles. These larger bubbles form in the minor U_3Si phase distributed throughout the major U_3Si_2 phase. The formation of some U_3Si is unavoidable in practice and does not negatively affect irradiation behavior when kept to a reasonably low

volume fraction. The high magnification scanning electron images of the fuel microstructure in Figs. 10 and 11 show, respectively, an oxide particle and the fission gas bubble morphology.

Figure 12 shows a longitudinal section through the trailing end of the U_3Si plate. This plate also exhibits a uniform fuel distribution, absence of dog boning, and the presence of some oxide particles. A representative microstructure of the U_3Si fuel is shown in Fig. 13. The gas bubble morphology is typical of U_3Si that is well below the breakaway swelling stage, as evidenced by the absence of large interconnected bubbles. The U_3Si bubble morphology is consistent with the swelling values shown in Fig. 3.

A small section from the center of U_3Si_2 plate RA-321 was spectrographically analyzed for U and Pu isotopic composition. The results of this analysis was used to calculate the burnup and fission density at the center of this plate. The average burnup of each plate was determined by integration of the longitudinal γ scans and normalization of these values to that of the spectrographically analyzed plate RA-321.

Finally, one U_3Si_2 plate was subjected to a blister annealing test. This test consists of annealing steps of 1/2 hour each beginning at 425°C and increasing by 25° intervals. Blistering at the edges of the fuel core was first detected after the 525°C annealing step. This is consistent with blister temperature measured for other U_3Si_2 plates.

4. SUMMARY AND CONCLUSIONS

CNEA miniplates loaded with 43 (33) vol.% of 19.75%-enriched U_3Si_2 (U_3Si), giving a uranium loading of 4.8 g/cm^3, were irradiated up to 81 at.% burnup of the ^{235}U. The behavior of all plates was excellent and consistent with that of plates irradiated previously in the RERTR program. In particular:

- the blister test showed few blisters beginning at 525°C.
- fuel swelling as a function of fission density compares well with previously irradiated mini plates.
- the microstructure shows a relatively uniform distribution of fission gas bubbles in the fuel grains.

- The single U_3Si plate shows larger fission gas bubbles as expected but the bubbles did not exhibit significant coalescence. As such the fuel did not enter the stage of break-away swelling and the plate did not approach pillowing.
- The U_3Si_2 fuel grain contains a fine distributed second phase, probably U_3Si, which appears as a consequence of the fabrication process. Given the fact that the fuel composition was on the U side of stochiometric U_3Si_2, some metallic U was likely present after casting. During the 72 hour anneal given the fuel, this U was transformed to the observed U_3Si phase. The gas bubbles in this second phase are much larger than in the U_3Si_2 phase, which is consistent with U_3Si behavior.
- Some oxidized particles were seen, primarily at the interface of meat and frame Such oxidized fuel particles have been previously identified as the nuclei of blisters during high temperature post irradiation blister tests. The quantity of oxidized particles is not considered excessive, and there is no reason for concern.
- The excellent behavior of the plates may be considered as a qualification of the CNEA plate fabrication process.

ACKNOWLEDGMENTS

The author's should like to thank Mssrs. G. L. Copeland, J. L. Snelgrove, and D. R. Giorsetti for their support and personnel of the ANL - A. G. Hotcell facility for carrying out the postirradiaton examiantion.

REFERENCES

1. J. L. Snelgrove, R. F. Domagala, G. L. Hofman, T. C. Wiencek, G. L. Copeland, R. W. Hobbs, and R. L. Senn, *The Use of U_3Si_2 Dispersed in Al Plate Type Fuel Elements for Research on Test Reactors*, Argonne National Laboratory Report, ANL/RERTR/TM-11 (October 1987).

2. G. L. Copeland, R. W. Hobbs, G. L. Hofman, and J. L. Snelgrove, *Performance of Low Enriched U_3Si_2 Al Dispersion Fuel Elements in the ORR Reactor*, Argonne National Laboratory Report, ANL/RERTR/TM-10 (October 1987).

3. ORNL Document No. Q-11821-ET-002-5-0, "*Fuel Plate Specification for RERTR Irradiation Test,*" Appendix A of R. L. Senn and M. M. Martin, Irradiation Testing of Miniature Fuel Plates for the RERTR Program, Oak Ridge National Laboratory Report, ORNL/TM-T161 (July 1981).

4. E. Perez, C. Kohut, D. Giorsetti, G. L. Copeland, and J. Snelgrove, *Irradiation Performance of CNEA UAl_x and U_3O_8 Miniplates*, Int. Meeting on Reduced Enrichment for Research and Test Reactors, Tokai-mura, Japan, October 17, 91983.

5. J. Gomez, R. Morando, E. E. Perez, D. R. Giorsetti, G. L. Copeland, G. L. Hofman and J. L. Snelgrove, *Postirradiation Examination of High-U-Loaded Low-Enriched U_3O_8, UAl_2 and U_3Si Test Fuel Plates*, Int. Meeting on Reduced Enrichment for Research and Test Reactors, Argonne, USA, Oct. 1984.

TABLE 1

CHARACTERISTICS OF CNEA MINIPLATES

Number	RA 311	RA 313	RA 316	RA 315	RA 321	RA 319	RA 320
Plate Weigh (g)	36.43	36.34	36.33	36.36	28.13	28.09	28.24
Plate Thick. (mm)	1.524	1.524	1.524	1.524	1.270	1.270	1.270
(in)	0.060	0.060	0.060	0.060	0.050	0.050	0.050
Fissile Bearing Compound	U_3Si	U_3Si_2	U_3Si_2	U_3Si_2	U_3Si_2	U_3Si_2	U_3Si_2
Meat Weight (g)	21.54	21.50	21.45	21.51	14.36	14.38	14.38
U Weight (g)	15.71	15.91	15.88	15.93	10.65	10.74	10.62
Enrich. (235) wt.%	19.70	19.70	19.70	19.70	19.70	19.70	19.70
Average Meat Thick.	0.775	0.776	0.776	0.776	0.558	0.558	0.558
Plate Vol. (cm^3)	8.7745	8.7565	8.7785	8.7784	7.3117	7.2929	7.3361
Meat Vol. (cm^3)	3.2637	3.2637	3.2715	3.2825	2.2154	2.2188	2.2066
U Density (cm^3)	4.812	4.876	4.856	4.853	4.809	4.838	4.838
Maximal (mg/cm^2)	43.18	44.32	44.05	44.03	27.95	28.06	28.09
U Surface Density							

TABLE 2

Plate, Thickness Before and After Irradiation In in. and mm

	Postirradiation			Pre. Irrad.
Plate	Average	Maximum	Minimum	Average
RA 311	0.0647 1.643	0.0650 1.651	0.0642 1.631	0.06 1.524
RA 313	0.0635 1.613	0.0641 1.621	0.0630 1.600	0.06 1.524
RA 315	0.0635 1.613	0.0640 1.626	0.0631 1.603	0.06 1.524
RA 316	0.0635 1.613	0.0639 1.623	0.0632 1.605	0.06 1.524
RA 319	0.0531 1.349	0.0537 1.364	0.0526 1.336	0.05 1.270
RA 320	0.0535 1.359	0.0540 1.372	0.0532 1.351	0.05 1.270
RA 321	0.0533 1.354	0.0537 1.364	0.0529 1.344	0.05 1.270

TABLE 2

Irradiation History of Module 30

Module in Position	Begin Irrad.	End Irrad.	Full-Power Days	Average Module Power, kW	Estimated U^{235} Burnup at End of Cycle, %
2	11/27/85	1/06/85	32.2	90	14
2	1/06/86	3/26/86	57.4	76	35
2	3/26/86	5/31/86	54.9	57	50
2	6/27/86	8/10/86	41.3	45	59
4	8/11/86	9/26/86	34.2	54	68
4	9/26/86	11/18/86	52.3	36	77

TABLE 3

Immersion Volume Measurements

Comp	Mod	No.	V_p^o %	V_f^o %	ΔV_m%	ΔV_f%	^{235}UBu	$FD_F(10^{21})$	$FD_m(10^{21})$
U_3Si	30	RA 311	7.75	33	5.20	39.2	77	5.2	1.7
U_3Si_2	30	RA 313	7.56	43	2.80	24.1	77	4.1	1.7
U_3Si_2	30	RA 315	8.01	43	1.81	22.8	77	4.1	1.7
U_3Si_2	30	RA 316	7.96	43	1.81	22.7	77	4.1	1.7
U_3Si_2	30	RA 319	8.76	34	1.49	23.8	78	4.1	1.8
U_3Si_2	30	RA 320	8.66	34	1.68	24.0	81	4.3	1.8
U_3Si_2	30	RA 321	9.11	34	1.52	24.7	80	4.2	1.8

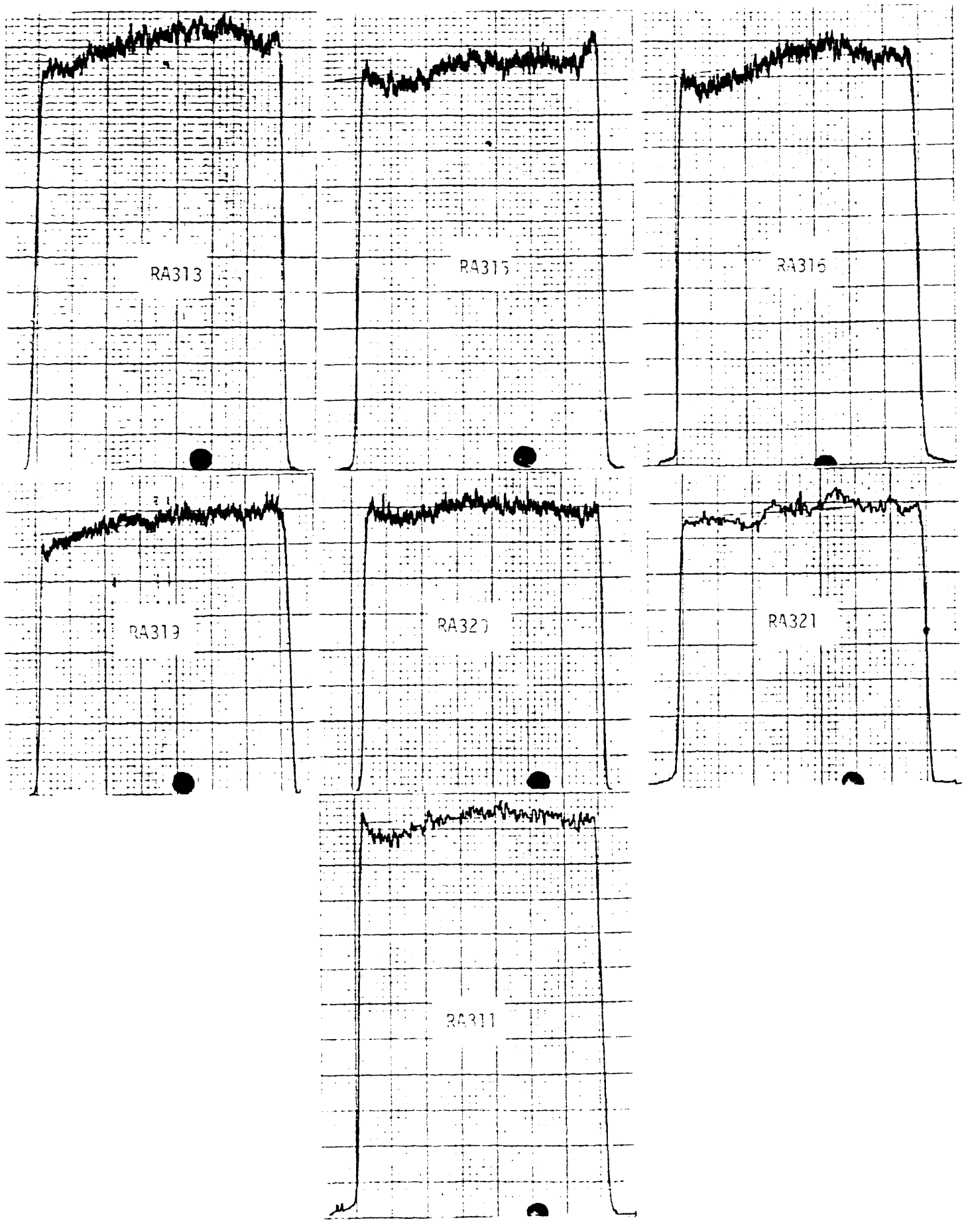

Fig. 1. Longitudinal Gross γ Scans of CNEA Silicide Miniplates

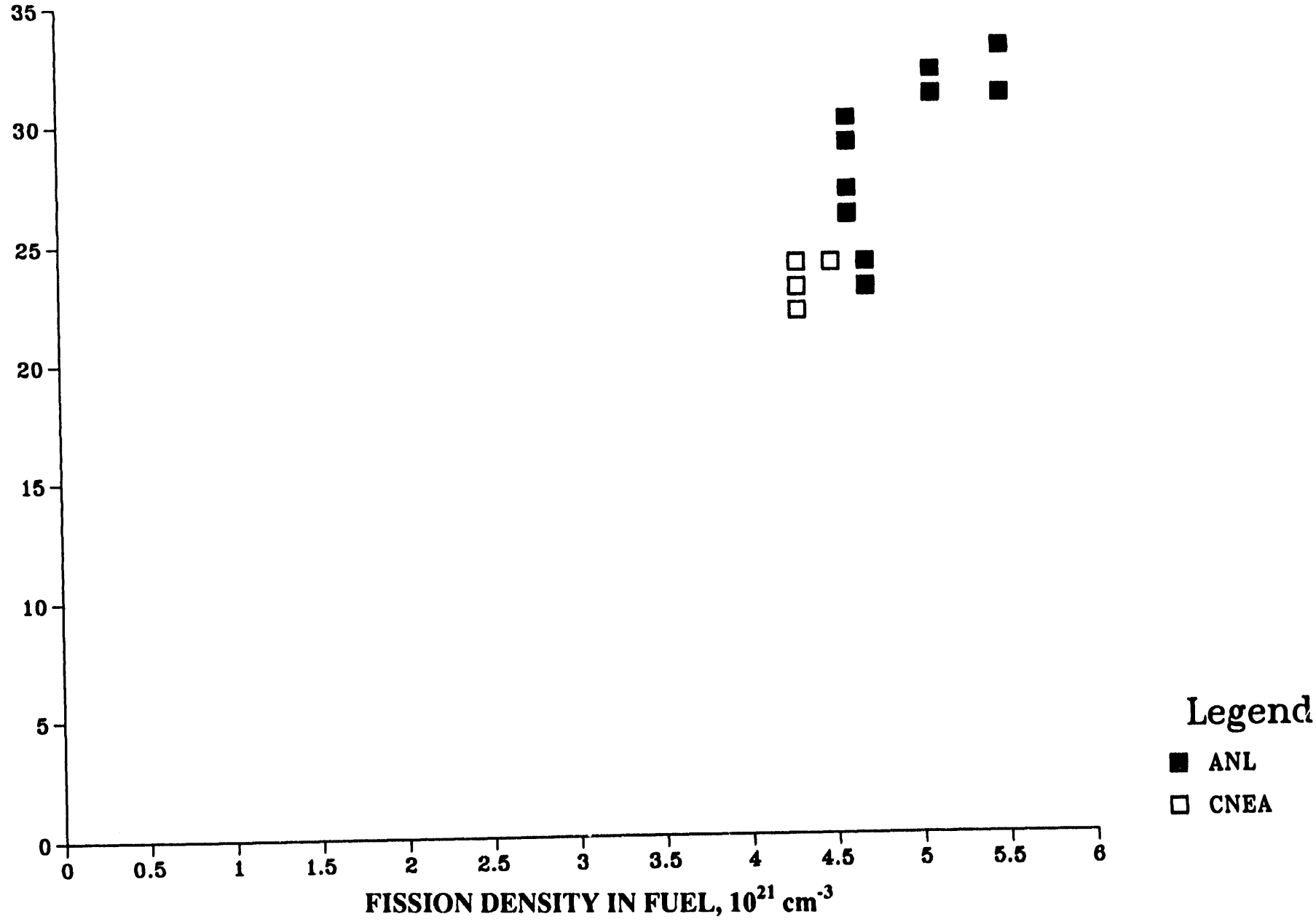

Fig. 2. Swelling of U_3Si_2 in ANL and CNEA Miniplates with LEU Loadings of up to 5.6 g cm^{-3}

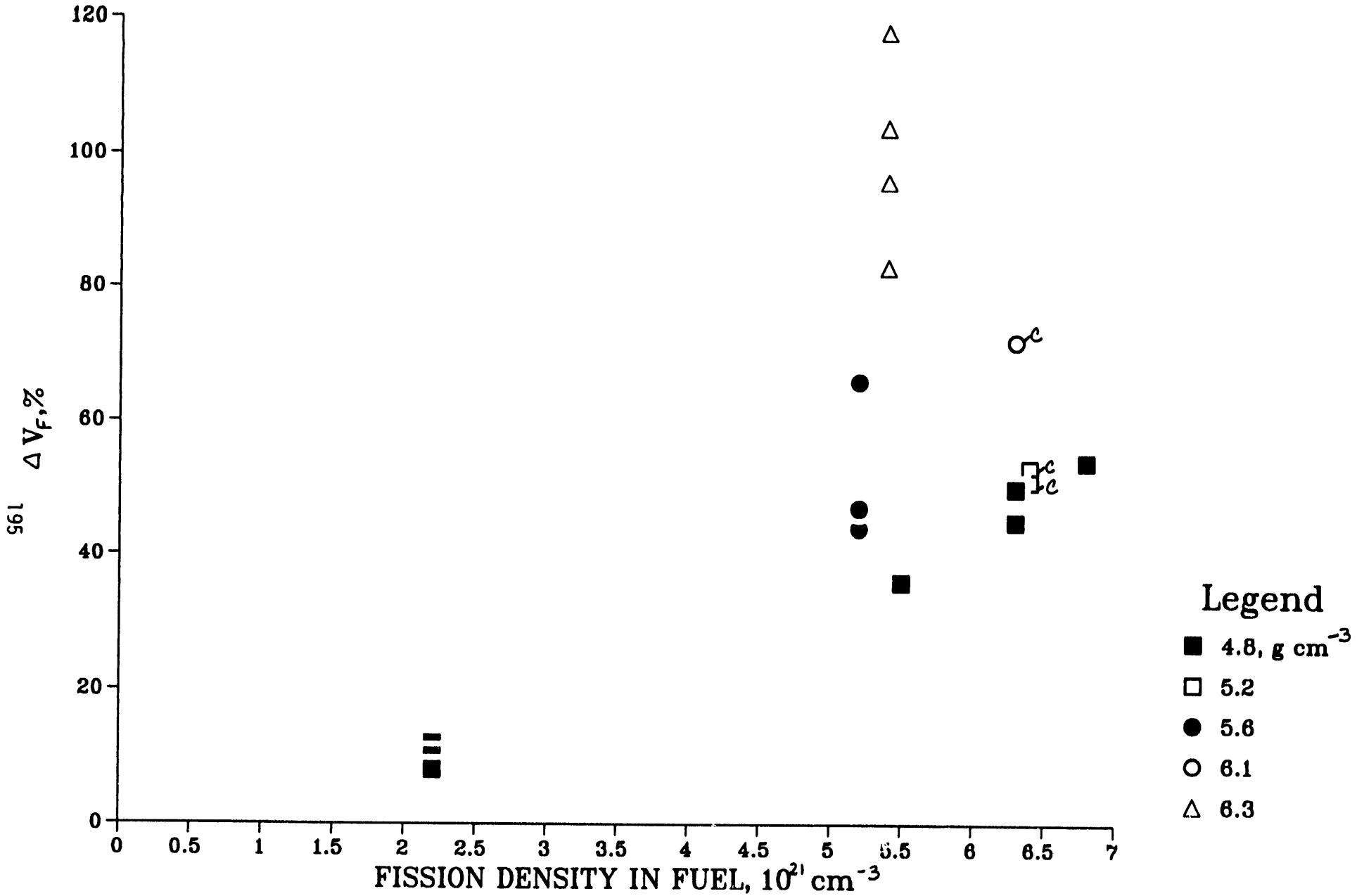

Fig. 3. Swelling of U_3Si in ANL and CNEA Miniplates with LEU Loadings from 4.8 to 6.3 g cm^{-3} (C indicates CNEA data)

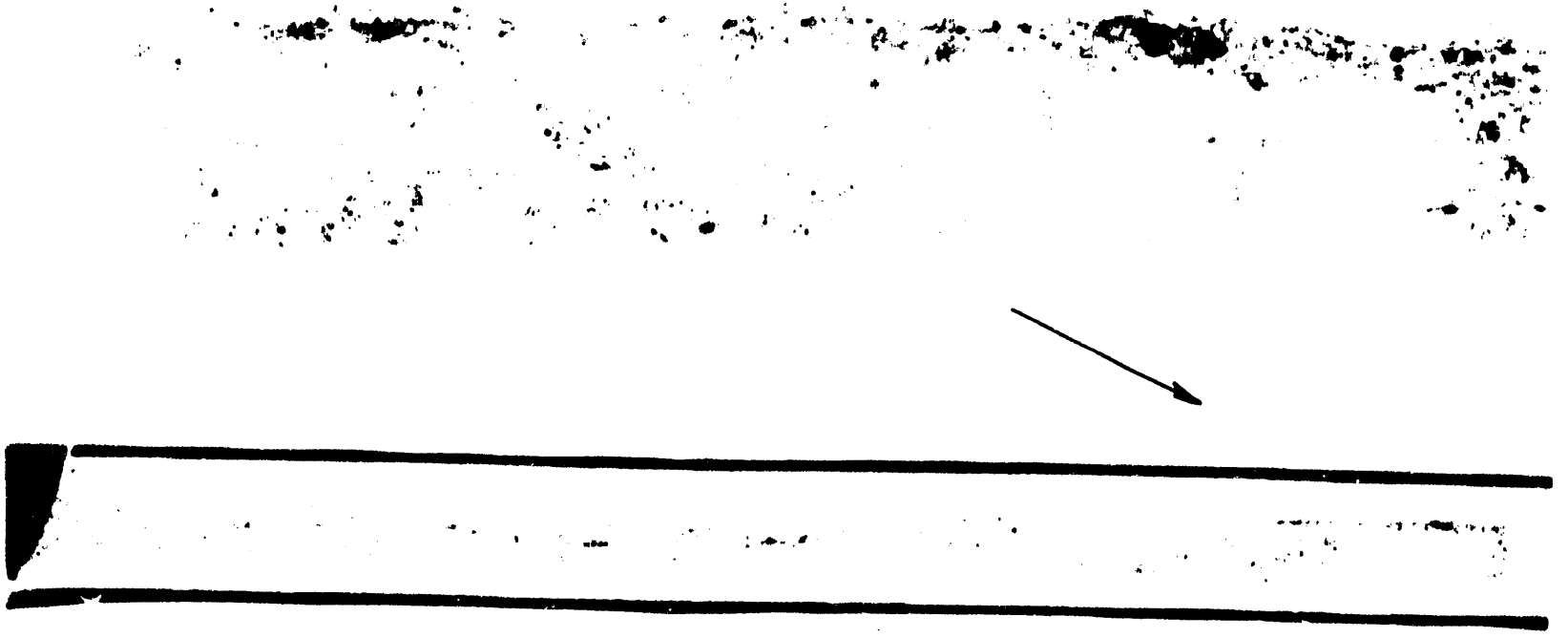

Fig. 4. Transverse Section of U_3Si_2 Plate RA 321, and Detail Showing Oxidation of Core Edge

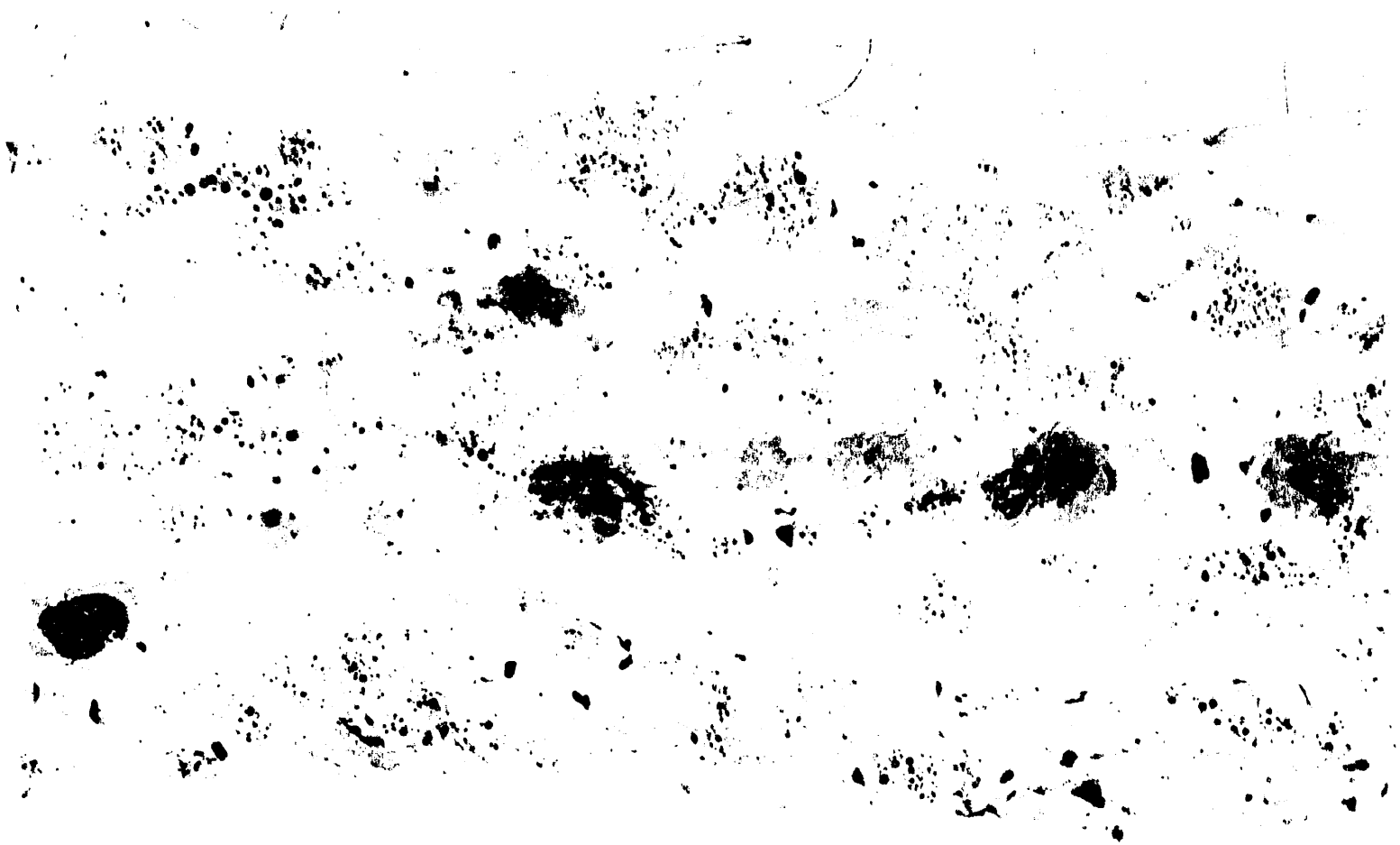

Fig. 5. Detail from Transverse Section of Plate RA 321, showing Fuel Microstructure and Oxidized Particles

Fig. 6. Longitudinal Section of Plate RA 321, Showing Minimal "Dogboning," Detail Showing Oxidized Fuel Particles

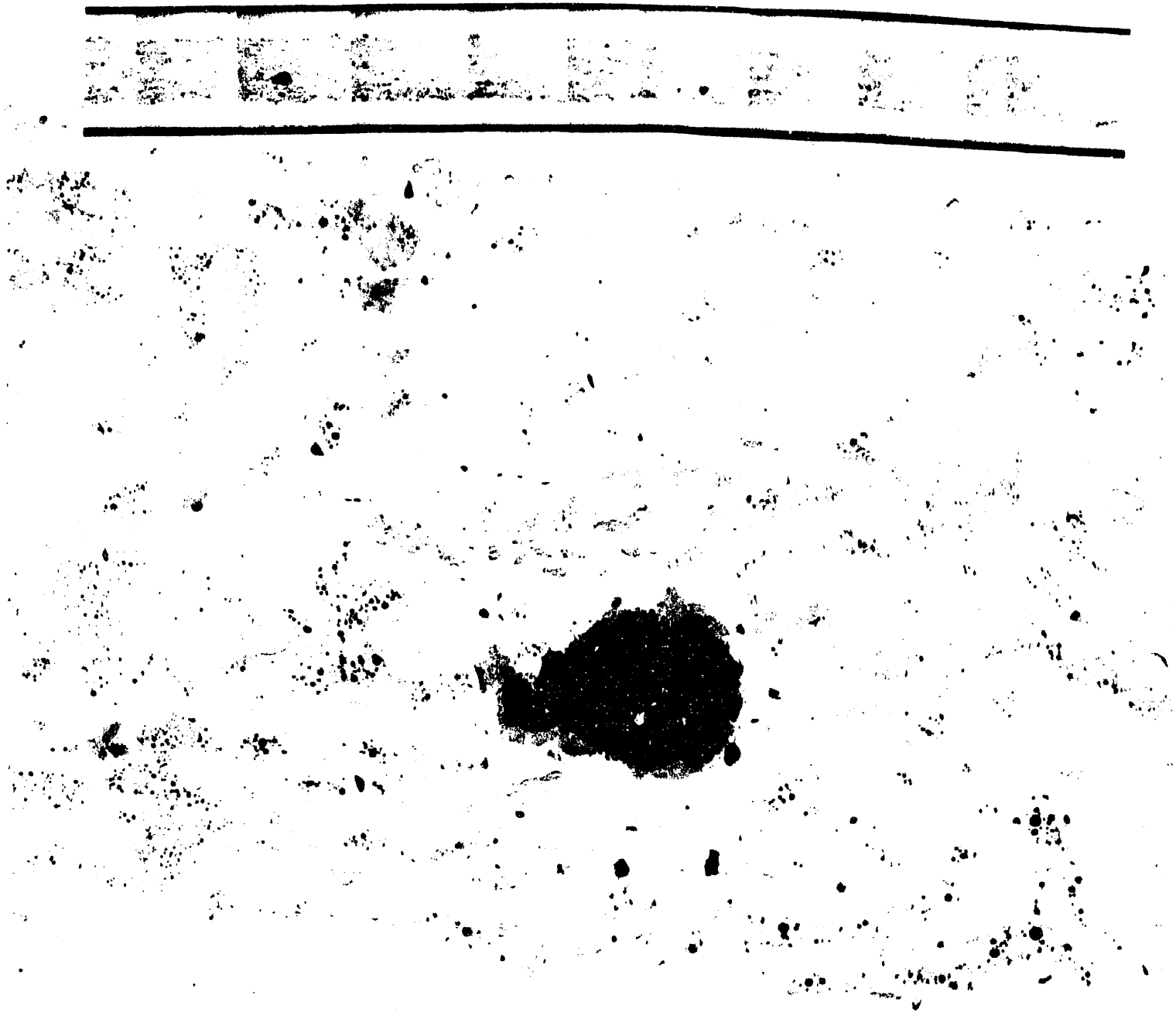

Fig. 7. Transverse Section of U_3Si_2 Plate RA 315, Showing Fuel Microstructure, Oxidized Fuel Particle, and Remnants of as-fabricated Porosity

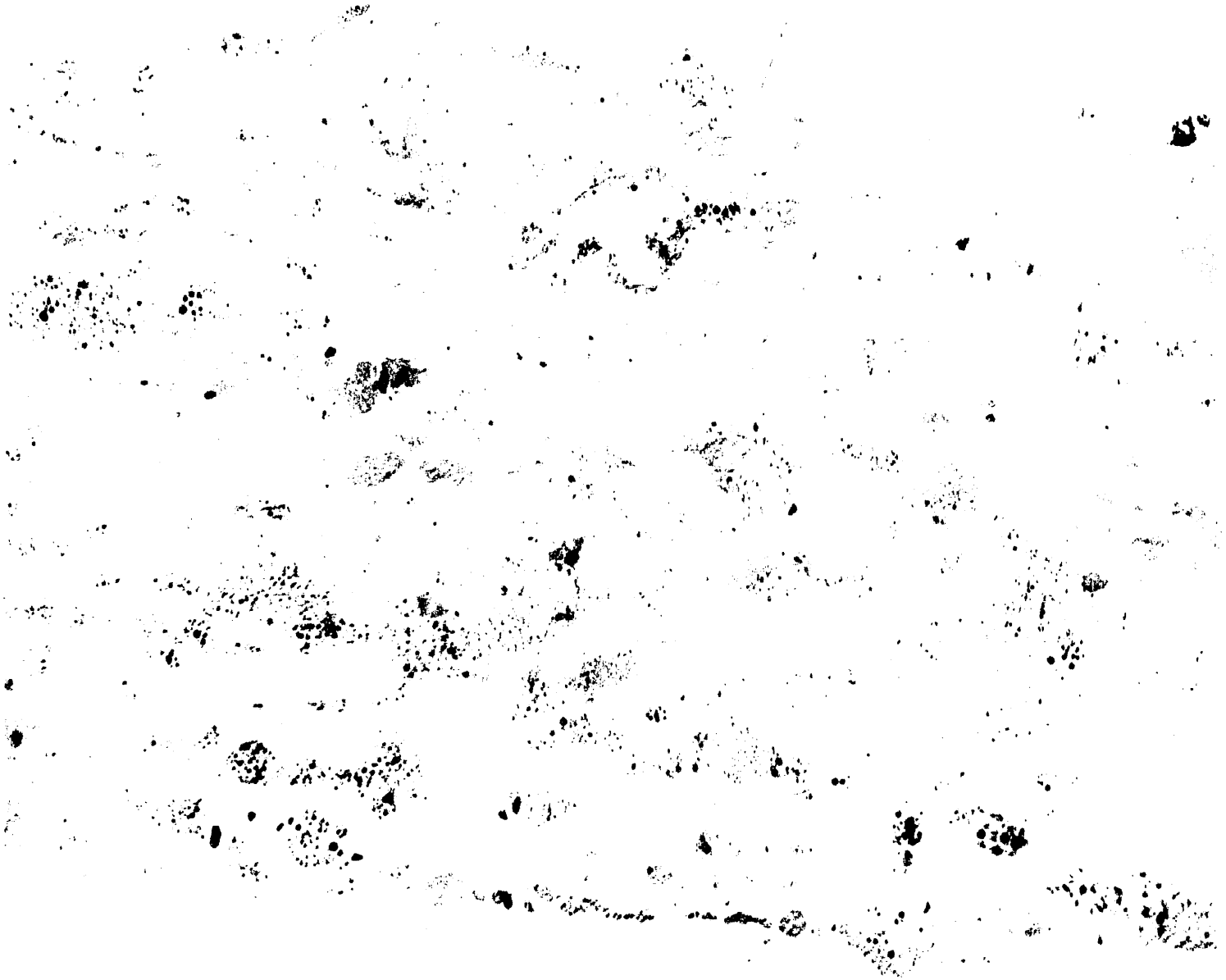

Fig. 8. Typical Fuel Microstructure of U_3Si_2 Plate RA 315

Fig. 9. Typical Fuel Microstructure of U_3Si_2 Plate RA 321

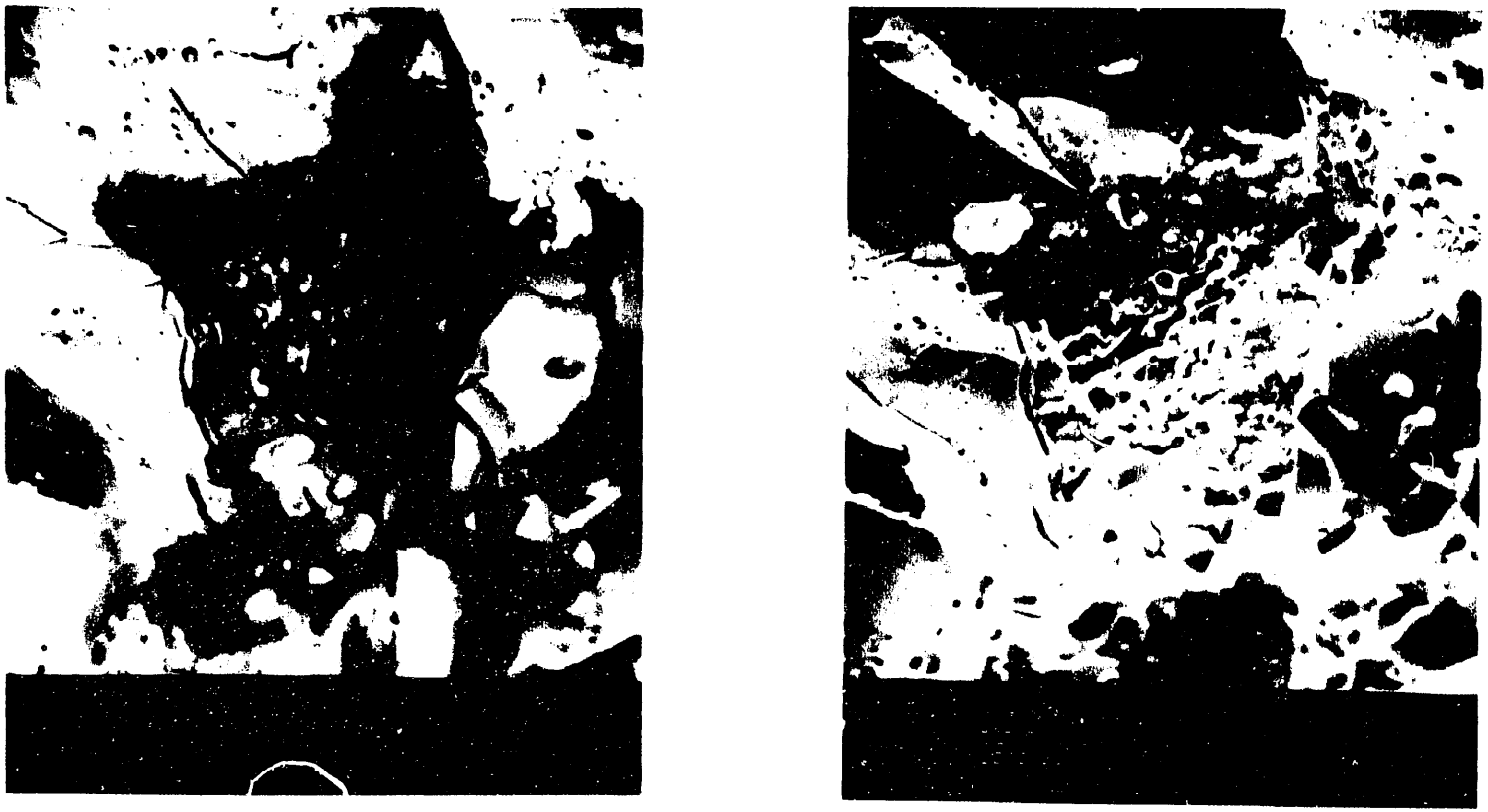

Fig. 10. SEM Image of Oxidized Fuel Particle (center) in U_3Si_2 Plate RA 321; left BSE, right SE

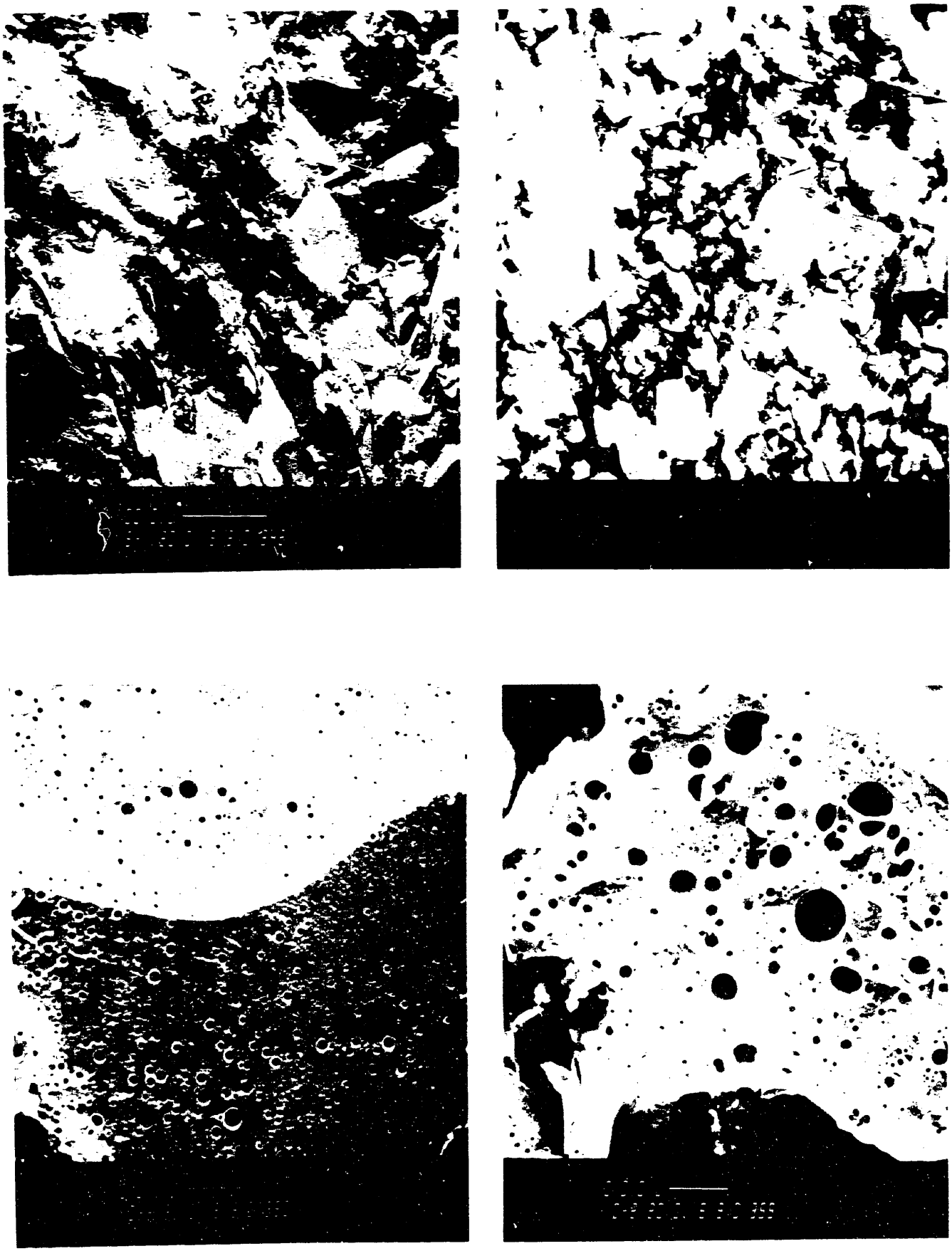

Fig. 11. SEM Images Showing Representative Fuel Microstructure and Bubble Morphology in U_3Si_2 Plate RA 321

Fig. 12. Longitudinal Section of U_3Si Plate RA 311, Detail Showing Oxidized Fuel at Core Edge

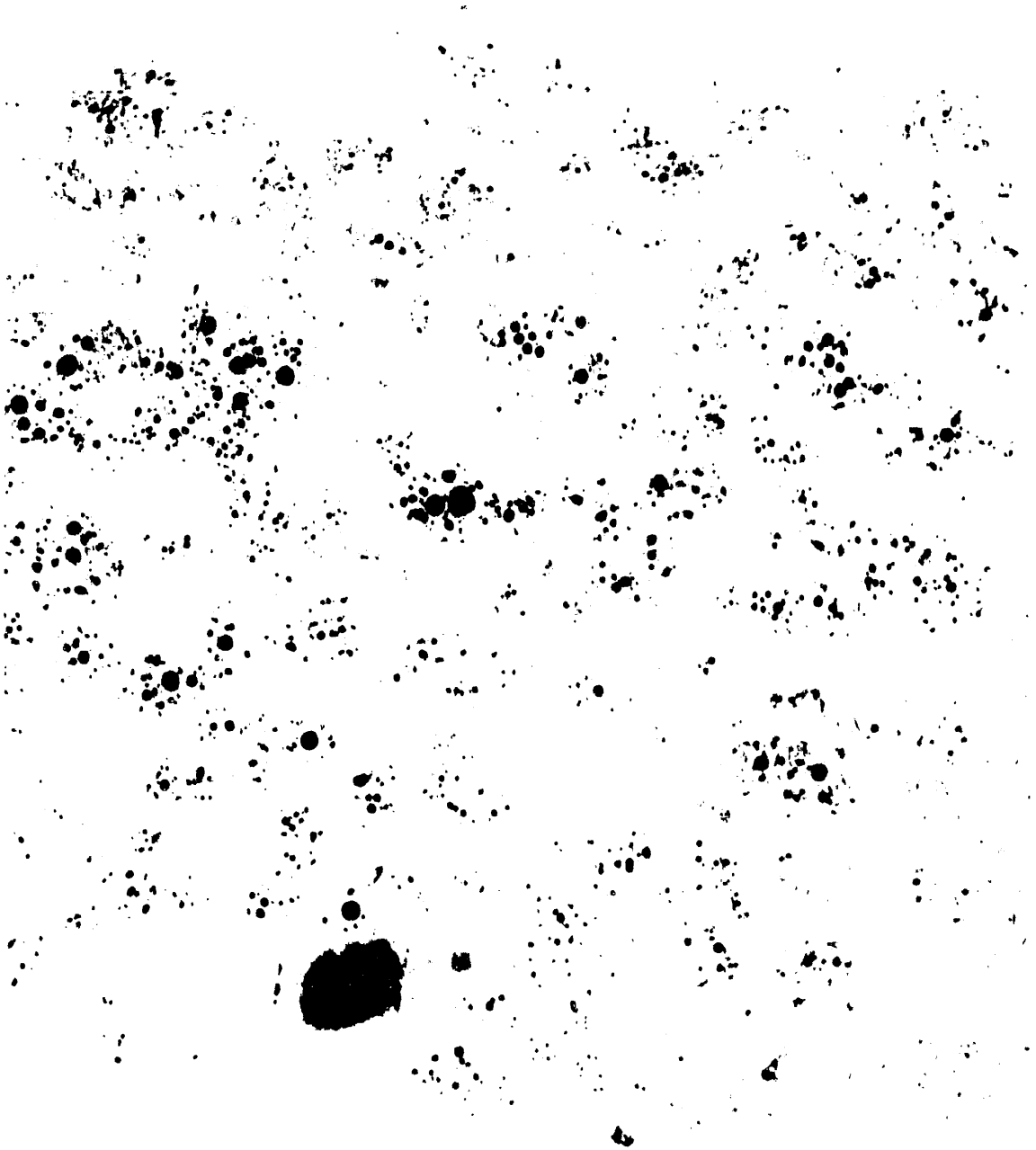

Fig. 13. Typical Fuel Microstructure Of U_3Si Fuel in Plate RA 311

SESSION IV

September 20, 1988

FUEL FABRICATION

Chairman:

W. Krull
(GKSS, Federal Republic of Germany)

ADAPTATION OF INSPECTION METHODS

TO LOW ENRICHED URANIUM FUEL

J.F. POUPARD
C.E.R.C.A.
ROMANS - FRANCE

ABSTRACT

Within the scope of RERTR Program, fuel plates up to 6 g/cm^3 have been manufactured by CERCA.

These changes in fuel density imply many changes in manufacturing and inspection procedures and equipments.

Some inspection methods have to be adapted, and new methods and/or new equipments have been designed to solve the problems met with the density increase.

We present here the problems met and the solutions found for three important inspection methods :

- U 235 content determination in fuel cores.
- Enrichment determination of fuel plates.
- Ultrasonic testing of fuel plates.

For each method, we will present the methods and the equipments in use at CERCA for Low Enriched Uranium fuel cores and fuel plates.

INTRODUCTION

The fuel plates production involves many inspection steps. When the production line has to be adapted from HEU fuel to LEU fuel, inspection methods and equipments have been reviewed.

As stated in Table 1, three major points of interest arised and we will present hereafter the adoption of inspection methods, new equipments developed.

Table 1. Inspection Methods for MTR Fuel

Methods used for HEU Fuel	Adaptation to LEU
Uranium Analysis	Unchanged
UAl_x Analysis	Adaptation to silicides
Grain Size Measurement	Unchanged
U235 Content of Fuel Cores by Gamma Counting	U235 Content of Fuel Cores by Weighing Method
Dimensional Inspection of Fuel Cores	Unchanged
	Enrichment Control of Fuel Plates
Ultrasonic Inspection of Fuel Plates	New Equipment for Core Edge Effect
X-Ray Inspection of Fuel Plates	Unchanged
Visual Inspection of Fuel Plates	Unchanged
Cladding Thickness Inspection	Unchanged
Dimensional Inspection of Fuel Plates	Unchanged
Surface Contamination of Fuel Plates	Unchanged
Fuel Elements Inspection	Unchanged

The Table 1 shows clearly that the efforts on inspection methods have been concentrated on U235 content determination (by gamma counting and by weighing method), enrichment control of fuel plates and ultrasonic inspection of fuel plates. In each case, new equipments have been designed by CERCA.

U235 CONTENT DETERMINATION

Basis of measurements

Gamma Counting Method

The measurement of U235 content in fuel cores is based on the measurement of gamma ray emission characteristic of U235 in the energy range of

185 keV. For this measurement, we use a NaI detector put in a lead shielding in order to prevent it from the background radiation. An electronic equipment allows counting of gamma rays in terms of number of pulses. This measurement is compared with countings obtained with standard cores containing a known content of U235. To reduce the effect of statistical dispersion of countings on standard, it is of common use to perform several measurements on standards and to take into account the main value of these several countings.

Weighing Method

Another method is based on recording the weights of powders added together in the manufacture of one fuel core and the weight of the fuel core. As the uranium content and the enrichment ratio in U235 is determined on the powder by chemical and isotopic analysis, we can calculate for every fuel core the U.total content and the U235 content. In order to prevent any mistake when reporting the results, the scales have been connected to computers and a special software developed by CERCA can give directly the inspection report.

Parameters of errors and dispersion

General Parameters of dispersion for gamma counting method

We present here a very brief summary of errors and dispersion of measurements made by gamma counting method. In fact, the gamma flux measured on a given equipment is a function of the following parameters :

- Gamma ray emission of U235.
- Self attenuation of gamma ray in the fuel core.
- Geometrical factors related to the location of fuel core and detector.
- Amplification factor of the electronic equipment.

The major parameters of errors are :

- Randomly statistical dispersion of the radiation emission (following a Poisson distribution). The variability of the method is still relatively high compared to the range of tolerances (.2 % compared to the range of tolerances ± 2 %).
- Interference radiation due to the fuel core itself (reflexion, diffusion, etc...) or due to external factors (background, cosmic radiation, etc...). As the measurement is performed by comparison, this does not affect the value measured just adding a very slight variability.

- Measurement errors due to dimensional and homogeneity dispersion. For dimension differences, these differences are measured and correction for thickness differences are calculated. Homogeneity differences could locally change **significantly** the contribution to gamma ray flux of the fuel core and therefore could affect the measurement and add a significant variability.

- Measurement errors due to calibration (accuracy of standard cores values, dispersion of calibration results, etc...). These errors are related to isotopic and chemical analysis variability for establishing the value of U235 content of the standards and to variability of countings on standards for periodical calibration.

General parameters of dispersion for weighing method

The errors and dispersion are due mainly to the following factors :

- Weighing variability that could be considered as fairly low, compared to the range of tolerances and decreasing in relative value when the weight is increasing.

- Powder homogeneity in order to take a representative sample and to give analytical values valid for each fuel core. For UAl_x and U3Si2 powders, the variability due to inhomogeneity is quite low and could be negligible.

- U. total content and U-235 isotopic analysis are the major factor of variability for this method.

Comparison of weighing and gamma counting for Low Enriched Uranium Fuel

When we have reviewed the causes of errors as stated hereabove, we have faced important factors when changing from High Enriched Uranium to Low Enriched Uranium Fuel. We have compared these causes of errors to those due to weighing method (weight of powder x U total content x enrichment ratio = U-235 content). As far as the weights of powders and fuel cores are increasing, the accuracy of weight measurement is better and if some other factors show that the accuracy of gamma counting is decreasing, we have thought that weighing method would be a good solution for Low Enriched Uranium Fuel.

These factors were :

Statistical variability of gamma ray emission : this variability would be the same as far as the number of countings measured would be the same. This increased the time of inspection or involved doubling the detector (one on each face of the fuel core).

Dimensional and homogeneity dispersion : the effect of dimensional variability is not changed, but the effect of homogeneity variability is different. We can say that local variability in homogeneity has a self attenuation effect double for U3Si2 fuel than for UAl_x fuel. As far as this cannot be corrected by calculation, it is a cause of variability from one core to another.

Equipment developed by CERCA

Principle

CERCA took the decision to develop an equipment based on weighing powders and cores and on isotopic and chemical analysis. The equipment is designed to give also support for the manufacturing operators preparing the mixing of powders and pressing the fuel cores.

We consider it as a "Computer Aided Weighing".

The scales are directly connected to computers linked in a local network. In this local network of computers a data base gives to the operator all the necessary informations to keep the manufacturing process under control and prevents any mistake from the operator.

Powder weighing station

At the powder weighing station, the operator puts together the UAl_x or U3Si2 powders with different grain sizes and the aluminium powder. All the powders weights are measured on scales directly connected to a computer. This allows to record directly on the working station all the powders weights and to reject directly mixing with incorrect proportion of powders.

Core Pressing Station

The press operator measures directly after pressing the weight and the dimensions of the fuel cores. Scales and dimensional equipments are connected directly to computer. So, for each fuel core, we have recorded the components weights and the fuel core weight.

Data Processing

Knowing, by isotopic and chemical analysis, the U.content and the U-235 ratio of the powder used, we can calculate the U-235 content and the U.total content of each core. The system allows to get directly the data printed for verification.

Development for the future

Some developments have been planned to put in this system other working stations and to give directly the data to uranium inventory system by data processing.

ENRICHMENT CONTROL OF FUEL PLATES

Purpose

In developing the Low Enriched Fuel manufacturing in the same facility that this used for High Enriched Fuel, CERCA has taken into account the risk of a mistake between fuel cores of different enrichments, even if a full identification and traceability program was applied. To avoid any consequences of this type of mistake, CERCA decides to inspect all the fuel plates for a recognition of enrichment. The main goal of this inspection is to discriminate between enrichments in the range of 93 % and enrichments close to 45 % and close to 20 %.

Basis of the measurement

Gamma Spectroscopy

The measurement is based on the gamma ray spectrography. For this, the gamma ray emitted by the fuel plates is measured and analyzed with a germanium detector. The data generated in the detector are computer processed for :

- automatic search of peaks,
- substracting of background,
- deconvolution of multiple peaks.

This computer process gives a spectrum, Number of pulses as a function of gamma ray energy in keV as measured during a given period of time.

Relationship with enrichment

From the gamma ray spectrum, we choose two peaks characteristics showing the effect of U-235 and U.total. The area of the gamma ray peak at 185.7 keV is representative of the U-235 amount.

The area of the X-ray peak at 98.4 keV is representative of the Uranium total content. This peak is due to self attenuation of gamma ray 185.7 keV for the total uranium present in the core. More uranium total implies more attenuation for the γray at 185.7 keV and more emission of X ray at 98.4 keV.

From this two areas, the computer software could calculate estimations for total amount of uranium, content of U-235 and therefore the enrichment ratio is estimated as a function of the ratio between the areas of the two peaks.

Calibration

The calibration is performed by use of real fuel plates with known U. content and isotopic analysis. From this known values, the relationship between enrichment ratio and the ratio of the areas of the two peaks will be determined and used for inspection.

Equipment designed by CERCA

The equipment designed by CERCA is based on a classical gamma spectrometer with a special software to allow the calculation of isotopic ratio.

This equipment is used to check the enrichment of all fuel plates produced in the workshop since five years, when CERCA has begun to work on mass production of different enrichments.

ULTRASONIC INSPECTION OF FUEL PLATES

Basis of the inspection

Principle of the inspection

The fuel plates are inspected by an ultrasonic testing method in immersion with focalized transducers. The inspection is based on the amplitude of the ultrasonic pulse after transmission through the fuel plate (double transmission with reflexion on a steel mirror). The transducers used are emitter/receiver type.

Defect Detection

After the double transmission through the plate, the ultrasonic pulse is electronically checked for amplitude. If there was no signal in the electronic gate used to follow the echo or if the signal was too attenuated, we consider that the ultrasonic beam has met a defect and has been reflected partly or totally.

Problem met with LEU Fuel

When the density in the fuel meat has been increased for UAl_x from 1.2 g/cm^3 to 2.2 g/cm^3 and up to 6.0 g/cm^3 for U_xSiy_3, the ultrasonic inspection of fuel plates has been limited by the core edge effect.

Core edge effect

The core edge effect is due to the presence of two areas with different ultrasonic speed.

At the limit of these two areas, there is a possibility of combination of two waves with different phases. This gives a combination/attenuation effect with amplitude maxima and minima (typical diffraction effect).

As the inspection equipment is based on the amplitude of the ultrasonic pulse, this is seen as a defect.

This core edge effect has been seen very clearly when the density of fuel has been increased. The core edge was detected as a "false reject" on the ultrasonic equipment.

New Equipment designed by CERCA

In order to solve the problem presented here above, CERCA has worked in relationship with a french specialized company to design a new machine.

Mechanical Equipment

The mechanical part of the new equipment is based on the same principle as the previous one :

- a stainless steel pool,
- a rotating disk supporting six transducers,
- a steel mirror at the bottom part of the pool,
- a driving mechanism for the translation of fuel plates between the transducers and the mirror.

This equipment allows settings of rotating speed and translation speed in order to adjust the step of inspection pattern. This is established to keep the sensitivity in accordance with specification.

Ultrasonic Equipment

The ultrasonic equipment is based on 6 transducers emitter/receiver type with a fully digital electronic. The electronic equipment could be programmed with more than 30 sets of parameters in memory. The frequency could be adjusted in a wide range between 1 and 20 MHz.

Data Processing and Monitoring Equipment

The monitoring and data processing functions are performed with a hard disk mass memory. The computer monitors all the inspection parameters for one type of plates : motor speeds, ultrasonic parameters, criteria. The data given by the ultrasonic equipment are processed by the computer. Defect information, if any, is analyzed for size and location to be compared to

the criteria. After data processing, this allows to have a quality certificate directly given by the printer connected to the computer.

Core edge information

As far as all informations coming from the ultrasonic unit are fully digital and related to a given location on the plate, it is possible to have a data processing in the core edge area. The core edge effect could be discriminated from the defect effect. This allows a full inspection of fuel plates with very high density fuel.

CONCLUSION

CERCA has made many efforts in research and development for inspection methods in the ten past years. These efforts have given new methods to inspect LEU Fuel and to improve the equipments in use at CERCA.

For the future, our intent is to continue those efforts in order to apply new techniques, to improve the reliability of the methods in use and to satisfy the customers' needs.

CERCA

INSPECTION METHODS FOR MTR FUEL

METHODS USED FOR HEU	ADAPTATION TO LEU
URANIUM ANALYSIS	UNCHANGED
UAlx ANALYSIS	ADAPTATION TO SILICIDES
GRAIN SIZE MEASUREMENT	UNCHANGED
U235 CONTENT OF FUEL CORES BY GAMMA COUNTING	U235 CONTENT OF FUEL CORES BY WEIGHING METHOD
DIMENSIONAL INSPECTION OF FUEL CORES	UNCHANGED
No inspection performed when only one enrichment	ENRICHMENT CONTROL OF FUEL PLATES
ULTRASONIC INSPECTION OF FUEL PLATES	NEW EQUIPMENT FOR CORE EDGE EFFECT
X-RAY INSPECTION OF FUEL PLATES	UNCHANGED
VISUAL INSPECTION OF FUEL PLATES	UNCHANGED
CLADDING THICKNESS INSPECTION	UNCHANGED
DIMENSIONAL INSPECTION OF FUEL PLATES	UNCHANGED
SURFACE CONTAMINATION OF FUEL PLATES	UNCHANGED
FUEL ELEMENTS INSPECTION	UNCHANGED

CERCA

MEASUREMENT OF U-235 CONTENT BY GAMMA COUNTING

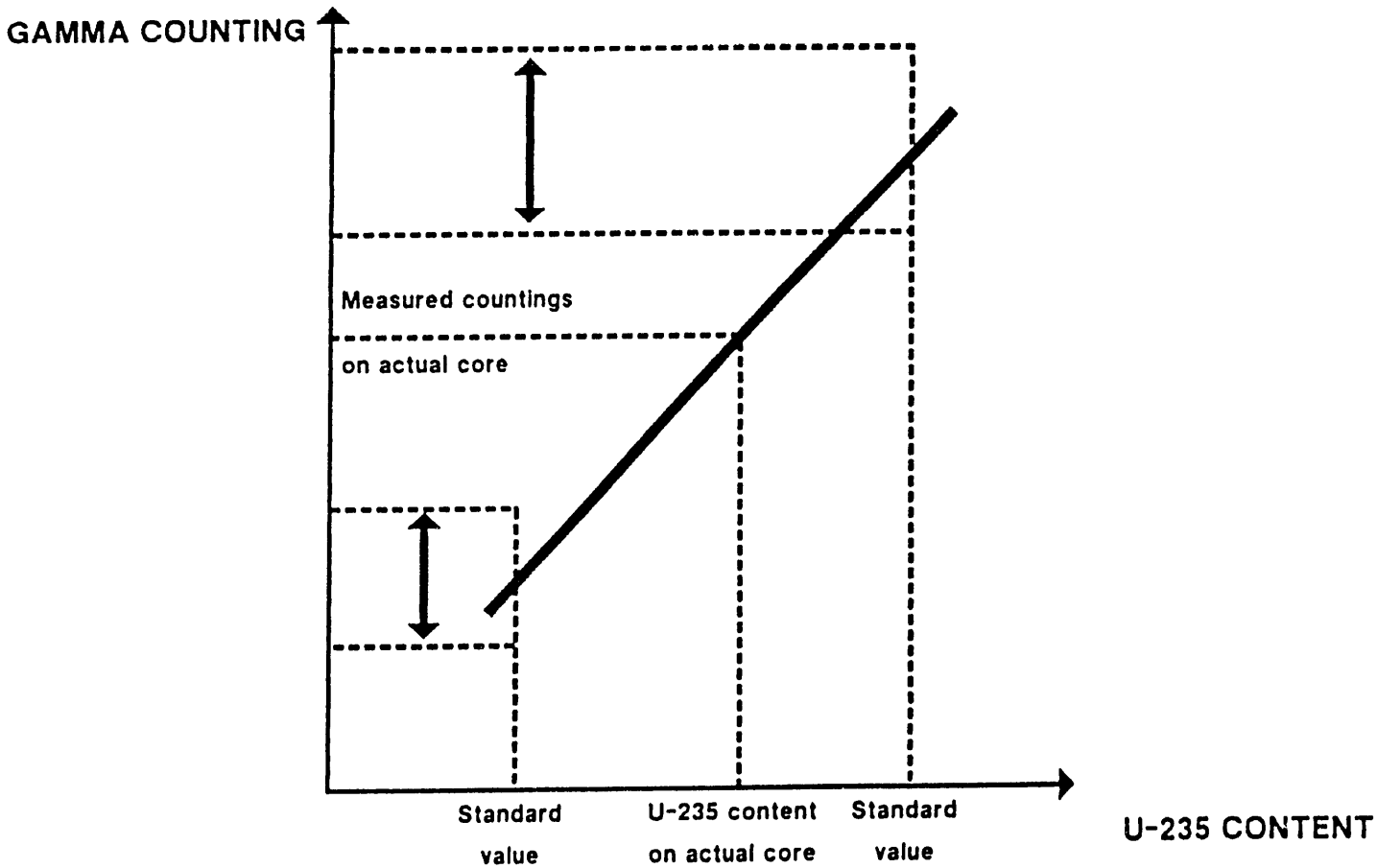

CERCA

GAMMA EMISSION SPECTRUM OF FUEL PLATES

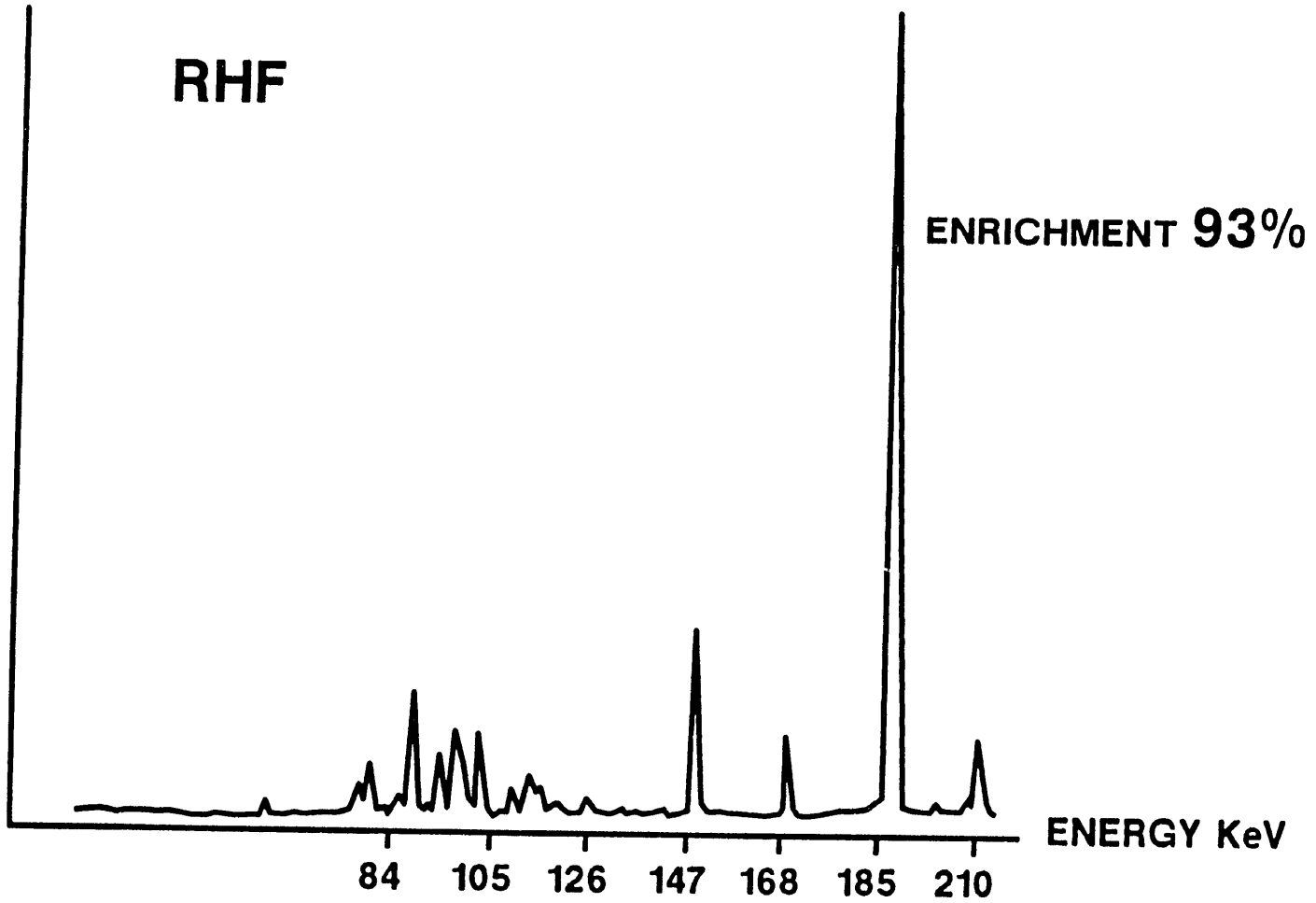

CERCA

GAMMA EMISSION SPECTRUM OF FUEL PLATES

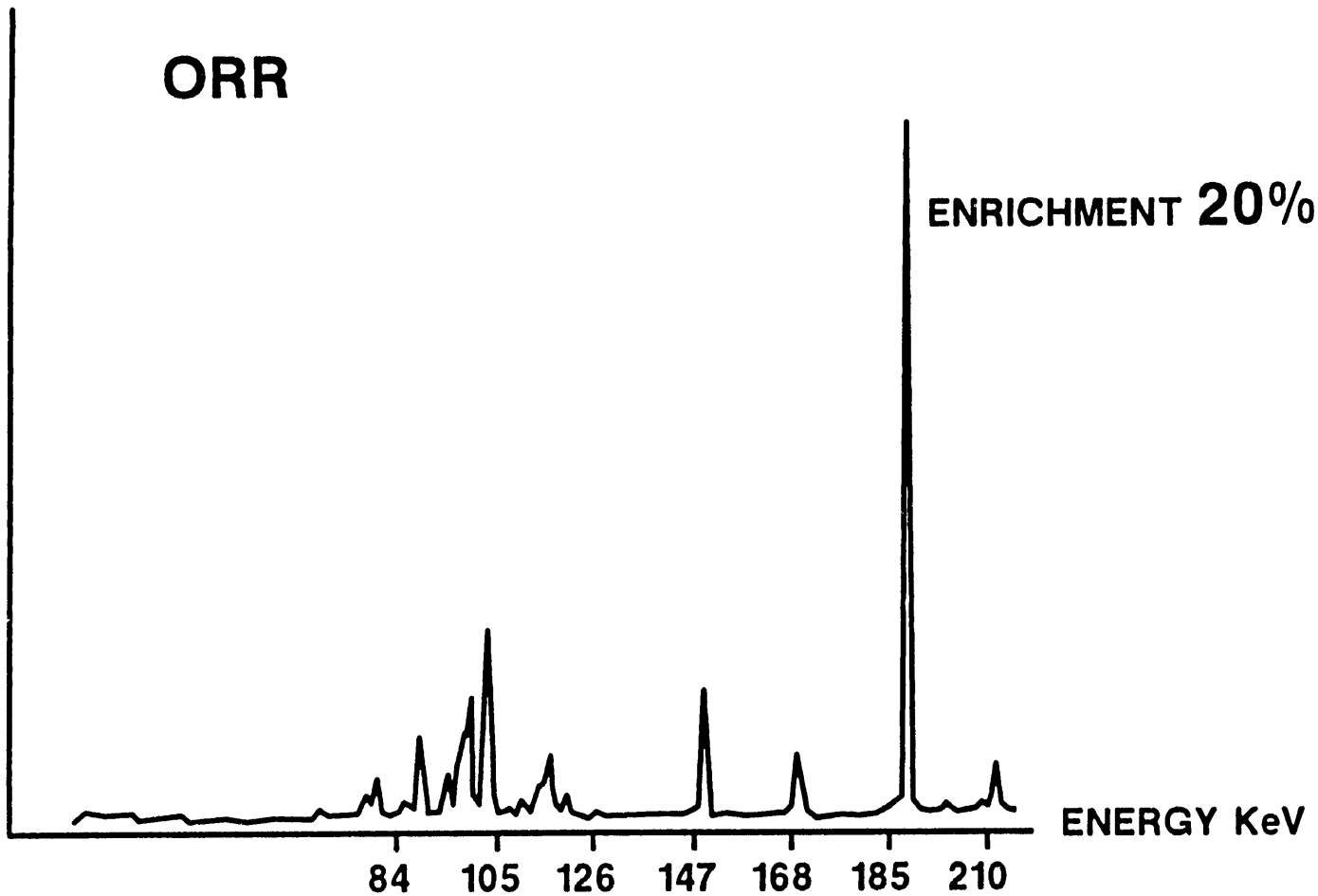

CERCA

FUEL PLATES ULTRASONIC INSPECTION
NORMAL INSPECTION

SEPT. 88

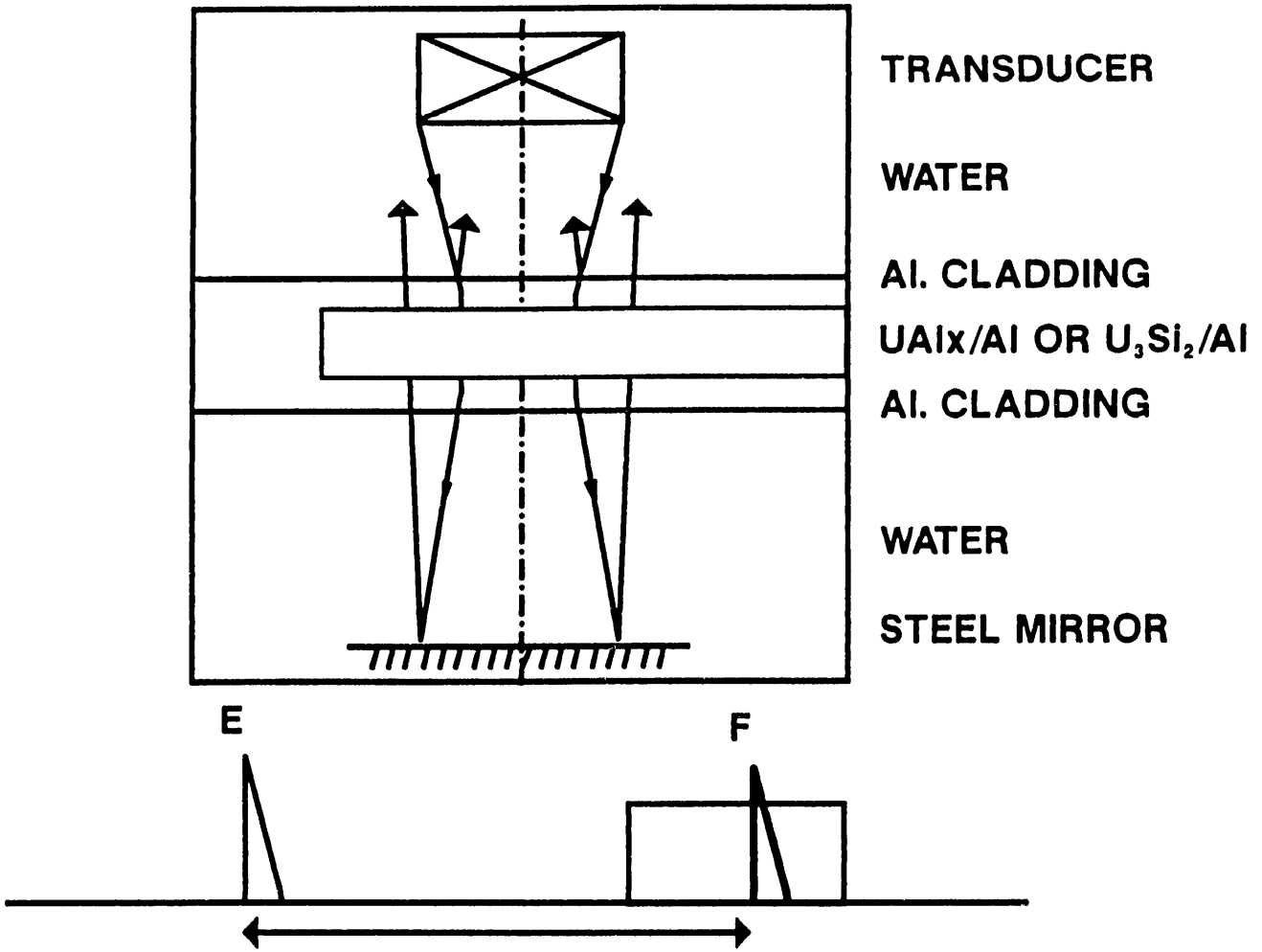

FUEL PLATES ULTRASONIC INSPECTION DEFECT EFFECT

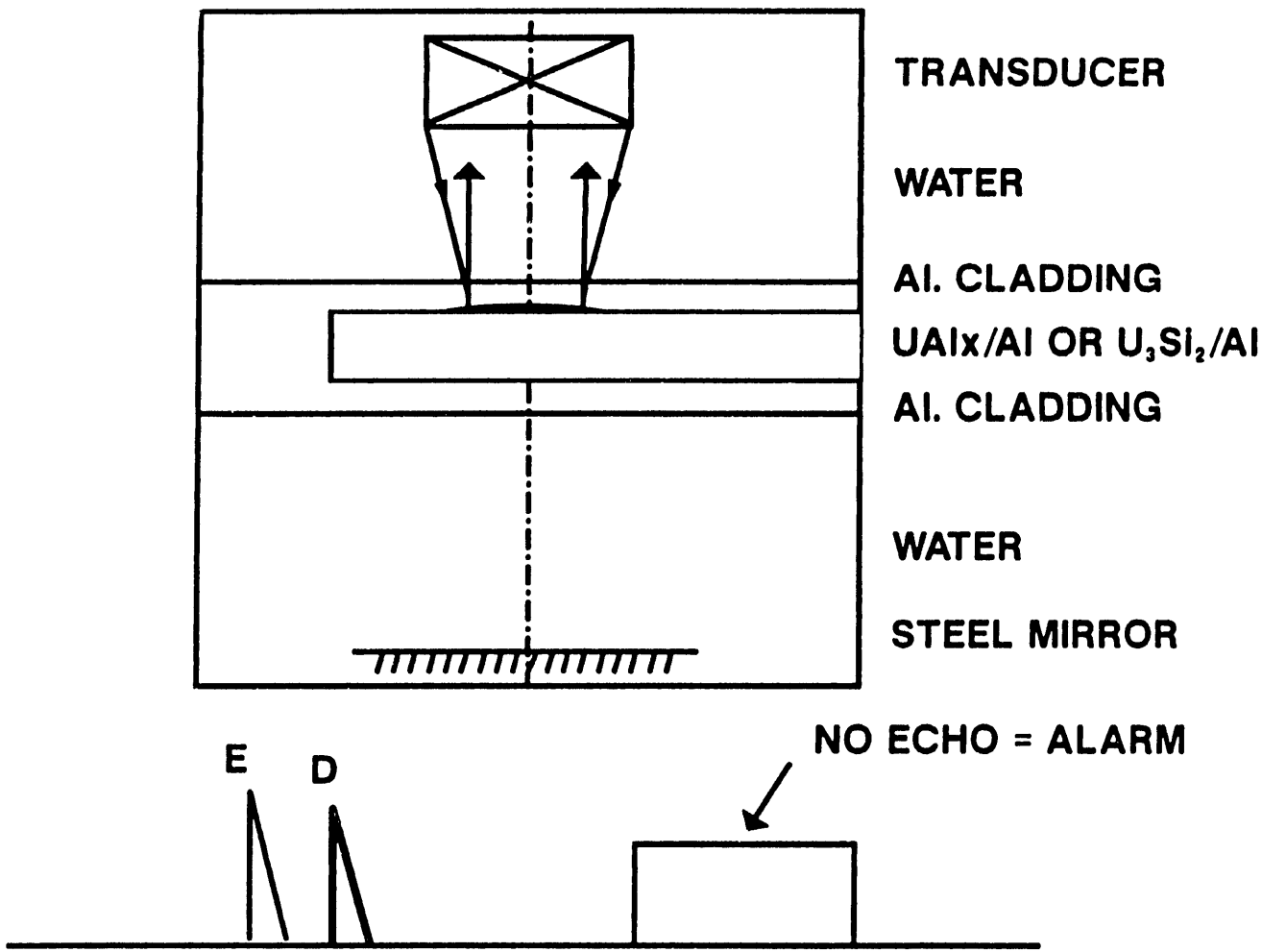

CERCA

FUEL PLATES ULTRASONIC INSPECTION
CORE EDGE EFFECT

SEPT. 88

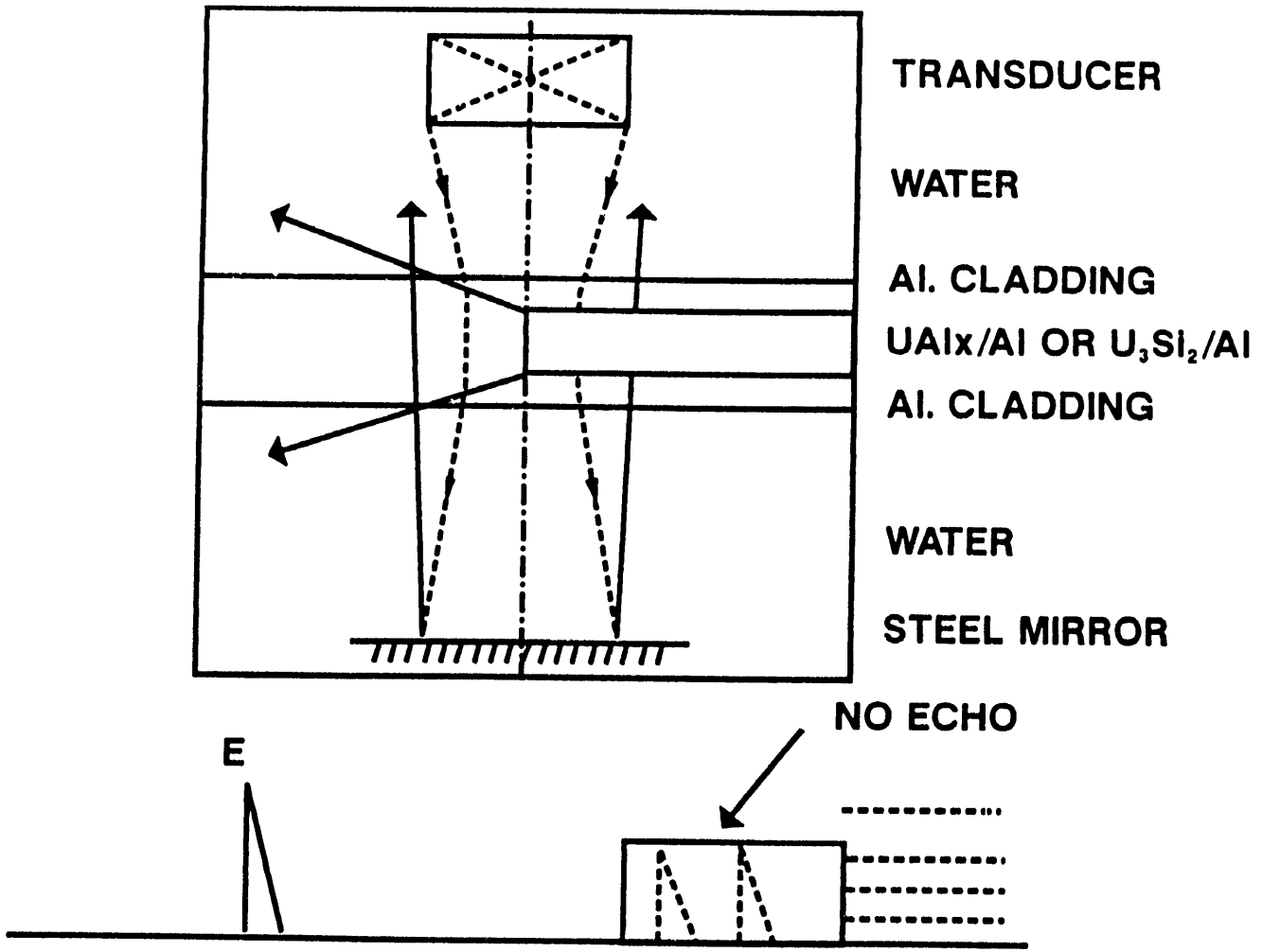

Manufacture of Research Reactor Fuels

R. W. Knight
Oak Ridge National Laboratory
Oak Ridge, Tennessee 37831
USA

Editor's Note

This paper summarized the information being published as Oak Ridge National Laboratory Report ORNL/TM-11809, "Observations in the Manufacture of Aluminum Based Research Reactor Fuel Elements." The abstract and table of contents of ORNL/TM-11809 are included in these proceedings in lieu of a summary paper. I encourage those with an interest in the subject to obtain the full report from the author.

Abstract

A large number of research reactor fuel elements are manufactured using aluminum. Configurations may vary, but the manufacturing sequence, problems, and philosophy are the same. Today, fuel forms are UAL^{x}, $U^{3}O^{8}$, or $U^{3}Si^{2}$. They are clad in aluminum and roll swaged into side plates, combs and end fittings are attached, and the unit is final machined. This report carries the reader through the manufacturing sequence and points out possible problems and solutions to problems in varying steps of the manufacture.

Contents

Abstract . . . . . .
Introduction . . . . . .
Material . . . . . .
Uranium . . . . . .
Aluminum Powder . . . . . .
Boron . . . . . .
Silicon . . . . . .
Powder Preparation . . . . . .
Weighing and Blending . . . . . .
Frames and Covers . . . . . .
Billet Assembly . . . . . .
Roll Bonding . . . . . .
Cold Rolling . . . . . .
Inspection . . . . . .
Homogeneity . . . . . .
Ultrasonics . . . . . .
Alpha Counting . . . . . .
Dimensional Inspection . . . . . .
Gamma Scanning . . . . . .
Boron Homogeneity . . . . . .
Destructive Examination . . . . . .
Fuel Elements . . . . . .
Conclusions . . . . . .
References . . . . . .

LEU FUEL ELEMENT PRODUCTION PLANT AT RISØ NATIONAL LABORATORY

P. Toft, J. Borring, E. Adolph
Metallurgy Department, Risø National Laboratory
DK-4000 Roskilde, Denmark

ABSTRACT

A production plant for fabricating LEU silicide fuel elements has been established at Risø National Laboratory. The first eight elements for the Danish reactor DR3 have been produced, based on 19.74 %-enriched U_3Si_2 powder. The production plant and the fabrication process has been set up without encountering major problems.

INTRODUCTION

Since the RERTR meeting in Gatlinburg November 3-6 1986, our main effort has been concentrated on finishing our HEU fuel element production. The three LEU fuel elements produced in our pilot plant (1) has been irradiated without incident (2).The current status is that we have stopped our HEU fuel element production and started our routine production of LEU fuel elements to the DR3 reactor.

FUEL ELEMENT DESIGN

The LEU fuel element is made with the same outer design as our HEU fuel element (Fig.1). The fuel content is increased from 150 g to 180 g U^{235} in order to compensate for the lower enrichment. The DR3 fuel element consists of 4 fuel tubes arranged concentrically. Each tube is made of 3 fuel plates welded together. All relevant fuel element data are shown in Table 1.

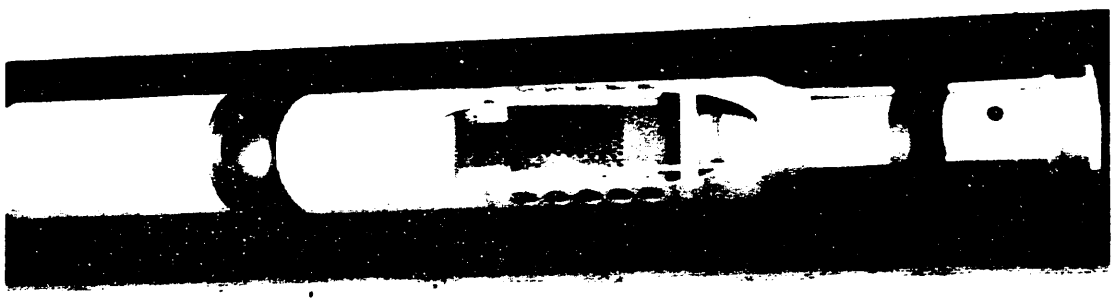

Fig 1. LEU fuel element

LEU FUEL ELEMENT PRODUCTION PLANT

The flow sheet in Fig. 2 and photos 1-13 give a general view of our LEU fuel element production plant. The plant has been established based on experience gained from our pilot plant production (1). During the spring 1988 we have fabricated eight elements without any major problems. Our annual production for the DR3 reactor is estimated to be fifty fuel elements.

CONCLUSION

Our LEU fuel element production plant has been established and is running satisfactorily. Process variables used in our pilot plant production (1) has shown a good reproducibility when implemented in our production plant.

Fig. 2

LEU Fuel Element Fabrication Line At Risø National Laboratory

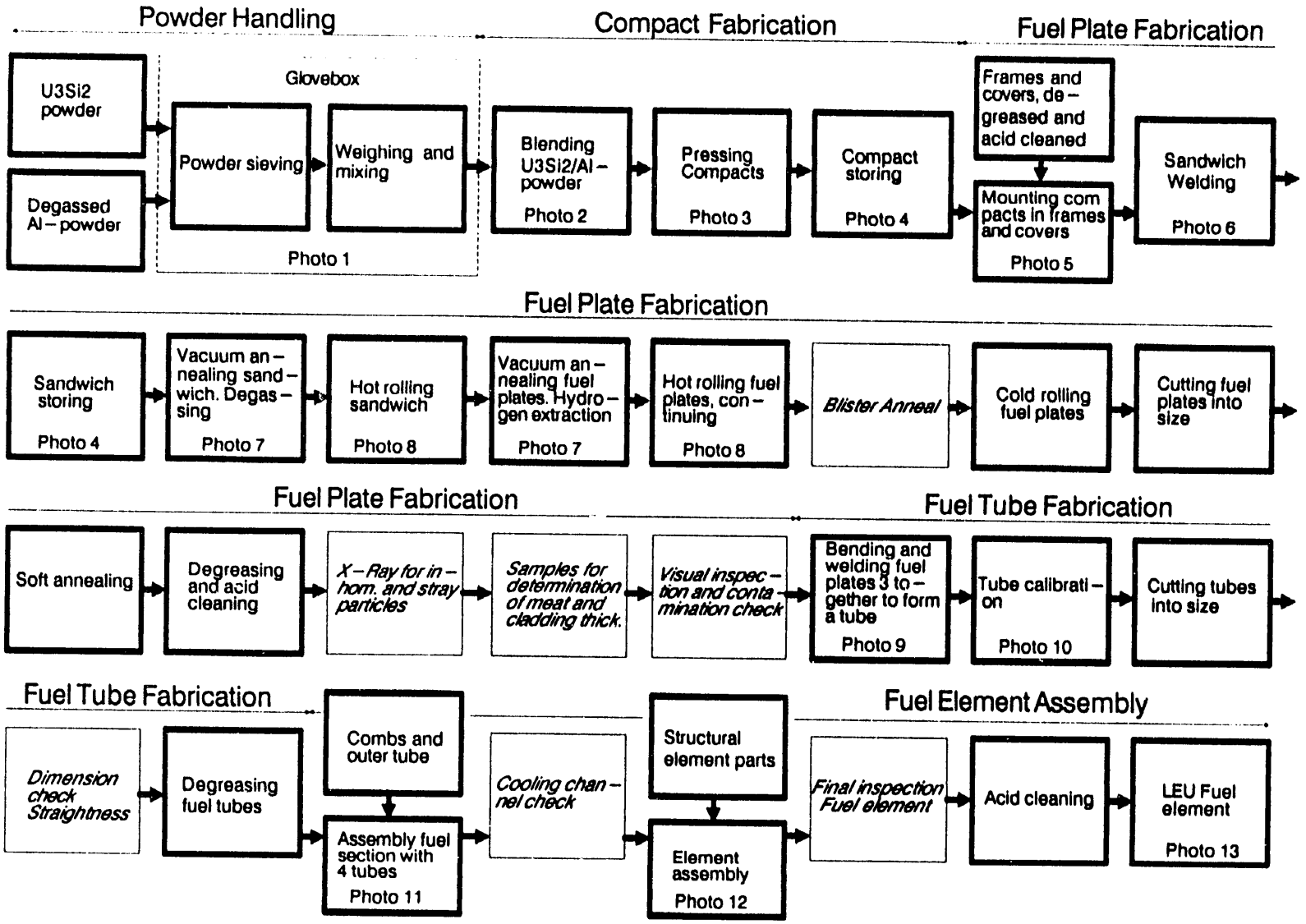

ACKNOWLEDGEMENT

The authors thank John Jespersen, Ole Olsen, Kjeld Sandsted and Erling Sørensen for their participation in our LEU silicide fuel work. We are indebted to The Argonne National Laboratory, The Babcox and Wilcox Company and The RERTR Project for their valuable contributions in connection with our conversion from HEU fuel element fabrication to LEU fuel element fabrication.

REFERENCES

1. P.Toft, J.Borring and E.Adolph, Metallurgy Department, Risø National Laboratory, DK-4000 Roskilde, Denmark. "Pilot plant production at Risø of LEU silicide fuel elements for the Danish reactor DR3" presented at the RERTR meeting in Gatlinburg, USA, November 3-6, 1986.

2. K. Haack, DR3, Risø National Laboratory, DK-4000 Roskilde, Denmark. "License approval of DR3's conversion to LEU" presented at the RERTR meeting in San Diego, USA, September 19-22, 1988.

Table 1: Fuel Element Data

Powder and Cladding Data	
U_3Si_2 Powder	−100+325 mesh; −325 mesh < =20%
Enrichment	19.74 % U^{235}
Al Powder	Alcan MD 101, −100 mesh
Cladding Material	AlMg1 (98% Al, 1% Mg, 1% Other)
Compact Data	
Compact Length	82.45 mm
Compact Width	57.70 mm
Compact Thickness	4.40/6.60 mm
Composition	w/o Al/U_3Si_2=33.6/66.4
Compacting Pressure	Approx. 80 tons
Uranium Density	3.3 g/cm^3
Fuel Tube Data	
Tube Length	660.4 mm
Core Length (nom.)	600.0 mm
Tube Thickness (nom.)	1.50 mm
Core Thickness (nom.)	0.56 mm
Cladd. Thickness (nom.)	0.47 mm
Diam. Fuel Tube 1	63.85 mm
Diam. Fuel Tube 2	73.65 mm
Diam. Fuel Tube 3	83.45 mm
Diam. Fuel Tube 4	93.25 mm

Powder Handling

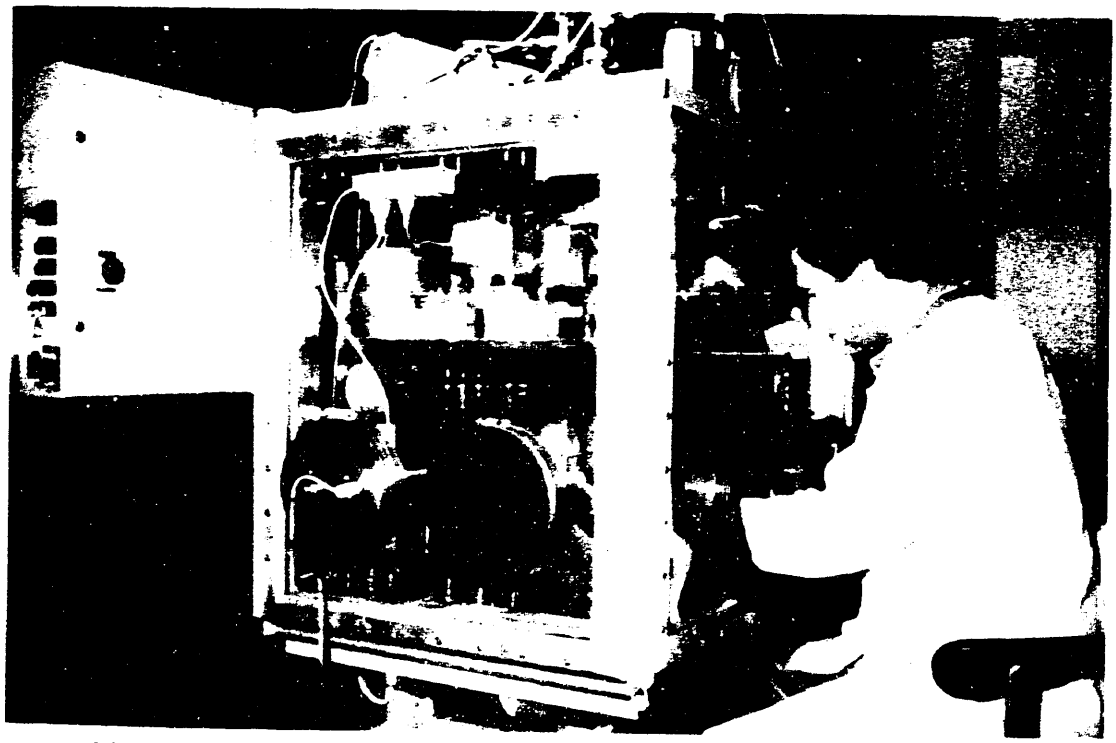

Photo 1: All powder handling is carried out in a glovebox containing an argon atmosphere with less then one percent oxygen.

Compact Fabrication

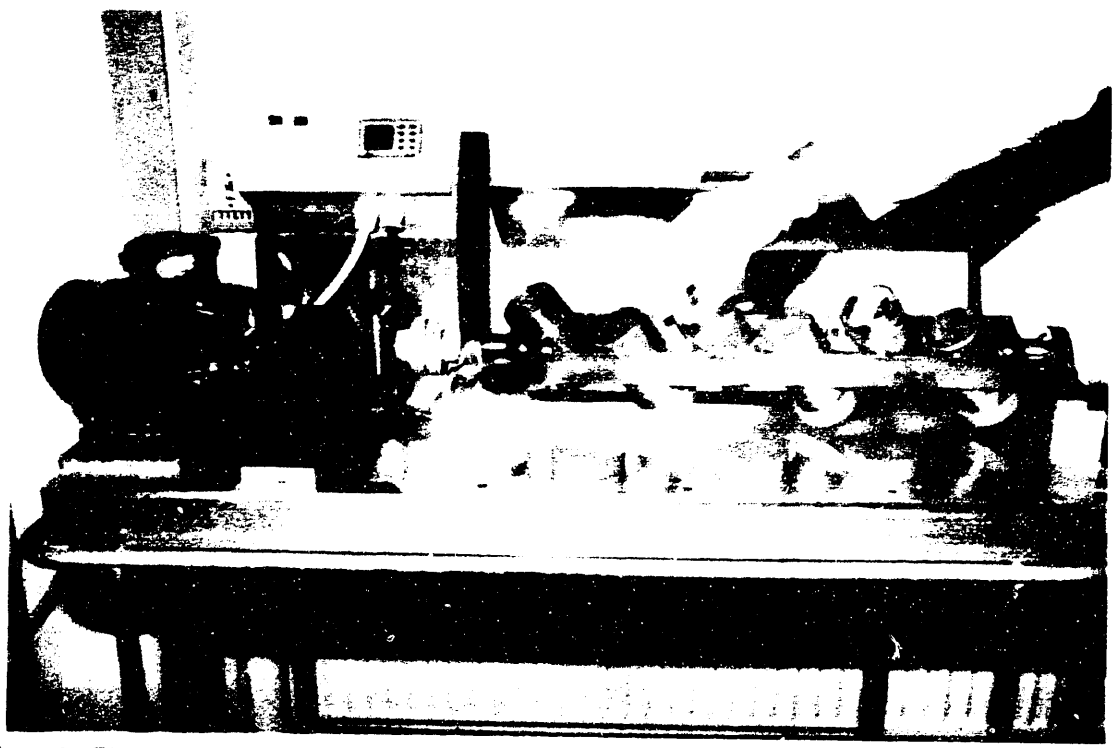

Photo 2: Blending of U3Si2/Al mixtures is carried out in a special blender.

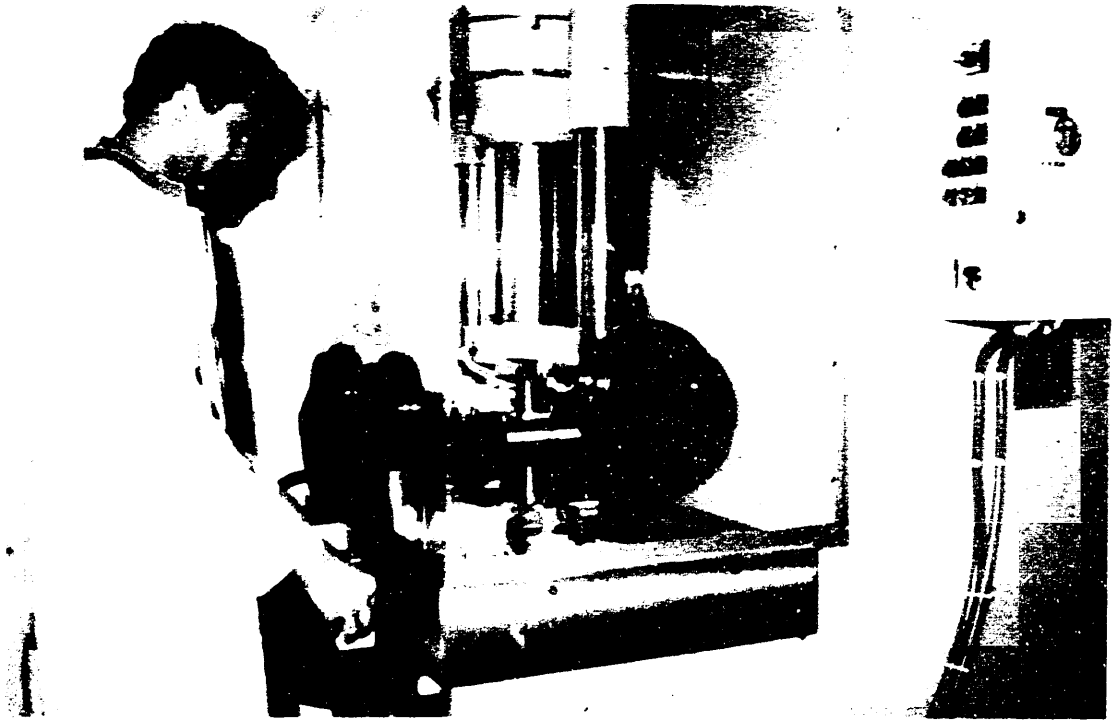

Photo 3: The pressing of U3Si2/Al compacts is carried out in a 250 t hydraulic press. All pressing operations are performed in a built in glovebox with a small negative pressure.

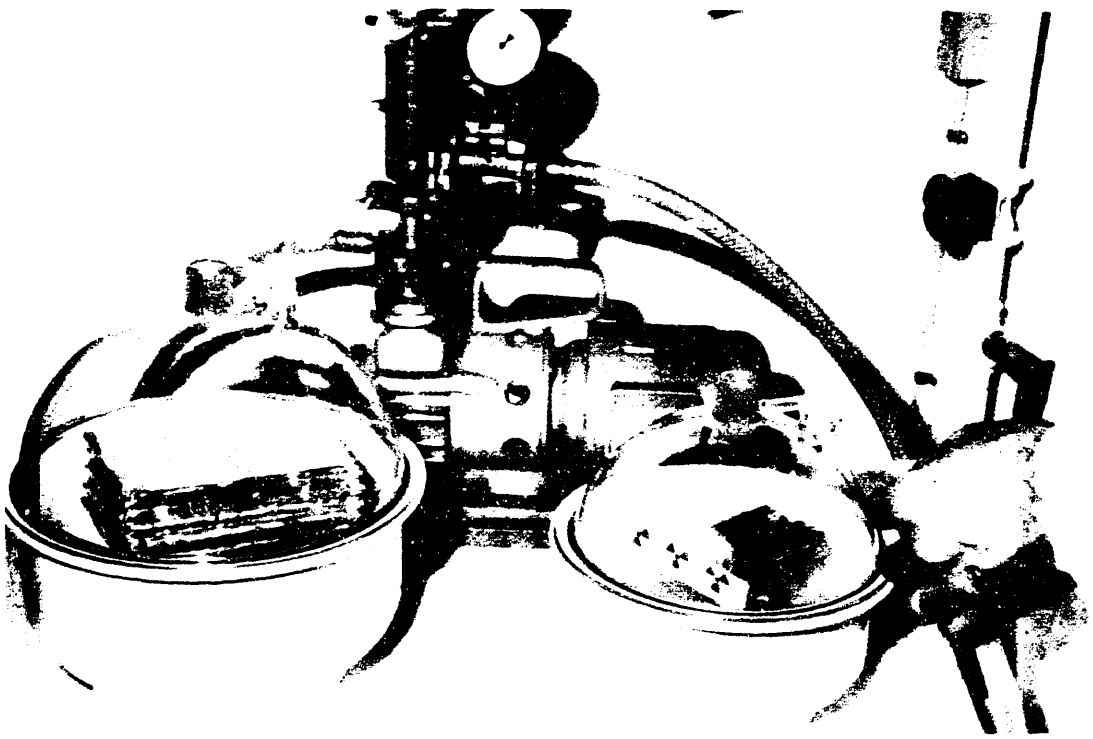

Photo 4: Compacts and sandwiches are stored in exicatores with a vacuum better than 10^{-2} torr.

Photo 5: Sandwiches are mounted in a fume cupboard. The frames are preheated to about 50 °C in order to ease the mounting , and to fit the frame/compact configuration, more closely.

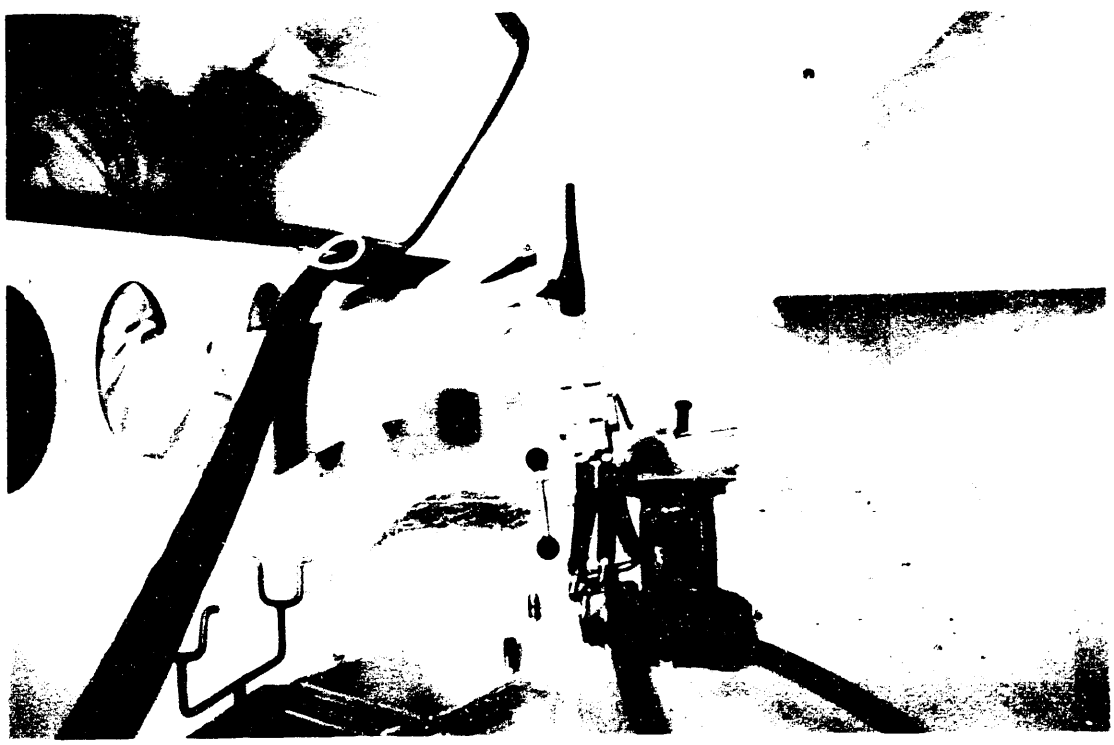

Photo 6: Sandwiches are welded in a fume cupboard with a controlled airflow. The sandwiches are mounted in a water cooled fixture which reduces the heat to the compacts during welding.

Photo 7: Sandwiches and semi finished plates are annealed in a vacuum furnace. Sandwiches are annealed in order to degass moisture absorbed during handling. Plates are annea–led in order to extract hydrogen from the core.

Photo 8: Sandwiches and plates are hot and cold rolled in a duo rolling mill.

Photo 9: Fuel plates are welded 3 together in a special fixture and bended to form a tube.

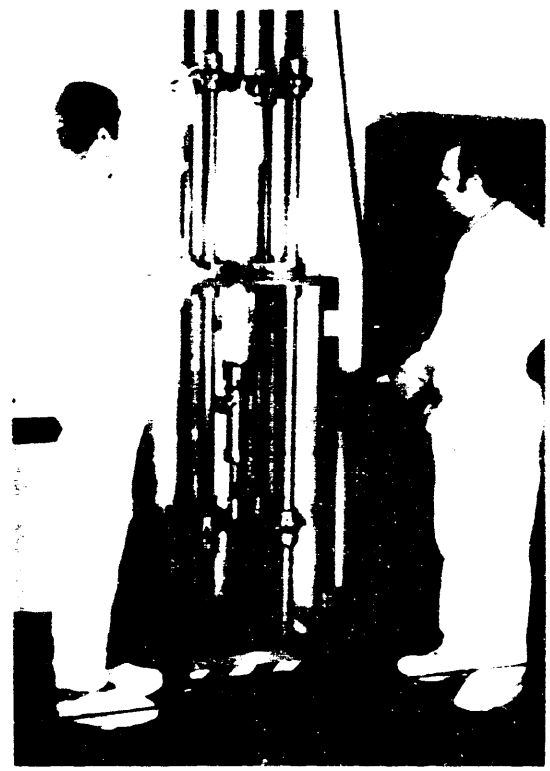

Photo 10: Calibration of fuel tubes to final shape

Fuel Element Assembly

Photo 11: Assembly of tubes into fuel sections.

Photo 12: Fuel element assembly.

Fuel Element Assembly

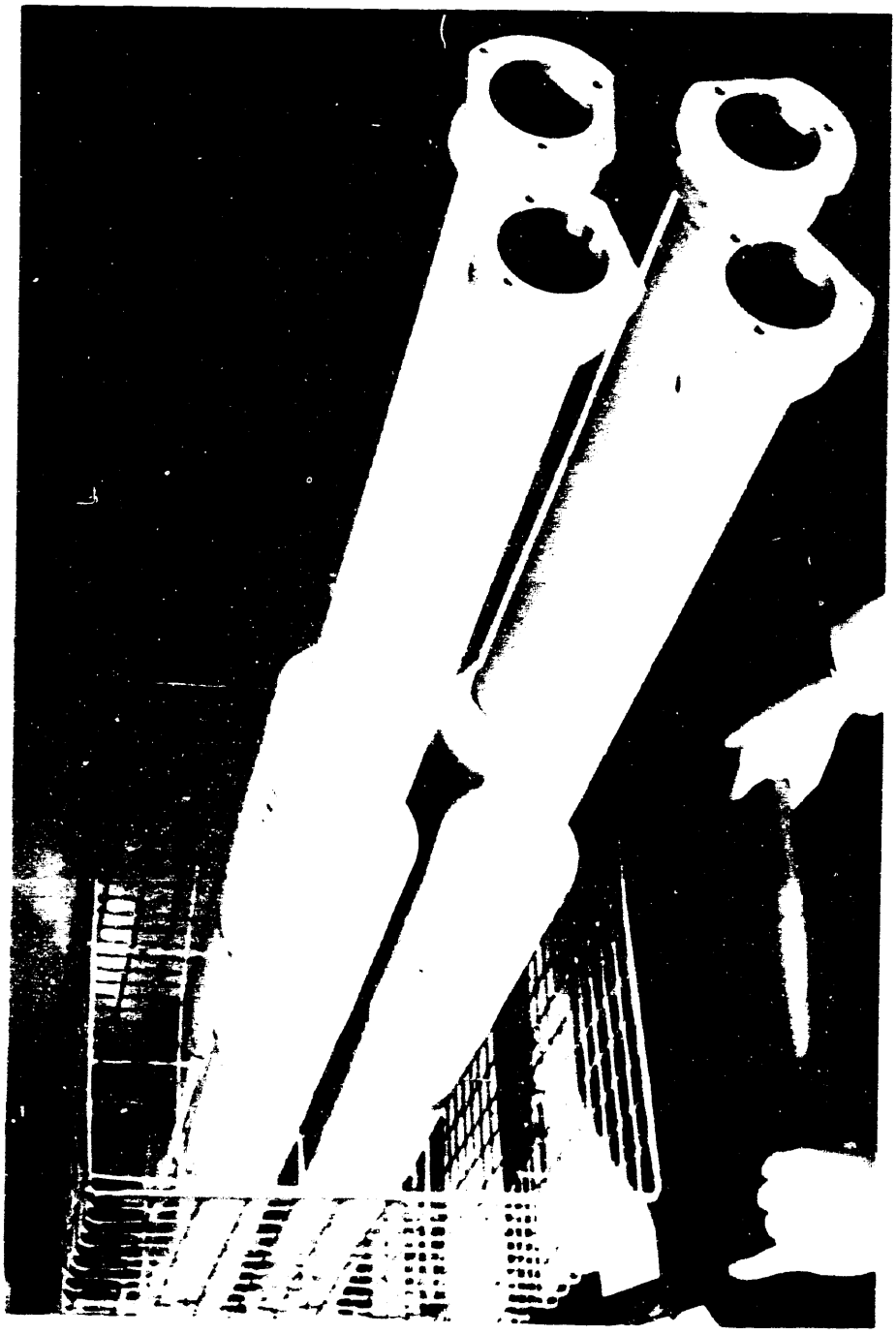

Photo 13: Four DR3 fuel elements with LEU

PREPARATION OF REDUCED ENRICHMENT FUELS FOR THE KOREA MULTI-PURPOSE RESEARCH REACTOR AND THE EFFORTS TO REDUCE THE DIFFICULTIES IN COMMINUTION OF U_3Si-Al DISPERSED FUEL

I.H.KUK, C.K.KIM, J.T.LEE
Korea Advanced Energy Research Institute
Daejeon, Korea

ABSTRACT

Fuels to be loaded in KMRR (Korea Multipurpose Research Reactor) will be similar to the pin type of the Canadian MAPLE-X. The fuel meat will consist of U_3Si_{1+x} dispersed in an Al matrix with enrichment of less than 20 %. Test fabrication of these fuel meats was made with depleted uranium in accordance with the conventional methods developed so far in the RERTR international program.<1>

It was experienced that the heat-treated blank with U_3Si_{1+x} was so tough, especially when x is close to 0, that particular equipment and labour had to be introduced in the following comminution. Better comminution was attempted by comminuting the as-cast ingot, composed of brittle U_3Si_2 and free uranium, prior to the heat-treatment. The concentration of uranium and silicon fluctuates in the cast ingot due to the formation of the primary U_3Si_2. The comminution below a certain size gives rise to inhomogeneities between particles. The size limit is decreased by reducing the size of the primary U_3Si_2 dendrites. For 10μm of the primary U_3Si_2 dendrites, the particles over 350μm contain sufficient numbers of primary phases for the homogeneity, resulting in a satisfactory heat-treatment which leaves no appreciable uranium or silicon-rich phase untransformed behind.

INTRODUCTION

KAERI made a plan to build a multi-purpose research reactor of 30 MWe. Design and construction are under way, and are scheduled to be completed by 1992. The reactor will be used in testing nuclear fuels and reactor components, production of radio-isotopes and neutron transmutation doped silicon, neutron activaton analyses of various materials, research employing neutron beams, neutron radiography, etc. The general layout of the reactor is as shown in Fig.1.<2>

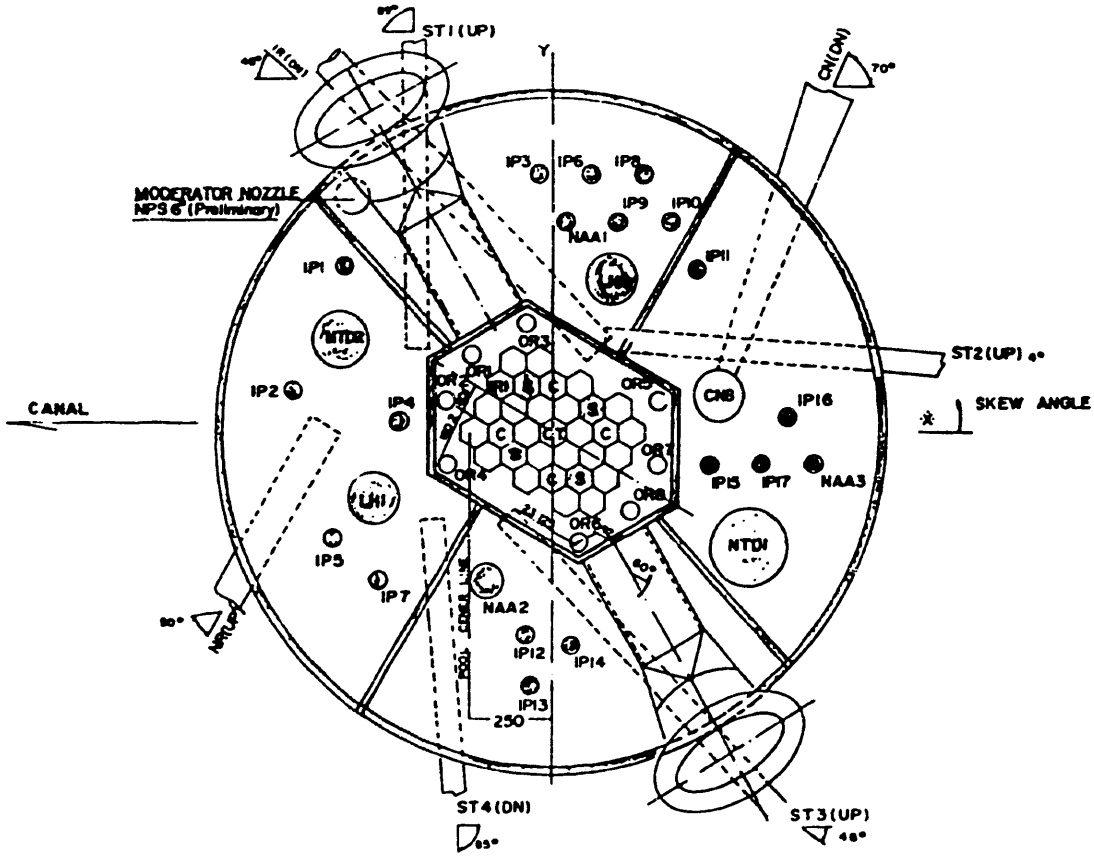

Fig.1 The plane view of the reactor and the experimental facilities (from proceedings of the 2nd appl. physics symp. on the phys in nucl. industry, Korean Physical Soceity, p 161)

The inner core has 31 honeycomb channels: 20 channels to accommodate the hexagonal driver fuel assemblies of 30 elements each ; 8 channels to accept the circular shim fuel assemblies of 18 elements each ; 3 sites, including the central flux trap, provided for testing rigs of fuels and materials. Both fuel assemblies, hexagonal with 30 elements and circular with 18 elements, have the same pin-type element design. Each element has an extruded fuel meat cladded with Al having 8 fins for better heat transfer. The fuel meat contains uranium silicide particles dispersed in an aluminum matrix.

Uranium silicide particles are fabricated in a composition of U_3Si_{1+x}, following the techniques developed so far in the RERTR program. X in the U_3Si_{1+x} will be minimized for higher loading, but the lower limit will be determined studying the performance at high burn-up. Extruded pins were made by casting the ingot with depleted uranium in arc or induction furnaces, heat-treating in vacuum, comminuting to the final size, blending with Al powders and extruding into the designed dimension.

It was pointed out that comminuting becomes more time-consuming, necessitating heavier equipment and several extra processes to be added, as x approaches 0 in U_3Si_{1+x}. This is due to the difference in toughness between U_3Si and U_3Si_2. U_3Si_2 is brittle enough to be comminuted easily even by hand, in mortar and pestle; on the other hand, U_3Si is so tough that heavy-duty equipment and a complicated pulverizer must be added in the process. Moreover powders and chips are left even after the end of the batch operation ; the products are mixed with impurities and some more undesirable labour is required. The difficulties in comminuting U_3Si can be reduced if the ingot is comminuted before the heat-treatment leading to the peritectoid reaction from U_3Si_2 to U_3Si. The cast ingot with U_3Si_2 + Uss is brittle and is comminuted easily. Thus, an attempt was made to exchange the order of heat-treatment and comminution processes. The process flows are compared in Fig.2.

However, the as-cast ingot always has micro-segregation due to the formation of the primary U_3Si_2 dentrite particles. Moreover, there occurs macro-segregation in the ingot obtained in induction melting and casting, and a small amount of segregation is produced in arc melting and casting as well. These segregations limit the size of the particles to be heat-treated. The particle which contains a relatively greater amount of U_3Si_2 is richer in Si, so that it may remain as it is even after the long heat-treatment. On the other hand, the particle which contains a relatively smaller amount of U_3Si_2, is rich in U, so that it leaves free uranium untransformed even after the long heat-treatment. These cause inhomogeneity between fuel particles, and may result in inhomogeneity in loading density and failure around the area of the free uranium.

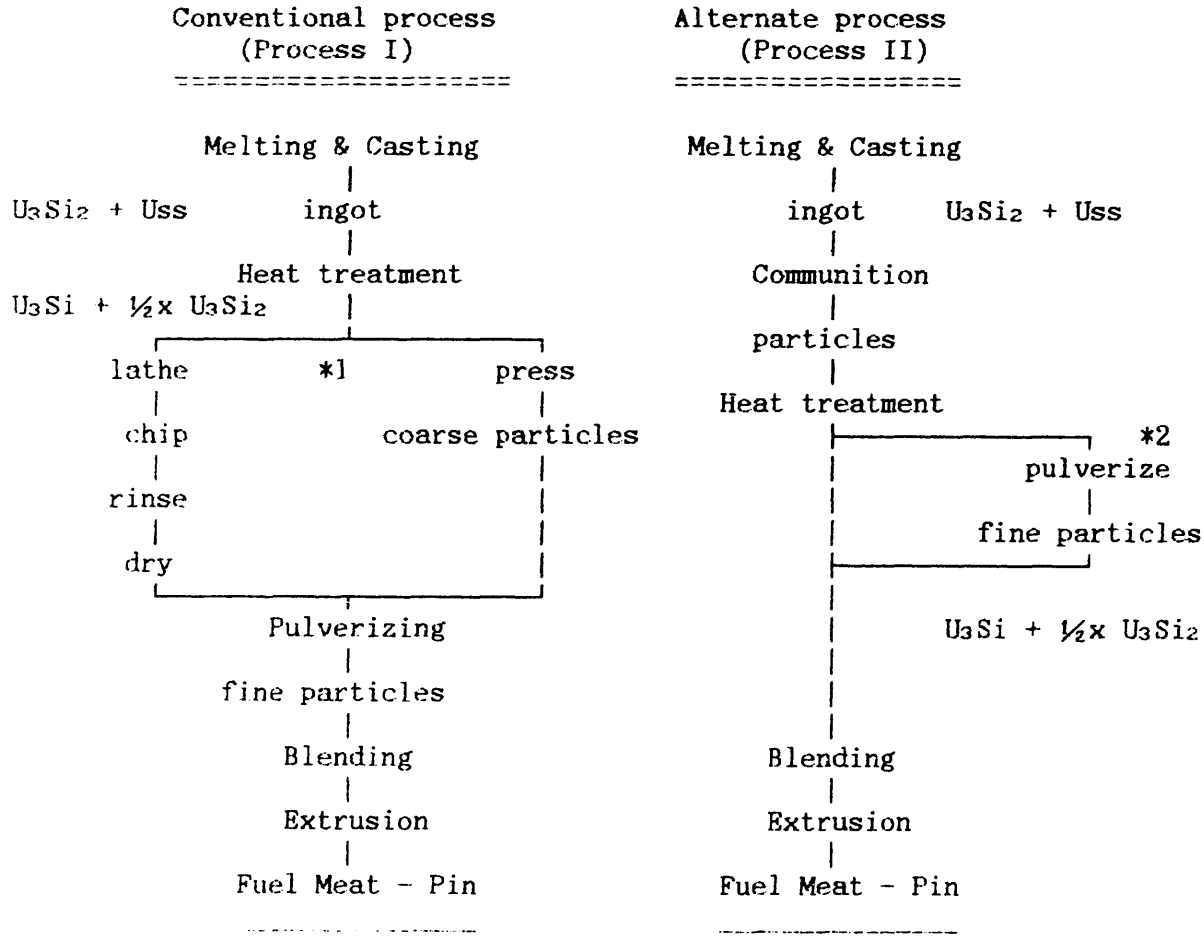

Fig.2 Comparison sheet of the process flows

*1 The ingot melted and cast in induction furnace is processed by lathe. The ingot melted and cast in arc furnace is processed by press and milling.

*2 If the heat-treated particles are fine enough, they can be used directly in blending.

The smaller the comminuted particles, the greater the inhomogeity between particles. Comminuting down to the size comparable with the primary U_3Si_2 dendrites, one particle may contain nothing but U_3Si_2 and another may contain all but free uranium. This type of inhomogeneity due to micro-segregation decreases as the average particle size increases. Above a certain size, the inhomogeneity due to the micro-segregation exists no longer. This will be called "the critical size". With an infinite size of material to be heat treated as is used in the conventional process, the micro-segregation can be reduced within a period of time. The critical size depends on the primary U_3Si_2 size. Fortunately, we can control the size of the primary U_3Si_2 dendrites by the cooling rate in solidification of the ingot.

Studies were made following process II in Fig.2; first, to find the dependence of the primary U_3Si_2 particle size on the cooling rate in solidification of the ingot; second, to find the critical size of the comminuted particle for a certain size of the primary U_3Si_2.

Experiments

The conventional process shows difficulties, as described above. Since process is well known, the detailed descriptions of process I in fig.2 is excluded here. Rather, process II is mainly described here.

Casting Alloys and the Measurement of Cooling Rate

Various cooling rates were obtained using both an arc melting furnace and an induction melting furnace. In induction melting, three ways of cooling were used; molten alloys were held at 960 °C to form eutectic U_3Si_2 and cooled; molten alloys were cooled controlling the cooling rate of the zirconia mold and graphite mold; molten alloys were cooled in a Cu mold cooled by running water. In arc melting, two ways of cooling were used; conventional cooling by introducing He/Ar to the molten ingot on the Cu hearth and rapid cooling by passing He/Ar through liquid nitrogen trap.

Depleted uranium (99.9 wt%) and silicon lump (99.9999 wt%) were charged in a weight ratio of, 96.1 / 3.9 in arc melting, 95.8 / 4.2 in induction melting. Alloy compositions were analyzed showing the results of silicon balance, 3.90 $\pm$ 0.05 wt % in arc melting, 4.12 $\pm$ 0.27 wt% in induction melting. The statistical deviation in silicon weight in induction melting is introduced by the negative segregation from top to bottom in the cast.

Cooling rates were measured in two ways; thermocouples were dipped in the molten cast ingot; and an optical pyrometer was pointed on the molten ingot and the reading was recorded automatically through the pyrometer system.

The sizes of the primary U_3Si_2 were measured metallographically by the image analyzer. Micro-variations of uranium and silicon were traced by EDX analysis.

Communition

The ingot cast in the induction furnace was in 25 mmϕ x 160 mm L. One group of ingots were crushed into a small segments by a 100 ton hydraulic press and were comminuted into various sizes by mortar and pestle of tool steel. The other group of ingots were machined into chips by lathe and were comminuted by mortar and pestle. Chips were rinsed and dried before comminution. The ingot cast in the arc furnace was made into a button shape of 70 mm wide and 8 mm thick. The ingot was crushed in the press and was comminuted by mortar and pestle.

Ingots were comminuted to 6 different size groups: +10, -10 / +20, -20 / +40, -40 / +100 meshes; 150 - 40 μm and below 40 μm.

The comminuted particles were mounted in an epoxy resin and were observed under the optical microscope and scanning electron microscope, to compare the size of the primary U_3Si_2 with the size of the comminuted particle and to find if there were any preferential sites propagating cracks between phases. The specimen observed in SEM was coated with gold. The fracture surface of the particles were also examined to find if crack propagating surface morphology may have any influence on the inhomogeneity between comminuted particles.

In a conventional process, the ingot from induction melting was heat treated in vacuum and the billet was machined to chips and pulverized to the required size. The ingot from arc melting was crushed by a press and a roll mill, and was pulverized in an impact mill.

Heat treatment

The comminuted particles were loaded on a steel boat and were heat-treated in a resistance furnace at 800 °C in vacuum 10E-6 torr for the various times, 1, 5, 24, 48 and 72 hrs. The heat-treated particles were mounted in an epoxy resin and the phase changes were examined under the optical microscope. The phase change was also analyzed by x-ray diffractometry. Uranium and silicon content were measured by line scanning of EDX on the SEM of the polished surfaces to identify the phases. The degree of inhomogeneity (I) is given by the ratio of the number of particles with free uranium remaining untransformed (Nu) to the total number of particles (Nt).

$$I = \frac{Nu}{Nt} \qquad (1)$$

Results and Discussion

The Size of the Primary U_3Si_2 Particles

Fig.3 shows the variation of the primary U_3Si_2 size with the cooling rate. Large dendritic particles are those obtained in an induction furnace and small particles below 10 μm in arc furnace. As is well known, the particle size decreases with the cooling rate.<3> It is noted that we can obtain dendritic particles close to 5 μm with a cooling rate over 50 °C/sec. The particle size approaches and levels out to 5 μm when the cooling rate is increased over 50 °C/sec. This indicates that we can reduce the dendritic particle size but no smaller than 5μm.

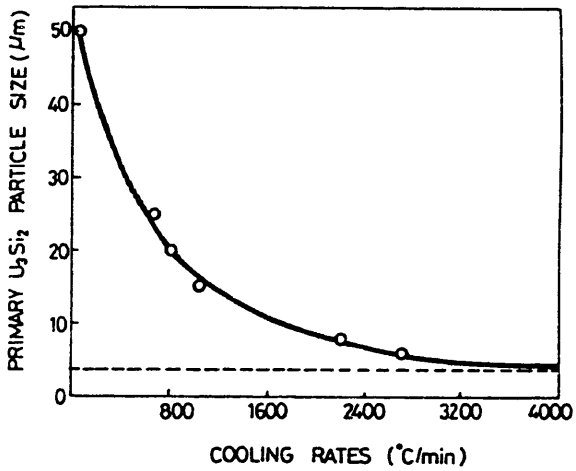

(Fig.3 Primary U_3Si_2 particle size vs. the cooling rate of the molten ingot.)

X-ray Analysis

As-cast ingots and the comminuted particles show all the similar results, as is in Fig.4. They consisting α-uranium, γ-uranium, U_3Si_2 primary dendrites, U_3Si eutectoid in free uranium matrix.

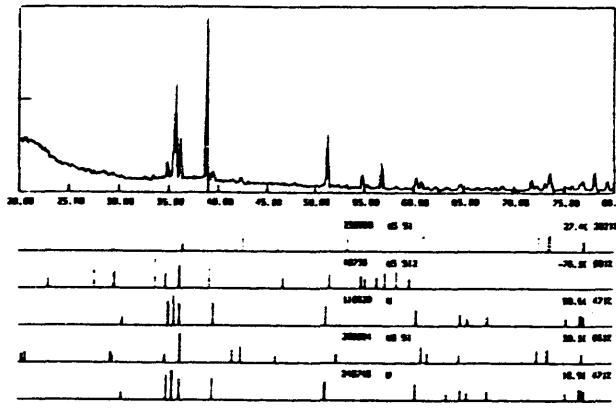

Fig.4. The result of x-ray diffractometry of as-cast ingot and of the comminuted particles.

As a convenience, the results are introduced first for the primary U_3Si_2 particle size 5- 30 μm, obtained in an arc melting furnace. The billet heat-treated at 800 °C for 72 hrs (in process I in Fig.1) shows no free uranium left untransformed and and negligible U_3Si_2, as shown in Fig.5a. All the remarkable peaks in this result stand for U_3Si. This indicate that the peritectoid reaction is completed leaving no free uranium. This result is compared with the particles over 40 mesh,i.e. , +10, -10/+20, -20/40 mesh, heat-treated at 800 °C for 24 hrs (Fig.5b) and for 72 hrs (Fig.5c). There is little difference between the three, Fig. 5a, 5b and 5c. This means that the particles over 40 mesh can be completely heat-treated within 24 hrs. The particles of size between 150 μm and 44 μm show evidently, in Fig.6a, that some untransformed free uranium was left. This indicates that some of the comminuted particles are smaller than 'the critical size'. It causes inhomogeneity so that one particle is poor in silicon and rich in uranium while the reverse is true in another particle. This phenomenon is found more obviously in Fig.6b where the result of the comminuted particles smaller than 44μm is shown.

With a primary U_3Si_2 size greater than 30 μm, untransformed free uranium was always left even after 72 hours at 800 °C, whatever the size of the primary U_3Si_2 may be. The x-ray results are quite similar to those of Fig.6b and are not shown here for simplicity.

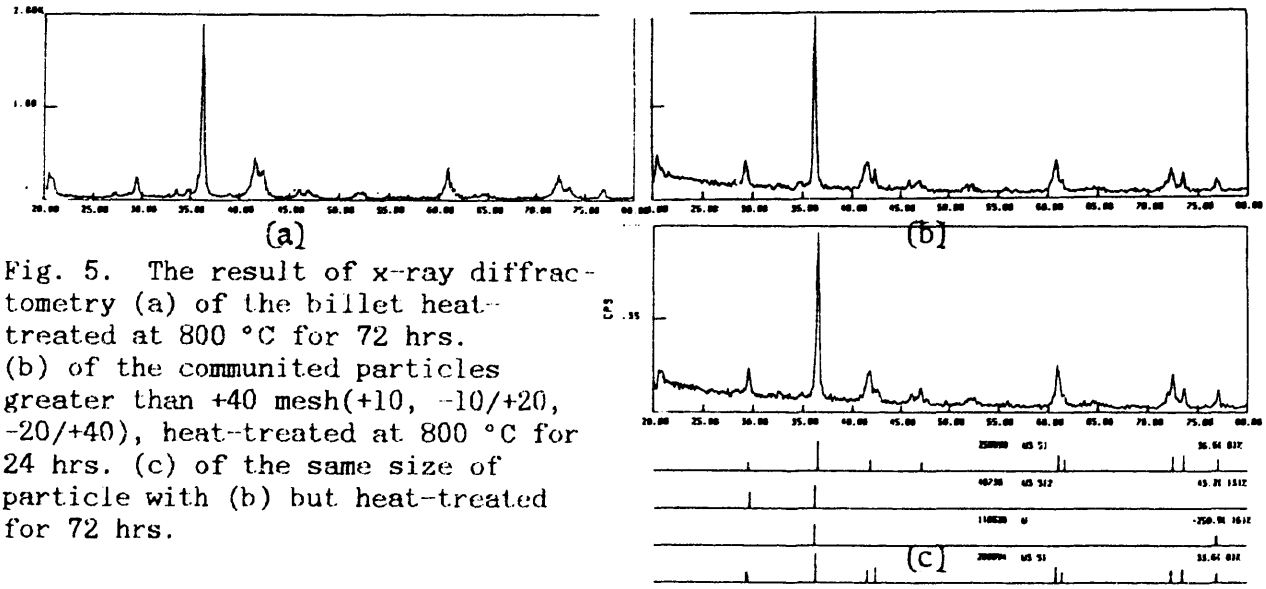

Fig. 5. The result of x-ray diffractometry (a) of the billet heat-treated at 800 °C for 72 hrs. (b) of the communited particles greater than +40 mesh(+10, -10/+20, -20/+40), heat-treated at 800 °C for 24 hrs. (c) of the same size of particle with (b) but heat-treated for 72 hrs.

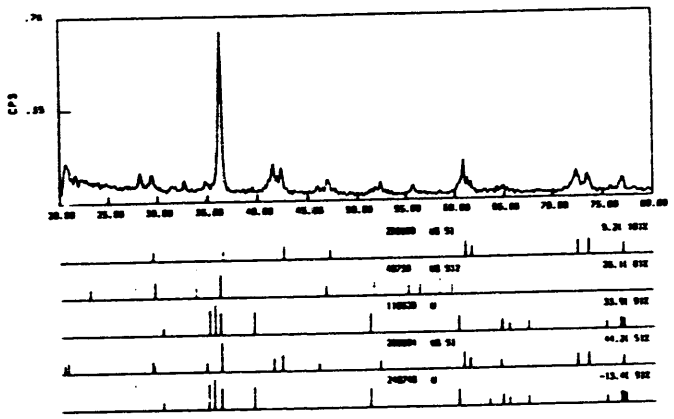

(a)

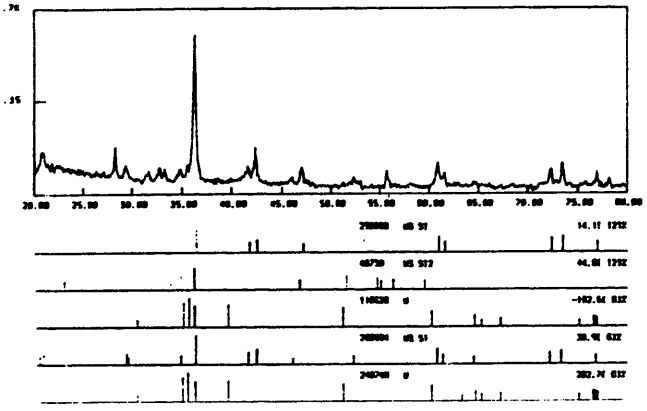

(b)

Fig. 6. The result of x-ray diffractometry (a) of the comminuted particles with sizes between 150 and 44μm heat-treated at 800 °C for 72hrs. (b) of the comminuted particles with sizes smaller than 44μm heat-treated at 800 °C for 72hrs.

Fracture surfaces of the comminuted particles

The ground and polished surface of the comminuted particle before heat-treatment were examined under SEM and analyzed by EDX. The polished surface shows that crack propagate randomly both through the primary U_3Si_2 particles and the free uranium matrix, in Fig.7a. Note the area in the circles of this micrograph. Cracks propagate transgranularly, not altering directions at the interface between phases. This is identified by the fracture surface observation in SEM. In Fig.7b, fracture surfaces are found to be dominantly transgranular. Therefore, the inhomogeneity between particles cannot be attributed to the crack propagating morphology on the surface of the comminuted particles. Consequently, it is proposed that the inhomogeneity between particles arises not from the fracture surface morphology but from the statistical relation of the population and size of the primary U_3Si_2 particles within the comminuted particle size.

Fig. 7a SEM shows the polished surface of communited particle. Note that cracks propagating in the circled area. Matrix is the uranium solid solution and the dark second phases are primary U_3Si_2 paritcles. (x200)

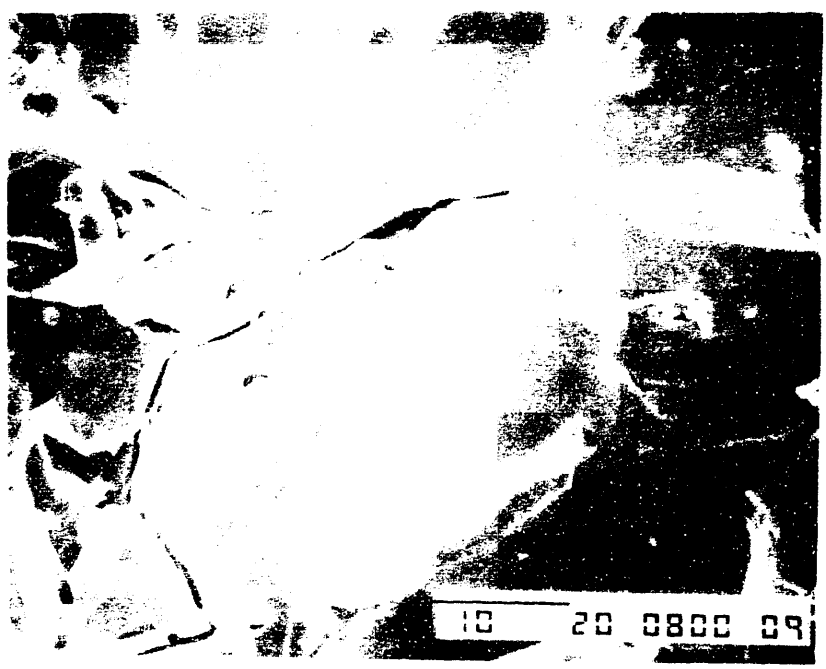

Fig. 7b Fracture surfaces of the communited particles.(x1000) The size of the particle is -10/+20 mesh.

Phase Identification by EDX

The ground and polished surface of the particle comminuted before heat-treatment was line scanned by EDX in SEM to analyze the content of uranium in different phases. Fig.8a is the result of EDX in the arc melted specimen. This result shows that uranium is in high concentration in the matrix where free uranium is mainly contained. In the middle of the micrograph, there are two holes where particles are missing. The content of uranium drops abruptly in this area, which implies that there were second phases, i.e., the primary U_3Si_2.

The specimen taken from the particle, comminuted after the casting in induction furnace, has a relatively greater size of the primary U_3Si_2, (see Fig.3). The polished surface of this specimen shows a microstructure as shown in Fig.8b. Si content is analyzed by line scanning of EDX on this surface. The dark phase is U_3Si_2, and the bright grey phase in the middle is the free uranium matrix in which small eutectic third particles spread all over. The result shows that Si is rich in the dark U_3Si_2 phase, but drops drastically in the free uranium matrix. Si content in the free uranium matrix shows three different levels. The uppermost levels are assumed to be U_3Si_2, the level of which seems to be lowered by the effect of using large a size beam in line-scanning. The middle level is assumed to be U_3Si and the lowest level seems to stand for free uranium.

Fig. 8a EDX line scanning of uranium content on the polished surface of as-cast ingot from arc furnace. Matrix is the uranium solid solution and the holes in the middle are the places where the U_3Si_2 phases are missed. Note that the uranium content drops in the holes (marked A).

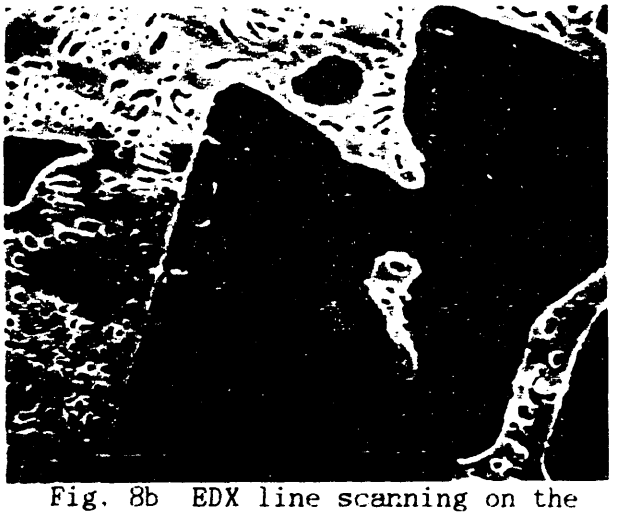

Fig. 8b EDX line scanning on the polished surface of as-cast ingot from induction furnace. Dark area shows the primary U_3Si_2 phase and the bright grey area shows uranium solid solution. Dark spots in the middle of the uranium solid solution are those of the third phase. Note that the silicon content drops to the lowest level in the matrix of uranium solid solution and to two levels in the places where the third phases located.

The comminuted particles smaller than 150μm with about 10μm primary U_3Si_2, have a distribution of phases as in Fig.10a; and the heat-treated particles show an inhomogeneity due to the fact that one has a great amount of untransformed free uranium and another has a relatively large amount of U_3Si_2 left, as is shown in Fig.10b. This inhomogeneity effect is reduced as the particle size increases. The particle -40/+100 mesh is in the middle of this trend showing some retained free uranium in Fig.11. The particles greater than +40 mesh complete the transformation within 24 hrs, as shown in Fig.12a. The particles greater than +20 mesh show no difference, as shown in Fig.12b.

These results of the metallographical analysis agree well with the x-ray analysis.

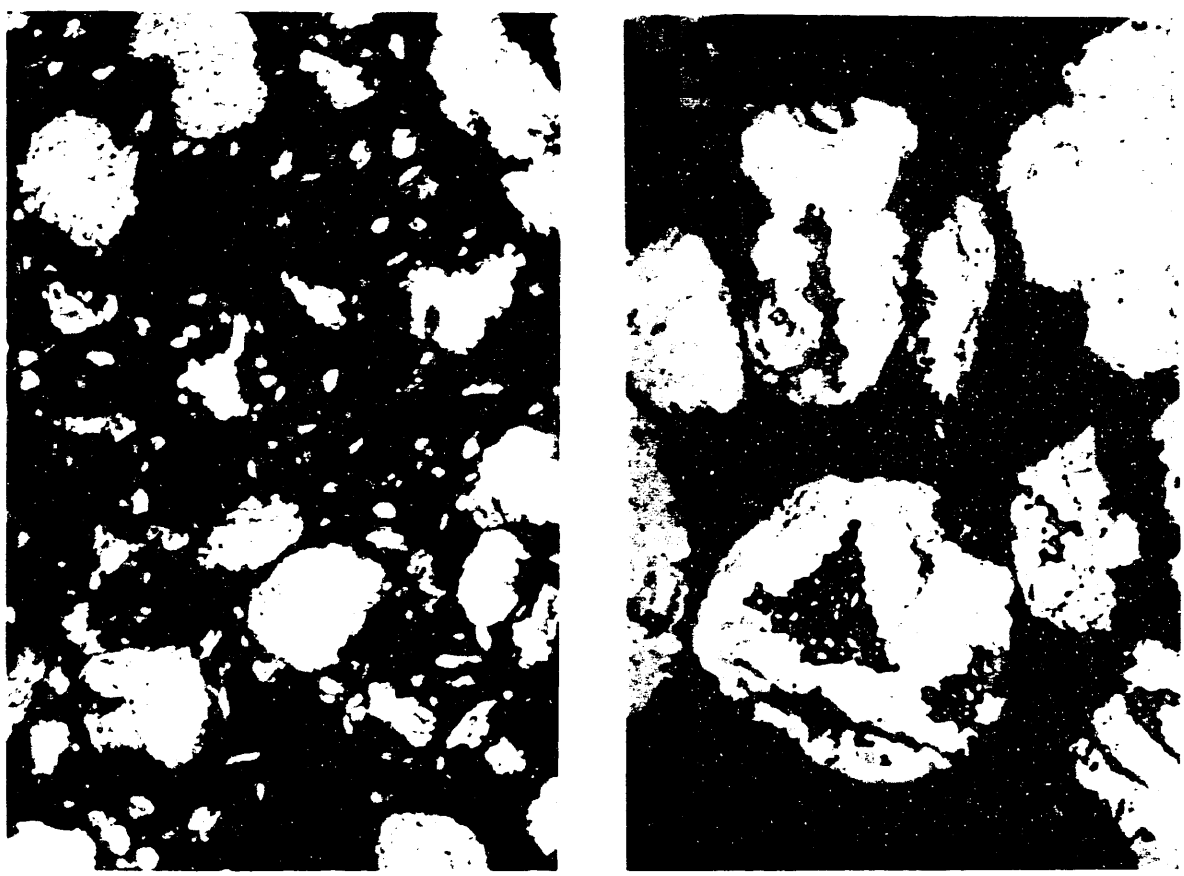

(a) (b)

Fig. 10 (a) The comminuted particle smaller than 44μm with primary U_3Si_2 phases of about 10μm. The particle size is compared with the size of U_3Si_2. (x400) (b) The heat-treated particles of the size smaller than 150μm with primary U_3Si_2 of 10μm. Note the evidence of inhomogeneity caused by free uranium left untransformed in some particles. The matrix is uranium solid solution and the small phases are U_3Si_2. Heat treated at 800 °C for 72 hrs.(x400)

Peritectoid Reaction of the Comminuted Particles

Heat-treatment was performed with six different comminuted particles and for 6 different primary U_3Si_2 sizes. The point is to find the formation of U_3Si and the amount of U_3Si_2 and free uranium retained after the heat-treatment. The amount of U_3Si_2 and free uranium left in the heat-treated particle shows the inhomogeneity of the chemical composition of a particle. The critical size of a particle is determined by the inhomogeneity factor (I in Equ.1), with respect to the primary U_3Si_2 size. In practice, the results are introduced here just for two extremely different sizes of primary U_3Si_2: one greater than 30 μm obtained in an induction furnace; and another about 10 μm obtained in an arc furnace. Other results are not important to the present purpose to find the smallest critical particle size for comminution.

The particle with the primary U_3Si_2 greater than 30 μm does not complete the tranformation leaving a great amount of untransformed free uranium and U_3Si_2 even after the long time of heat-treatment. The micro structures are shown in Fig.9a (for a particle machined into chips and comminuted before heat-treatment) and in Fig.9b (for a particle after heat-treatment).

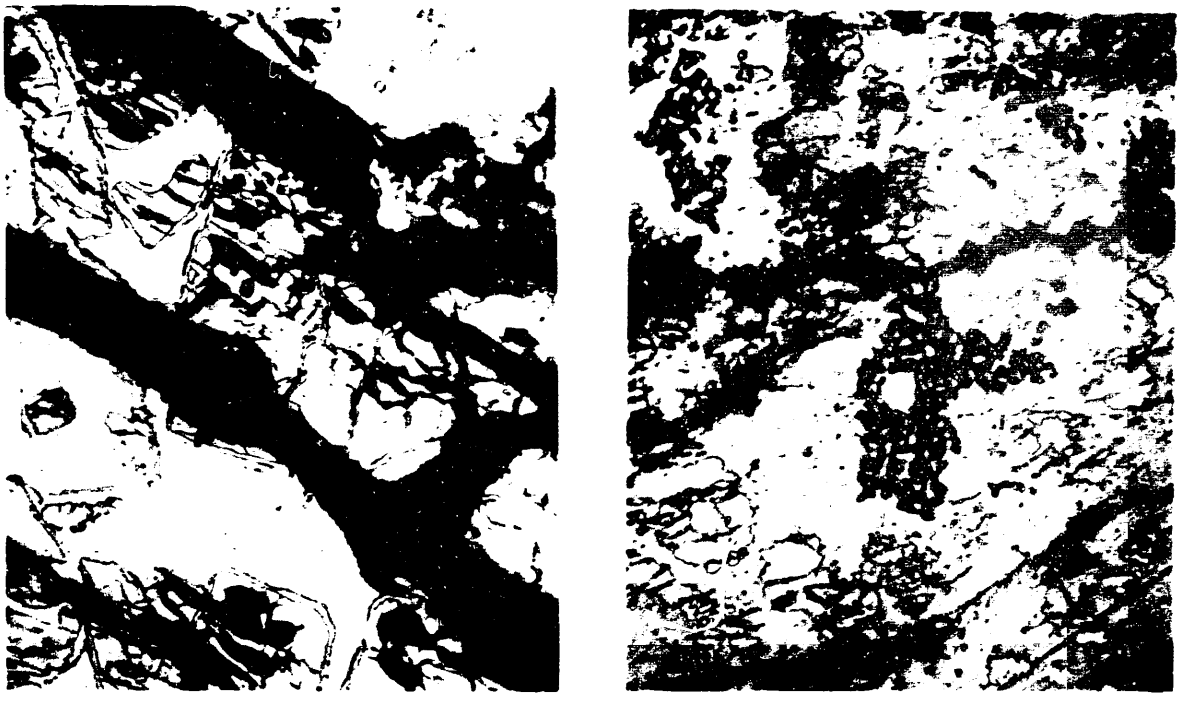

(a) (b)

Fig.9 (a) The machined and comminuted particles from the ingot cast in an induction furnace showing the microstructure of large U_3Si_2. (x400)
(b) The heat treated particle from induction melting. Note that the peritectoid reaction is not completed even after the long time of heat-treatment and that free uranium is left. (x400) The dark grey area is the matrix of uranium solid solution and the bright area is U_3Si_2. Heat-treated at 800 °C for 72 hrs.

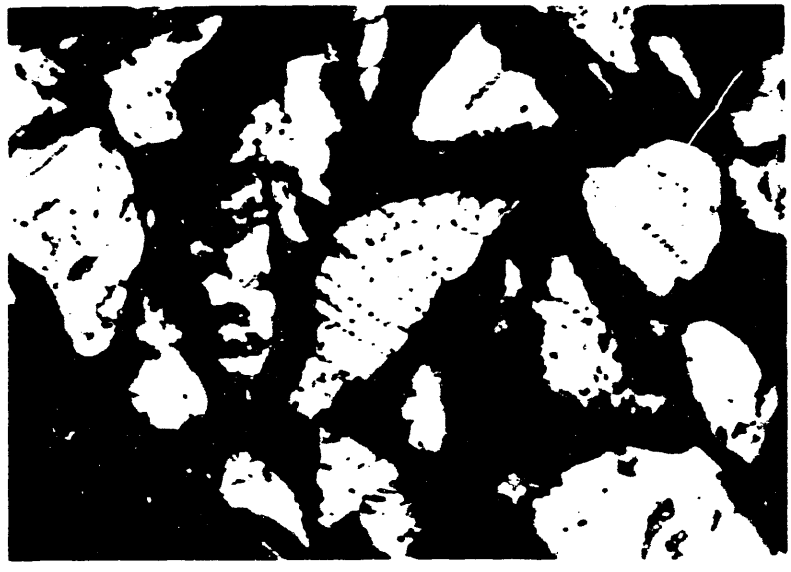

Fig. 11 The heat-treated particles of the size -40/+100 mesh show less inhomogeneity than the particles of 150 μm. Heat-treated at 800 °C for 72hrs.(x75)

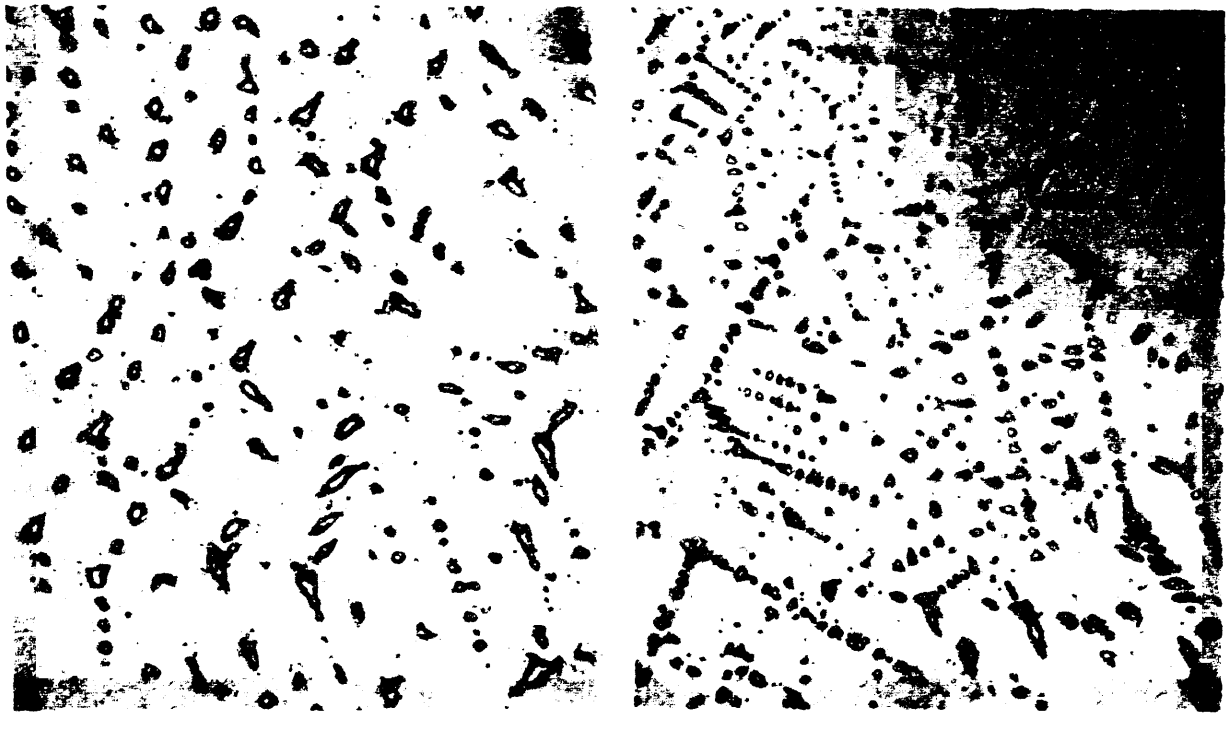

(a) (b)

Fig. 12 (a) The particles of the size +40 mesh heat-treated at 800 °C for 24hrs show completion of the phase transformation. (x400) (b) The particles greater than +20 mesh heat treated at 800 °C for 24hrs. (x400)

The above results are shown quantitatively in Fig.13 in terms of I in Equ.1. It is found that the inhomogeneity decreases with the size of the comminuted particle. The crititcal size for 10 μm primary U_3Si_2 is about 350μm. However, the critical size varies with the size of the primary U_3Si_2. Therefore, it is proposed that the critical can be reduced by reducing the size of primary U_3Si_2 but no smaller than 5μm.

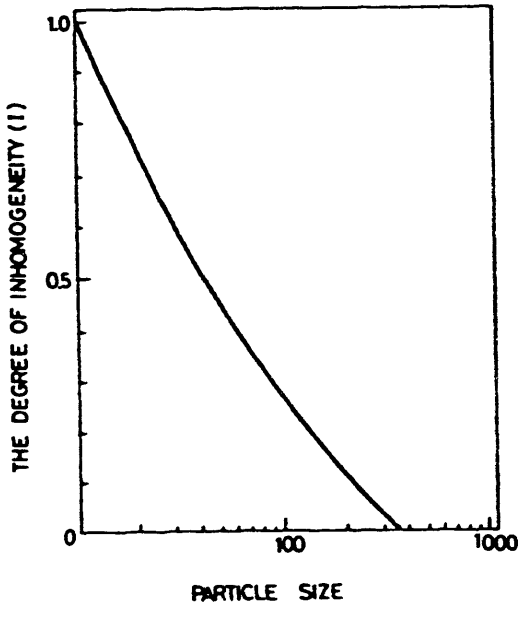

Fig. 13 The degree of inhomogeneity vs. the comminuted particle size, counting the number of particles containg free uranium / total number of particles.

CONCLUSION

Test fabrication of KMRR fuel was made with depleted uranium in accordance with the fuel development procedure of RERTR program.

Communition of the heat-treated U_3Si_{1+x}, especially when x is close to 0, is difficult, necessitating particular equipment and labour. Communition is performed before the heat-treatment.

(1) The primary U_3Si_2 dendritic particle is decreased in order to reduce the critical size in order to achieve homogeneity of the comminuted particles. The particle size of primary U_3Si_2 decreases with the cooling rate, but cannot be made smaller than 5 μm.

(2) The fracture surface of the comminuted particle shows trans-granular fractures. The inhomogeneity in chemical composition of the comminuted particles is not attributed to the fracture morphology but to the statistical relation of the size and population of the primary U_3Si_2 particles within the size of the comminuted particles.

(3) Particles with the primary U_3Si_2 greater than 30 μm do not complete the peritectoid reaction, leaving free uranium untransformed.

(4) The smaller the particles comminuted, the greater the inhomogeneity in chemical composition between particles.

(5) For particles with primary U_3Si_2 of 10 μm, the critical size for the homogeneity is found to be about 350 μm.

(6) The critical size can be reduced if the primary U_3Si_2 particle size is reduced by increasing the cooling rate in solidification of the molten ingot.
(7) With a particle size greater than the critical size for homogeneity, the peritectoid reaction can be completed within 24 hrs at 800 °C, even faster than the conventional process.

REFERENCES

1. 'Fuel development and Fabrication' in proceedings of the 1980, 1982, 1984 and 1986 Intl. Meeting on Reduced Enrichment for Research and Test Reactors. ANL/RERTR/TM-3,4,6 and 9 CONF801144, 821155, 8410173 and 861185.

2. S.K. Oh, S.Y. Kim and D.H. Kim "Design Characteristics of KMRR and its utilization" in Proceedings of the 2nd Appl. Phys. Symp. on the physics in Nuclear Industry, KPS, 2, 147 (1987)

3. L.C. Berthiaume and B.S. Wyatt "Effect of Primary U_3Si_2 particle size and distribution on the peritectoid reaction in uranium / silicon alloys." CRNL, AECL-3222, Dec. 1968)

SESSION V

September 20, 1988

CONVERSION EXPERIENCES

Chairman:

F. Merchie
(CEA-CEN, France)

FUEL ELEMENT POWERS, ^{235}U MASSES, AND BURNUPS FROM GAMMA-SCANNING DATA (PRELIMINARY ANALYSIS OF IRRADIATED ORR LEU FUEL ELEMENTS)

M. M. Bretscher and J. L. Snelgrove
Argonne National Laboratory
Argonne, Illinois 60439 USA

and

R. W. Hobbs
Oak Ridge National Laboratory
Oak Ridge, Tennessee 37831 USA

ABSTRACT

Fuel elements used in the ORR whole-core LEU fuel demonstration have been gamma-scanned to determine axial distributions of ^{149}La and ^{137}Cs fission product activities. This data has been analyzed to determine cycle-averaged fuel element powers, residual ^{235}U masses, and burnups of discharged fuel elements. Methods used to analyze the data are discussed and results are presented for the LEU fuel elements. Measured and calculated fuel element powers agree to within 5%, residual ^{235}U masses to within 2%, and burnups to within 3%. These results are somewhat preliminary and await improved burnup calculations and independent calibration data to be based on the destructive analyses of a number of irradiated fuel elements.

INTRODUCTION

After each cycle of operation during the whole-core LEU demonstration, fuel elements from the 30 MW Oak Ridge Research Reactor (ORR) were removed from the core to allow for xenon decay. During these intercycle periods the fuel elements were scanned along their centerlines to measure the ^{140}La fission product activity. Because of the relatively short half lives involved, this information was used to determine fuel element powers and burnups which occurred during the previous operating cycle. In addition, discharged fuel elements were gamma-scanned using the ^{137}Cs activity. Because of the 30-year half life of ^{137}Cs, this measurement integrates the activity over all previous cycles of operation and so gives information regarding the ^{235}U mass and burnup in the discharged fuel.

Figure 1 shows a schematic drawing of the fuel element gamma scanning apparatus which is anchored at the edge of the reactor pool. The fuel element is placed horizontally in a tray located at the bottom of the pool. Under computer control, the element is moved beneath a 1/2-diameter voided vertical tube to each of 16 predetermined counting locations along the element axis. The tube extends upward through about 16 feet of water to a lead collimator one foot long with a 1/16-inch diameter hole. Gamma rays are detected in a

lithium-drifted germanium crystal (58 cm^3) and the results of a gamma-peak fitting routine for each axial location scanned are stored on floppy disks. Figure 2 shows a measured gamma spectrum of irradiated LEU fuel.

This paper describes methods used to analyze the gamma scanning data. Results are presented for LEU fuel elements used during the ORR whole-core demonstration. However, these results are still somewhat preliminary. The final calibration of the gamma-scanning system awaits burnup data to be based on destructive analyses of several ORR fuel elements. With the exception of core 179A, the last core to operate in the ORR, new burnup calculations are needed to:

1) use improved cross section sets

2) use improved estimates of ^{235}U masses in the HEU fuel elements

3) account for voided beam tube effects

4) correct an error which occurred in some of the initial burnup calculations when a few beryllium reflector elements were unintentionally overlayed with a water/aluminum mixture.

Some earlier evaluations of the gamma scanning data are given in the first three references.

DATA ANALYSIS METHODS

The fission product chains which lead to the production of ^{140}La and ^{137}Cs are

$$^{140}I(0.86s) \rightarrow ^{140}Xe(13.6s) \rightarrow ^{140}Cs(63.7s) \rightarrow ^{140}Ba(12.79d) \rightarrow ^{140}La(40.26h) \rightarrow ^{140}Ce(\text{stable})$$

$$^{137}Te(4s) \rightarrow ^{137}I(24.5s) \rightarrow ^{137}Xe(3.84m) \rightarrow ^{137}Cs(30.17y) \rightarrow ^{137}Ba(\text{stable})$$

with cumulative fission yields of 6.28% and 6.22%, respectively. For ^{140}La, the gamma ray yield is 95.6% for the 1596 kev line. In the case of ^{137}Cs, the 662 kev gamma ray has a yield of 84.6%. These are the gamma rays used in the gamma-scanning analysis system. Because of interfering gamma rays, the ^{137}Cs scans cannot be recorded until most of the short-lived fission product activities have decayed away.

The equations which govern the population densities of ^{140}Ba, ^{140}La, and ^{137}Cs during the irradiation cycle are given below.

$$\frac{d}{dt} N_B = Y_B \bar{F} - \lambda_B N_B - \sigma_B \bar{\phi} N_B$$

$$\frac{d}{dt} N_L = \lambda_B N_B - \lambda_L N_L - \sigma_L \bar{\phi} N_B$$

$$\frac{d}{dt} N_C = Y_C \bar{F} - \lambda_C N_C - \sigma_C \bar{\phi} N_C$$

Here the subscripts B, L, and C refer to ^{140}Ba, ^{140}La, and ^{137}Cs, respectively. $\bar{F}$ is the cycle-averaged fission rate per unit volume and Y the fission yield. In all cases neutron capture losses ($\sigma\Phi$) are negligibly small relative to the λ decay constants. These equations determine the specific activity of ^{140}La and ^{137}Cs at a given point $\underline{r}$ in the fuel. Thus, the ^{140}La specific activity, $A_L(\underline{r})$, may be written as

$$A_L(\underline{r}) = Y_B\bar{F}(\underline{r})\ BDF_L(\underline{r}) = CR_L(\underline{r})/V_S E_L \ . \tag{1}$$

$BDF_L(\underline{r})$ is the buildup-decay factor for ^{140}La and is given by

$$BDF_L = \sum_{i=1}^{m} \frac{\lambda_L\left(1-e^{-\lambda_B t_{ei}}\right)e^{-\lambda_B t_{wi}} - \lambda_B\left(1-e^{-\lambda_L t_{ei}}\right)e^{-\lambda_L t_{wi}}}{\lambda_L - \lambda_B} \tag{2}$$

Here, m is the number of reactor startups for a given irradiation cycle, t_{ei} is the exposure time (in equivalent full-power days) for the ith startup, and t_{wi} is the wait interval (days) from the ith reactor shutdown until the ^{140}La activity is counted. The values for t_{ei} and t_{wi} are obtained from the count times and detailed power histories for each irradiation cycle. In Eq. (1) $CR_L(\underline{r})$ is the observed count rate associated with the decay of ^{140}La and corrected for any residual activity from earlier irradiation cycles. E_L is the probability that a ^{140}La decay occurring in the volume V_S "seen" by the detector will result in a count. It follows from Eq. (1) that the residual ^{140}La count rate at time t_c after n irradiation cycles is

$$RCR_L(t_c) = \sum_{i=1}^{n-1} CR_L(t_{ci})\ \frac{BDF_L(t_c)}{BDF_L(t_{ci})}\ \frac{RE(t_{ci})}{RE(t_c)} \tag{3}$$

where $RE(t_c)$ is the relative efficiency of the detector system at time t_c. These relative efficiency factors account for possible long term changes in detector efficiency and were measured by periodically counting the ^{137}Cs activity of fuel element C021. Note that the net count rate in Eq. (1) has been normalized (divided) by the appropriate relative efficiency factor.

The fuel element power and burnup depend on the total fission rate in the fuel element, which is the volume integral of the fission density. Thus,

$$\int_{fuel}\bar{F}(\underline{r})d\underline{r} = V_M\langle\bar{F}\rangle = \langle CR_L/BDF_L\rangle/Y_B G_L \tag{4}$$

where the overall geometric efficiency $G_L = (V_S/V_M)E_L$. V_M is the volume of the fuel in the element and $\langle\bar{F}\rangle$ is the volume-averaged fission density. If transverse gradients are neglected, $\langle CR_L/BDF_L\rangle$ may be evaluated by numerically integrating (trapezoidal rule) the axial count rates divided by the corresponding values of BDF_L.

Because of the 30.17 yr half life of ^{137}Cs, the specific cesium activity is directly related to the total fission density, TF.

$$A_C(\underline{r}) = Y_C\lambda_C\ TF(\underline{r})\ BDF_C(\underline{r}) = CR_C(\underline{r})/V_S E_C \tag{5}$$

where the subscript C is used to denote ^{137}Cs quantities and where the buildup-decay factor is given by

$$\begin{aligned} BDF_C(\underline{r}) &= \sum_{j=1}^{n} \bar{F}_j\left(1-e^{-\lambda_C t_{ej}}\right) e^{-\lambda_C t_{wj}} \Big/ \lambda_C \sum_{j=1}^{n} \bar{F}_j\, t_{ej} \\ &\approx \sum_{j=1}^{n} t_{ej}\, e^{-\lambda_C t_{wj}} \Big/ \sum_{j=1}^{n} t_{ej} \end{aligned} \tag{6}$$

In Eq. (6) n is the number of irradiation cycles during which the fuel element was activated. As for the case of ^{140}La, CR_C in Eq. (5) is the measured ^{137}Cs count rate divided by the appropriate relative efficiency factor. The total fissions which occurred in the discharged fuel element are given by the volume integral of $TF(\underline{r})$.

$$\int_{fuel} TF(\underline{r})\, d\underline{r} = V_M\langle TF\rangle = \langle CR_C/BDF_C\rangle/\lambda_C Y_C G_C \tag{7}$$

$G_C = \left(\frac{V_S}{V_M}\right) E_C$ is the overall geometric efficiency factor for the detection of ^{137}Cs gamma rays. Assuming the effects of transverse gradients are negligible, $\langle CR_C/DBF_C\rangle$ may be evaluated by numerically integrating the axial distribution of ^{137}Cs count rates divided by the appropriate value of BDF_C.

The fuel element cycle-averaged power ($\bar{P}$) is directly proportional to the total fission rate.

$$\bar{P}(MW) = V_M\langle\bar{F}\rangle E_R = E_R\langle CR_L/BDF_L\rangle/Y_B G_L \tag{8}$$

E_R is the recoverable energy per fission and has a value of 3.152×10^{-17} MW-sec/fiss for the thermal fission of ^{235}U.

The ^{235}U burnup depends on the total number of fissions, N_F, which occurred in the fuel element. Thus,

$$\Delta^{235}M = (1 + {}^{235}\bar{\alpha})\ N_F({}^{235}F/F)\ {}^{235}AW/N_A \tag{9}$$

where ${}^{235}\bar{\alpha}$ is the spectrum-averaged ^{235}U capture-to-fission ratio, $^{235}F/F$ the fraction of fissions due to ^{235}U, ^{235}AW the atomic weight of ^{235}U, and N_A is Avogadro's number. Because ${}^{235}\bar{\alpha}$ and $^{235}F/F$ vary somewhat as a function of burnup, $\Delta^{235}M$ was obtained from a least squares polynomial fit of the form

$$\Delta^{235}M = \sum_{i=1}^{6} a_i N_F^{i-1} . \qquad (10)$$

If the geometric efficiencies G_L and G_C are known, N_F can be evaluated from both the ^{140}La and ^{137}Cs count rate data using the equations already developed.

EVALUATION OF $G_L(^{140}La)$ AND $G_C(^{137}Cs)$

During the ORR whole-core LEU fuel demonstration seven cores operated at full power (30 MW) using only LEU 19-plate fuel elements. For each of these cores it is possible to derive a value for G_L by requiring that the measured power summed over all the fuel elements be equal to $30(1-PF_{FF})$MW where PF_{FF} is the calculated power fraction developed in the fuel follower portions of the shim rods. From Eq. (8) it follows that

$$G_L(^{140}La) = \frac{E_R}{Y_B} \sum_{i=1}^{n} \langle CR_L/BDF_L \rangle_i \Big/ 30(1-PF_{FF}) \qquad (11)$$

where n is the number of standard fuel elements in the core. Table I lists the values of G_L obtained for each of the seven cores. The average value is

$$\bar{G}_L(^{140}La) = (3.944 \pm 0.030)\ 10^{-13}$$

where the error is the standard deviation of the mean. Note that the calculated power fractions PF_{FF} are in the range of 0.13 to 0.16.

For a given fuel element the accumulated total fissions obtained from the ^{140}La counting data must equal that obtained from the ^{137}Cs data. This fact allows a determination of the ratio $G_C(^{137}Cs)/G_L(^{140}La)$ for each fuel element. From Eqs. (4) and (7) it follows that

$$G_C(^{137}Cs)/G_L(^{140}La) = \frac{\langle CR_C/BDF_C \rangle / \lambda_C Y_C}{\sum_{i=1}^{n} \langle CR_L/BDF_L \rangle_i t_{ei}/Y_B} \qquad (12)$$

where the summation extends over the n cycles of irradiation. For all the irradiated LEU fuel elements (68) the average value of this ratio is

$$\langle G_C(^{137}Cs)/G_L(^{140}La) \rangle = 7.448 \pm 0.015$$

where again the error is the standard deviation of the mean. Combining these results gives

$$\bar{G}_C(^{137}Cs) = (2.937 \pm 0.023)10^{-12} .$$

RESULTS

Using the methods just described, powers, end-of-cycle (EOC) ^{235}U masses, and burnups have been evaluated from the gamma-scanning data for each of the LEU fuel elements used in the demonstration. Approximate correction factors have been applied to the calculations for the voided beam tube effects and beryllium overlay errors mentioned in the Introduction. These correction factors were obtained by re-calculating a few representative cores in which the beam tubes were explicitly modeled and the beryllium overlay errors corrected. Thus far, however, the volume integrations of the gamma-scanning data have been performed assuming transverse gradient effects are negligibly small.

Table II summarizes the irradiation history of a typical LEU fuel element (B044). For this element calculated and measured powers agree to within 4% or less for each of the seven irradiation cycles. The calculated and measured end-of-cycle ^{235}U masses agree to better than 1% for each cycle. Discharge burnups based on REBUS-3[4] calculations, ^{140}La counting, and ^{137}Cs counting are 50.45%, 50.40%, and 50.04%, respectively.

Figure 3 shows the C/E (calculated-to-experiment) ratios for the cycle-averaged powers in ORR core 179A. For all but three elements these ratios differ from unity by 5% or less. Similar results are shown in Fig. 4 where all the C/E ratios at each grid position are averaged over the seven LEU cores. Again, all but three of the ratios fall within the 5% range.

Measured end-of-cycle (EOC) ^{235}U masses, burnups, and corresponding C/E ratios for the 179A core are shown in Figs. 5 and 6. In all cases the calculated and measured masses are equal to within 2%. For a fresh LEU fuel element the ^{235}U mass is either 339 or 340 grams. Discharge fuel masses obtained from ^{140}La counting data are very consistent with those gotten from ^{137}Cs counting. This is illustrated in Fig. 7 where the EOC ^{140}La-to-^{137}Cs ^{235}U mass ratio is shown for the fuel elements in core 179A.

The calculated and measured axial distributions of ^{235}U masses and burnups were obtained by dividing the fuel column into six segments of equal height (10.0 cm). Table III shows ^{140}La and ^{137}Cs C/E mass ratios for each segment averaged over the fuel elements in core 179A. Generally speaking, the measured and calculated axial mass distributions are in good agreement. The maximum burnup occurs in fuel segment C (20.0-30.0 cm from the bottom of the core). For fuel element B044 (see Table II) the average discharge burnup is 50.04% (^{137}Cs data) whereas the measured value for segment C is 63.21% with a corresponding C/E ratio of 1.02.

CONCLUSIONS

For reasons given in the Introduction, these results are still somewhat preliminary. New REBUS-3 burnup calculations are needed

a) to take advantage of more accurate cross sections recently generated,

b) to explicitly model the voided beam tubes and to use an improved core box treatment,

c) to remove beryllium-overlay errors, and

d) to use more accurate ^{235}U mass data for the partially burned HEU fuel elements used in the HEU/LEU transition cores. This information will soon be obtained from an analysis of the gamma scanning data for these HEU elements using procedures described in this paper.

A quasi-experimental method, described earlier, was used to determine numerical values for the geometric efficiencies $G_L(^{140}La)$ and $G_C(^{137}Cs)$ for LEU fuel. In principle, these same techniques can be used to find the corresponding efficiencies for HEU fuel. Alternatively, the HEU/LEU ratio of gamma attenuation in the fuel may be calculated from appropriate gamma interaction cross sections. However, a direct determination of the efficiency factors must await the PIE results from the destructive analyses of several ORR fuel elements.

The results presented earlier neglect corrections for possible transverse gradients in the measured fuel element fission rates. By counting fuel elements at ±1/2 inch displacements from the center line and by taking data with both the convex and concave sides of the fuel plates facing the detector, R. W. Hobbs has obtained experimental data from which it may be possible to determine position-dependent gradient correction factors for four of the LEU cores. These results, together with supporting calculations, need to be carefully studied before gradient correction factors are applied to the gamma-scan data.

Because of the above limitations, the results given in this paper must be regarded as preliminary. Nevertheless, they are very encouraging. These analyses suggest that gamma scanning of irradiated fuel elements for ^{140}La and ^{137}Cs activities provides a method for measuring cycle-averaged fuel element powers, end-of-cycle ^{235}U masses and corresponding burnups. Measured and calculated fuel element powers agree to within 5% or less, ^{235}U masses to within ±2%, and burnups to ±3%. In addition, ^{235}U masses in discharged fuel elements obtained from the ^{140}La data are very consistent with results based on ^{137}Cs counting.

REFERENCES

1. R. W. Hobbs, M. M. Bretscher, R. J. Cornella, and J. L. Snelgrove, "The Transition Phase of the Whole-Core Demonstration at the Oak Ridge Research Reactor," Proceedings of the 1986 International Meeting on Reduced Enrichment for Research and Test Reactors, pp. 269-286, Gatlinburg, Tennessee, Nov. 3-6, 1986, ANL/RERTR/TM-9, CONF-861185.

2. R. W. Hobbs, "Fuel Element Gamma Scanning at the Oak Ridge Research Reactor," Trans. ANS 55, 195 (Nov. 1987).

3. L. Robinson, R. W. Hobbs, F. F. Dyer, L. P. Pugh, J. L. Snelgrove, and N. A. Teasley, Jr., "An Automated Fuel Element Scanning System," J. Radioanal. Nucl. Chem., Articles, in press.

4. B. J. Toppel, "A User's Guide for the REBUS-3 Fuel Cycle Analysis Capability," Argonne National Laboratory Report ANL-83-2 (March 1983).

Table I. Evaluation of $G_L(^{140}La)$

Core	$G_L(^{140}La)$
177D	4.047×10^{-13}
178A	4.047×10^{-13}
178C	3.867×10^{-13}
178D	3.944×10^{-13}
178H	3.848×10^{-13}
178J	3.903×10^{-13}
179A	3.949×10^{-13}

$$\bar{G}_L(^{140}La) = (3.944 \pm 0.030)10^{-13}$$

Note: The error in $\bar{G}_L$ is the standard deviation of the mean.

Table II. Irradiation History of Fuel Element B044

Cycle	Grid	FPD's*	Power - MW			EOC ^{235}U Mass - g		
			Calc.	Exp.	C/E	Calc.	Exp.	C/E
176B	E8	21.864	1.080	1.054	1.025	309.9	310.8	0.997
176D	E4	19.446	1.356	1.303	1.041	277.1	279.2	0.993
177B	F3	18.516	1.081	1.114	0.970	252.7	253.8	0.996
177D	B7	15.334	0.969	0.962	1.007	234.8	236.0	0.995
178C	E6	11.782	1.243	1.283	0.968	217.5	218.1	0.997
178H	C6	20.277	1.029	1.050	0.980	193.5	193.1	1.002
179A	E5	20.169	1.088	1.056	1.030	168.5	168.6	0.999
						^{137}Cs: 168.5	169.9	0.992

*Cycle length in full-power (30-MW) days.

Table III. ORR Core 179A

Axial Distribution of EOC C/E U-235 Mass Ratios

Fuel Segment*	Elements Having Burnup <35%		Elements Having Burnup >35%		All Elements in Core	
	La-140	Cs-137	La-140	Cs-137	La-140	Cs-137
A	0.98	0.99	0.96	0.98	0.97	0.99
B	0.99	1.00	0.99	1.01	0.99	1.00
C	1.00	1.01	1.02	1.02	1.01	1.01
D	1.01	1.01	1.05	1.02	1.02	1.01
E	1.01	1.00	1.04	1.01	1.02	1.01
F	1.00	0.99	1.01	0.98	1.00	0.99
All	1.00	1.00	1.01	1.00	1.00	1.00

*Fuel segments of equal height (10.0 cm) with Segment A at bottom of core.

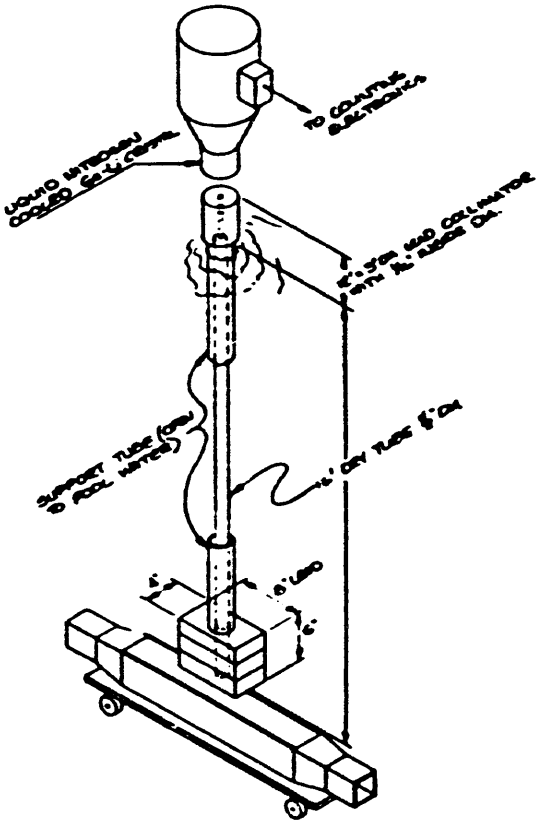

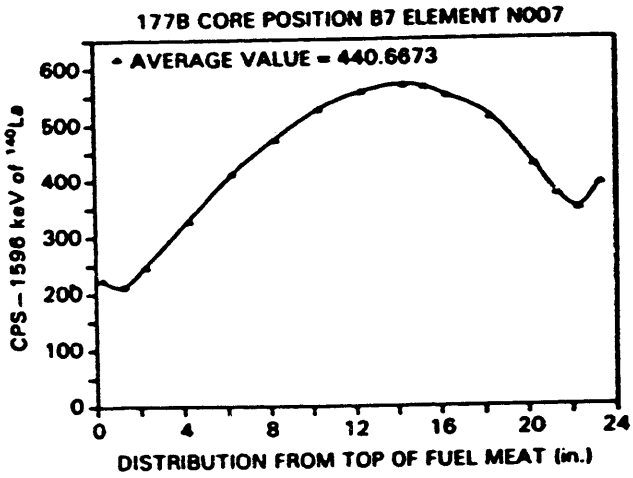

Fig. 1. Fuel Element Gamma Scanning Apparatus and Typical Axial Scan.

GAMMA SPECTRUM OF LEU FUEL

Middle of Element B084 2-3-87

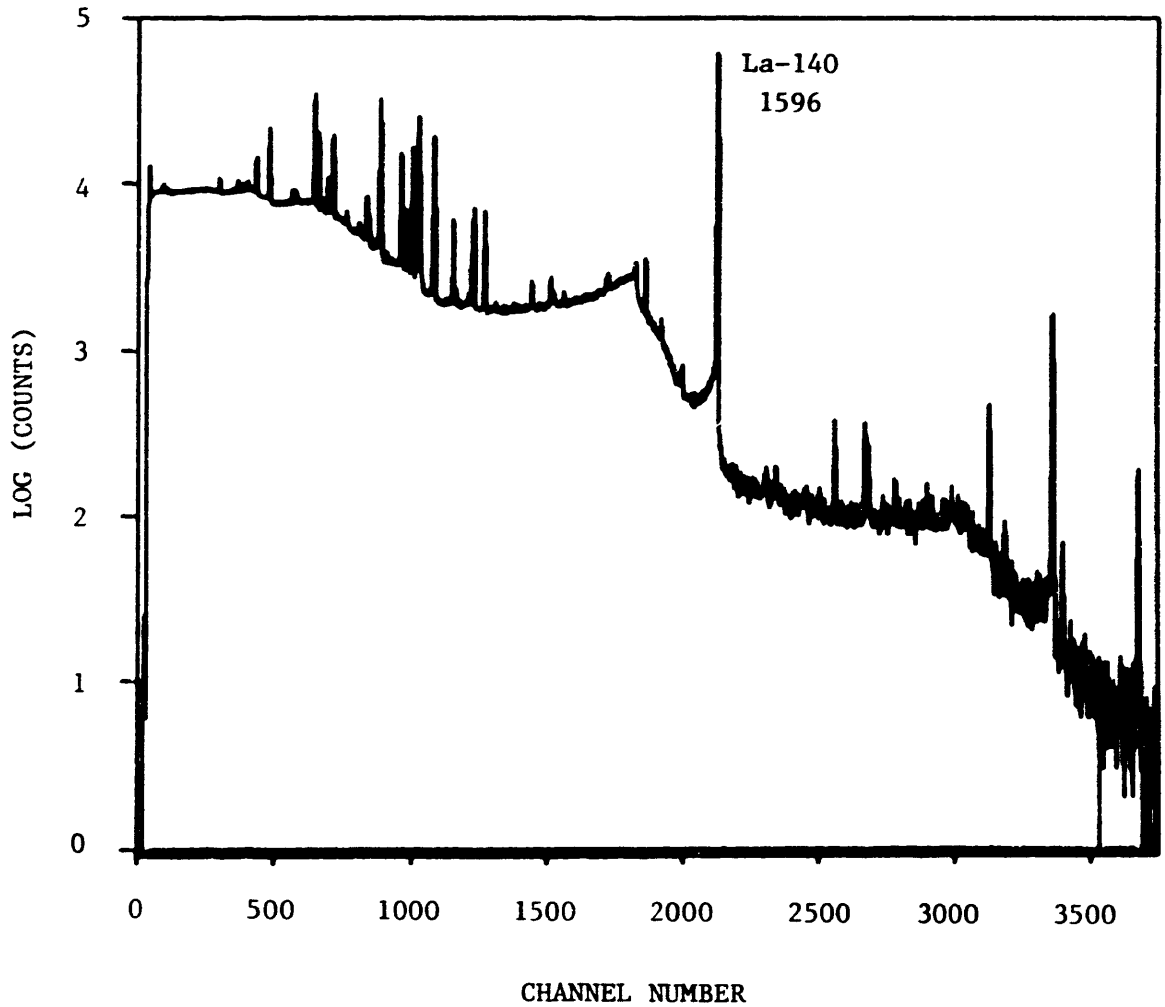

Fig. 2

ORR CORE 179A
Cycle-Average Power C/E Ratios

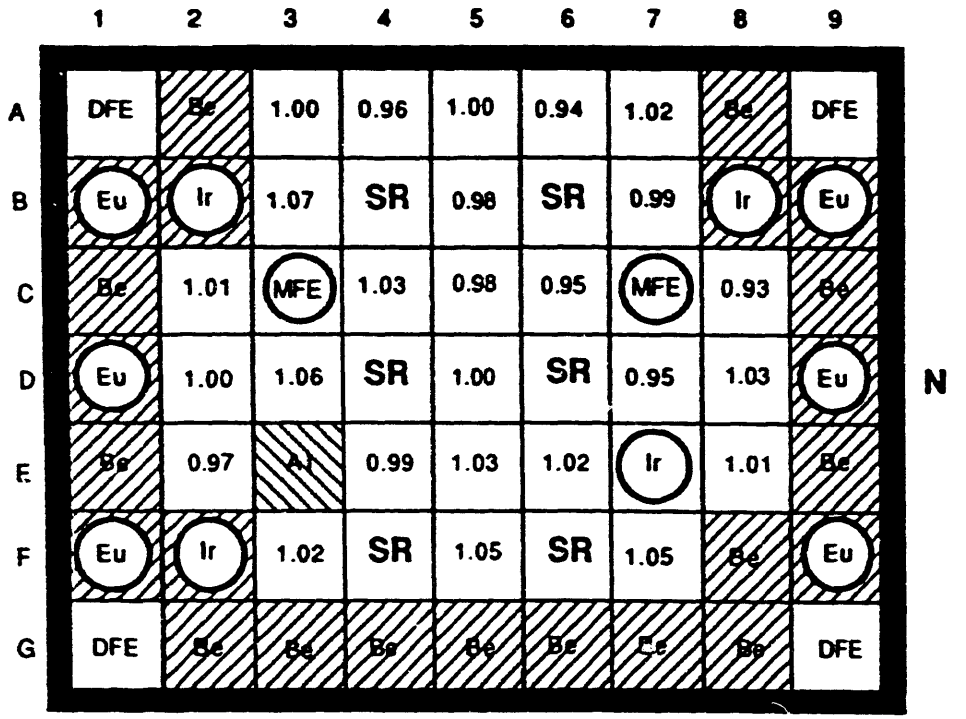

SR ≡ Shim Rod Assemblies

MFE ≡ Magnetic Fusion Experiment

Al ≡ Aluminum Block

Ir, Eu ≡ Irradiation facility for activating iridium or europium samples

DFE ≡ Dummy Fuel Element

Fig. 3

C/E Power Ratios Averaged Over the Seven LEU Cores

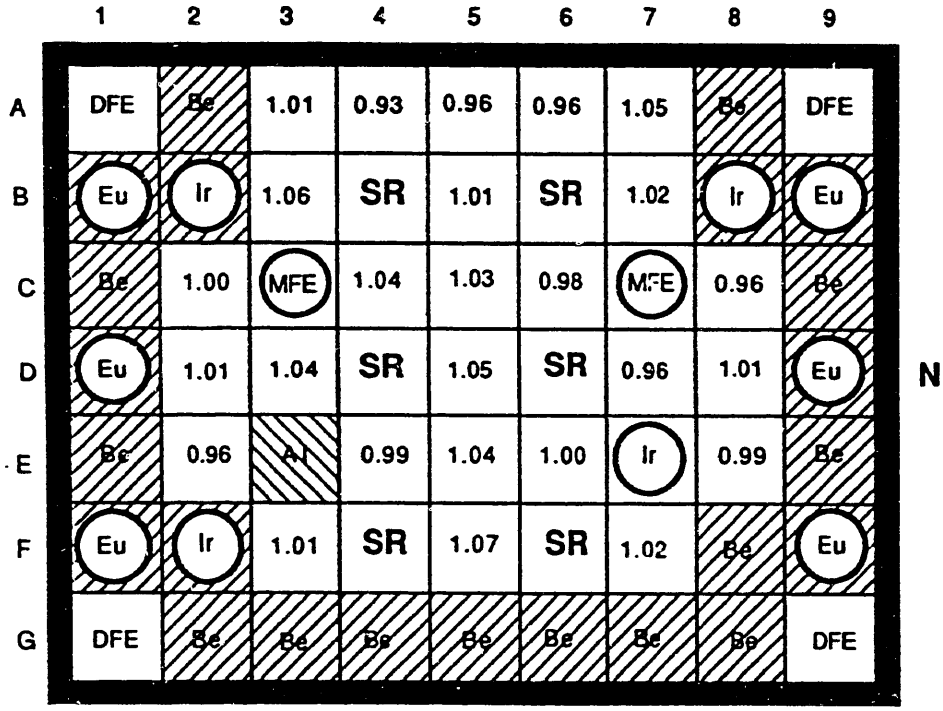

SR ≡ Shim Rod Assemblies

MFE ≡ Magnetic Fusion Experiment

Al ≡ Aluminum Block

Ir, Eu ≡ Irradiation facility for activating iridium or europium samples

DFE ≡ Dummy Fuel Element

Fig. 4

ORR Core 179A

Measured EOC U-235 Masses and Corresponding C/E Ratios

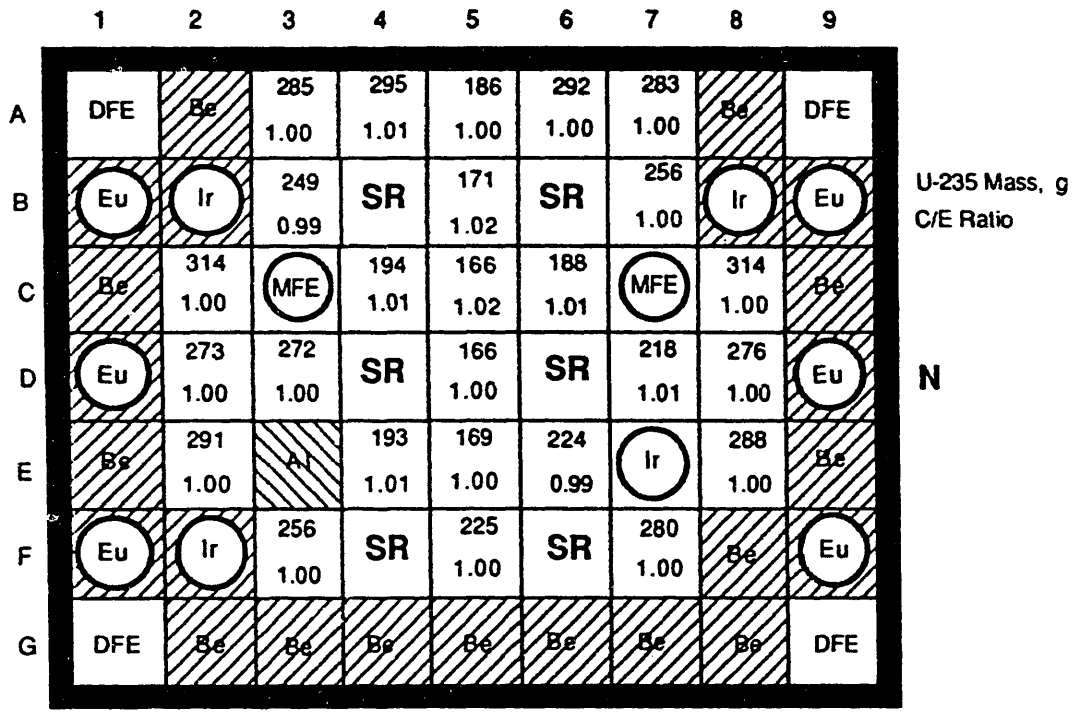

SR ≡ Shim Rod Assemblies

MFE ≡ Magnetic Fusion Experiment

Al ≡ Aluminum Block

Ir, Eu ≡ Irradiation facility for activating iridium or europium samples

DFE ≡ Dummy Fuel Element

Fig. 5

ORR Core 179A

Measured EOC U-235 Burnups and Corresponding C/E Ratios

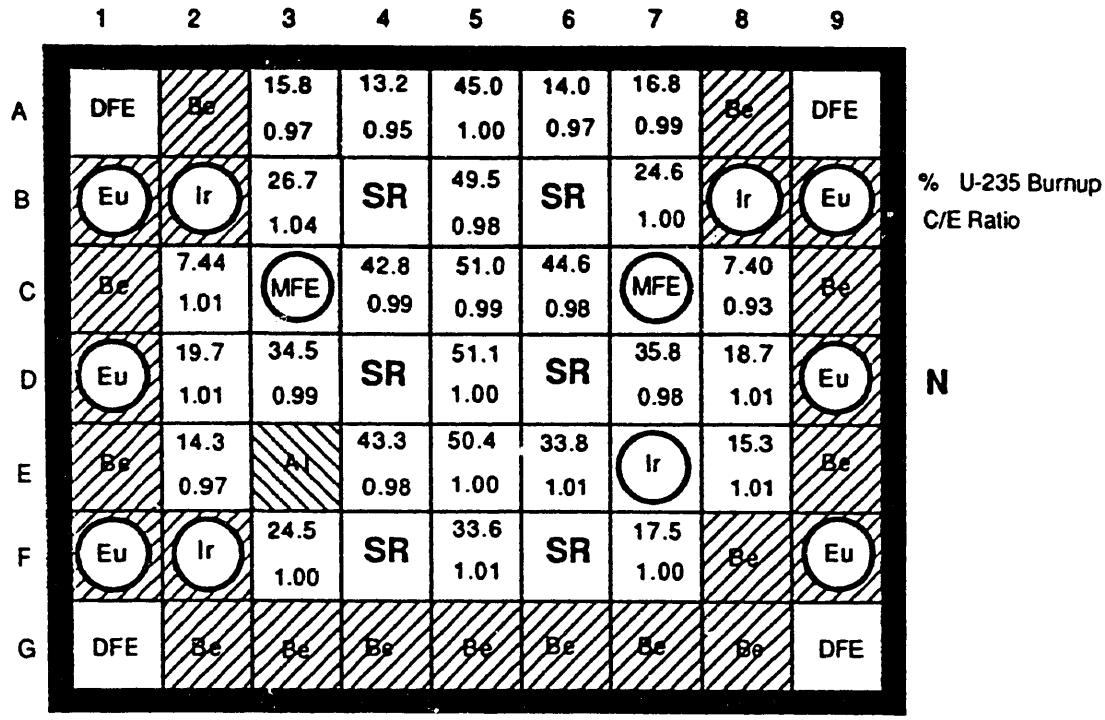

SR ≡ Shim Rod Assemblies

MFE ≡ Magnetic Fusion Experiment

Al ≡ Aluminum Block

Ir, Eu ≡ Irradiation facility for activating iridium or europium samples

DFE ≡ Dummy Fuel Element

Fig. 6

ORR Core 179A

EOC La-140/Cs-137 U-235 Mass Ratio

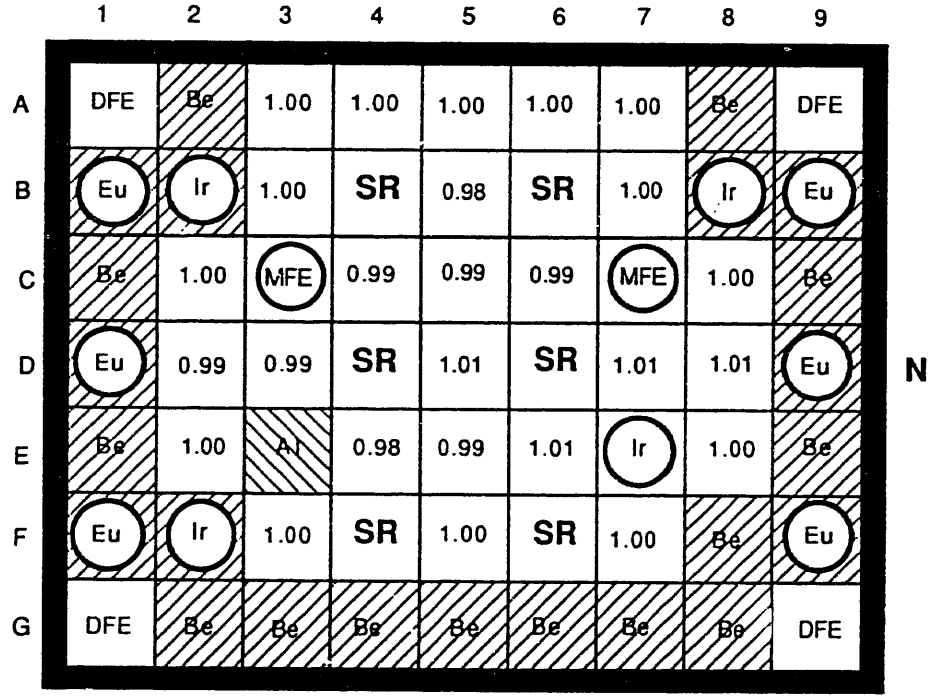

SR ≡ Shim Rod Assemblies

MFE ≡ Magnetic Fusion Experiment

Al ≡ Aluminum Block

Ir, Eu ≡ Irradiation facility for activating iridium or europium samples

DFE ≡ Dummy Fuel Element

Fig. 7

ENRICHMENT REDUCTION ACTIVITIES FOR THE FRG-1 AND FRG-2 RESEARCH REACTORS

W. Krull

GKSS Forschungszentrum Geesthacht GmbH

Geesthacht, Federal Rupublic of Germany

ABSTRACT

The GKSS research centre is participating since 1980 in the national and international efforts on enrichment reduction to clarify the needs on safety and licensing issues, to decide on fuel tests, to perform fuel tests and conversion calculations. These efforts are being made within the IAEA working groups, the German AF-program and the GKSS R & D program.

There are successfully tested fuel elements with 45 % and 20 % enrichment; UAl_x, U_3O_8 and U_3Si_2 fuel meat; U-densities up to 3.7 g U/cc and fission densities up to 1.25×10^{21} fissions/cc (ex. Pu) and five U_3Si_2 fuel plates ($\rho(U) = 4.75$ g/cc).

A safety report for the conversion of the FRG-1 to LEU fuel (U_3Si_2, $\rho = 3.7$ g U/cc) has been submitted to the licensing authority. After examining the safety report by independent experts (TÜV) and the licensing authority the license for the conversion has been granted in May 1988.

78 fuel elements have been fabricated and delivered to GKSS with difficulties. The FRG-1 is ready for conversion to LEU fuel.

Two fuel elements are instrumented with 8 thermocouples to perform loss of flow and fuel plate temperature measurements. GKSS has performed already reactivity, microflux, flux distribution, fuel plate temperature and loss of flow measurements.

1. Present situation and future needs

The GKSS research centre Geesthacht GmbH operates the two MTR-type swimming pool research reactors FRG-1 (5 MW) and FRG-2 (15 MW). These reactors in operation since 30 resp. 25 years are used for fundamental and applied research, mainly in materials testing and development. Main efforts are made (e.g. installation of a cold neutron source /1/, backfitting /2/) to have today and in future a high utilization, availability and safety standard. Both reactors are operated in one reactor hall in a connecting pool sy-

stem with at present ca. 800 MWd/a resp. 3200 MWd/a. The fuel elements used are identical: 23 plates, UAl_x, standard geometry, 93 % enriched and 180 g U-235/element, meat dimensions 0.51 x 62.8 x 600 mm^3, canning thickness 0.38 $\pm$ 0.08 mm, canning material AlMg1.

The 5 MW FRG-1 will be used in future with higher availability and to a greater percentage for beam tube experiments. Therefore the installation of a cold neutron source in one of the beam tubes will be supported by reducing the core size. Reducing the core size, enlarging the burnup and the fuel cycle length can be made only if the fuel loading is increased and the control rod design is changed from the old oval type to fork type absorbers.

The 15 MW-FRG-2 is and will be used mainly for materials testing. The present program (testing of large specimens of pressure vessel steel) require a core size with 7 x 7 positions and last til the the end of 1991.

Increase in fuel loading can and will reduce fuel cycle cost significantly and (or) enables to reduce the core size due to changing experimental needs. Therefore the tendency is to increase fuel loading and to change control rod design. As our two reactors are operated in one pool system with the same fresh and spent fuel storage we intend to have the same fuel elements for both reactors in the future, too. This makes design and decisions a little more complicate.

2. Fuel testing

After discussions with the independent experts (TÜV* = consultants of the licensing authority) and the licensing authority it was agreed to have a procedure for fuel development and fuel testing showing five steps and starting from no knowledge and finishing with the conversion of the reactor. The tests of prototype fuel elements should be done in the reactor under consideration /3/. If these prototype fuel element tests are not performed in the reactor under consideration, the conversion procedure will be extremely stretched as operation has to be interrupted by fuel element inspection.

Fuel tests in the FRG-2 reactor were made within the German AF-program (RERTR) and for our own conversion needs: investigation of fabricational limits and qualification of fuel elements.

a. Investigation of fabricational limits

Swelling may depend on the amount of fine grain (grain size $< 40\ \mu$). 5 plates containing U_3Si_2 fuel with fine grain content up to 40 % and an U-density of 4.75 g U/cc were irradiated to a burnup of ca. 63 % which corresponds to 1.27×10^{21} fissions/cc (ex. Pu). Fission product release was measured on line. No defects were observed.

---

*) TÜV = Technischer Überwachungsverein

b. Qualification of fuel elements (details see table 1)

- 10 fuel elements, 45 % enrichment, UAl_x, ρ = 1.41 g U/cm³, 280 g U-235 were burned up to 64 %, test reason: backup variant;
- 7 fuel elements, 20 % enrichment, U_3O_8, ρ = 3.1 g U/cm³, 270 g U-235 are burned up to 66 %, test reason: fabricational limits and backup variant;
- 4 fuel elements, 20 % enrichment U_3Si_2, ρ = 3.7 g U/cm³, 323 g U-235 are burned up to 68.5 %, test reason: prototype for the conversion of our research reactors.

3. Experimental program

a. Qualification of fuel elements

During the qualification tests of fuel elements especially the following experiments were performed: reactivity measurements (comparison with present fuel), "micro"thermal neutron flux distribution, fuel plate temperature at normal operation and during loss of flow experiments, flux mapping and fission product release /3/.

b. Investigation of fabricational limits

The five fuel plates were investigated in our hot cells /4/. The following investigations were made: visuell inspection, dimension and volume change, γ-scan (total and nuclide specific), blister test and metallography. These results were obtained

- no peculiarities were observed during visuell inspection
- overall swelling was below 1 % $\Delta V/V$ per plate (the porosity was between 6 % and 8.4 %), meat swelling is below 5.4 %
- the total γ and Cs-137 γ-scans are showing identical profiles with characteristic peaks at the top and buttom of the fuel plate due to fuel inhomogeneities and neutron flux peaking
- two blister temperatures were measured between 520 °C and 540 °C
- Al-fuel interactions were found in a narrow zone around the fuel particles. The size of this zone is comparable to the fission product recoil thickness in Al (≈ few µm)
- nearly no remaining porosity was observed
- very small fission gas bubbles could be seen ($\simeq$ 0.1 µm)
- an increase in bubble size up to a few µm and in some cases an agglomeration of bubbles were found
- no differences were found between fuel plates with low (17 %) and increased (40 %) fine grain content.

All these results are an excellent confirmation of results presented by Hofman and Snelgrove /6/.

4. Conversion of the FRG-reactors

The conditions for the conversion of our research reactors are as follows: same fuel elements for FRG-1 and FRG-2, unchanged geometry (23 plates), reduction of fuel cycle cost and increase of excess reactivity (higher U-235 loading, Be-reflector, fork type absorbers), increase of neutron flux in the experimental positiors of the FRG-1 (reduction of core size).

A safety report for the conversion of the FRG-1 and FRG-2 research reactors was submitted to the licensing authority. Especially the following points were discussed:

a. applied changes

- fuel elements
  enrichment 90 %, 93 % to 19.75 %
  fuel meat UAl_x to U_3Si_2
  U-density 0.44 g U/cc to 3.7 g U/cc
  canning material AlMg1 to AlMg2
  fuel loading 180 g U-235 to 323 g U-235
- control rods
  Hf fork type absorbers shall be used instead of oval Cd-B_4C absorbers
- conversion of the FRG-1
  fuel elements and 5 (instead of 4) control rods as described.
  The conversion procedure is discussed in detail.
- conversion of the FRG-2
  No detailed procedure was discussed. As one of the conditions of the existing operation license is that a new reactor core configuration has to be approved by a safety commitee it was believed to get a more general license for the conversion of the FRG-2.

b. qualification of the fuel and the fuel elements

It was decided to use U_3Si_2 fuel with ca. 3.7 g U/cc. For 100 % U-235 burnup the fission density is 1.57×10^{21} fission/cc (ex. Pu). Due to investigations made by G. Hofman and J. Snelgrove /6/ it was very easy to show that the swelling is below 6 %. The porosity was limited in the specifications to 4 % - 11 % as swelling is depending on it /5/. As the fabricator was not able to reach the specified value a porosity of 2 % was accepted. A major step for the qualification was the successful test of the 4 prototype fuel elements. Therefore it could be demonstrated that U_3Si_2 is qualified for the conversion of the FRG-1 and the FRG-2 research reactors.

For the qualification of U_3Si_2 fuel and fuel elements a detailed report has to be written describing the test program and procedure, corrosion experiments, swelling behaviour, blister temperature, metallographic investigations, exothermic reaction etc. Within this qualifying discussion fuel specs and fuel fabrication was of main interest, too. The IAEA-TEC-DOC-467 /5/ will be helpful.

c. fork type absorbers

The present FRG control rods are central absorbers of the oval type with Cd and B_4C as absorbing material. For some reasons we want to switch over to uncanned Hf fork type absorbers

- fork type absorbers
  more reactivity per control rod
  qualified type
- Hf
  no canning necessary
  no Ag contamination possible
  approximately the same reactivity worth as Ag-In-Cd.

d. FRG-1 conversion

First the general conversion aspects have to be discussed. These aspects are described in the IAEA-Guidebook on safety and licensing aspects due to research reactor core conversion, which is under preparation since 1980. Within the five volumes of this guidebooks there is enough information, which shall not be repeated at this place.

In addition calculations were made by GKSS and Interatom /7/ for the conversion procedure and the reactor core under consideration: startup accident, reactivity balance, conversion procedure, max. permissible power or max. form factor, flow instability. Fig. 1 shows the present and the future reactor core configuration. Some details of the calculations are given in the IA- paper presented by Strömich at this meeting /7/.

e. FRG-2 conversion

No detailed calculations are presented at this time as the idea was to follow one of the conditions of the existing operation license.

f. licensing procedure

In following § 7 of the German Atomic Energy Act an Ordinance gives exactly conditions when a license application needs a public hearing procedure. These conditions are: increase of activity release above given values, change of safety features of material structures, changes of the reactor protection systems, increase of thermal power or fission product inventory or storage capacity by more than 10 %. Only the increase of fission product inventory (if actinides are included) is of interest. This increase is between 3 % and 5 %. Therefore there exist no demands having a public hearing procedure getting a license for the conversion of the FRG research reactors.

Beside this it is of course at all time within the decision of the licensing authority to have a public hearing if there may be concerns that in connection with the applied changes negative conditions for the public exist. Comparing the pros and cons it is believed that the negative influence

- increase of fission product inventory,
  is by far over compensated by
- increasing the shut down reactivity,
  (fork type absorbers and (for FRG-1) the number of control rods)
- prompt (Doppler) negative temperature coefficient*,
- greater negative void coefficient*,
- proliferation risk reduced.*

Therefore the licensing authority decided that there is no need having a public hearing.

5. License

After a detailed expertise of the presented safety report by the independent consultants (TÜV) of the licensing authority and by the authority itself, the license for the conversion of the FRG-1 has been granted in May 88 with the following demands

- an experimental program for the conversion procedure has to be presented one month in advance. Main points are: shut down reactivity, reactivity speed and fuel plate temperature.

- experimental results have to be presented to the licensing authority and the TÜV before startup of the following fuel cycle

- the fluence dependence of the reactivity worth of the Hf fork type absorbers has to be presented to the authority in due time.

As mentioned GKSS is installing a cold neutron source in a new Be block reflector at the FRG-1 research reactor. The cold neutron source and the reactor (first with old fuel) are ready for startup but the reconstruction of the beam tube experiments will take til early 1989. Therefore the conversion of the FRG-1 will start not before 1989.

Today the future utilization of the FRG-2 research reactor is under discussion. Therefore the decision for the future operation, utilization, core configuration and conversion of the FRG-2 is pending.

*) LEU instead of HEU fuel

Literature:

/1/ W. Krull, K. Hansen, J. Stein: The cold neutron source for the FRG-1 research reactor at the GKSS research centre, IAEA-SR-119/27, Kopenhagen 9.-13. September 1985

W. Krull: Die Kalte Neutronenquelle am Forschungsreaktor FRG-1, Atomwirtschaft 33 (1988) 43-47

/2/ W. Krull: Backfitting- und Upgrading-Maßnahmen für Forschungsreaktoren, Reaktortagung Aachen 9.-11. April 1986

W. Hajek, H.-J. Kriks, W. Krull: Backfitting-Maßnahmen bei den Forschungsreaktoren in Braunschweig (FMRB) und Geesthacht (FRG-1 und FRG-2), Atomwirtschaft, to be published

/3/ W. Krull: Reduced enrichment activities at GKSS, RERTR-meeting, Petten 14.-16. October 1985

/4/ J. Müllauer: private communication 1988

/5/ W. Krull: Standardization of specifications and inspection procedures for LEU plate-type research reactor fuel, RERTR-meeting, Gatlinburg 3.-6. November 1986
IAEA-TECDOC-467 (1988)

/6/ G. Hofmann, L. Neimark, F. Olquin: The effect of fabrication variables on the irradiation performance of uranium silicide dispersion fuel plates, RERTR-meeting, Gatlinburg 3.-6. November 1986

J. Snelgrove et al.: The use of U_3Si_2 dispersed in Aluminium in plate-type elements for research and test reactors, ANL/RERTR/TM-11, 1987

/7/ A. Strömich: paper presented at this meeting

Table 1: Fuel Elements Qualification

	I	II	III	IV
Weight U-235 (g)	180	280	270	323
Weight U (g)	193, 200	622	1357	1635
Enrichment (%)	93	45	20	20
Meat material	UAl_x	UAl_x	U_3O_8	U_3Si_2
Density (g U/cc)	0.44	1.41	3.1	3.7
Canning material	AlMg1	AlMg1	AlMg2	AlMg2
Number	1000	10	7	4
Goal average burnup (%)	45	60	65	65
Burnup MWd	64.8	134.4	140.4	168.0
Test status	present fuel	finished	finished	finished
Test finished	open	April 84	Autumn 86	Spring 87
Max peak burnup 10^{21} fissions/cc (ex Pu)	0.66	1.01	1.00	1.25
Average U-235 burnup (%)	45	58.9-64.0	58.3-66.0	66.3-68.5

F	F	F	F	F	F	F	F
F	F	F	F	F	F	F	X
F	F	T	F	T	F	F	X
F	F	F	IF	F	IF	F	X
F	F	T	F	T	F	I	X
F	F	F	IF	F	F	F	X
F	F	F	F	F	F	I	X
X	X	X	X	X	X	X	X
X	X	X	X	X	X	X	X

old FRG-1 core

F = fuel element
X = Be-metal reflector element
T = control rod with partially fuel element
I = Irradiation position

F	F	F	F	F	F	F	X
F	T	F	T	IF	F	F	X
IF	F	T	F	T	F	XI	X
F	F	F	IF	F	F	X	X
X	XI	X	X	XI	X	X	X
X	X	X	X	X	X	X	X

new FRG-1 core

Fig. 1: present (93 %) and future (20 %) FRG-1 core

LICENSE APPROVAL ON THE CONVERSION OF DR 3 TO LEU

Karsten Haack
Risø National Laboratory
DK-4000 Roskilde, Denmark

ABSTRACT

The license application for conversion of the danish DR 3 reactor from the use of highly enriched uranium (HEU) to low enriched uranium (LEU) and for a power increase from 10 to 12 MW, was forwarded September 1986 to the authorities: The Danish Nuclear Inspectorate, the National Institute of Radiation Hygiene and the Danish Labour Inspection Service. The application was based on 155 pages of amendments to the safety documentation.

The amendments were discussed and explained on a series of meetings between reactor and authority representatives during 1987.

A framework approval was issued by the authorities in June 1988. The reactor management expects to have fullfilled the frames for the start of the conversion by supplementary reports and investigations before the scheduled date for start of conversion: October, 14th, 1988.

The mixed core operation schedule is presented. Full-core LEU operation is expected around May 1990.

THE APPLICATION

On September 18th, 1986, Risø applied to the Danish authorities for 12 MW LEU operation of reactor DR 3.

The accompanying documentation was based on 15 MW operation because it turned out during the revision of the safety documentation, that 15 MW operation would be feasible within the authorized conditions of operation. This would facilitate an eventual later power increase above 12 MW as well.

The application was based on amendments to the DR 3 safety documentation, concerning following subjects:

- Flow stability evaluation
- Initial events safety analysis

OF
1.0
2.8
2.5
3.2
2.2
3.6
1.1
2.0
1.8
1.25
1.4
1.6

- Analysis of cold coolant accidents initiated by the primary cooling system
- Analysis of cold coolant accidents initiated by the secondary cooling system
- Evaluation of emergency cooling system capability at a loss-of-coolant accident
- Analysis of loss of all primary cooling after reactor shut-down
- Coarse control arm failure analysis
- Evaluation of the tertiary cooling system (fjord cooling water) capability at 15 MW power
- Re-evaluation of the shut-down margin
- Analysis of reactivity accidents at low power
- Calculation of individual and population doses from core melt-down accidents at DR 3
- Reference data ammendments collection.

Evaluation of the mixed core operation phase and proposals for revisions on 7 items of the "authorized conditions for operation of DR 3" were enclosed.

CLEARING-UP AND SUPPLEMENTARY DOCUMENTATION

During 1987 the Nuclear Inspectorate raised a series of supplementary questions in meetings and in letters. The main topics were:

1) Maximum fuel element power and power peaking

We had proposed to vouch for the flow stability of the fuel elements by setting a limitation on the fuel element power, because the fuel element power distribution can be measured on-line by means of the built-in thermocouples at the fuel element exit ports when the flow through each fuel element is known. We had measured the flow distribution of the core for each of the three combinations of two main circulators in June 1986. The inspectorate demanded an evaluation of the probability that a 1000 kW limit on the 180g fuel element could be infringed, and they required a calculation of the power peaking factor in a 1000 kW fuel element.

2) Flow instability factor

The 1000 kW limit was based on a flow instability factor of 1.3. Earlier we had applied a factor of 1.5 because the core flow distribution was not known for certain after the change from a box type to an annular type of fuel element. The flow distribution measurements in 1986 provided the base for decreasing the factor to 1.3.

The Nuclear Inspectorate required information on flow instability factors of other DIDO/PLUTO-type reactors.

Re 2) We asked Harwell (UK), Jülich (FRG) and Lucas Height (NSW, Australia), for which instability factors they apply, and their kind replies confirmed that our choice (1.30) was reasonable and safe.

3) Void coefficients in a LEU core
Calculation of void coefficients of DR 3 was a part of the benchmark calculations on heavy water research reactors in the guidebook IAEA-TECDOC-324. The authorities required a separate report.

4) Reactivity transients in a LEU core
The authorities required recalculations of all transients calculations in the DR 3 safety documentation. We had argued that because of the higher temperature coefficients in a LEU core, reactivity transients would be smaller than in a HEU core.

5) Wigner energy deposition in the graphite reflector
The authorities required an updating of the previous report on this subject, because of the power increase applied for in the application for the conversion to LEU.

6) Lifetime of the coarse control arm (CCA) system
The burn-up of the CCA's is faster at a higher power. The authorities wanted to know the estimated lifetimes of the 7 CCA's and they required a schedule for the exchange of the CCA connecting rods, which are exposed to the damage flux in the reactor.

Re 6) We made an inquiry on demand of the authorities, to our sister-reactors on the lifetime of their CCA connecting rods. Unfortunately their operation conditions and maintenance schedules were very different from ours, so our programme for exchange of the rods had to be made rather conservatively.

7) LOCA design basis accident
The loss-of-coolant-accident (LOCA) upon which the emergency cooling system design was originally based, was a longitudinal rupture of one of the main tubes in the heavy water plant room. This accident has for many years been considered incredible owing to the thick stainless steel walls of the tubes and the low pressure in the system. The revised report evaluating the emergency cooling system at increased power in connection with the conversion to LEU was based on a more probable rupture caused by fatigne stresses in a welding seam of one of the stainless steel tubes. This would cause a smaller leak rate, of course, which made the authorities suspicious. They asked for an evaluation by an independant body on credible ruptures of the primary system pipework, and required measurement of the emergency cooling water flow to each fuel element.

Re 7) We asked the danish institute for welding research and development "Svejsecentralen" to evaluate the D_2O pipework. They made a thorough examination and concluded that a risk for small leakages would exist after so many years of operation, but the probability for large ruptures in the main pipes was very small and insignificant. This conclusion confirmed our proposal for an amended design basis for the emergency cooling system.

The emergency cooling water flow to each individual fuel element was measured during the extended shut-down prior to the conversion.

8) Cooling system temperatures at increased power levels
The authorities required a set of diagrams showing the temperatures in all cooling systems at steady conditions at power levels of 10, 12 and 15 MW.

9) PIEs of the three danish LEU test fuel elements
The authorities required post-irradiation examinations (PIE) of the three danish manufactured test elements. We had argued that very thorough PIEs had been carried out on mini plates and full scale test elements at ORNL and the authorities had copies of the reports from the RERTR-meetings. We had pointed out that PIEs on our test elements would undoubtedly not add new information to the existing documentation.

Re 9) We arranged a meeting between dr. Jim Matos from the RERTR-programme, ANL and our Nuclear Inspectorate (NI). Jim Matos reported on the experiences obtained by PIEs under the RERTR programme. NI was satisfied by the information, but stuck to the demand for a series of fuel tube wall thickness measurement on the 3 test elements, combined with a visual inspection for blisters. The thickness measurements and the visual inspections have been carried out in our shearing pond. No swelling within an accuracy range of ± 0.02 mm was detected, and no blisters were seen neither in the visual inspection nor in the photographical documentation.

10) Guarantee for reprocessing
The authorities demanded a written obligation from the USDOE that they would recieve the used LEU fuel elements for reprocessing and final store of the high-active waste. We had given them a copy of the US Federal Register/Vol 51 No. 32/Tuesday, February 18, 1986/Notice, but they wanted a more obligatory statement.

Re 10) This subject was also discussed between Jim Matos and NI. It was finally decided to ask the EURATOM supply agency for assistance on obtaining a written obligation from USDOE for reprocessing and final store of the fuel. Until now we have not got such an obligation.

11) Conversion approval for other reactors
The authorities required statements from such reactors which have got the permission to convert to LEU or were expecting the permission in a near future.

Re 11) We asked mr. Winkler (SAPHIR reactor, Switzerland), dr. Burtscher (ASTRA reactor, Austria) and dr. Krull (FRG-1, FRG-2, DFR) to inform us on the state of their conversions. Our authorities were happy to learn (Nov. 1987) that the swiss and the austrian reactor allready had obtained their license for LEU-operation and that the Geesthacht reactors would have their license in a couple of months.

12) Argumentation for non-amended "Authorized Conditions of Operation" (ACO)

We had given written proposals for amendments to 7 ACO's which we found to be the only which had to be amended owing to the LEU-conversion and the power increase. The authority required a written argumentation for each of the remaining 80 ACO's, on the reason why they should not be amended.

13) Safety at low-power operation

The DR 3 safety documentation contains a chapter about reactivity transients starting from low power (< 50 kW) where the temperature coefficients have no effect.

The authorities required a revision with the changed temperature coefficients of LEU taken in consideration.

14) Earliest time of withdrawal of used fuel elements from the core

By increasing the reactor power the maximum fuel element power is also increased. This extend the time after shut down needed to ensure that the residual heat of the fuel element can be removed by convection in free air if the cooling fails. We had proposed to replace the time limit (37 hours after shut-down) by a limit of 1.9 kW residual power. This is the residual power 37 hours after shut-down in a fuel element which had been operating at 700 kW just before shut-down.

The authorities required a device for measurement of the individual fuel element powers, so that we just before shut-down could measure the powers of those fuel elements which have to be changed during the shut-down.

Re 14) We provided a delta-T-times-flow measurement channel for the power of each fuel element. The individual flows were allready known for all 3 main circulator combinations, and the outlet temperatures were accessible through the built-in outlet thermocouples in the fuel elements. The inlet temperatures were obtained by statistical treatment of data collections from previous operation. The control room computer was coded to supply the fuel element powers on demand.

We have supplied most of the additional information required by the authorities. Only a few items were lacking when the authorities decided to isue a preliminary approval:

THE FRAMEWORK APPROVAL

Early 1988 the authorities issued an "evaluation report" with a "framework approval", e.g. an approval under conditions that some demands were fullfilled before the conversion starts and other demands were fullfilled before a full LEU core were established.

Required by the authorities before the conversion starts:

- Thickness measurements of test elements
- Emergency cooling flow measurements
- Recomputation of reactivity transients
- Schedule for exchange of the CCA connecting rods

Required march 1989, before full LEU-core is established:

- Instruction for measures against LOCAs
- Analysis on loss-of-lead-shield-cooling-accident
- Reanalysis on max. energy release by transients
- Calculation of reactivity increase by D_2O-filling of the He-volume in the top of the reactor tank
- Recalculations of transients and safety absorber reactivity worths with a series of different core configurations
- Revised proposals for "authorized conditions of operation"
- Reevaluation of LEU-operation based on experience obtained during the mixed-core operation.

During the mixed-core operation period we are obliged to precalculate thermal and fast neutron flux densities and power distributions in the core before the start of each reactor cycle, and to verify these calculations by measurements during each cycle. The results shall be presented in a report to the authorities after establishment of the full LEU-core. This report shall also contain results from calibrations of the safety absorbers (safety rods and coarse control arms), measurements of temperature coefficients and an evaluation of operation conditions in the pure LEU-core after the conversion.

MIXED-CORE OPERATION SCHEDULE

At start-up on October 14. 1988 eight 180g LEU fuel elements will be present in the core in the positions shown below (figure 1).

When these LEU fuel elements burn-up (at about 50% of the initial U235-content) they will be replaced by new LEU fuel elements in the same positions.

The remaining 18 core positions will contain HEU fuel elements until the stock is empty, which is expected about November 1989 ("K1"-period in the figure).

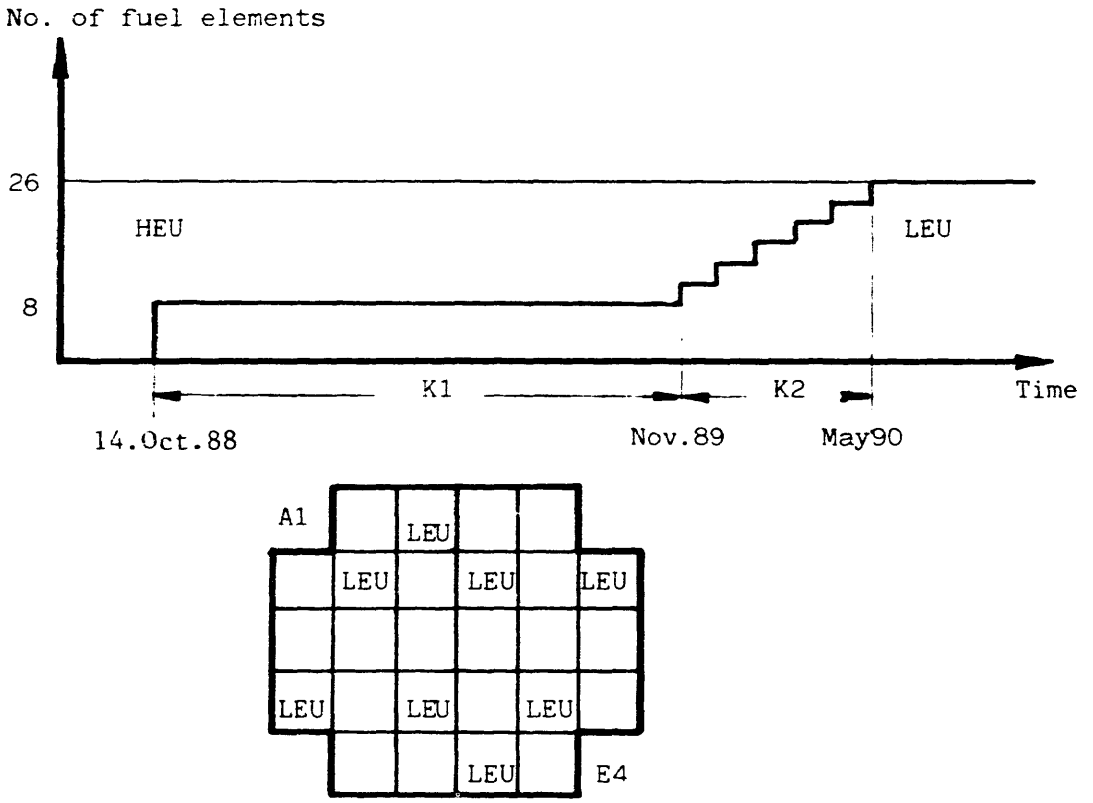

The core during the K1-period

Figure 1

The last core positions will be converted from HEU to LEU around May 1990.

There are two reasons for this conversion schedule:

1) The experimenters will have steady and foreseeable irradiation conditions during the K1-period.

2) If failures in the first production series of LEU fuel elements show up during the K1-period, we will still have the possibility to replace the 8 LEU fuel elements by 8 HEU fuel elements and continue the operation while new LEU fuel elements are produced.

REFERENCES

1. K. Haack, Irradiation of MEU and LEU Test Fuel Elements in DR 3 Page 203, Proceedings of the International Meeting on Reduced Enrichment for Research and Test Reactors, 24-27. Oct- 1983, Tokai, Japan.

2. K. Haack, Study on Al-alloy or Silicide LEU for DR 3 in Denmark. Page 337, Proceedings of the 1984 International Meeting on Reduced Enrichment for Research and Test Reactors, Argonne, Illinois, Oct. 15-18, 1984.

3. K. Haack, Selection of Fuel Type and Core Pattern and Application for LEU-Licensing of the Danish Reactor DR 3. Page 359, Proceedings of the 1986 International Meeting on Reduced Enrichment for Research and Test Reactors, Gatlinburg, Tennessee, Nov. 3-6, 1986.

Tryk: Grafisk Service, RISØ

SESSION VI

September 20, 1988

CONVERSION PLANS AND STUDIES

Chairmen:

K. Kanda
(KURRI, Japan)

F. DiMeglio
(RINSC, USA)

FULL CORE MEU FUEL DEMONSTRATION IN THE JRR-2

Yoshiaki Futamura, Junsaku Tsunoda and Takashi Koganezawa
Japan Atomic Energy Research Institute
Tokai-mura, Ibaraki-ken 319-11, Japan

ABSTRACT

In 1980, when JRR-2 was planned to convert from HEU to LEU, the LEU fuel being adopted in JRR-2 had not been qualified yet. So the MEU fuel was selected for JRR-2 conversion.

The integrity of MEU fuel element was confirmed with the irradiation test in JRR-2 and PIEs of irradiated fuel.

From the safety review on the base of LWR criteria, some modifictions and installations of additional equipment were required.

In November 1987, JRR-2 was converted to MEU and in January 1988, the full core MEU fuel demonstration test has been successfully completed and the JRR-2 has been satisfactorily operated with MEU fuel since that time.

INTRODUCTION

The Japan Research Reactor No.2 (JRR02) is a heavy water moderated and cooled 10 MW tank type reactor using both ETR type and cylindrical type fuel elements, and has been utilized for wide purpose such as irradiation for reactor fuels and materials, radioisotope production, neutron beam experiments and so on since October 1960. The characteristics of JRR-2 in shown in Table 1.

For converting from HEU to medium enriched uranium (MEU) fuel, the following guidelines were set up for the fuel element design.

(1) The reactor characteristic is equivalent to that of the previous core.
(2) The dimensions and the configuration of the fuel elements should be unchanged.
(3) The number of the fuel elements loaded in the core and the core configuration should be unchanged.
(4) The U-235 content per fuel element should be sufficient to allow operation with the fuel life-time and the reactivity of the core being less than those of previous one respectively.

Under the above mentioned guideline, MEU aluminum dispersed fuel with uranium density 1.6 gU/cm^3 in the fuel meat was adopted.

The MEU and HEU reactor core characteristics of JRR-2 are shown in Table 2, and the specifications of the MEU and HEU fuel elements are shown in Table 3. The structure of the MEU fuel element is shown in Fig. 1, and the JRR-2 core configuration is shown in Fig. 2.

For converting to MEU fuel, the following tests and equipment installation had been carried out.

(1) Irradiation test of full sized MEU fuel elements.
(2) Installation of required equipment on considering the safety review.

The full core conversion to MEU fuel was permitted by Japanese Government on November 5th 1986.

The criticality examinations and reactor characteristic examinations including rated power demonstration test with full core MEU fuel were successfully performed from November 1987 to January 1988. Since the time, JRR-2 has been satisfactorily operated with MEU fuel.

Installation of Additional Equipment on Considering the Safety Review Evaluation

By the results of required safety review evaluation analysis for the reactor systems on the base of LWR safety criteria, some reactor systems were found not to satisfy with the single failure criteria. Therefore, the following systems were additionally installed.

JRR-2 cooling system and emergency cooling system in shown in Fig. 3.

(1) An emergency heavy water supply system.
(2) Scram circuits "Flux High at low power mode" and "Fuel Failure".
(3) Re-establishment of two vital electical power supply systems (if one system not available, another one can be put into in use).

The emergency heavy water supply system consists of a heavy water reserver tank (ET-1) with 6 m^3 of heavy water, two supply pumps (Ep-2, Ep-2A) with redundancy and pipings. It functions to recover the coolant level decrease in the reactor at the postulated loss of coolant accident. The reactor coolant level being decreased to the preset level due to any cause, one of two supply pumps is automatically started. Then the pump supplies the heavy water from the reserver tank to the reactor core to keep it in the water (refer to Fig. 3). The additional sump pit recirculation pump is installed to reinforce the current recirculation system in consideration of redundancy. The two scram circuits has been installed with redundancy respectively. As a prevent measure of the start-up accidents, the "Flux High at low power mode" initiates trip circuits for reactor shut down when the flux level is exceeded the preset point equivalent to 0.44 % rated power (440 KW) at the low power operation mode. The "Fuel Failure" initiates the trip circuits

when the count rate of the fuel failure detectors (FFD) is exceeded the preset point corresponding to the value of ten times higher than the back ground.

There must be redundancy in the power supply for the engineering safety features, so the electric power must be separately supplied to the two pumps in those systems.

Irradiation Tests

Two MEU fuel elements fabricated by CERCA were irradiated, and they had the same specifications as those of the driver fuel element to be loaded in JRR-2. Concerning with the irradiation test, the following items were expected to be confirmed.

(1) Reactivity of fuel element.
(2) Integrity during operation.
(3) Burnup warranty.

The MEU fuel element (cylindrical type fuel element) had a comparable reactivity with that of HEU fuel. For example, the reactivity of the MEU fuel is 2.02 % ΔK/K and that of HEU is 1.96 % ΔK/K when each fuel was separately loaded at the same position (B ring) of the reactor core. Both reactivity are found to be almost same.

These two MEU fuel elements were loaded in the core for irradiation from September 1984 to December 1985. They had been irradiated with good behavior, such as no fission gas detected.

After the irradiation, post irradiation examinations (PIEs) for one MEU fuel element were carried out, such as (a) visual inspection (b) dimension measurement (c) X-ray radiography (d) gamma scanning (e) dlister test (f) mechanical properties (g) metallography (h) absolute burnup (i) SEM and XMA.

The results of PIEs showed satisfactory with no indication of irradiation behavior for using as reactor fuel element.

Full Core MEU Fuel Demonstration

The full core demonstration with MEU fuel was carried out November 25, 1987 through January 30, 1988 with satisfactory results. The following examinations and measurements were performed.

(1) Excess reactivity.
(2) One rod stuck margin.
(3) Shut down margin.
(4) Temperature coefficient.
(5) Neutron flux.

(6) Control rod worth.
(7) Moderator dump effect.
(8) Xenon poisoning effect.

The main results are shown in Table 4 and 5, and xenon poisoning effects is shown in Fig. 4.

Conclusion

The full core demonstration with MEU fuel in JRR-2 had been successfully completed with results sufficient to operate JRR-2 safely. Some neutronics data and reactor core characteristics data such as excess reactivity, shut down margin, temperature coefficient, etc. were measured and compared with calculation values. Those measurement results show almost consistency with its respective calculation value. The results were satisfactory.

During the reactor operation, fission products leakage was carefully checked by the monitoring of the primary coolant and the cover gas He. No fission products were observed.

REFERENCES

1. T. Sato, M. Sato, Y. Asahi, T. Koganezawa, S. Yamaguch and J. Tsunoda, LOSS-OF-COOLANT ACCIDENT OF JRR-2 IN A SAFETY ANALYSIS FOR CORE CONVERSION, JAERI-memo 63-220, 1986.

2. M. Kurosawa and Y. Torii, NEUTOONICS DESIGN OF MEDIUM-ENRICHED URANIUM CORE OF THE RESEARCH REACTOR, JRR-2, JAERI-M 86-052, 1988.

3. CHARACTERISTIC MEASUREMENTS OF JRR-2 AFTER MODIFICATION JRR-2 OPERATION SECTION, JAERI-M 6943, 1977.

4. Y. Futamura et. al., "Post-Irradiation Examination of Low Enriched UAlx-Al Fuel Element in JAERI" in 10th RERTR Meeting, Buenos Aires, Argentina, Sep. 28 ∿ Oct. 2, 1987.

Table 1. Characteristics of JRR-2

Type	Tank type
Power	10 MW thermal
Moderator/coolant material Pressure temperature coolant velocity	 D_2O Atmosphere 44°C (Inlet). 50°C (Outlet) 3 ~ 4 m/s (water ch.)
Reflector	D_2O
Fuel material enrichment loading type	 UAl_x 93 % 24 element Cylindrical type and MTR
Control rod	6 rods (Cd)
Neutron flux (In-core irradiation hole of cylindrical type:6B)	5.5×10^{13} ϕf (max.) 7.0×10^{13} ϕth (max.)
Power density	30 kw/ℓ (ave.)

Table ?. Reactor core characteristics of the MEU and HEU fuel

	MEU core	HEU core
Excess reactivity %Δk/k	18	16
Total control rod worth %Δk/k	31	37
Highest control rod worth %Δk/k	10	12
Shut down margin %Δk/k	14	22
One rod stuck shut down margin %Δk/k	4	10
Temperature coefficient (27°C ~ 52°C) Δk/k/°C	$-(0.23 \sim 1.2) \times 10^{-3}$ (17 ~ 127°C)	-0.37×10^{-3} (27 ~ 52°C)
Prompt neutron life time s	2.6×10^{-4}	$(2.8 \sim 3.1) \times 10^{-4}$

Table 3. Specifications of MEU and HEU fuel

		MEU fuel	HEU fuel
Meat	Material	$UA\ell_x$-Al dispersien	U-Al alloy
	Enrichment (%)	45	93
	Thickness (mm)	0.51	0.51
	U-Density (g/cm^3)	1.6	0.7
Clad	Thickness (mm)	0.38	0.38
Fuel plate	Thickness (mm)	1.27	1.27
Fuel element	Number of fuel plate	15	15
	U-235 Content (g)	220	195
	Dimension (cylindrical type) (mm)	$108^{\Phi} \times 950$	$108^{\Phi} \times 950$

Tbale 4. Measurement values of demonstration test comparing with calculated ones

		Measured	Calculated
Excess reactivity	%Δk/k	17	18
Total control rod worth	%Δk/k	33	31
Highest control rod worth	%Δk/k	6.4(C1)	10(C1)
Shut down margin	%Δk/k	16	14
One rod stuck shut down margin	%Δk/k	10	4
Moderator dump effect	%Δk/k	-0.71	-0.59
Temperature coefficient (27°C ~ 52°C)	%Δk/k/°C	-0.017 ~ -0.045 (16 ~ 56°C)	-0.023 ~ -0.12 (17 ~ 127°C)

Table 5. Measured neutron fluxes in MEU and HEU fuel core

Typical irradiation facilities \ Cores			MEU core	HEU core
Neutron flux $10^{13}/cm^2s$	In-core irradiation holes	6B	5.8/5.2	7.0/5.5
		6C	4.7/3.6	5.4/4.0
	Vertical experimental thimble	VT-1	13/2.8	20/2.5
	Pneumatic tube	Pn-2	8.1/0.3	8.0/0.25

* The neutron flux are given as Thermal Neutron Flux / Fast Neutron Flux.

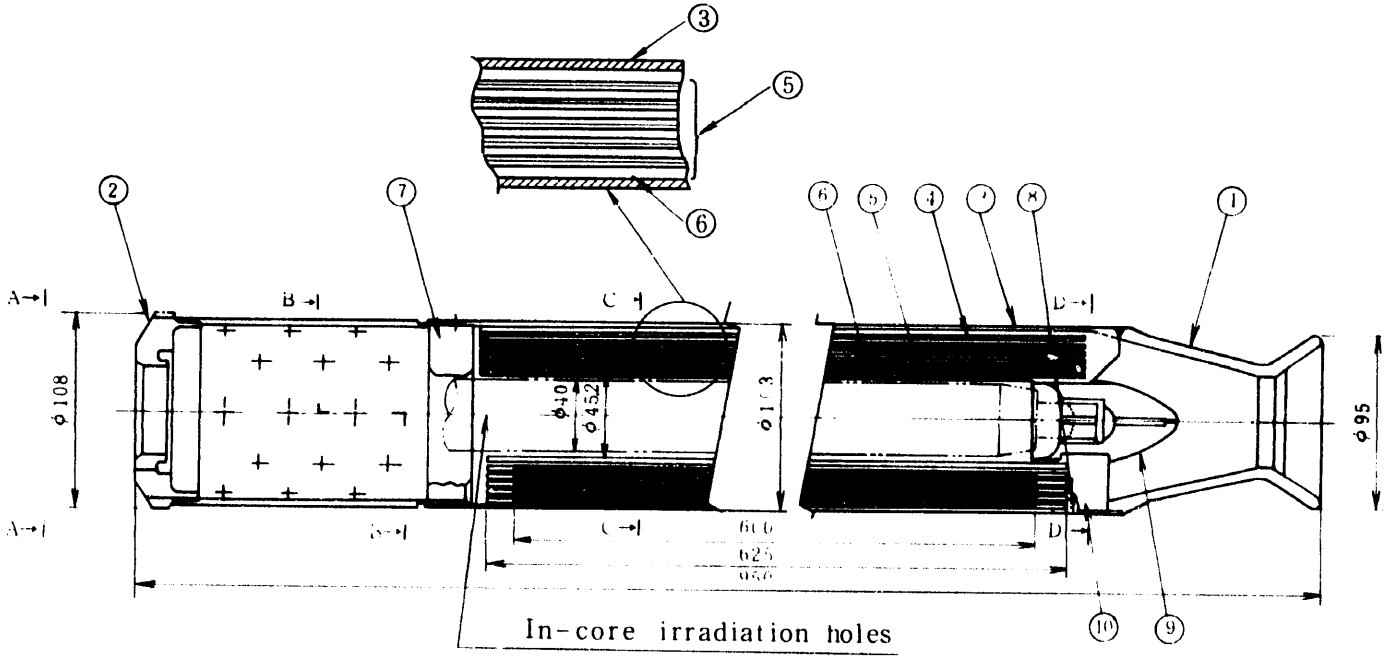

10	Comb
9	Capsule guide
8	Support pin
7	Upper capsule guide
6	Inner plate
5	Fuel plate
4	Fuel plate support
3	Outer tube
2	Upper adapter
1	Lower adapter

Fig. 1. JRR-2 MEU cylindrical fuel element

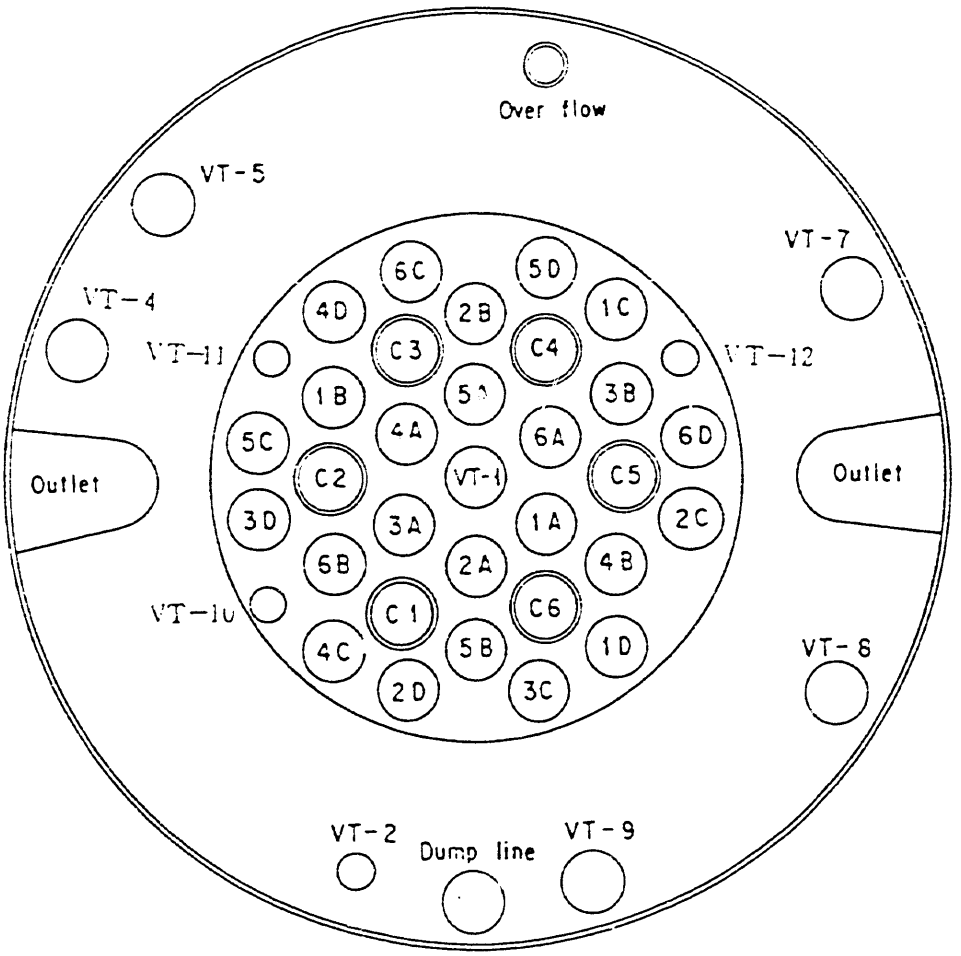

○ Fuel element (1A~6D)

○ Vertical experimental thimble (VT)

◎ Control rod

Fig. 2. JRR-2 core configuration

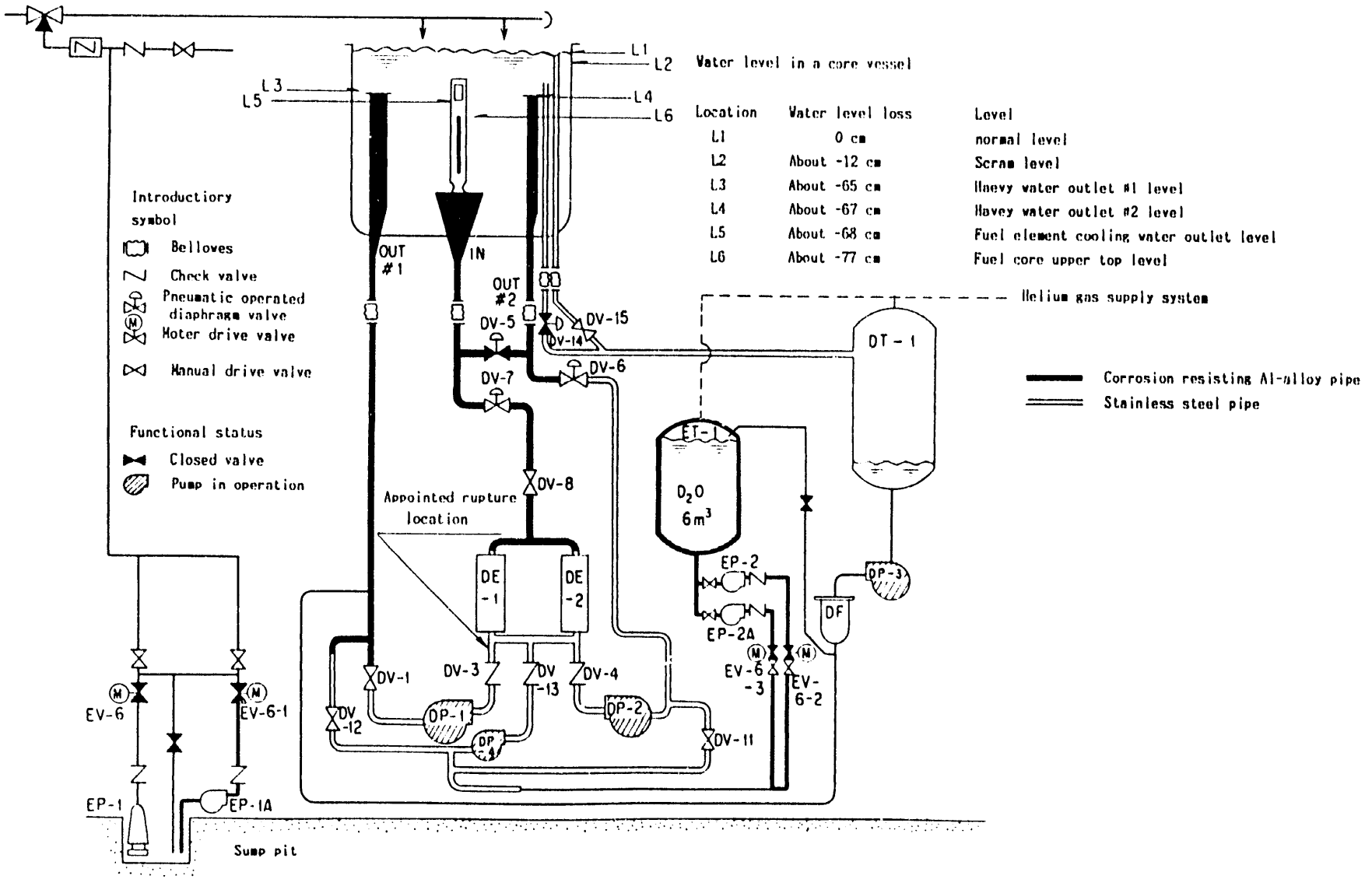

Fig. 3. JRR-2 cooling system and emergency core cooling system

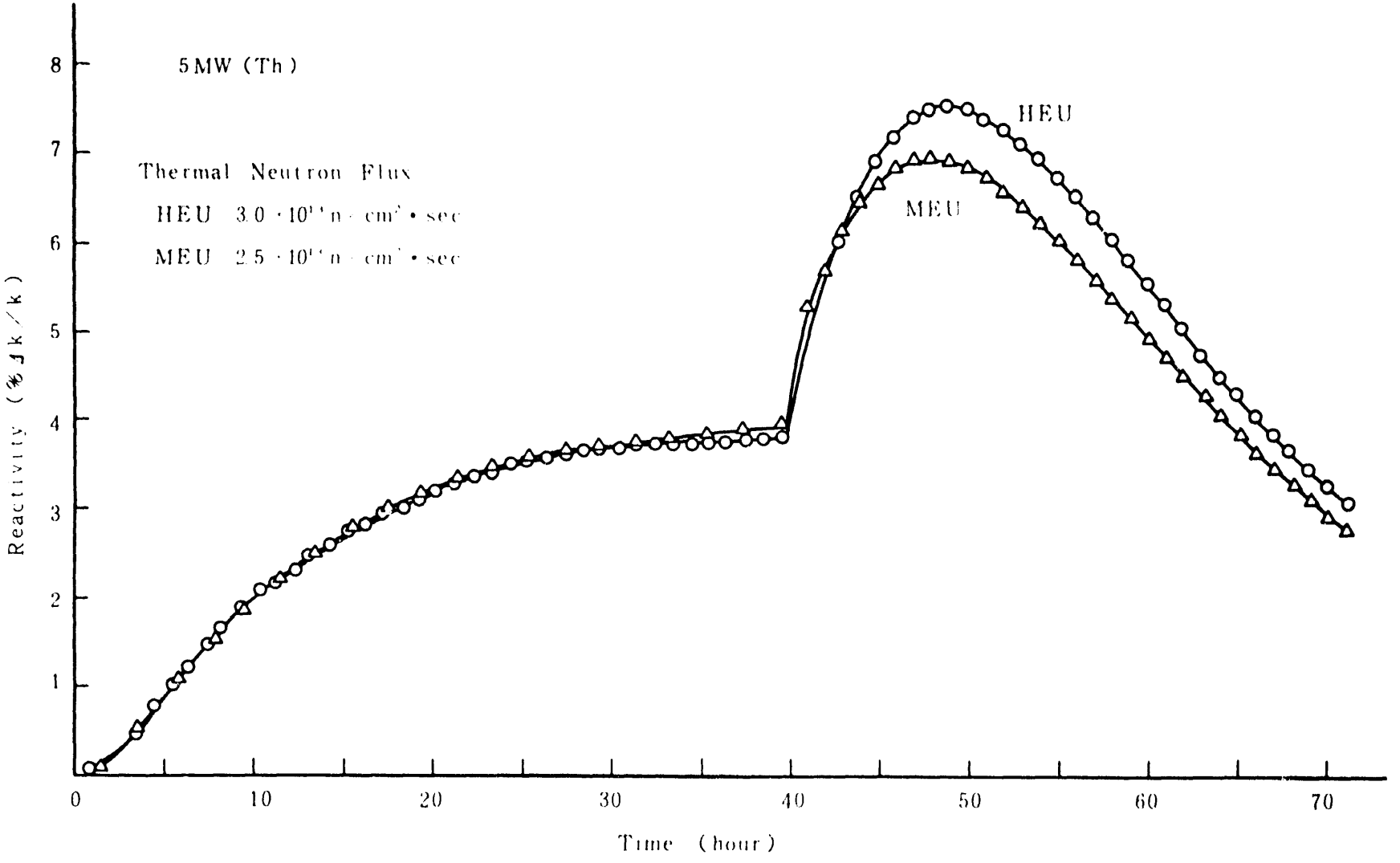

Fig. 4. XENON POISONING IN JRR-2 CORE (MEASURED)

Reduced Enrichment Fuel Conversion Efforts at the Swedish R2 Research and Test Reactor

E. Kaffehr and K. Saltvedt
Studsvik AB, Sweden

Abstract

Studies on the feasibility of operating the R2 reactor with LEU fuel have been in progress since 1982.

STUDSVIK is at present irradiating LEU silicide demonstration fuel elements with two different fuel densities. Two of the high density elements initially containing 490 g U^{235} and with a meat density of 4.8 kg U^{235}/cm^2 are manufactured by B & W. CERCA and NUKEM have each manufactured one element with the same fissile loading.

Three elements with an initial fissile loading of 320 g U^{235} are manufactured by B & W. The high density elements have reached burnup in the range from 11.6 to 22.6%. One of the elements with a lower fuel density has reached 50% burnup.

Introduction

Comprehensive studies on the feasibility of operating the R2-reactor with LEU fuel were carried out from 1982 to 1985. A large part of this work was done by the RERTR-project staff in Argonne and part of the work has been reported at previous RERTR-meetings (1).

The conclusion of these preliminary calculations was that the fuel cycle costs would be about the same with LEU elements as with HEU elements, if the LEU elements were loaded with approximately 50% more U^{235} than the HEU elements. The manufacturing cost for LEU elements was then assumed to be about 1.4 times that of the HEU elements. The performance reduction was calculated to be 5 - 15% for experiments requiring thermal neutrons and was almost unchanged for irradiation damage experiments. The calculations also indicated that fissile loading as high as 490 g U^{235} could be used and that this would give a substantial reduction in the fuel cycle costs.

Irradiation of LEU demonstration elements in the R2 reactor

In 1984 STUDSVIK made an agreement with ANL to irradiate four LEU demonstration fuel elements, each of them with a fissile loading of 490 g U^{235}. Two of the elements were manufactured by B & W and the two other by CERCA and NUKEM. In addition STUDSVIK also ordered three elements from B & W with a lower fuel loading. The elements were manufactured according to essentially the same specifications.

Design data for the elements are given in Table 1.

Table 1 Design data for the LEU demonstration elements irradiated in R2

Manufacturer	U^{235} content g	Fuel composition	Meat thickness mm	Cladding thickness mm	ρ_u g/cm^3
CERCA	490	U_3Si_2	0.76	0.38/0.57	4.8
NUKEM	490	U_3Si_2	0.76	0.38/0.57	4.8
B & W	490	U_3Si_2	0.76	0.38/0.57	4.8
B & W	320	U_3Si_2	0.76	0.38/0.57	3.1

Four of the B & W elements were already delivered in June 1984. The CERCA and NUKEM elements were delivered to Studsvik during the spring of 1986. The irradiation testing of these elements has however been much delayed compared with the initial planning. There are several reasons for the delay. Some of them are due to the replacement of the reactor vessel which was performed during the second half of 1984 and the first quarter of 1985.

The reason for the replacement was that ductility measurements on irradiated samples of the reactor vessel material showed unexpectedly low values. Lacking documentation on the manufacturing quality of the vessel STUDSVIK was not able to show that rupture of the reactor vessel and consequent sticking of the control rods could not occur.

To fulfil present design requirements and safety criteria the new vessel had to be modified in several respects compared to the old one. One of the major modifications was that the core lattice was changed from a 10 x 10 configuration to a 8 x 10 configuration. The Be-reflector was omitted on two sides of the core. Because of this the two fixed test loops for LWR fuel, each occupying two lattice positions, had to be moved to core positions with higher neutron fluxes.

The change of the core geometry and reflector composition had a large effect on the conditions for core loading and fuel shuffling.

After restart of the reactor with the new vessel we had difficulties in loading the heavy B & W element in the core without either exceeding the stated peak power limits or impairing the conditions for the experiments in the core. This problem was mostly related to the long term experiments designed for the old core.

After receiving the CERCA and NUKEM elements we performed a series of low power measurements aiming at verification and validation of the core physics calculation methods and establishing loading criteria for these heavy elements.

The license to operate the elements at high power was obtained after reporting the results of the measurements to the safety authority.

The most important limitation stated in the operating license is that if the core calculation previous to the loading shows a peak power in the element exceeding 70% of the maximum permissible level the calculation must be verified by adequate measurements. This requirement implies a great problem for the reactor operation.

It has generally not been possible to find more than one or occasionally two core positions where those heavy elements could be accepted without previous neutron flux measurements, either with consideration to the peak power criteria or to the effects on the experiments in the core. Neutron flux measurements including evaluation of the results do however reduce the fuel power availability of the reactor by 30 - 40 hours.

To reduce the operating costs the reactor has for approximately two years been operated by a reduced number of staff and with reduced availability.

Because of this the operating schedule has been very busy and it has not been considered acceptable to carry out flux measurements more frequently than every third or fourth period.

Lower power activation measurements have in addition to the initial campaign been performed on two later occasions.

Detailed neutronic calculations of possible configurations for irradiation testing of LEU prototype elements in the R2 HEU core have been performed both at ANL and in Studsvik.

It was not possible however to reproduce the core loadings which were assumed for the ANL calculations with sufficient accuracy to allow a detailed comparison between the ANL calculations and the measurements to be made. We attempted a comparison by calculating the effects of the differences between actual and assumed core loadings.

The preliminary conclusions from the comparisons between the measurements and the calculations made by Argonne and STUDSVIK are:

- We generally found good agreement between the Argonne calculations of the power distribution in the core and the measurements after corrections of the differences in the core loading. We did not however

find the element power peaking factors, i.e. maximum power density in an element to the average power density in the element, to be as high as was predicted by Argonne.

- When we compared the measurements and the calculations made in Studsvik the agreement was mostly acceptable. It seems however as if the predictions overestimate the neutron flux in the periphery of the core and especially in the corner positions where we found calculated to measured ratios up to 1.33. We also noticed a tendency to underestimate the neutron fluxes in HEU elements adjacent to the LEU elements.

  Also the STUDSVIK calculations predicted higher element power peaking factors than were measured. We believe that this is the same effect which has been observed by comparisons between calculations and measurements made in ORR reported by Cornella, Bretcher and Hobbs at the 1986 RERTR-meeting (2). They found that the neutron flux in the center of an element was overpredicted and underpredicted near the sideplates of the element.

  Figure 1 shows average ratios between calculated and measured neutron flux in the LEU elements which have been irradiated up to now, and also some typical values in some HEU elements. The figure also shows the ratios between calculated and measured power peaking factors in the LEU elements. Unfortunately we do not have a sufficient number of qualified wires from the measurements in the HEU elements to evaluate the power peaking factors in those elements.

The irradiation data of the LEU demonstration elements up to the beginning of September 1988 are shown in Table 2.

Table 2 Irradiation data for LEU demonstration elements in the R2 reactor (1988-09-01)

Manufacturer	Initial U^{235} g	Firr days	Pelement kW	Burnup U^{235} %
CERCA	490	110	800	22.6
B & W	490	62	770	12.2
B & W	320	194	660	50.6
NUKEM	490	62	730	11.6

The U^{235} content in the elements has dropped to a level where it will be easier to load the elements in to the core, and we expect the burnup to be substantially quicker in the future.

All three high density elements above will reach 50% burnup before the end of 1989, and the target fluence which is twice the fluence necessary to achieve 50% burnup can be reached during the spring of 1990. The second high density B & W element will reach approximately 35% burnup at the end of 1989.

One of the elements will be brought to the Hot Cell Laboratory for destructive examination after the 50% burnup.

Visual inspection and measurements of meat volume changes

The elements have been visually inspected in the reactor pool after each operating period. The only noticeable observation so far is a very light red-brown coating mainly on the sideplates on the NUKEM element.

In order to detect volume changes of the fuel plates the elements are weighed after every third operation period. The weight can be determined with an accuracy of 0.1 g which corresponds to a volume change in the meat of all the fuel plates of 0.1%

No significant volume changes have been observed so far in the high density LEU elements.

we have however observed a volume decrease of approximately 1% in the B & W element which has reached 50% burnup.

The core conversion plan for the R2 reactor

The conversion of the R2 core will be achieved by gradually replacing the fully burned HEU elements by LEU elements. The start of the conversion process will be determined with consideration to the inventory of HEU elements.

During the first phase of the transition it will be necessary to replace the burned HEU elements by a mixture of unirradiated HEU and LEU elements in order to obtain an acceptable uranium distribution in the core.

The past transition equilibrium state is reached when the inventory of partially burned elements corresponds to two core loadings.
The number of HEU elements needed for the whole transition process corresponds to approximately one core loading.

STUDSVIK plans to start with the transition in September 1988, and the equilibrium state will be reached two years later.

The studies which were based on the previous mode of operation, which means 6300 operating hours per year and a cycle length of 24 days, indicated that an element loading of 400 g U^{235} would be a good compromise between considerations to fuel economy and performance.

With the present mode of operation, which means 4400 operating hours per year and a cycle length of 17 days, we might have to reduce the loading in the elements. Calculations are in progress and the final decision will be made within the next few months.

Figure 1 Average calculated to measured neutron flux and power peaking ratios in mixed LEU/HEU cores

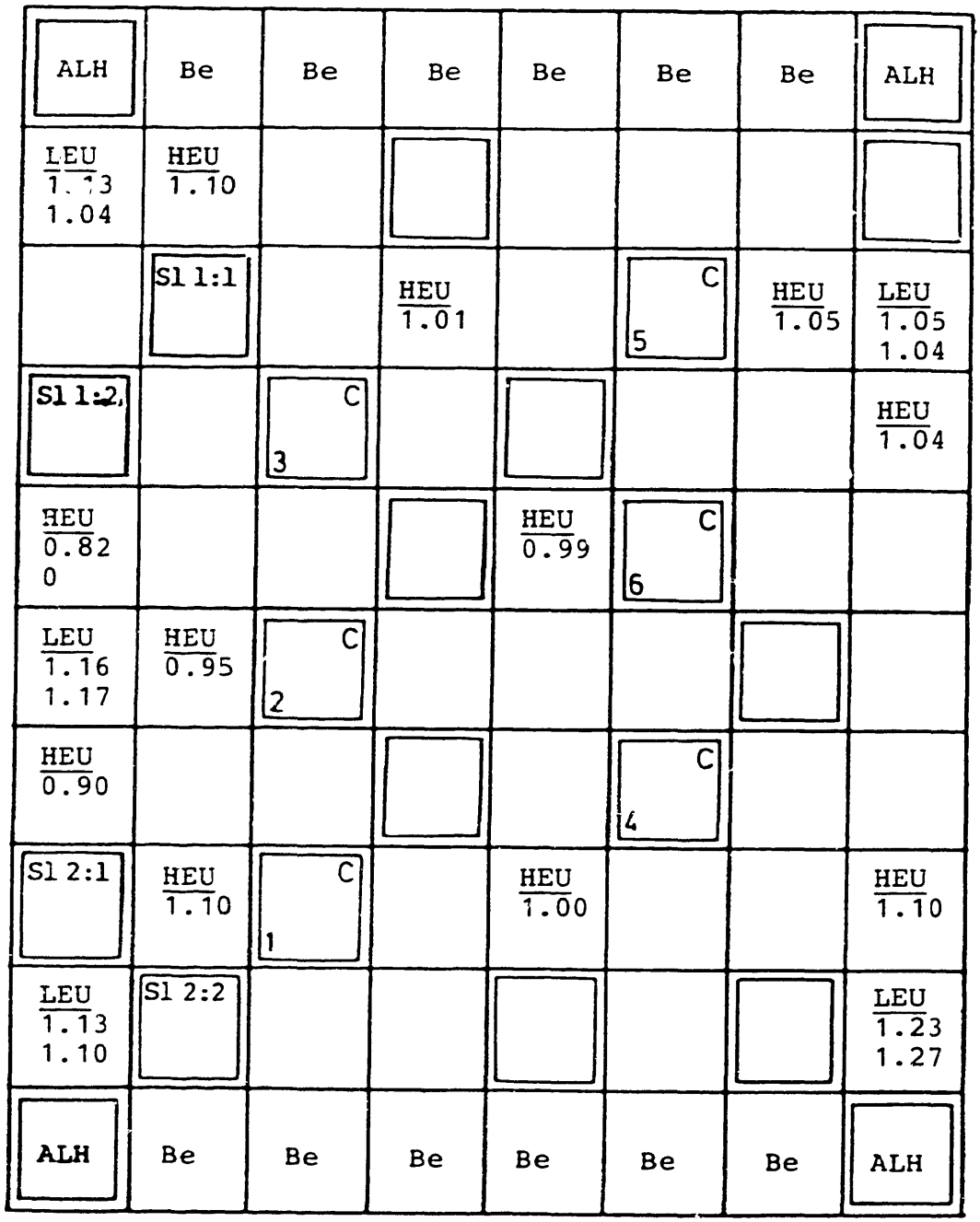

References

1. R. B. Pond, K. E. Freese and J. E. Matos "Performance and Fuel Cycle Costs Study of the R2 reactor with HEU and LEU fuels" in Proceeding of the International Meeting on the RERTR Program, Argonne, October 15 - 18 1984.

2. R. J. Cornella, M. M. Bretcher and R. W. Hobbs "Comparison of calculated and measured irradiated wiredata for HEU and mixed HEU/LEU cores in the ORR.

LEU FUEL CYCLE ANALYSES FOR THE BELGIAN BR2 RESEARCH REACTOR

James R. Deen and James L. Snelgrove
Argonne National Laboratory
Argonne, Illinois

ABSTRACT

Equilibrium fuel cycle characteristics were calculated for reference HEU and two proposed LEU fuel cycles using an 11-group diffusion-theory neutron flux solution in hexagonal-Z geometry. The diffusion theory model was benchmarked with a detailed Monte Carlo core model. The two proposed LEU fuel designs increased the ^{235}U loading 20% and the fuel meat volume 51%. The first LEU design used ^{10}B as a burnable absorber and the second used Cd wires as an alternative burnable absorber. Either proposed LEU fuel element would provide equilibrium fuel cycle characteristics similar to those of the HEU fuel cycle. Irradiation rates of Co control followers and Ir disks in the center of the core were reduced 6 ± 1% in the LEU equilibrium core compared to reference HEU core.

INTRODUCTION

The Reduced Enrichment Research and Test Reactor (RERTR) Program and the Centre d'Etude de l'Energy Nucléaire (CEN/SCK) have been engaged in a joint study to determine the most suitable LEU fuel element design for the BR2 reactor in Mol, Belgium.[1-3] The previous fuel cycle analyses were performed using a five-group diffusion theory model. Comparisons of the diffusion and Monte Carlo models in hexagonal-Z geometry of fresh and equilibrium cores indicated the need for improvements to the diffusion model. Presented in this paper are the equilibrium fuel cycle characteristics calculated using the improved diffusion theory model for two proposed LEU fuel designs.

REACTOR DESCRIPTION

The BR2 core is cooled and moderated with pressurized light water with an average pressure of 12 bar. The reference steady state power level is 56 MW, but the reactor has the cooling capacity to permit operation at 125 MW. The beryllium matrix has 79 cylindrical holes in a hexagonal lattice of 9.644 cm pitch at the midplane of the core. The holes are filled with fuel elements, control rods, various experiments or Be plugs. There are 64 standard channels of 84 mm diameter, 10 small channels of 50 mm diameter, and five large channels of 200 mm diameter. All core elements are placed at a slight angle from a perfectly vertical position relative to the core midplane in order to permit easier

access to core elements. The cosine of this non-vertical placement of element varies from 0.9981 to 0.9844 and does not significantly affect smeared material densities except in the upper and lower reflectors.

Core configuration 10D, which has 31 fuel elements with six shim and two regulating control rods as shown in Figure 1, has been chosen for these anlayses. No actual experiments have been modeled in these fuel cycle analyses. All core positions have been modeled using Be central plugs.

Fuel Element Description

The standard HEU fuel element has six concentric fuel rings with an active fuel length of 762 mm placed in an 84 mm diameter channel in a Be hexagonal matrix. Each fuel ring is formed by three fuel plates secured in position by a mechanical connection along their edges to three equally spaced radial Al webs (corresponding to the side plates of box-type elements) as shown in Figure 2. The water gap between the fuel plates is 3 mm and the fuel plate thickness is 1.27 mm with a fuel meat thickness of 0.51 mm. Each HEU fuel element contains 400g ^{235}U with 3.8g B from B_4C and 1.4g Sm from Sm_2O_3 as burnable absorbers homogeneously mixed into the UAl_x fuel meat.

Control Rod Description

The six shim control rods are divided into three axial zones: a cadmium control zone; a ^{59}Co zone, 12.15 cm in length; and a Be follower zone. The annular Cd section has an outer diameter of 60 mm and an inner diameter of 50 mm as shown in Figure 3. The two regulating control rods are similar to the shim rods but have a thinner annular cadmium control zone with outer diameter of 39 mm and inner diameter of 34 mm and no cobalt annular zone.

GENERATION OF CROSS SECTIONS FOR FUEL AND CONTROL RODS

TABLE I

Broad-Group Neutron Energy Structure for Neutronic Analyses

Neutron Group	Upper Energy Boundary (eV)
1	1.0×10^{7}
2	0.821×10^{6}
3	5.531×10^{3}
4	1.855
5	6.249×10^{-1}
6	1.427×10^{-1}
7	8.197×10^{-2}
8	4.276×10^{-2}
9	3.061×10^{-2}
10	2.049×10^{-2}
11	6.325×10^{-3}

The EPRI-CELL[4] code was used to generate all neutron cross sections for use in the fuel cycle calculations. EPRI-CELL uses one-dimensional integral transport theory with 35 neutron groups below 1.8 eV (similar to THERMOS) and 68 neutron groups above 1.85 eV in a homogeneous mixture (similar to GAM). The fine group cross sections were collapsed into 11 broad groups with three groups above 1.85 eV and eight below for use in broad-group diffusion-theory fuel cycle calculations as shown in Table I. A cylindrical representation of the fuel element was developed assuming that no web material was present and that the outer Be filler block could be represented as an

Fig. 1. BR2 Core Configuration 10D

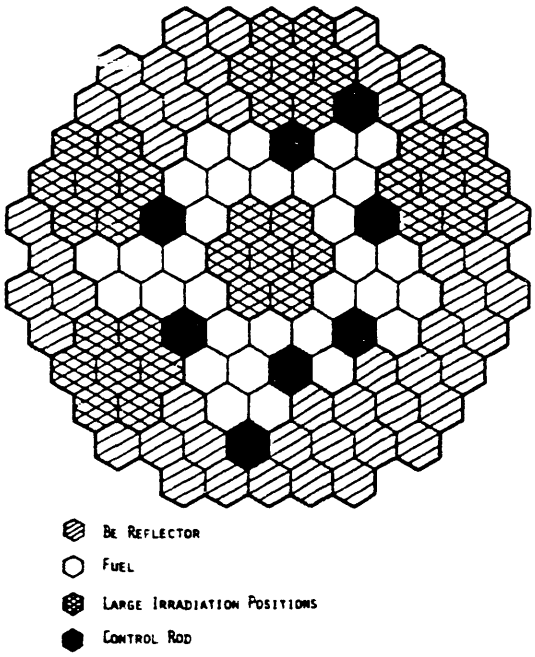

Fig. 2. BR2 HEU Fuel Element Cross Section at Core Midplane

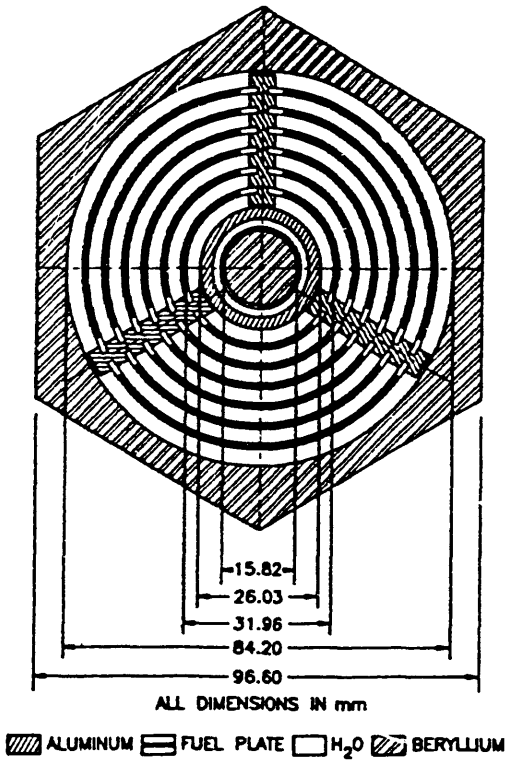

Fig. 3. BR2 Control and Follower Sections of Shim Control Rod

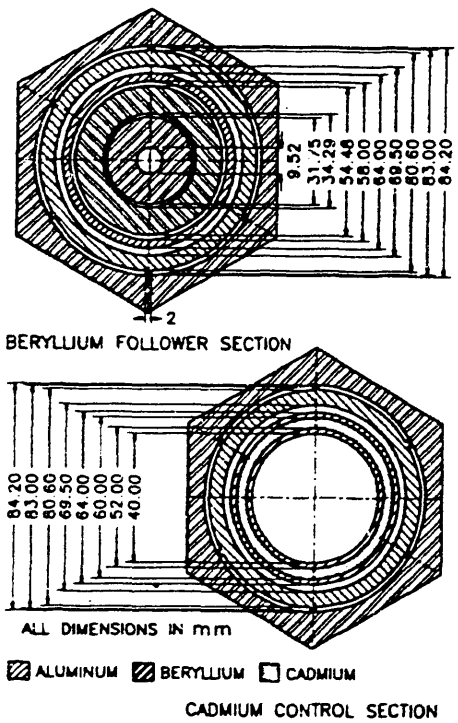

Fig. 4. EPRI-CELL Model for Cd Wire Depletion

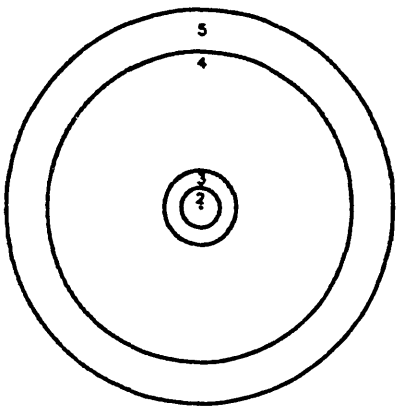

OUTER RADII OF EACH ANNULAR ZONE

r_1 = 0.2 mm – Cd WIRE

r_2 = 2.5 mm – Al WEB

r_3 = 4.3 mm – Al/H_2O

r_4 = 19.3 mm – FUEL

r_5 = 24.8 mm – Be

annulus. Each fuel meat, clad, and moderator zone was modeled separately with one mesh point used in each zone. A total of 44 mesh points was required for this model to calculate burnup-dependent cross sections for each isotope in each fuel plate of the fuel element. Each axial zone of the control rod was represented by a cylindrical model surrounded by an outer zone of homogenized fresh fuel.

Generation of Cross Sections for Cd Wires

The EPRI-CELL model for depletion of Cd wires consisted of four different zones surrounding a single Cd wire as shown in Figure 4. The first of these zones consisted of Al, representing any wire cladding and those parts of the web and fuel plate edge cladding closest to the wire, and had a radius equal to the distance from the center of the wire to the closest moderator. The second annular zone consisted of Al and H_2O, representing a volume-averaged mixture of web, fuel plate edge cladding, and moderator within a radius equal to the distance from the center of the wire to the closest fuel meat. The third zone was a homogeneous mixture of fuel, cladding, and moderator materials. The last zone was Be to represent the presence of Be filler block and inner plug material.

The key variables in the development of this model for accurately following the changes in composition of Cd from beginning to end of life were the volumes of the outer two zones (fuel and Be). Increasing the volume of fuel would harden the neutron spectrum while Be volume increases would soften the thermal spectrum without much effect on the higher energy groups. The main criterion for achieving a good EPRI-CELL model for Cd depletion was to create a neutron spectrum over the entire volume of the wire that would be as close as possible to the spectrum calculated by an exact VIM[5] model of the fuel element with each Cd wire explicitly represented. Once this spectrum was achieved, the EPRI-CELL calculated Σ_{a_5} of the unirradiated wire was within ±1% of the VIM result averaged over all wire locations in the element.

FUEL ELEMENT BENCHMARK COMPARISONS USING VIM AND DIF3D

In order to determine the adequacy of the cross section data generated by EPRI-CELL for use in whole-core diffusion calculations, it was necessary to benchmark the data using VIM. This benchmarking activity was needed because of the unusual geometry of the standard fuel element as well as the departure from infinite lattice boundary conditions caused by numerous fuel-non-fuel interfaces in the core. Initial VIM-DIF3D comparisons were made with infinite lattice boundary conditions before whole-core comparisons were begun.

The VIM model of the fuel element was an exact geometrical representation of the location of each fuel plate, Be plug and matrix block, and water channel using the standard combinatorial geometry option. The fuel element was modeled assuming no axial leakage and perfect reflector boundary conditions for all neutron energies at all radial surfaces.

The initial comparisons of fuel cross section data were made in an infinite lattice environment with a single homogeneous-composition, 11-broad-group diffusion calculation using a nodal method[6] DIF3D[7] flux solution. The key items for comparison of the two models were k_∞ and isotopic absorption rates

normalized to unity, as shown in Table II. Also included in Table II with the HEU fuel element are the comparisons for the two proposed LEU fuel element designs. LEU design #1 was loaded with 480 g ^{235}U/element and 2.85 g B and 1.4 g Sm mixed into the fuel meat. LEU design #2 has the same ^{235}U and Sm loading but with the boron burnable absorber replaced by 36 Al-clad Cd wires (0.4 mm in diameter) placed in the Al support webs of the element. Each of the VIM cases had accumulated 100,000 neutron histories, resulting in standard deviations for the most significant isotopic absorption rates presented in Table III of less than ±2%. The standard deviation for the VIM k_∞ was ±0.003 Δk_∞.

The results of the VIM and DIF3D models were in good agreement for the case of fresh HEU or LEU fuel in an infinite array of like elements. The only adjustment that was necessary for achieving this agreement for the elements using boron as a burnable absorber was to replace the EPRI-CELL $\sigma_1(n,2n)$ for Be with the VIM $\sigma_1(n,2n)$ in the DIF3D model. With 32% of the fuel element volume occupied by the Be matrix and central plug, the n,2n scattering in Be was a significant contribution to the element reactivity with approximately four n,2n scattering events occurring for every 100 absorption events. Since the strongly absorbing Cd wires in LEU design #2 occupy a very small volume relative to the fuel element, the EPRI-CELL microscopic thermal cross sections for ^{113}Cd required adjustment until the ^{113}Cd absorption rate in DIF3D was equivalent to the VIM model prediction. Once the ^{113}Cd absorption rate was forced to be equal to the VIM rate and the VIM $\sigma_1(n,2n)$ for Be utilized, all other isotopic absorption rates in the element were brought into good agreement using unadjusted EPRI-CELL cross section data. Four additional infinite lattice VIM-DIF3D comparisons were necessary for LEU elements using Cd wires so that the thermal absorption cross sections for ^{113}Cd could be properly adjusted throughout the lifetime of the wires.

WHOLE CORE MODEL COMPARISONS USING VIM AND DIF3D

In order to benchmark the DIF3D core model, six comparisons were made with a detailed VIM core model, three each with HEU fuel and with LEU fuel. Four of the six comparisons were for all-fresh fuel with no axial leakage both with and without control rods inserted and two were hexagonal-Z core models with beginning-of-equilibrium-cycle loadings and partially inserted control rods.

The VIM BR2 core model was an exact representation of each fuel plate, water region, web, Cd wire, Be plug in planar or hexagonal-Z geometry. The only approximation to the actual core geometry was the assumption that all elements were perfectly orthogonal to the horizontal mid-plane of the core. A total of 1876 zones were required for the HEU equilibrium cycle core and 2186 zones for the LEU equilibrium cycle core. Each VIM case required 300,000 neutron histories to obtain absorption rate standard deviations $<\pm 2\%$ for each significant isotope in each fuel element. Lumped fission products were simulated using concentrations of ^{135}Xe and ^{99}Mo. One axially averaged fuel meat concentration was used per element to reduce the volume of input that several axially dependent compositions would require. The shim rods were all positioned with the end of the 12.15 cm-long cobalt follower section at 2.5 cm above the core mid-plane. The regulating rods were pulled such that their Cd section tips were

TABLE II

Benchmark Comparisons of VIM and Single-Composition Infinite Lattice DIF3D Models of Fresh 400 g ^{235}U HEU Reference Fuel and Fresh 480 g ^{235}U LEU Fuel

Isotopic Absorption Rates Normalized to Unity

	HEU Element		LEU Element No. 1		LEU Element No. 2	
Isotope	VIM	DIF3D	VIM	DIF3D	VIM	DIF3D
^{235}U	0.6686	0.6662	0.6529	0.6551	0.6878	0.6865
^{238}U	0.0044	0.0047	0.0774	0.0780	0.0785	0.0780
^{27}Al	0.0225	0.0214	0.0180	0.0172	0.0185	0.0188
^{10}B	0.1634	0.1655	0.1344	0.1354	-	-
Si	-	-	0.0006	0.0006	0.0006	0.0005
^{149}Sm	0.0525	0.0530	0.0428	0.0419	0.0450	0.0446
^{1}H	0.0689	0.0688	0.0543	0.0537	0.0531	0.0531
^{16}O	0.0013	0.0011	0.0011	0.0010	0.0012	0.0011
^{9}Be	0.0184	0.0192	0.0185	0.0180	0.0180	0.0202
^{113}Cd	-	-	-	-	0.0974	0.0972
k_∞	1.3918	1.3914	1.3682	1.3710	1.4396	1.4411

TABLE III

Comparison of Isotopic Absorption Rates Calculated Using VIM and Several DIF3D Nodal Models for the BR2 BOL HEU Core

Isotopic Absorption Rates Normalized to Unity

Isotope	VIM	DIF3D 20 gr	DIF3D 11 gr	DIF3D 5 gr	DIF3D* 20 gr	DIF3D* 5 gr
^{235}U	0.5821	0.5826	0.5833	0.5867	0.5860	0.5893
^{238}U	0.0033	0.0034	0.0034	0.0034	0.0034	0.0034
^{9}Be	0.0570	0.0594	0.0590	0.0578	0.0583	0.0570
^{10}B	0.1451	0.1465	0.1466	0.1477	0.1474	0.1485
^{1}H	0.1313	0.1280	0.1275	0.1250	0.1251	0.1226
^{27}Al	0.0322	0.0315	0.0315	0.0312	0.0310	0.0308
^{149}Sm	0.0476	0.0476	0.0476	0.0472	0.0479	0.0475
k_{eff}	1.1581	1.1590	1.1601	1.1636	1.1663	1.1691

*Finite difference with 64 triangles per hexagon mesh.

alsc 2.5 cm above the core mid-plane, which corresponds to a rod position of 505 mm of withdrawal. A no-return current boundary condition was placed at axial planes 30 cm above and below the active core zone and at the outer radial boundary of seven hexagonal rings.

The DIF3D core model required 127 hexagonal unit cells for the seven hexagonal rings in each of the 21 axial mesh planes for the 31-fuel-element core. The microscopic cross sections were burnup dependent for all heavy metal and burnable absorber materials. The nodal method of flux solution to the diffusion equations using 11 broad groups was used for this model. The rationale for this selection can be deduced by a comparison of the isotopic absorption rates and k_∞ data using finite difference and nodal methods with different group structures as shown in Table III. The comparison presented in Table III was for an all-fresh HEU core with all control rods fully withdrawn. Although the finite difference and nodal methods yielded identical flux solutions in infinite lattice single fuel element DIF3D cases, the nodal method yielded better predictions of absorption rate and k_∞ for every group structure tested in whole core calculations. Increasing the number of groups below 0.625 eV using the nodal method yielded closer agreement with VIM. A finer group structure above 0.625 eV was also compared with VIM fine group neutron spectra but found to be unnecessary to improve any reaction rates or neutron spectral comparisons.

The whole-core reactivity comparisons using the VIM and DIF3D models are presented in Table IV. In each case the k_{eff}'s agree to within $\pm 0.003\ \Delta k_{eff}$. The isotopic absorption rate comparisons for the entire core followed the same trends presented in Table III for the fresh core comparisons. The hydrogen absorption was underpredicted consistently in HEU and LEU cores but the bias is reduced upon insertion of all control rods. Most other isotopic absorption rates were predicted well except for Be, whose absorption rate is consistently larger than for VIM. The only adjustment to the microscopic cross section data was a further adjustment to the $\sigma_1(n,2n)$ of Be compared to infinite lattice comparisons. Although the k_{eff} comparisons for the equilibrium HEU and LEU cores were as good as the fresh core comparisons, the agreement in the isotopic absorption rates was not as favorable. Although all heavy metal and burnable absorber absorption rates were predicted to within $<\pm 2\%$, the hydrogen absorption was overpredicted by 3.9% in the HEU core and 6.5% in the LEU core. These differences did not affect the core reactivity because the absorption in the steel axial reflector material was underpredicted by a similar amount.

The average fission rate per element predicted by DIF3D was within ±3.3% of the VIM result for all elements in the HEU core. The average bias was reduced to ±2.5% for the DIF3D prediction of element fission rates in the LEU core relative to VIM. The peak element fission rate has been lowered in the LEU core relative to the HEU core by 5.4% because of the small shift in power out of the central ring.

FUEL CYCLE ANALYSES

The fuel management strategy used for these equilibrium fuel cycle calculations was based upon the burnup distribution and fuel cycle length of 19.8 days observed for configuration 10D. Six of the eight fresh elements loaded into the core at the beginning of each cycle were located in the fourth hexagonal ring, along with all six shim control rods. The other two fresh

elements were loaded into the fifth ring. The third ring consisted of second- and third-cycle-residence fuel in which nearly half of the total core power is produced, providing a large source of neutrons for the central irradiation position. The core power peak usually occurred in this third ring. The nominal core thermal power was 56 MW but calculations were also performed at 20% above this average power because significant portions of the BR2 operating history have been at higher-than-average power levels.

One of the primary fuel cycle objectives, in addition to minimizing LEU fuel density and power peaking, was to preserve or reduce the movement of control rods during the fuel cycle. Reduced control rod motion provides constant irradiation conditions for the in-core experiments. This was achieved through the careful selection of burnable absorber materials, concentrations and locations. The use of the rapidly depleting ^{149}Sm in the fuel meat reduced the startup control rod motion until ^{135}Xe and ^{149}Sm had reached equilibrium concentrations. The use of ^{10}B reduced the total control rod travel during a cycle by placing more absorber control material at the beginning of the cycle and depleting a significant portion of it before the end of cycle was reached. Cd wires performed much the same as ^{10}B except the difference in absorber worth from beginning to end of cycle was greater owing to the faster ^{113}Cd depletion rate.[8,9]

Equilibrium fuel cycle characteristics were obtained using the REBUS3[10] code with 11 group, burnup-dependent cross sections. The EPRI-CELL burnup-dependent cross sections were fit to different order polynomials using the least-squares method. The DIF3D model developed by benchmark comparisons with VIM was used in REBUS3 to perform all nodal diffusion theory solutions. A summary of the equilibrium fuel cycle characteristics using HEU and LEU fuels is presented in Table V. The BOEC k_{eff} was a simulated startup reactivity with saturated Sm in previously burned fuel and no ^{135}Xe. The EOEC k_{eff} assumed equilibrium concentrations of ^{135}Xe and ^{149}Sm. All control rods were fixed at their mid-cycle positions, 505 mm. By comparing the EOEC k_{eff} for the reference HEU cycle and the LEU cycle using 2.85 g B/element, the use of LEU meat with 4.9 Mg/m^3 meat density would provide ~0.7% Δk_{eff} more reactivity. Similarly when ^{10}B was replaced by Cd wires in the LEU fuel cycle, the increase in Δk_{eff} was 2.0% Δk_{eff}. This reactivity increase was caused by less burnable absorber material present at EOEC in the Cd case compared to the boron case. The required LEU fuel density was slightly higher when using the Cd wires clad with Al, but the minimum LEU density could be reduced to ~4.8 Mg/m^3 by reducing the ^{235}U loading by 6%. This would bring the reactivity performance of the LEU and HEU cycles closer together while using the ORR U_3Si_2-Al demonstrated LEU fuel density.[11] The comparison of the HEU and LEU fuel cycles operating at 67.2 MW demonstrated an increasingly favorable reactivity bonus for LEU fuel cycle operating at higher burnups. Pu fission replaces more of the reactivity lost by ^{235}U burnup in LEU fuels with higher burnups compared to the HEU fuel cycle.

The reactivity change from BOEC to EOEC increased 42% in the LEU cycle using ^{10}B absorbers and 21% using the Cd wires for operation at 56 MW relative to the reference HEU cycle. This reactivity change is an indication of the distance control rods must travel to preserve criticality during the cycle. When the power was increased to 67.2 MW, the control rod travel was reduced by ~6% in the LEU cycle relative to the HEU cycle. A further reduction in reactivity change from BOEC to EOEC could be achieved through the addition of more burnable absorber material or by operation at higher power levels.

TABLE IV

BR2 Whole Core Reactivity Comparisons for Fresh and Equilibrium HEU and LEU Cores

Enrichment	Core Burnup	All Control Rods	Whole Core k_{eff} VIM	Whole Core k_{eff} DIF3D
LEU	BOL	withdrawn	1.2160	1.2157
LEU	BOL	inserted	1.0801	1.0771
LEU	BOEC	505 mm*	1.1405	1.1390
HEU	BOL	withdrawn	1.1581	1.1601
HEU	BOL	inserted	1.0340	1.0348
HEU	BOEC	505 mm*	1.1245	1.1268

*Near core midplane position of 480 mm.

TABLE V

Summary of BR2 HEU and LEU Equilibrium Fuel Cycle Characteristics

Enrichment	HEU	HEU	LEU	LEU	LEU
Core Power (MW)	56	67.2	56	56	67.2
^{235}U/element (g)	400	400	480	480	480
Burnable Absorber	^{10}B	^{10}B	^{10}B	^{113}Cd	^{113}Cd
Meat U Density (Mg/m^3)	1.3	1.3	4.9	5.1	5.1
k_{eff} (BOEC)	1.1242	1.1108	1.1388	1.1556	1.1484
k_{eff} (EOEC)	1.1061	1.0779	1.1125	1.1331	1.1153
Discharge Burnup (%)					
Average	44	52	35	35	42
Peak	65	75	53	53	60

The peak nodal power for the LEU cores relative to the HEU cores has increased ~2 to 3% according to DIF3D predictions. Referring back to the VIM-DIF3D equilibrium core benchmark, VIM predicted an average fission rate reduction in the peak element of 5% while DIF3D predicted no change in the same peak element. Therefore the LEU peak power is probably slightly lower relative to HEU equivalent-fuel-management cores if credit is taken for the slight redistribution in the radial power from the central core to the periphery in the LEU cores.

Changes in Co and Ir Irradiation Rates

The irradiation rates of ^{59}Co and natural Ir in an LEU core were compared to an HEU equilibrium core using VIM. For the core provided by the BR2 staff, Co and Ir were the primary materials used for isotope production. Most of the Co was located in the six shim control followers and the Ir disks were located in the central large irradiation hole, H1. The capsule used for irradiation of the Ir disks was 75 mm in height located near the axial flux peak of the core. Each disk contained 35 mg of Ir and was attached to the exterior of an Al annulus 21 mm in diameter with a central water hole. There were 228 disks placed around each of three Al annuli located 106.4 mm from the center of the H1 irradiation hole. Each of these disks was modeled in exact detail in the VIM equilibrium core model. It was necessary to model Ir as a combination of ^{197}Au and ^{6}Li owing to the absence of Ir from the VIM library, assuming a resonance integral of 2000 barns and thermal absorption cross section of 426 barns for Ir.

The relative absorption rates for Co and Ir were found to be reduced by 6 ± 1% in LEU relative to an HEU core. The correction for fission source differences in adjacent power-producing elements was less than 2%. The reductions in the Ir and Co irradiation rates followed the thermal flux reduction computed for LEU relative to HEU cores without any experiments present.

CONCLUSIONS

The equilibrium HEU-LEU fuel cycle comparisons have indicated that LEU fuels with meat densities of ~4.8 Mg/m^3, comparable to the LEU density used in the LEU-ORR demonstration core, would provide fuel cycle characteristics similar to current operational characteristics. A change from the use of ^{10}B in the fuel meat to Cd wires placed in the webs would provide ~2% Δk_{eff} more excess reactivity at EOEC. Fast neutron fluxes are slightly higher in LEU cores while thermal flux reductions are less than 10% in irradiation positions adjacent to a fuel element or in the reflector. Power peaking changes would require more detailed study, but indications from these analyses were that power shifts caused by a harder neutron spectrum near the core center reduced the LEU peak power. The change in the location of the burnable absorbers from the fuel meat to the web also served to reduce local power peaking within the element. Control rod worth changes were minimal. Reductions in Ir and Co irradiation rates were less than 10%.

Detailed benchmark comparisons of the DIF3D model were required using VIM because of the unusual core and fuel element geometry and the large volume of in-core Be. The Be $\sigma_1(n,2n)$ was found to be location dependent and a neutronically important parameter for determination of core reactivity requiring

careful benchmarking with VIM. Most research reactor core analyses have been possible using one thermal group below 0.625 eV. With the presence of more Be, the BR2 core model needed a few more thermal groups to accurately determine reaction rates and reactivity. With the completion of extensive benchmark comparisons for the BR2 core diffusion model, one can have greater confidence in the fuel cycle predictions of reactivity and reaction rates.

REFERENCES

1. J. M. Baugnet, et al., "The BR2 Materials Testing Reactor and the RERTR Program, Present Status and Future Trends," *Proc. of 1984 International Meeting on Reduced Enrichment for Research and Test Reactors*, ANL/RERTR/TM-6, CONF-8410173, 423-445 (1985).

2. J. R. Deen and J. L. Snelgrove, "Preliminary LEU Fuel Cycle Analyses for the Belgian BR2 Reactor," *Proc. of the 1986 International Meeting on Reduced Enrichment for Research and Test Reactors*, ANL/RERTR/TM-9, CONF-861185, 345-358 (1986).

3. J. R. Deen and J. L. Snelgrove, "LEU Fuel Cycle Analyses for the Belgian BR2 Reactor," *Trans. Am. Nucl. Soc.*, 56, 581 (1988).

4. B. A. Zolotar et al., "EPRI-CELL Description," *Advanced Recycle Methodology Program System Documentation*, Part II, Chap. 5, Electric Power Research Institute (Sept. 1977); EPRI-CELL code supplied to Argonne National Lab. by Electric Power Research Institute, Palo Alto, California (1977).

5. "VIM - A Continuous Energy Monte Carlo Code at ANL," *A Review of the Theory and Application of Monte Carlo Methods, Proc. Seminar-Workshop* April 21-23, 1980, ORNL/RISC-44, Oak Ridge National Lab.

6. R. D. Lawrence, "The DIF3D Nodal Neutronics Option for Two- and Three-Dimensional Diffusion Theory Calculations in Hexagonal Geometry," ANL-83-1, Argonne National Lab. (Mar. 1983).

7. K. L. Derstine, "DIF3D: A Code to Solve One, Two, and Three-Dimensional Finite Difference Diffusion Theory Problems," ANL-82-64, Argonne National Lab. (Apr. 1984).

8. J. R. Deen and J. L. Snelgrove, "Comparison of Boron and Cadmium Burnable Absorbers in Research Reactors," *Trans. Am. Nucl. Soc.*, 35, 570 (1980).

9. J. R. Deen and J. L. Snelgrove, "Advantages of Cadmium Burnable Absorbers in Research Reactors," *Trans. Am. Nucl. Soc.*, 38, 287 (1981).

10. B. J. Toppel, "A User's Guide for the REBUS-3 Fuel Cycle Analysis Capability," ANL-83-2, Argonne National Lab. (Mar. 1983).

11. M. M. Bretscher, J. L. Snelgrove, and R.W. Hobbs, "The ORR Whole-Core LEU Fuel Demonstration," *Trans. Am. Nucl. Soc.*, 56, 579 (1988).

CONVERSION AIMS ON THEIR WAY FROM PHYSICS TO ECONOMY

A. Strömich, H.-J. Roegler
Interatom GmbH
Bergisch Gladbach, Germany

ABSTRACT

Within the German AF-Program all the calculational efforts related to the planned core conversion of research reactors in Germany were overtaken by Interatom. Ten reactor HEU-cores had to be analysed and treated for conversion to LEU-fuel during the course of this program up to now. As time went on aspects of economics generated complications arising from the extreme increase of U 235 loading together with the change of enrichment to compensate for the high fabrication costs of the new fuel. Dependent on the development since 1979 with respect to operation and use of research reactors in Germany in the program up to now five cores remained for conversion including licensing and the related calculational tasks. For one core the conversion license is already achieved, the residual four are in different stages of licensing procedure. Another LEU-core calculated by Interatom in detail is the core of the MPR 30 in Indonesia, erected by Interatom 1984 - 1987.

INTRODUCTION

In the framework of the German AF-Program from its start in 1979 all calculational work related to the planned conversions of German research reactors has been performed by Interatom. This includes the pure nuclear calculations for defining suitable fuel and fuel elements with low enriched uranium as well as performance and safety-related aspects as they are essential for scientists, for operations and for licensing bodies. Subsequently more complications were generated by economical aspects due to the extreme increase of U 235 loading per fuel element in the planning of the operators together with the change of enrichment. Target of this U 235 loading increase was to compensate for the high fabrication costs of the new fuel. Moreover, the operators influenced the work at Interatom by additional demands towards upgrading, reflector improvements, power density increase etc.

A parallel task for Interatom since 1980 has been the design, licensing and supply of a modern multipurpose research reactor for Indonesia foreseen to use LEU-fuel from the beginning of its operation (August 1987).

TASKS FOR CONVERSION CALCULATIONS

The members of the AF-Program have agreed upon a catalogue of tasks for conversion calculations which are classified into

- basic studies
- licensing-specific studies
- operating specific studies

Standard tasks which are nearly equal for each reactor are:

- basic studies
  - . recalculation of core status with HEU
    - .. reactivity levels
    - .. burnups
  - . complete fixation of the REU-fuel and control elements
    - .. geometry
    - .. U loading
    - .. target burnup
  - . fixation of related absorbers (old/new)
    - .. type
    - .. absorbing material
    - .. geometry
  - . analysis and definition of the LEU-core
    - .. configuration
    - .. burnup and cycle length
    - .. power density distribution
    - .. shut down margin
    - .. neutron fluxes (core/reflector/irradiation positions)
  - . transition phase analysis
    - .. optimum mixed cores
    - .. LEU first core plus subsequent LEU transition cores
    - .. respective safety related characteristics

- licensing-specific studies
  - . reactivity coefficients
  - . selected kinetics parameters
  - . fission product inventory
  - . accident analysis
    - .. new calculations or plausibility evaluations based on new feed back coefficients
    - .. assessment with references to guide books

Non-standard Tasks arise from special demands of the licensing authorities or demands of the operator with respect to reactor operation after conversion:

- licensing-specific studies
  - . calculational prove of all variations of LEU-core for future flexibility of operation for the actual license (most plants)
  - . calculations for experimental test of fuel elements with small changes in fabrication procedure with HEU before converting (FRJ-2)
  - . comparison of burn-up behaviour of different absorbers (FRG-1)
  - . determination of inventory of actinides

(separately to fission inventory; FRG-1, BER-II)
. fission product release on basis of new source terms (BER-II)
. analysis of the hypothetical accident of fuel melting by propagation (BER-II)

- operating-specific studies
  . operator demands on input data for station codes
    .. fluxes
    .. cross sections
    .. other parameters

ANALYSED CORES

In the course of the AF-Program ten different HEU-cores of seven research reactors were the starting point for conversion investigations. These cores are shown in Fig. 1.

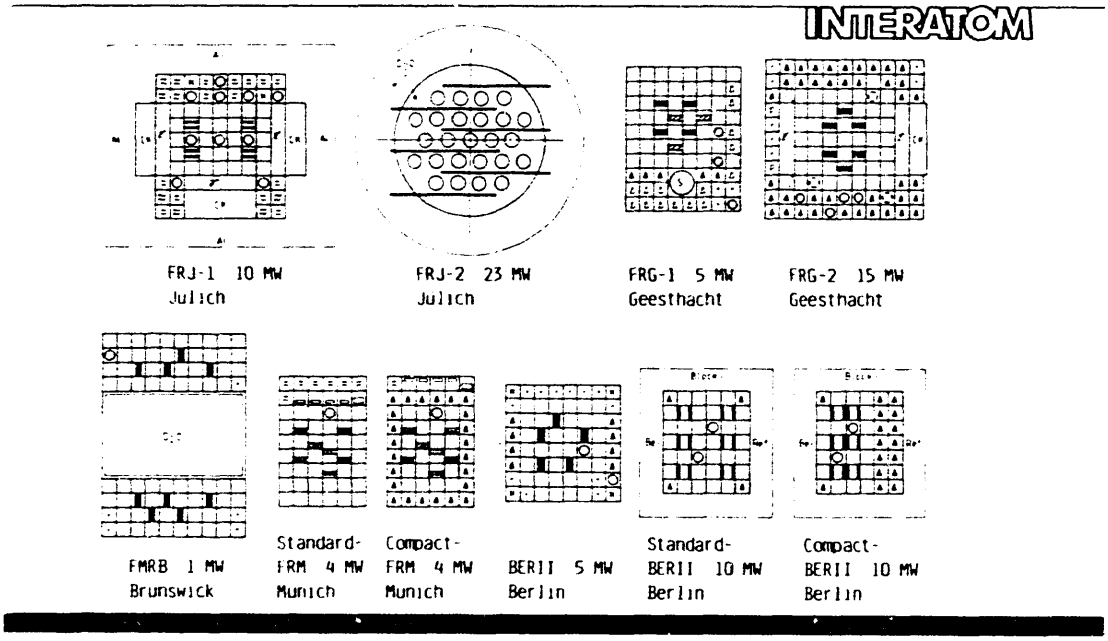

FIG.1 COMPILATION OF CORES
CALCULATED FOR CONVERSION TO LOWER ENRICHMENT

The calculations had to comprise different moderators H_2O, D_2O, all types of reflectors C, Be, D_2O, H_2O and different types of absorbers such as oval central absorber, fork type absorber and a three-rod type absorber. Moreover, a lot of irradiation inserts had to be treated. Before starting the conversion investigations each of these HEU-cores were recalculated in order to assure that the used methods and models treat the special core and the core related components correctly. The calculated data had to be compared with a data set of good measurements of excess reactivity, shut down reactivity, neutron fluxes, power distribution etc. An example for the recalculation of a FRG-2 core is given in Fig. 2.

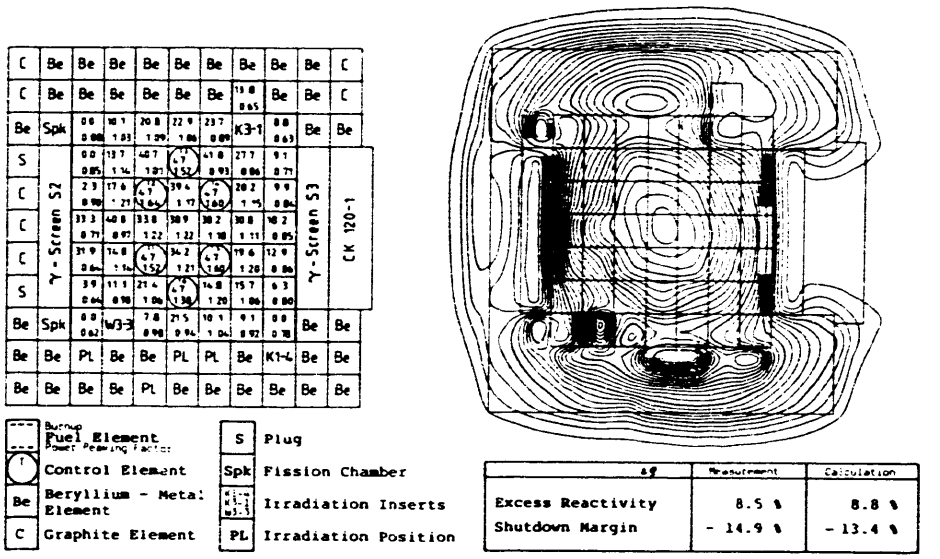

FIG. 2 STATUS OF THE HEU-REFERENCE CORE BY RECALCULATION (EXAMPLE FRG-2)

CHOICE OF LEU-FUEL ELEMENT

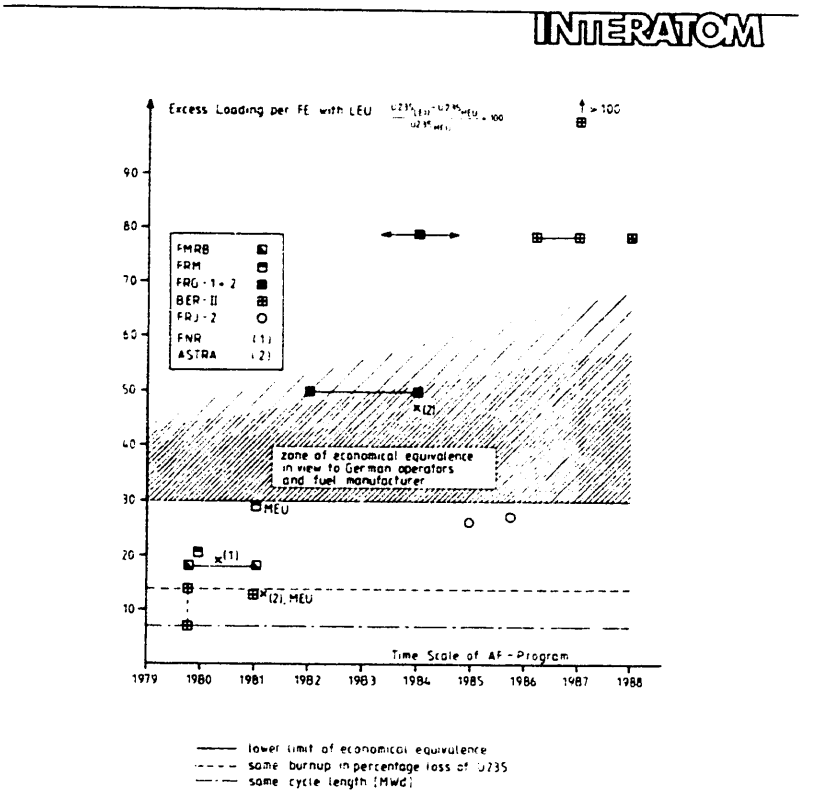

FIG. 3 U235-EXCESS LOADING DEVELOPMENT VS. TIME IN THE AF-PROGRAM

During the AF-Program for most of the reactors there was a development towards high or even extremely high U 235 loadings per LEU-fuel element in order to compensate for the high fabrication costs. This was possible as a consequence of the success in development and fabrication and the favourable irradiation results of U_3Si_2-fuel. The development of the U 235 loading with time for the German research reactors is demonstrated in Fig. 3.

A clear trend is displayed away from the two lower loading levels resulting from reactor physics. The trend leads to a zone with distinctly increased loading determined by economical considerations regarding fabrication and fuel cycle costs. Each of the three stations GKSS-Geesthacht (FRG-1, FRG-2), HMI-Berlin (BER-II), KFA-Jülich (FRJ-2) shows its own path of U 235 excess loading gradient. From the beginning GKSS has been on the highly economical path. HMI followed with a delay of time, in an intermediate stage even going to an extremely high U 235 loading but soon stepping back to the same U 235 loading as GKSS. The path of KFA is rather smooth and ends with a relatively moderate excess loading. For the residual German reactors no more conversion calculations had to be performed since 1981. Table 1 compiles characteristics of HEU- and MEU-elements used for calculations of HEU- or MEU-target cores.

Table 1: Compilation of LEU- and MEU-elements

LEU-Element						
FRJ-2	200	g/FE	3.1	g U/cm^3	meat	U_3Si_2
	180	g/FE	2.8	g U/cm^3	meat	U_3Si_2
	225	g/FE	3.5	g U/cm^3	meat	U_3Si_2
FRG-1/2	270	g/FE	3.1	g U/cm^3	meat	U_3O_8
	323	g/FE	3.7	g U/cm^3	meat	U_3Si_2
BER-II	206	g/FE	2.36	g U/cm^3	meat	U_3O_8
	204	g/FE	2.34	g U/cm^3	meat	U_3O_8
	402	g/FE	4.6	g U/cm^3	meat	U_3Si_2
	323	g/FE	3.7	g U/cm^3	meat	U_3Si_2
FRM	262	g/FE	3.0	g U/cm^3	meat	U_3O_8
FRMB	165.5	g/FE	1.85	g U/cm^3	meat	U Al_x
MEU-Element						
FRM	280	g/FE	1.41	g U/cm^3	meat	U Al_x

LEU TARGET CORES AND THEIR DEVELOPMENT

From the starting point of HEU-cores which had to be converted at the beginning of the AF-Program 1979 (upgrading of BER-II was not yet decided) there remained 5 cores for the complete calculational task of conversion:

- GKSS-Geesthacht FRG-1, FRG-2
- KFA-Jülich FRJ-2
- HMI-Berlin BER-II Standard Core, BER-II Compact Core

FRG-1 Conversion

The conversion of the FRG-1 is licensed. The LEU-Elements of 323 g U 235 have been fabricated and are ready for insertion. Fig. 4 shows a typical HEU-core and the LEU-Target core[1]. The number of fuel elements of the LEU-core is reduced to about 50 % of the HEU-core. The oval central absorbers will be replaced by fork type absorbers. A beryllium block reflector is designed for better neutron physics adjustment to the core of beam tubes and the new cold neutron source. All conversion calculations have been performed; the only exception is the investigation of the burnup of the absorbers.

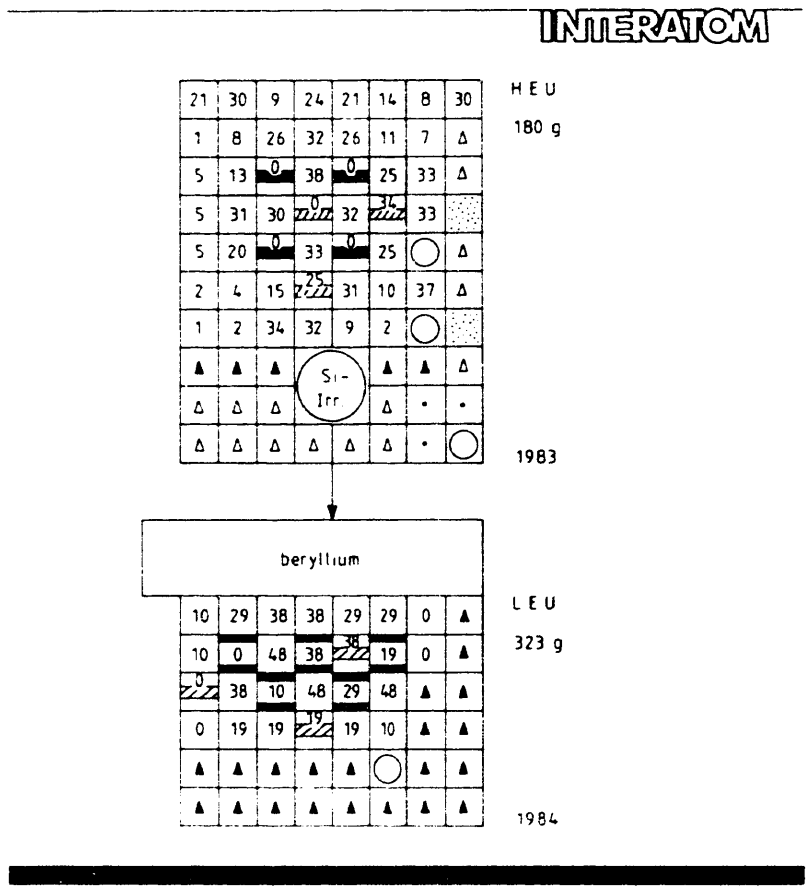

FIG. 4 FRG-1 - CONVERSION

FRG-2 Conversion

The fuel elements, control elements and absorbers for the FRG-2 (HEU) are the same as for the FRG-1 (HEU) and so it will be for the respective LEU cores. Thus the high flexibility of fuel management for both FRG-reactors will be maintained. The number of fuel elements of the FRG-2 LEU-core will be a little smaller and the reflector region contains three γ-screens and three irradiation inserts compensating the reactivity excess from the higher U 235 loading (cf. Fig. 5).

The LEU-license still depends on supplementary contributions by analysis.

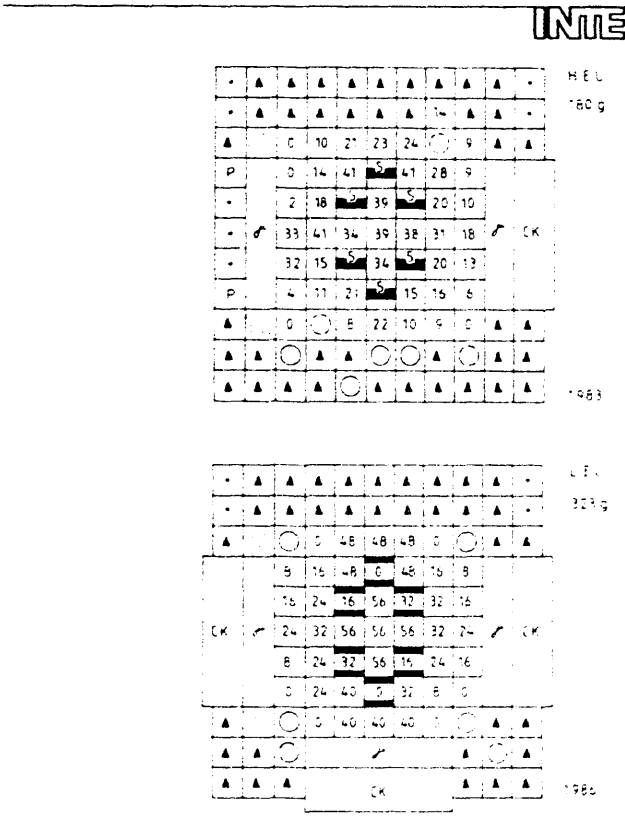

FIG. 5 FRG-2- CONVERSION

INTERATOM

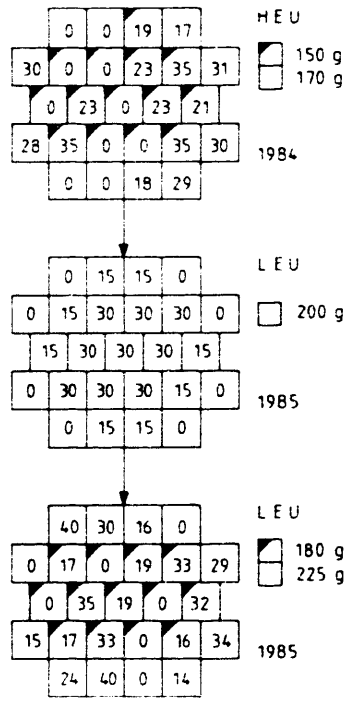

FIG. 6 FRJ-2: TWO ATTEMPTS TO CONVERT

KFA-Jülich did not intend to obtain major changes of the core and reflector configuration. Therefore the decision for a LEU-element could be straight forward. The HEU-core is set up of fuel elements with two different U 235 loadings. The attempt to convert the core to LEU-elements with only one U 235 loading failed[2] under the boundary condition that fuel element shuffling should not be necessary (equal to HEU). Consequently, LEU fuel elements with two different loadings (180 g, 225 g) were chosen for the conversion of FRJ-2 (Fig. 6). Concerning the status of the conversion calculations: Basic investigations are finished, investigations specific for licensing and for operation after conversion have been started.

BER-II Conversion

For BER-II three HEU-cores had to be investigated for conversion. In Fig. 7 the complicated conversion planning (including dead ends) for BER-II is demonstrated. Complication arose from the upgrading of the BER-II from 5 MW to 10 MW and from its reconstruction. 1980 the conversion of the 5 MW-core was investigated. After the decision of HMI for the upgrading to 10 MW and after the fixation of the corresponding HEU-core with a newly designed beryllium block reflector was established a LEU-core was determined using the conversion criterion of the same cycle length in percent U 235 burnup. This criterion led to a low U 235 loading of 204 g for the LEU-element. In the course of development of LEU-fuel it turned out that such a low U 235 loading will lead to a significant increase of the fuel cycle costs.

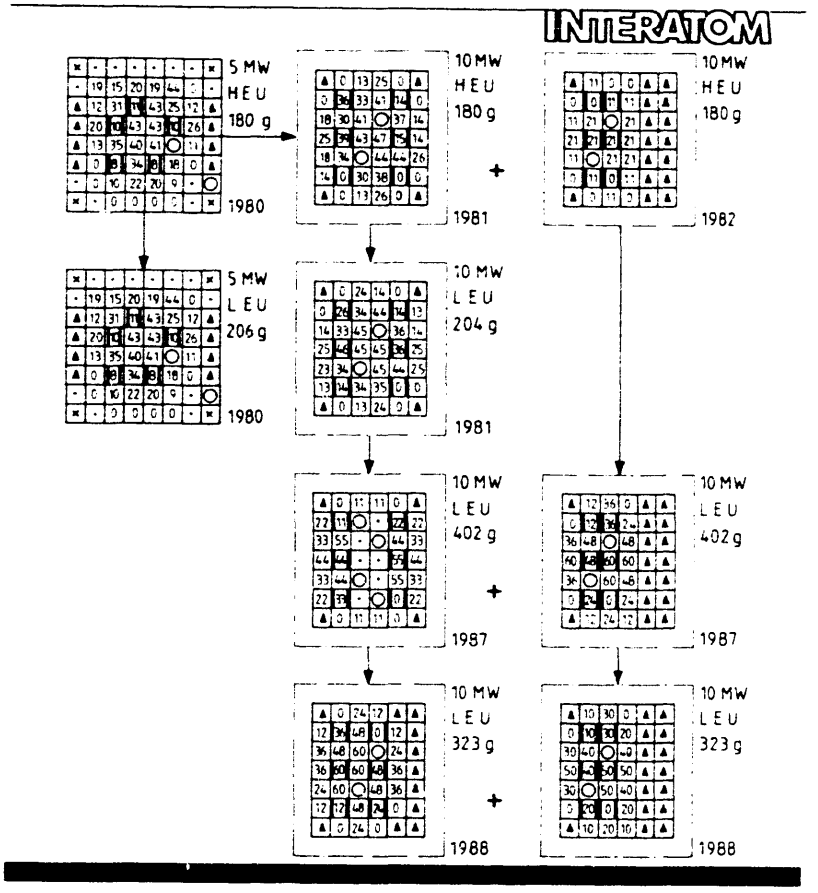

FIG.7 BER II - CONVERSION PLANNING INCL. DEAD ENDS

Additionally, 1982 an alternative HEU-core, the compact core, was designed with a reduced number of fuel elements to about 65 % of the reference (standard core). Both cores - standard core and compact core - shall be operated alternatively. Consequently both cores shall be converted to LEU-fuel. To compensate for the significant increase of fuel

fabrication costs HMI 1985 selected the fuel element with the same U 235 loading of 323 g as GKSS, but switched lateron 1987 even to a LEU-element with 402 g U 235 loading. The choice of the 402 g U 235 per fuel element led for the standard core to a ring core with 6 graphite reflector elements and four irradiation positions in the core centre in order to compensate for the high reactivity resulting from the high U 235 content. The choice of the 402 g fuel element was a pure economical solution. But it was really unfavourable from the physics point of view. There will be no use for four irradiation positions in the core centre in the future operation. On the other hand the graphite elements do not contribute to an increase of neutron flux in the reflector. They will be heated up to high temperatures. Consequently HMI stepped back to the 323 g-element. New references for standard core and compact core were designed.

For these reference cores with the 323 g-element the basic investigations, most of the licensing-specific and a part of operating-specific work are performed. An intermediate report dealing with all safety-related aspects of the conversion is transferred to the licensing authorities. This report proves that with the conversion of BER-II there are no major problems to be expected and no considerable backfitting measures necessary. The work at Interatom for the preparation of a final safety analysis report for the conversion is going on.

Concerning the work for the conversion of BER-II two facts were very time consuming:

- the upgrading and reconstruction of the reactor with the related licensing procedure for HEU-fuel.
- the significant increase of fuel cycle costs with respect to LEU-fuel which can only be compensated by a U 235 loading per element as high as possible.

CONCLUSIONS

Within the AF-Program five cores remained up to now for the conversion to LEU-fuel. For all cores the basic studies have been finished. For the GKSS (FRG-1/FRG-2) the licensing- and operating-specific studies have been worked out finally. For HMI (BER-II) the licensing-specific studies have been mostly performed, the operating-specific are still under way. Operating- and licensing-specific studies for KFA (FRJ-2) have been started recently since the FRJ-2 has still to run through the phase of demonstrating the qualification of the way of the LEU-fuel element manufacturing. The conversions will be performed with LEU-elements of relatively high uranium densities and U_3Si_2-Al fuel. The Conversion investigations for the German research reactors interacted with the work for the development, licensing and construction of a new reactor with LEU-fuel from its start-up (August 1987), the MPR 30 in Indonesia. A report on this subject we are pleased to leave to the experts of BATAN at a coming conference on research reactors.

REFERENCES

1. H.-J. Roegler
   Conversion Planning for the Two FRGs of the GKSS-Research Centre
   Proceedings of the International Meeting on Reduced Enrichment from Research and Test Reactors
   24 - 27 October 1983, Tokai, Japan, JAERI-M 84-073 (May 1984)

2. A. Strömich, Ch. Siebertz, M. Wickert
   The Conversion of the DIDO-Type Reactor FRJ-2 - Studies and Conclusions
   Reduced Enrichment for Research and Test Reactors
   Proceedings of an International Meeting, Petten 1985
   D. Reidel Publishing Dordrecht

ANALYTICAL, ENGINEERING AND LICENSING ASPECTS OF THE OSURR LEU CONVERSION/UPGRADE

T. Aldemir, J. W. Talnagi, D. W. Miller
The Ohio State University
Columbus, Ohio, U.S.A.

ABSTRACT

The efforts for the LEU conversion of the 10 kW Ohio State University Research Reactor (OSURR) with a simultaneous power upgrade to 500 kW have been underway since August 1985. The details of the analytical/experimental design studies have been reported at the previous RERTR meetings and elsewhere. These studies are summarized and put into perspective with regard to the conversion/upgrade objectives. The physical system changes and licensing process for the conversion/ upgrade are described.

INTRODUCTION

The Ohio State University Research Reactor (OSURR) is a 10 kW, natural-convection-cooled reactor using 14.0 g ^{235}U per 2.74 mm thick, flat-plate, HEU UAl-alloy MTR-type fuel elements. In August 1985, funding was obtained from the U.S. Department of Energy, with matching funds from The Ohio State University (OSU), for the LEU conversion of OSURR with a simultaneous power upgrade to 500 kW. The conversion/upgrade will take place with 1.27 mm thick U_3Si_2-Al "standardized"[1] plates which have a nominal loading of 12.5 g ^{235}U. Natural convection core cooling mode will be maintained in the power upgrade and a pool heat removal system (PHRS) will be installed.

The details of the analytical/experimental design studies for the conversion/upgrade of OSURR have been reported at previous RERTR meetings and elsewhere[2-10]. The objectives of this paper are: a) to summarize the previously reported studies and to put them into perspective with regard to the conversion/upgrade objectives, and b) to describe the physical system changes and licensing process for the conversion/upgrade.

ANALYTICAL/EXPERIMENTAL STUDIES

The change in fuel plate characteristics requires the determination of a new fuel geometry and core configuration for the conversion/upgrade of OSURR. Also, measures have to be taken to limit the pool top ^{16}N activity (PTNA) to allowable levels. The analytical/experimental studies consisted of both neutronic and thermal-hydraulic work towards the following design objectives[10]:

1. Allow sufficient excess reactivity to compensate for experiment worth (0.7% $\Delta k/k$), temperature and xenon feedback and other burnup effects while maintaining a minimum 1% $\Delta k/k$ cold, clean shutdown margin with the highest worth rod stuck out.

2. Allow a minimum 20% margin to onset of nucleate boiling (ONB) in the hot channel under steady-state operation.

3. Maximize the thermal neutron flux at the central irradiation facility (CIF) and the beam tube positions.

4. Minimize the PTNA.

5. Maximize the water temperature at the inlet to the primary side of the PHRS to enhance heat exchanger efficiency.

The LEU fuel element geometry was fixed as 16 and 10 standardized plates per standard and control element, respectively. Each standard and control element also contains two unfueled plates. The function of the unfueled plates in the standard fuel elements is to reduce core loading without a substantial reduction in core size and increase in coolant channel thickness (which reduces the ONB margin under natural convection). The unfuelled plates in the control elements serve as guides for the control rods.

Neutronic Studies

The first phase of the neutronic studies involved benchmarking the computational core model for the existing HEU fueled core by comparing the predicted results for excess reactivity, control rod worths, and flux distribution against measured values. The core was modeled as having 13 and 16 material zones for the 2- and 3-D diffusion calculations, respectively, using 2DB[11] with a 67 X 72 mesh, and UMDIF (University of Michigan 3-D version of 2DB) with a 67 X 72 X 39 mesh. The 4-group diffusion parameters for each material zone (except the control rods) were determined by the LEOPARD[12] code. Effective absorption cross sections for the control rods were found by matching the absorption rates predicted by Monte-Carlo and diffusion calculations on a supercell containing the control rod[13]. The Monte-Carlo calculations were performed by the Argonne National Laboratory (ANL) RERTR Program using VIM[14]. Comparison of the computed and experimentally determined data showed excellent agreement[3], with 0.18% $\Delta k/k$ difference in excess reactivity and a maximum difference of 0.25% $\Delta k/k$ in individual safety rod worth.

Next, 15 LEU core configurations were analyzed[5] to determine the configuration which satisfies the design objectives #1 #3. One 17 and two 18 standard fuel element cores, with excess reactivities, radial peaking factors and thermal neutron flux levels at the CIF/beam tube positions in the ranges 1.57-1.91% $\Delta k/k$, 1.36-1.41, and 1.40-1.44 X 10^{13}/7.2 8.0 X 10^{12} neutrons/cm^2/second, respectively, were identified as possible options[3]. Comparison of the diffusion calculation results for excess reactivities and rod worths for the 17 element and one of the 18 element LEU cores to the results of full core Monte-Carlo simulations (performed by ANL RERTR

Program) again showed excellent agreement. Transient analyses using PARET[15] indicate that these possible LEU cores can accomodate step reactivity insertions of up to $1.00 with a minimum burnout ratio of 4.02 (burnout heat flux/maximum heat flux the during transient), assuming no scram occurs. Due to the similarity of the predicted core characteristics and in view of fuel fabrication tolerances, it was not found to be physically meaningful to choose one of these options as the optimal configuration with regard to design objective #3.

Thermal-Hydraulic Studies

The thermal-hydraulic studies involved both computational and experimental work. The 3-D steady-state velocity and temperature distributions in the OSURR pool were simulated using the COMMIX-1A code[16], considering various arrangements to meet the design objectives #1 and #5. The flow domain was modeled partly as continuum and partly as porous medium, using 10496 computational cells and 3360 surface elements[4,7]. All the major pool components were explicitly described in the simulations and three different flow models were used to assess the effects of local turbulence on global pool dynamics. The simulations showed that a sufficiently deep stagnant water layer could be created below the pool surface by the conventional measure for limiting PTNA in natural-convection-cooled research reactors (i.e. plume dispersion by a flat water jet directed across the top of the core, with the PHRS inlet away from the core) to yield an estimated ^{16}N dose rate of <1 mrem/hr at the pool surface[8]. However, the simulations also showed that this conventional measure is infeasible in view of objective #5. A better option was found to be to contain the core outflow in a shroud (an 75 cm tall open box) and to place the PHRS inlet within the shroud at the core outlet. There is no appreciable change in the PTNA compared to the conventional measure, but the coolant temperature at the PHRS inlet increases from 25°C to 38°C.

Experimental studies were undertaken to investigate the validity of the currently used correlations for predicting the ONB heat flux in plate-type fuel element channels[17] under low velocity, upward flow conditions, and thereby to reduce the uncertainty in the determination of the ONB margin towards objective #2. Channel surface roughness, height (~65 cm), width (~7 cm), and heat source distribution along the channel (truncated cosine) for the experiments simulated expected operating conditions[4,6]. The results for 2 to 4 mm thick channels and upward flow velocities in the range of 2 to 15 cm/second showed that the currently used correlations can over- or underestimate the ONB heat flux by as much as a factor of 10. A new correlation was obtained which predicts the experimental results within 13% and which is valid in the local pressure range of 1.40 to 1.46 atmospheres[9]. The ONB margins for the possible OSURR LEU core configurations were found to be in the range of 50 to 60 percent.

PHYSICAL SYSTEM MODIFICATIONS

Changes to the reactor system are required for both the fuel conversion and power upgrade. The LEU elements were specified to be identical to the

existing HEU elements in regard to their outer dimensions and structural material makeup (6061 Al) to minimize variation in physical characteristics. The LEU elements will also have end boxes and side plates identical to those of the current HEU elements. Flat-plate fuel geometry will be maintained and the fuel plates will be swaged to the side plates as it is done with the existing HEU elements. Other mechanical joining will be done with welds. The control elements will be fabricated to accommodate the existing OSURR control rods, with a nearly identical gap for the control rod movement compared to that of the HEU elements (for similar control rod stroke and drop time characteristics).

Since the possible LEU core configurations all require a reduction in core size (resulting from the higher fuel loading of the LEU elements), several grid plate positions will be vacant. In addition, all of the current graphite isotope irradiation elements will have be removed to meet the design objective #1. Thus, up to 8 grid plate positions may be unoccupied. The vacant grid plate positions will be plugged with aluminum boxes having outer dimensions identical to fuel elements. These plugs will prevent excessive bypass coolant flow and improve the thermal-hydraulic core performance.

Several options were examined for the PHRS and the PHRS was designed using the following criteria:

1. The PHRS must not significantly perturb the natural convection flow through in the core (i.e. lead to upward forced convection).

2. The PHRS must be capable of removing the full core heat load under a variety of environmental conditions.

3. The PHRS design should be kept as simple as possible for reliable operation.

4. The instrumentation for the PHRS operation and monitoring must interface with the reactor safety system.

5. The PHRS cost should be minimized while satisfying criteria #2-#4.

Criterion #1 is motivated by procedural considerations rather than technical. Although upward forced convection cooling (such as used in Canadian MAPLE systems) improves the ONB margin, its implementation necessitaties a new construction license for the upgrade of OSURR. However, the power upgrade is regarded as a license amendment if the current core cooling mode is maintained.

Consideration of criterion #5 above resulted in early elimination of the somewhat traditional research reactor cooling system components of a wet cooling tower and a tube-and-shell heat exchanger. Instead, a dry cooling system with a forced-draft 8-fan unit (drycooler) and two plate-and-frame heat exchangers (one using a mixture of ethylene-glycol as the working fluid and the other water) was designed. These heat exchangers provide relatively large heat transfer surface in a compact package, enhance simplicity and reduce total system cost. The ethylene-glycol mixture allows operation of the system under low outdoor temperatures.

Figure 1 shows a simplified schematic diagram of the PHRS. The drycooler is sized so that the entire 500 kW heat load can be rejected to the atmosphere if the air temperature is 23°C and the entire available volume of secondary fluid flows through the drycooler. If the air temperature is lower than 23°C, the bypass leg in the secondary loop can be used for reducing the excess heat removal capacity while still maintaining a constant total volumetric flow rate. The heat removal capacity can be also adjusted by varying the number of fans operated at a time (4 or 8). In addition, the secondary loop pump has adjustable capacity to allow a range of flow rates during initial setup and shakedown of the system. When the outdoor air temperature exceeds 23°C, the auxiliary heat exchanger provides additional cooling capacity to remove 500 kW. The auxiliary heat exchanger uses city water as its heat sink. The primary loop pump has constant capacity, but the flow rate through the loop can be adjusted by a modulating valve for different power levels in view of criterion #1.

The primary coolant is drawn from the top of the core through a plenum containing a manifold which has numerous suction points to allow relatively uniform withdrawal of heated water at the core outlet. Above the suction manifold is the shroud, which contains the heated water rising from the top of the core and limits bypass flow of cooler pool water into the PHRS. The primary coolant is first directed through a decay tank located within the reactor pool. The decay tank provides a delay time of about 70 to 80 seconds for the primary coolant and removes almost all ^{16}N via radioactive decay. The decay tank is insulated to reduce heat loss from the primary coolant to the cooler reactor pool and thus decrease in heat exchanger efficiency. The system configuration avoids expensive and cumbersome shielding of the primary system piping, heat exchanger and the decay tank itself. The cooled primary water is returned to the reactor pool at a point above the core, through a disperser nozzle. The disperser creates a downward-directed jet of water to prevent the core outlet water which may leak outside the shroud from reaching the pool top. The nozzle is located and directed so that outward flow from the nozzle does not affect the natural convective coolant flow through the core.

Criterion #4 above requires the addition of several reactor trip functions and alarm readouts related to operation of the PHRS. The reactor will trip on: a) low pool water (<610 cm from the bottom of the pool), b) high core inlet temperature (>35°C) and c) loss of flow in the primary or secondary coolant loops if the reactor power is above 120 kW. The last trip function assures that the PTNA is limited to operationally tolerable levels and cooling capacity is available for heat removal from the pool. Warning alarms are activated on changes in: a) flow rates in the primary and secondary loops, b) temperatures at various locations around the PHRS, c) pressure drops across certain system components (e.g., heat exchangers), d) outdoor air temperature, and e) the status of pumps and fans (i.e. on/off).

Other instrumentation modifications required for the power upgrade include: a) extending the range of the startup power range monitoring (SPRMC) channel, b) installing a more sensitive, digital electrometer in the linear power monitoring channel (LPMC), c) installing of a second gaseous effluent monitor to measure ^{41}Ar concentration in the exhaust stream of the pneumatic transfer system (rabbit) and d) adding one or more area radiation monitor (ARM) channels to the existing ARM system. The range of the SPRMC

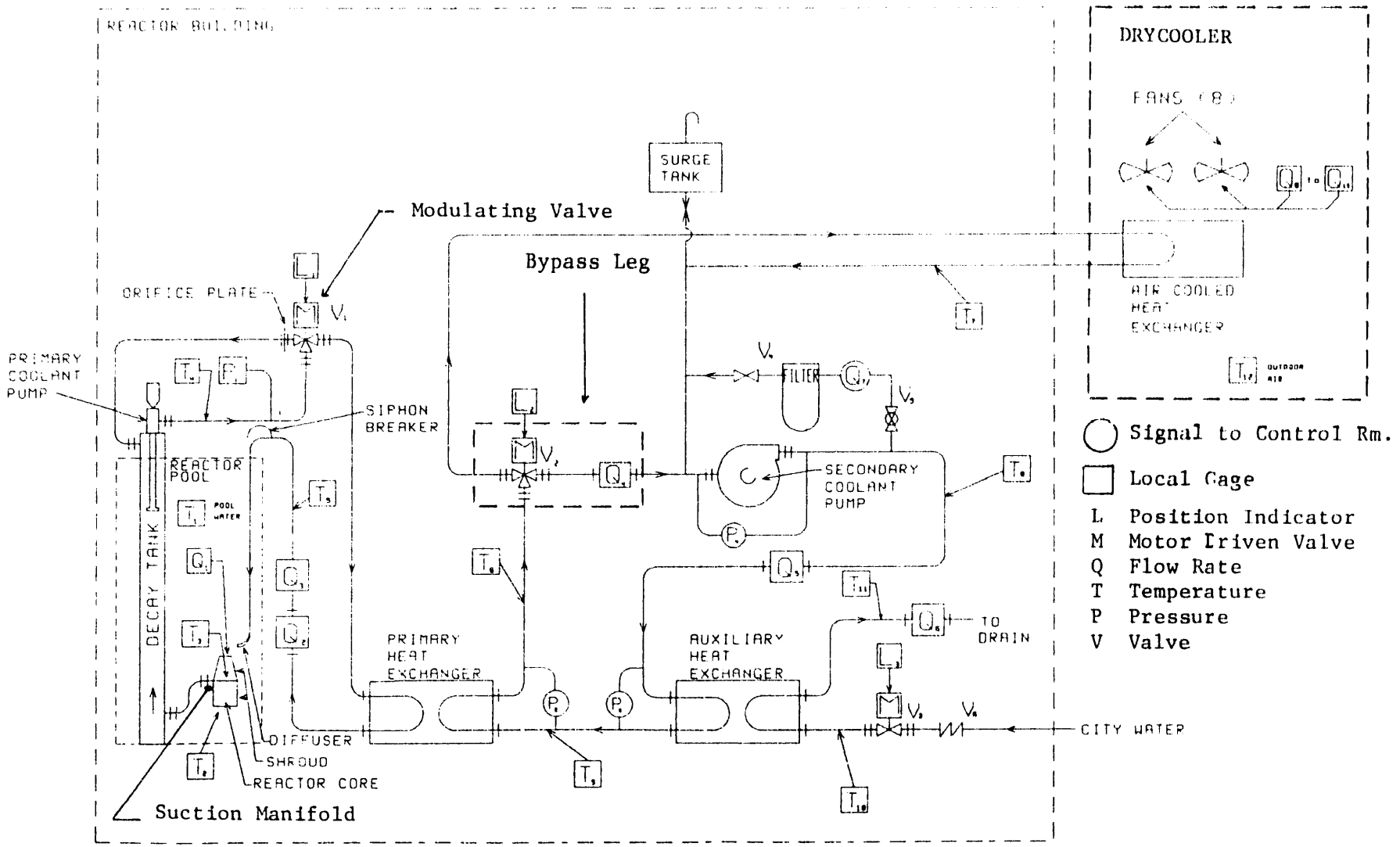

Fig.1 Simplified Schematic Diagram of the OSURR Pool Heat Removal System

can be extended by simply providing for a longer stroke in the movement of the neutron sensor (fission ion chamber) away from the core during power ascension. The LPMC neutron sensor (compensated ion chamber) has adequate response characteristics to provide meaningful information on reactor power over the anticipated range, but the existing tube-based electrometer has insufficient resolution to display the sensor signal over this range. A solid-state digital electrometer has been installed to improve the display resolution. The rabbit exhaust effluent monitor consists of: a) a shielded sample volume, b) a high-sensitivity beta scintillator, c) an air pump or blower to pass exhaust stream effluent through the sample volume at a known volumetric flow rate, d) a programmable digital ratemeter with various warning and alarm setpoints (located in the control room), and e) a stripchart recorder. Each added ARM channel will utilize a G-M radiation detector of appropriate sensitivity, a digital ratemeter similar to that used in the rabbit exhaust effluent monitor and an analog ratemeter display at the sensor location with various warning and alarm annunciators and indicators.

Uncertainties in delivery of the LEU fuel, as well as possible delays in the U.S. Nuclear Regulatory Commission (NRC) approval to use the LEU fuel, make shipment of HEU fuel prior to receipt of LEU fuel an unattractive option. Severe economic penalty can result from an extended facility shutdown. The current conversion/upgrade schedule calls for: a) receipt and interim storage of the LEU fuel, b) unloading and interim storage of the HEU fuel from the reactor core, c) installation of the LEU core, and, d) startup and testing of the LEU fueled OSURR. This approach also allows the HEU fuel elements to undergo their required decay prior to shipment while the LEU core is being loaded and tested, further reducing facility outage. Although the OSURR has a fuel storage pit recessed into the floor of the pool, it was decided to keep this pit available for the LEU fuel prior to loading into the core and an additional storage rack was designed. Built from aluminum, the storage rack will hold 16 fuel elements in a 2 X 8 array, with a nominal element pitch of 15 cm, and will be placed in the bulk shielding facility (BSF) pool adjacent to the OSURR pool. A criticality analysis of the storage rack indicates that it will have an infinite multiplication factor of less than 1.0 when fully loaded with standard OSURR HEU fuel elements. A fuel transfer cask has been built from carbon steel and lead to allow shielded transfer of the HEU fuel elements one at a time from the reactor pool to the BSF pool.

LICENSING PROCESS

Operation of the OSURR with LEU fuel at an increased power level requires the approval of the revised technical specifications (TS) and the safety analysis report (SAR) which describe the modified reactor system and changes in operational characteristics. Early in the conversion/upgrade effort, the NRC decided that the order for conversion would include the reactor modifications related only to the fuel change, while any other changes would be dealt with through the usual license amendment process. The OSU has prepared a unified SAR which addresses the modifications brought about both by the fuel change and the power upgrade. A preface to the SAR identifies the sections dealing with the following items:

- Changes related only to fuel conversion (e.g. k_{eff}, rod worth).
- Changes related only to power upgrade (e.g. effluent production rate, dose rates).
- Changes related to both fuel conversion and upgrade (e.g. changes in channel thermal-hydraulics, plate temperature distributions, transient core performance).
- Updates and changes which are not related to either fuel conversion or power upgrade (e.g. demographics, instrumentation upgrades completed since the last license renewal and reformatting of TS to meet the guidelines of ANSI/ANS 15.1-1982).

The TS were also revised to reflect operation of the OSURR at an increased power level, but the sections related to power upgrade were prefaced with the notation "This section not applicable for 10 kW operation". This approach to the licensing process allows the NRC the flexibility to issue a fuel conversion order based on those sections of the SAR which deal only with changes related to the fuel conversion while addressing the other aspects through the normal license amendment process. It also allows the OSU to perform the analytical efforts as a single task and to generate and submit a single set of documents describing all changes, avoiding duplication of effort.

CONCLUSION, STATUS AND FUTURE PLANS

The analytical/experimental studies performed to date have identified three LEU cores and a system configuration which allow operating the OSURR at a steady-state power level of up to 500 kW. These studies have also provided:

- a quantitative understanding of natural-convection-cooled research reactor pool dynamics with plume dispersion, resolving the difference in opinion regarding the feasibility of power upgrades while maintaining the core cooling mode,[18]
- a new technique for simultaneously minimizing the PTNA and maximizing the coolant temperature at the primary cooling loop suction point, thereby maximizing heat exchanger efficiency and reducing cooling system costs, and
- an improved correlation for predicting the ONB heat flux in plate-type natural-convection-cooled research reactors.

Based on results of the analytical/experimental studies and system design efforts, the revised TS, together with the supporting SAR, were submitted to the NRC for approval in October 1987. The SAR also includes the results of calculations performed to assess the possible radiological consequences of controlled and uncontrolled releases. An initial set of questions concerning those aspects of the license modifications related only to fuel conversion has been received and answered. Action by NRC on the OSU

response is expected shortly. Additional questions and comments concerning issues related to the power change have been also received. These questions and comments are being studied at the present time. Formal responses are planned to be submitted to NRC in the next few months. Procurement of equipment and materials needed for the fuel change and power upgrade is proceeding. Some equipment has been installed, with utilization pending licensing action. Until definite action is taken on the pending license changes, operation of the OSURR will continue with the existing systems.

Initially, it was expected that LEU fuel could be loaded into the OSURR during the Summer of 1988. This schedule would have minimized the impact of a facility outage on reactor users, since courses utilizing the reactor were rescheduled for the Spring quarter. However, delays resulting from the extended negotiation of the fuel fabrication contract have led to postponment of the plans. Optimistically, fuel loading could begin sometime in late Fall 1988. Otherwise, the next available time is Summer of 1989. Because of heavy facility utilization Winter and Spring, a facility outage during these times is undesirable. Once again, courses normally scheduled to use the reactor during the Summer of 1989 will have to be shifted to Spring. Upon the receipt of the NRC approval for fuel and/or power change, a startup plan will be developed to outline those steps to be taken to accomplish the specified change. The conversion/upgrade of OSURR is expected to be completed in December of 1989.

ACKNOWLEDGEMENT

The authors would like to acknowledge Dr. J. E. Matos (ANL) and the RERTR Program staff for their cooperation since the inception of the OSURR conversion/upgrade project and for their contribution to neutronic studies. The contribution of the OSU Nuclear Engineering Program students (M. Belhadj, J.-J. Ha, M. D. Seshadri, H. S. Aybar) and faculty (Drs. R. N. Christensen and D. Richards) is recognised through the cited references. In addition, the authors would like to thank Dr. M. Caner (SOREQ, Israel) for installing LEOPARD, 2DB and UMDIF on the OSU computer system, A. P. Clark (Assurance Technical Services) for his assistance in cooling system specification and design, and R. D. Myser (OSURR) for his assistance in drafting the revised technical specifications. The study was partly supported by the U.S. Department of Energy Grant No. DE-FG02-85ER75201.A000.

REFERENCES

1. H. H. Young, K. R. Brown, J. E. Matos, "Conversion and Standardization of University Reactor Fuels Using Low-Enriched Uranium - Plans and Schedules", ANL/RERTR/TM-9, 31-41, Argonne National Laboratory (1988).

2. M. Caner, T. Aldemir, "Preliminary Neutronics Calculations For the OSURR LEU Conversion/Upgrade Program", *Reduced Enrichment For Research and Test Reactors*, D. Reidel Publishing Co., 273-285 (1986)

3. M. D. Seshadri, H. S. Aybar, T. Aldemir, "Neutronic Design of An LEU

Core for The Ohio State University Research Reactor", to appear in the Proceedings of the 1987 International RERTR Meeting, Buenos Aires, Argentina (Sept. 28-Oct. 2, 1987).

4. J.J. Ha, M. Belhadj, T. Aldemir, R.N. Christensen,"Feasibility of Maintaining Natural Convection Mode Core Cooling in Research Reactor Power Upgrades", to appear in the Proceedings of the 1987 International RERTR Meeting, Buenos Aires, Argentina (Sept. 28-Oct. 2, 1987)

5. M. D. Seshadri, T. Aldemir, "Neutronic Scoping Calculations for OSURR Core Design With Standardized U_3Si_2 Fuel Plates", ANL/RERTR/TM-9, 410-421, Argonne National Laboratory (1988).

6. M. Belhadj, R.N. Christensen, T. Aldemir, " Experimental Investigation of Onset of Nuclear Boiling in Thin, Rectangular Channels", Proceedings of the 1986 International RERTR Meeting, ANL/RERTR/TM-9, 461-472, Argonne National Laboratory (1988)

7. J.J. Ha, T. Aldemir, "Thermal-Hydraulic Analysis of the OSURR Pool for Power Upgrade With Natural Convection Core Cooling", Proceedings of the 1986 International RERTR Meeting, ANL/RERTR/TM-9, 473-487, Argonne National Laboratory (1988)

8. J.-J. Ha, T. Aldemir, "Pool Dynamics of Natural Convection-Cooled Research Reactors", *Nucl. Technol., 79*, 297-310 (1987).

9. M. Belhadj, T. Aldemir, R. N. Christensen, "Onset of Nucleate Boiling in Thin, Rectangular Channels Under Low-Velocity, Upward-Flow Conditions", *Nucl. Technol. 82*, 330-340 (1988).

10. T. Aldemir, "Neutronic/Thermal-Hydraulic Studies for the LEU Conversion/Upgrade of OSURR", *Trans. Am. Nucl. Soc. 56*, 572-573 (1988).

11. W. W. Little, Jr., R. W. Hardie, "2DB User's Manual - Revision 1", BNWL-831, REV1 (1969).

12. R. F. Barry, "LEOPARD - A Spectrum-Dependent Non-Spatial Depletion Code for the IBM-7094", WCAP-3269-26 (1963).

13. M. M. Bretscher, "Blackness Coefficients, Effective Diffusion Parameters, and Control Rod Worths for Thermal Reactors", ANL/RERTR/TM-5, Argonne National Laboratory (1984).

14. E. M. Gelbard, R. E. Prael, "Monte Carlo Work at the Argonne National Laboratory", ANL-75-2, p. 201, Argonne National Laboratory (1975).

15. W. L. Woodruff, "A Kinetics and Thermal-Hydraulics Capability for the Analysis of Research Reactors", *Nucl. Technol, 64*, 196-206 (1984).

16. H. M. Domanus, R. C. Schmitt, W. T. Sha, V. L. Shah, "COMMIX-1A: A Three-Dimensional Transient Single-Phase Computer Program For Thermal-Hydraulic Analysis of Single and Multicomponent Systems, Volume I: User's Manual", NUREG/CR-2896 Vol. I (1983).

17. "Research Reactor Core Conversion from the Use of Highly Enriched Uranium to the Use of Low Enriched Uranium Fuels - Guidebook", IAEA-TECDOC-233, 96, 368, International Atomic Energy Agency, Vienna, Austria (1980).

18. F. Merchie (CEN/Grenoble-France), H. Winkler (EIR-Switzerland), A. F. DiMeglio (RINSC-USA), Private Communication (Nov. 5, 1986).

STATUS OF THE UNIVERSITY OF VIRGINIA REACTOR CONVERSION TO LEU FUEL

R.A. Rydin, M. Fehr, S. Wasserman, D. Freeman and B. Hosticka
Dept. of Nuclear Engineering and Engineering Physics
University of Virginia
Charlottesville, Virginia, USA

ABSTRACT

The University of Virginia is preparing to convert the 2MWT UVAR reactor from 18-curved plates/element high-enriched fuel to comparable flat plate low-enriched fuel. Scoping studies have taken into account the unique features of the UVAR: its flexibility to use various size core arrangements, different reflectors, and a variety of external experiments. Benchmarking studies against a previously measured core confirmed our ability to calculate criticality, control rod worths, and temperature coefficients. Depletion studies of low enriched cores suggest that the use of 22 plates/element in a 4-by-5 array will give a considerably longer core life and a generally higher thermal flux than direct replacement with 18 plates/element. Thermal hydraulic calculations indicate that these cores are acceptable with only small changes in safety system settings.

DESCRIPTION OF THE UVAR FACILITY

The UVAR is a 2 MWT swimming pool-type research reactor. It is made up of plate-type MTR fuel elements mounted on an 8-by-8 grid plate that is suspended from a movable bridge above a large open pool of water. The reactor can be moved to either end of the pool while the other pool half is drained for maintenance purposes. But only when the core is mounted on the South end, directly above a coolant funnel that provides forced down-flow circulation, can it be operated at full power. This position is shown in Figure 1, which also shows the location of the experimental beam ports.

The original UVAR design was done by J.L. Meem [1], circa 1960, using analytical two-group theory. The Technical Specifications (TS) require maintenance of a minimum shut-down margin of 0.4% $\Delta k/k$ with the largest worth shim rod fully withdrawn. Any core arrangement that will fit on the grid plate, and that meets this TS, can be used, providing that the control rods are experimentally recelebrated each time a new core arrangement, which was not previously tried, is assembled. The UVAR has been operated for more than twenty years using experimental techniques, essentially without benefit of computational modeling. During this time, both 12-flat-plate fuel elements and 18-curved-plate fuel elements have been used in separate cores, and arrangements having anywhere from 16 to 27 fuel elements have been operated. Some cores have been entirely water reflected, others graphite reflected, while cores in the EPRI sponsored studies of radiation damage to pressure vessel steels have had water on some sides and graphite on the others. Some such arrangements are shown in Figures 2-4.

It is not really to our advantage to allow the UVAR core size to become as large as 27 elements, because the thermal flux available for experiments is correspondingly reduced. We believe that a more practical future strategy would be to try to operate with a core arrangement that is essentially fixed in a 4-by-5 array, with the shim rods placed close to the core center, as illustrated in Figure 5, to provide a high shutdown margin. We also believe that a planned fuel shuffling pattern should be used in place of our current ad hoc procedure of trying to obtain equal burnup for each element in inventory.

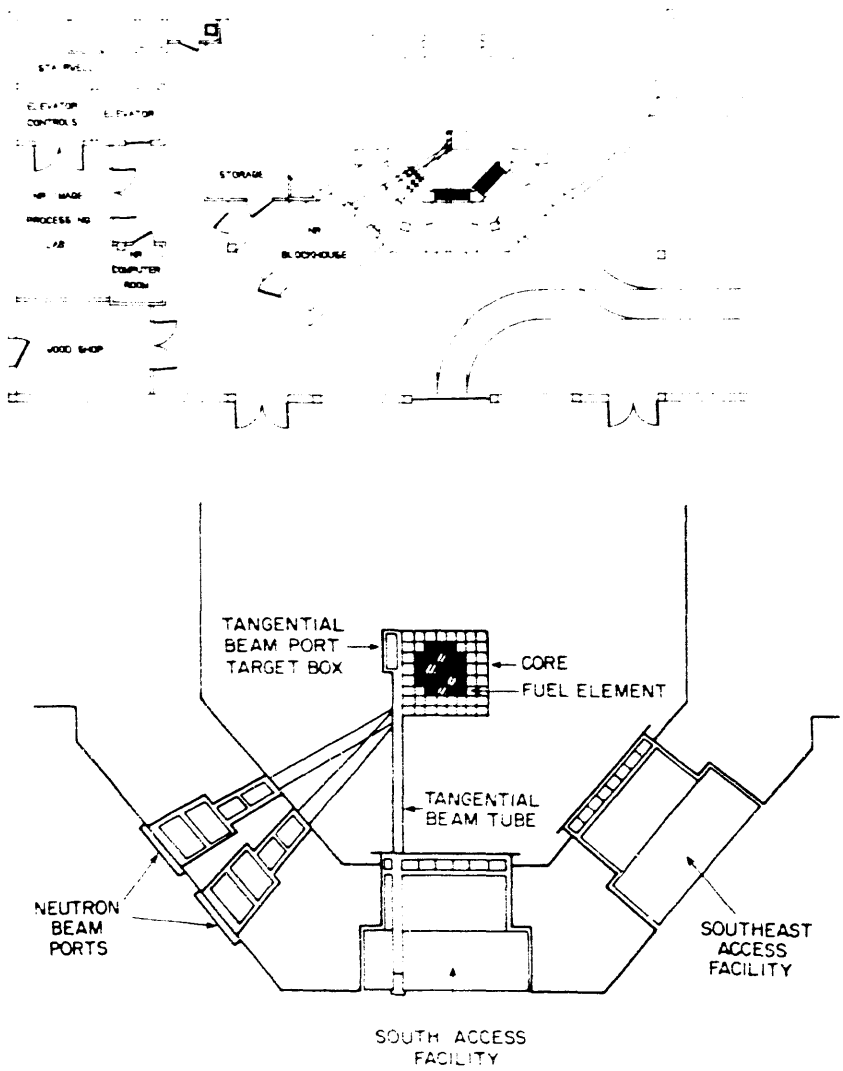

Figure 1. Sketch of UVAR Pool Showing 8-by-8 Grid Plate

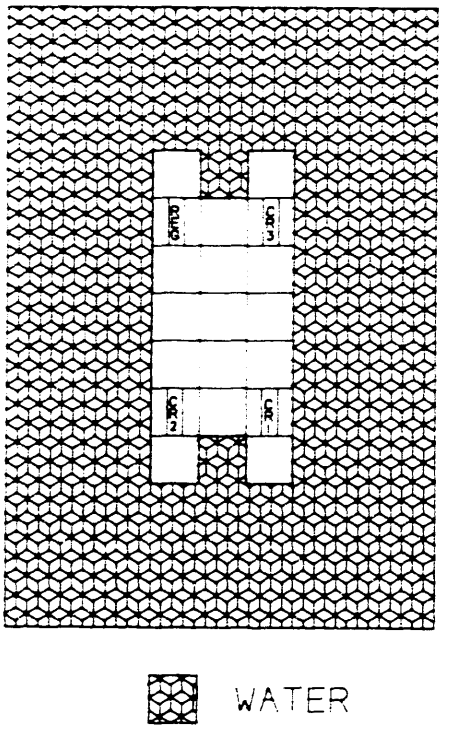

Figure 2. Long Core Experiment

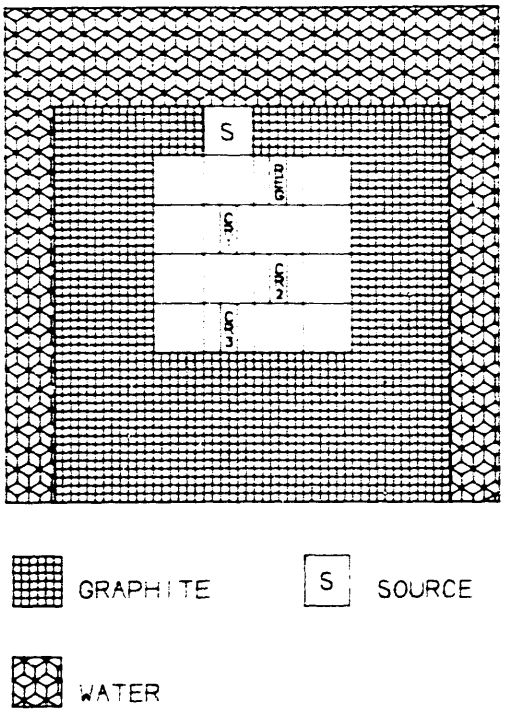

Figure 3. 1975 Texas A&M Core

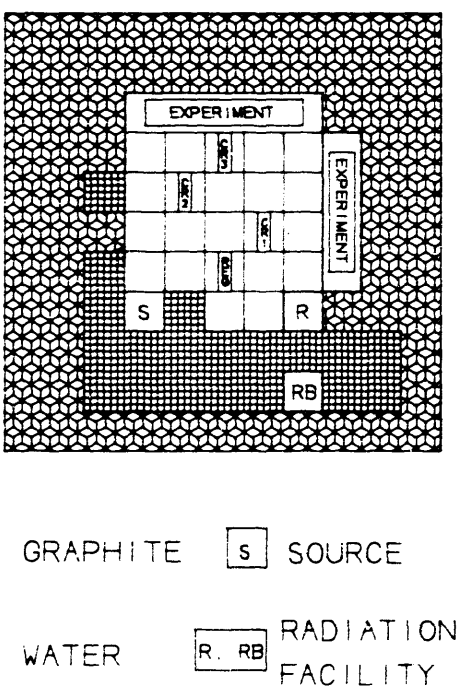

Figure 4. Sample Core from EPRI Experiments

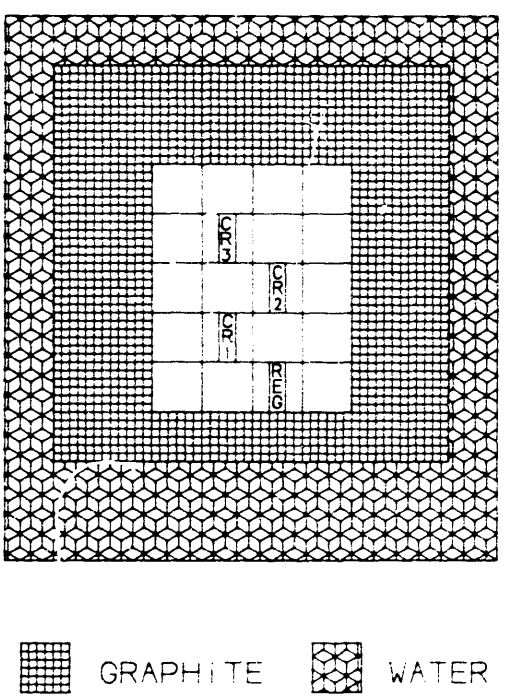

Figure 5. Ideal LEU UVAR Core Configuration

BENCHMARK CALCULATIONS

The most recently measured UVAR-core configuration that met the conditions of being clean, unburned, and fully documented, was an initial 1975 loading of 18-plate Texas A&M fuel elements. This arrangement, shown in Figure 3, was a 4-by-4 element array, asymmetrically surrounded by graphite. Almost all other recent UVAR core arrangements have contained fuel elements having only an approximately known individual burnup history, making them unsuitable for benchmark purposes.

Available data for the Texas A&M core included measured individual control rod worth curves, an implied measured excess reactivity worth with all control rods withdrawn from the critical position, an approximate temperature defect worth obtained from single warm-up and cool-down swings, and an implied measured equilibrium xenon worth. Since the control rod worth curves are measured by repositioning any three control rods at equal depth to incrementally measure the fourth, some control rod interaction effects are built into the measurements. Integral rod worths may still be accurately determined in this manner, but the differential rod worth curves are probably somewhat tilted to the bottom of the core causing measurements, based upon subtraction from the critical position, to be somewhat in error.

Effective Control Rod Cross Sections

Control rods are strongly absorbing bodies having relatively small planar dimensions. They must be treated using transport theory, which must also take into account thermal spectrum hardening. We have developed effective diffusion theory cross sections in two groups, for both the boron steel shim rods and the stainless steel regulating rod, by applying the following procedure.

A transport theory model of a control rod surrounded by fuel material was made in slab geometry using the THERMOS thermalization code. Thermal group absorption fractions in both the fuel and absorber regions were obtained from this model. Fast group absorption fractions for the same regions were then obtained using the GAMTEC slowing down and thermalization code in cylindrical geometry; the GAMTEC thermal group result was cross checked against THERMOS. A cell model was then made using the 2D diffusion theory code EXTERMINATOR, and the fast group and thermal group absorption cross sections were iteratively varied until both the thermal and fast group absorption fractions matched those from THERMOS and GAMTEC. Finally, these effective cross sections were used with the same mesh spacings in the 2DBUM diffusion theory code for our reactor design studies.

Control Rod Worths

The procedure for obtaining effective control rod cross sections was applied separately to both HEU and LEU models. Within the uncertainties of the iterative process, the results were essentially the same for both. When these values were used in 2DBUM models of the 4-by-4 Texas A&M core (called HEU-18) the results shown in Table 1 were obtained.

Table 1. Control Rod Worths for the 4-by-4 Texas A&M Core and Replacements

Case	Rod 1* $	Rod 2* $	Rod 3* $	Rod 4* $
HEU-18 Expt. ($gm^{235}U$/elem	4.75	5.00	3.06	0.57
HEU-18 (192gm)	4.75	4.89	2.79	0.71
LEU-18 (225gm)	4.73	4.87	2.84	0.75
LEU-22 (275gm)	4.79	4.92	2.96	0.83

*Experimental and Computational Uncertainties are ±5%

The integral rod worths for all three shim rods were predicted within the experimental accuracy of the measurements, while the regulating rod was predicted slightly high. Experimental uncertainties of ±5% are attributed to inaccuracies in period measurements and to uncertainties in the precise value of beta-effective, which was taken to be $\beta_{eff} = 0.008$.

Calculations were also made for LEU replacement cores having 18 plates/element (LEU-18) and 22 plates/element (LEU-22). The predicted control rod worths are also given in Table _, where it is seen that they do not differ markedly from the HEU-18 results.

When the critical control rod positions for a core are entered into the experimentally measured integral control rod worth curves, the excess reactivity available for removing the rods entirely is determined. The sum of these values for the Texas A&M core experiment is reported in Table 2. The value of k_{eff} that is obtained from the corresponding 2DBUM model of the same core, using axial B^2 values obtained from an ANL 3D model, is approximately 0.02 higher. The ANL B^2 value is consistent with the B^2 determined by Meem [1], and with that determined from an RZ model of the core.

Table 2. Beginning-of-Life Unrodded k_{eff} for Texas A&M UVAR Core

CONDITION	K_{EFF}
EXPERIMENTAL,* HEU-18	1.036 ± 0.005
2DB CALC, δ = 7.8 CM, B^2 = .0017	1.062

* Implied From Control Rod Worth Curves

The difference between the calculated and experimental values is probably caused by the use of a 2D model to represent a 3D situation. The experimentally determined total control rod worths agree well with the calculated values, but the experimental sigmoid-shaped integral worth curves are probably tilted towards the bottom of the core due to the method used to determine them. The effect of such a tilt is an implied low experimental result for an unrodded core, in agreement with observation. We plan to analyze the experiment using a partially-rodded 3D model to try to resolve this discrepancy.

Feedback Effects

Experimental values are also available for the Texas A&M core for the worth of equilibrium xenon-samarium and for the moderator temperature coefficient. The xenon-samarium worth was obtained from the differences in the critical control rod positions for the no-xenon case as implied from the measured integral control rod worth curves. This value probably suffers from the same difficulties mentioned previously. The temperature coefficient was implied from a single heat-up experiment and a corresponding cool-down experiment whose worths differed by about 50%. Xenon buildup was also ignored. Hence, this value cannot be considered to be anything but an order of magnitude estimate.

The experimental Texas A&M core feedback results are given in Table 3, where they are compared with calculated results for both HEU and LEU models. The calculations of temperature coefficients were made both directly from LEOPARD cell models and from 2DBUM models of the full core, with comparable results.

The experimentally derived xenon-samarium worth is about .004 lower than the calculated worth, which again implies that the experimental control rod worth curves are tilted toward the bottom of the core. The calculated temperature coefficients are lower than the measured value by more than a factor of two, but this is not considered bad agreement due to the inaccuracy of the measurements. The LEU cores have very slightly lower moderator coefficients than the HEU core, but they pick up a Doppler coefficient due to the increased ^{238}U loading.

Table 3. Feedback Effects for the 4-by-4 Texas A&M UVAR Cores and Replacements.

Case	Xenon-Samarium Worth $\Delta\rho$	Temperature* Defect $\Delta\rho$ ($\times 10^4$)	Moderator* Coefficient $\Delta\rho/\Delta T(°C)$ ($\times 10^4$)	Doppler Coefficient $\Delta\rho/\Delta T(°C)$ ($\times 10^5$)
HEU-18Expt*	-1.9%	-19.	-5.2	———
HEU-18	-2.3%	-7.6	-1.9	-0.09
LEU-18	-2.3%	-7.3	-1.8	-1.0
LEU-22	-2.4%	-6.8	-1.7	-1.2

*Experimental Measurements are ±50%

SCOPING STUDIES

Part of the conceptional difficulty in studying future UVAR performance is caused by its almost random past history. Not only has the UVAR core size varied from 16 to 27 fuel elements, but also the philosophy that has been used to move fuel has involved constituting new cores from elements having roughly equal burnup. We refer to this scheme as flat burnup.

In order to make the problem tractable, we picked three fixed arrays (4-by-4, 4-by-5 and 5-by-5) as the bases of comparison, and did calculations with HEU-18 plate fuel and LEU-18 and LEU-22 plate replacement fuel. We initially tried to simulate the flat burnup shuffling pattern, but found that this scheme was counterproductive compared to an unshuffled core burnup that achieves a certain amount of natural power flattening.

The 2-dimensional burnup calculations were each initially done with a fixed average axial B^2 in all planar regions. The calculations were later rerun with spatially dependent B^2 values obtained from ANL, but the results were qualitatively similar. The comparisons are shown in Figures 6-8, where several comments of a general nature can be made.

First, all LEU cores start out with a somewhat lower k_{eff} than the corresponding HEU cores because they have a harder neutron spectrum and a consequently greater leakage. The burnup curves for LEU are less steep than for HEU, and therefore the excess reactivity curves eventually cross as depletion increases. However, for the 4-by-4 core, the lower initial k_{eff} of LEU-18 fuel cannot be made up by the decreased burnup slope before the excess reactivity crosses zero, and therefore LEU-18 fuel will not last as long as HEU-18 fuel. On the other hand, LEU-22 fuel will have comparable performance to HEU-18 fuel.

For a 4-by-5 array, one finds that both the LEU-18 and HEU-18 fuel reach an asymptotic behavior, and these cores attain essentially equal burnup at the same point in life where the excess reactivity crosses zero. On the same basis, LEU-22 fuel lasts about 50% longer than LEU-18 fuel, even though the uranium loading is only 20% greater.

A similar behavior is seen for the 5-by-5 core models. Again, the HEU-18 and LEU-18 cores have essentially the same endpoint, while the LEU-22 core lasts about 50% longer. But the most interesting result is that the LEU-22 core in a 4-by-5 array lasts almost as long as an LEU-18 core in a 5-by-5 array. This means that an LEU-22 core can be kept in a 4-by-5 configuration, with attendant higher average thermal flux for experimental purposes, and still operate almost as long as our previous larger cores.

ANL[2] has independently calculated all of the 4-by-5 cases using a 3-dimensional model, and has verified that a 2-dimensional model gives similar results when the correct spatially-dependent axial B^2 values are used. Their results are shown in Figure 9. We find that our HEU results are in almost exact agreement with theirs, while our LEU results are offset low by about 1% in k_{eff}.

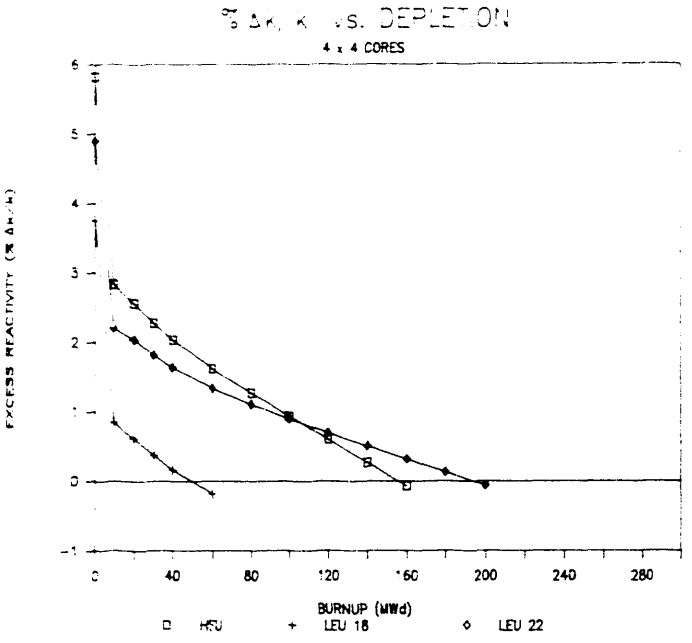

Figure 6. Unshuffled 4-by-4 Depletion of HEU and LEU Cores Using 2DBUM

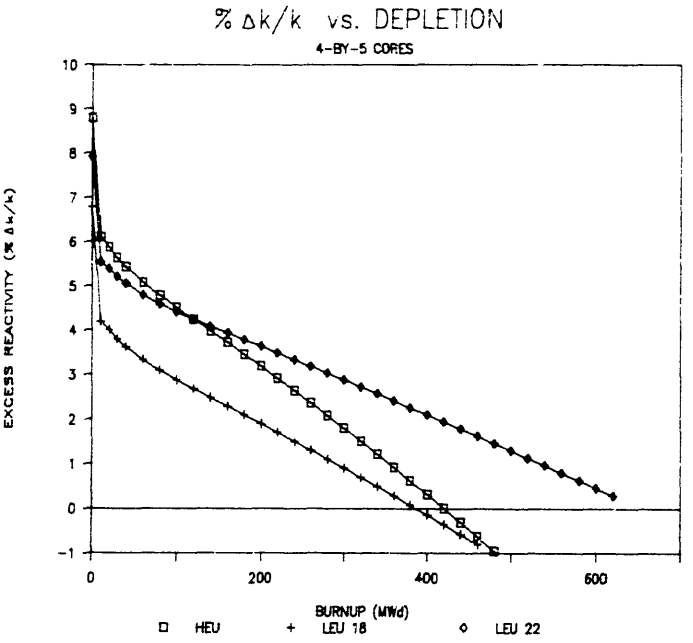

Figure 7. Unshuffled 4-by-5 Depletion of HEU and LEU Cores Using 2DBUM

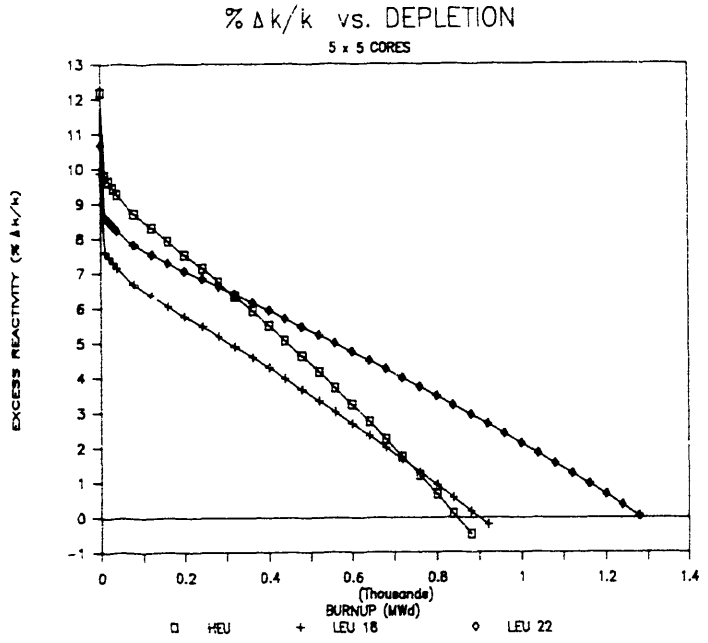

Figure 8. Unshuffled 5-by-5 Depletion of HEU and LEU Cores Using 2DBUM

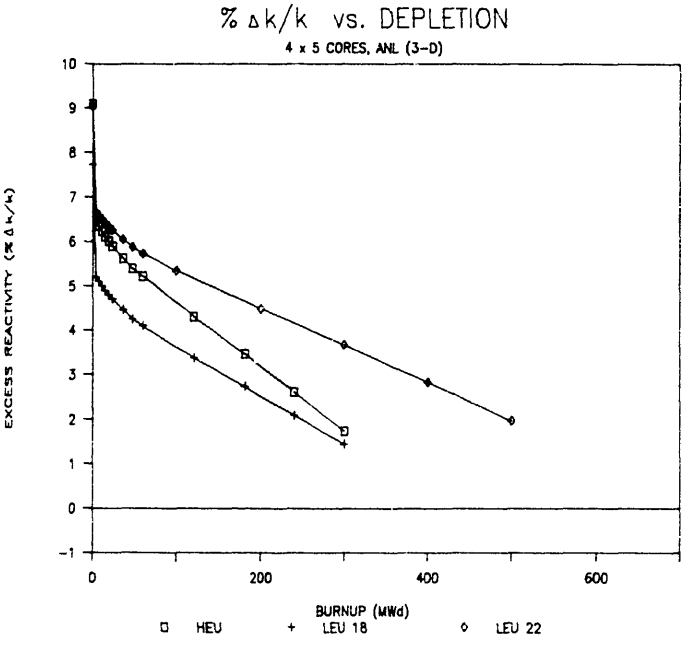

Figure 9. Unshuffled 4-by-5 Depletion of HEU and LEU Cores by ANL in 3D

Only minor differences exist between the UVA and ANL 4-by-5 LEU models. UVA included a small amount of ^{234}U and ^{236}U in the LEU fuel specification, whereas ANL used only ^{238}U. This change essentially accounts for the difference in results. The qualitative conclusions are still the same: LEU-22 fuel is a superior replacement, relative to LEU-18 fuel, for use in the UVAR.

ANL has also suggested that we consider using an equilibrium-cycle shuffling pattern, based upon the adoption of a fixed 4-by-5 core array. This cycle appears to be very attractive for the UVAR, if LEU-22 fuel is indeed used to replace our present HEU-18 fuel. This option is under serious consideration, although we would like to retain the right to use bigger cores, if needed.

THERMAL HYDRAULIC ANALYSIS

The UVA thermal hydraulic analysis makes use of two basic computer code packages, PARET and THERHYD. The PARET code from ANL is used to calculate an envelope of maximum achievable power transients, based upon pump coastdown and period trips, all accompanied by Scram. The net result of all of the PARET analyses is the fact that the control rod release and insertion times are the limiting factors for the UVAR, and that temperature feedback plays only a minor role. The responses for both HEU and LEU cores are quite similar. Transients not accompanied by Scram are argued to fall within the SPERT Experiment envelope.

The main tool for our analysis is the THERHYD code[3], developed at UVA in 1967. This code is used to calculate limiting-power versus system-flow envelopes for the UVAR, below which all PARET transients must lie. The code handles forced convection down-flow, using an axial power distribution fit and planar peaking factors from 2DBUM. The limiting condition is given using a burnout ratio of 1.49 (99% confidence that burnout will not occur) and taking into account channel and loading tolerances and bypass flow.

The peaking factors obtained from 2DBUM are shown in Table 4 for all of the cores that have been analyzed. Also shown is an older experimental measurement[4,5], scaled up to an 18-plate HEU fuel element. In general, the calculated peaking factors are a bit larger than the measured value, but lie within the experimental uncertainty.

Table 4. Planar Power Peaking Factors

CORE CONFIGURATION	CALCULATED	EXPERIMENTAL*
HEU-18 4-BY-4	1.58	1.45 ± 0.15
LEU-18 4-BY-4	1.62	
LEU-22 4-BY-4	1.67	
LEU-18 4-BY-5	1.66	
LEU-22 4-BY-5	1.71	

*Scaled From 12-Plate Measurement

Some of the more important data used in the THERHYD analysis are tabulated in Table 5. When these data are employed, we obtain limiting-power versus system-flow curves, such as shown in Figure 10. In general, the inclusion of reasonable tolerances in fuel element manufacture causes the limiting envelope to approach the actual transient results from PARET. We conclude that reasonable control must be exercised on the process of making LEU fuel, especially for the LEU-22 assemblies.

Table 5. Data And Parameters For Thermal Hydraulic Analysis

	LEU-18		LEU-22	
Core size	4x4	4x5	4x4	4x5
Number of Plates	252	324	308	396
Number of Channels	238	306	294	378
Radial Peaking Factor	1.62	1.67	1.66	1.71
(For Comparison)	HEU-18		HEU-12	
Core Size	4x4	4x5	4x4	4x5
Number of Plates	252	324	168	216
Number of Channels	238	306	154	198
Radial Peaking Factor	1.45	Not Determined	1.37	1.57

Axial Power Distribution: Exit Peak as defined by 5th order polynomial in Dahlheimer's Thesis.

Inlet Temperature: 111°F
Pool Depth to Core Center: 20.36 Ft.
Flow Distribution Factor: 16.5%

Reference Non Element Flow Parameters:
- Core: 4x4 12 Plate HEU
- System Flow: 940 GPM
- Element Flow: 48 GPM
- Dynamic D.P.: 0.0776 psi

Element Dimensions:

	18 plate	22 plate	Tolerances
Channel Gap	0.1244"	0.0927"	(both +/- .007&.002")
Channel Width	2.621"	2.621"	(+/- 0.013")
Fuel Width	2.395"	2.395"	(+/- 0.075")
Fuel Loading U235	12.5 g	12.5 g	(+/- 0.35 g)
Plate Thickness	0.05"	0.05"	

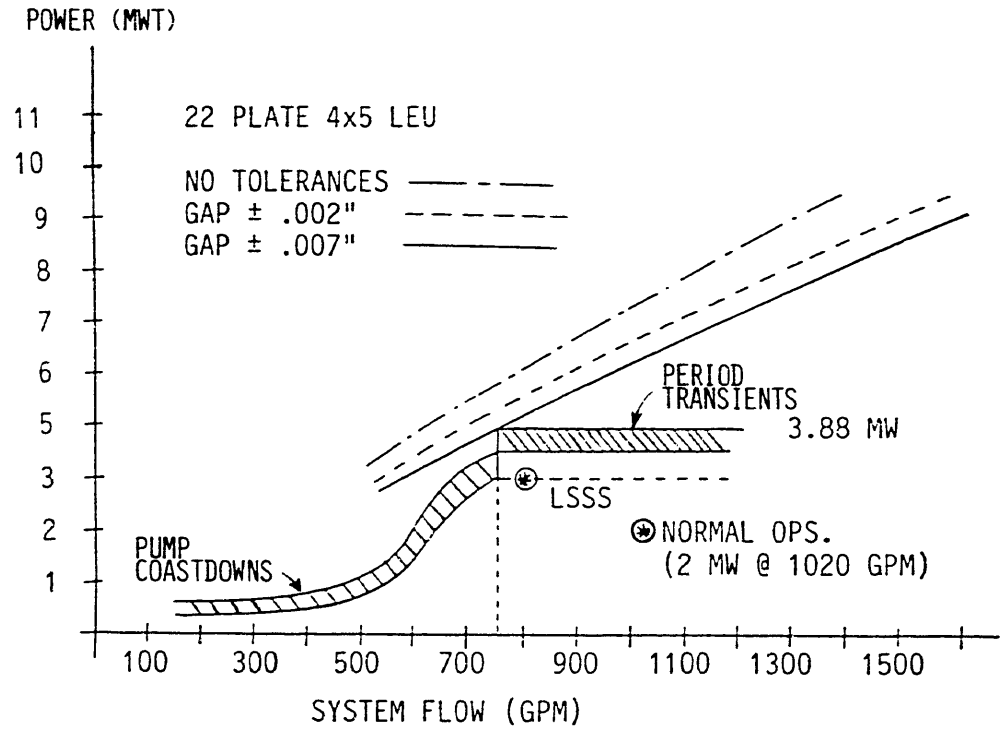

Figure 10. Limiting Power vs. Flow, 4-by-5 LEU-22 Plates/Element

The overall conclusion is that the LEU fuel is only slightly worse than HEU fuel from a thermal hydraulic standpoint. This result will require a small upward revision in the minimum safety system settings for the UVAR when it is converted. Otherwise, the small 4-by-4 core is more limiting than the larger 4-by-5 core (due to a higher average heat flux), and the 22-plate fuel element is more limiting than the 18-plate fuel element (due to manufacturing tolerances).

CONCLUSIONS

We conclude that the LEOPARD-LINX-2DBUM package of computer codes is in good working order at UVA and provides a reasonable basis of predicting the future performance of LEU replacement cores in the UVAR. However, the present 2D analysis does not appear to be sufficient for predicting the exact critical configuration of a partially-rodded core, due to an inability to include the axial flux-tilt effect on the control rod curves. For this purpose, we plan to use the DIF3D code on our new IBM-3090 computer. We believe that our present method of computing effective cross sections for control rods works well, but we plan to check these results against ANL.

The best replacement option for the UVAR appears to be the use of 22-plate LEU fuel assemblies in a fixed 4-by-5 core array. We will seriously consider the adoption of the shuffle pattern recommended by ANL. On the other hand, it is to our advantage to retain the flexibility of loading UVAR cores to meet experimental needs.

Finally, all of the postulated LEU UVAR replacement cores meet the required thermal-hydraulic conditions for safe operation. However, we will have to make slight changes in current UVAR limiting safety system settings and pay close attention to the manufacturing tolerances placed on the new fuel.

REFERENCES

1. J.L. Meem, Two Group Reactor Theory, Appendix A, Gordon and Breach Science Publishers, New York, N.Y., 1964.

2. J.E. Matos, Private Communication from Argonne National Laboratory, August 1988.

3. J.A. Dahlheimer, "Thermal-Hydraulic Safety Analysis of Pool Reactors", M.S. Thesis, University of Virginia, 1967.

4. W.K. Brunot, "An Analysis of Fuel Element Surface Temperature and Coolant Flow Rate in the University of Virginia Reactor," M.S. Thesis, University of Virginia, 1961.

5. R.L.J. McGuinness, "Thermal-Hydraulic Safety Analysis of 18-Plate Reactor Fuel Elements", B.S. Thesis, University of Virginia, 1973.

NEUTRONIC CALCULATIONS FOR THE IAN-R1 RESEARCH REACTOR CORE CONVERSION

I. A. Concha
Instituto de Asuntos Nucleares
Bogotá, Colombia

ABSTRACT

This paper presents the neutronic analysis for the conversion of the 10 Kw IAN-R1 research reactor from HEU (90%) to LEU (20%). By changing the number of LEU plates per standard element, five different LEU protoipe cores are found acceptable in excess reactivity, and deeper studies with the lowest and higest $\Delta K/K\%$ are carried out.

INTRODUCTION

The Instituto de Asuntos Nucleares (IAN) has proposed the project of changing the core of the IAN-R1 research reactor to perform the core conversion from HEU to LEU and to rice the power from 10Kw to 1Mw. To reduce the costs of the core conversion, a minimun of geometrical and structural changes must be done, and the new fuel could be any usual density and uranium content LEU fuel.

This calculations were done at Argonne National Laboratory in developing an IAEA fellowship, with the EPRI-CELL and DIF3D codes which has been deeply prooved by the RERTR-Program staff. The thermal-hydraulics calculations and safety analysis will be done in the inmediate future, just based on this neutronics calculations. I want to thank the colaboration I received from all RERTR program staff, and specially Dr. Jim Matos, whom drove me during the time I spent at Argonne doing this calculations.

REACTOR AND FUEL ASSEMBLIES DESCRIPTION

The IAN-R1 research reactor is a swiming pool type facility, light water moderated, natural convection cooled and graphite reflected (Figure 1). Standard fuel elements consist of a 10 MTR flat plate array as shown in Figure 2.

The core is a 4x4 array of fuel assemblies surrounded by 20 graphite reflector elements; 3 of the 16 fuel assemblies are control elements (6 fuel plates/control element) and one row of six of the graphites contain circular irradiation spaces. Tables 1 and 2 shows the main caracteristics of the core and the fuel elements.

Figure No. 1

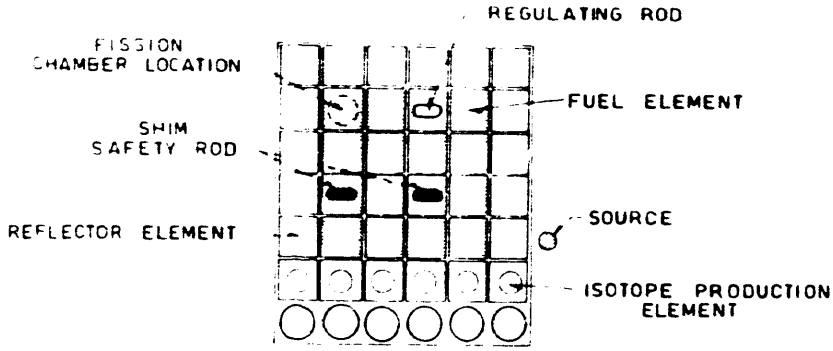

CORE ARRANGEMENT

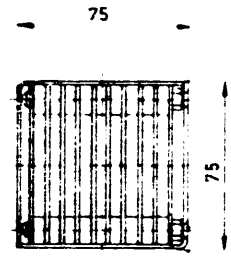

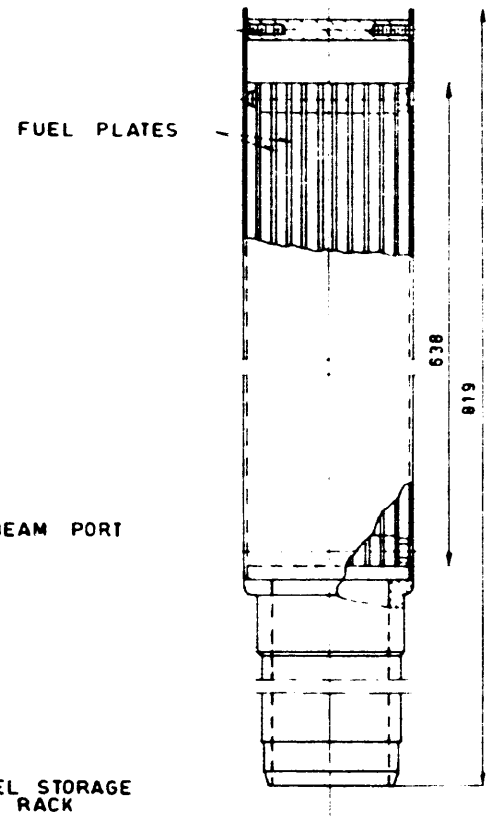

FUEL ELEMENT

All dimensions in mm

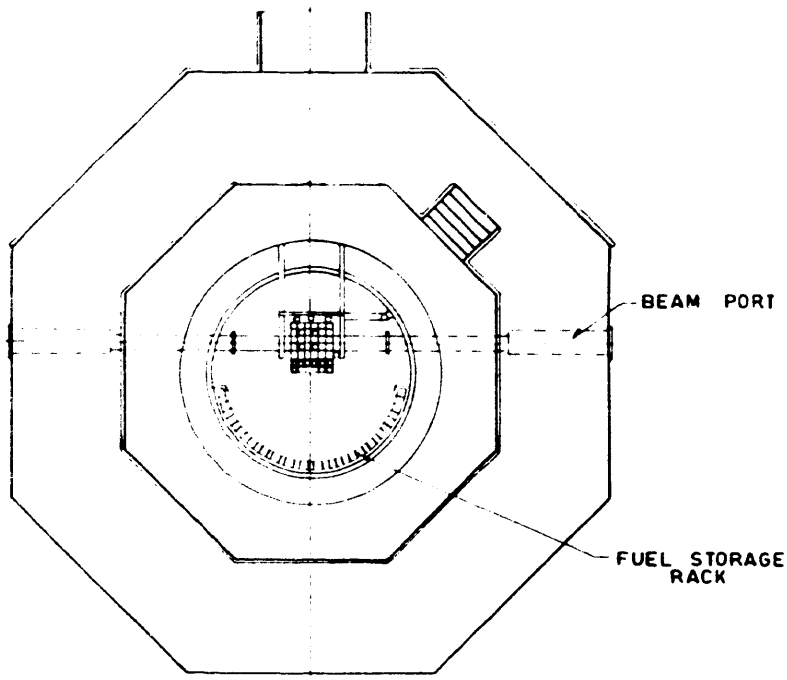

HORIZONTAL SECTION REACTOR IAN-R 1

Figure No. 2

IAN-R1 STANDARD FUEL ELEMENT H.E.U.(90%)
(All dim in cm)

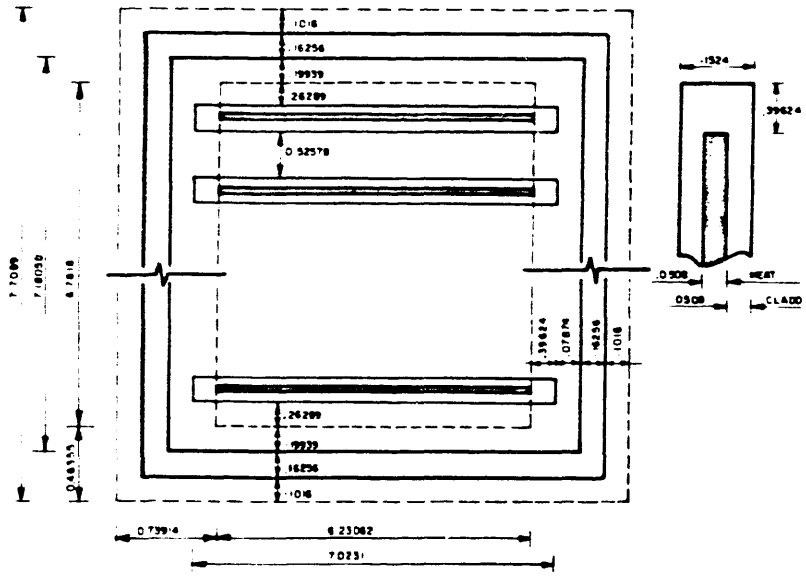

Table 1. IAN-R1 Core Description.

Reactor type	Swiming pool, MTR
Nominal Power	10 Kw
Plates per standard element	10
Plates per control element	6
Critical U235 mass (Kg)	2.167
Core loading U235 mass (Kg)	2.1819
Safety absorbing material	Boron-SS (2 rods)
Regulating absorbing material	SS-holow water filled
Grid perforations	6x6
Grid pitch	7.71 cm
Cooloing-moderating material	Light water
Average water temperature	30 deg-C
Maximun water temperature	38 deg-C
Reflector material	Graphite

Table 2. Fuel Element Description.

Enrichment %	90
Plate type	Flat MTR
Fuel element dimensions (cm)	7.62x7.62x71.45
Plate dimensions (cm)	0.1524x7.023x63.82
Fuel meat dimensions (cm)	0.0508x6.23x59.37
Water channel thickness (cm)	0.526
Cladding thickness (cm)	0.0508
Plates/Standard element	10
Plates/Control element	6
Fuel type	U-Al1100 alloy
U-density	0.8916 grs/cc
U-fraction	0.2677
U-235/plate	15.06 grs

NEUTRONIC CALCULATIONS

The macroscopic problem-dependent cross sections for each of the different regions of the reactor were generated using EPRI-CELL code with normal group structure used at Argonne National Laboratory colapsed to 5 or 7 energy groups, modeling different unit cells for each of the regions of the reactor. The generated cross sections sets were used in 2 and 3-dimensional difusion calculations with the DIF3D difusion code. Zone dependent energy promediated extrapolation lengths were used while XY difusion calculations by using the EXTRAP code. In Table 3 main features of HEU core elements are shown. Figure 3 shows the geometrical representation of the core used for the input of the difusion code. Because of in XYZ geometry the code does not accept circular regions, the irradiation spaces were transformed into squares preserving the area. Figures 4 and 5 are control elements and graphite reflector/irradiation elements.

Figure No. 3

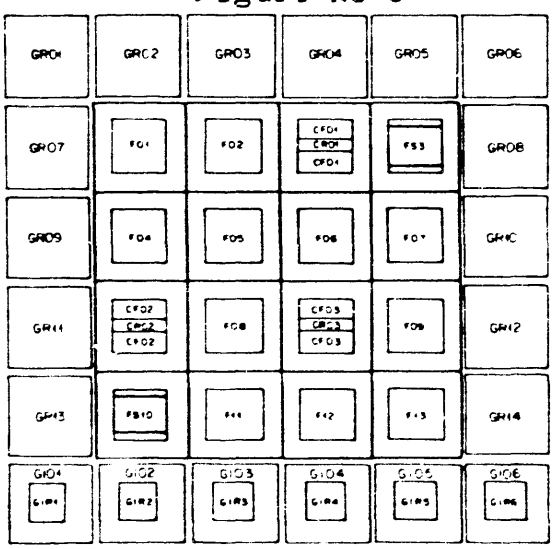

Figure No. 4

IAN-R1 GRAPHITE IRRADIATION/REFLECTORS

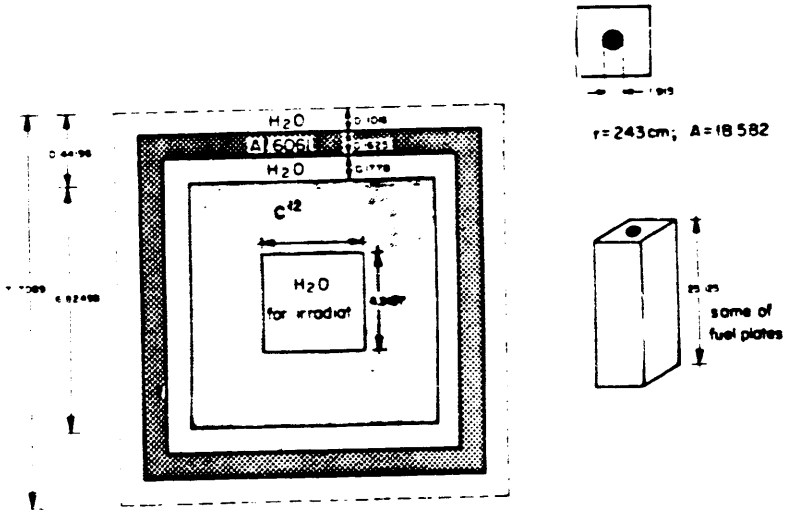

GRAPHITE SIDE PLATE AREA 12.846787 cm

VAl 4.77308 H_2O 0.6284612

Al 6061 0.3715388

Figure No. 5

IAN-R1 LEU CONTROL ELEMENT

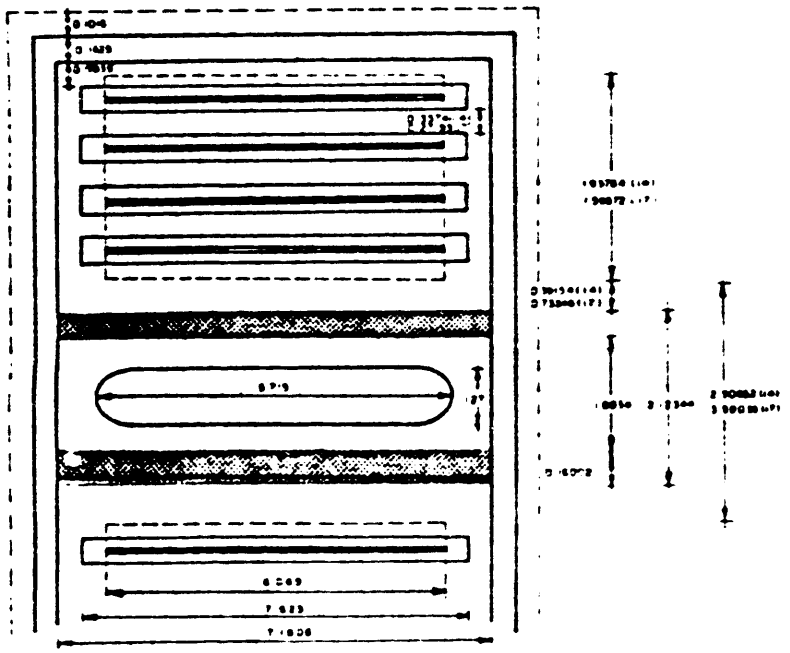

GR01 to GR14 are normal graphite reflector elements, GI01 to GI06 are graphite irradiation-reflector elements where irradiation spaces are water filled and represented as GIR01 to GIR06. F01 to F13 are standard fuel elements, CF01 to CF03 are control elements where control rod spaces are represented by CR01 to CR03. FS3 and FS10 are special fuel elements where the first and the last fuel plates were replaced by dummy plates when starting the reactor in 1964 in order to fix the K_{EFFEC} to the value of 1.00603. The side plates are presented as square frames of the fuel elements because the fuel plates are located into aluminum boxes, attached at the top and bottom by screws across the array. This kind of "side plates" are not very usual in research reactor thecnology.

The fresh core (20 deg-c) XYZ five groups calculated value for the K_{EFFEC} was 1.0147021 (1.449 $\Delta K/K\%$). Even the calculated value is about 0.8% $\Delta K/K$ higher than the experimental value the conclusions to be drawn from the following calculations will not be afected by this "bias", because of the diferences in excess reactivity will hold, and this diferences are the quantities to be considerated in the analisys.

Recently, as a magister tesis work, thermal fluxes were measured inside irradiation spaces (GIR1 to GIR6) at Z coordinates coincident with those of the XYZ DIF3D code input. Figures 6 and 7 shows experimental and calculated values, where a very good agreement can be seen. The reactor was calculated at 10 Kw, and the measurements were done at the same power.

Table 3. HEU Zone Volumes and Compositions

Zones	Area Cm^2	Volume Cm^3	Fraction
Standard Fuel:			
- Total	42.254818	2508.7741	-
- Meat	3.165149	187.9228	0.0749082
- Cladding	6.3303098	375.85155	0.1498148
- Moderator	32.75936	1945.0051	0.775281
Standard Side Plate:			
- Total	17.1544	1018.4996	-
- Aluminum	5.9807798	355.09384	0.348644
- Moderator	11.173627	663.4061	0.6513562
Control Region:			
- Total	16.901927	1003.5096	-
- Aluminum	1.9940476	118.39159	0.1179775
- Moderator	14.90778	885.11216	0.8820116
Control Side Plate:			
- Total	17.1544	1018.4996	-
- Aluminum	5.80325	344.55346	0.3382951
- Moderator	11.35115	673.94615	0.6617048

Fig No. 6 IAN-R1 HEU (z = 14 cm)
THERMAL FLUX vs IRRADIATION HOLES

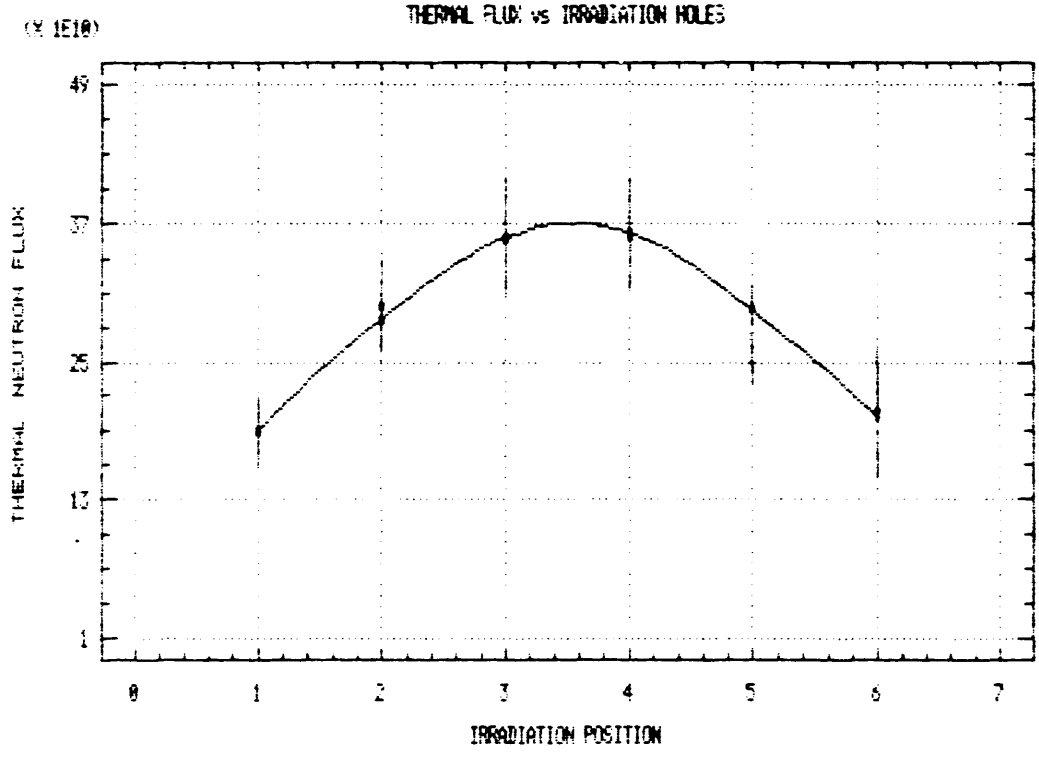

Fig No. 7 IAN-R1 HEU (z = 5 cm)
THERMAL FLUX vs IRRADIATION HOLES

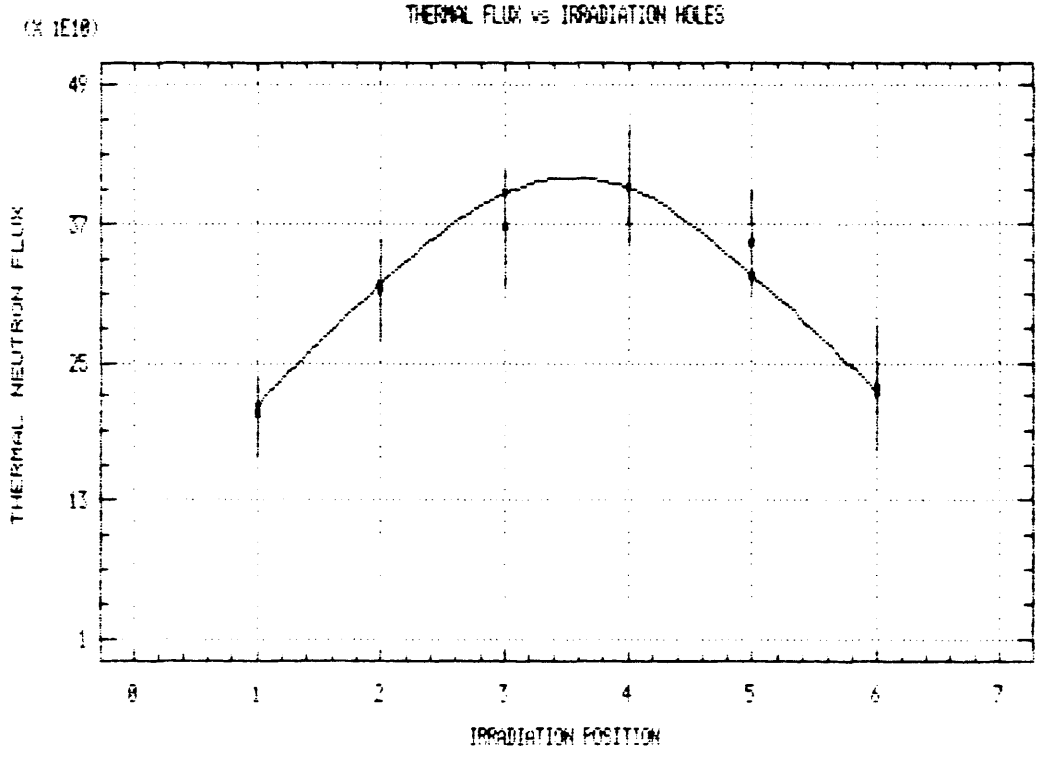

LOW ENRICHED URANIUM CALCULATIONS

In order to reduce core conversion costs, a typical low-enriched fuel plate was chosen with the following main caracteristics:

-Fuel plate dimensions (cm)	0.127x7.0231x63.817
-Fuel meat dimensions (cm)	0.0508x6.065x59.05
-Fuel type	U_3Si_2-Al
-Enrichment %	19.75
-U235 grs/plate	12.50
-Cladding aluminum type	Al-6061

The external LEU fuel plate dimensions are compatible with the IAN-R1 fuel boxes, so the present core geometry and equipment do not need to be changed for the core conversion.

To perform the LEU calculations the dimensions of the fueled region in the plate-to-plate direction was fixed at the same value of the HEU core (water chanels were adjusted), but the width was transformated to the new value. Because of the plate thickness is fixed, the water channel between plates decreased when the number of plates per standard fuel element was increrased. Also a total of 8 plates per control element was fixed for all the 5 cases analyzed; in this way, the guide tubes for the control absorbers has the same dimensions in HEU as in LEU control elements so that the present control rods can also be used in the future core.

The main features of the elements that were studied are shown in tables 4,5,6,and 7.

Table 4. Standard LEU Element Designs

No.plates/sfe	U235 grs	Water channel cm
13	162.5	0.39468
14	175.0	0.35741
15	187.5	0.32512
16	200.0	0.29686
17	212.5	0.27193

Table 5. Standard LEU Element Volume Fractions

No. Plates	Meat	Clad	Moderator
13	0.0973782	0.1460674	0.7565544
14	0.1048689	0.1573033	0.7378278
15	0.1123595	0.1685393	0.7191012
16	0.1198501	0.1797752	0.7003747
17	0.1273408	0.1910112	0.681648

Table 6. Control Reflector Zones

No. Plates	C.R.Thick.	VF Aluminum	VF Moderator
14	2.90652	0.1101074	0.8898926
15	3.16484	0.1011108	0.8988892
16	3.39092	0.0943696	0.9056304
17	3.59036	0.0849338	0.9150662

Table 7. Standard Side Plates

No. Plates	VF Aluminum	VF Moderator	Ext.Reg.Tk.
13	0.3473452	0.6526548	0.2320454
14	0.3539959	0.6460041	0.2154676
15	0.3606466	0.6393534	0.2011048
16	0.3672974	0.6327026	0.1885347
17	0.3739481	0.6260519	0.1774457

The respectives EPRI-CELL and DIF3D inputs were prepared for each of the cases mentioned above and run to obtain the excess reactivity curve shown in Fig. 8.

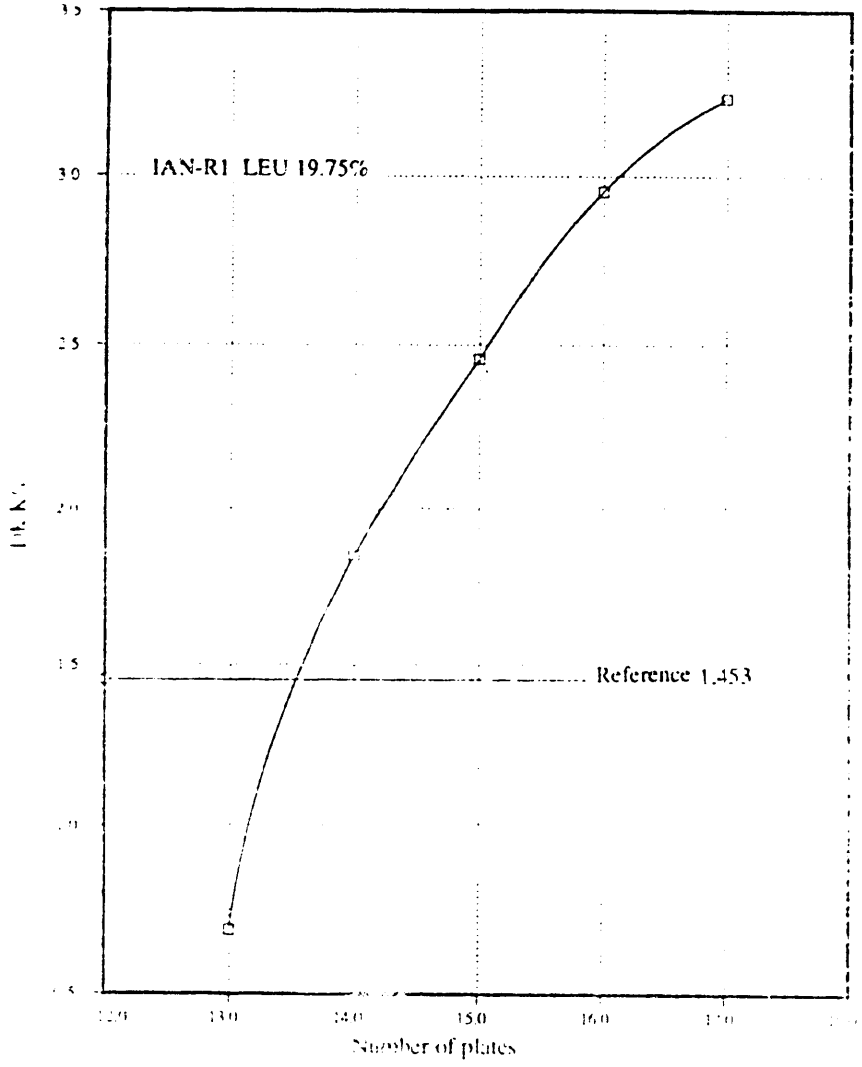

This results were done for 5 energy groups. It can be seen that to obtain a LEU core with at least the same excess reactivity as the actual HEU core, a minimum of 14 plates per standard fuel element must be included. If it is desired to increase the reactor power, then to compensate the burnup reactivity loss, a standard element with 15-17 plates is desirable. All the possibilities in figure 3 are reasonable choices for the IAN-R1 LEU core.

SOME COMPARATIVE STUDIES FOR THE HEU CORE AND TWO LEU CORES

In the following, all the LEU studies are for the 14 and 17 plates per standard fuel element prototype cores.

Borom Impurity Content in the Cladding

The boron impurity content of the aluminum cladding must be taken into account in selecting an apropiated fuel element design for core conversion. It was found a linear excess reactivity loss with increasing of the B10 content in the cladding. Also, all the aluminum impurities can be represented as an equivalent natural boron amount. For both LEU cases the loss is about 0.15ΔK/K% per 10ppm boron:

ppm B10 added	14-LEU ΔK/K%	17-LEU ΔK/K%
0	2.604	3.967
10	2.455	3.814
20	2.307	3.662

Control Rod Worth

The IAN-R1 core has two shim safety rods and one regulating rod. The regulating rod is a SS tube with an eliptical shape and a cross section of 5.715x1.27 cm. The experimental regulating rod value is -0.4% ΔK/K. Generating macroscopic cross sections for the SS in cilindrical geometry preserving areas to make it to correspond to the real geometry of the control rod position, the 2d-difusion calculation was run whith the rods into the core:

CORE	ROD POSITION	ΔK/K	ROD WORTH
HEU	OUT	1.650	-
	IN	1.056	-0.594
14-LEU	OUT	2.455	-
	IN	1.916	-0.539
17-LEU	OUT	3.814	-
	IN	3.267	-0.547

Prompt Neutron Life Time and Effective Delayed Neutron Fraction

These two core physical parameters were evaluated for the HEU and the two LEU prototype cores using the DIF2D computer code and also using the 1/v absorber insertion method which essentially consist in a serie of different calculations adding a small amount of suitable neutron 1/v isotope absorber in the whole reactor to apply the perturbation theory formula:

$$\ell_p = \lim_{N\ 0} (\delta k/k)/N.C$$

via graphical extrapolation. The resuslts folows (time is given in micro seconds):

CORE	β_{EFE}	ℓ_{DIF2D}	$\ell_{1/V}$
HEU	0.00774	87.06	75.16
14-LEU	0.00771	79.59	63.58
17-LEU	0.00773	77.16	60.21

Isothermal Feedback Reactivity Coefficients

These coefficients were determinated by comparing the excess reactivity changes as a function of the temperature, considering the following effects: (a) The hardness of the neutron spectrum due to the rice of the water temperature only. (b) The increasing of the fast neutron leakage due to the diminution of the water density while increasing its temperature. (c) The Increasing of the resonant absorption of the U238 due to the rice of the meat temperature (Doppler effect).

The calculations for the water temperature coefficient were done using 7 energy groups, while the others whith only 5 energy groups. The results are shown in Figures 9 to 13.

CONCLUSIONS

The work presented in this paper is just the begining of the complete package of the core conversion study for the IAN-R1 research reactor. Most of the results are still on the code outputs or being analyzed at the present, eg. neutron fluxes among others, wich are the basis for next calculations.

The experimental work recently done by P. Reyes (Magister Student of the National University of Colombia, Bogotá) and E. Ramírez, (Physics Section-IAN) shows a nice agreement between calculated values and measurements, increasing the worth of this calculations. This work is going to be presented in the next furure at the University. I want to thank them for their permision to put some results here.

IAN-R1 CORE
Isothermal Reactivity Feedback Coefficients

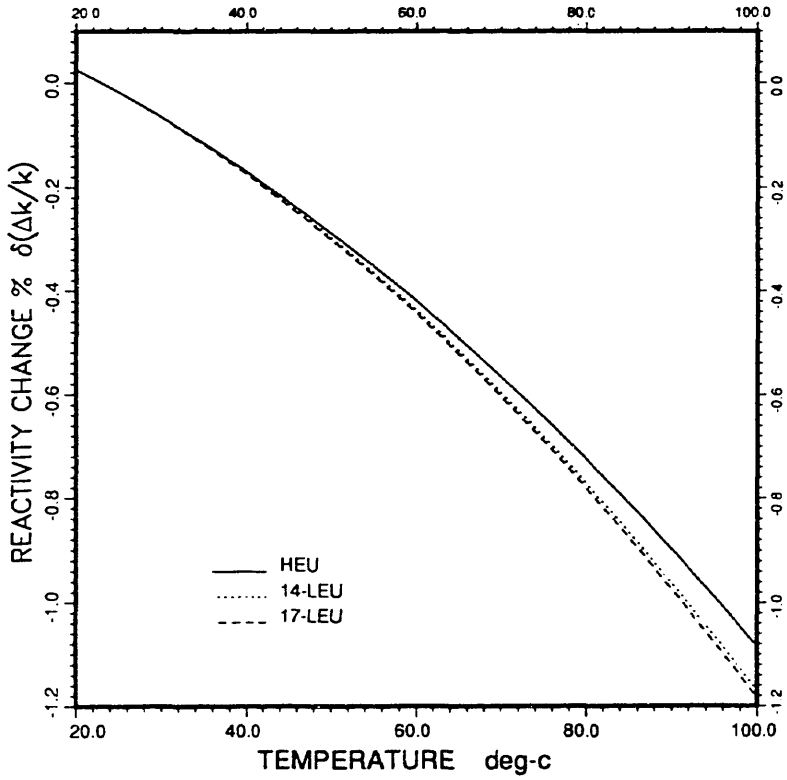

IAN-R1 CORE
Doppler Effect

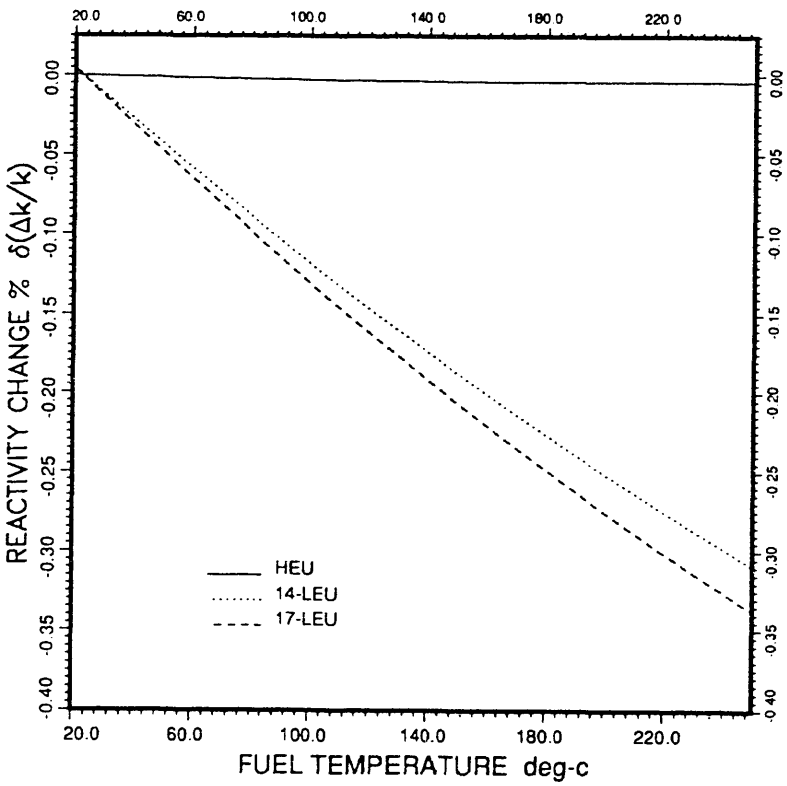

IAN-R1 HEU
Isothermal Reactivity Coefficients

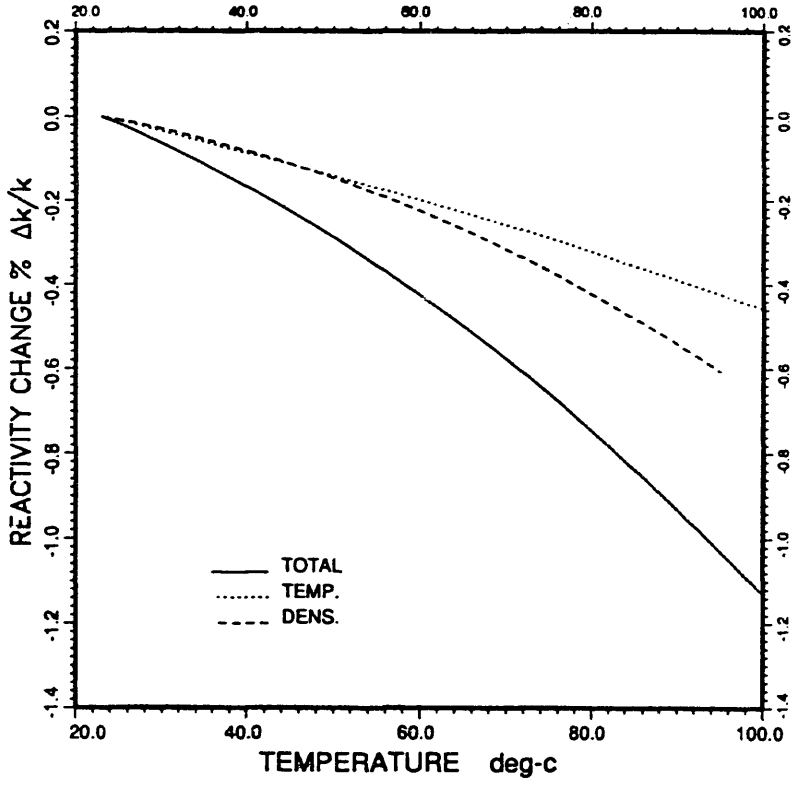

IAN-R1 14-LEU
Isothermal Reactivity Coefficients

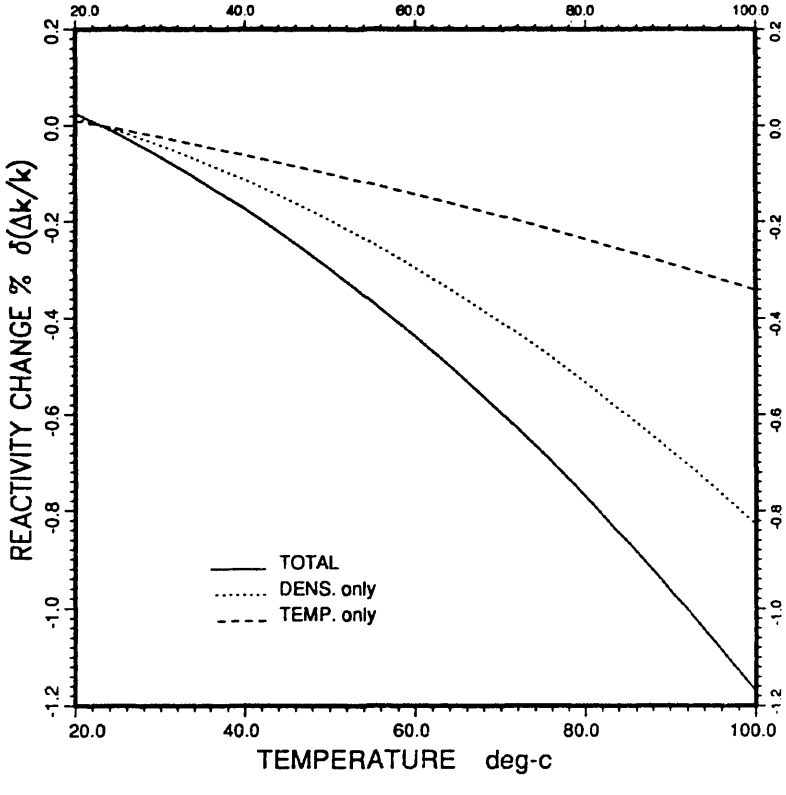

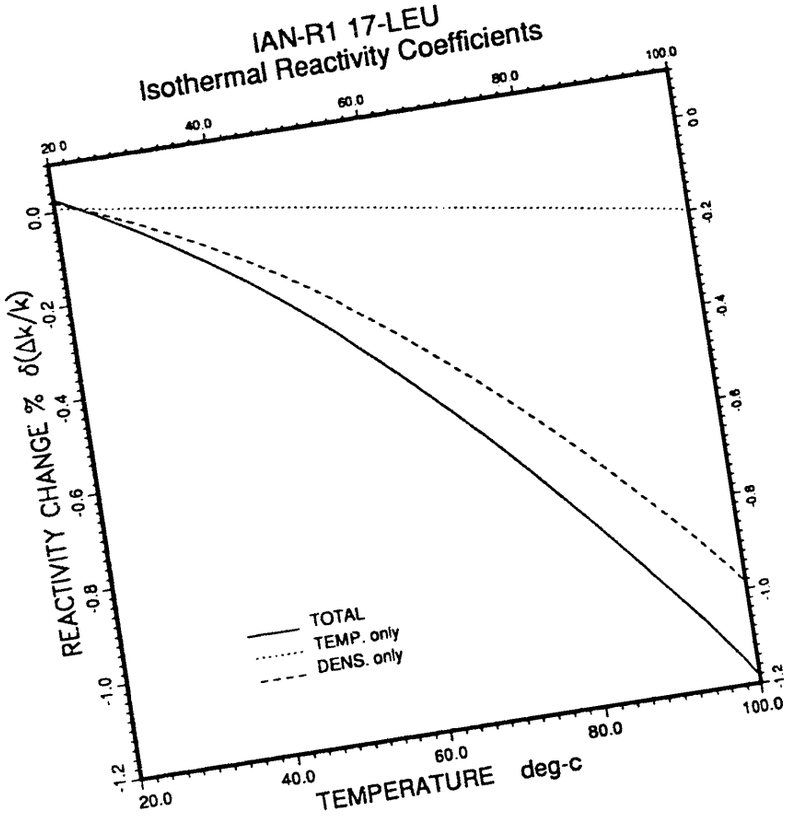
IAN-R1 17-LEU
Isothermal Reactivity Coefficients
REACTIVITY CHANGE % δ(Δk/k)
TEMPERATURE deg-c
TOTAL
TEMP. only
DENS. only
20.0
40.0
60.0
80.0
100.0
0.0
-0.2
-0.4
-0.6
-0.8
-1.0
-1.2

SESSION VII

September 21, 1988

CONVERSION PLANS AND STUDIES

Chairman:

A. Beeckmans
(CEN-SCK, Belgium)

PRELIMINARY SAFETY ANALYSIS FOR JMTR CORE CONVERSION TO LEU FUEL

Fumio SAKURAI, Etsuo ISHITSUKA, Hiroei ANDO, Minoru SAITO
and Rokuro OYAMADA
Japan Atomic Energy Research Institute
Oarai Research Establishment
Oarai-machi, Ibaraki-ken, Japan

ABSTRACT

Japan Materials Testing reactor(JMTR, 50MWt) has been successfully operated with the MEU(45% enriched uranium)fuel since July 1986. The effort is still continued to convert the core from MEU to LEU fuel. The safety assessment in the application for the JMTR core conversion to LEU fuel is being allover revised based on light water power reactor(LWR)-base criteria. This paper provides the analyses carried out for the three of the design basis events ; loss of A-C power, primary and secondary coolant pump shaft seizures. The analyses predicted that those design basis events can meet the design basis criteria defined based on the criteria of the LWR and the characteristics of research reactor.

INTRODUCTION

In recent safety review for research reactor installation including reactor modification like the core conversion with reduced enriched fuel, LWR-base criteria are translated in most cases. For this reason, the safety assessment in the application of safety review for the JMTR core conversion to LEU fuel is required to be allover revised based on LWR-base criteria.

In the present application, the anticipated operational transients(AOT) are included in the postulated accidents(PA), and no judgment criteria for PA are set up.

In the revised application, the judgments shown in Table 1 will be set up. Items of AOT and PA being discussed are listed in Table 2.

The safety analyses for the design basis events shown in Table 2 are being carried out in order to estimate whether each event can meet the design basis criteria shown in Table 1 without changing the safety system setting currently adopted in the JMTR. The analyses are being carried out using the thermo-hydraulic transient analysis code THYDE-W developed at JAERI. A full plant simulation is used in the analyses for the transient behavior of the JMTR.

This paper describes analytical results of (1) loss of A-C power, (2) primary coolant pump shaft seizure and (3) secondary coolant pump shaft seizure and some of matters for the safety review for the JMTR core conversion to LEU fuel presented in this meeting.

MAJOR FEATURES OF JMTR THERMOHYDRAULICS

The JMTR is a light water moderated and cooled 50MW tank type reactor. Figure 1 shows the core configuration of the JMTR. The core consists of 22 standard fuel elements, 5 control rods with fuel followers, and Be and Al reflectors with irradiation holes. Table 3 shows the characteristics of the JMTR.

Figure 2 shows the schematic diagram of the standard fuel element with burnable absobers of Cd wires to be used in the JMTR . JAERI decided to use the LEU silicide fuel element with burnable absobers of Cd wires in the JMTR in order to (1) extend the core life from 11 days in the present MEU fuel core to 24 days in the LEU core, and (2) reduce the reactivity swing during the cycle.

Figure 3 shows the schematic diagram of the primary cooling system. In the primary cooling system, four main circulation pumps are installed parallel with one another, and the three pump of them are operated during the reactor operation. Two emergency cooling pumps are installed parallel with the main circulation pumps, and the power to the pumps is supplied from the diesel generator. The one of emergency cooling pumps is always operated during the reactor operation. In order to prevent the core from being not covered with water in case of loss-of-coolant accidents(LOCA) due to a pipe break, syphon break valves, connecting valves and recycling system are installed.

ANALYTICAL RESULT AND DISCUSSION

Loss of A-C Power

Analysis Condition

The loss of A-C power is assumed to be occurred when the reactor is in the full power normal operation. Three main circulating pumps installed in the primary cooling system and three circulating pumps installed in the secondary cooling system stop immediately, and their coastdown is started. On the other hand, an emergency cooling pump installed in the primary cooling system keeps operation with the rated rotation, and an auxiliary cooling pump installed in the secondary cooling system starts to operate.

Following the loss of reactor coolant flow caused by the loss of A-C power a reactor trip is actuated on a trip signal shown in Table 4. The reactor trip settings used in the analyses are the same as the one currently adopted in the JMTR. The time from the initiation of a trip signal to initiation of control rod motion is conservatively assumed to be 0.4 second. For conservatism, the reactivity feedback effects are not taken into account.

Results and Discussions

Figure 4 shows the transients of the primary and secondary coolant flows, the core inlet and outlet pressures. The core inlet pressure decreases due to the loss of the main circulating pump at power, and the core outlet pressure increases due to a decrease in the differential pressure between the core inlet and outlet caused by a decrease in the primary coolant flow.

Figure 5 shows the reactor power, the coolant flows in the hot and average channels and the differential pressure between the core inlet and outlet. It can be seen that a reactor trip is actuated on a signal of the low differential pressure between the core inlet and outlet at about 0.8 second after initiation of the transient, and the reactor power is rapidly reduced by the control rod insertion.

Figure 6 shows the transients of the coolant, fuel centerline and fuel surface temperatures at the hot spot. The maximum coolant, fuel centerline and fuel surface temperatures of 118 ℃, 224 ℃ and 205 ℃, respectively, are reached at about 1.2 seconds after initiation of the transient. At the same

time, a minimum DNB ratio of about 2.4 is reached, too. This value is calculated by using Bernath correlation.

It became clear from the analyses that the loss of A-C power transient can meet the criteria for AOT without changing the reactor trip settings currently adopted in the JMTR.

Primary coolant Pump Shaft Seizure

Analysis Condition

The shaft of the one of the main circulating pumps is assumed to be instantaneously seized when the reactor is in the full power normal operation. The coolant flow through the seizured pump is rapidly reduced, leading to a reactor trip on a signal shown in table 4.

In the analyses, a seizure of No.1 main circulating pump shaft is assumed to occur, NO.2 and No. 3 circulating pumps and NO.1 emergency cooling pump are assumed to keep operation with the rated rotation during the accident.

Results and Discussions

Figure 7 shows the transients of pump flows. The coolant flow through No.1 pump is rapidly reduced and kept at zero by the effect of a check valve installed at the discharged side of the pump since about 0.5 second after initiation of the accident. The coolant flows through No.2 and No.3 pumps that keep operation with the rated rotation increase due to a decrease in the pressure loss in the primary coolant system following a decrease in primary coolant flow caused by the seizure of No1. pump shaft.

Figure 8 shows the primary coolant flow, the core inlet and outlet pressure. The primary coolant flow decreases to 4,800 m^3/hr at about 0.4 second after initiation of the accident, and is after then maintained. The core inlet and outlet pressures reach 13.7 Kg/cm^2G and 11.1 Kg/cm^2G, respectively, at about 0.4 second after initiation of the accident, and are after then maintained.

Figure 9 shows the reactor power, the primary coolant flows in the hot and average channels, the differential pressure between the core inlet and outlet. A reactor trip is actuated on a signal of the low differential pressure between the core inlet and outlet at about 0.7 second after initiation of the accidents.

Figure 10 shows the transients of the coolant, fuel centerline and surface temperatures at the hot spot. The highest fuel temperature of 198 ℃, the highest fuel surface temperature of 178 ℃ and the highest coolant temperature of 99 ℃ are reached at about 0.7 second after initiation of the accident, i.e. at the initiation of control rod insertion. At this time, the minimum DNB ratio of about 3.5 is reached, too.

It became clear from the analyses that the primary coolant pump shaft seizure accident can meet the criteria for AOT without changing the reactor trip settings currently adopted in the JMTR, even in the accident condition.

Secondary Coolant Pump Seizure

Analysis Condition

The shaft of the one of the circulating pumps is assumed to be instantaneously seized when the reactor is in the full power normal operation.

In the analyses, a seizure of No.1 circulating pump shaft is assumed to occur, and NO.2 and No.3 circulating pumps are assume to keep operation with the rated rotation.

Results and Discussions

Figure 11 shows the transients of pump flows. The coolant flow through No.1 pump is rapidly reduced and kept at zero by the effect of a check valve installed at the discharged side of the pump since about o.3 second after initiation of the accident. The coolant flows through No.2 and No.3 pumps that keep operation with the rated rotation increase due to a decrease in a pressure loss in the secondary coolant system.

Figure 12 shows the heat removal from the primary cooling system, the secondary coolant flow and the reactor power. It can be seen that in case of this accident a reactor trip is not actuated. The heat removal from the primary cooling system decreases with decrease in the secondary coolant flow at the early stage of the accident, but it recovers to the initial level.

Figure 13 shows the coolant and fuel temperatures at the hot spot. These temperatures reach another steady values at about 1,000 seconds after initiation of the accidents. In this steady state, the fuel centerline

temperature and the DNB ratio are calculated to be about 180 °C and 3.6. respectively.

It became clear from the analyses that in case of the secondary coolant pump shaft seizure accident the reactor safety can be kept without a reactor trip.

MATTERS TO BE SOLVED FOR SAFETY ANALYSES

Establishment of Neutronics Calculation Method for Fuel Element with Cd Wires

The accurate evaluation of the neutronic effect of Cd wire upon the core is very important in order to estimate the nuclear characteristics of the JMTR LEU fuel core. Therefore, the following modeling of the fuel element with Cd wires is under examination now.

The fuel element is modeled with separated fuel and nonfuel regions for the core burnup calculation. The nonfuel region contains Cd wires. In order to generate proper cross sections for the nonfuel region, it is necessary to develop an adequate model for Cd depletion due to burnup. The main criterion for an adequate model for Cd depletion is to create a neutron spectrum over the entire volume of the wire that would be as close as possible to the practical spectrum. The spectrum calculated by Monte Carlo calculation code VIM is used as a reference spectrum. This modeling will be validated experimentally using the critical facility JMTRC.

Experimental Validation of DNB Heat Flux Correlation

Most DNB heat flux correlations for the thermal-hydraulic design of research reactors have been produced under the normal operational conditions with high coolant velocities. Therefore, before those correlations are used in the analyses of AOT or PA with loss of coolant velocity, it is necessary to evaluate the applicabilities of them under low coolant velocity conditions.

JAERI developed a DNB heat flux correlation that is applicable to the low coolant velocity and low pressure condition in order to design the upgraded JRR-3. Therefore, this correration cannot be used in the analyses of AOT and PA in the JMTR whose coolant is pressurized to 14 Kg/cm^2G without any corrections.

OF
1.0
2.8
2.5
3.2
2.2
3.6
1.1
2.0
1.8
1.25
1.4
1.6

It is necessary to investigate the DNB heat fluxes under the JMTR AOT and PA conditions in the experiments. The experiments will be carried out in 1989.

Measurements of LEU Silicide Properties

Integrity of the fuel must be kept even in case of AOT as mentioned above. Therefore, temperature-dependent property data up to 400 ℃ are necessary for the fuel meat, because the maximum temperature allowed from view point of the blister-threshold temperature is 400 ℃ in case of AOT. The measurements will be carried out in 1988.

CONCLUDING REMARKS

This paper presents the preliminary analyses carried out for the three of the design basis events of the JMTR and some of matters for the safety review for the JMTR core conversion to LEU fuel.

The analyses show the following results.

(1) The loss of A-C power transient can meet the design basis criteria for AOT without changing the reactor trip settings currently adopted in the JMTR.
(2) The primary and secondary coolant pump seizure accidents can meet the design basis criteria for AOT without changing the reactor trip settings currently adopted in the JMTR, even in the PA condition. In case of the secondary coolant pump shaft seizure accident, the reactor safety can be kept without a reactor trip.

The following matters must be solved for the safety analysis of the JMTR LEU fuel core.

(1) Establishment of neutronics calculation method for the fuel element with Cd wires.
(2) Experimental validation of DNB heat flux correlation.
(3) Measurement of LEU silicide fuel properties.

REFERENCES

1. R. Oyamada, M. Saito, A .Yamamoto and H .Sakurai, "Licensing Aspect of Reduced Enrichment Program for JMTR Fuel," in Proceedings of the International Meeting on Reduced Enrichment for Research and Test Reactor, Buenos Aires, Argentina, 28 Sep - 2 Oct, 1987.

2. K. Kanda, et al., "Status of Reduced Enrichment Program for Research and Test Reactor Fuels in Japan," these proceedings.

3. Y. Nagaoka, R .Oyamada, J.E. Matos and W.L. Woodruff, "Neutronic Analysisof The JMTR with LEU and Burnable Poison," in Proceedings of th Internat ional Meeting on Reduced Enrichment for Research and Test Reactor,Argonne, Illinois, U.S.A., October 18, 1984, ANL/RERTR/TM-6, CONF-8410173.

4. Y. Sudo, K. Miyata, H. Ikawa, et al., "Core Heat Transfer Experiment for JRR-3 to Be Upgraged at 20 MW · Part Ⅱ," JAERI-M85-126,(in Japanese), 1985.

5. J.R.Deen and J.L.Snelgrove, "Preliminary LEU Fuel Cycle Analyses for the Belgian BR2 Reactor," in Proceedings of the International Meeting on Reduced Enrichment for Research and Test Reactor, Argonne.Illinois ,U.S.A., November 3-6,1986.

Table 1 Design Basis Criteria in the JMTR

Judgement criteria for AOT

The core must be kept so as to be able to revert to the normal operational conditions without damage when AOT occurs.

* Minimum DNB ratio ≧ 1.5 .
* Fuel core maximum temperature ≦ Blister threshold temperature(400℃).
* NO significant deformation of fuel plate.
* Pressure loaded to the primary coolant system ≦ 1.1 X Maximum operational pressure(1.8 MPa).

Judgement criteria for PA

* The reactor core must be covered with water in any cases.
* The reactor core must not be led to significant damage, and can be cooled enough.
* Pressure loaded to the primary coolant system ≦ 1.2 X Maximum operational pressure(1.8 MPa).
* NO significant risk of radiation dose to the public.

Table 2 Items of Design Basis Events to be revised

AOT

* Uncontrolled positive reactivity insertion by reactivity control system from low power start up condition.
* Uncontrolled positive reactivity insertion by reactivity control system at the rated power.
* Positive reactivity insertion by sudden temperature drop of the primary coolant.
* Single and multiple reactor coolant pump trips.
* Pressure drop of the primary coolant.
* Loss of A-C power.

PA

* Core channel flow blockage.
* Reactor coolant pump shaft seizure.
* Loss-of-coolant accident resulting from the postulated primary coolant pipe breaks.

Table 3 Characteristics of the JMTR

Type	Tank Type	
Power	50 MW thermal	
Heat Flux (ave.)	115 W/cm^2	
Neutron Flux ($\times 10^{14}$ n/cm^2), (max.)		
	fast(>1 Me)	thermal
fuel region	4	4
reflector region	1	4
Fuel Element		
standard	22	
follower	5	
Moderator/Coolant		
material	H_2O	
inlet pressure	14 Kg/cm^{2}G	
inlet temperature	≦ 49 ℃	
coolant velocity	10 m/s	
Reflector		
material	Be, Al	

Table 4 Tripping Functions Considered in the Analysis

Tripping Function	Limiting Trip Point
High Core Inlet Pressure	17.1 Kg/cm^{2}G
Low Core Inlet Pressure	12.0 Kg/cm^{2}G
Low Primary Coolant Flow	4,000 m^3/hr
Low Differential Pressure between Core Inlet and Outlet	2.2 Kg/cm^{2}G
High Coolant Temperature Difference between Core Inlet and Outlet	10.5 ℃

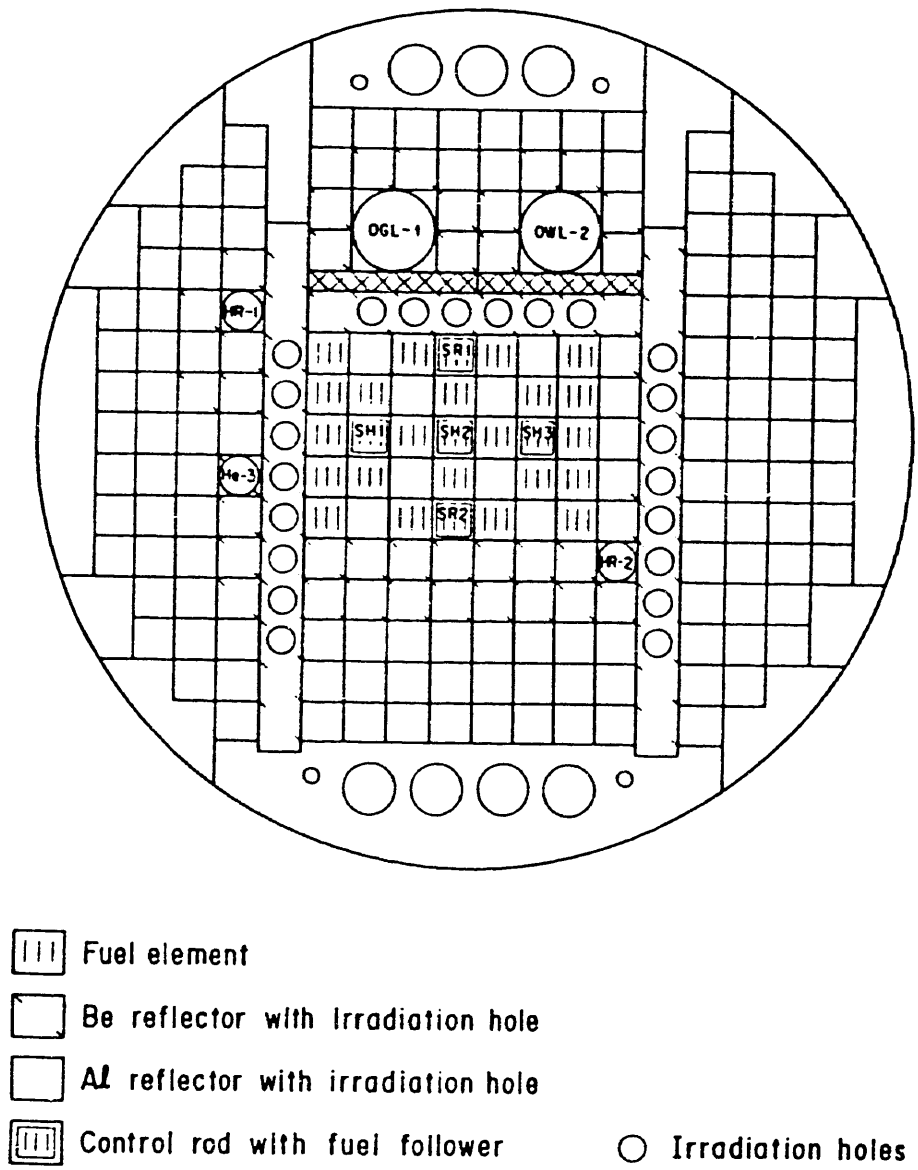

Fig. 1 JMTR Core Configuration

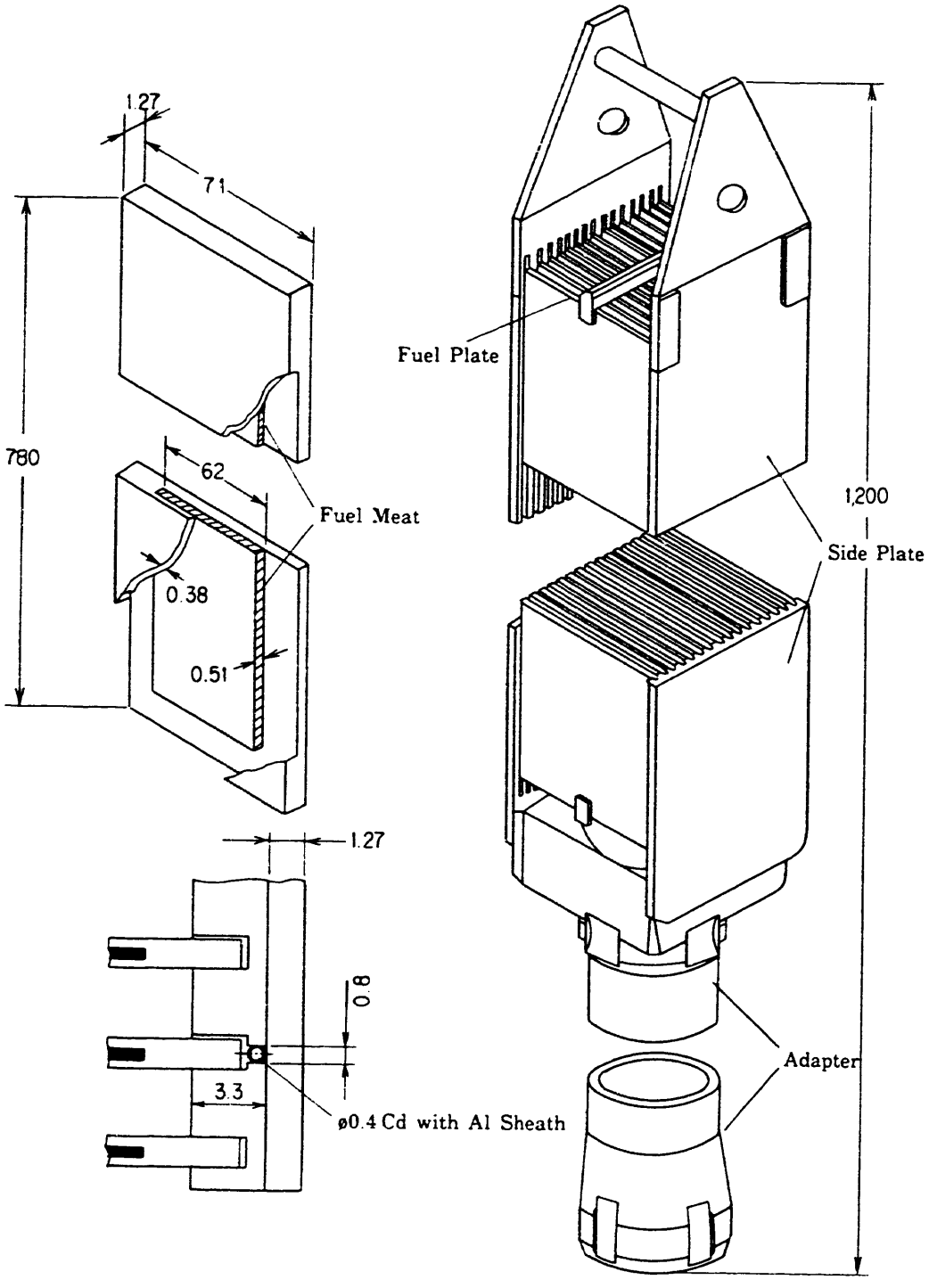

Fig. 2 Schematic Diagram of the Standard Fuel Element

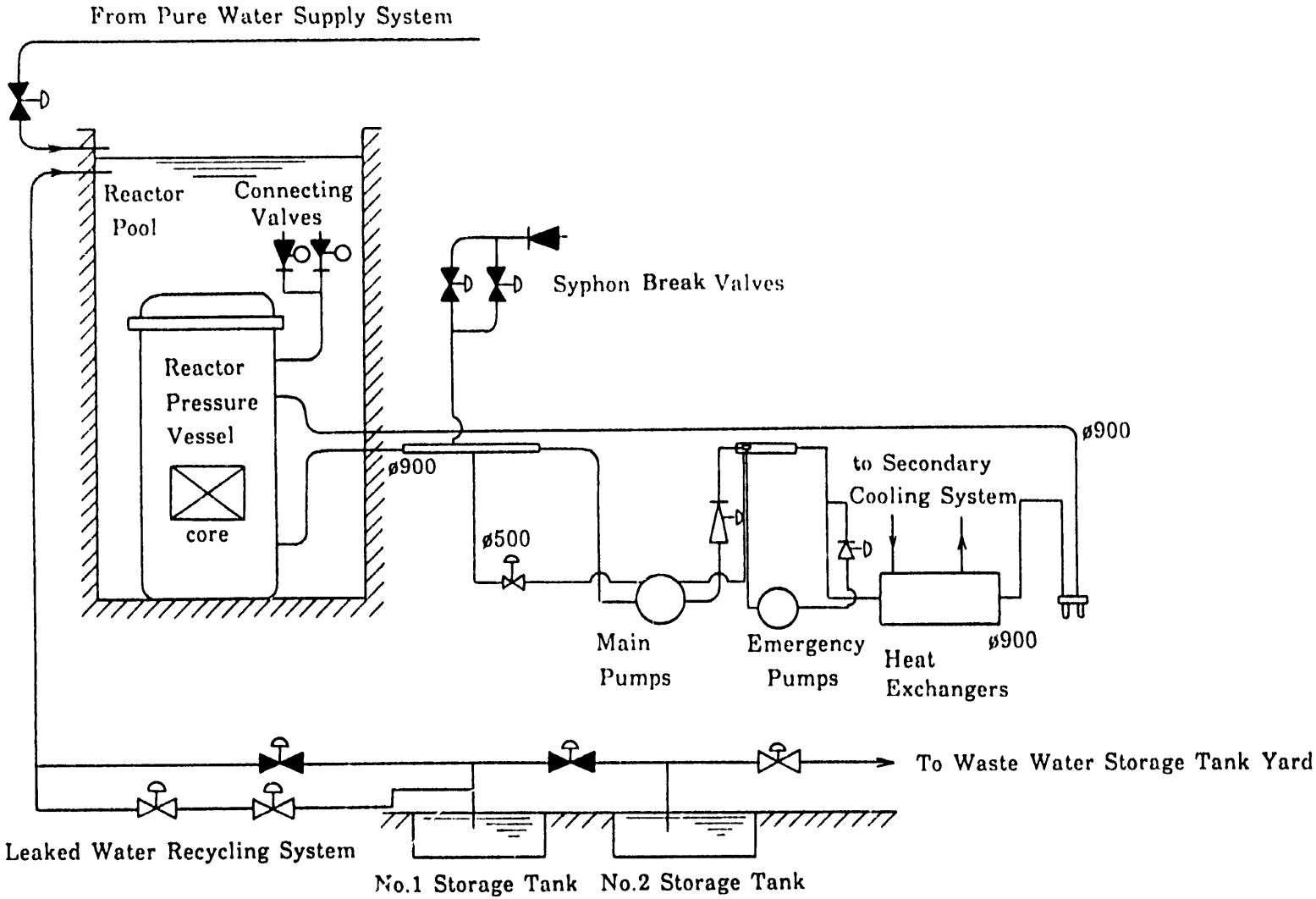

Fig. 3 Schematic Diagram of Primary Cooling System

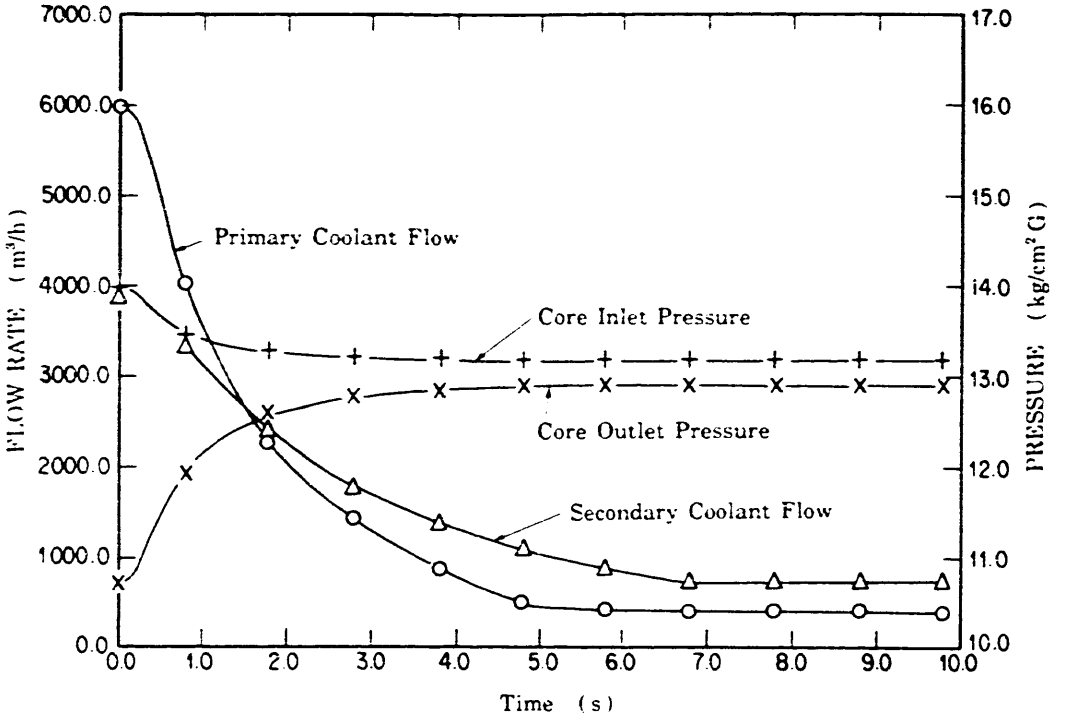

Fig. 4 Core Inlet and Outlet pressures, Primary and Secondary Coolant Flows
(Loss of A−C Power)

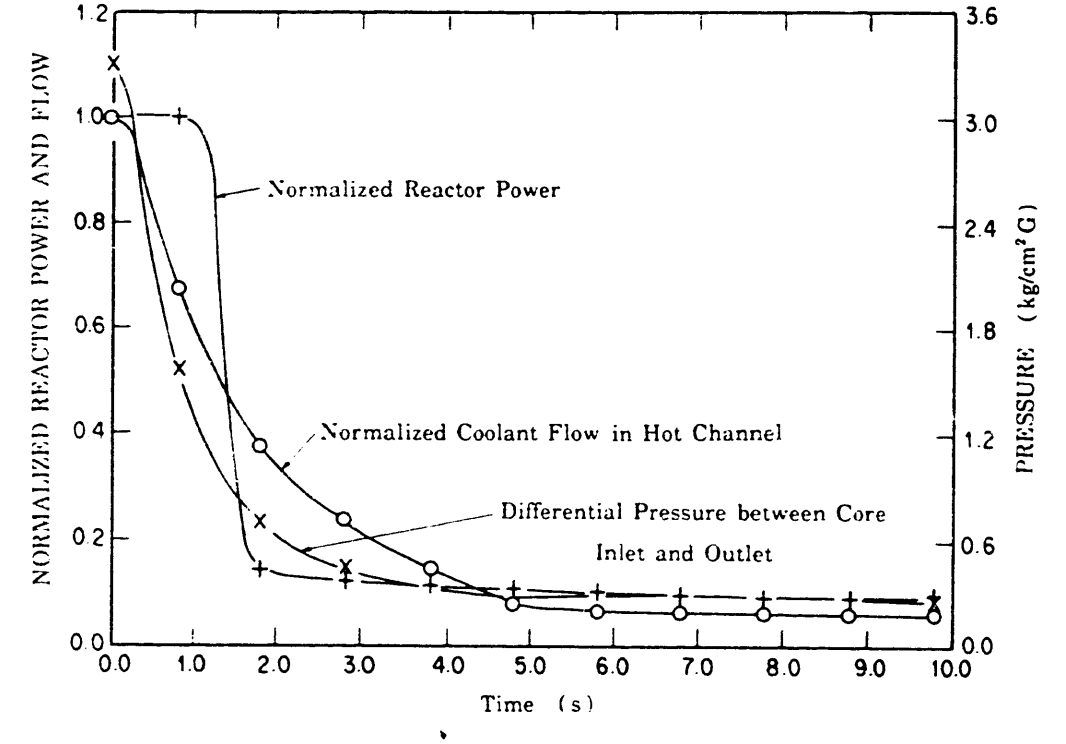

Fig. 5 Normalized Reactor Power and Coolant Flow in Hot Channel, Differential Pressure between Core Inlet and Outlet
(Loss of A−C Power)

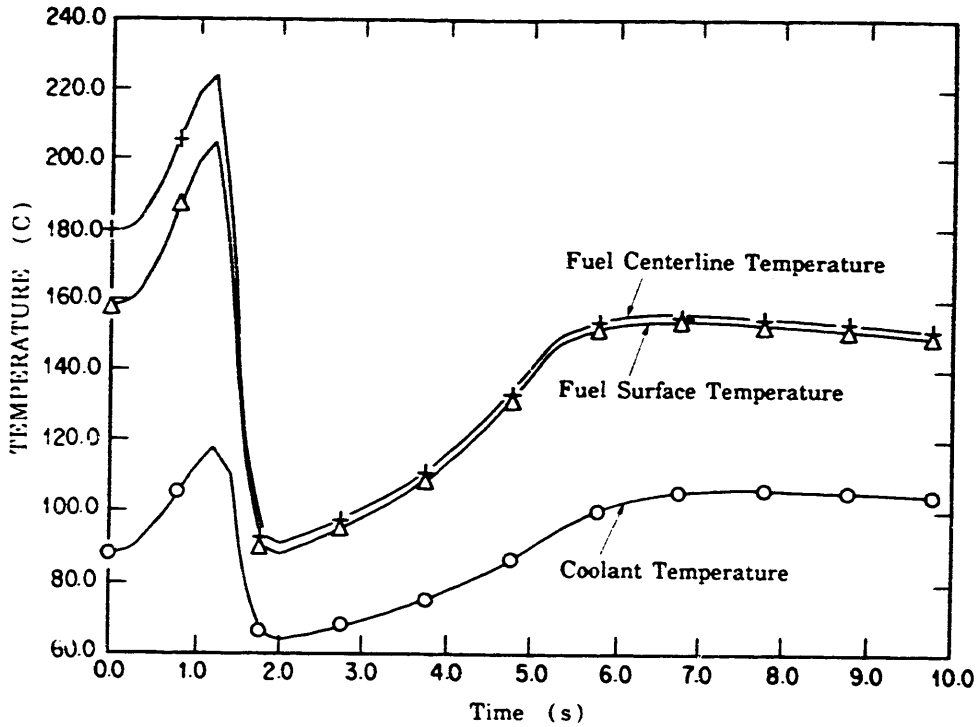

Fig. 6 Coolant, Fuel Centerline and Surface Temperatures at Hot Spot
(Loss of A–C Power)

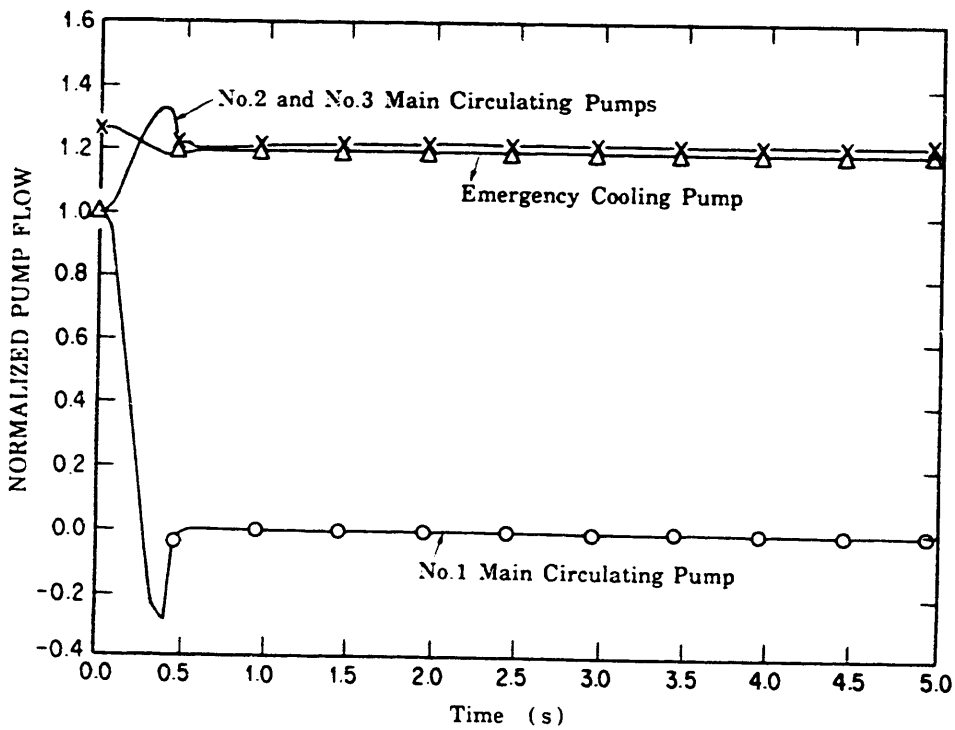

Fig. 7 Pump Flow in Primary Cooling System
(Primary Coolant Pump Shaft Seizure)

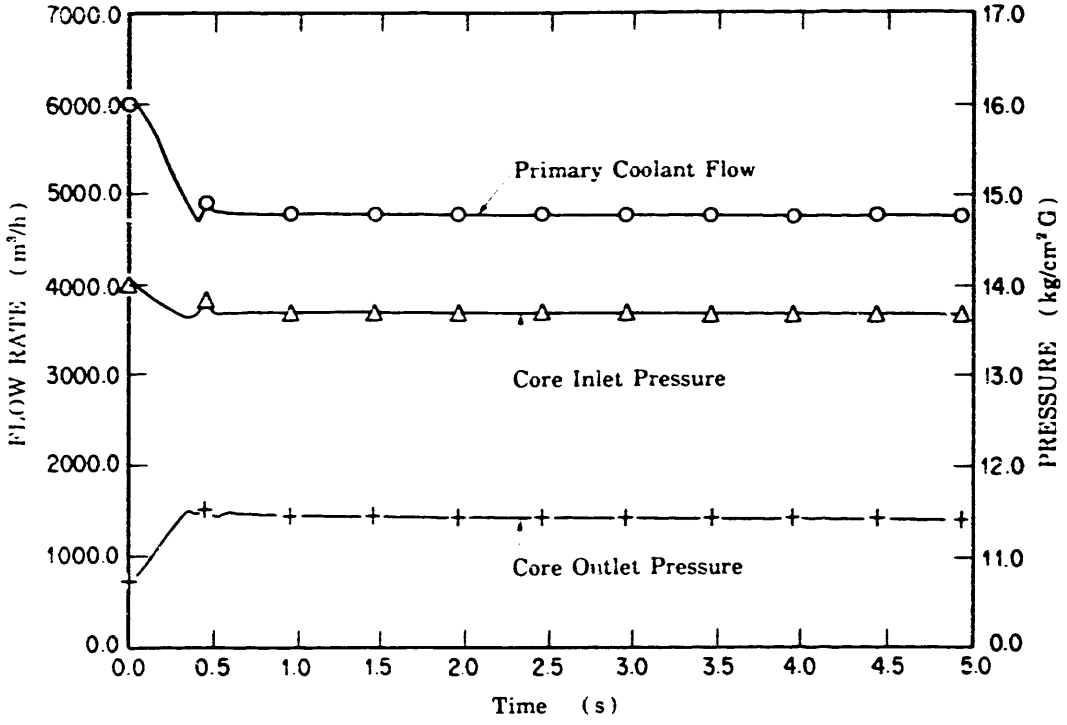

Fig. 8 Primary Coolant Flow, Core Inlet and Outlet Pressures
(Primary Coolant Pump Shaft Seizure)

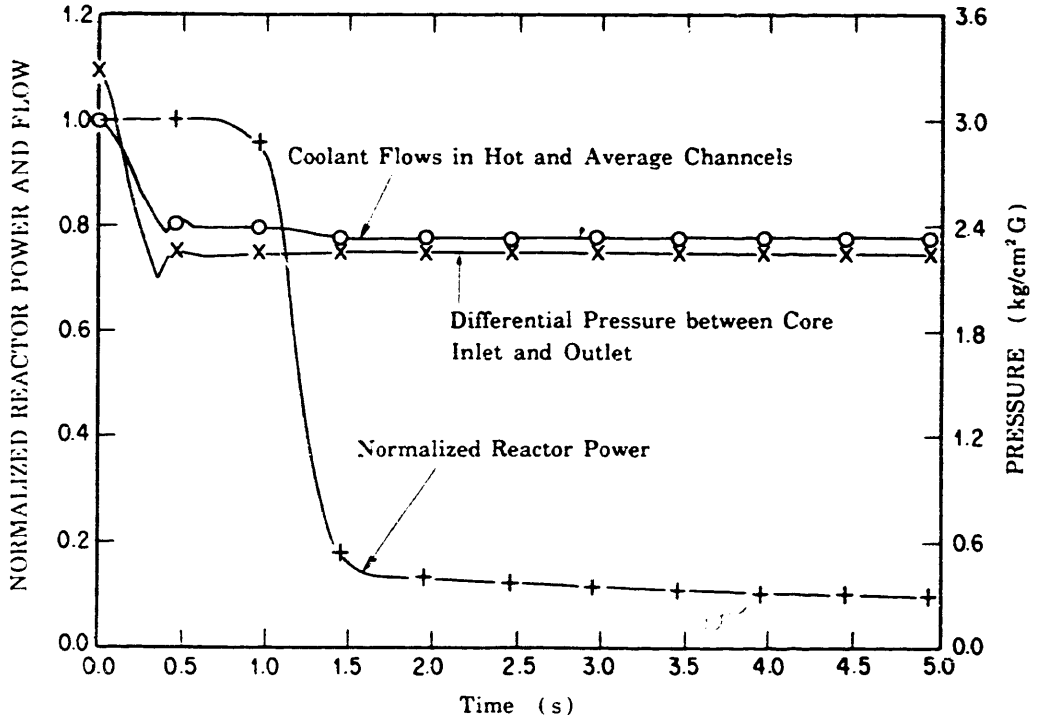

Fig. 9 Differential Pressure between Core Inlet and Outlet, Normalized Reactor Power and Coolant Flows in Hot and Average Channels
(Primary Coolant Pump Shaft Seizure)

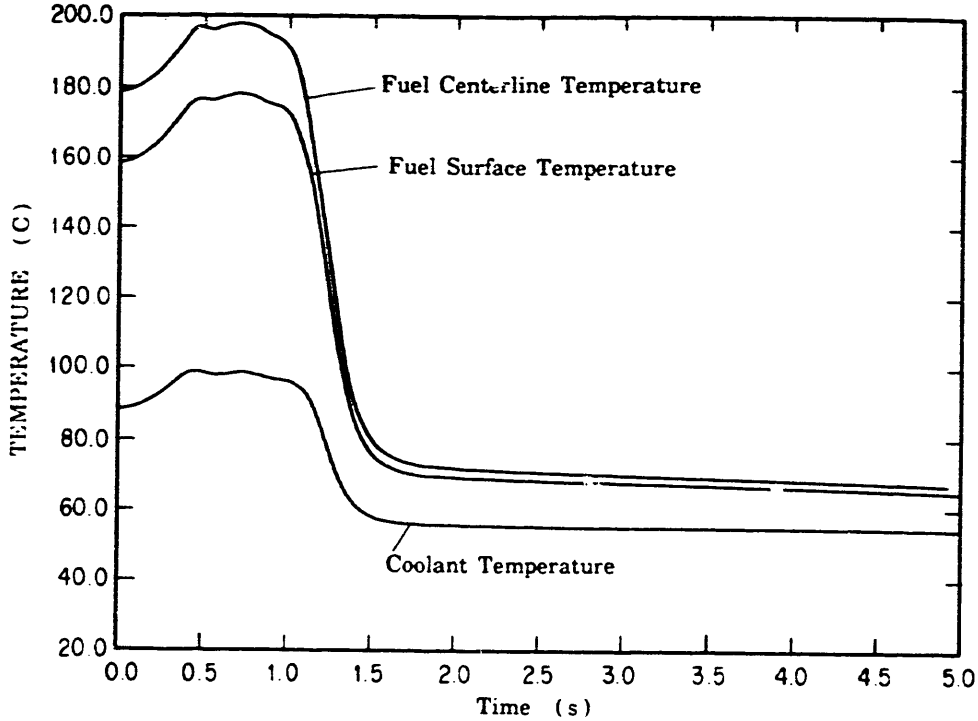

Fig.10 Coolant Temperature, Fuel Centerline and Surface Temperatures at Hot Spot
(Primary Coolant Pump Shaft Seizure)

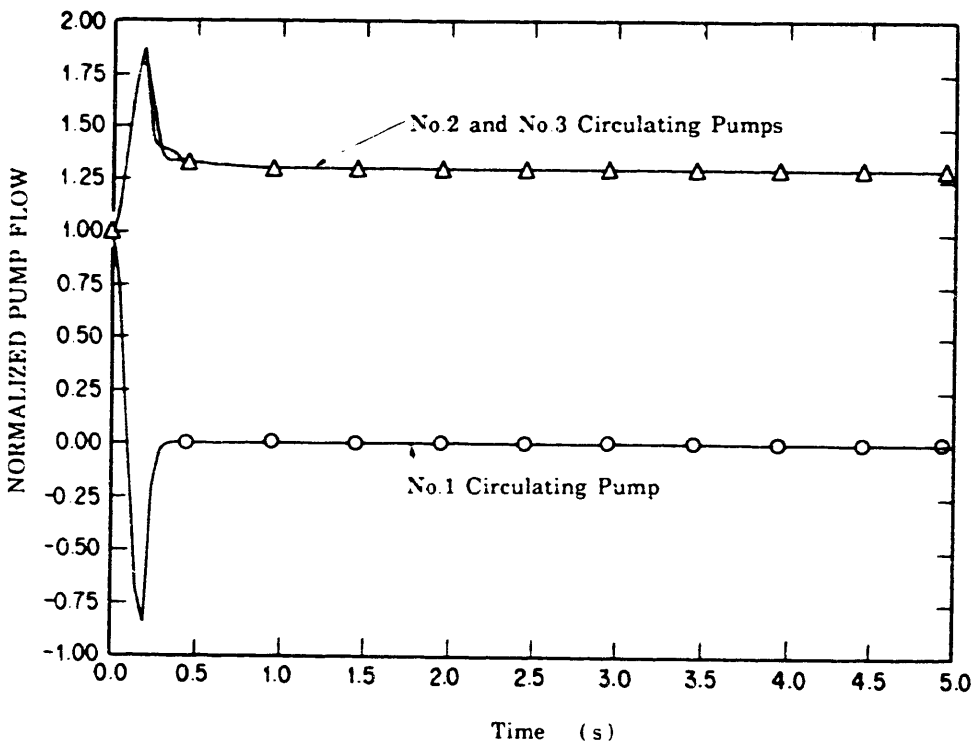

Fig. 11 Pump Flows in Secondary Cooling System
(Secondary Coolant Pump Shaft Seizure)

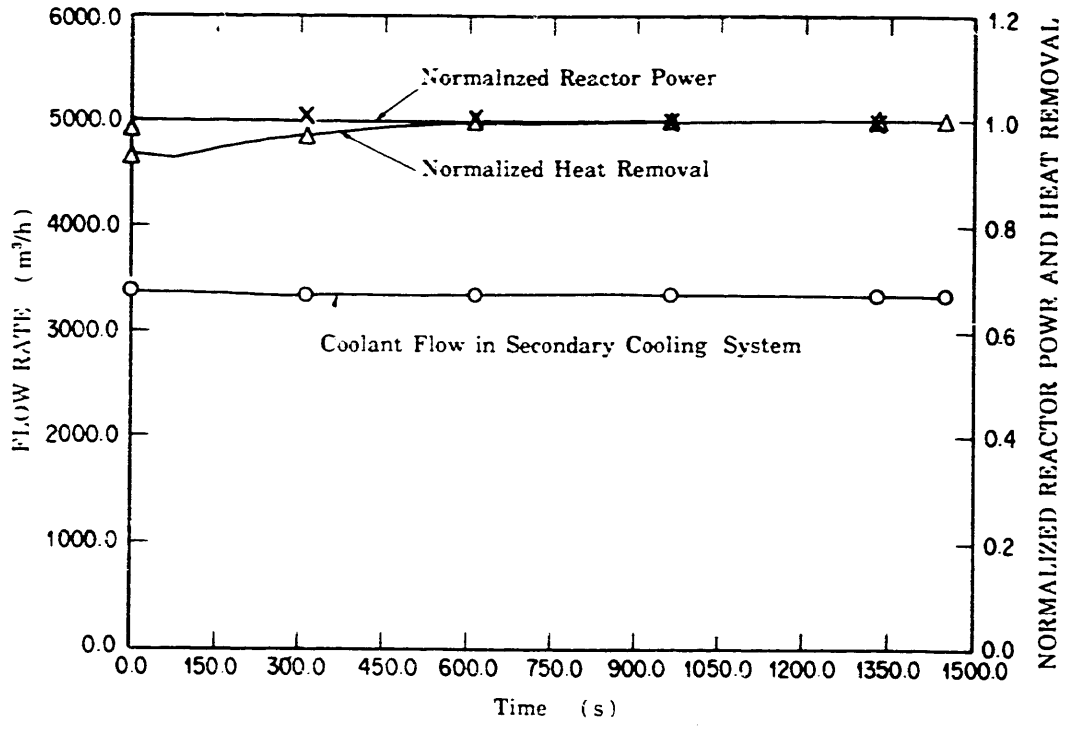

Fig. 12 Coolant Flow in Secondary Cooling System, Normalized Reactor Power and Heat Removal
(Secondary Coolant Pump Shaft Seizure)

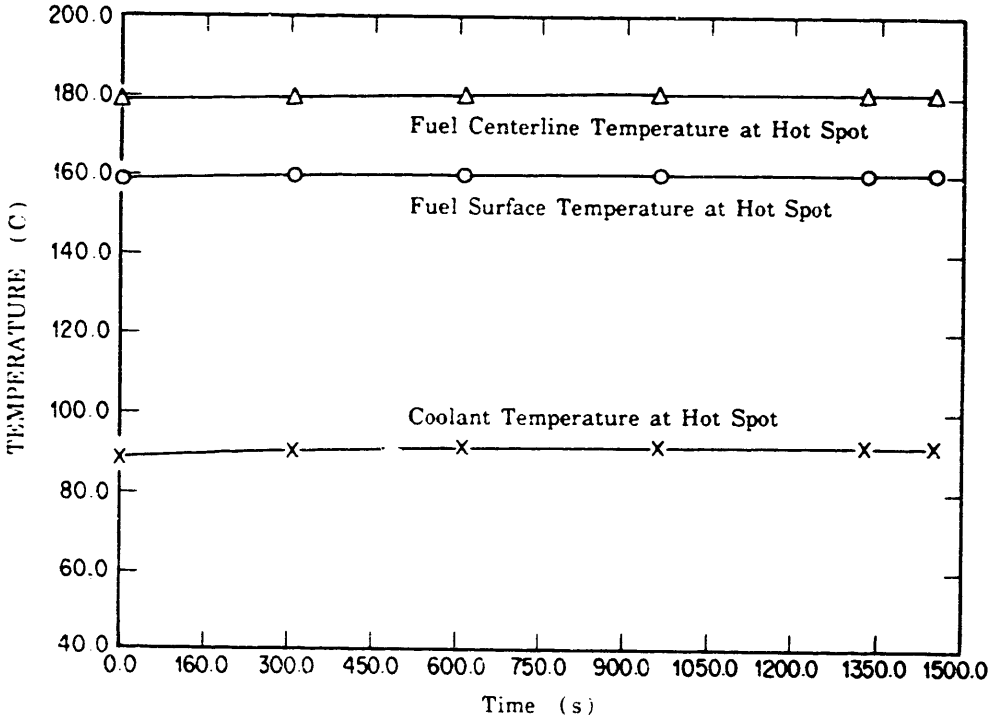

Fig. 13 Coolant, Fuel Centerline and Surface Temperatures at Hot Spot
(Secondary Coolant Pump Shaft Seizure)

PHYSICS OF THE MUNICH COMPACT CORE DESIGN

K. Böning, W. Gläser*, A. Röhrmoser

Fakultät für Physik E21, Technische Universität München,
D-8046 Garching, Germany

ABSTRACT

The project of a new research reactor in Germany aims at realizing an efficient neutron source optimized primarily for neutron beam applications. Since the reactor power has to be low from reasons of economy and public acceptance, our optimization studies have resulted in a particularly compact, light water cooled reactor core which is surrounded by a large heavy water moderator tank. This concept leads to high values of the thermal neutron flux in a large useable volume outside of the core - with an unperturbed flux maximum of about $8 \cdot 10^{14} \cdot cm^{-2} \cdot s^{-1}$ at only 20 MW power.

PHYSICAL OPTIMIZATION PRINCIPLE

A new national neutron source is planned to be constructed in the immediate neighbourhood of the existing Munich Research Reactor FRM at Garching. The idea was born some time ago and was first presented in 1981 [1]. In the design of this source highest priority has been given to its optimization with respect to beam tube applications. That is, the new reactor should provide a large useable volume with nigh flux levels and pure spectra of thermal neutrons outside of the core. These slow neutrons could then be used for many kinds of applications, out of which scattering experiments by means of beam tubes are most important. A particularly impressive example of an existing neutron source of this type is the high-flux reactor of the Institut ILL at Grenoble [2], which operates at nearly three times the power as has been set here for the new source and which provides a maximum thermal neutron flux (unperturbed) of about $1.5 \cdot 10^{15} \cdot cm^{-2} \cdot s^{-1}$.

The physical optimization principle can be described as follows. According to Fig. 1 we assume a relatively small cylindrical reactor core which is placed in the center of a large heavy water moderator tank. If we keep the reactor power P constant and reduce the active core volume V, as far as this is possible considering the requirement of safe core cooling, the average power density increases and so does the fission neutrons density. Since this small core is highly undermoderated, a large fraction of these fast neutrons immediately leaks out through the core surface and slows down in the surrounding high-quality moderator (D_2O). After thermalisation these

---

* present address: Institut Laue-Langevin, 156 X, F-38042 Grenoble, France

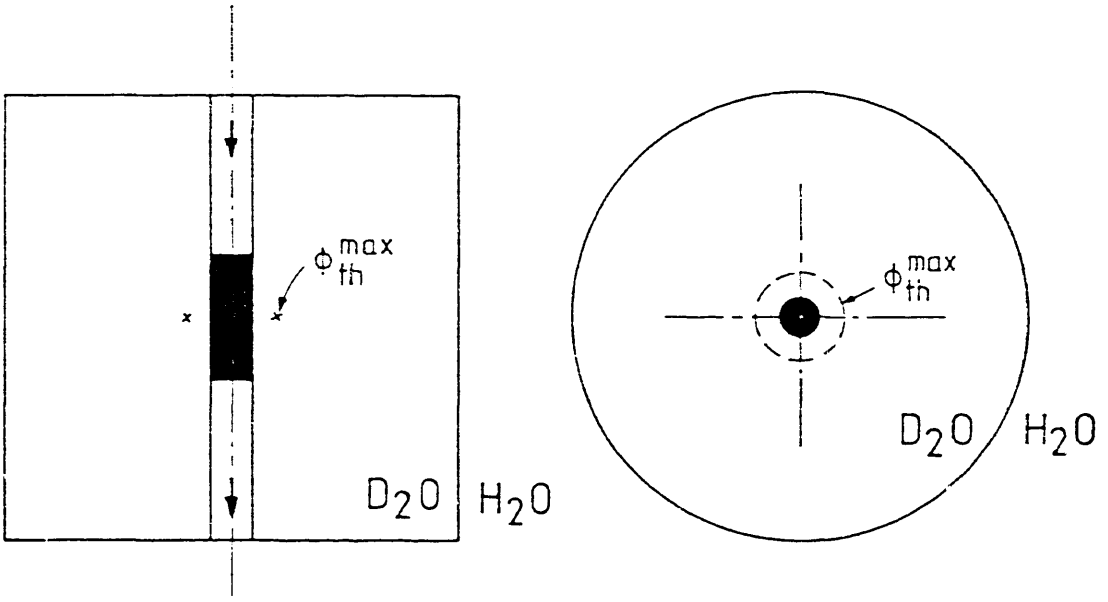

Fig. 1 Schematic view of a typical "inverse flux trap" research reactor (vertical cut at left, horizontal cut at right). The cylindrical core is shown in full black. In the heavy water (D_2O) moderator tank the position of the thermal flux maximum Φ_{th}^{max} is indicated but the beam tubes and other experimental or reactor installations were left out.

neutrons lead to the high thermal flux Φ_{th} and a very pure thermal spectrum in a large useable moderator volume as is required for their experimental utilization ("inverse flux trap", see Fig. 1). In this way the ratio of thermal flux in the region of the beam tube noses to reactor power assumes a high value, which means that a high flux level can be realized at low power.

Important contributions to this behaviour arise from the fact, that the effective neutron slowing-down volume in the D_2O moderator decreases and - additionally - the probability of neutrons diffusing back into the core decreases also when the core dimensions are reduced. This follows just from simple geometrical reasons. On the other hand, the choice of a smaller reactor core leads to problems such as a low multiplication factor or short reactor cycle, a high power density, the requirement of fuel with high U235 density, etc.. These and other aspects will be further discussed in the next section.

The physical arguments just given can easily be checked and confirmed by numerical calculations. In the unperturbed case of Fig. 1, i.e. without consideration of the experimental installations in the moderator tank, the whole arrangement has cylindrical symmetry (R,Z) whence 2-dimensional calculations allow a very realistic study of the core behaviour. As an example Fig. 2 shows in a comparison of those calculations that heavy water D_2O is the best material for our purpose since it provides both a large volume of high thermal flux and a large multiplication factor - as compared to the other moderator materials beryllium, graphite and light water H_2O.

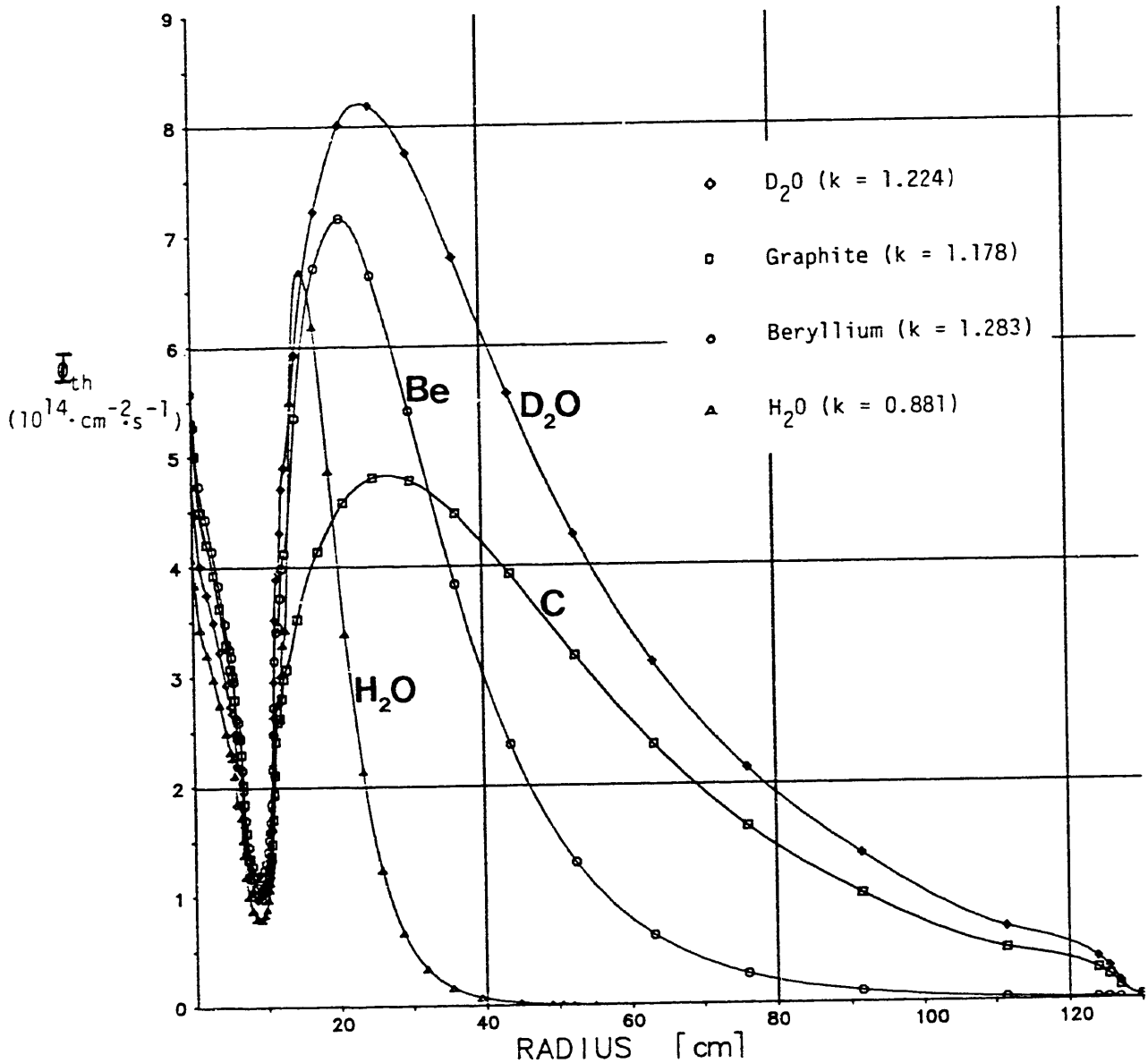

Fig. 2 Radial cut in the core mid-plane (Z = 0) through the whole core-moderator-arrangement for different materials of the moderator outside of the core as indicated. The thermal neutron flux Φ_{th} at 20 MW power is plotted and the values of the effective multiplication factor k are given for all the 4 cases considered. The core is always the same as discussed later in this paper (KKE7, but with constant uranium density and without boron absorber ring), compare Fig. 4, with the central control rod in its out-of-core position and the beryllium reflector inside of the core.

In another series of calculations the inner and outer radii of cores with otherwise identical geometry were varied in a way as to keep the active core volume constant. These calculations again clearly yielded the highest thermal flux maximum Φ_{th}^{max} for the smallest core. On the other hand some cycle-days are being lost in this case, because the reactivity at begin of life is somewhat smaller for the smaller core than for a core with a larger inner diameter. To compensate for this effect one could abandon the criterion of identical core volume; that means that the outer diameter of the smaller cores could be expanded until the same cycle length would be obtained for the different cores. The results then are without strongly significant differences. If the inner core diameter is increased in this way from 6.5 cm to 9.0 cm the neutron flux maximum would be obtained to be lower by about 4 %. The integral heating of the water in the hot flux line resulted to be identical at the begin of the cycle for the two cases considered here, which both guarantee the same cycle lenght as just discussed [3].

COMPACT CORE

The new high-flux research reactor which shall be optimized primarily for beam-tube experiments is being designed in Germany by a group at the Technical University of Munich. Since the reactor power has to be low from reasons of economy and public acceptance, its value has been fixed to P = 20 MW only. So the goal was to develop a particularly "efficient" neutron source. As a result, our studies have led to a particularly compact, light water cooled reactor core in a large heavy water moderator tank. The concept also has to provide a relatively long reactor cycle length of about 50 full power days, which was mostly an economical but also an experimental requirement. Fig. 3 shows the latest design of the compact core (version "KKE7"). The high enriched fuel (93 %) is contained in 113 involute-shaped plates with 0.60 mm meat thickness and 0.38 mm Al cladding on both sides. The active core volume of V = 17.6 liter is defined by inner and outer radii of 67.5 and 112.0 mm, respectively, and by 700 mm of height; it contains a total of 7.54 kg U235. Allowing for additional fuel-free zones with a radial span of 5 mm on both sides of the plates and for a thickness of the inner and outer Al core tubes of 6 and 7 mm, respectively, the radial dimensions of the complete core are 59.0 and 121.5 mm as indicated in Fig. 3. In the axial direction the fuel-free plate extensions are 15 mm wide on either end. As a consequence of the involutes the H_2O cooling channels between the plates have constant thickness, in this case 2.2 mm.

If we assume for simplicity that the reactor power P will be fully deposited in the active core volume V the average power density comes out to be P/V = 1.15 MW/liter; this value is of the same order as that of the HFR Grenoble or of the HFIR Oak Ridge. Flattening of the power density profile over the volume of the compact core will be achieved by two means. First, the density of the uranium in the new U_3Si_2/Al dispersion fuel will be radially graded into two zones: 3.0 g/cm^3 up to a radius of 105.6 mm and 1.5 g/cm^3 otherwise. That means that the U density will be significantly reduced in the outer core region where the thermal flux is particularly high because of the neutrons diffusing back from the D_2O tank. This discontinuous method to flatten the radial power density profile is considered to be better reproducible and more economical than grading the fuel continuously which would otherwise be superior.

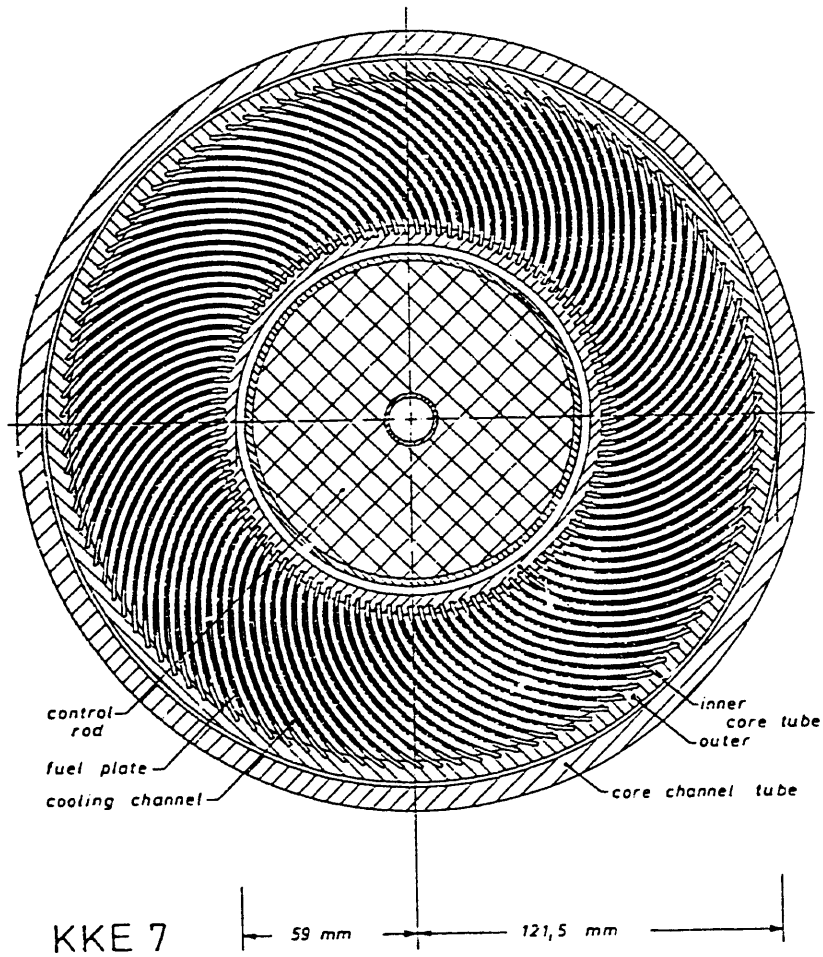

Fig. 3 Horizontal cut through the compact core (version KKE7) placed within the core channel tube which separates the H_2O region (inside) from the D_2O region (outside). The central control rod is in its out-of-core position, i.e. shown in this figure is the beryllium follower with its Al cladding.

The second means to flatten the power and fission density profiles refers to the axial direction. Here it is a ring of burnable poison, i.e. of an Al-cladded B/Al cermet with preliminary dimensions of 3 mm thickness and about 50 mm height, which is inserted into the outer core tube immediately below the lower end of the fuel plates. Initially this ring contains about 10 g of boron in its natural isotope composition. This solution is a very simple way to reduce the power density, especially at the axial core end, where a narrow peak is generated by the light water in the core channel tube. The alternative way of putting the poison into all the fuel plates would be more expensive [4].

Fig. 4 gives a schematic vertical cut through the central region of the reactor [5]. Shown are the plates (not the tubes) of the compact core and the boron ring B. The core channel tube CCT separates the H_2O primary coolant from the D_2O moderator regions (the full dimensions of the D_2O tank are both 2.5 m diameter and height). The reactor will be controlled by a central control rod CR, which according to the present design status is a cylinder of natural hafnium with 56 mm outer radius, 2.5 mm thickness and 820 mm height. Additionally there will be 5 or 6 safety absorber rods which

can be shot into the D_2O tank in case of emergency but which are fully withdrawn during regular reactor operation. The Hf cylinder of the central control rod is filled with aluminium (Al) and followed by a central reflector of beryllium (Be), the height of which is 900 mm.

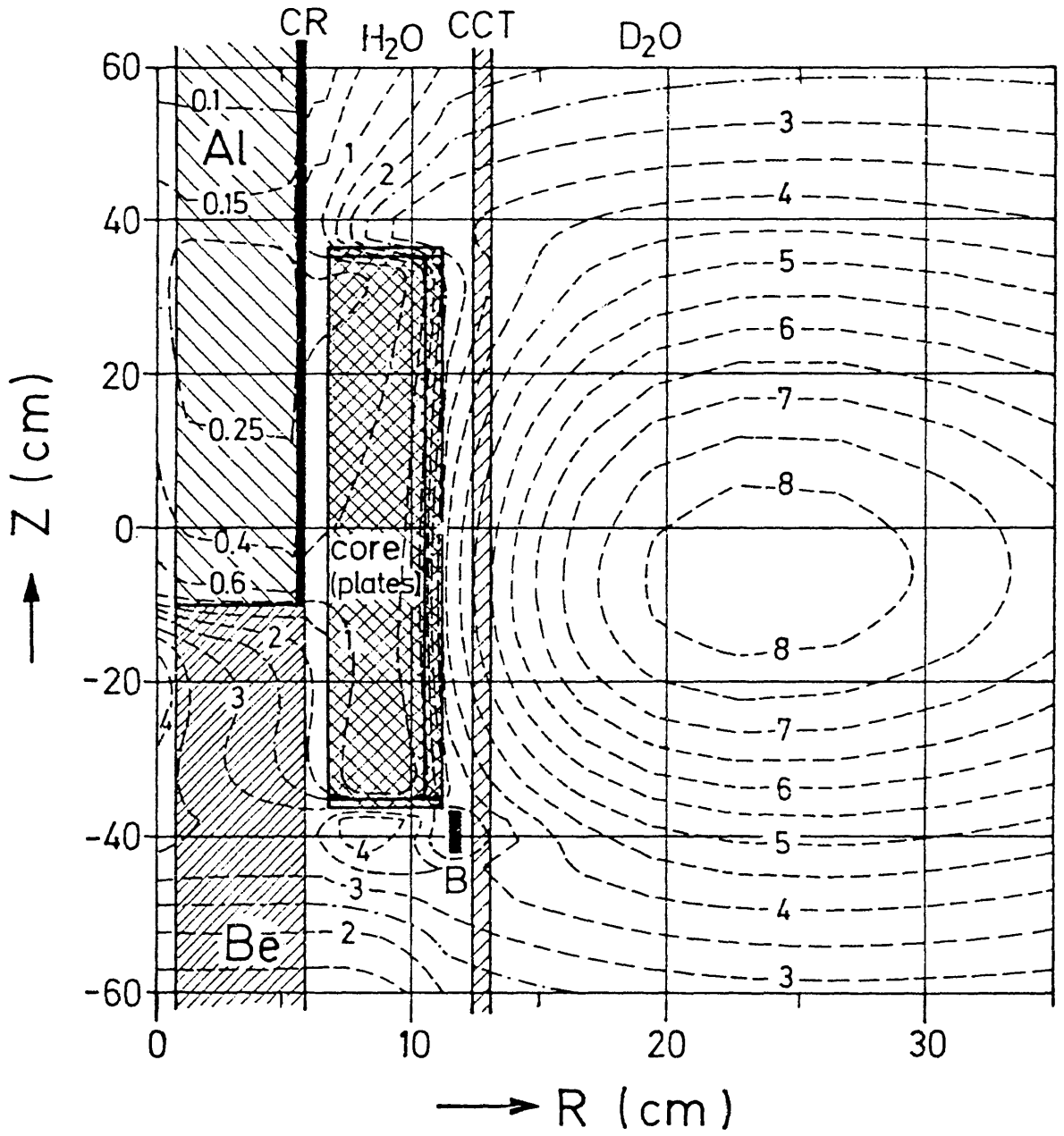

Fig. 4 Vertical cut through the whole arrangement. One can see the compact core KKE7 (only the fuel plates of which are shown here) with the boron ring B. The core channel tube CCT separates the H_2O coolant from the D_2O moderator. The control rod CR is shown in its position at the begin of the cycle (begin of life BOL), with its Al filler and Be follower. The contour lines represent the thermal neutron flux in units of $10^{14} \cdot cm^{-2} \cdot s^{-1}$ at 20 MW power.

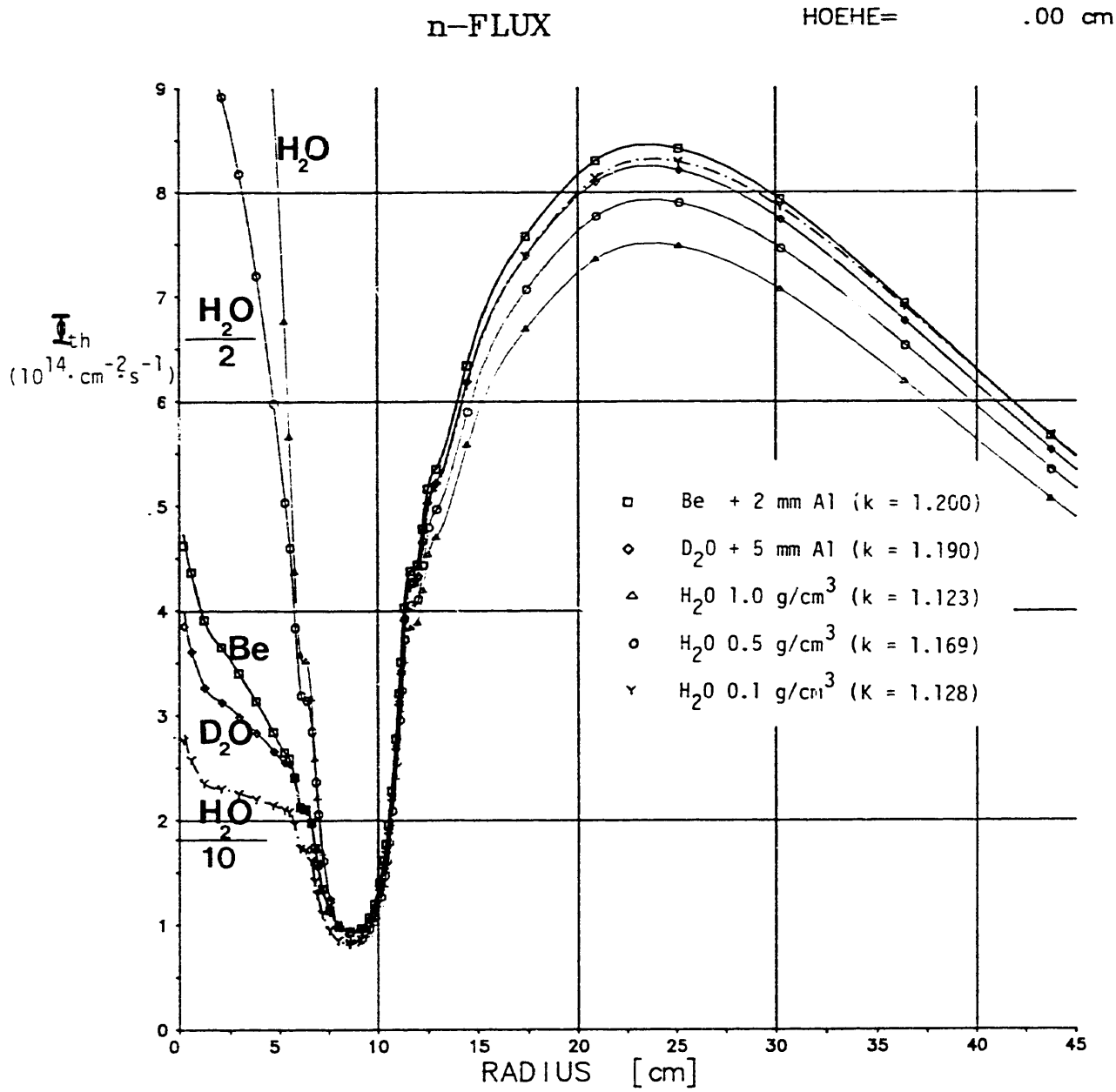

Fig. 5 Radial cut in the core midplane (Z = 0) through the whole core-moderator-arrangement for different materials of the reflector inside of the core as indicated. The thermal neutron flux Φ_{th} at 20 MW power is plotted and the values of the effective multiplication factor k are given for all the cases considered. The core is the compact core KKE7 as in Fig. 3 with the moderator outside of the core being always D_2O. The inner reflectors beryllium and heavy water are discussed inside an alu-bottle of 2 mm respectively 5 mm, and the case of light water is shown for 3 different densities.

As already mentioned in the first section, a particular problem of such a compact reactor core lies in achieving a value of the multiplication factor being large enough to allow a sufficiently long reactor cycle. So it is essential that the new high-density uranium-silizide fuel will be used with high enrichment in order to provide a sufficient U235-loading of the core. Further, core cooling by light water H_2O - instead of D_2O - is not only very attractive from operational and economical reasons, but is also necessary from physical arguments: the enhanced slowing-down strength of H_2O increases the in-core part of neutron moderation and so the multiplication factor (nevertheless the compact core is still highly undermoderated). In the central core channel below the control rod light water would not represent a good choice of a reflector material, since both beryllium and D_2O give rise to a longer reactor cycle. This is illustrated in Fig. 5. One can also see that the multiplication factor k shows a complicated behaviour if the H_2O density decreases in the central core channel, which comes from the variation in the balance of the neutron slowing down and absorption rates in H_2O. So the void coefficient of the light water inner reflector would be initially (down to a water density of about 0.4 g/cm^3) positive —— in contrast to the void coefficient of the (undermoderated) core itself which is always strongly negative. From these reasons the light water in the central core channel has been replaced by the beryllium reflector which is designed as a follower of the control rod.

Numerical neutron diffusion and transport calculations have been performed for the compact core reactor [3]. In the unperturbed case, i.e. without consideration of the experimental and reactor installations in the D_2O tank, and once the homogenized results of the fuel lattice cell calculations have been obtained, this is a problem of purely 2-dimensional geometry (R,Z). For the hypothetical case of the control rod being fully withdrawn from the core (i.e. if its lower end would be at Z = 45 cm in Fig. 4) the calculations yield a value of the multiplication factor of k = 1.192 for the fresh core at operating temperatures; this value would have been larger by 1.0 % without the boron ring. The position Z = - 9.8 cm of the control rod as shown in Fig. 4 corresponds to the situation at the beginning of the cycle, however with k kept at a fixed value about 4 % higher than the critical value of 1.0 . This is to compensate the reactivity reducing effect of the D_2O tank installations and also of some other details which have not been considered in these calculations. Contour lines of the thermal flux Φ_{th} at 20 MW have been obtained for this situation; they are also plotted in Fig. 5 and show how the neutrons concentrate in that part of the core which is not directly affected by the control rod absorber and that a maximum thermal flux of about $\Phi_{th}^{max} = 8 \cdot 10^{14} \cdot cm^{-2} \cdot s^{-1}$ piles up in the D_2O moderator. At the end of the reactor cycle - which comes out to be about 50 full power days - the control rod will be withdrawn from the core and the position of Φ_{th}^{max} will be more or less exactly on the core midplane (Z = 0).

Fig. 6 shows the local power density in the compact core at 20 MW as a function of the axial coordinate Z. The various curves refer to different radii as specified. The distinct power density maxima at both axial ends (Z = + 35 cm) are a consequence of the strong reflector peak of the thermal flux in the H_2O (compare Fig. 4). Due to the high thermalisation strength of H_2O this reflector peak is steeper and closer to the fuel zone as in the case of D_2O. This effect would be particularly distinct at the beginning of the cycle (BOL) as shown in Fig. 6 when the thermal flux is highly asymmet-

ric in Z because of the control rod. However, it is exactly for this situation that the boron ring has its strongest effect and - indeed - the power density maximum at the lower core edge (which would otherwise be of the order of 3.5 MW/liter) has been reduced to about 2.5 MW/liter. At the end of the reactor cycle the B10 absorber in the boron ring has practically disappeared ('burnt', remaining concentration about 7 %) and the control rod is withdrawn from the core; the power density curves are nearly symmetric in Z, then, their maximum being reduced to about 2.3 MW/liter and situated on the upper core edge, now. Finally, the two uppermost power density curves in Fig. 6 belong to the hot channels of the two core regions

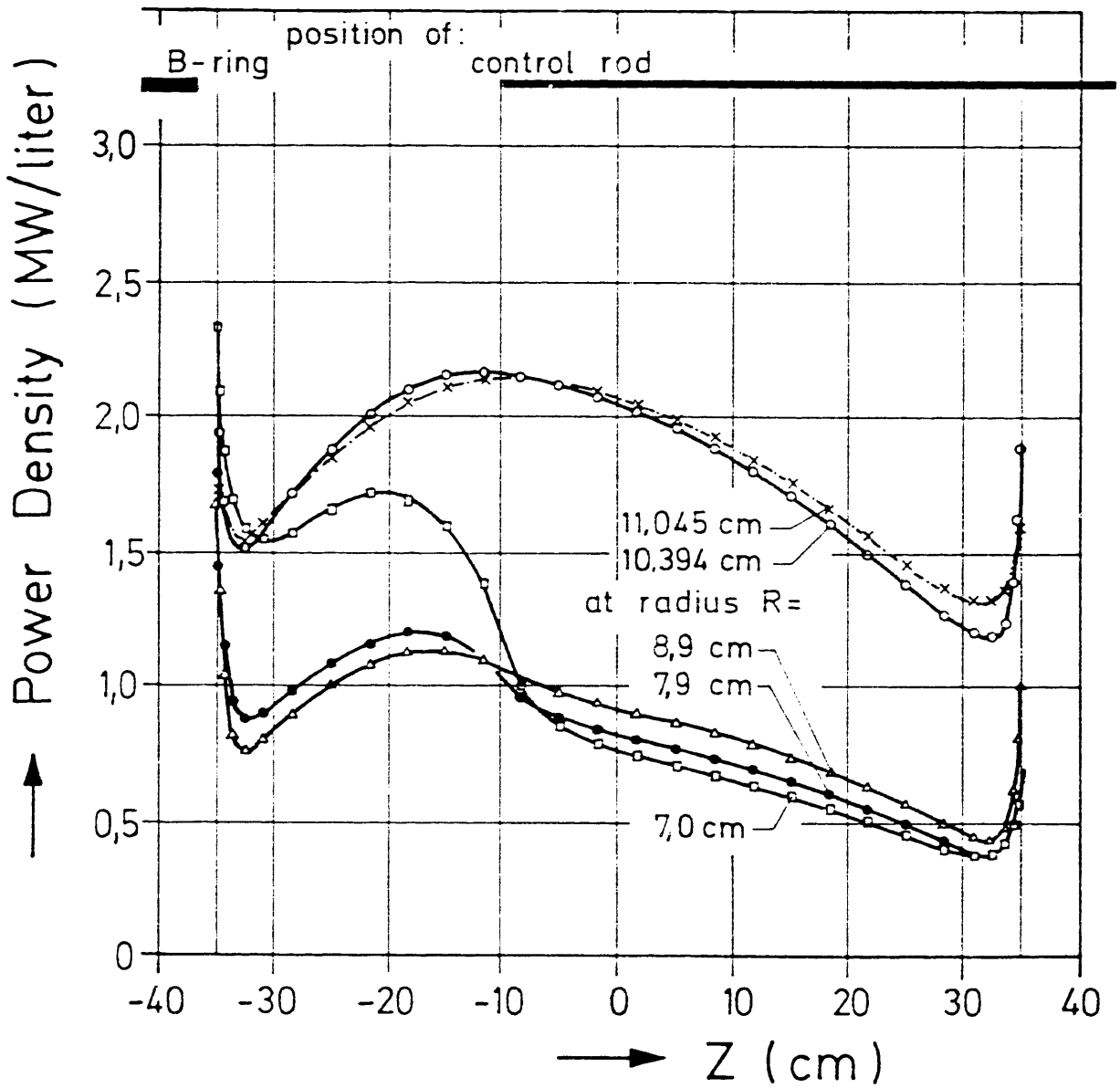

Fig. 6 Axial dependence of the local power density in the compact core KKE7 at 20 MW power. The various curves refer to different radii as specified. The position of the control rod is again that at the begin of the cycle (BOL); it is indicated on the top of the figure together with the axial position of the boron ring B (compare Fig. 4).

with different U density in the meat - apparently these two curves are virtually identical which demonstrates that the radial fuel grading is very effective and has been properly adjusted. During the reactor cycle the curve belonging to the largest radius decreases faster than the other one since the fuel burnup is stronger in the outer core region. At the end of the cycle the local maximum of the fission density in the meat amounts to $1.85 \cdot 10^{21}$ fissions/cm^3.

The primary cooling water will be flowing downwards through the core from technical reasons (core support and handling, etc.). There are in principle two possible directions to move the control rod during the reactor cycle. The first one would be to move it downwards, i.e. in the direction of the flow of the cooling water. This would be a good choice with respect to the begin of the cycle where most of the reactor power is produced in the upper half of the core where the cooling water has both a lower temperature and a higher pressure to improve the cooling conditions. However, the axial asymmetry of the power-density distribution is not very distinct at the begin of the cycle as a consequence of the flattening effect of the boron ring (Fig. 6). Further, at the end of the cycle the power density profile becomes rather symmetric, as has already been mentioned. So it is also possible - as far as core cooling is concerned - to move the control rod upwards, i.e. opposite to the directions of both the flow of the cooling water and the force of gravitiy. It is this latter solution which has been adopted now since it is considered to be strongly superior with respect to reactor safety. That means, even in the hypothetical case of a mechanical break of the control rod drive the absorber will be quickly forced down in its shut-down position by the combined action of the flowing water and of gravity.

The large dimensions of the D_2O moderator tank of both 2.5 m diameter and height (as at the HFR Grenoble) are essentially a consequence of the requirement to provide sufficient volume for the installation of the experimental (and some reactor) facilities. Of main interest in this context is, of course, a large useable volume with high thermal flux values as defined in the first section of this paper. Additionally, however, there are many applications where high thermal flux levels do not represent the essential requirement as compared to, e.g., the details of the neutron spectrum or the possibility to irradiate large or strongly absorbing samples. Applications of this kind can be performed in the outer regions of the D_2O tank - with only negligible influence on the neutronics of the core.

Final remark: the planned compact core reactor will be characterized by an unperturbed maximum thermal flux of about $8 \cdot 10^{14}$ cm^{-2}s^{-1} outside of the core at only 20 MW power - and by a flux to power ratio which is higher than at any existing reactor.

ACKNOWLEDGEMENTS

This work was supported by the German Bundesministerium für Forschung und Technologie BMFT.

REFERENCES

1. K. BÖNING, W. GLÄSER, J. MEIER, "Vorschlag einer Modernisierung des Forschungsreaktors München FRM", Internal Report of the Physik-Department der Technischen Universität München, Munich (1981)

2. K. SCHARMER, H.G. ECKERT, "FOEHN - Das kritische Experiment für den Deutsch-Französischen Hochflußreaktor", Report of the Kernforschungszentrum Karlsruhe, KFK 1064 (1971)

3. A. RÖHRMOSER, Ph. D. Thesis at the Technical University of Munich (in preparation)

4. L.BUTH, M. KÜCHLE, "Das Brennelement des HFR-Grenoble mit Festbor in den Rohren statt in den Platten", Internal Report of the Kernforschungszentrum Karlsruhe (1978)

5. K. BÖNING, W. GLÄSER, J. MEIER, G. RAU, A. RÖHRMOSER und L. ZHANG, "Status of the Design of the Munich Compact Core with Involute-Shaped Fuel Plates, in Proc. Int. Meeting on Reduced Enrichment for Research and Test Reactors (RERTR), Gatlinburg, Tenn., USA, Nov.1986, published as an ANL-Report

SOME OBSERVATIONS REGARDING RESEARCH REACTOR COMPARISONS TO THE SPERT TRANSIENT EXPERIMENTS

W. L. Woodruff
Argonne National Laboratory
Argonne, Illinois 60439 USA

ABSTRACT

The SPERT I experiments have been used in the Safety Analysis Reports of many research reactors to define safety limits on the maximum reactivity insertion. Comparisons for selected reactor cores show that transient parameters are quite sensitive to flow channel thickness, reactor size, and the pressure or coolant depth over the core. For example, higher operating pressures can in fact contribute to higher peak clad temperatures. Comparison of current HEU reactor designs with low power and large flow channels and proposed LEU designs show that the LEU designs will provide larger safety margins for reactivity insertions because of a higher void/density feedback and the addition of Doppler feedback.

INTRODUCTION

In the late 1950s and early 1960s, a wide range of reactivity insertion transients were carried out in the SPERT I series of cores[1] including destructive tests in the D-12/25 core.[2] Since these cores were similar in design to many of the light water cooled and moderated, MTR type, research reactors, the results of these experiments have been used in the Safety Analysis Reports (SARs) of many research reactors to define safety limits for reactivity insertion or maximum excess reactivity. These experimental data have also been used to evaluate various analytical[1] and computational[3] methods for the analyses of reactor transients.

The PARET code[3] is capable of computing results that give good agreement with the SPERT I tests. The code provides a means of comparing some types of research reactors with "similar" SPERT cores.

The International Atomic Energy Agency (IAEA) 10MW benchmark core[4] is representative of a large class of research reactors, and the clad melting threshold predicted by the PARET code has been found to compare favorably with that predicted by the D-12/25 tests.[3] The benchmark core is also compared with the B-24/32 SPERT core, which has a similar geometry.

A number of low power research reactor designs have fuel elements with only ten plates and rather large channel spacing. These reactors are most

similar to the D-12/25 core with twelve plates per element, but there are significant differences. Comparisons are provided which show the impact of some of these differences.

RESULTS AND DISCUSSION

The current version of the PARET code has been used to generate all of the results shown here. A $1.50 step insertion has been used as a convenient transient for comparison.

Two examples of research reactors are compared with the SPERT I D-12/25 and B-24/32 cores: 1) A small research reactor with 10 fuel plates in each standard element, referred to as RR10, and 2) The IAEA benchmark reactor with 23 plate standard elements. All of the reactors have Highly Enriched Uranium (HEU) fuel. RR10 represents an extreme case with a small core and a large channel thickness, while the IAEA benchmark reactor is more typical. Some of the geometric and kinetics characteristics are shown in Table I.

Table I. A Comparison of SPERT I, RR10, and Benchmark Properties

Reactor	Total No. of Plates	Coolant Channel, cm
SPERT D-12/25	270	0.455
SPERT B-24/32	768	0.165
RR10, HEU	169	0.658
Benchmark	551	0.223

Reactor	Neutron Gen. Time, μs	Beta Eff.	Density/void Coef., $/% void	Coolant Temp. Coef., $/K*100
SPERT D-12/25	60.0	0.0070	0.4214	2.801
SPERT B-24/32	50.0	0.0070	0.3571	2.527
RR10, HEU	60.9	0.0078	0.2710	0.732
Benchmark	56.0	0.0076	0.2992	1.646

The D-12/25 core has larger coolant channels and fewer plates than the B-24/32 core, but the D-12/25 core also has larger feedback coefficients. The RR10 core has an even larger channel spacing and even fewer plates than the D-12/25, while the feedback coefficients for both voiding and coolant temperature are considerably smaller. The void/density coefficient is about 2/3 of the D-12/25 value, and the temperature coefficient is only about 1/4 of that of the D-12/25 core. The other kinetics parameters for the prompt neutron generation time and beta effective are also somewhat larger and result in a larger inverse period, alpha, for the same reactivity insertion (see Table II).

Table II. Results with $1.50 Step Insertion of Reactivity

Reactor	P, MW	E_{tm}, MWs	Alpha, s^{-1}	T_{tm}, °C	Peak T, °C
D-12/25	225	4.94	65.8	238	325
RR10	219	3.87	74.2	267	496
D-12/25*	258	5.14	65.8	247	366
D-12/25**	286	5.16	75.6	248	356

*Using feedback coefficients from RR10 in SPERT D-12/25 core.
**Using feedback coefficients, beta effective and neutron generation time from RR10.

The RR10 with the HEU fuel does not behave like the D-12/25 SPERT core under similar transient conditions, as shown for a $1.50 step reactivity insertion in Table II. While the peak power (P) and the energy deposited to the time of peak power (E_{t_m}) are similar, the clad temperature at the time of peak power (T_{tm}) and the peak clad temperature (Peak T) are substantially higher for the RR10.

Kinetics Parameter Differences

Table II also shows the use of RR10 kinetics parameters with the SPERT I D-12/25 core. The smaller feedback coefficients in D-12/25* increases the peak temperature from 325°C to 366°C, but power and energy have also increased with these changes. The D-12/25** case with matching alpha shows a slight decrease in the peak clad temperature. The modified D-12/25 cases still have no film boiling and thus good heat transfer from the clad, while the RR10 has significant film boiling over the course of the transient and poor heat transfer. The feedback for the RR10 and the D-12/25 cores is substantially different even with the same parameters imposed.

The feedback for the RR10 and the D-12/25 reactors is compared at approximately the same energy deposition in Table III. Both the voiding and temperature feedback are substantially lower in the RR10. The voiding feedback is still high in the last case even with the lower coefficient from the RR10. Clearly other differences are contributing to these results.

Core and Channel Size Differences

While the differences are not independent and difficult to evaluate, an attempt has been made to isolate the sources of the differences noted. The power in the RR10 HEU case is distributed over far fewer plates, and with larger channel spacing the same voiding is a smaller percentage of the volume. These differences would contribute to a higher clad temperature, and if the temperature is high enough to initiate film boiling, the poor heat transfer can produce even higher clad temperatures.

Table III. Feedback and Energy Deposition Comparison

Reactor	E, MWs	Peak T, °C Ch. 1 / Ch. 2	Feedback Voiding / Temp., $
D-12/25	3.82	184 / 123	0.099 / 0.072
RR10	3.78	261 / 168	0.337 / 0.026
D-12/25	5.49	268 / 152	1.762 / 0.134
RR10	5.61	396 / 238	1.004 / 0.038
D-12/25	6.12	312 / 158	2.454 / 0.210
RR10	6.15	449 / 259	0.921 / 0.064
D-12/25*	6.13	304 / 168	2.185 / 0.039

*Using feedback coefficients, beta effective and neutron generation time (kinetics parameters) from RR10.

The SPERT I D-12/25 core with the RR10 kinetics parameters is used here as a reference case. The total number of plates in D-12/25 can be reduced from the original 270 toward the 169 in the RR10 as shown in Table IV with the channel spacing held constant. This could be taken as a reduction in the number of fuel elements in the core, but no effort has been made to make the numbers necessarily correspond to any physically realizable cases. Also the loading in the cases with fewer plates would have to increase to preserve reactivity, and this in turn would result in changes in the conductivity and volumetric heat capacity of the fuel meat. These changes have not been included but should be of only minor importance. The kinetics parameters would also change with core size but have been held constant. In the last two cases in Table IV, the channel spacing is increased to match the RR10 value.

The cases with fewer and fewer plates result in the clad and coolant heating up faster, more feedback, and a lower peak power and energy deposition to time of peak power. The power and energy deposition in the fuel, however, are just proportional to the number of plates in the core (172/270 * 286 MW = 182 MW vs 181 MW shown in table). Thus, the clad temperatures are about the same for all cases. The film boiling finally reached in the 172 plate case is rather modest and the energy stored in the fuel is still low. The threshold for film boiling has been reached. The RR10 results exhibit a significant degree of film boiling as noted earlier.

Increasing the channel spacing has more influence on the clad temperature as shown in Table IV. This increase in coolant volume reduces the feedback and allows the power following the peak to remain higher, and a higher clad temperature is reached. Table V compares the 172 plate model with and without the increased channel spacing over the course of the transient. The peak clad temperatures reached still do not compare with the RR10 case shown in Table II, and other differences must be found.

Table IV. Performance Variation with Number of Elements (Plates)

D-12/25 Case	P(P/Plate), MW	Peak T, °C	Boiling
270 Plates	286 (1.06)	360	Transition
235	249 (1.06)	360	Transition
200	211 (1.06)	360	Transition
180	191 (1.06)	360	Transition
175	185 (1.06)	360	Transition
172	181 (1.06)	360	Film
175*	196 (1.12)	400	Film
172*	192 (1.12)	400	Film

*Channel spacing increased from 0.455 cm to 0.658 cm matching RR10.

Table V. Effects of Increasing the Channel Spacing in D-12/25

172 Plate Data: With Channel Increase / Without Increase

t, s	P, MW	E, MWs	T_C, °C	Void/Dens. Feedback, $
0.285	76.8 / 75.9	1.20 / 1.19	113 / 112	0.0043 / 0.0054
0.290	105 / 103	1.65 / 1.63	142 / 141	0.0066 / 0.0084
0.295	143 / 140	2.26 / 2.24	173 / 172	0.0177 / 0.0228
0.300	184 / 177	3.08 / 3.04	231 / 230	0.1785 / 0.2320
0.301	191 / 181	3.27 / 3.22	245 / 244	0.2540 / 0.3570
0.302	192 / 179	3.46 / 3.40	260 / 259	0.5393 / 0.7848
0.304	171 / 144	3.83 / 3.72	291 / 288	1.2536 / 1.6925
0.306	133 / 98.9	4.14 / 3.97	319 / 313	1.5527 / 2.1169
0.308	99.6 / 63.9	4.37 / 4.12	342 / 331	1.6075 / 2.1094
0.310	74.4 / 41.6	4.54 / 4.23	360 / 343	1.5462 / 2.1255
0.315	38.9 / 16.4	4.81 / 4.36	388 / 358	1.4156 / 1.8420
0.320	22.3 / 8.0	4.96 / 4.42	401 / 358	1.2244 / 1.5803
0.325	14.3 / 4.8	5.05 / 4.45	400 / 350	1.2172 / 1.4027
0.330	9.8 / 3.8	5.11 / 4.47	398 / 348	1.2206 / 0.8818

Operating Pressure Differences

Other differences such as the direct heating source to the coolant, plate width, inlet coolant flow rate, and fuel conductivity were considered but were not found to be significant contributors. The difference noted in the operating pressure of 113.3 kPa for SPERT and 169.6 kPa for RR10 (deeper pool) was found to be significant. Table VI shows the effect of changing only the operating pressure in the initial D-12/25 core to that of the RR10 core. The peak clad temperature increases by 62°C. The peak power and energy deposition also increase.

Table VI. Effects of Increasing Operating Pressure in D-12/25

Press, kPa	P, MW	E_{tm}, MWs	T_{tm}, °C	Peak T, °C
110.0	224	4.90	236	321
120.0	229	5.04	243	337
130.0	234	5.19	250	347
140.0	239	5.29	254	354
150.0	243	5.43	261	363
160.0	247	5.55	266	373
170.0	248	5.59	268	383

While a higher operating pressure gives a larger margin to the onset and departure from nucleate boiling, the dynamics of the reactivity insertion transient and the benefits of surface boiling to heat transfer and feedback must also be considered. By increasing the pressure in the SPERT model, boiling (voiding) is suppressed and the lower feedback results in an increase in the clad temperature. Also, heat transfer in single phase is generally lower than two phase (until film boiling is reached), and this contributes to a higher clad temperature.

The cumulative effects of changing the SPERT I D-12/25 core parameters to the values for the RR10 HEU core are summarized in Table VII. The third through fifth cases all have 172 plates rather than the 169 in the RR10. A peak clad temperature was not reached in the case with increased operating pressure. With a reduction to 169 plates this case would more nearly agree with the RR10 results. The two cases still have differences in the axial distributions and peaking factors that contribute to some of the differences observed. The peaking factor for the SPERT core is 1.83 compared to a value of 1.65 for the RR10 core. The importance of operating pressure on the void/density feedback to the transient behavior of the reactor has been clearly demonstrated.

Table VII. Cumulative Effects of RR10 Values in SPERT D-12/25

Case	P, MW	E_{t_m}, MWs	T_{t_m}, °C	Peak T, °C
Ref. (270 Plates)	225	4.94	238	325
Kinetics Parms.	286	5.16	248	356
& 172 Plates	181	3.27	248	360
& Ch. Increase	192	3.41	255	402
& Press. Increase	225	3.99	297	547+*
RR10, HEU	219	3.87	267	496

*Peak temperature not reached in this case.

Differences with LEU Fuel

The proposed LEU conversion fuel for the RR10 class of reactors has an 18 plate standard element and a much smaller channel spacing than the HEU case. The characteristics of the two cores are shown in Table VIII. The density/void coefficient is larger for the LEU case, but the coolant temperature coefficient is lower. The most important difference is the significant Doppler coefficient in the LEU fuel. The results of a $1.50 step insertion are also compared in Table VIII. The peak clad temperature is much lower for the LEU core and more comparable to the SPERT values at a similar pressure. The HEU SPERT cores, however, should not be used for comparison in the LEU cases.

Table VIII. RR10 with Proposed LEU Fuel

Fuel	Plates/ Standard Element	Total No. of Plates	Coolant Channel, cm	Neutron Gen. Time.	Beta Eff.
LEU	18	301	0.316	50.5	0.00787
HEU	10	169	0.658	60.9	0.00785

Feedback Coefficients

	Density/Void Coef., $/%	Coolant Temp. Coef. $/K*100	Doppler Coef. $/K*100
LEU	0.2991	0.245	0.186
HEU	0.2710	0.732	0.0

Transient Results

	P, MW	E_{t_m}, MWs	T_{t_m}, °C	Peak T, °C
LEU	234	4.52	257	358
HEU	219	3.87	267	496

Benchmark Comparison

As shown in Table I, the channel spacing for the benchmark core is somewhat larger than the B-24/32 SPERT core, while the core size (number of plates) is smaller. The feedback coefficients for the benchmark are smaller than either of the SPERT cores considered here. The operating pressure for the benchmark core is 170 kPa as in the RR10 case and higher than that in the SPERT cores. The benchmark core has forced flow.

Again a $1.50 step insertion is used with the benchmark core, and the results are compared with both SPERT cores in Table IX. Although the benchmark core would appear to be more similar to the B-24/32 core, the result are considerably different. The agreement is more favorable for the D-12/25 core, and as noted earlier the threshold for clad melting in the benchmark agrees very well with the results from the D-12/25 tests.

Both SPERT cores predict a higher clad temperature than that computed for the benchmark core, and the case where the pressure is reduced to match that of the SPERT cores gives even lower values. At least in these cases a SPERT comparison would be conservative.

The benchmark core with LEU fuel has been shown[3] to give a peak clad temperature that is 45°C lower than the HEU case. The threshold for clad melting was predicted to be $2.35 for HEU and $2.80 for LEU in the benchmark core and $2.30 for the D-12/25 SPERT core (in excellent agreement with the experimental results). Another study[5] has predicted a step of $3.7 as the threshold for clad melting in the B-24/32 core and values in excess of $3 for most of the other cores in the SPERT I series. These values, however, disagree with the D-12/25 and benchmark results. The other cores in the SPERT series, did not include destructive tests. Thus, experimental data in this range is not available for direct comparisons.

Table IX. Benchmark Core Comparison with SPERT Cores

Reactor	P, MW	E_{t_m}, MWs	T_{t_m}, °C	Peak T, °C
D-12/25	225	4.94	238	325
B-24/32	576	11.8	215	301
Benchmark	342	6.61	204	271
Benchmark*	308	5.82	179	242

	Clad Melting Threshold, $
D-12/25	2.30
Benchmark, HEU	2.35
Benchmark, LEU	2.80

*Operating pressure reduced from 170 kPa to 113.3 kPa.

CONCLUSIONS

Based on these results, a somewhat atypical 10 plate/element RR10 HEU core shows significant differences when compared to the SPERT I D-12/25 core; the differences observed appear to be the result of an accumulation of differences in feedback, reactor size, channel spacing, and operating pressure. In the HEU cores the void/density feedback is the most important component. The void/density coefficient is less important in the LEU case because Doppler feedback plays a significant role. The proposed LEU fuel also has a more typical channel spacing and number of plates per element. Thus, the LEU fuel has a much lower peak clad temperature than the HEU case.

With the IAEA benchmark core, though more typical, the transient results still do not compare well with the SPERT I cores. The peak clad temperature for both SPERT cores is higher than that for the benchmark core. In earlier work the PARET code was found to give good agreement with the SPERT I tests including the prediction for clad melting in the D-12/25 core for a $2.30 step insertion. A slightly higher clad melting threshold of $2.35 for the benchmark core is consistent with the peak clad temperature estimates. Estimates by others of in excess of $3 for the B-24/32 and other SPERT I cores would seem to be out of line with these findings. Again the LEU fueled core requires a larger reactivity insertion to initiate melting than the HEU case.

Some differences between research reactors and the SPERT I cores that at first may seem unimportant can contribute to some substantial differences in the transient behavior. The strong influence of the operating pressure on the transient response is one such example. These differences do not always contribute to a conservative safety margin when comparison are made to the SPERT cores. Most research reactors have set very conservative reactivity insertion limits that are well below limits reported for any of the SPERT I tests. Since the SPERT I series did not include LEU cores, the results cannot be used for direct comparison to the LEU conversion cores. The conversion to LEU fuel in most cases leads to larger safety margins, but some additional analysis may be useful.

ACKNOWLEDGEMENTS

This author is very grateful to Mr. K. E. Freese of ANL for his contributions to the computation of kinetics parameters for this work and to Dr. J. E. Matos for his many helpful discussions.

REFERENCES

1. S. G. Forbes, et al., "Analysis of Self-shutdown Behavior in the SPERT I Reactor," IDO-16528, Idaho National Engineering Laboratory (1959).

2. A. H. Spano and R. W. Miller, "SPERT I Destructive Test Program Safety Analysis Report," IDO-16790, Idaho National Engineering Laboratory (1962).

3. W. L. Woodruff, "A Kinetics and Thermal-hydraulics Capability for the Analysis of Research Reactors," Nucl. Tech., 64, 196-206 (1983).

4. "Research Reactor Core Conversion from the Use of Highly Enriched Uranium to the Use of Low Enrichment Uranium Fuels Guidebook," IAEA-TECDOC-233, International Atomic Energy Agency (1980).

5. Reactor Physics Constants, ANL-5800 (Second Edition), Argonne National Laboratory (1963).

SESSION VIII

September 21, 1988

TARGETS

Chairman:

J. Matos
(ANL, USA)

PRODUCTION CYCLE OF FISSION MOLYBDENUM-99

Sameh A. Ali and H. J. Ache
Nuclear Research Center Karlsruhe
Institute of Radiochemistry
7500 Karlsruhe, P. O. Box 36 40, D - 7500 Karlsruhe, FRG

ABSTRACT

Technetium-99m for human organ function tests has to fulfill high quality standards such as nuclear purity, maximal specific activity and radionuclid concentration. This can be only realized by using technetium, generated from fission molybdenum-99 separated from irradiated shortly cooled nuclear fuel targets. The actual world-wide used uranium targets with U-235-enrichments of about 90 - 93 % has to be reduced under 20 % due to nonproliferation aspects. Expected handicaps such as higher irradiation and waste treatment costs, resulting from the enrichment depth can be overcome by replacing the actual used UAl_x-targets by U_3Si_2-silicides keeping the same target dimensions by using low enriched uranium. Due to the alkaline digestion behavior of uran-silicide remarkable modifications in the existing production processes are needed. Basing on first experiences with unirradiated U_3Si_2-targets of MTR-type expected changes in the KfK-production cycle presented will be discussed.

INTRODUCTION

The most frequently used radioisotope in medical organ function tests is technetium-99-m. The chemical versatility of the pertechnetate anion, the γ-decay energy and the half-life of Tc-99m allow optimum conditions for its application in clinical diagnostics. Due to its short half-life the delivery of this isotop all over the country is not possible at a reasonable price. This shortcoming was effectively eliminated by introduction of the generator technique, a procedure long practiced in radiochemistry, according to which the longer-lived parent nuclide is absorbed on a chemically and radiation resistant matrix. The continuously produced daughter nuclide is eluted with a suitable solution. The parent nuclide of Tc-99 is molybdenum-99. Because of its half-life of 66 hours, the mentioned concept can be realized [1]. The advantages offered by Tc-99m can be fully utilized only if highest chemical purity, specific activity and concentration can be ensured. This requirement can be met only if it is fulfilled by the parent nuclide, molybdenum-99, too. Solely fission molybdenum attains the by far highest specific activities. It is obtained by processing of irradiated and shortly cooled U-235 containing targets. Many process variants published [2 - 9] reflect the growing interest in its practical application.

The most commonly used targets are rather small fuel elements of the type used in material testing reactors. They are processed after irradiation with thermal neutrons and short periods of cooling down. In order to achieve the highest possible product yields, targets enriched to approximately 90 - 93 % U-235 are used. The steadily growing demands for fission nuclides in nuclear medical applications is accompanied by a corresponding increase in the amounts of highly enriched uranium which must be handled. The wider dissemination of this sensitive material inevitably resulting from the growing demands constitutes an ever increasing serious problem. The substitution of highly enriched uranium by fuels of less than 20 % enrichment is steadily aimed and has been successful in modifying reactor core loads. It was possible to compensate the lower enrichment levels by using silicide containing fuel elements of high fuel density and to avoid in this way losses in neutron flows. Considerations to the effect that these positive experiences could be transferred to the similar irradiation targets employed in Mo-99 production meet with the refusal by the producers of radioisotopes. Their arguments are being backed by experience accumulated so far in the chemical treatment of the irradiated elements. Uranium silicide targets have shown to react at much slower rates compared to the presently used aluminides, both in the process of digestion with alkali hydroxide solutions and in the course of direct dissolution in nitric acid. Abandoning the silicides and retaining the aluminides despite their low levels of enrichment - on account of the greater amounts of targets then needed - would imply major drawbacks in terms of the costs of irradiation, transport and waste treatment. Considering these aspects, the KfK Radiochemistry Institute (IRCH) adapted under a Technology Transfer Program the process of fission product molybdenum separation developed at the Institute to the application of silicide targets. This process will be described together with the integrated nuclear fuel recycling and the target fabrication. Modifications of the flowsheet expected from the use of silicide targets will be explained.

Molybdenum separation

The targets consist of an aluminium cladded uranium/aluminium alloy of the approximate composition UAl_3; since the aluminium content in the compound is variable, the term UAl_x is mostly used. To achieve the highest possible fission product yields uranium enriched to 90 - 93 % is used. The individual plates are irradiated jointly in one rig exposed to thermal neutron fluxes of approximately 5×10^{13} - 1×10^{-14} n/s cm^2 for five to ten days with forced cooling. Figure 1 shows a picture of the fuel element plates in the irradiation holder.

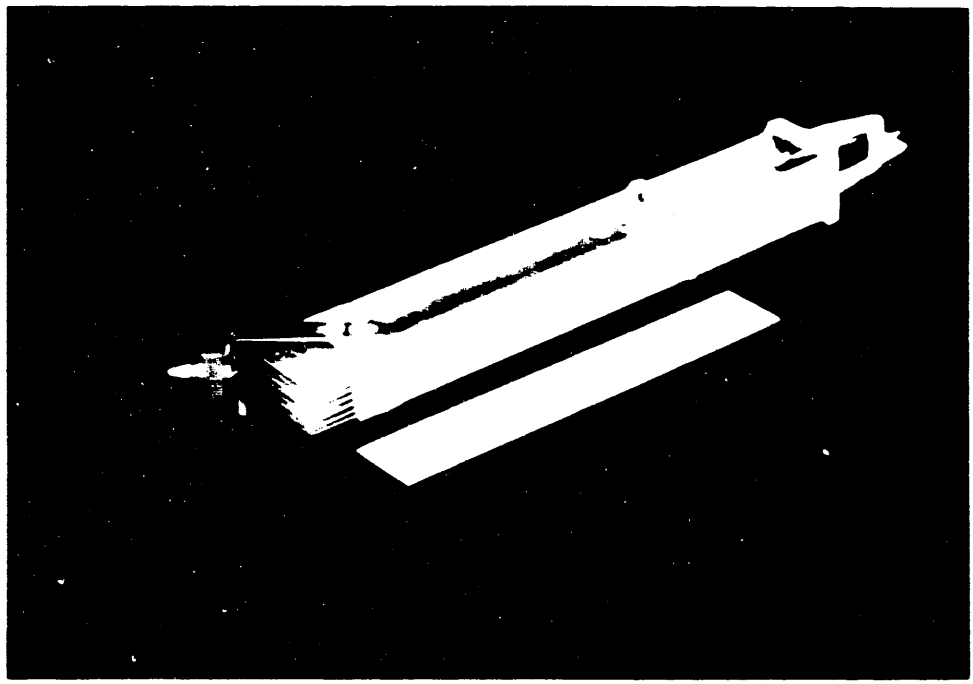

Fig. 1. Fuel element targets in the aluminium irradiation holder. The dimensions of the plates are: 220 mm in length, 40 mm in width and 1.3 mm in thickness. The dimension of the fuel meat inside is 200 mm in length, 300 mm in width and 0.5 mm in thickness.

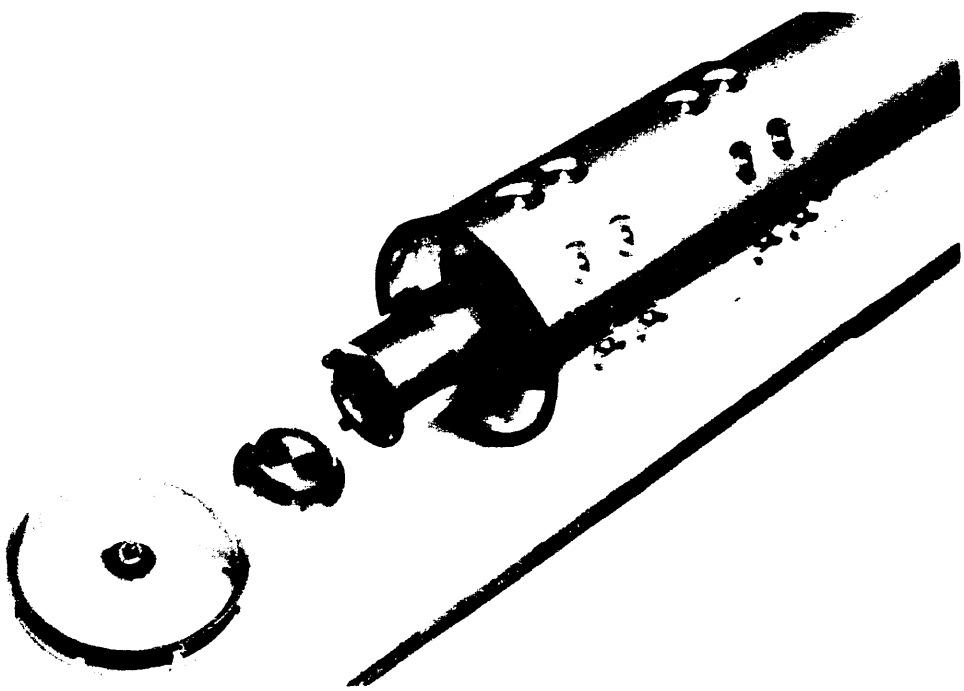

Fig. 2. α-tight transportation- and connection system

To minimize decay losses of the desired nuclide the targets are transported to the processing plant after a minimum decay period of about twelve hours. Figure 2 shows the α-tight transportation- and connection system. The first chemical step normally consists in the alkaline digestion of the target using 3 - 6 M NaOH respectively KOH. After a minimum decay period of about twelve hours, a simplified scheme of the complete Mo-99 production process including the subsequent recycling of nuclear fuel, developed at KfK, is showed in Figure 3.

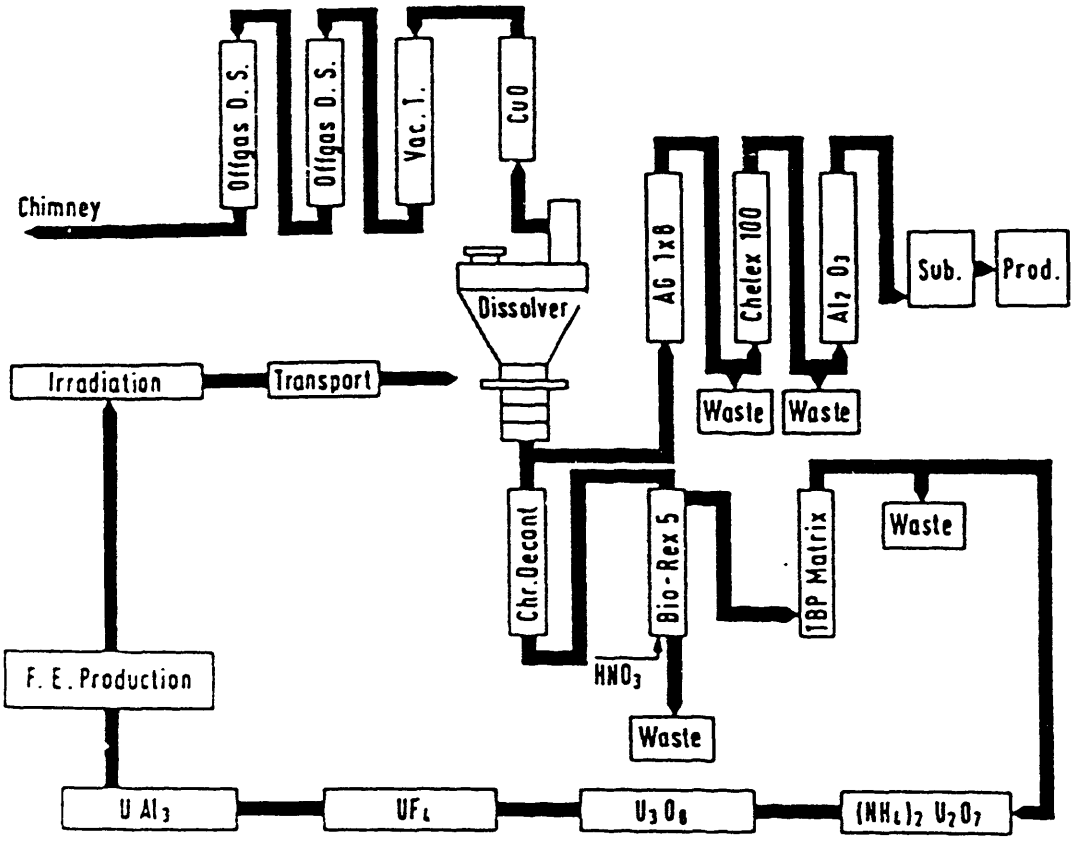

Fig. 3. Scheme of the complete Mo-99-production including fuel recycling and target fabrication.

During the alkaline digestion the main constituents of the plate are dissolved namely aluminium and the fission products soluble in this medium such as alkaline and alkaline earth cations as well as antimony, iodine, tellurium, tin, and molybdenum. The volatile fission products with Xenon-133 as the main carrier of activity leave the dissolver at its upper end passing through a reflux condenser together with the hydrogen generated in the digestion process and driven by a nitrogen stream. The hydrogen is oxidized to H_2O via CuO at 350 - 400°C and the resulting water condensed. Xenon is collected together with nitrogen in preevacuated stainless steel tanks and later on carried to the xenon delay section (D. S.) passing deep bed carbon filters. To guarantee a safe, leakage-free process all equipment used in this extremely hot part of the process are made of stainless steel. Figure 4 shows a picture of the digestion equipment [10] and the first Mo-purification column.

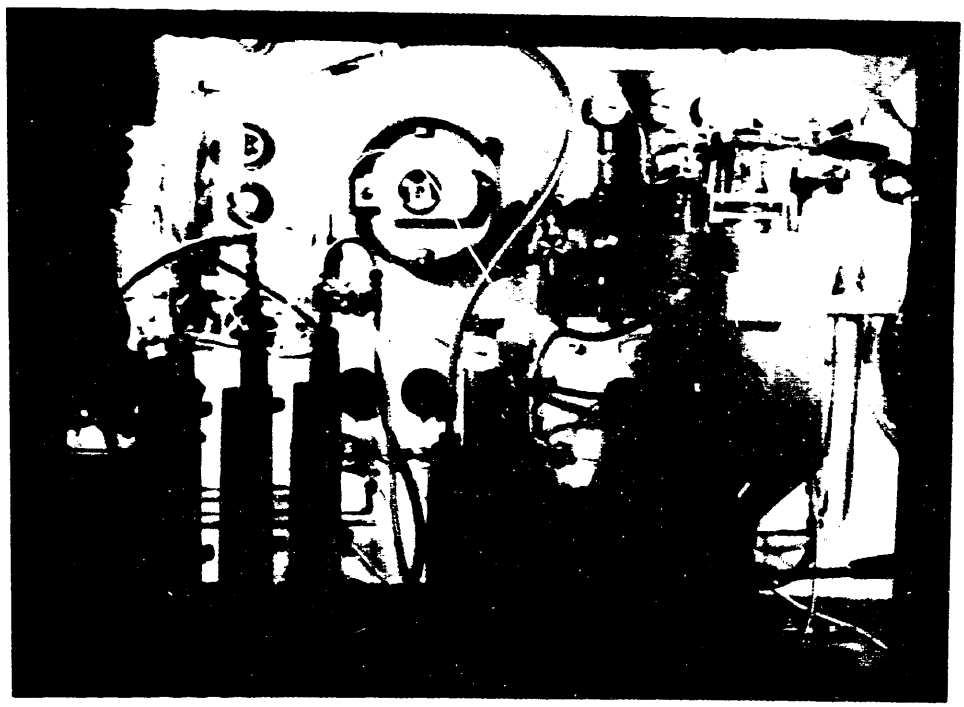

Fig. 4. Stainless steel digestion equipment in operation in the hot cell.

The alkaline solution containing molybdenum passes through a column of the strong basic exchanger AG 1 x 8, 50 - 100 mesh. Molybdenum is quantitatively adsorbed on the exchanger together with a significant part of fission products. Cationic impurities as caesium, strontium, and barium pass through the column together with hydroxaluminate, tellurit and iodine anions. After washing the column with sodium hydroxide molybdenum and the main part of the accompanying fission products are eluted with 1 - 1.5 M sulfuric acid and subsequently with a solution of 0.5 M ammonium hydroxide and 1 M sodium sulfate. This solution is transferred to the Mo-purification cell. Figure 5 shows a picture of this installation part.

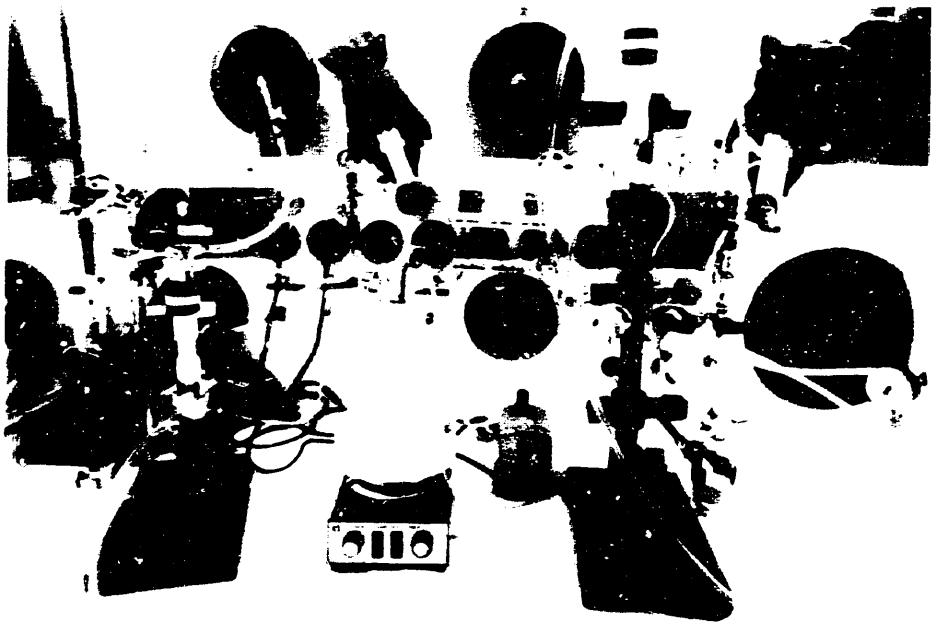

Fig. 5. Fission molybdenum purification cell used in Karlsruhe.

The process solution is subsequently treated with solutions of ammonium thiocyanide, potassium iodide, sodium sulphite and finally acidified with sulphuric acid up to 1 1.5 - 2.0 M H_2SO_4. Under these conditions the molybdenum will be reduced and forms an extremely stable anionic $[Mo(SCN)_6]^{3-}$-complex with the thiocyanide ions. From this medium molybdenum can be retained quantitatively on ion exchangers with functional nitrilodiacetate groups such as chelex-100 [11]. In Figure 6 the distribution coefficients of molybdenum on chelex-100 in thiocyanate, sulphite and HCl respectively H_2SO_4 containing solutions are shown.

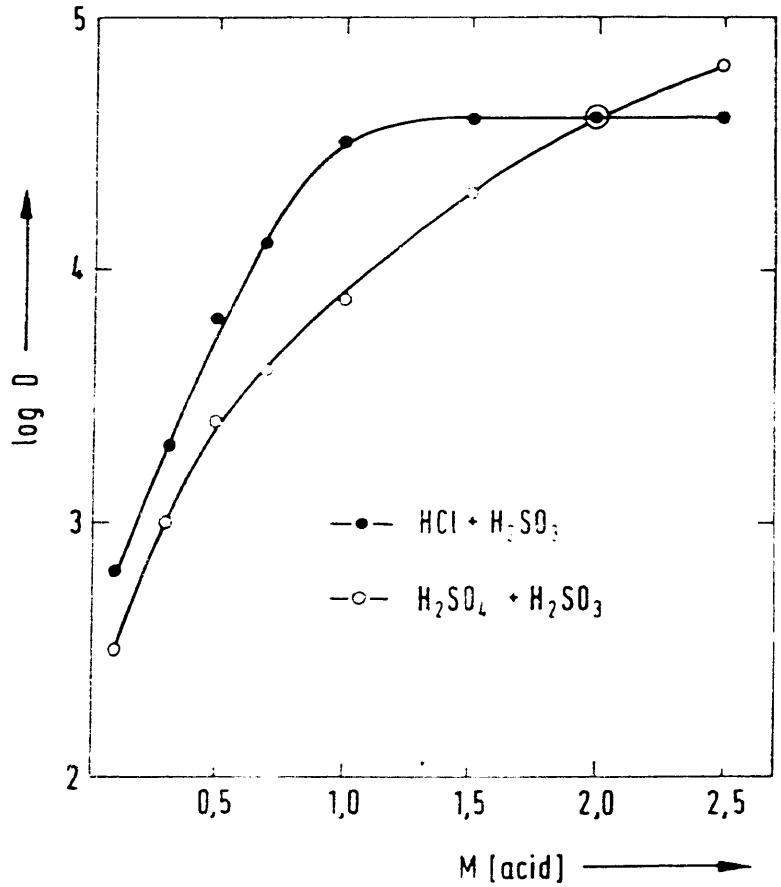

Fig. 6. Distribution coefficients of molybdenum thiocyanate complex as a function of the acid concentration on Chelex-100 50 - 100 mesh.

It should be mentioned that under these conditions all fission products which accompany the molybdenum have distribution coefficients of approximately 1 on chelex-100 that means, in one column a decontamination factor of about 10^5 can be practically gained.

In the following step the column is subsequently washed with thiocyanide containing sulphuric acid, sulphuric acid and water. The molybdenum elution from the column is carried out with 1 M NaOH. To guarantee a product of highest purity the procedure is repeated on a second smaller chelex-100 column. The described process is schematically presented in Figure 7. The eluate of the second column will be acidified with the calculated amount of nitric acid to adjust a pH-value of the solution between 1.8 - 3.5.

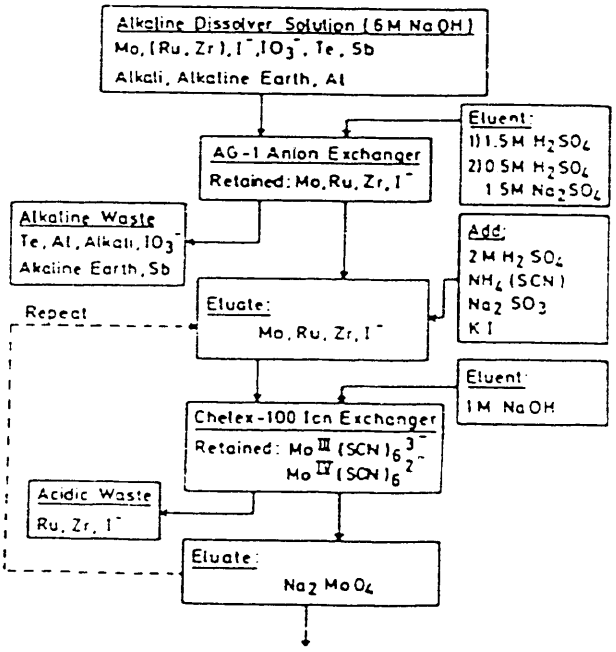

Fig. 7. Flowsheet of the fission molybdenum separation process.

To avoid retention of corrosion products from the metal equipment on the Al_2O_3 column the solution has to pass first a cation exchange AG 50 x 8 100 - 200 mesh column before it enters a chromatographic column filled with aluminium oxide. The Al_2O_3-column is useful to purify molybdenum from nonvolatile sodium salts and from possible traces of contamination. After washing the column with 0.01 M HNO_3 and finally with water, the molybdenum is eluted with 1 M ammonium hydroxide and transferred to the sublimation cell. The molybdenum solution is evaporated in a stainless steel apparatus and afterwards placed into a platinum crucible. The residue is evaporated on an electric hot plate and the crucible with the completely dried residue slowly heated up to about 700°C in a quartz glass apparatus inside a resistance furnace. At this temperature all organic impurities possibly introduced from the ion exchangers into the product are removed. The last process is the sublimation of the molybdenum oxide. The sublimation is started after a quartz glass condensation device is placed over the quartz vessel in the furnace and the temperature increased to about 1150°C. The molybdenum volatilization is finished in about 30 minutes. In the upper parts of the quartz device the molybdenum trioxide is deposited. After removal of the crucible the oxide is dissolved with ammonia vapour. The molybdenum solution is mixed with sodium hydroxide and ammonia is removed by boiling. The solution obtained in that way represents the final product. The flowsheet of this process part is shown in Figure 8.

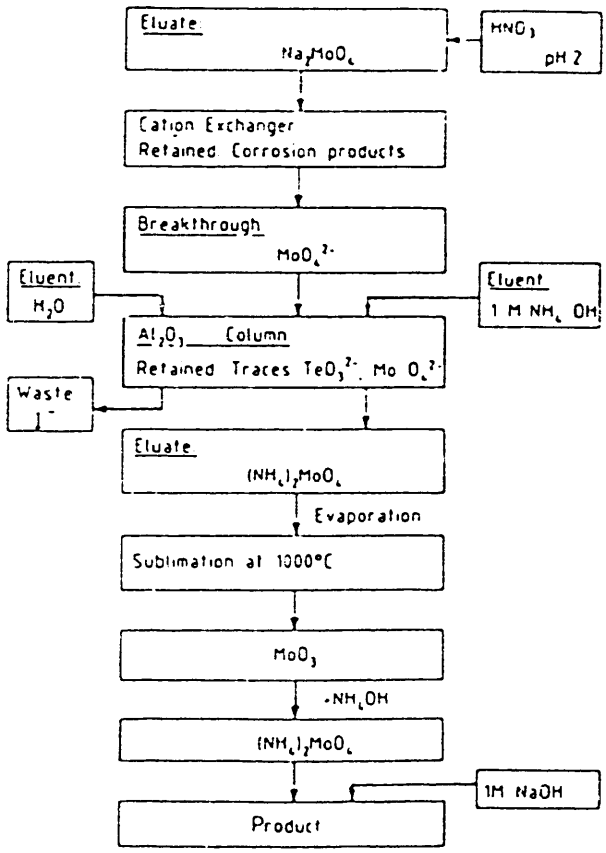

Fig. 8. Flowsheet of the purification procedure on cation exchanger/ aluminium oxide system and the MoO_3-sublimation.

The sublimation step is an integral part of most Mo-separation processes because it guarantees that the product is not contaminated by organic impurities. The disadvantage of this procedure: It is labor intensive in operation and time consuming since the evaporation of the Mo-containing solution has to be carried out very carefully to prevent overboiling. These aspects initiated a research program to simplify the volatilization process. The basic idea was to find a suitable adsorber-matrix, which is able to retain the molybdenum quantitatively from aqueous solutions and which permits a thermal desorption of the molybdenum(VI) oxide by applying high temperatures [12].

The mentioned aim succeeded and an efficient system basing on the Mo-adsorption on SnO_2 and the subsequent thermal desorption of molybdenum oxide in a H_2O-stream containing oxygen, was developed [13]. The total yield was found to be better than 97 % and the process time was reduced to one hour.

Recycling of the nuclear fuel

The insoluble residue contains about 99 % of the initially irradiated uranium in the form of uranium dioxide and alkaline diuranate together with the insoluble fission product species, above all ruthenium, zirconium and the lanthanides. Under aspects of economy and safety the nuclear fuel must be recycled, targeted and reirradiated. To minimize the investment costs for fuel and installation protection the amount of enriched U-235 has to be as low as possible with the consequence that the fuel cooling times will not be longer than few weeks. In this case the digestion residues still contaminated in Ci-scale with I-131 and Xe-133 kept in some undissolved uranium/aluminium alloy particles, under these conditions the other wise proven dissolution in nitric acid followed by the Purex Process [14 - 16] cannot be recommended. The drawback of using HNO_3 in hot installations filtered by activated carbon is fire risk caused by No_x generated during the dissolution. Charcoal is by far the most effective material for Xenon delay at room temperature and it shows an excellent iodine retention behavior in combination with practical advantages such as adequate resistance to wear and economic efficiency. The described difficulties were successfully avoided by dissolving the uranium dioxide and diuranate residues in HCO_3^-/CO_3^{--} medium and chromatographic decontamination of the fuel solution by passing through exchanger columns.

The presented process is based on the formation of soluble negativ charged uranyltricarbonato-complexes. Figure 9 shows the uranium solubility as a function of the carbonate molarity.

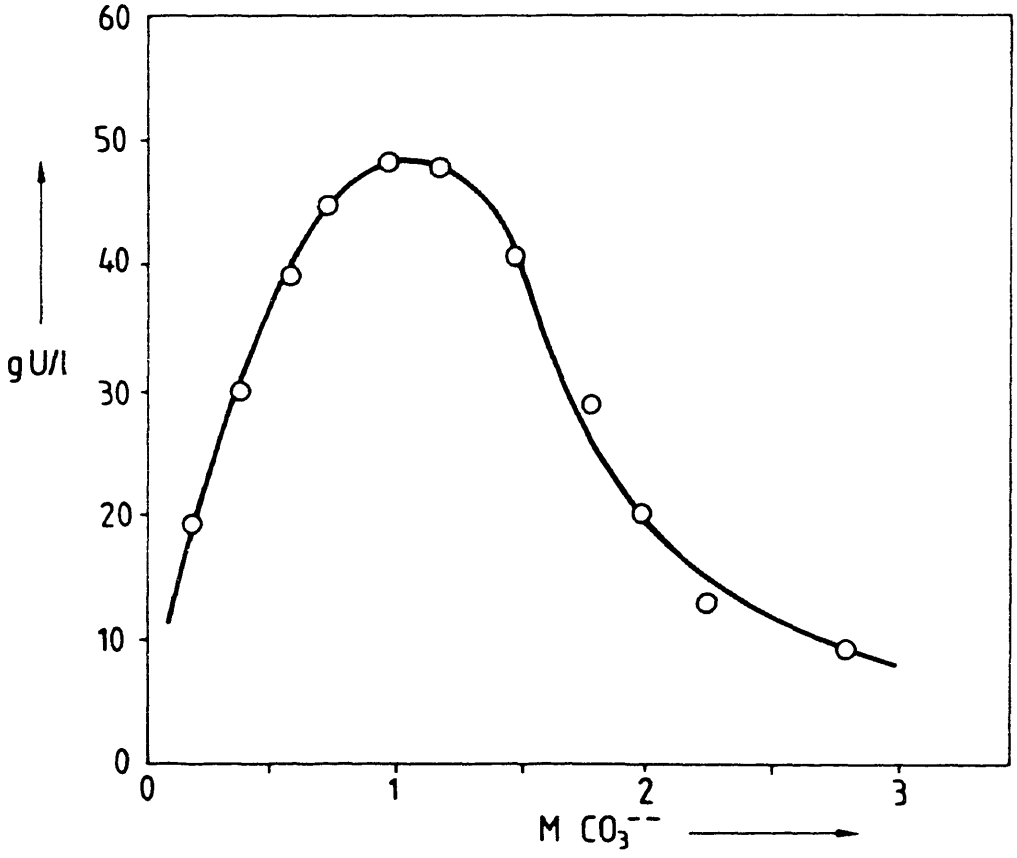

Fig. 9. Solubility of uranium in carbonat media as a function of the CO_3^{--}-concentration.

The decontamination of the fuel solution is carried out on radiation resistent inorganic adsorbers. Several commercial available exchangers, mainly metaloxides, were found out to realize efficient purification of the uranium solutions [17]. Figure 10 shows the highest distribution coefficients of cesium, cerium, strontium and zirconium on their individual best adsorbers as a function of the HCO_3^-/CO_3^{--} ratio in batch experiments.

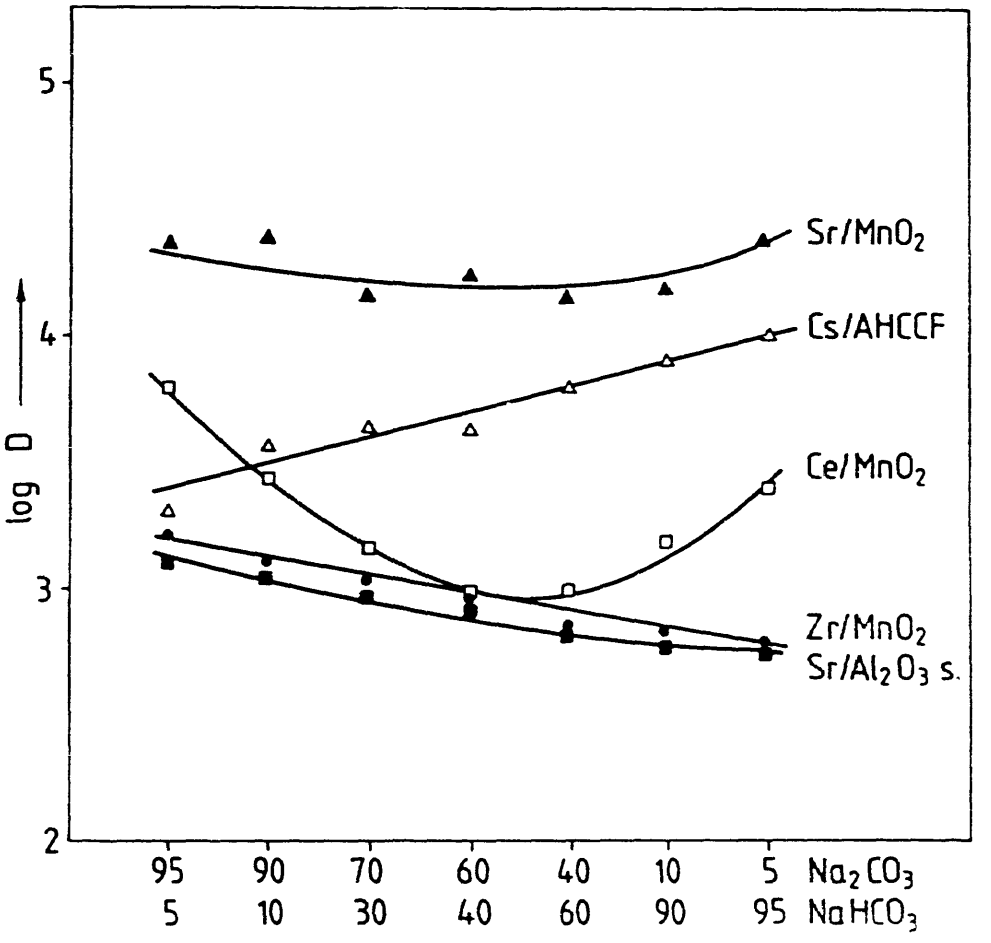

Fig. 10. Distribution coefficients of Cs on AHCCF = $(NH_4)_2$ [$CoFe(CN)_6$], Ce, Sr, Zr on MnO_2 and Sr on Al_2O_3 in different HCO_3^-/CO_3^{--} ratios total carbonate molarity.

The adsorption behavior of the mentioned exchangers for fission products permits suitable separation possibilities from solutions containing high carbonate concentrations. Following dynamic experiments with different stationary phases demonstrated their efficiency. The table includes the determined breakthrough in percent of Ce, Cs, Ru, Sb, Sr and Zr on columns of AHCCF = $(NH_4)_2$ [$CoFe(CN)_6$], acidic Al_2O_3, MnO_2 and SnO_2 by passing fission product tracers dissolved in 1 M HCO_3^-/CO_3^{--} solutions. The loaded columns were washed subsequently with hydrogencarbonate/carbonate of the same molarity.

Table

Fiss. Prod.	Ce	Cs	Ru	Sb	Sr	Zr
Al_2O_3	100	60	94	38	100	0
AHCCF	98	100	31	0	0	100
MnO_2	100	7	82	100	100	100
SnO_2	95	0	6	0	100	63

loading sol. = 10 ml
washing sol. = 15 ml
total carbonat conc. = 1.0 M
HCO_3^-/CO_3^{--} = 2 : 1

column:
diameter = 9,7 mm
bed volume = 5,5 ml
Cond. rate = 0,84 m · n^{-1} · cm^{-2}

The percentage data underline the efficiency of inorganic exchangers for fission product separation in carbonat systems. Only ruthenium is not completely retained on the named adsorbers. The best Ru-decontamination was carried out on Al_2O_3 columns. The detailed breakthrough behavior of Ru on Al_2O_3, $(NH_4)_2$ $CoFe(CN)_6$, MnO_2 and SnO_2 columns during the loading and washing steps is plotted in Figure 11.

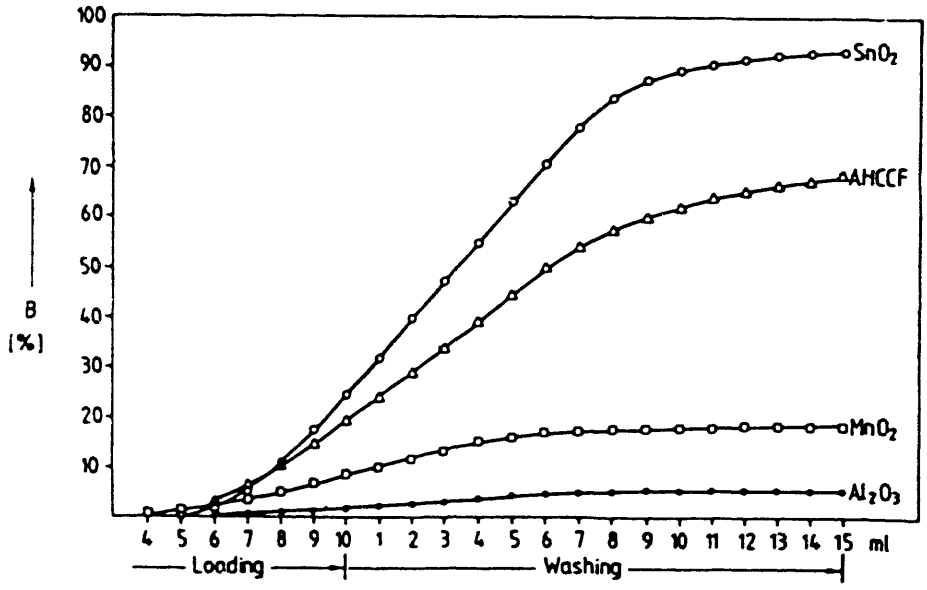

Fig. 11. Breakthrough curves of Ru-carbonat species on columns of $(NH_4)_2$ $[CoFe(CN)_6]$, acidic Al_2O_3, MnO_2 and SnO_2

Experimental conditions similar to the Table

Further experiments were carried out to study the influence of higher uranium concentrations on the retention behavior of the mentioned exchangers. They showed significant increases of the adsorption behavior for the relevant fission products. Particularly remarkable was the increase of cerium and zirconium retention on MnO_2. The dynamic breakthrough of cerium on MnO_2-columns in uranium free and 35 g uranium per liter containing HCO_3^-/CO_3^{--}-solutions are plotted in Figure 12. The comparable data for zirconium are showed in Figure 13.

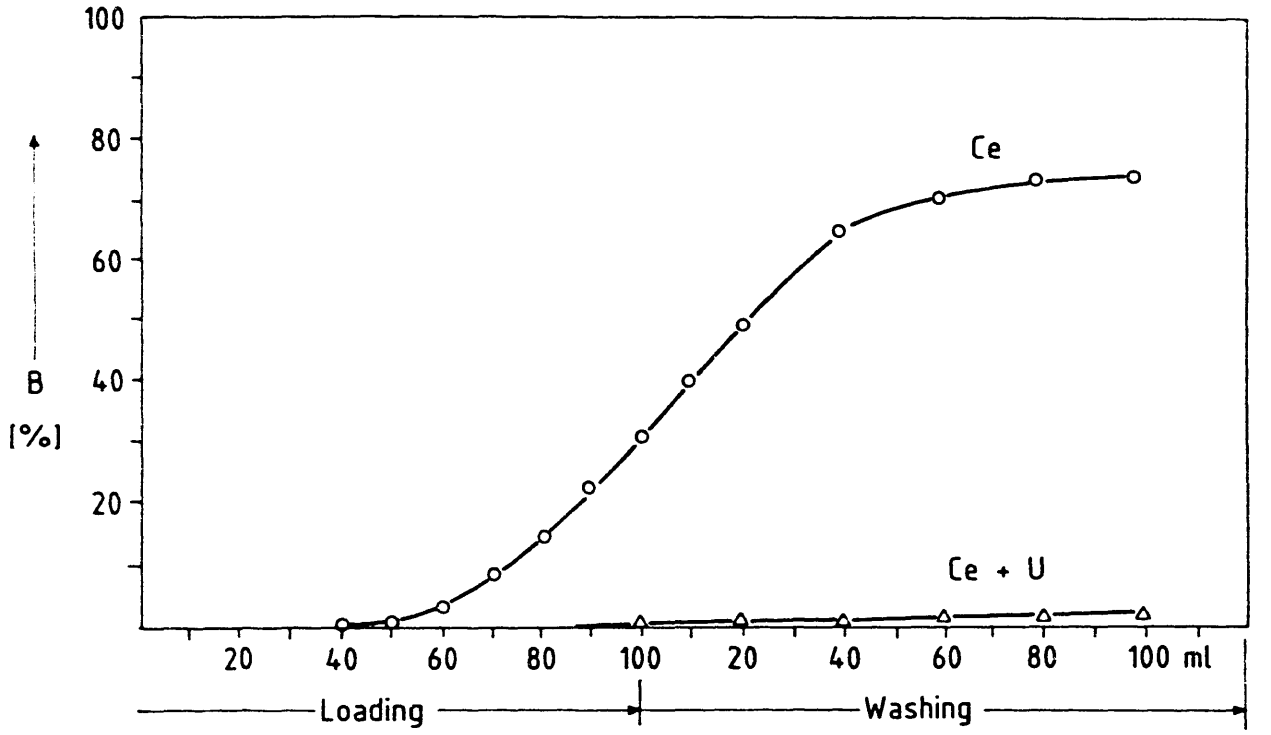

Fig. 12. Breakthrough in % of Ce by loading on MnO_2-columns from uranium containing and uranium free HCO_3^-/CO_3^{--} solutions.

Total HCO_3^-/CO_3^{--} molarity:	1
Adsorber:	MnO_2
Adsorber amount:	5 g
Column dimensions:	9,7 mm ⌀
	75 mm length
Loading solution:	100 ml
Washing solution:	50 ml

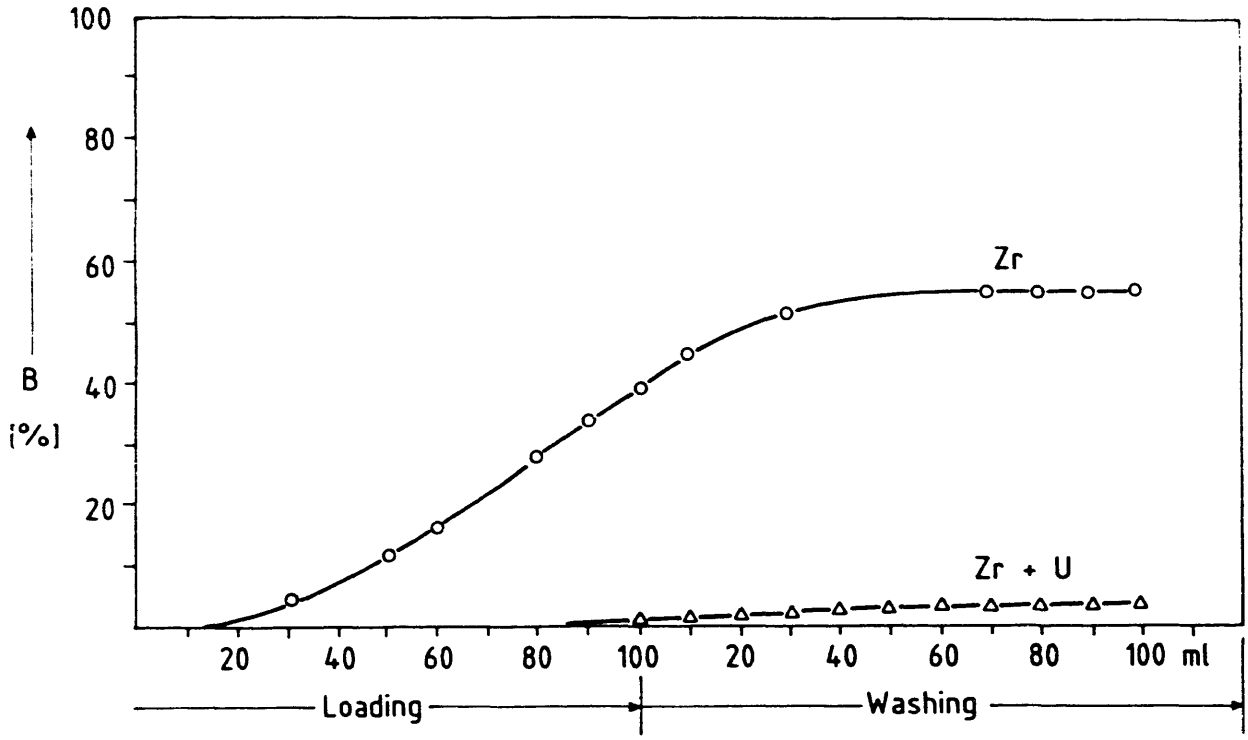

Fig. 13. Breakthrough in % of Zr by loading on MnO_2-columns from uranium containing and uranium free HCO_3^-/CO_3^{--} solutions.

Total HCO_3^-/CO_3^{--} molarity:	1
Adsorber:	MnO_2
Adsorber amount:	5 g
Column dimensions:	9,7 mm ⌀ 75 mm length
Loading solution:	100 ml
Washing solution:	50 ml

The plotted data in both figures demonstrate the high efficiency of MnO_2-columns for the fuel decontamination in carbonate media. The presence of uranium leads to significant increase of the retention capacity for the mentioned nuclides. The most probable explanation of this effect is that by the formation of uranyltricarbonatocomplexes the excess of free HCO_3^-/CO_3^{--}-ions is reduced. This minimizes the formation of negativ charged fission product spezies of high carbonate coordination which are not retained properly. The decontaminated fuel solution is passed through a column of the intermediate basic exchanger Bio-Rex 5 [18, 19]. Uranium is retained quantitative by loading degrees below 250 g / kg exchanger.

After subsequently washing of the stationary phase with ~ 0.1 M hydrogencarbonate/carbonate solution and water, uranium is eluted with 4 M nitric acid. The final fuel purification is carried out on tributyl phosphate loaded organic stationary phases [20, 21]. The eluted uranium is precipitated as diuranate in ammonia. The dried ammoniumdiuranate is converted to U_3O_8, subsequently to UF_4 and finally to U_3Si_2. The powdered alloy is used for the production of target material by MTR-technique.

U_3Si_2 - targets and expected process modifications

Alkaline digestion experiments in 3 - 10 M sodium- and potassium hydroxide solutions with unirradiated uranium silicide targets showed extremely low solubility of the alloy. Corresponding to this behavior low molybdenum yields have to be expected. Sufficientincrease of the fission Mo-yields can only be obtained by a following dissolution step. Two processes appear practical:

- The oxidation with hydrogen peroxide in basic media
- Dissolution of the alloy in 3 M HNO_3 and precipitation of the uranium and fission products with NaOH.

Actually the acid dissolution is favoured. The molybden containing stream will be combined with the other part separated from the alkaline digestion and retained on a cationic adsorber. The adjusted eluate will be loaded on the Chelex column and the process can be continued as presented in the flow sheet.

REFERENCES

1. W. D. Tucker, M. W. Greene, A. P. Murrenhoff, Atompraxis 8 (1962) 163.
2. L. G. Stang (Coordinator): BNL 864 (T-347) (1964).
3. P. Richards: USAEC, 323 (1966).
4. C. L. Ottinger: ORNL, 34 (1970).
5. Y. Kawakami: Isotope News 6 (1977).
6. W. Heyne: Isotopenpraxis 10 (13) (1977) 343.
7. C. K. Sivaramakrishnan, A. V. Jadhav, K. Raghuraman, S. Raman, P. S. Nair, M. U. Ramanish: BARC-847 (1976).
8. H. Arino, H. H. Kramer: Int. J. Appl. Radiat. Isot. 29 (1978) 97.
9. O. Hladik, G. Bernhardt, W. Boessert, R. Münze, Tech. Comm. Meeting organized by IAEA, Karlsruhe (1987).

10. Sameh A. Ali, K. Sauermann: German Patent PS 2306 592 (1981)

11. Sameh A. Ali, J. Knapp, J. Reinhardt: German Patents: PS 2610 948 (1979), PS 2758 783 (1980), US Patent: PS 4044 953 (1978).

12. J. Bürck, Sameh A. Ali, H. J. Ache: KfK-3754 (1984).

13. J. Bürck: KfK-4095 (1986).

14. R. G. Wymer, B. L. Vondra, CRC Press (1981).

15. T. V. Healy, H. A. C. McKay, Trans. Faraday Soc., 52, 633, (1959).

16. K. Alcock, G. F. Best, E. Hesford, H. A. C. McKay, J. Inorg. Nucl. Chem., 6, (1958), 328.

17. Sameh A. Ali, U. Berndt, W. Rottmann, W. Leifeld, U. Kaminski, Int. Conf. "RECOD '87", Paris, Vol. 1, 451 - 458.

18. J. Haag: KfK-3460 (1983).

19. Sameh A. Ali, J. Haag: German Patent: PS 3144 974.

20. R. Kroebel, A. Maier, Int. Solv. Extr. Conf. Lyon 35, (1974) 2095.

21. H. Eschrich, W. Ochsenfeld, Sep. Science and Technology 15, (1980), 697

PROCESSING OF LOW-BURNUP LEU SILICIDE TARGETS*

Jane D. Kwok, George F. Vandegrift, and James E. Matos
Argonne National Laboratory
9700 South Cass Avenue
Argonne, Illinois 60439

ABSTRACT

Currently much of the world's supply of ^{99m}Tc for medical purposes is produced from ^{99}Mo derived from the fissioning of high enriched uranium (HEU). Substitution of low enriched uranium (LEU) silicide fuel for the HEU alloy and aluminide fuels used in current target designs will allow equivalent ^{99}Mo yields with no change in target geometries. In these studies, targets were irradiated to low burnup (10^{-5}%) to produce fission products and ^{239}Np at concentrations conveniently measured by gamma spectroscopy.

Processing was done by dissolution of LEU targets in acid or base followed by alumina column recovery of ^{99}Mo. Acid dissolution is more rapid, but precipitation of silica results in loss of ^{99}Mo. Dissolution of U_3Si_2-Al targets in base requires more processing steps than the current process for UAl_x-Al fuel. A two-step process of first dissolving the 6061Al cladding and fuel meat aluminum, and then dissolving the U_3Si_2 fuel particles, has the advantage of eliminating the aluminum from further processing. Loss of ^{99}Mo during the aluminum dissolution is attributed to recoil of ^{99}Mo out of the silicide particles during irradiation. A larger particle size would decrease this ^{99}Mo loss.

INTRODUCTION

Technetium-99m for medical purposes is a decay product of ^{99}Mo, which is produced in nuclear reactors from the fissioning of ^{235}U or from neutron capture in ^{98}Mo. This continuing effort is related only to fission-product ^{99}Mo.

The purpose of this study is to assess the feasibility of substituting LEU for HEU in targets for production of fission-product ^{99}Mo. Switching from HEU (93% ^{235}U) to LEU (<20% ^{235}U) while maintaining ^{99}Mo yields and target geometries requires a denser fuel. Uranium silicide dispersed in aluminum (U_3Si_2-Al) with a uranium density of 4.8 g/cm^3 is currently the fuel of choice. Its approval by the NRC for use as a reactor fuel also makes it attractive as a ^{99}Mo target fuel.[1]

*Work supported by the U.S. Department of Energy, SST Program under Contract W-31-109-Eng-38.

In this study, targets of U_3Si_2 and U metal were irradiated and chemically processed by either an acidic or basic dissolution. Nuclide behaviors could then be monitored throughout the processing. Alumina column separation of molybdenum was done after dissolution of the irradiated targets. Alumina column runs were also preformed with tracer ^{99}Mo only.

The current process for basic dissolution involves dissolving the entire target in $NaOH/NO_3$ solution.[2] During the dissolution, uranium and various fission products precipitate as hydrated hydroxide salts. This mixture is diluted and filtered, and the solution is acidified for purification of the molybdenum on an alumina column. The dissolution of U_3Si_2 is extremely slow with $NaOH/NO_3$ solution alone, so the current process must be modified. As suggested in an earlier progress report, the dissolution can be done in two steps.[3] The first step dissolves the 6061Al cladding and the aluminum matrix in a 3M NaOH solution, leaving behind the U_3Si_2 particles. The high density of the U_3Si_2 (12 g/cm^3) allows the basic aluminum-containing solution and the precipitated hydroxide/salt components of the aluminum alloy cladding to be decanted easily from the silicide particles. The U_3Si_2 can then be dissolved separately in $NaOH/H_2O_2$. Uranium stays in solution as a peroxo complex until the peroxide is destroyed. Once the uranium has precipitated, the process is the same as that currently in use.

The acidic dissolution of UAl_x is done with nitric acid in the presence of Hg^{2+} as a catalyst.[4] Once the target is dissolved, the pH is adjusted for the alumina column procedure. The biggest difference in switching to U_3Si_2 is the precipitation of the silicates during acidic dissolution. Researchers at the Atomic Energy of Canada, Ltd., report that this finely divided precipitate tends to plug the alumina column, as well as adsorb ^{99}Mo. Irradiation of the silicide tended to make the particles even finer and the problem worse.[4]

EXPERIMENTAL

Irradiation

Targets were irradiated in the 180 kW JANUS reactor at ANL for 80 minutes at 1/4 power. This low burnup, which produced approximately 0.9 mCi of ^{99}Mo and 3 mCi of ^{239}Np, was chosen so that the nuclide activities would be high enough to be measured by gamma spectroscopy but low enough for processing in an unshielded hood. Targets were either one-quarter of a U_3Si_2 miniplate or uranium metal foil (0.2-mm thick, 4.5 g) wrapped in aluminum foil. They were electron-beam welded under vacuum into an 1100Al capsule, which was then placed in a secondary 1100Al container for introduction into the reactor.

Basic Dissolution (U_3Si_2)

The sample was digested in 3M NaOH to dissolve the 6061Al cladding and the aluminum of the fuel matrix (henceforth referred to as the aluminum fraction). The aluminum fraction, including its hydroxide precipitates,

was removed, leaving the dense fuel particles. The fuel was dissolved by adding 20 mL aliquots of 1.5M NaOH/15%H_2O_2 and heating, pouring off solution before each addition. After destruction of the peroxide through heating, the hydroxides (including uranium) were separated from the solution by centrifugation.

The supernate from the uranium hydroxide precipitation was acidified with HNO_3 to a pH of 0.32 for loading onto the alumina column. The alumina column procedure for the irradiated samples was the same as that for the ^{99}Mo-only samples, except that the columns were not thermostated. Molybdenum was eluted with concentrated NH_4OH.

Acidic Dissolution (U_3Si_2)

The acidic dissolution began with the sample being placed into a solution of 3M HNO_3 plus $Hg(NO_3)_2$ as a catalyst. This resulted in a fairly violent reaction that soon subsided. Concentrated HNO_3 was added to sustain the reaction rate. The dissolution solution was gravity filtered to remove the precipitate (mostly silicates). The solution pH was adjusted upward with NaOH solution for loading onto the alumina column. Molybdenum was eluted with 1M NH_4OH instead of concentrated NH_4OH.

Dissolution of U Metal

The uranium metal foil, wrapped in aluminum, was cut in two. One piece was treated by the acidic dissolution procedure. This dissolution was fast, and the resulting solution was taken through the alumina column procedure.

The second piece of uranium metal was combined with all of the aluminum foil and heated with 3M NaOH. This solution was decanted, and the uranium metal was dissolved in 1.5M NaOH/15% H_2O_2. This dissolution was very slow. At its completion, the remaining peroxide was destroyed by heating. The hydroxides were centrifuged, and the solution pH adjusted for loading onto the alumina column.

Alumina Column Procedure

For the ^{99}Mo-only experiments, a 2.7 Curie ^{99m}Tc generator from DuPont NEN was used as a source of ^{99}Mo.

A circulating bath was connected to a water jacket enclosing a 0.9 cm diameter column for temperature control at 25 or 50°C. The column had two adjustable syringes: one on top to avoid solvent mixing above the alumina, and one on the bottom to support the alumina. The column bottom was connected to a peristaltic pump and finally to a sample collector.

Alumina (3.0 g) was washed three times with water. The column was prepared and preconditioned with the appropriate molarity of nitric acid, depending on the loading solution. Either a ^{99}Mo spiked HNO_3 solution or a

dissolved target solution of pH 0.32 was then loaded onto the alumina. Flow rates were 1.2 mL/min unless specified otherwise. After loading, the column was washed with 25 mL of the appropriate nitric acid solution followed by 50 mL of water. Then the column was washed with 25 mL of 0.01M NH_4OH and eluted with either 1M or concentrated NH_4OH. For the run at 50°C, the eluting temperature had to be lowered to 25°C to avoid boiling of the concentrated NH_4OH.

Gamma Counting

Samples were counted on either a Packard Biogamma automatic gamma counting system using a NaI detector or on a germanium detector equipped with an automatic sample changer and a Nuclear Data 66 multichannel analyzer. For counting on the NaI detector, the Mo double peak at 739 and 778 keV was used to avoid overlap with the Tc peak at 141 keV.

RESULTS AND DISCUSSION

Basic Dissolution

The foremost benefit for using basic digestion of irradiated uranium targets for ^{99}Mo production is the high degree of separation achieved. During target digestion, as ^{99}Mo is dissolved, it is purified from U, Np, Pu, and many of the fission products that have insoluble hydroxide salts. A second benefit is that radioxenon can be collected separately from radioiodine (recovered during acidification). These benefits appear to remain when HEU aluminide is substituted by LEU silicide.

Chemical Partitioning

As expected from their chemistries, many radionuclides precipitate during the basic dissolution as hydroxides (Fig. 1). Nuclides remaining in solution include Mo, Ru, Rh, Te, I, Cs, and (inexplicably) Ce. With the exception of Cs, some of each of these nuclides is associated with the precipitate. This is probably due to their complex chemistry (Ru) or adsorption by the hydroxides (Mo).

Activation products of minor metals in the 6061Al cladding (Zn, Ti, Mn, Mg, Fe, Cu, and Cr) were not observed in the target solutions. Their activities were calculated to be under background levels except for ^{64}Cu, which was borderline. Activity from these nuclides should not be important to the purity of the final ^{99}Mo product.

Mo-99 Loss

From Fig. 2, we see that about 15% of the fission products (including ^{99}Mo) is lost during the first basic dissolution step to the aluminum fraction. Four possible mechanisms for this loss are the following:

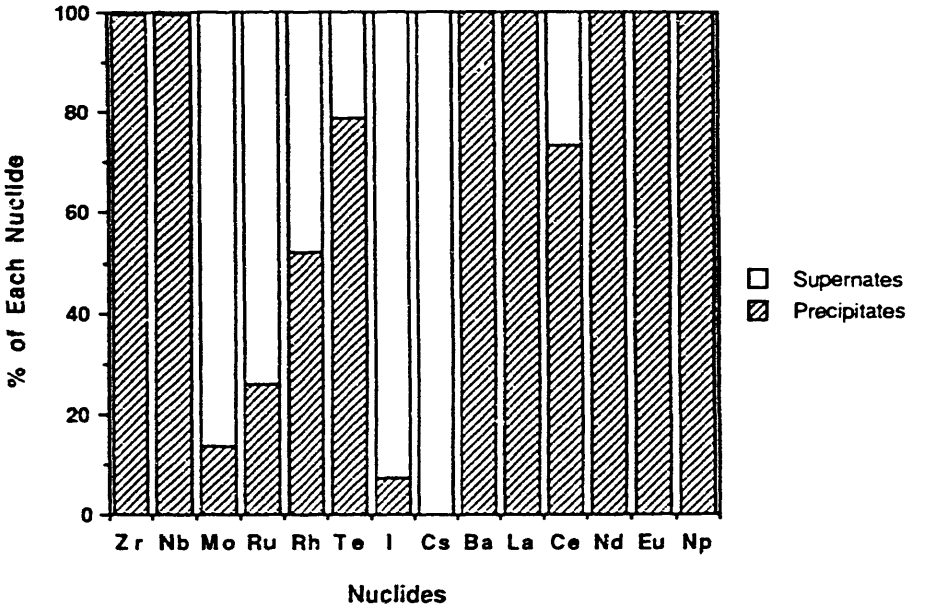

Fig. 1. Distribution of Nuclides during the Two-Step Basic Dissolution.

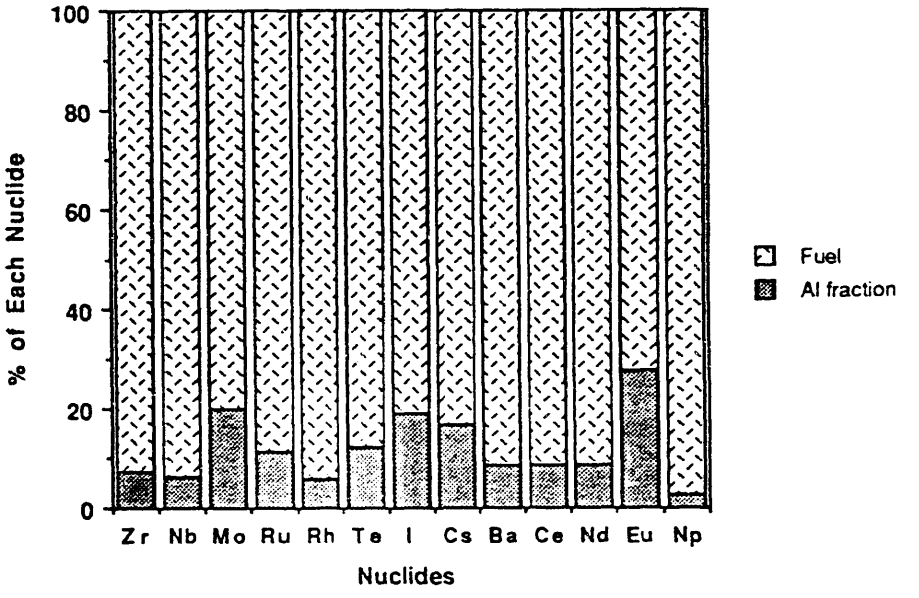

Fig. 2. Loss of Nuclides to Aluminum Fraction during First Step of Basic Dissolution.

(1) recoil due to fission energy from the uranium silicide particles into the aluminum matrix, (2) loss of U_3Si_2 fine particles due to carryover during transfer of the aluminum fraction away from the fuel, (3) dissolution of U_3Si_2 in NaOH-only solutions, and (4) dissolution of a "shell" of UAl_x around the U_3Si_2 particles that is formed during irradiation. Because these shells have only been seen at very high ^{235}U burnups (>30%), the fourth mechanism should not be important.

The ^{99}Mo loss due to recoil can be calculated based on the particle size distribution of the fuel, which relates to the total fuel surface area.[5] The fission fragment range, or the distance a fission product will travel, was estimated at 9.4 μm, the value for UO_2.[6] This value is probably an overestimate, since the value for U metal is 6.8 μm. Calculated and experimental losses for ^{99}Mo and ^{239}Np are presented in Table 1.

Table 1. Loss of ^{99}Mo and ^{239}Np to the Aluminum Fraction during Dissolution with Sodium Hydroxide

	% ^{99}Mo Loss		% 239 Np Loss	
	Exp.	Calc.[a]	Exp.	Calc.[a]
U_3Si_2	20	19	3	0
U metal	3.3	2.7-6.2[b]	0	0

[a]Using 9.4 μm (value for UO_2) for fission fragment range.
[b]Range is an artifact of experimental procedure, not the calculation itself.

Neptunium-239 is an activation product rather than a fission product; therefore, its calculated recoil loss is 0%. The experimental value for the aluminum fraction but could also be due to dissolution of U_3Si_2. Because ^{239}Np does not recoil, its loss should also be a measure of the loss of U, ^{239}Pu, and other activation products. For the processing of U metal, the experimental ^{239}Np loss was 0%, as expected. Because the metal was present as a foil, ^{99}Mo loss due to carryover of fines would not occur. The calculated ^{99}Mo loss for the metal foil is smaller than that for the U_3Si_2 particles because of its smaller surface area. Agreement with experimental values in both cases is good.

With larger particles sizes, the loss of ^{99}Mo during the two-step basic dissolution would decrease; less ^{99}Mo would escape due to recoil, fewer fines would carry over to the aluminum fraction, and less U_3Si_2 would dissolve.

Loss of ^{99}Mo during acidic dissolution is a result of silicate precipitation.[4] At our low target burnups, we saw 6% loss of the ^{99}Mo, likely due to its association with the silicates.

Alumina Columns

In column runs using ^{99}Mo tracer only, excellent recoveries were obtained with the alumina columns (Table 2). There was no significant temperature effect with loading at 50°C rather than 25°C. Loading solutions were either 0.5 or 1M HNO_3, with the lower concentration being possibly better.[3,4]

Results for the alumina column separation of Mo after dissolution of the irradiated targets are shown in Figs. 3 and 4. These clearly show the advantage of the initial basic hydroxide separation prior to the column procedure. The acidic dissolution final eluant had several nuclides eluting with ^{99}Mo, including Rh, I, Te, Nd, and Eu. The basic dissolution eluant contained only ^{131}I and ^{99}Mo.

Table 2. Experimental Conditions and Results from Alumina-Column Experiments Using ^{99}Mo Only.

Run	Temp. (°C)	Loading [HNO_3] (M)	Flow Rate mL/min	FWHM[b] (mL)	% ^{99}Mo in Effluent	% Yield ^{99}Mo
1	25	0.5	1.2	-	0.12	144[a]
2	25	0.5	0.67	2.3	0.025	104
3	25	0.5	1	4.5	0.031	102
4	25	0.5	1.2	2.4	-	96
5	25	1	1.2	5	0.89	108
6	50	1	1.2	4	-	104

[a]High yield probably due to counting interference with ^{99m}Tc peak.
[b]Full width at half maximum.

CONCLUSIONS

There are several factors important to a decision on the best way to process U_3Si_2. An acidic dissolution in HNO_3 is amenable to a batch dissolver because concentrated HNO_3 can be added to sustain the reaction rate. The acidic dissolution is faster, but silicates will precipitate and cause problems during the alumina column procedure.

Due to the rapid decline of the reaction rate of U_3Si_2 in $NaOH/H_2O_2$, this dissolution would be more appropriate to a continuous flow dissolver. Basic dissolution allows the separation of I and Xe radionuclides, avoids silicate precipitation, and allows the initial separation from other fission products, U, Np, and Pu. This would also reduce uranium losses. A two-step dissolution process, where the cladding and fuel matrix aluminum are dissolved first in NaOH and separated from the fuel dissolution process, removes the bulk of the Al from further processing. This, in turn, reduces processing volumes and transuranic waste. This advantage is somewhat offset by the ^{99}Mo loss during the first step of the dissolution but may be countered by increasing U_3Si_2 particle size. No problems with the alumina column procedure are anticipated with the basic dissolution.

Future work will be performed to test our finding of ^{99}Mo loss during the basic dissolution process and to set conditions for processing a full-burnup target under plant conditions.

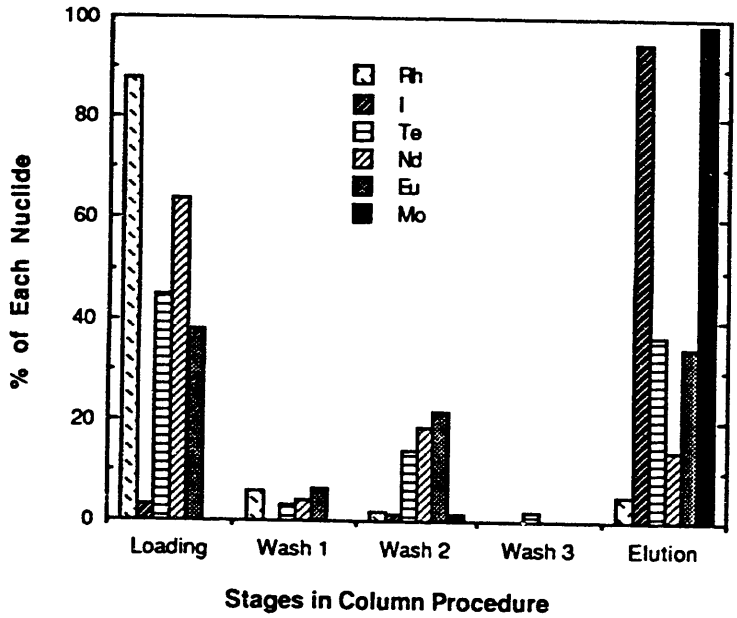

Fig. 3. Distribution of Nuclides from Alumina Column after Acidic Dissolution. Loading onto column in 0.5M HNO_3. Wash 1 is 0.5M HNO_3, Wash 2 is H_2O, Wash 3 is 0.01M NH_4OH, Elution by 1M NH_4OH.

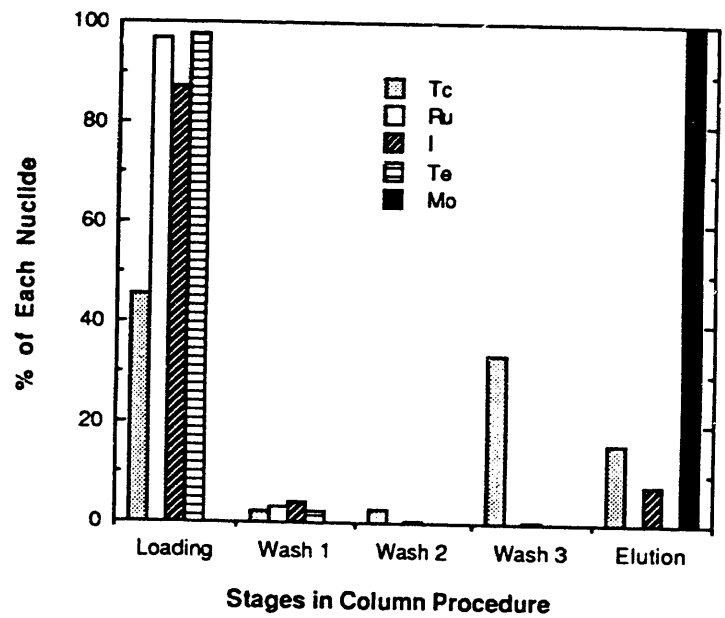

Fig. 4. Distribution of Nuclides from Alumina Column after Basic Dissolution. Loading onto column in 0.5M HNO_3. Wash 1 is 0.5M HNO_3, Wash 2 is H_2O, Wash 3 is 0.01M NH_4OH, Elution by concentrated NH_4OH.

REFERENCES

1. U.S. Nuclear Regulatory Commision, "Safety Evaluation Report Related to the Evaluation of Low-enriched Uranium Silicide-Aluminum Dispersion Fuel for Use in Non-power Reactors," NUREG-1313 (July 1988).

2. J. Salacz, "Reprocessing of Irradiated Uranium 235 for the Production of Mo-99, I-131, Xe-133 Radioisotopes," Revue IRE Tijdschrift 9(3) (1985).

3. G. F. Vandegrift, J. D. Kwok, S. L. Marshall, D. R. Vissers, and J. E. Matos, "Continuing Investigations for Technology Assessment of ^{99}Mo Production from LEU Targets," Proc. 1987 International Meeting on Reduced Enrichment for Research and Test Reactors, in press.

4. K. A. Burrill and R. J. Harrison, "Report on Technical Committee Meeting on Fission Molybdenum for Medical Use," October 13-16, 1987, Nuclear Research Centre Karlsruhe, Federal Republic of Germany, to be published.

5. J. C. Wood, J. T. Foo, L. C. Berthiaume, L. N. Herbert, J. D. Schaefer and D. Hawley, "Reduced Enrichment Fuels for Canadian Research Reactors--Fabrication and Performance," Proc. 1986 International Meeting on Reduced Enrichment for Research and Test Reactors, ANL/RERTR/TM-9 CONF-861185 (1986).

6. C. E. Weber and H. H. Hirsch, "Dispersion-Type Fuel Elements," Proc. 1955 Geneva Conf. on Peaceful Uses of Atomic Energy, Vol. 9, #P561.

CONTINUING INVESTIGATIONS ON ELECTROCHEMICAL PREPARATION OF LEU TARGETS FOR ^{99}Mo PRODUCTION

S. L. Marshall, L. Redey, D. R. Vissers, G. F. Vandegrift
and J. E. Matos
Chemical Technology Division, Argonne National Laboratory
Argonne, IL 60439-4387, U.S.A.

ABSTRACT

Continuing investigations of uranium electrodeposition from molten salts, as a possible method for the preparation of low-enriched uranium targets for ^{99}Mo production, are described. Potential-pulse plating has been applied with two electrolytes: (1) a UCl_3-LiCl-KCl mixture close to the eutectic composition and (2) 4 w/o UF_4 in LiCl-KCl-LiF ternary eutectic. The widest range of operating conditions is provided by the second electrolyte at 504°C. This electrolyte is economically attractive owing to its low uranium content. Dendrite-free, well-bonded uranium films have also been produced with bipolar current-pulse plating on substrates. Current densities sufficient to plate 6-mil coatings in 8 hours have been achieved without loss of coating uniformity or adhesion. This process was demonstrated on a cylindrical mock target that was approximately 1/3 the size of a commercial target.

INTRODUCTION

The substitution of low-enriched uranium (LEU) for the high-enriched uranium (HEU) presently used in cylindrical targets (design patented by Arino et al.[1,2]) for ^{99}Mo production will probably require replacement of the uranium oxide film by uranium metal.

Electrodeposition of uranium from molten-salt mixtures consisting of 20 w/o UCl_3 in LiCl-KCl eutectic, onto nickel and tantalum substrates, has been described elsewhere.[3,4] The reversible deposition kinetics of uranium results in a strong tendency towards formation of dendritic (irregular, tree-like) deposits. Dendrite formation must be avoided to generate coatings satisfying the surface uniformity standards required of targets for ^{99}Mo production.

Dendrites are usually formed under constant-potential or constant-current plating conditions.[3,4] A pulsed potential method involving application of a potential V_2 for time τ and a second potential, $V_1 = 0$, for time $r\tau$ was

examined. Faster deposition was achieved by increasing V_2 and decreasing r, but only to the point where dendrite formation was avoided. Conditions for avoidance of dendrites were determined previously by a two-level factorial experiment.[4] For each value of τ, these conditions imply a linear relation between r and V_2.

The subject of this paper is the determination of "dendrite-free" plating conditions in electrolytes other than 20 w/o UCl_3 in LiCl-KCl. Current-pulse plating is also discussed, and a successful plating demonstration of a commercial-type tubular uranium target for ^{99}Mo production is described.

EXPERIMENTAL

Electrolytes and Electrodes

To avoid the well-known deleterious effects of oxygen and moisture in molten-salt electroplating,[5,6] work was carried out in a glove box (Vacuum Atmospheres Corp.) under helium, with oxygen and moisture content below 1 ppm. Depleted uranium was used throughout this work. Electrolytes were prepared as follows:

(1) Reaction of 221.75 g KCl (Alpha), 227.76 g LiCl-KCl eutectic, 182.80 g $FeCl_2$, and 6.40 g LiCl (Anderson Physics Laboratory) with 228.78 g U metal produced UCl_3:

$$2U + 3FeCl_2 = 2UCl_3 + 3Fe \qquad (1)$$

The final composition of the electrolyte was UCl_3 11.8 m/o (42.1 w/o), LiCl 30.8 m/o (13.5 w/o), KCl (57.4 m/o). This is close to the ternary eutectic with composition UCl_3 12.0 m/o (42.4 w/o), LiCl 29.5 m/o (12.8 m/o), KCl 58.5 m/o (44.8 w/o), and melting point 335°C.[7]

(2) Reaction of excess U metal with a 4.5 w/o solution of UF_4 (supplied by the Y-12 Plant of Oak Ridge National Laboratory) in a ternary eutectic with composition LiCl 56.0 m/o (43.3 w/o), KCl 40.5 m/o (55.1 w/o), and LiF 3.5 m/o (1.6 w/o) formed U^{3+} according to the reaction:

$$3U^{4+} + U = 4U^{3+} \qquad (2)$$

Uranium anodes in the form of rods or discs were used, with a stainless steel rod serving as a current collector. Potential-pulse plating experiments

were carried out on a nickel disc (area 0.178 cm^2) cathode, described in Refs. 3 and 4. Bipolar current-pulse plating experiments used cylindrical nickel coupons with a total area of 7.74 cm^2. A uranium rod served as the reference electrode. Electrical control of the cell in experiments with these small disc and coupon electrodes was provided by a potentiostat and function generator (Princeton Applied Research, models 173 and 175).

Tubular Cathode Plating Assembly

For uranium electrodeposition experiments on a cathode resembling a commercial target, a two-electrode plating cell was developed. Electrolyte (1) was contained in a 1.5-in. i.d. alumina crucible, surrounded by a stainless steel secondary crucible. The cathode (101 cm^2 area) was made from 5 in. length of nickel tubing, 1-in. i.d. and 1.25-in. o.d., with opposing external grooves cut in the walls to facilitate separation of the tube into two halves after the experiment, and examination of the electrodeposit. Nickel tubing, 1/8-in. i.d. and 1/4-in. o.d., welded to the upper rim of the cathode, served as the current collector and thermocouple gland.

A 5/16-in. dia uranium anode was positioned coaxially with the cathode (using a boron nitride insulator with center hole, lying on the bottom of the alumina crucible). The entire assembly, with the heat reflectors for the furnace well, is shown in Fig. 1.

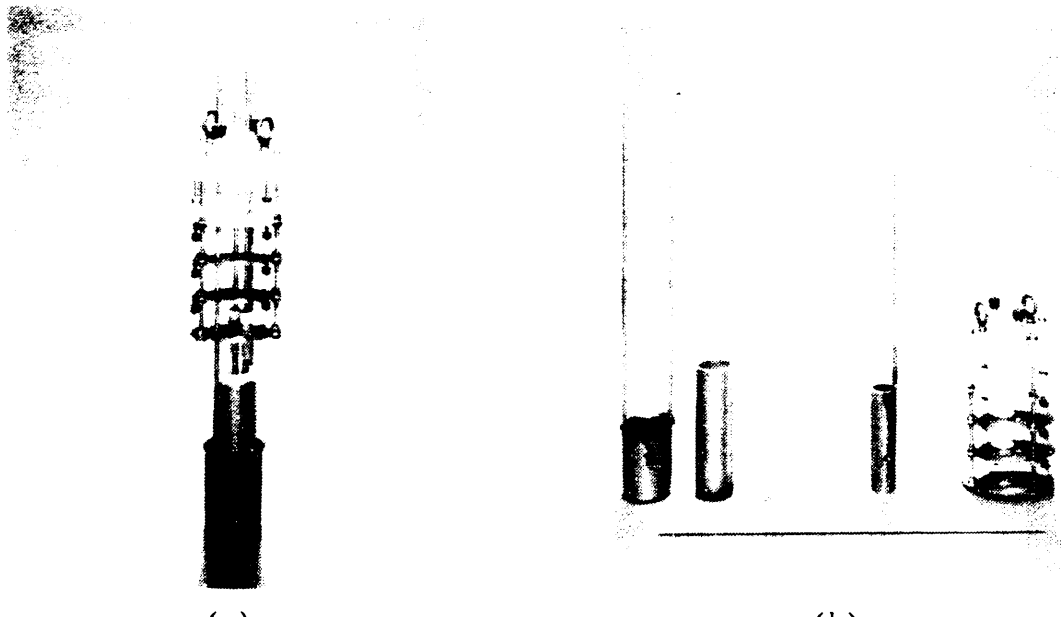

(a) (b)

Fig. 1. Photograph showing cell components (a) and assembled cell (b). The cell components in Fig. 1a are from left to right: cell hanger, steel crucible, Al_2O_3 crucible, BN insulator, Ni tube cathode, heat shield unit, BN insulator sleeves, and a 5/16-in. dia rod in front of the other components.

RESULTS AND DISCUSSION

Potential-Pulse Plating Experiments

To decrease plating times under pulsed-potential conditions, one can increase the voltage pulse (V_2) or decrease the time, $r\tau$, that the system is resting. However, those variables can be optimized only in a region where dendrite formation is avoided.

Dendrite formation under pulsed potential control was assessed by visual estimation of the length, **d** (in mm), of the largest dendrite present after application of the potential signal for 20 minutes. In Refs. 3 and 4, the conditions for which **d** = 0 were expressed by a linear relation between **r** and V_2 for each τ. In the present study, linearity was not assumed, and the desired relation between **r** and V_2 was determined for τ = 1 ms. If the conditions of each experiment are represented as points with coordinates **r** and V_2, the values of **d** define a surface above the **r**-V_2 plane (Fig. 2). It is then possible to determine the region in this plane where **d** = 0.

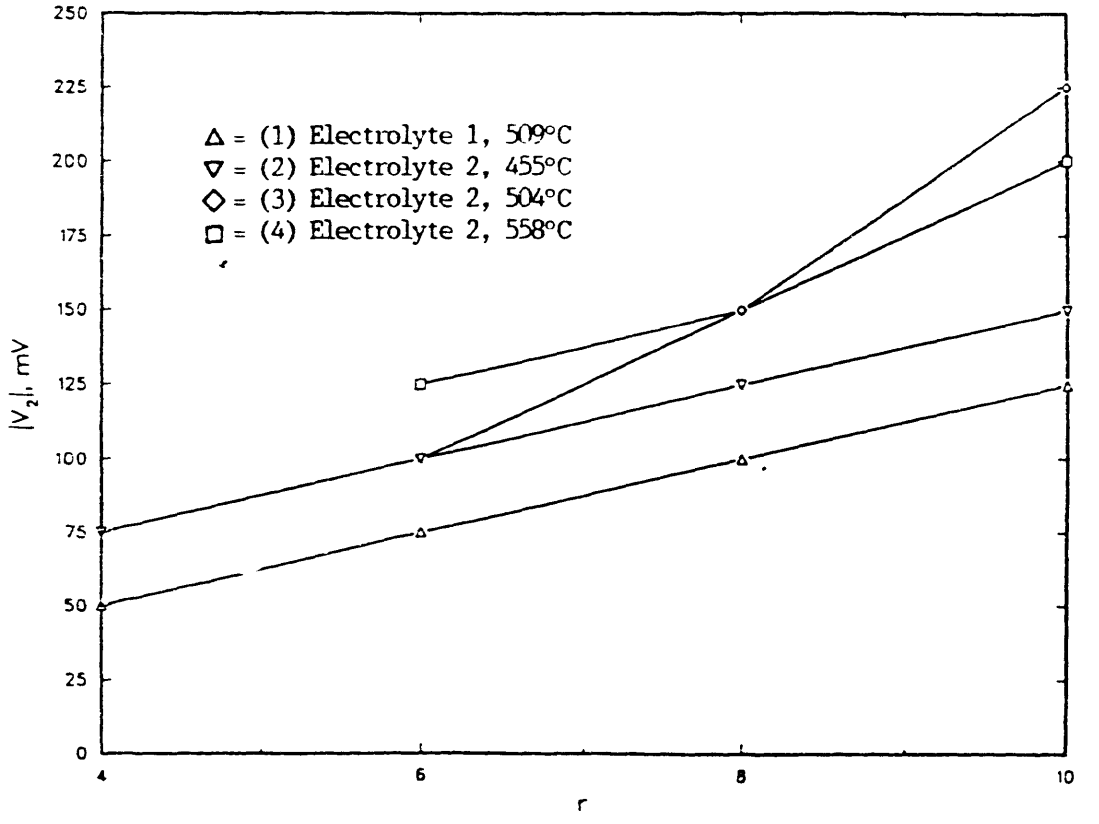

Fig. 2. Boundaries of dendrite-free V_2,R regions for (1) electrolyte 1 at 509°C, (2) electrolyte 2 at 455°C, (3) electrolyte 2 at 504°C, and (4) electrolyte 2 at 550°C. Regions above the curve are dendrite free; below the curves dendrites form.

Results are shown in Fig. 2 for electrolytes (1) and (2) at several temperatures. Dendrites are formed for (r, V_2) values lying above the curve appropriate to the given conditions. For instance, at the point (10, 200), dendrites were formed in electrolyte (1) at 509°C (curve 1) but not in electrolyte (2) at 504°C (curve 3). The largest dendrite-free region was observed with electrolyte (2) at 504°C (curve 3), and the smallest with electrolyte (1) at 509°C (curve 1). Comparison of curves 2 and 3 shows that elevation of the temperature from 455°C to 504°C in electrolyte (2) results in an enlargement of the range of accessible values of r and V_2. Further improvement does not, however, result from increasing the temperature to 558°C, as shown by comparison of curves 3 and 4.

It may be concluded that the mixed chloride-fluoride electrolyte (2) provides a wider range of operating conditions than the all-chloride electrolyte (1). This result is also significant in demonstrating the successful use of an electrolyte of lower uranium concentration and, consequently, lower cost.

Current-Pulse Plating Experiments

The potential-pulse technique mentioned in the preceding section was the most convenient method for screening pulse parameters for dendrite formation. Industrial electroplating is, however, commonly carried out under controlled-current conditions, since the extent of electrodeposition is more conveniently determined. Although the simple application of a constant cathodic current may be used in most cases, periodically interrupted currents can produce plated coatings of finer grain size and superior coherence.[8]

The technique used here involved alternate application of cathodic current density i_c for time t_c and anodic current density i_a for time t_a. This technique results in the removal of a fraction of the material deposited during each cathodic pulse; the reciprocal of this fraction is given by

$$q = i_c t_c / i_a t_a \tag{3}$$

In terms of q, the ratio of pulse lengths $R = t_c/t_a$, and the average current density $\langle i \rangle$, values of i_a and i_c are given by

$$i_a = \langle i \rangle (1 + R)/(1 + q) \tag{4}$$

$$i_c = \langle i \rangle q(1 + R)/R(1 + q)$$

Uniformity of coverage was found to be favored by q values close to -1. For R = 2 and $\langle i \rangle = -7$ mA·cm^{-2}, the optimal ranges are -20 to -40 mA·cm^{-2} for i_c and 30 to 40 mA·cm^{-2} for i_a; thus, q is between -1.3 and -1.5.

Experiments of this type in electrolyte (1) were preceded by a nucleation pulse of -1.0 A·cm^{-2} for 2 s, which was intended to ensure uniform coverage of the substrate with crystal nuclei. The coupon shown in Fig. 3 was plated with $i_c = -74.9$ mA·cm^{-2}, $t_c = 4.17$ ms, $i_a = 107.0$ mA·cm^{-2}, and $t_a = 2.08$ ms. These conditions result in R = 2, $\langle i \rangle = -14.3$ mA·cm^{-2}, and q = -1.400. The values of i_c and t_c correspond to the deposition of about a monolayer of uranium per plating pulse, of which 1/1.4 = 71.4% is removed in the following dissolution pulse. Plating time in this case was 8 hours, so that the average thickness is 6.9 mil. Relatively high deposition rates can, therefore, be achieved without adverse effects on the morphology or adhesion of the deposit.

Fig. 3. Uranium Plated Nickel Coupon.

Tubular Cathode Plating Experiment

Since uranium electrodepostion requires one ampere-minute per square centimeter per mil, 10 Ah is required for a 6-mil coating of the cathode. The plating conditions of the coupon in Fig. 3 were used in electrolyte (1). A nucleation pulse was not used in this study because of the high currents (100 A) involved. After plating, the cathode was halved longitudinally, rinsed with deionized water, dried with methanol, and photographed (Fig. 4).

With small coupons, nucleation pulses generally improve the uniformity of the deposit, but their omission in this study did not seem to affect the quality of the deposit. Differences in the anode-cathode separation (respectively, 1/8 and 11/32 in.) and the current distribution probably exerted more effect. With the exception of some dendrites, the quality of the deposit in the tubular cathode configuration was as good or slightly better than that observed on the small coupons (see Fig. 4).

The dendrites are seen to be concentrated on the side opposite the current collector. Heat conduction along this heavy-walled tube could have caused a temperature gradient, which, in turn, would have resulted in electrolyte convection and uranium concentration gradients. Such an effect would have been compounded by the radiative, rather than conductive, heating of the crucible in the furnace well.

This experiment has demonstrated the simplicity and feasibility of uranium electrodeposition as a method for LEU target production. Still required are more detailed consideration of temperature- and current-distribution effects and optimization of current-pulse plating conditions. Further work with the tubular cathodes will be carried out to optimize the cell design and plating regime.

Fig. 4. Uranium Plated Tubular Cathode.

ACKNOWLEDGMENTS

This work was supported by the U.S. Department of Energy under contract Nos. W-31-109-Eng-38 and DE-AC05-840R21400.

REFERENCES

1. H. Arino, H. H. Kramer, J. J. McGovern, A. K. Thornton, "Production of High Purity Fission Product Molybdenum-99," U.S. Patent 3,799,883, March 28, 1974.

2. H. Arino, F. J. Cosolito, K. D. George, A. K. Thornton, "Preparation of a Primary Target for the Production of Fission Products in a Nuclear Reactor," U.S. Patent 3,940,318, February 24, 1976.

3. G. F. Vandegrift, J. D. Kwok, S. L. Marshall, D. R. Vissers and J. E. Matos, Proceedings of the International Meeting on Reduced Enrichment for Research and Test Reactors, Buenos Aires, Argentina, September 1987.

4. S. L. Marshall and D. R. Vissers, Electrochemical Society 173rd Meeting, Atlanta, GA, May 1988, Extended Abstract No. 280.

5. M. Kolodney, J. Electrochem. Soc., **129**: 2438 (1982)

6. M. Broc, "Etude de Revêtements Métalliques Prêparés par Electrolyse Ignée", French Atomic Energy Commission Report CEA-R4291 (1978).

7. V. N. Desyatnik and B.V. Dubinin, J. Appl. Chem. USSR, **48**: 885 (1975)

8. The Canning Handbook of Surface Finishing Technology, 23rd ed., published by W. Canning plc in association with E. and F. N. Spon Ltd, Birmingham (1982).

L. Woodruff, W. Woodruff (ANL), and P. Ernst (McMaster University)

K. Parker (UKAEA, UK), D. Thom (UKAEA, UK), A. Wares (UKAEA, UK), and G. Gruber (NUKEM, FRG)

I. Kuk (KAERI, Korea), O. Gailar (Purdue University), and J. Talnagi (Ohio State University)

Y. Futamura (JAERI, Japan), F. Sakurai (JAERI, Japan), and S. Fukushima (Nissho Iwai, Japan)

A. Sameh (KFK, FRG), H. Tschiesche (Transnuklear, FRG), and D. Sears (AECL, Canada)

T. Michaels (NRC), F. DiMeglio (RINSC), and K. Brown (EG&G)

A. Travelli (ANL) and L. Woodruff

S. Ceja (DOE) and D. Giorsetti (CNEA, Argentina)

A. Travelli (ANL), F. Merchie (CEA/CEN, France),
R. Muranaka (IAEA, Austria), and J. Jaspert (EURATOM, Belgium)

D. Giorsetti (CNEA, Argentina), S. Ceja (DOE),
J. Colton (ACDA), A. Travelli (ANL),
F. Merchie (CEA/CEN, France), and
R. Muranaka (IAEA, Austria)

R. Muranaka (IAEA, Austria), J. Jaspert (EURATOM, Belgium),
K. Kanda (KURRI, Japan), and R. DeLaBarre (OES/NEC)

A. Travelli (ANL), F. Merchie (CEA/CEN,
France), R. Muranaka (IAEA, Austria).
J. Jaspert (EURATOM, Belgium), K. Kanda
(KURRI, Japan), and R. DeLaBarre (OES/NEC)

Giorsetti (CNEA, Argentina), S. Ceja (DOE), Thom (UKAEA, UK), and J. Colton (ACDA)

D. Thom (UKAEA, UK), J. Colton (ACDA) and G. Thamm (KFA, FRG)

A. Travelli (ANL), F. Merchie (CEA/CEN, France), and R. Muranaka (IAEA, Austria)

R. Muranaka (IAEA, Austria), R. DiMeglio, and F. DiMeglio (RINSC)

R. Muranaka (IAEA, Austria), "Gabi," and L. Woodruff

E. Adolph (Riso, Denmark), H. Preble (B&W), J. Marks (B&W), J. Borring (Riso, Denmark), and K. Borring

A. Snelgrove, K. Kanda (KURRI, Japan), C. Simpson (ANL), S. Mo (ANL), and L. Woodruff

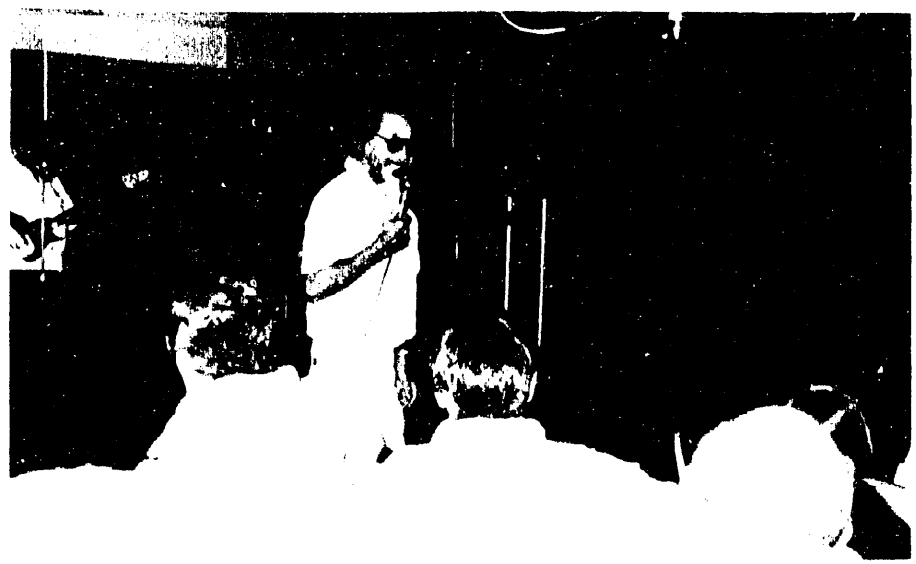

R. Muranaka (IAEA, Austria) sings "Tiny Bubbles"

P. Ernst (McMaster University), H. Tschiesche (Transnuklear, FRG), J. Marguin (CERCA, France), P. Porte (CERCA, France), and H. Fuchs (CERCA/NUKEM, FRG)

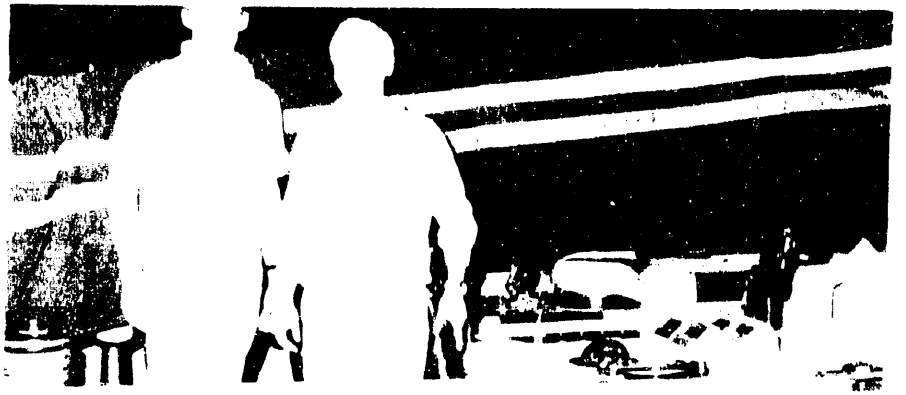

I. Kennedy (AECL/CRNL, Canada) and J. Schreader (AECL, Canada)

G. Copeland (ORNL) and K. Brown (EG&G)

C. Simpson (ANL) and E. Johnson (ANL)

P. Porte (CERCA, France), E. Bauer (Institut Laue-Langevin, France), and J. Poupard (CERCA, France)

I. Kuk (KAERI, Korea), R. Domagala (ANL), and D. Domagala

J. Marks (B&W) and E. Adolph (Riso, Denmark)

A. Travelli (ANL), D. Giorsetti (CNEA, Argentina), R. Rydin (University of Virginia), and K. Saltvedt (Studsvik Energiteknik, Sweden)

I. Kennedy (AECL/CRNL, Canada), I. Bornstein (ANL), J. Colton (ACDA), and I. Kuk (KAERI, Korea)

A. Lissier (CERCA, France), W. Byszewski (IAEA, Austria), J. Poupard (CERCA, France) and P. Porte (CERCA, France)

D. Giorsetti (CNEA, Argentina), S. Ceja (DOE), D. Thom (UKAEA, UK), J. Colton (ACDA), G. Thamm (KFA, FRG), and A. Travelli (ANL)

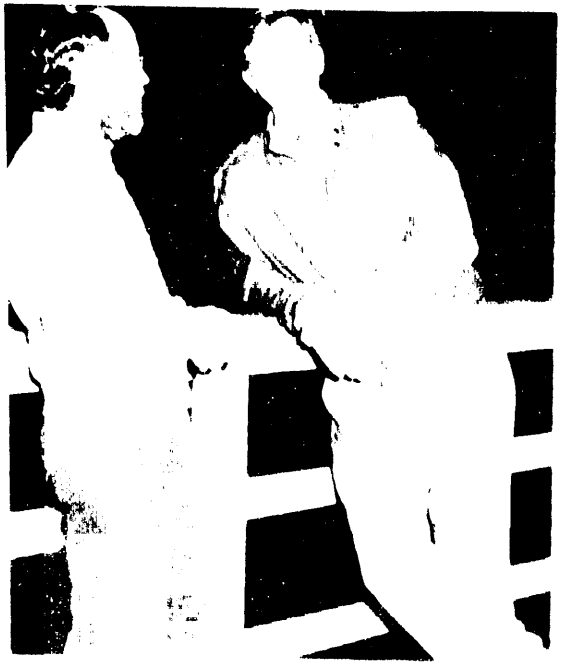

B. Horn (NRC) and J. Matos (ANL)

TRANSNUCLÉAIRE INTRODUCTION TO THE TRANSPORTATION PANEL

I have the pleasure to represent at this meeting TRANSNUCLÉAIRE, a French Transport and Engineering Company as well as its affiliated companies established in 8 countries with major nuclear programs.

TRANSNUCLÉAIRE was founded 25 years ago and followed the growth of the world's nuclear industry. Its expertise is specifically related to :

- the Transport of radioactive material
- the Design and procurement of the appropriate packagings and equipments

Through a permanent network of affiliated companies, TRANSNUCLÉAIRE operates on a worldwide basis, providing each customer with a full "door to door" transport arrangement. This is important as all transport operations have distinctive features and the following steps must be performed accurately:

- Obtaining Regulatory authorizations, package licenses and license validations in different countries concerned with the transport.
- Selecting the best routes and the most reliable transport companies.
- As necessary, drawing up customs declarations, providing import/export licenses and delivery verification certificates, complying with physical protection requirements, supplying nuclear liability coverage, providing loss and damage insurance, representing consignor for transports performed under exclusive use, establishing emergency plans and providing technical assistance in case of accident, etc...

In addition TRANSNUCLÉAIRE can rent standard equipments (in particular shielded casks) for transport or storage, develop new ones and provide assistance to reactors for operating the equipment or train their staff, maintaining quick connection with reprocessors within the framework of a reprocessing contract or provide the reactor operators with a complete transport/reprocessing package.

One of the first casks developed by TRANSNUCLÉAIRE was the Pegase cask which contains up to 40 standard MTR elements with a cooling time of 4 months. This development was made at the request of the French Atomic Energy Commission who ordered 6 units. Now, the casks are the property of COGEMA who performs the maintenance in specialized shops, but they remain available through TRANSNUCLÉAIRE, in particular for the transport of MTR spent fuel to US reprocessing plants.

As a matter of fact, just during the past decade, TRANSNUCLÉAIRE used the casks for more than 110 shipments to Savannah River and Idaho. The transports originated mainly from France, Belgium and Denmark but TRANSNUCLÉAIRE has also transported spent MTR fuel from Sweden, Holland, Spain, Italy, Switzerland, Turkey and South Africa, to various reprocessing plants, using different types of shielded casks, in particular, the TN1 and TN7 models.

TRANSNUCLÉAIRE has also developed various shielded casks which are currentlyu owned by themselves or customers to serve different test reactors throughout the world and especially to transport fuel or material specimens for postirradiation examinations (PIE). Of course, TRANSNUCLÉAIRE has new casks currently under development: cen of them is an extra large capacity cask for the transport of MTR fuel with one year cooling time. As concerns the unirradiated MTR fuel, TRANSNUCLÉAIRE currently transports some enriched UF6 but mainly delivers enriched metallicuranium to CERCA Plant in France and transports the completed elements to the various customers of CERCA throughout the world, using different packaging generally supplied by the customers or CERCA.

Let me quickly give TRANSNUCLÉAIRE positions concerning the recent changes and trends affecting MTR transport business.

- First, I want to mention the impact of the 1985 revision of the IAEA regulations for the transport of radioactive materials. One feared in particular that the reduction by a factor 5 of the A2 value for Uranium above 5% enrichment would affect the licensability of some existing packaging for fresh MTR assemblies (such as CERCA FS13 model). In fact this is not the case, as even for the new reduced A2 value, the activity of the fuel matrix does not exceed the allowable limit for LSA III materials, whichever is the enrichment of the fuel elements. Nevertheless, the margin for highly enriched fuel is now so slim that any foreseeable change in the regulation to take into account the activity of uranium impurities may reverse the above conclusion. More generally, one may consider that the implementation of 1985 IAEA regulations which is foreseen in 1990 will not significantly affect MTR transports, even if some very old casks risk to become obsolete due to a lack of Q.A. records or poor maintenance.

  One also may question the impact on transport business of the reduction of fuel enrichment from about 93% to less than 20%, together with the foreseeable increase of uranium in the fuel elements.

  From a criticality point of view, there should be no problem, except in some instances the need to perform new criticality calculations to support package license extensions.

  We can also mention that even for expected extended burnups the neutron dose rate at the surface of spent fuel casks will remain negligible.

  A positive consequence of the enrichment reduction is linked to the physical protection of unirradiated fuel as the armed escorts and air force planes required above 20% enrichment will not be necessary any more: this will greatly simplify transport coordination and speed up deliveries, especially with international transports.

- To complete this quick survey of trends concerning MTR fuel management, I should mention that to deal with difficulties for renewal of reprocessing contracts, TRANSNUCLÉAIRE can offer economical storage casks or storage/transport casks allowing reactors to wait for a satisfactory solution to the problems linked to reprocessing of MTR fuel.

Final List of Attendees

1988 International Meeting on Reduced Enrichment for Research and Test Reactors

Argonne National Laboratory
September 19-22, 1988

Adolph, Eivind (Mr.)
Metallurgy Department
Risø National Laboratory
Post Box 49
DK-4000 Roskilde
Denmark

Phone: 45-2-37-1212
Telex: 43 116
Facsimile: 45-2-35-1173

Ahlf, Jürgen (Dr.)
Commission of the European Communities
Joint Research Centre
P.O. Box 2
1755 ZG Petten
The Netherlands

Phone: 31-22-46-5101
Telex: 57211 REACP
Facsimile: 31-22-46-1002

Aldemir, Tunc (Dr.)
Department of Nuclear Engineering
The Ohio State University
206 West 18th Avenue
Columbus, Ohio 43210
USA

Phone: 614-422-4627
Telex: None
Facsimile: 614-292-3163

Axmann, Anton (Dr.)
Hahn-Meitner-Institut
Glienicker Str. 100
D-1000 Berlin 39
Federal Republic of Germany

Phone: 49-30-8009-2740
Telex: 185 763
Facsimile: 49-30-8009 2999

Ballagny, Alain (Mr.)
Services des Piles
CEA-Centre d'Etudes Nucleaires de Saclay
91191 gif sur Yvette
Cedex
France

Phone: 33-1-69-08-41-95
Telex: ENERG 604641F
Facsimile: 33-1-69-08-65-11

Bauer, Ekkehardt (Dr.)
Institut Laue-Langevin
Avenue des Martyrs
BP 156X
F38042 Grenoble
France

Phone: 33-76-487000
Telex: 320621F
Facsimile: 33-76-483906

Beeckmans de West-Meerbeeck, Andre, (Dr.)
Belgian Nuclear Research Centre
Centre d'Etude de l'Energie Nucleaire
CEN/SCK
200 Boeretang
B-2400 Mol
Belgium

Phone: 32-14-311801
Telex: 31922 ATOMOL B
Facsimile: 32-14-315021

Blum, Paul (Mr.)
Transnucléaire
11, rue Christophe Colomb
75008 Paris
France

Phone: 33-1-47.23.78.50
ts
Telex: 280992
Facsimile: 33-1-47.20.26.08

Bornstein, Ira (Mr.)
RAS-208
Argonne National Laboratory
9700 So. Cass Avenue
Argonne, Illinois 60439
USA

Phone: 312-972-4673 (Comm. & FTS)
TWX: 910-258-3285 US DOE-CH ARGN
Facsimile: 312-972-5318

Borring, Jan (Mr.)
Atlas Advanced Engineering Division
Atlas-Danmark/Risø National Laboratory
P.O. Box 49
DK-4000 Roskilde
Denmark

Phone: 45-2-37-12-12, Ext. 5738
Telex: 43116A RISOE DK
Facsimile: 45-2-35-11-73

Bretscher, Manuel M. (Dr.)
RERTR/AP-207
Argonne National Laboratory
9700 S. Cass Avenue
Argonne, Illinois 60439
USA

Phone: 312-972-8616 (Comm. & FTS)
TWX: 910-258-3285 US DOE-CH ARGN
Facsimile: 312-972-5161 or 4007

Brown, Keith R. (Mr.)
EG&G Idaho, Inc.
P.O. Box 1625
Idaho Falls, Idaho 83415
USA

Phone: 208-526-1181
583-1181 (FTS)
TWX: None
Facsimile: Unknown

Byszewski, Witold (Mr.)
International Atomic Energy Agency
Wagramerstrasse 5
A-1400 Vienna
Austria

Phone: 43-222-2360, X-2655
Telex: 112645 ATOM A
Facsimile: Unknown

Ceja, Salvador (Mr.)
Office of International Affairs
and Energy Emergencies
U.S. Department of Energy
M/S 7-G-046, Forrestal Bldg.
Washington, D.C. 20585
USA

Phone: 202-586-1883
896-1883 (FTS)
TWX: 710-822-0176 DOEFRSTAL WSH
Facsimile: 202-586-2707

Colton, J. Phillip (Mr.)
Nuclear Safeguards and Technology Div.
Arms Control and Disarmament Agency
320 21st Street, N.W.
Main State Room 4664
Washington, D.C. 20541
USA

Phone: 202-647-1140 (Comm. & FTS)
Telex: ITT-44080, WI-WUI-64144
Facsimile: 202-647-6721

Copeland, George L. (Dr.)
Oak Ridge National Laboratory
Bldg. 4508, MS-6089
P.O. Box X
Oak Ridge, Tennessee 37831-6089
USA

Phone: 615-574-3909
624-3909 (FTS)
TWX: 810-572-1076 US DOE OKRE
Facsimile: 615-574-7721

Cundy, Michael R. (Mr.)
Commission of the European Communities
Joint Research Centre - Petten
P.O. Box 2
1755 ZG Petten
The Netherlands

Phone: 31-22-46-5332
Telex: 57211 REACP NL
Facsimile: 31-22-46-1002

Deen, James R. (Dr.)
RERTR/AP-207
Argonne National Laboratory
9700 S. Cass Avenue
Argonne, Illinois 604239
USA

Phone: 312-972-4853 (Comm. & FTS)
TWX: 910-258-3285 US DOE-CH ARGN
Facsimile: 312-972-5161 or 4007

DeFelice, John D.
Precision Components Corporation
Box M-101, 500 Lincoln Street
York, Pennsylvania 17405
USA

Phone: 717-848-1126
Telex: None
Facsimile: Unknown

DeLaBarre, R. Robin (Mr.)
Department of State
OES/NEC, Rm. 7820
2201 C Street, N.W.
Washington, D.C. 20520
USA

Phone: 202-647-2245 (Comm. & FTS)
Telex: 440511 IBGC UI
Facsimile: 202-647-6510

DeVries, Jacob W. (Mr.)
HOR/IRI
Interuniversitair Reactor Institut
Mekelweg 15
NL 2629 JB Delft
The Netherlands

Phone: 31-15-781402
Telex: 38214 IRI NL
Facsimile: 31-15-786422

DiMeglio, Francis A. (Mr.)
Rhode Island Nuclear Science Center
Rhode Island Atomic Energy Commission
South Ferry Road
Narragansett, Rhode Island 02882-1197
USA

Phone: 401-789-9391
Telex: None
Facsimile: Unknown

Domagala, Robert F. (Mr.)
RERTR/MCT-212
Argonne National Laboratory
9700 S. Cass Avenue
Argonne, Illinois 60439
USA

Phone: 312-972-5197 (Comm. & FTS)
TWX: 910-258-3285 US DOE-CH ARGN
Facsimile: 312-972-4798

Ernst, Peter C. (Mr.)
Nuclear Reactor
McMaster University
1280 Main Street West
Hamilton, Ontario L8S 4K1
Canada

Phone: 416-525-9140, Ext. 4279
Telex: 061-8347
Facsimile: 416-528-5030

Fanjas, Yves (Mr.)
CERCA
BP-1114
Les Berauds
26104 Romans, Cedex
France

Phone: 33-75-05-6061
Telex: FCOMB A 345155F
Facsimile: 33-75-05-6078

Fuchs, Heinrich (Mr.)
Compagnie Europeenne de Combustible
CERCA-NUKEM
c/o NUKEM GmbH
Postfach 110080
645 Hanau 11
Federal Republic of Germany

Phone: 49-6181-58-2350
Telex: 4184780 NUKM D
Facsimile: Unknown

Fukushima, Shounosuke (Mr.)
Nuclear Industry Section 2
Nuclear Energy Department
Nissho Iwai Corporation
4-5, Akasaka 2-chome
Minato-ku, Tokyo 107
Japan

Phone: 81-3-588-2794
Telex: 22233
Facsimile: 81-3-588-4216/4924

Futamura, Yoshiaki (Dr.)
Japan Atomic Energy Research Institute
Tokai-mura, Ibaraki-ken
Japan 319-11

Phone: 81-292-82-5318
Telex: J24596
Facsimile: Unknown

Gailar, Owen (Dr.)
School of Nuclear Engineering
Purdue University
West Lafayette, Indiana 47907
USA

Phone: 317-494-5754
Telex: Unknown
Facsimile: Unknown

Giorsetti, Domingo (Mr.)
Comisión Nacional de Energia Atomica
Departamento Combustibles Nucleares
Avenida del Libertador 8250
1429 Buenos Aires
Argentina

Phone: 541-707-713
Telex: 26110 CAC AR
Facsimile: 541-752-4722

Gruber, Gerhard (Mr.)
MTR Fuel Services
NUKEM GmbH, Alzenau Branch
P.O. Box 1313, Industriestr. 13
D-8755 Alzenau
Federal Republic of Germany

Phone: 49-6023-500-609
Telex: 4188233 NUKA D
Facsimile: 49-6023-500-600

Guiheux, Jean-Michel (Mr.)
COGEMA
2, rue Paul Dautier
B.P. 4 - 78141 Velizy-Villaccublay
Cedex
France

Phone: 33-1-39-46-96-41
Telex: 697 833 F
Facsimile: 33-1-34-65-1377

Haack, Karsten (Mr.)
Risø National Laboratory
Postbox 49
DK-4000 Roskilde
Denmark

Phone: 45-2-37-1212
Telex: 43116A RISOE DK
Facsimile: 45-2-75-5052

Hassel, Horst W. (Mr.)
NUKEM GmbH
Postfach 110080
D-6450 Hanau 11
Federal Republic of Germany

Phone: 49-6181-58 x2336
Telex: 4184780 NUKM D
Facsimile: Unknown

Hejian, Mao (Mr.)
Southwest Center for Reactor
Engineering Research & Design
P.O. Box 291-106
Chengdu, Sichuan
Peoples Republic of China

Phone: 825 Special Line 4416
Telex: 222315 FACNC CN881020/ICD
Facsimile: Unknown

Hofman, Gerard L. (Dr.)
RERTR/MCT-EBR-II-310
Argonne National Laboratory
9700 S. Cass Avenue
Argonne, Illinois 60439
USA

Phone: 312-972-6683 (Comm. & FTS)
TWX: 910-258-3285 US DOE-CH ARGN
Facsimile: 312-972-6788

Horn, Brian G. (Mr.)
U.S. Nuclear Regulatory Commission
Mail Stop 881-SS
Washington, D.C. 20555
USA

Phone: (301) 427-4271 (Comm. & FTS)
Telex: 908142 NRC-BHD-WSH
Facsimile: Unknown

Jaspert, Jürgen F. W. (Mr.)
Euratom Supply Agency
Rue de la Loi, 200
B-1049 Brussels
Belgium

Phone: 32-2-235-1248
Telex: 21877 COMEUR BRU
Facsimile: 32-2-235-0527

Kanda, Keiji (Dr.)
Kyoto University
Research Reactor Institute
Kumatori-cho, Sennan-gun
Osaka 590-04
Japan

Phone: 81-724-52-0901
Telex: 5397073 KURRIA J
Facsimile: 81-724-53-0360

Kennedy, Ian C. (Mr.)
Atomic Energy of Canada Ltd.
Chalk River Nuclear Laboratories
Chalk River, Ontario K0J 1J0
Canada

Phone: 613-584-3311, X-3028
Telex: 053-34555 AECL B CKR
Facsimile: 613-589-2039

Knight, Rodney W. (Mr.)
Operations Division
Oak Ridge National Laboratory
Bldg. 7910
P.O. Box X
Oak Ridge, Tennessee 37831-6387
USA

Phone: 615-574-5713 (Comm.)
FTS: 624-5713 or 624-6916
Telex: 810-572-1076 US DOE OKRE
Facsimile: Unknown

Krug, Wolfgang (Dr.)
Zentralableitung Forschungsreaktoren
Kernsforschungsanlage Jülich GmbH
Postfach 1913 D-5170
Jülich 1
Federal Republic of Germany

Phone: 49-2461-613197
Telex: 833556 KFA D
Facsimile: 49-2461-615327

Krull, Wilfried (Dr.)
Forschungszentrum Geesthacht
GKSS Reaktorstrasse 7-9
Postfach 1160
D-2054 Geesthacht
Federal Republic of Germany

Phone: 49-4152-87-1200
Telex: 218712 GKSS G
Facsimile: 49-4152-87-1618

Kuk, I. H.(Dr.)
Radiation Shielding Material
Fabrication Research Division
Korea Advanced Energy Research Institute
P.O. Box 7, Daeduk-Danji
Choong-nam
Korea 300-31

Phone: 42-820-2334
Telex: KAERI K-45553
Facsimile: Unknown

Kung, Hsien-tzu (Mr.)
Institute of Nuclear Energy Research
P.O. Box 3-14
Lung-tan, 32500
Taiwan, R.O.C.

Phone: 886-2-3145384, X-4148
Telex: 34154 CAEC
Facsimile: 886-3-471-1064

Kwok, Jane (Ms.)
RERTR/CMT-205
Argonne National Laboratory
9700 South Cass Avenue
Argonne, IL 60439
USA

Phone: 312-972-7699 (Comm. & FTS)
TWX: 910-258-3285 US DOE-CH ARGN
Facsimile: 312-972-5287

Madariaga, Marcelo (Mr.)
Comision Nacional de Energia Atomica
Centro Atomico Bariloche
Bariloche
Argentina

Phone: Unknown
Telex: 80739 INVAP AR
Facsimile: Unknown

Marguin, Jean-Claude (Mr.)
CERCA
9-11 Rue Georges Enesco
94000 Creteil, Cedex
France

Phone: 33-14-377-1263
Telex: 213051 F CERCA
Facsimile: Unknown

Marks, John A. (Mr.)
Babcock & Wilcox
Naval Nuclear Fuel Division
P.O. Box 785, Mail Code 61
Lynchburn, Virginia 24505
USA

Phone: 804-522-5340
Telex: 901640 B&W NNFD LY
Facsimile: 804-522-5922

Matos, James E. (Dr.)
RERTR/AP-207
Argonne National Laboratory
9700 S. Cass Avenue
Argonne, Illinois 60439
USA

Phone: 312-972-6758 (Comm. & FTS)
TWX: 910-258-3285 US DOE-CH ARGN
Facsimile: 312-972-5161 or 4007

Merchie, Francis (Mr.)
Research Reactors Division
CEA/CEN-Grenoble
P.O. Box 85
38041 Grenoble, Cedex, France

Phone: 33-76-88-44-00
Telex: 320323 F ENERG A
Facsimile: Unknown

Michaels, Theodore S. (Mr.)
U.S. Nuclear Regulatory Commission
Mail Stop 11H3
Washington, D.C. 20555
USA

Phone: 301-492-1102 (Comm. & FTS)
Telex: 908142 NRC-BHD WSH
Facsimile: 301-492-7142

Mo, Sai Chi (Dr.)
RERTR-207
Argonne National Laboratory
9700 S. Cass Avenue
Argonne, Illinois 60439
USA

Phone: 312-972-6054 (Comm. & FTS)
TWX: 910-258-3285 US DOE-CH ARGN
Facsimile: 312-972-5161 or 4007

Muranaka, Richard G. (Mr.)
Department of Research and Isotopes
Division of Research & Laboratories
IAEA - Rm. 2372
Wagramerstrasse 5
P.O. Box 100
A-1400 Vienna, Austria

Phone: 43-222-2360, X-1751
Telex: 112645Z ATOM A
Facsimile: 43-123-4564

Parker, Keith A. (Mr.)
United Kingdom Atomic Energy Authority
Commercial Directorate, Rm. E443
Risley, Warrington,
Cheshire, WA3 6AT
United Kingdom

Phone: 44-925-31244 x-2631
Telex: 629301 ATOMRY G
Facsimile: 44-925-31244, X-2563

Perdomo, Ismael Antonio Concha (Mr.)
Area de Fisica
Instituto de Asuntos Nucleares
Avenida Eldorado Carrera 50
Apartado Aereo 8595
Bogota, D.E.
Colombia

Phone: Unknown
Telex: 42416 IANBG CO
Facsimile: Unknown

Porte, Philippe (Mr.)
CERCA
9-11, Rue Georges Enesco
94008 Creteil, Cedex
France

Phone: 33-43-77-12-63
Telex: 264276
Facsimile: 33-43-99-96-59

Poupard, Jean. F. (Mr.)
CERCA
Les Berauds, B P 1114
26104 Romans, Cedex
France

Phone: 33-75-75-05-60-00
Telex: FCOMB A 345155F
Facsimile: Unknown

Preble, Harry E. (Mr.)
Naval Nuclear Fuel Division
Babcock & Wilcox
P.O. Box 785
Mt. Athos Road
Lynchburg, Virginia 24505-0785
USA

Phone: 804-522-5660
Telex: 901640 B&W NNFD LY
Facsimile: 804-522-5922

Rest, Jeffrey (Dr.)
MCT-212
Argonne National Laboratory
9700 South Cass Avenue
Argonne, Illinois 60439
USA

Phone: 312-972-5026 (Comm. & FTS)
TWX: 910-258-3285 US DOE-CH ARGN
Facsimile: 312-972-4798

Röhrmoser, Anton (Dr.)
Physik-Department, E21
Technische Universitaet München
8046 Garching
Federal Republic of Germany

Phone: 49-89-32092151
Telex: Unknown
Facsimile: 49-89-32092112

Ruzicka, William G. (Mr.)
Cintichem, Inc.
P.O. Box 816
Tuxedo, New York 10987
USA

Phone: 914-351-2131, X-234
TWX: 710-577-2881
Facsimile: Unknown

Rydin, Roger A. (Dr.)
Reactor Facility
University of Virginia
Charlottesville, Virginia 22901
USA

Phone: 804-924-7136
Telex: Unknown
Facsimile: Unknown

Sakurai, Fumio (Dr.)
Japan Atomic Energy Research Institute
Tokai-mura, Ibaraki-ken
Japan 319-11

Phone: 81-292-67-4111
Telex: J24596
Facsimile: Unknown

Saltvedt, Kristian (Mr.)
Fuel Technology Department
Studsvik Energiteknik AB
S-611 82 Nyköping
Sweden

Phone: 46-155-21000
Telex: 64013 STUDS S
Facsimile: 46-155-63070

Sameh, A. Ali (Dr.)
Kernforschungszentrum Karlsruhe
Institut für Radiochemie
Postfach 3640
Weberstrasse 5
D-7500 Karlsruhe 1
Federal Republic of Germany

Phone: 49-7247-82-2664
Telex: 17724716-KFK
Facsimile: Unknown

Schreader, Jack W. (Mr.)
Atomic Energy of Canada Ltd.
Chalk River Nuclear Laboratories
Chalk River, Ontario K0J 1J0
Canada

Phone: 613-584-3311, X-4350
Telex: 053-34555 AECL B CKR
Facsimile: 613-589-2039

Seymour, L. Kenneth (Mr.)
EG&G Idaho, Inc.
P.O. Box 1625 - MS 7114
Idaho Falls, Idaho 83415
USA

Phone: 208-526-0203
FTS: 583-0203
TWX: 910-977-5915 US DOE IDAH
Facsimile: 208-526-4715

Snelgrove, James L. (Dr.)
RERTR/AP-207
Argonne National Laboratory
9700 S. Cass Avenue
Argonne, Illinois 60439
USA

Phone: 312-972-6369 (Comm. & FTS)
TWX: 910-258-3285 US DOE-CH ARGN
Facsimile: 312-972-5161 or 4007

Strömich, Alfred (Dr.)
Interatom GmbH
Friedrich-Ebert-Strasse
5060 Bergisch Gladbach 1
Federal Republic of Germany

Phone: 49-2204-842677
Telex: 8878457 IAGL D
Facsimile: Unknown

Talnagi, Joseph W. (Mr.)
The Ohio State University
Nuclear Reactor Laboratory
1298 Kinnear Road
Columbus, Ohio 43212
USA

Phone: 614-422-6755
Telex: Unknown
Facsimile: 614-730-4271

Thamm, Gerd H. (Dr.)
Zentralableitung Forschungsreaktoren
Kernsforschungsanlage Jülich GmbH
Postfach 1913 D-5170
Jülich 1
Federal Republic of Germany

Phone: 49-2461-61-5055
Telex: 833556-20 KF D
Facsimile: 49-2461-61-3841

Thom, David (Mr.)
Dounreay Nuclear Power Development
Establishment
Northern Division
United Kingdom Atomic Energy Authority
Thurso
Caithness KW147TZ
Scotland

Phone: 44-847-62121, X-677
Telex: 75297
Facsimile: 44-847-63167, X-648

Tissier, Antoine (Mr.)
CERCA
Les Berauds
26104 Romans-sur-Isere
France

Phone: 33-75-70 02 22
Telex: FCOMB A 345155F
Facsimile: Unknown

Travelli, Armando (Dr.)
RERTR/AP-207
Argonne National Laboratory
9700 S. Cass Avenue
Argonne, Illinois 60439
USA

Phone: 312-972-6363 (Comm. & FTS)
TWX: 910-258-3285 US DOE-CH ARGN
Facsimile: 312-972-5161 or 4007

Tschiesche, Horst (Mr.)
Nuclear Cargo & Service GmbH
Rodenbacher Chaussee 6
Postfach 11 00 30
D-6450 Hanau 11
Federal Republic of Germany

Phone: 49-6181-58-2427
Telex: 418[illegible]3 TNH D
Facsimile: 49-6181-58-2081

Vandegrift, George F. (Dr.)
RERTR/CMT-205
Argonne National Laboratory
9700 S. Cass Avenue
Argonne, Illinois 60439
USA

Phone: 312-972-4513 (Comm. & FTS)
TWX: 910-258-3285 US DOE-CH ARGN
Facsimile: 312-972-5287

Visser, Donald R. (Dr.)
CMT-205
Argonne National Laboratory
9700 S. Cass Avenue
Argonne, Illinois 60439
USA

Phone: 312-972-4331 (Comm. & FTS)
TWX: 910-258-3285 US DOE-CH ARGN
Facsimile: 312-972-5287

Wares, Alexander (Mr.)
Dourneay Nuclear Power Development
Establishment
Northern Division
United Kingdom Atomic Energy Authority
Thurso, Caithness KW14 7TZ
Scotland

Phone: 44-847-62121, X-677
Telex: 75297
Facsimile: Unknown

West, Gordon B. (Mr.)
General Atomics
TRIGA Reactor Division
P.O. Box 85608
San Diego, California 92138
USA

Phone: 619-455-2292
Telex: 695065 GA TECH SDG
Facsimile: 619-455-4169

Wiencek, Thomas C. (Mr.)
RERTR/MCT-212
Argonne National Laboratory
9700 S. Cass Avenue
Argonne, Illinois 60439
USA

Phone: 312-972-5020 (Comm. & FTS)
TWX: 910-258-3285 US DOE-CH ARGN
Facsimile: 312-972-4798

Woodruff, William L. (Dr.)
RERTR/AP-207
Argonne National Laboratory
9700 S. Cass Avenue
Argonne, IL 60439
USA

Phone: 312-972-8634 (Comm. & FTS)
TWX: 910-258-3285 US DOE-CH ARGN
Facsimile: 312-972-5161 or 4007

DISTRIBUTION FOR ANL/RERTR/TM-13 (CONF-8809221)

Internal:

A. Schriesheim
C. E. Till
P. I. Amundson
D. W. Cissel
W. L. Deitrich
M. H. Derbidge
L. G. LeSage
R. B. Poeppel
R. J. Teunis
A. Travelli (75)
D. C. Wade
All ANL Attendees (15)
TIS Files (1)

External:

ANL East Library

ANL West Library

DOE-OSTI, for distribution per UC-940 (99)

Manager, Chicago Operations Office, DOE

Director, Technology Management Div., DOE-CH

Engineering Physics Division Review Committee:

Robert J. Budnitz, Future Resources Associated
Michael J. Driscoll, Massachusetts Institute of Technology
George H. Gillespie, G.H. Gillespie Associates
W. Reed Johnson, University of Virginia
James E. Leiss, Consultant
Warren F. Miller, Jr., University of California
Gerold Yonas, Sandia National Laboratories

All Non-ANL Attendees and Participants (67)

END

DATE
FILMED
3/10/94